THÈSE

Présentée pour obtenir le grade de

DOCTEUR DE L'UNIVERSITÉ DE STRASBOURG

par

Rafael BALLESTEROS GARRIDO
Ingénieur ECPM

Synthesis of New Triazolopyridine and Triazoloquinoline Based Ligands and Application as Fluorescence Sensors

Synthèse des Nouveaux Ligands à base de Triazolopyridines et Triazoloquinoléines et Application comme Capteurs de Fluorescence.

soutenue publiquement le 9 Octobre 2009
devant la commission d'examen composée de :

Dr Frédéric LEROUX	*Directeur de thèse*
Pr. Françoise COLOBERT	*Directeur de thèse*
Pr. Paul KNOCHEL	*Rapporteur Externe*
Pr. Miguel YUS	*Rapporteur Externe*
Pr. Mir Wais HOSSEINI	*Examinateur*
Pr. Belén ABARCA	*Examinateur*

Résumé de la thèse de doctorat

Discipline : Chimie (42000 03)

Spécialité : Chimie Organique

Présentée par : Rafael Ballesteros Garrido

Titre : Synthesis of New Triazolopyridine and Triazoloquinoline Based Ligands and Application as Fluorescence Sensors

Unité de Recherche : UMR 7509
Chimie moléculaire

Co-Directeur de thèse : Pr. Françoise COLOBERT

Co-Directeur de thèse : Dr Frédéric LEROUX, HDR

Grade Localisation: École Européenne de Chimie, Polymères et Matériaux. Laboratoire de Stéréochimie (UMR 7509). 25, Rue Becquerel F-67087 Strasbourg

1. Introduction : chimie de la [1,2,3]triazolo[1,5-*a*]pyridine

À l'heure actuelle, les hétérocycles aromatiques sont des composés clé dans de nombreux domaines de la science. Ils constituent le squelette d'un grand nombre de médicaments et de produits employés dans l'agrochimie. On les rencontre également en chimie de coordination et dans les matériaux moléculaires[1].

La [1,2,3]triazolo[1,5-*a*]pyridine est un composé constitué par un triazole et une pyridine[2]. En dépit de sa simplicité structurale, cette substance possède une réactivité très particulière du point de vue synthétique mais aussi théorique. Sa chimie a été développée par les groupes de Jones (Université de Keele, Grande Bretagne)[2] et d'Abarca[3] (Université de Valence, Espagne) dans les années 80. Depuis, de nombreux travaux ont permis de connaitre sa réactivité ainsi que ses propriétés. Ainsi, la [1,2,3]triazolo[1,5-*a*]pyridine peut être considérée comme le précurseur de pyridines 2,6 disubstituées[4,5] ou de 2,2'-bypiridines[6].

Un des intérêts majeurs de la [1,2,3]triazolo[1,5-*a*]pyridine est la possibilité de fonctionnaliser sa position 7 par métallation[4] avec des bases comme le BuLi ou la LDA suivi d'un piégeage avec un électrophile, ce qui permet de créer une grande diversité moléculaire. En effet, la position 7 dans une triazolopyridine est équivalente à la position 2 d'une pyridine. Néanmoins, l'activation de l'hydrogène 2 de cette dernière nécessite l'emploi de la base de Caubère (BuLi-LiDMAE) ou la protection de l'azote de la pyridine sous forme de *N*-oxyde, de complexe *N*-BF_3 ou *N*-hexafluoroacétone par exemple. A noter également qu'à partir de 2-(aldéhyde ou cétone)pyridines, les [1,2,3]triazolo[1,5-*a*]pyridines peuvent servir d'intermédiaires à la synthèse de pyridines 2,6-disubstituées lorsqu'elles sont soumises à un traitement acide[6] (**Schéma 1**).

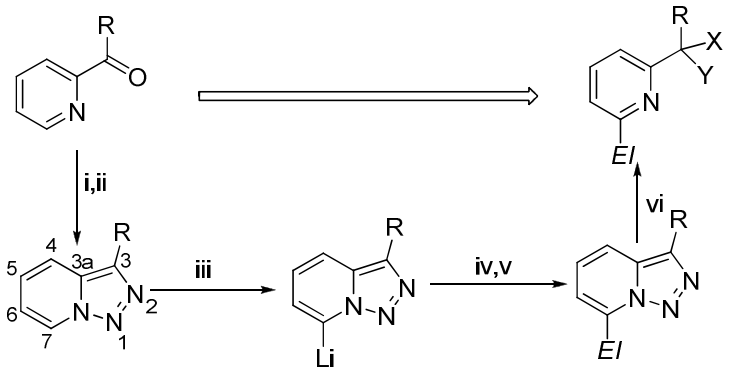

i= NH_2NH_2 ; ii= MnO_2,CH_2Cl_2; iii=BuLi,Toluène,-40 °C; iv= Électrophile; v= NH_4Cl, H_2O
vi= AcOH (X = H, Y = OAc), Acide Sufurique (X = H, Y = OH)....

Schéma 1 : Obtention de pyridines 2,6-disubstituées à partir de la [1,2,3]triazolo[1,5-*a*]pyridine.

La deuxième propriété remarquable de ces systèmes est le dynamisme[7] du système triazole dans la 3-(2'-pyridyl)-[1,2,3]triazolo[1,5-*a*]pyridine. Il peut en effet se présenter sous 2 formes A et B (**Schéma 2**). Les observations expérimentales ont été corroborées par les études[8] théoriques réalisées par Abarca , Elguero *et al* à l'ICM à Madrid.

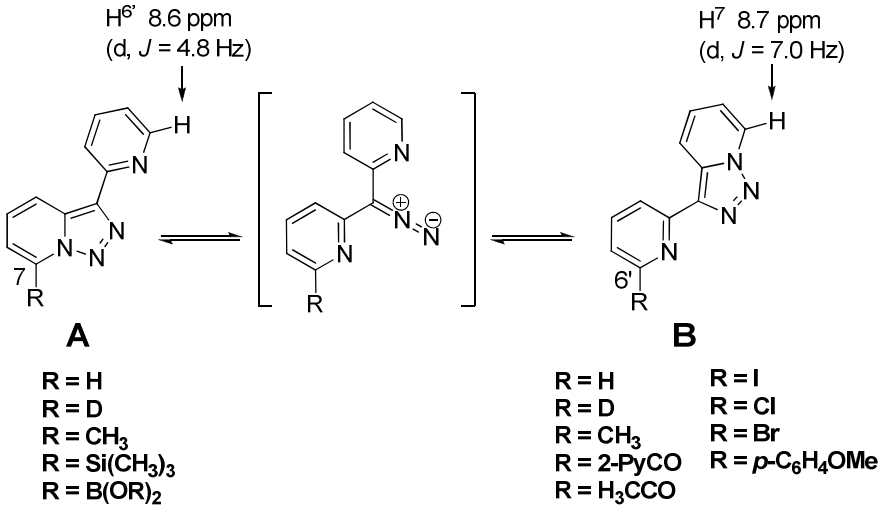

Schéma 2 : Réarrangement de la 3-(2'-pyridyl)-[1,2,3]triazolo[1,5-*a*]pyridine.

Des études ont montré que les substituants électron-donneurs favorisent une structure de type A (pas de réarrangement) alors que les substituants électron-accepteurs conduisent à une structure de type B (réarrangement). Par ailleurs, certains substituants (H, D et CH_3) ont fourni des mélanges dans diverses proportions. D'autre part, ce réarrangement donne la possibilité d'obtenir des structures tridentates (structure B) grâce à l'introduction d'électrophiles accepteurs coordinants (**Schéma 3**):

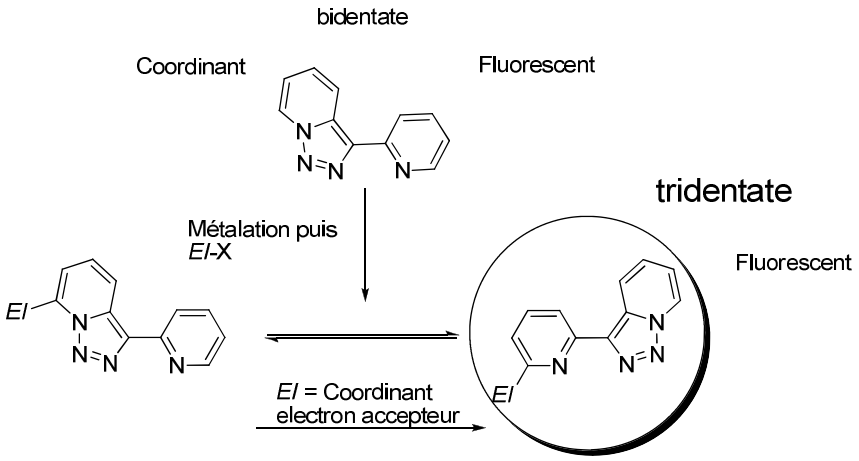

Schéma 3 : Obtention de structures fluorescentes tridentates.

Dans ce contexte et en collaboration avec le groupe d'Abarca, nous avons mis au point la synthèse de nouvelles familles de triazolopyridines possédant différents substituants pouvant avoir une importance biologique (sulfoxydes et dérivés de la fenchone) et catalytique (phosphines). Nous nous sommes également intéressés à la chimie d'un analogue : la triazoloquinoléine, ce qui nous a ouvert l'accès à des 2,8-quinoléines di-substituées. Nous avons également mis en évidence un nouveau réarrangement avec la triazoloquinoléine-pyridine.

Enfin, nous avons étudié les propriétés fluorescentes de ces structures[9] qui se sont révélées être d'excellents capteurs de métaux, d'anions et d'acides aminés. Elles nous ont également permis d'effectuer de la reconnaissance chirale par fluorescence.

2. Synthèse des triazolopyridines chirales : vers l'obtention de pyridines 2,6 di-fonctionnalisées

Comme décrit précédemment, lorsque le noyau triazole est traité par un équivalent de butyllithium, on peut effectuer une métallation sélective[5,6] en position 7. Nous avons ensuite introduit un auxiliaire chiral par piégeage de l'intermédiaire lithié avec la (-)-fenchone et le (*R*)-*p*-toluènesulfinate de menthyle (**2**, **3B** et **5**, **6B**). Nous espérions ensuite réaliser l'ouverture du triazole avec transfert de chiralité afin d'accéder à des pyridines 2,6-di-fonctionnalisées chirales (**Schéma 4** et **5**).

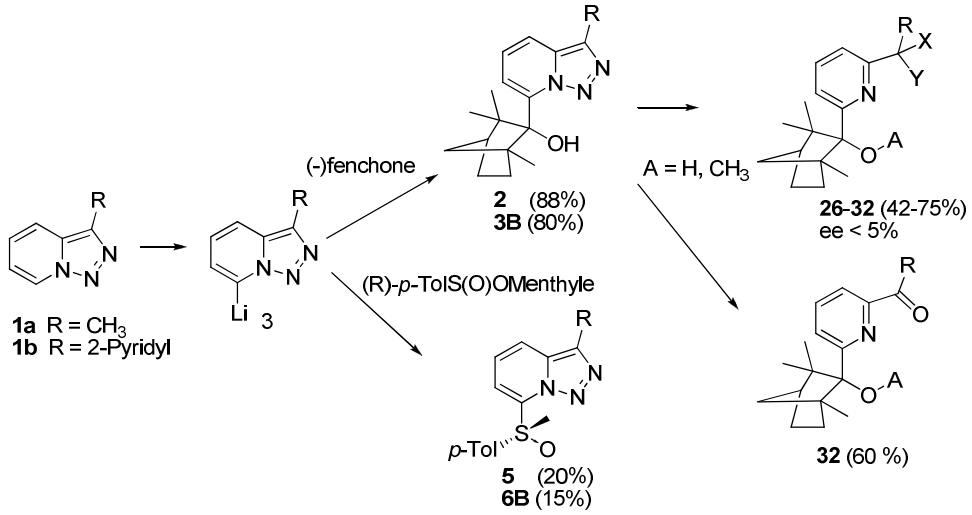

Schéma 4 : Obtention de pyridines 2,6-di-fonctionnalisées chirales.

Les dérivés de la fenchone ont été obtenus avec des bons rendements contrairement à ceux du sulfoxyde[10]. Afin d'accéder à ces structures de façon plus efficaces, nous avons utilisé la sulfoxydation catalysée au palladium initialement développée par Poli[11] sur des substrats de type iodoaryles. Nous avons étendu cette méthode à des substrats de type hétérocycliques (pyridine, thiophène, ..) et nous avons également montré qu'il était possible d'effectuer la réaction non pas à partir de iodures mais de bromures[12,13] (**Schéma 5**).

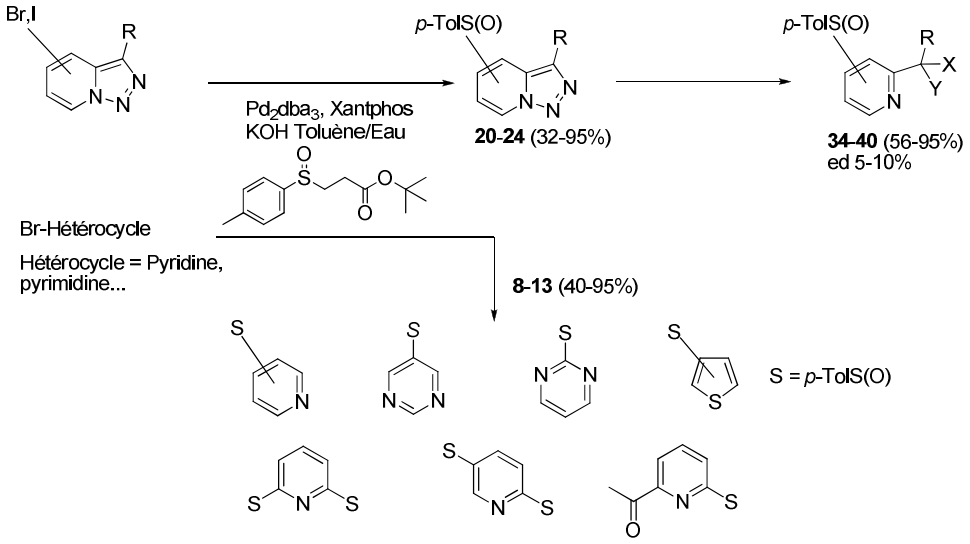

Schéma 5 : Obtention des sulfoxydes par voie catalytique.

Malheureusement, lors de l'ouverture des triazoles nous avons pu constater que le transfert de chiralité généré par la présence de la fenchone ou du sulfoxyde est limité. En effet, nous avons obtenu les

pyridines 2,6-disubstituées avec des excès énantiomériques ou diastéréomériques inférieurs à 10 %. Des tests biologiques sont actuellement en cours dans le laboratoire de Céline Tarnus à Mulhouse afin de déterminer une activité potentielle de ces composés.

3. Etudes autour d'un autre noyau : la [1,2,3]triazolo[1,5-*a*]quinoléine

3.1. Synthèse de quinoléines 2,8-disubstituées à partir de la [1,2,3]triazolo[1,5-*a*]quinoléine

La chimie de la [1,2,3]triazolo[1,5-*a*]quinoléine[14] (**44**) est restée inexplorée depuis les années 80 et possède une réactivité différente de la triazolopyridine vis-à-vis des métallations[14] (**Figure 1**).

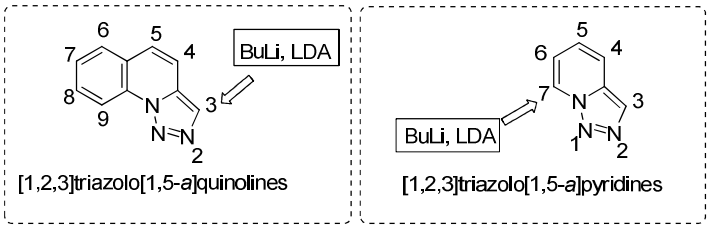

Figure 1 : Réactivité envers le BuLi et la LDA de la triazoloquinoleine et la triazolopyridine.

Notre objectif a été de fonctionnaliser sélectivement la position 3 de la [1,2,3]triazolo[1,5-*a*]quinoléine afin de générer des structures fluorescentes. Nous y sommes parvenus avec succès par traitement avec LiTMP dans le THF (4**5a-e**). D'autre part, lorsque la [1,2,3]triazolo[1,5-*a*]quinoléine (**44**) est mise à réagir avec 3 équivalents de butyllithium dans le THF, la position 9 est également métallée et il est donc possible d'introduire deux groupements fonctionnels ou atomes identiques dans ces positions (**47a-d**). Enfin, nous avons observé que les triazoloquinoléines dihalogénées ainsi obtenues peuvent facilement être converties en aldéhyde (**51a-c**) dans des conditions acides par ouverture du triazole (**Schéma 6**). Ce résultat est particulièrement intéressant compte tenu du fait que les quinoléines 2,8-disubstituées ne peuvent pas être directement synthétisées par métallation de la quinoléine déjà fonctionnalisée en position 2 par métallation de la position 8. Par ailleurs la fonctionnalisation des quinoléines a un intérêt synthétique certain étant donné que ce motif est fréquemment rencontré dans des composés biologiquement actifs[15].

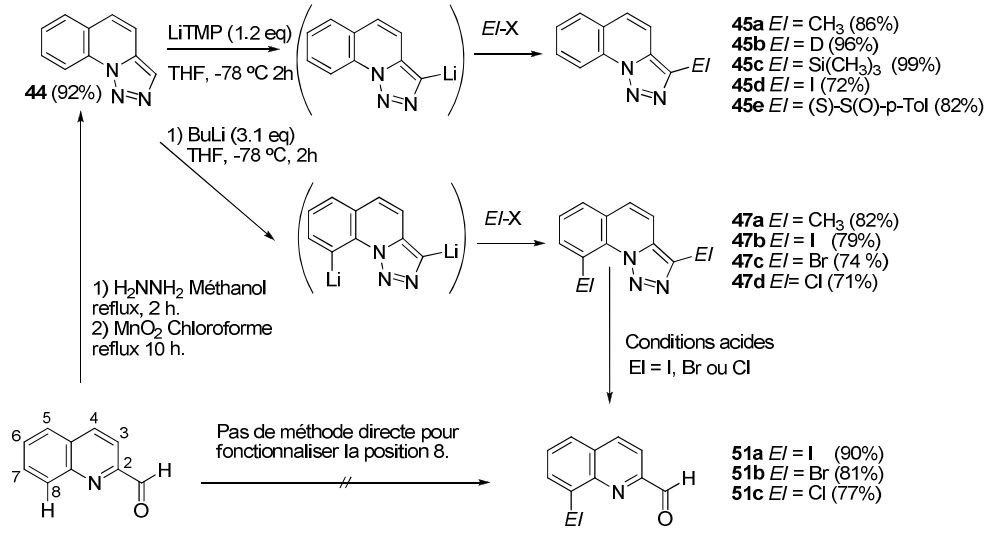

Schéma 6 : Fonctionnalisation de la triazolquinoléine obtention des quinoléines 2,8-disubstituées.

3.2. Mise en évidence d'un nouveau réarrangement

Finalement, nous nous sommes également intéressés à un analogue de la triazolopyridine-pyridine mais basé sur un noyau triazoloquinoléine : la 3-(2'-pyridyl)- [1,2,3]triazolo[1,5-*a*]quinoléine (**53**). Ce dernier a été synthétisé à l'aide des méthodes classiques à partir de la 2-bromopyridine. (**Schéma 7**)

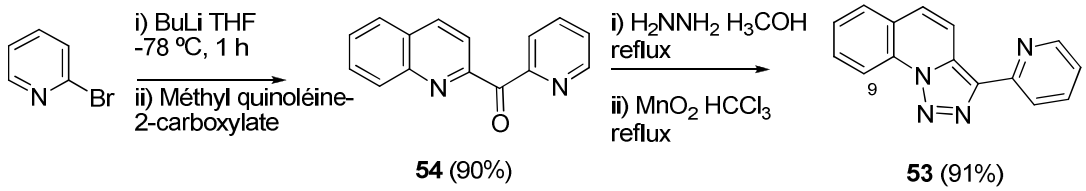

Schéma 7: Synthèse de la 3-(2'-pyridyl)- [1,2,3]triazolo[1,5-*a*]quinoléine (**8**).

Lors de la métallation de la 3-(2'-pyridyl)-[1,2,3]triazolo[1,5-*a*]quinoléine (**53**), la position 9 est la plus réactive. Après l'introduction de divers substituants, nous avons encore une fois obtenu un mélange des deux structures isomères **A** et **B**, dans des rapports différents comme dans le cas de la triazolopyridine-pyridine (**Schéma 8**).

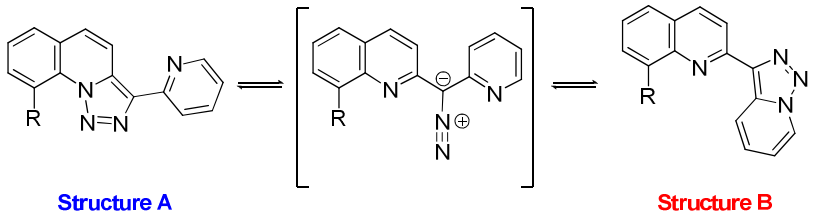

		Ratio [%]		
53A	R = H	> 99 : 1	**53B**	R = H
55A	R = D	> 99 : 1	**55B**	R = D
56A	R = I	< 1 : 99	**56B**	R = I
57A	R = CH_3	52 : 48	**57B**	R = CH_3
58A	R = Br	< 1 : 99	**58B**	R = Br
59A	R = Cl	< 1 : 99	**59B**	R = Cl
60A	R = F	17 : 83	**60B**	R = F
61A	R = $C(OH)(CH_3)_2$	< 1 : 99	**61B**	R = $C(OH)(CH_3)_2$
62A	R = OH	> 99 : 1	**62B**	R = OH
63A	R = $B(OR)_2$ pinacol ester	> 99 : 1	**63B**	R = $B(OR)_2$ pinacol ester
64A	R = OCH_3	8 : 92	**64B**	R = OCH_3
65A	R = O^{i}Pr	15 : 85	**65B**	R = O^{i}Pr

Schéma 8 : Réarrangement de la 3-(2'-pyridyl)-[1,2,3]triazolo[1,5-*a*]quinoléine (**9**).

En collaboration avec Pr. Elguero, Pr. Alkorta and Dr. Blanco nous avons effectué une nouvelle étude théorique[7,8] afin de comprendre le réarrangement qui se produit sur ce noyau. En particulier, nous avons déterminé que dans ce cas l'encombrement stérique joue un rôle (favorise les structures **B**) mais aussi que la formation des liaisons d'hydrogène peut modifier cet équilibre. Les propriétés électroniques du substituant introduit jouent aussi un rôle : les électron-donneurs favorisent une structure de type **A** (pas de réarrangement) alors que les substituants électron-accepteurs conduisent à une structure de type **B** (réarrangement).

4. Synthèse de triazolopyridines-phosphines et application

4.1 Triazolopyridine-pyridine comme senseur des propriétés électroniques de phosphines

Nous avons employé l'isomérisation de la triazolopyridine-pyridine **1b** pour observer le profil électronique des phosphines. Or cette substance est connue pour subir un réarrangement entre deux structures isomères selon la nature du substituant porté en position 7. Ces dernières sont facilement identifiables par analyse du spectre RMN ^{1}H. Les substituants donneurs favorisent la forme **A** alors que les substituants attracteurs conduisent préférentiellement à la forme **B** (**Schéme 9**).

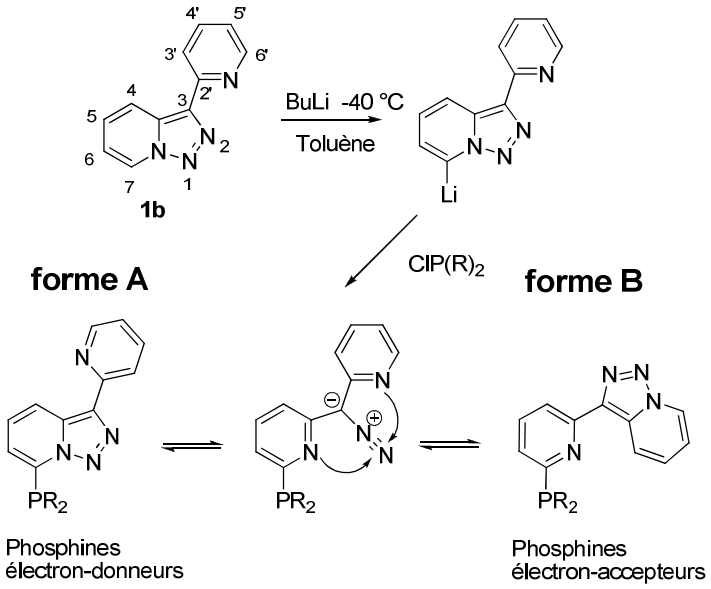

Schéma 9 : Réarrangement du système triazolopyridine-pyridine avec des phosphines.

Or les phosphines sont connues pour avoir un caractère mixte σ-donneur et π-accepteur. Ainsi, l'étude du réarrangement (**Schéma 8**) des triazolopyridinephosphines **69(a-g)** synthétisées nous a permis d'établir un classement des phosphines PR_2 en fonction du ratio entre les deux structures A/B mettant en évidence le profil électronique global (**graphique 1**) de ces dernières sans modification du phosphore (par oxydation en séléniде ou coordination à un métal).

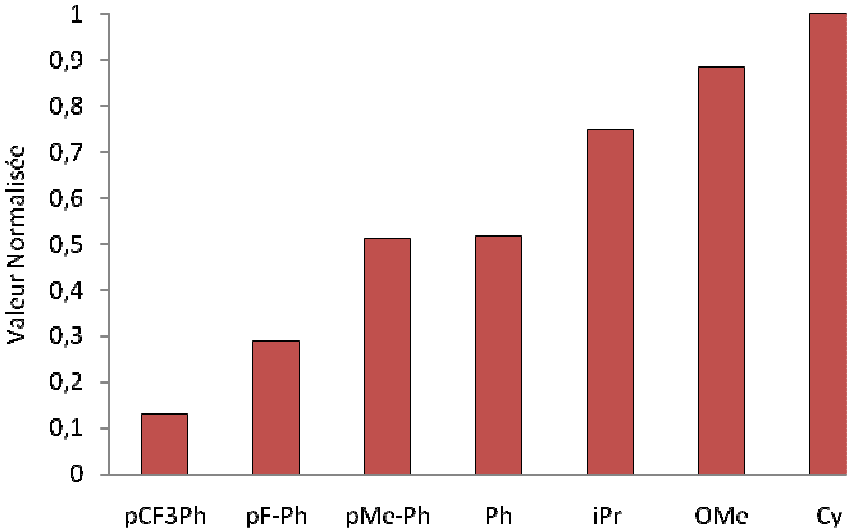

Graphique 1 : Classement des phosphines en fonction des valeurs normalisées des ratios A/B (|| A/B||) en fonction du type de phosphine.

4.2 Synthèse triazolopyridine-phosphines

En 2005, Zhang a rapporté l'utilisation de phosphines basées sur un noyau triazole[16a-b] et leur utilisation en couplage de Suzuki-Miyaura, d'autre cote il existe une croisante demande des ligands phosphorés pour la préparation de systèmes photoluminescents.[16c] Dans ce contexte, nous avons décidé de créer une nouvelle famille de ligands avec une structure triazolopyridine substituée en position 3 par un groupement R= H, CH_3 et Ph et un groupement phosphine en position 7 portant différents substituants de type aryle (**75a-c**) et de type alkyle (**76a-b** et **77a-c**) (**Schéma 10**). Ce travail a été réalisé en collaboration avec M[elle] Bonnafoux, doctorante au laboratoire de stéréochimie.

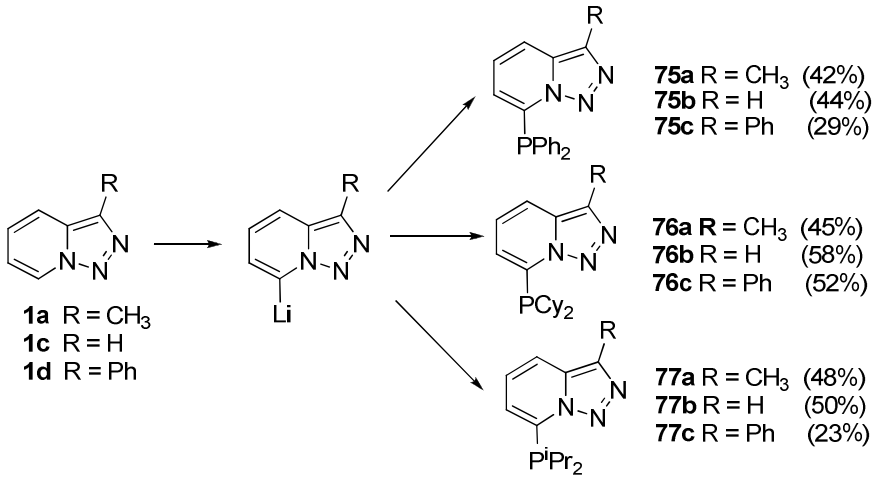

Schéma 10 : Préparation des phosphines à base de triazolopyridines.

Des tests sont actuellement en cours afin de déterminer leurs activités catalytiques dans des couplages de Suzuki-Miyaura, en comparaison à celles de ligands classiques comme la **S-PHOS** qui est à l'heure actuelle une des meilleures monophosphines permettant le couplage encombré d'halogénures d'aryle avec des acides boroniques. Par contre nous avons observé des différences importantes sur les spectres de RMN du proton et du carbone associables à l'isomérie rotationnelle a travers la liaison phosphine-triazolopyridine (**Figure 2**).

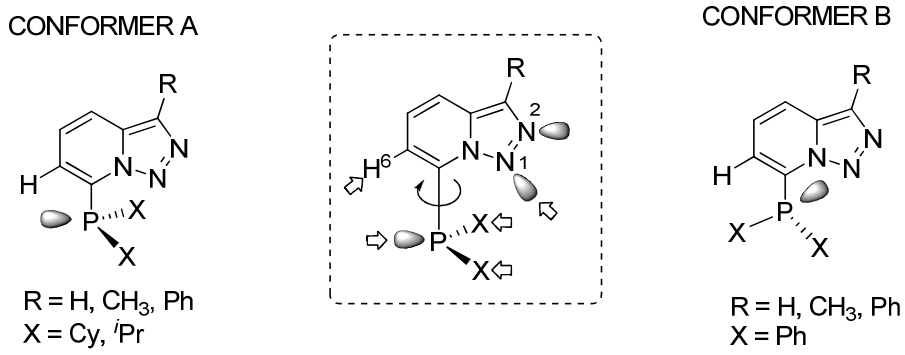

Figure 2 : Différents conformères observées en fonction du type de phosphine.

En collaboration avec le group du Pr Elguero et du Pr. Alkorta nous avons montré de façon expérimentale et théorique que pour les alkyl phosphines le conformer A est plus favorable, par contre les aryl phosphines adoptent une conformation type B.

5. Utilisation des triazoles pour la reconnaissance des métaux, des anions et des acides aminés par fluorescence.

La synthèse des composés fluorescents est aujourd'hui un domaine en pleine expansion. Leur utilisation est très diversifiée que ce soit en chimie, en biologie en médecine ou en génétique. Leur intérêt a été reconnu cette année par l'attribution du Prix Nobel de chimie à Dr. Osamu Shimomura, Dr. Martin Chalfie et Dr. Roger Y. Tsien pour l'utilisation des GFP (Green Fluorescence Proteins). En chimie, les composés fluorescents sont utilisés comme nouveaux capteurs de métaux et d'anions. Durant les dernières années, les systèmes comme le BODIPY, les fullerènes, le BINOL ou des systèmes polyaromatiques (anthracène, phénanthrène, pyrène…) ont été employés comme source de fluorescence. Par ailleurs, la fluorescence des systèmes triazoles a été mise en évidence ces dernières années. En 2004, le groupe du Pr. Abarca a développé des capteurs de métaux et d'anions à base de [1,2,3]triazolo[1,5-*a*]pyridine[17] (**1a**)(**Figure 3**).

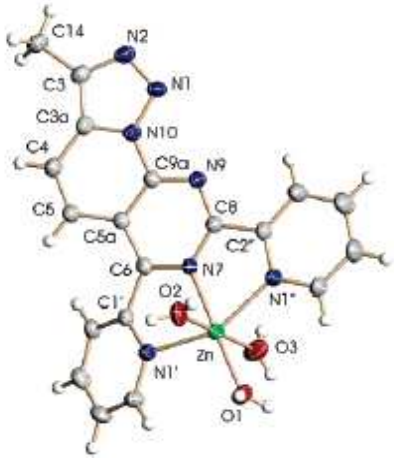

Figure 3 : Premier capteur de métaux et d'anions à base de [1,2,3]triazolo [1,5-*a*]pyridine (1a)

En effet, ce motif agit comme donneur de densité électronique vers un système tridenté. Cependant, le système développé n'employait alors pas le système triazole comme structure coordinante et fluorescente, mais comme fluorophore. Au cours des travaux de thèse, nous avons mis au point la synthèse d'une nouvelle famille des ligands bidentés/tridentés fluorescents (**Figure 4**) où la triazolopyridine est employée comme source de fluorescence (fluorophore)[9] mais aussi comme groupe coordinant[18]

Pour réaliser des tests de fluorescence, nous avons sélectionné différentes molécules tridentées ou bidentées synthétisées au cours des dernières années et nous avons comparé leur réponse en fonction de l'ajout de $Zn^{2\oplus}$ ou $Cu^{2\oplus}$. Pour effectuer les tests de reconnaissance des métaux, les ligands ont été mis en solution dans l'éthanol (10^{-5}M) et ont été titrés avec des métaux en solution aqueuse ($Zn^{2\oplus}$ et $Cu^{2\oplus}$ 10^{-3}M) (Graphique 2). Les changements les plus représentatifs ont été observés avec le $Zn^{2\oplus}$ qui augmente la fluorescence et le $Cu^{2\oplus}$ où une perte totale de la fluorescence a été observée pour tous les ligands sauf pour le **TPOA** qui est quenché. Dans le cas du **TPF** des problèmes de solubilité ont été

rencontré lors de l'addition de l'eau. Les meilleurs ligands, *i.e.* ceux pour qui la réponse est la meilleure, sont le **TPT** et le **TPON**.

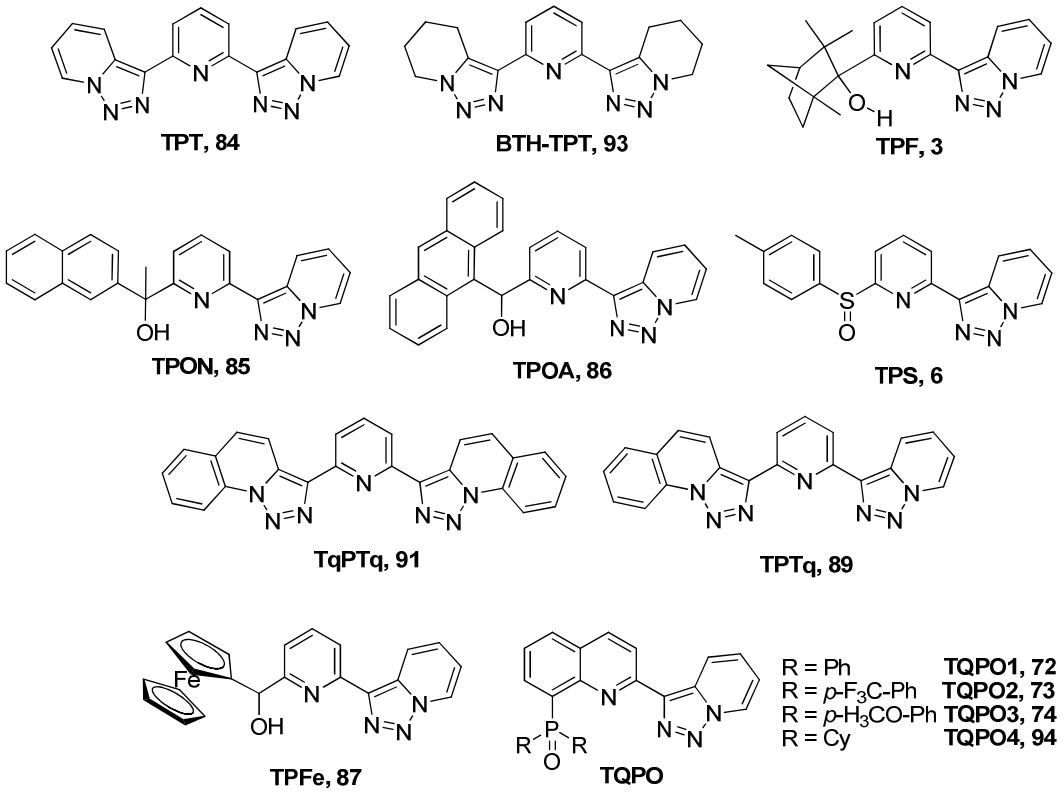

Figure 4 : Ligands (L) développés au cours de nos travaux.

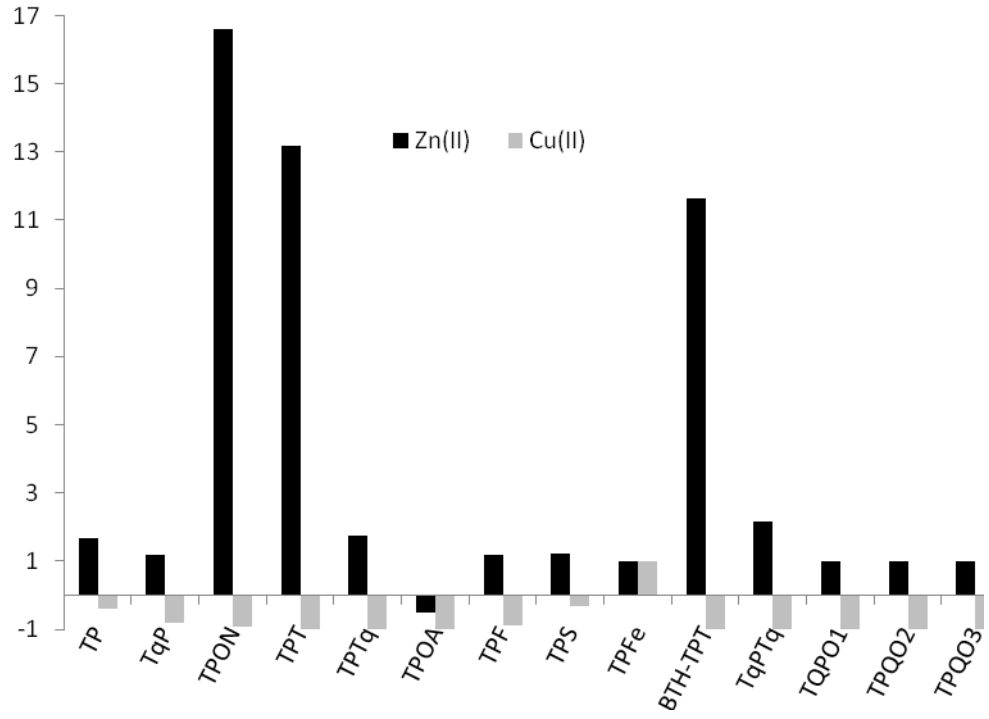

Graphique 2 : Intensité de $M(L)^{2\oplus}$ / Intensité initiale de L

Etant donné que le **TPT** est un composé de symétrie C_2, le système **TPT**$Zn^{2\oplus}$ devrait être le moins complexe à analyser au cours d'une première approche. Nous avons donc réalisé des tests de reconnaissance des anions et des acides aminés avec le système **TPT**$Zn^{2\oplus}$. Les valeurs calculées pour les anions sont fournies dans le tableau 1. L'addition d'un anion ou un acide aminé provoque toujours la perte de fluorescence (quenching). A noter également que cette réponse est dépendante des propriétés coordinantes de l'anion choisi:

	$FF^{\ominus}$	$VCl^{\ominus}$	$BBr^{\ominus}$	$II^{\ominus}$	$CCN^{\ominus}$	$SSCN^{\ominus}$	$NNO_2^{\ominus}$	$NNO_3^{\ominus}$
Log(K)	**44.85**	44,08	44,23	44,58	33.87	44,88	55,07	33,5
	$\mp\mp$	$\mp\mp$	$\mp\mp$	$\mp$	$\mp$	$\mp\mp$	$\mp\mp$	$\mp\mp$
e	0.05	0.04	0.02	$\mp$0.02	$\mp$0.09	0.04	0.03	0.02

Tableau 1 : Valeurs des constantes K calculées pour les différents anions avec le système $TPTZn^{2+}$.

Le système est capable de reconnaitre des anions avec différentes constantes (K). De plus, compte tenu de la différence entre les valeurs obtenues pour les nitrates et les nitrites, il est possible de doser les nitrites sans interférence avec les nitrates. En ce qui concerne les acides aminés, nous avons observé aussi une variation de la réponse de fluorescence en fonction du nombre d'équivalents ajoutés (graphique 3).

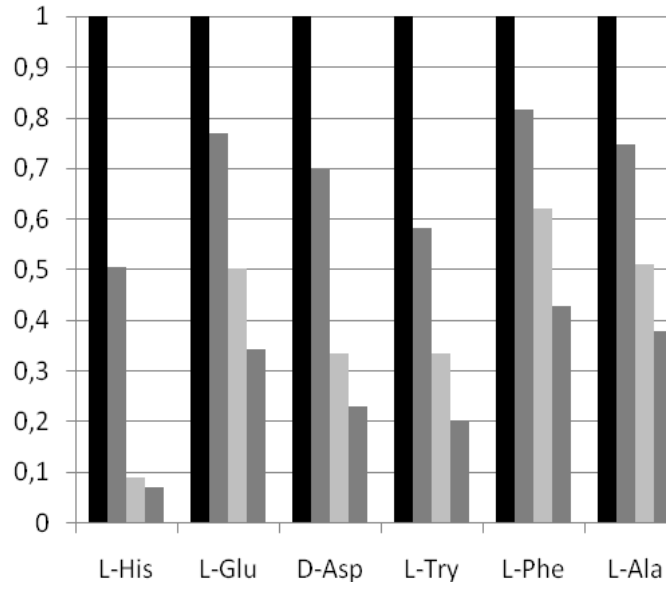

Graphique 3: Réponse du système $TPTZn^{2+}$ après l'addition d'un, deux ou trois équivalents d'acide aminé

Finalement, nous sommes actuellement en train de développer des méthodes de reconnaissance chirale soit à l'aide de fluorophores chiraux (séparation par HPLC chirale des énantiomères de **TPON**) soit par l'utilisation d'auxiliaires chiraux. Dans ce cas, nos premiers résultats sont très encourageants puisque en employant le complexe **TPT**Zn(L-Histidine) comme capteur, nous sommes parvenus à obtenir différentes

réponses entre le D-acide glutamique et le L-acide glutamique (Schéma 11, Graphique 4). Enfin, des résultats similaires on été obtenus en employant le (*R*,*R*) diamino cyclohexane au lieu de la L-histidine.

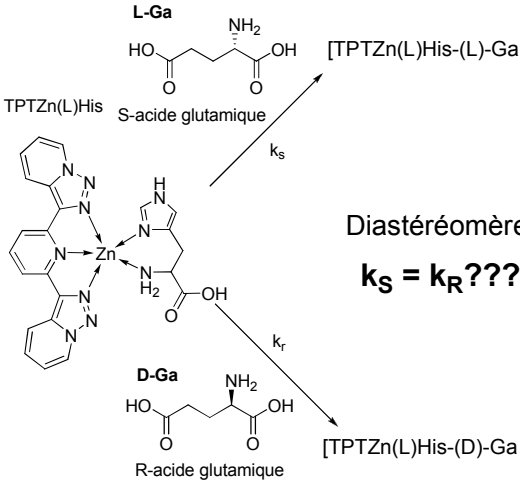

Schéma 11: Utilisation de la L-Histidine comme auxiliaire chiral.

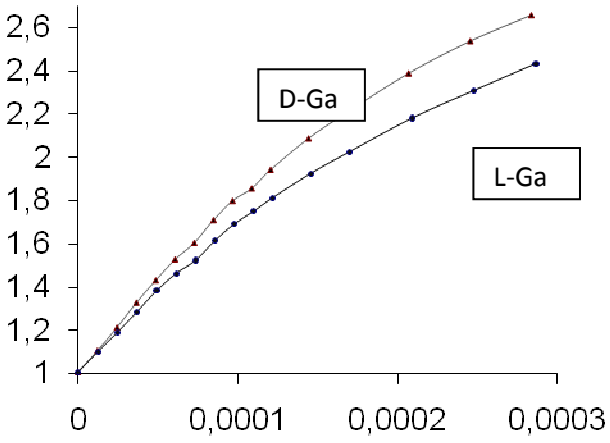

Graphique 4: Représentation Stern-Volmer (Io/I *vs* concentration (M) d'acide aminé) pour le système TPTZn-L-(His) avec les deux énantiomères de l'acide glutamique.

Références

1. Katritzky, A.R.; Rees, C.W.; Scriven, E.F.V. *Comprehensive Heterocyclic Chemistry* I,II,III Ed. Elsevier Science Ltd.
2. a) Jones, G. *Adv.Het.Chem*. **1983**, *34*, 81. b) Jones, G. *Adv.Het.Chem*. **2002**, *83*, 1.
3. Abarca, B. *J.Enz. Inh. Med. Chem.* **2002***, 17*, 359.
4. Jones, G.; Sliskovic, R. *J. Chem. Soc. Perkin I* **1982**, 967. b) Jones, G.; Sliskovic, D. R. *J. Chem. Soc. Perkin Trans.I* **1982**, 967.
5. a) Jones, G.; Sliskovic, D. R.; Foster, B.; Rogers, J.; Smith, A. K.; Wong, M. I.; Yarham, A. C. *J.Chem. Soc.Perkin Trans.I* **1981**, 78. b) Jones, G.; Mouat D.J.; Tonkinson, D.J. *J. Chem. Soc. Perkin Trans. 1*, **1985**, 2719. c) Abarca, B.; Ballesteros, R.; Jones, G.; Rodrigo, G.; Veciana, J.; Gancedo, J. V. *Tetrahedron* **1998,** *54*, 9785.
6. a) Jones, G.; Pitman, M.A.; Lunt, E.; Lyghgoe, D.J.; Abarca, B.; Ballesteros, R.; Elmasnouy, M. *Tetrahedron* **1997**, *53*, 8257. b) Abarca, B.; Ballesteros, R.; Elmasnouy, M. *Tetrahedron* **1998**, *54*, 15287.
7. Blanco, F.; Alkorta, I.; Elguero, J.; Cruz, V.; Abarca, B.; Ballesteros, R. *Tetrahedron* **2008**, *64*, 11150.
8. Abarca, B.; Alkorta, I.; Ballesteros, R.; Blanco, F.; Chadlaoui, M.; Elguero, J.; Mojarrad, F. *Organic & Biomolecular Chemistry* **2005***, 3*, 3905.
9. Abarca, B.; Aucejo, R.; Ballesteros, R.; Blanco, F.; García-España, E. *Tetrahedron Lett.* **2006**, *47*, 8101.
10. Abarca, B.; Ballesteros, R. ; Ballesteros-Garrido, R.; Colobert, F. ; Leroux, F. R. *Tetrahedron* **2007**, *63*, 10479.
11. Maitro, G.; Vogel, S.; Prestat, G.; Madec, D.; Poli, G. *Org. Lett.* **2006**, *8*, 5951.
12 . Colobert, F.; Ballesteros-Garrido, R.; Leroux, F. R.; Ballesteros, R. ; Abarca, B. *Tetrahedron Lett.* **2007**, *48*, 6896.
13. Abarca, B.; Ballesteros, R.; Ballesteros-Garrido, R.; Colobert, F.; Leroux, F. R. *Tetrahedron* **2008**, *64*, 3794.
14. a) Abarca, B.; Ballesteros, R.; Gomez-Aldaravi, E.; Jones, G., *J. Chem. Soc. Perkin Trans. I* **1985**, 1897.b) Abarca B., Gomez-Aldaravi B.; Jones G. *Journal of Chemical Research, Synopses* **1984**, 140.
15. a) Wiesner, J.; Ortmann, R.; Jomaa, H.; Schlitzer, M. *Angew. Chem. Int. Ed. Engl.* **2003**, *42*, 5274. b) Duffour, J.; Gourgou, S.; Desseigne, F.; Debrigode, C.; Mineur, L.; Pinguet, F.; Poujol, S.; Chalbos, P.; Bressole, F.; Ychou, M. *Cancer Chemother. Pharmacol.* **2007**, *60*, 383.
16. a) Dai, Q.; Gao, W.; Liu, D.; Kapes, L. M.; Zhang, X., *J. Org. Chem.* ***2006****, 71,* 3928. b) Lui, D.; Gao, W.; Zhang, X., *Org. Lett.* **2005**, *7*, 4907**.** C) O. Moudam, A. Kaeser, B. Delavaux-Nicot, C. Duhayon, M. Holler, G. Accorsi, N. Armaroli, I. Séguy, J. Navarro, P. Destruel, J. F. Nierengarten, *Chem. Commun.* **2007**, 3077
17. Chadlaoui, M.; Abarca, B.; Ballesteros, R.; Ramirez de Arellano, C.; Aguilar, J.; Aucejo, R.; Garcia-Espana, E. *J. Org. Chem.* **2006**, *24*, 9030.
18. a) Ballesteros R.; Abarca B.; Samadi A.; Server-Carrió J.; Escrivá E. *Polyhedron* **1999**, *18*, 3129. b) Niel V.; Gaspar A. B.; Muñoz M. C.; Abarca B.; Ballesteros R.; Real J. A. *Inor. Chem.* **2003**, *42*, 4782. c) Abarca B.; Ballesteros R.; Chadlaoui M.; Ramírez de Arellano C.; Real J.A. *Eur. J. Inorg. Chem***. 2007**, 4574.

General introduction

John Maddox[1] suggested in his book: "...*these observations of what has happened in science in this century illustrate two important truths. First, new understanding does indeed spring from current understanding, and usually from contradictions that have become apparent. Second, while it may be possible confidently to guess in which fields of science new understanding will be won, the nature of the discoveries that will deepen understanding of the world cannot be perfectly anticipated*"

This PhD thesis concerns the chemistry of a relative simple heterocyclic compound: the [1,2,3]triazolo[1,5-*a*]pyridine. The background of this compound contains 40 years of devoted research being mainly and exhaustively developed by Pr. Abarca and Pr. Jones. During this time, and with the aim to understand its reactivity, the domain concerning the chemistry of [1,2,3]triazolo[1,5-*a*]pyridines has been reported and analyzed. Despite of its simple structure, this molecule has revealed as an extremely versatile compound: ligand design, drug preparation or fluorescence applications are only a few examples of those that had been appearing in the literature. The main objective of this PhD could be associated to the preparation of triazolopyridine based fluorescent compounds to perform metal and anion recognition as well as chiral recognition. However, in the course of this, we have been interested in the understanding and the analysis of the obtained results in order to contribute as much as we could into the general knowledge of triazolopyridine chemistry.

The first part of this research involved two domains from two different laboratories: Triazolopyridines and Chirality. As starting point of this international collaboration we focused

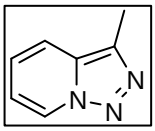

on the preparation of the first chiral triazolopyridines and the study of the effects of chirality into the triazole system under ring opening conditions. Needless to comment about the choice of the chiral source, being a student at the Laboratoire de Stereochimie. <the chiral sulfoxide was presented as a key compound in the preparation of chiral triazolopyridines. The chosen strategy involved the introduction of a chiral sulfoxide on the triazolopyridine moiety ant then the study of the transmission of this chirality while the generation of a second asymmetric carbon by a triazole ring opening reaction. However, "*...the nature of the discoveries that will deepen understanding of the world cannot be perfectly anticipated"*. Low yields and side reactions transformed the first syntheses (that were supposed to reach 90% yield) in a small 17% yield. Although it was not a good start, at least it was a start. This disappointing yield forced us to find alternatives, to introduce other chiral compounds, as for example (-)-fenchone were we reached 88%! and we developed a catalytic sulfenation (reaching 82%) also focusing on the expansion of this methodology towards other heterocycles. Finally we prepared a family of triazolopyridine- and pyridine- sulfoxide and fenchone derivates.

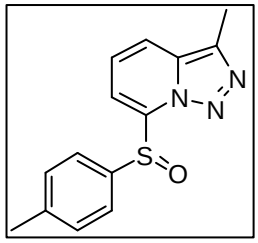

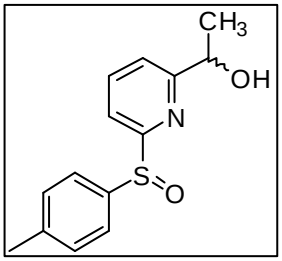

[1] *What Remains to Be Discovered*. John Maddox. Touchstone, New York, 1998.

At the end of the synthesis of these compounds we realized that some of them had an interesting tridentate structure and were fluorescent. For these reasons, we studied, in collaboration with Pr. García España the fluorescent properties of these compounds, finding that one compound could be used to detect zinc, or anions. This compound had already been

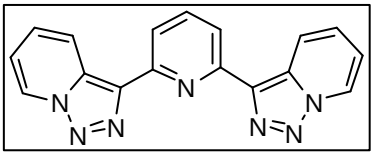

prepared by Abarca, but had never been studied as fluorescent ligand, however, it revealed as an excellent sensor.

Back to Strasbourg, we decided to prepare analogues of this compound increasing the electron density of the system by adding an extra aromatic ring to the triazolopyridines. In this way we focusedon [1,2,3]triazolo[1,5-*a*]quinoline. This compound has been less studied and presented "*contradictions that have become apparent*" compared to triazolopyridines, the metalation was regioselective but at a different position. We tested different bases and at the end we succeeded opening a new and fast way to 2,8-disubstituted quinolines. Once the metalation studies were finished, we started to prepare our fluorescent

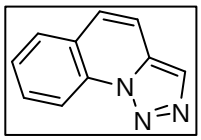

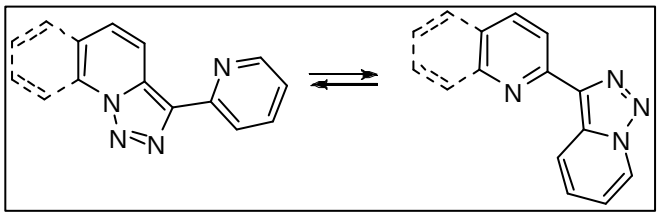

analogues. However, these systems had some properties that must be always taken into account, the ring-chain isomerisation. We had already used this isomerisation with triazolopyridine-pyridines to obtain tridentate ligands. However, triazoloquinoline-pyridines were different and required a completely new study. In collaboration with Pr Elguero and Pr Alkorta (who already had studied the triazolopyridine-pyridine isomerisation) we analyzed experimentally and theoretically how this equilibrium was affected by the introduction of different substituents. We decided to understand this compound before continuing with the preparation of fluorescent analogues. And the ideas associated with these isomerizations (the old one with triazolopyridine-pyridines and the new one with triazoloquinoline-pyridines) suggested, that these compounds could be used as sensors for the electronic profile of compounds bonded to them. The new isomerisation was affected by electronic and steric effects.

The diversity of subjects studied in the Laboratoire de Stereochimie (fluorine chemistry, total synthesis, chiral sulfoxides, phosphines...) offers an excellent scientific atmosphere to mix ideas. In this way, it required less than 2h to create Nitrogen-Phosphorus project. In collaboration with Laurence Bonnafoux (now Dr. Bonnafoux) we decided to introduce phosphines onto the triazolopyridine moiety. At the beginning, this was a win/win strategy,

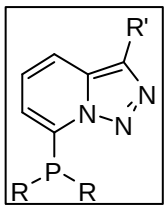

phosphines are classic donor-acceptor compounds (so the previous isomerisation may be able to evaluate these properties) but also a background of ligands for catalysis and molecular materials which encouraged us to prepare a family of triazolopyridine phosphines (having also an interest from a "*fluorescent*" point of view). What at the beginning was classified as a fast project ended with two months of NMR assignation, theoretical calculations, X-ray structures and a new way to observe the electronic profile of phosphorus atoms as well as to observe the rotational dependence of P-C ^{13}C-NMR coupling constants. Furthermore, some of these compounds had strong fluorescent blue emission, which already encouraged us to study them as copper (II) sensors.

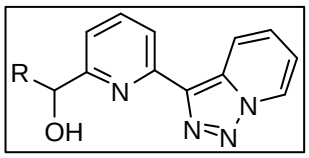

Then, we took finally the time and prepared fluorescent analogues. The isomerisation of the triazolopyridine-pyridine ring helped us to obtain tridentate fluorescent compounds. However, the isomerisation of triazoloquinoline-pyridines, rendered this objective difficult and we designed different synthetic approaches to obtain the target molecules.

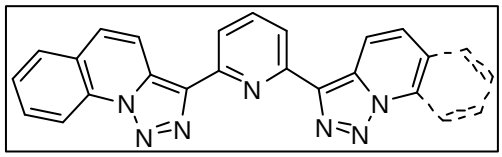

Back to Valencia we studied the fluorescent properties of the newly prepared compounds. Some of them were able to detect zinc(II) and copper(II), some of them were useless, however the study of these properties furnished a complete idea about the possible application of these compounds, for example as OLED's, cell imaging and anion detection.

As some of the prepared ligands were chiral compounds, we became interested in the possible enantio-discrimination by means of fluorescent spectroscopy with them. The interaction between chiral compounds with a chiral target molecule would provide diastereomers (depending on the chirality of the selected target molecule) and maybe differences could be observed in the fluorescence tests. Once again discoveries *"cannot be perfectly anticipated"* and no chiral recognition was obtained with chiral fluorophores. Thus we tried to do it with non-chiral fluorophores (which was already a challenge) and by adding a chiral compound to our fluorescent system. We obtained a chiral fluorescent sensor which allowed (finally) the enantio discrimination of glutamic acid by means of fluorescence spectroscopy.

The present manuscript presents the research developed during three years. In the first part a general introduction concerning the chemistry of triazolopyridines is presented to provide the key reactions that will be employed later. The ring chain isomerisation is also explained in order to clarify this phenomenon due to the fact that it has been present in many parts of the work performed. The second chapter is devoted to the preparation of chiral triazolopyridines with fenchone and sulfoxide groups, as well as the synthesis of 2,6-disubstituted pyridines. The third chapter involves the chemistry of triazoloquinoline, in the first part affording a new route to 2,8-disubstituted pyridines and secondly the study of a new ring-chain isomerisation is presented with the new triazoloquinoline-pyridine system. Chapter four involves all work performed with phosphines, in a first part concerning the isomerisation as a tool to evaluate the electronic profile of phosphorus atoms. In a second part we studied the effects of the phosphine-triazolopyridine bond rotation and its consequences with ^{13}C-NMR spectra. The last chapter is devoted to fluorescence. Starting with a general introduction concerning luminescence, this chapter presents the results concerning the fluroescent properties, metal recognition and anion/amino acid recognition. Then, the last part explains how the enantio-sensing was performed with non-chiral fluorophores.

Acknowledgement

First of all, I would like to express my deepest gratitude to Pr. Hosseini, Pr. Knochel and Pr. Yus for accepting to evaluate the present manuscript and being members of this jury. It's a honour for me to have the chance to present you the results concerning my PhD research.

I want to thank Pr. Colobert who was my organic chemistry professor and then one of my PhD directors. She already found in me a possible PhD student while I was not able to say more than 5 words in French. I also thank her for suggesting me to do a PhD in her team and for accepting me in his laboratory, as well as for all the facilities afforded while the development of the Strasbourg-Valencia collaboration and for her help with my industrial stage. I really want to thank both of my PhD directors (Pr. Colobert and Dr. Leroux) for guiding me, especially by forcing me to finish things before starting developing new ideas. Without this, the present manuscript would be a complete chaos about triazolopyridines with no logic. Finally, I want to thank Pr. Colobert for her trust in me while I was performing fluorescence studies in Valencia as well as her support during these five years in Strasbourg and the correction of this manuscript.

I would like to thank Dr. Leroux for giving me a work methodology that is responsible of all results obtained ("*3 reactions each day, 3 new products each week*"...I did my best!). Five years have passed since you directed me in the practical class courses. Thanks for your enormous and great patience with me, thanks for the corrections in the publications, in the PhD manuscript, in the lab and in almost everything I have done during the last three years. I know that sometimes it has not been easy for you to deal with someone like me (and *vice versa*!!!), however after this time I am proud to have had the chance to belong to your team and to learn from you. Thank you for your support, your suggestions, your help and your trust in me. You have always said that my molecules gave you headache, so I supposed that a full PhD manuscript should have been close to migraine... I excuse for that!!! It has been a pleasure to work with you, so the three last years passed so fast. You know, I tried several times to convince my triazolopyridines to provide arynes but they said no...I hope one day the will obey me until now it is just a project. During these years you have always been present to provided solutions, ideas and I have learned more in three years than in the five years I spent studying chemistry. It has been a great pleasure for me to be directed by you.

I would like to thank Pr. Abarca and Pr. García España for their help during my PhD with triazolopyridines and fluorescence, and also for accepting me as student in their teams. I also thank Pr. Abarca for evaluating this manuscript and for the help while the development of the Strasbourg-Valencia collaboration.

I thank Dr. Blanco, Pr. Alkorta and Pr. Elguero for their advices and work concerning all the theoretical calculations.

I really want thank Dr. Rafael Ballesteros, my father. You dedicated to me your PhD a few days before I was born, now I dedicate you this work, my PhD.

A mi madre. Desde el pragmatismo de Kant al mejor de los mundos posibles de Leibniz, tenías razón (para variar). Puede que seas la persona que más ha oído hablar de triazolopyridinas y que menos haya pisado un laboratorio, muchas gracias por poner las cosas en su sitio, por tus mítines y por leerme a Platón cuando era pequeño, eso deja marca!!!

A Mariate. Esto no sería posible sin ti y… tú también tenías razón. Gracias por haber estado todo este tiempo conmigo, por tu forma de ver las cosas, por tu confianza y por estar a mi lado cuando nos separan 1500 km, termina aquí una época de mi vida y poco a poco vamos bajando hacia casa, deshaz la bufanda (era un sudario, pero bueno) unos cuantos meses más.

I thank Dr Bonnafoux (Lolo), it has been a pleasure to work with you during this years and thanks for adding phosphorus to my triazolopyridines, thanks for being there in the good and in the bad times, for the phosphination weekends, thanks for your corrections (oh oui, là il y en a eu plain). Now you have left Strasbourg... I hope you will be “cool“ in Zurich!!! Thanks for your generous gift of chemicals and distilled solvents (I always wanted to say this), for many days in the lab laughing and for your ideas and support. The phosphorus-nitrogen project would not be the same without you. Thanks for BuLi titration... for the patience with me while you were doing your four hours *tert*-BuLi drop-wise addition and I was explaining you my mad theories. Thank you for being yourself even in presence of someone like me, we really had a great time in the lab.

Pauline (Dr. Burger): You, me and the end of the world have a deal that requires being finished! However I think we can wait. Thank you for being as you are, for your smile each morning at the friendship coffee, for the flam’s invitation. I hope you will have a nice time in Montpellier!!! Thank you for being an excellent friend all these years.

Alex (Slovakgirl): Darling you are not small, just concentrated (27 M), it has been a pleasure to meet you, thank you for all the coffee breaks, the mskt nights, the please stop reading my brain. I really love your “yes, but in Slovakia is normal”. Thank you for your help, especially with my English and listening to my mad theories, good luck with flavones.

Rafeta (R2): Un amigo y un compañero de piso excelente, trabajamos juntos 5 meses, no sé cómo al jefe no le dio una crisis cardiaca!!! Aun te quedan dos años por aquí, disfruta, dale caña a las ciclodextrinas que el tiempo pasa volando, hay mucha gente que hace una tesis y que publica y que saca rayos x “sin querer” pero solo hay dos personas lo suficientemente locas como para haber fundado un club en su propia casa (LC19) y hasta aquí puedo leer.

David (Dr. Rodríguez o poz3): Tu también estás para que te encierren, muchas gracias por tus consejos, por tu alegría en el labo, por los sushis attacks hasta explotar, por muchas reuniones de carácter lúdico y por estos años que hemos pasado juntos, siempre has sido nuestro compañero de piso aunque tu casa estuviera a 500 metros.

Esther, Joseph, Alfonso y al resto de la familia: Muchas gracias por estos años (y por adoptarme de forma espiritual!!!) que tengáis mucha suerte.

Lab. triazolopyridinas: Cuando llegué no había nadie, Fernando pasó algunos días. Desde entonces hasta ahora Rosa, Sonia, Empar y Cristina han tenido que convivir conmigo (pobres) ha sido un placer marearos cuando pasaba por allí, cuidaros y cuidado con el BuLi.

Lab. Supramol: Vosotros sí que lo tenéis bien montado!!! Fanny, Salva, Jorge, Javi2, Marc, MariPaz, Raquel, Sandrita, Juan, Teresa Jose Miguel, Conxa...Os pido disculpas por haber robado el fluorímetro de forma indiscriminada cada vez que pasaba por Valencia, muchas gracias por vuestra ayuda y consejos. Por marearos e invadir vuestro espacio de forma indiscriminada y por el frasco de etanol que perdí en la máquina de rendimientos cuánticos.

Lab. Stereochimie: Sabine, Gilles, Agnès, Marie, Irene, Nico, Arlette, Mercedes, Didier, Bouchra, Baptiste, Charlote, Vinc, Christophe, Maryam, Leti, Vicky, Maggie…and all people who passed during the last three years. Thank you for this excellent time, for the coffee breaks, the coffee pause, the beer days, and for your help and your patience with me during my PhD. Thank you for not killing me each time I used your NMR time to pass my samples, for the excellent ambiance, for the meals joking, and for having an excellent time with all of you.

Lab 2: Vinc, you must control yourself, you must be awarded that if you do more than three “7 grams chromatography columns” at the same time the whole universe will be destroyed. Good luck in your second post-doc. Baptiste, John Petrucci is probably the best guitar player in the world!!! I told you that liquid nitrogen cannot be used to cool drinks, especially beer!!! Good luck with your manuscript and take care when you use HF. Charlotte.... degage... you were the last one who arrived and you will be there when we will leave, be careful with SbF_5, thank you for the morning coffee.

Present and Past R4: Michel, Carol, Bene, Katia, Juanjo, Pititia, Julien, Maida, Laure, Don Antoine, Isabelle, Damien and all these master students that I don’t remember their names (and also Lab’s directors), thank you for these years, for being my secret coffee place!

Michel, Estelle and Sales, thank you for the thousands of NMR and HRMS performed during these years and for your help. I would also like to thank Lydia Brelot from the X-ray service for the crystal analysis.

To the “coffee” friends: Those that like the coffee at 7.00 (Agnes, Lolo, Pauline, Rafa2, Charlotte, Christophe...) it has been a pleasure to wake up like this.

The Strasbourg-n-people: Matsou, Bertrand, ECPM, Jean Loup, Antoine, Ishmael, Alexis, Marie, Silvia, Omar, Juanito, Jose, Lina, Erick, Dan, SECO 45...

Table of contents

General Part

I: State of the Art

II: Chiral Triazolopyridines

Towards chiral 2,6-disubstituted pyridines

III: [1,2,3]Triazolo[1,5-*a*]quinoline

IV: Triazolopyridine-phosphines

V: Fluorescence

VI: General conclusion and Outlook

Experimental Part

VII: Experimental part

General Part

I: State of the Art

1.1 The Triazolopyridine family

The family of triazolopyridines is composed of five heteroaromatic compounds: three [1,2,3]triazoles and two [1,2,4]triazoles. A nitrogen atom is common to both cycles in three of them. The position of the nitrogen atoms provides very important differences between them, especially concerning their synthesis and reactivity (**Figure I-1**).

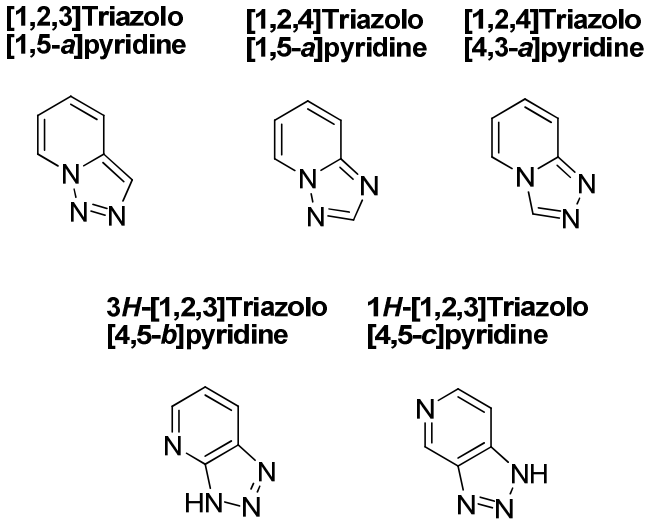

Figure I-1: Triazolopyridine family.

Triazolopyridines are known since 1950. However, their chemistry has been less studied compared to other heteroaromatic compounds. The discovery of the [1,2,4]triazolopyridine *Trazadone* (**figure I-2**), a serotonin reuptake inhibitor was the starting point of research on these structures.

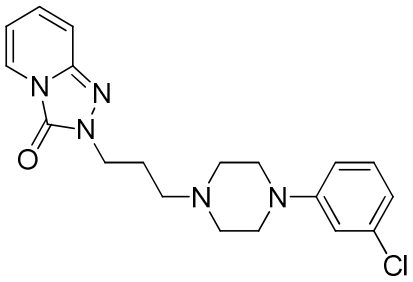

Figure I-2: *Trazodone* structure.

Up to now, the synthesis and reactivity of triazolopyridines have been revised several times. The first paper was published in 1961 by Mosby.[1] The second revision was performed by Jones[2] and Sliskovicin 1983 with all references concerning these compounds until 1981. In Comprehensive Heterocyclic Chemistry, 1st and 2nd Edition, the most important synthetic ways towards triazolopyridines are described. [3, 4] Later, Jones revised the bibliography concerning these systems until 2002[5] and Abarca published a review concerning the chemistry of [1,2,3]triazolo[1,5-*a*]pyridine[6] the same year.

1.2. Synthesis of [1,2,3]triazolo[1,5-*a*]pyridines

[1,2,3]Triazolo[1,5-*a*]pyridines are generally prepared starting from pyridines. The most common method consists in the oxidation of the corresponding hydrazone from the 2-pyridylcarboxaldehyde derivative. Numerous analogues bearing a substituent at the C^3-position were synthesized (**Scheme I-1**).

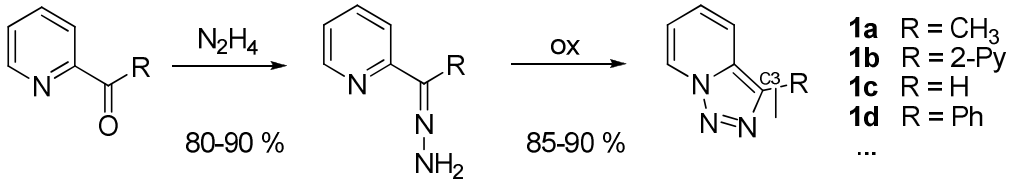

Scheme I-1: Synthesis of 3-substituted triazolopyridines.

Boyer, Borgers and Wolford[7] published the first synthesis of [1,2,3]triazolo[1,5-*a*]pyridines. Hydrazones were oxidized using Ag_2O to give the diazo-intermediate (**Scheme I-2**) which undergo an intramolecular cyclization affording [1,2,3]triazolo[1,5-*a*] pyridines.

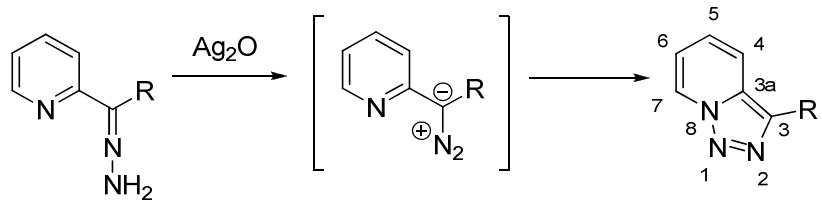

Scheme I-2: First synthesis of triazolopyridines.

This methodology was also applied to synthesize various 3-phenyl-[1,2,3]triazolo[1,5-a]pyridines (R = aryl) (**Scheme I-3**) by Mayor and Wentrup.[8]

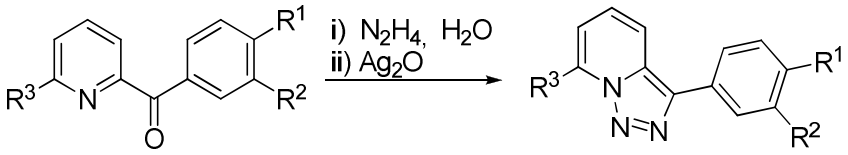

	a	b	c	d[a]	e[a]	f	g	h	i
R_1	H	OCH_3	Cl	NO_2	CN	H	H	H	C_4H_4
R_2	H	H	H	H	H	NO_2	OCH_3	H	
R_3	H	H	H	H	H	H	H	CH_3	H
Yield	71%	30%	71%	10%	73%	60%	40%	36%	37%

Scheme I-3: Mayor and Wentrup aryl derivatives. a) MnO_2 was employed as oxidant.

Although Ag_2O provided triazolopyridines in good yields, Bower and Ramage[9] replaced it by potassium ferrocyanide. Under these conditions, they obtained mixtures of [1,2,3]triazolo[1,5-*a*]pyridine , 3-methyl[1,2,3]triazolo[1,5-*a*]pyridine and other side products like azines. Using this procedure, Jones[10, 11] and Sliskovic[10] synthesized the corresponding 7-methyl and 4-methyl derivative (**Scheme I-4**). Many other oxidants, like nickel peroxide, lead tetraacetate, copper (I) salts, have been tested[2, 5].

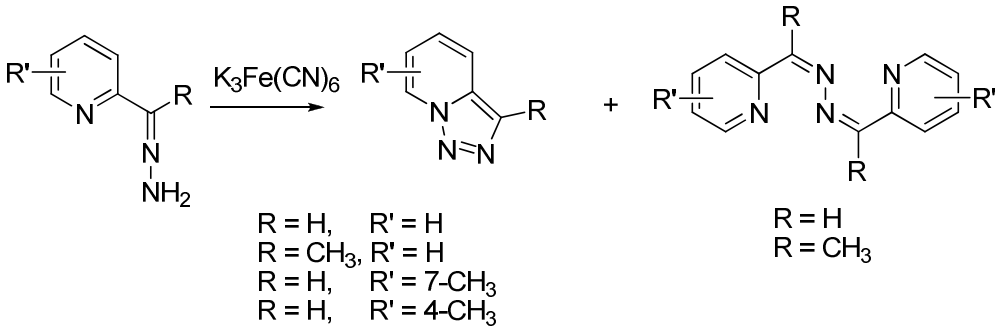

Scheme I-4: Potassium ferrocyanide oxidation.

Some examples concerning the air oxidation of the corresponding hydrazones.[12, 13]can also be found In the bibliography. However the low yield remained as the most important problem. Comparing all published synthetic ways to obtain [1,2,3]triazolo[1,5-*a*]pyridines using pyridyl ketones or aldehydes as starting reagent, and hydrazine, the oxidation with manganese (IV) oxide (MnO_2) due to its low cost, (0.53 €/g) and the good and reproducible yields (**Scheme I-5**) made it the reagent of choice. Manganese oxide was successfully employed by B. Abarca[14] to prepare triazolopyridines on gram scale.

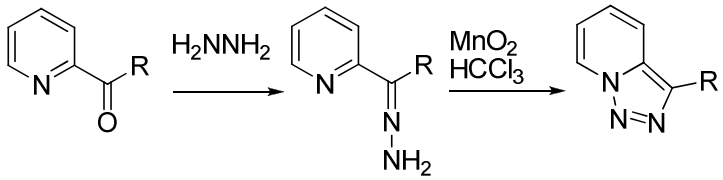

Scheme I-5: Hydrazine/MnO_2 strategy for the preparation of triazolopyridines.

In order to avoid the oxidation step, Boyer and Goebel[13] developed another approach to obtain triazolopyridines. They were synthesized after condensation of tosylhydrazine with the corresponding 2-pyridyl aldehydes or ketones, followed by a basic treatment with NaOH or KOH. In this way they acceded to the 3-phenyl, 3-picolinoyl, and [1,2,3]triazolo[1,5-*a*]pyridine in high yield without oxidizing agent. (**Scheme I-6**). Other bases like morpholine were also employed to prepare, for example, 7-methyltriazolopyridine[10] , 5-methoxytriazolopyridine[15] bromo analogues[16].

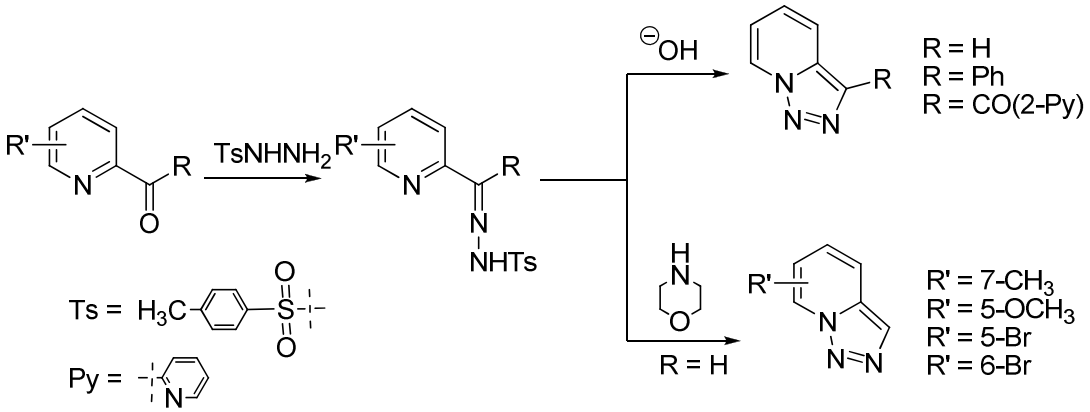

Scheme I-6: Non oxidative synthesis of triazolopyridines.

Reimlinger[17] *et al*. tried to trap the diazo intermediate in order to confirm the reaction mechanism. However, they never succeed and proposed a non-diazonic mechanism based on the nucleophilic attack of the free doublet of the non-protected nitrogen atom to the carbonyl group followed by cyclization (with release of water) and detosylation (**Scheme I-7**).

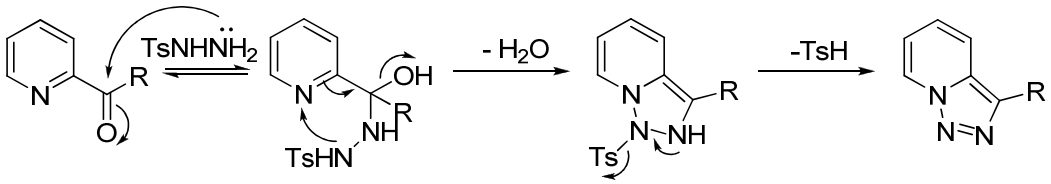

Scheme I-7: Reimlinger mechanism for the non oxidative synthesis.

Regitz also obtained triazolopyridine derivatives (**Scheme I-8**) with moderate to high yields (50-80%) by reaction of the 2-acylmethylpyridines with tosylazide (TsN_3) in presence of sodium ethoxide.[18, 19]

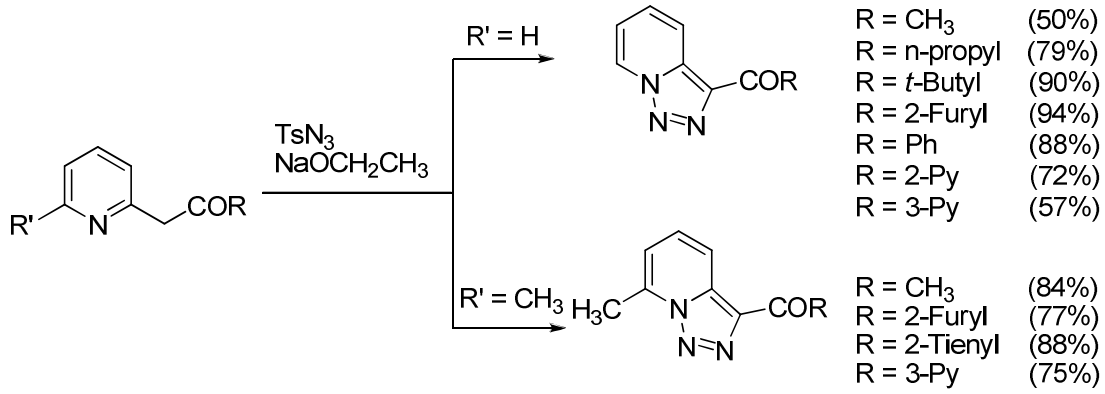

Scheme I-8:Regitz derivatives.

Regitz proposed a mechanism and assumed that, first the deprotonation of CH_2 by sodium ethoxide[18] occurs, followed by reaction of the newly formed enolate with tosyl azide to provide the diazo compound (**Scheme I-9**).

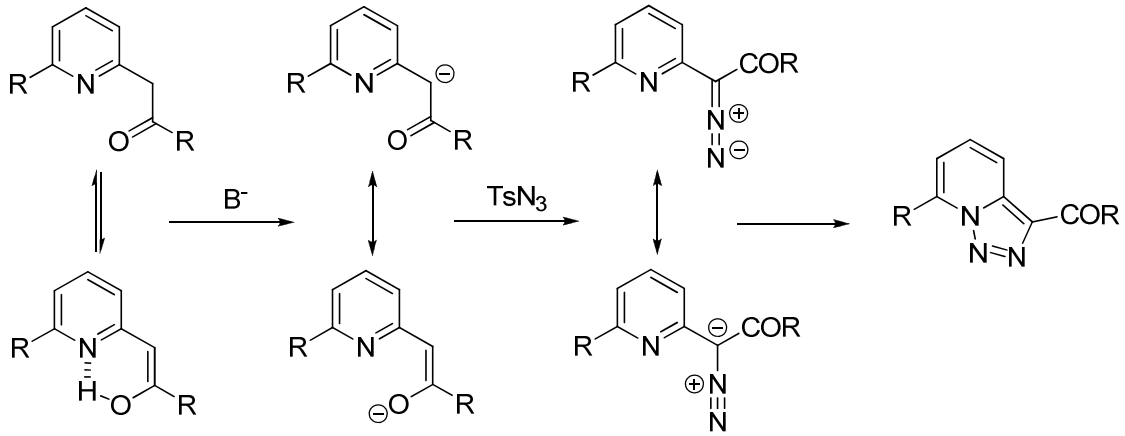

Scheme I-9: Proposed mechanism with TsN_3.

The same procedure was used by Abarca *et al* in order to prepare ethyl [1,2,3]triazolo[1,5-a]pyridine-3-carboxylate[15] (**figure I-3**) and by Jones to synthesize [1,2,3]triazolo[1,5-*a*]pyridine-3-carbonitrile in 46% yield (Scheme I-10). In the latter case, sodium hydride was used as a base instead of sodium ethoxide[20].

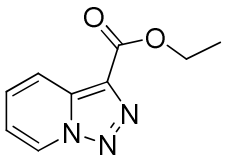

Figure I-3: Ethyl [1,2,3]triazolo[1,5-a]pyridine-3-carboxylate.

This compound was also prepared with different azides, (**Scheme I-10**) like 2-azide-1-ethylpyridiniumtetrafluoroborate[21] or 2-azide-3-ethylbenzothiazolium tetrafluoroborate. [22] Triazolopyridine-phosphine oxide was also prepared using phenyllithium as a base[23].

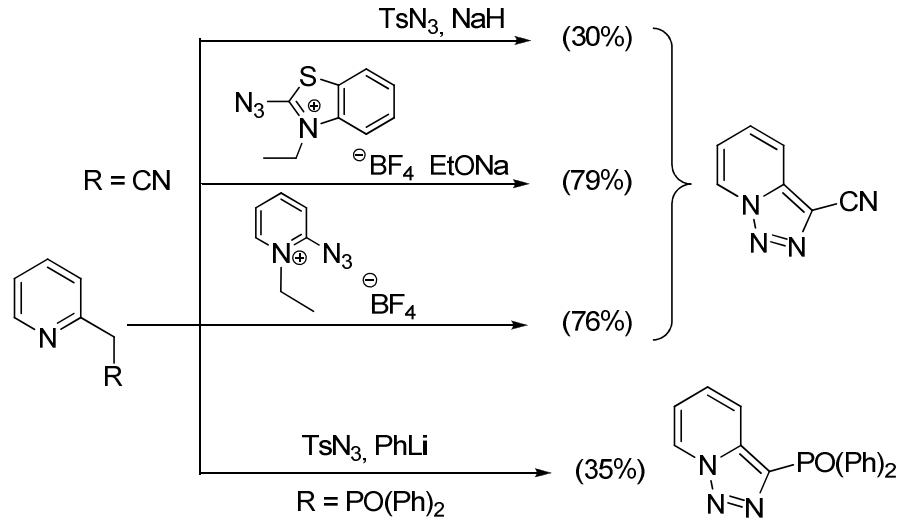

Scheme I-10: Triazolopyridine synthesis with different R-N_3 sources.

Another synthesis, proposed by Tamura *et al.* is based on an intramolecular cyclization of *N*-amine salts from the corresponding oximes[24], by treatment with polyphosphoric acid (PPA) (**Scheme I-11**).

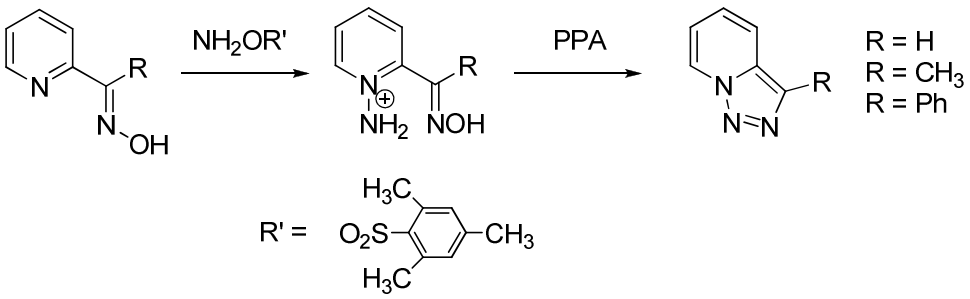

Scheme I-11: Tamura synthesis.

1.3 Reactivity of [1,2,3]triazolo[1,5-*a*]pyridines

As mentioned previously, Boyer and Woldford prepared for the first time 3-methyl[1,2,3]triazolo[1,5-*a*]pyridine and [1,2,3]triazolo[1,5-*a*]pyridine in the late fifties. These compounds were described as solid products, water soluble, soluble in organic solvents and crystallizable in hexane. Since then, an important number of researchers, including Jones, Sliskovik and later Abarca and Ballesteros have contributed to the development of the chemistry of triazolopyridines. The reactivity of [1,2,3]triazolo[1,5-*a*]pyridines (**Figure I-4**) has been methodically and systematically studied by these groups, providing a solid comprehension and knowledges on the chemistry of these compounds. Furthermore, theoretical calculations were recently performed by Elguero, Alkorta and Blanco in order to explain the unusual chemistry of [1,2,3]triazolo[1,5-*a*]pyridines.

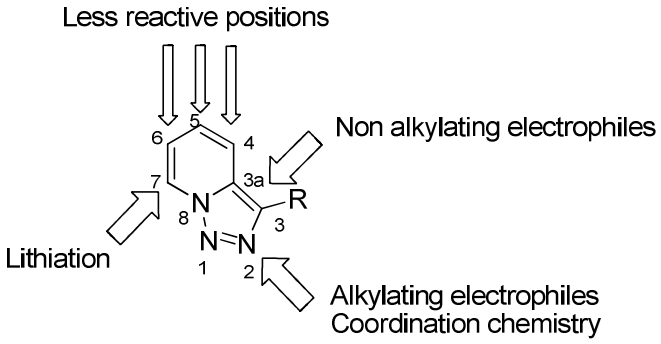

Figure I-4: Reactivity of [1,2,3]triazolo[1,5-*a*]pyridine

1.3.1 [1,2,3]Triazolo[1,5-*a*]pyridines towards non alkylating electrophiles

The [1,2,3]triazolo[1,5-*a*]pyridines can undergo two different reactions with electrophiles depending on their nature (**Scheme I-12**).

a) By substitution at the C^3 position (only for R = H).

b) By ring opening reaction with loss of nitrogen.

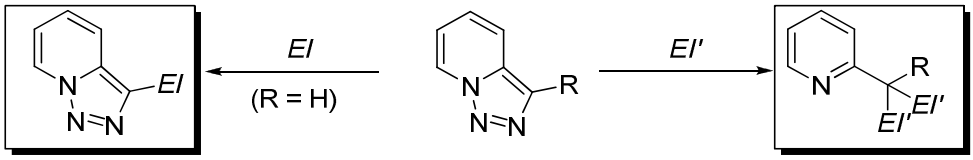

Scheme I-12: Reaction with non alkylating electrophiles.

The first paper concerning the reactivity towards electrophiles was published by Boyer and Wolford in 1958. In their study[25], they showed that the protonation at room temperature with mineral acids takes place at the N^1 atom. However, with carboxylic acids and phenols at high temperature the triazole ring degradates with loss of nitrogen to provide esters in

moderate yields. The following mechanism for the ring opening reaction based on the protonation of N^1 was proposed. (**Scheme I-13**)

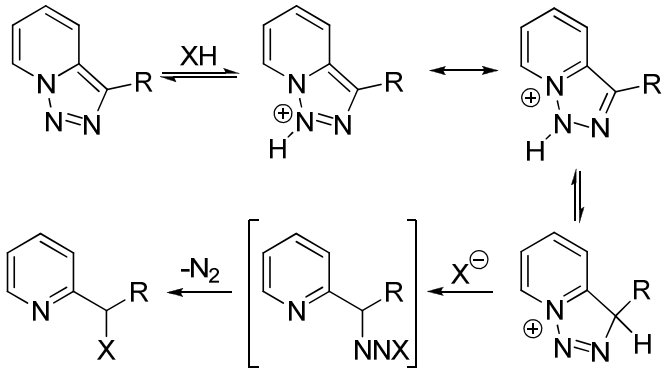

R	XH	Yield
H	H_3CCO_2H	20%
H	$CH_3CH_2CO_2H$	19%
H	$PhCO_2H$	29%
H	p-$NO_2C_6H_4CO_2H$	25%
H	3,5-$(NO_2)_2C_6H_3CO_2H$	33%
H	PhOH	22%
Ph	H_3CCO_2H	44%
Ph	$PhCO_2H$	69%

Scheme I-13: Mechanism for the ring opening reaction.

Later, Boyer and Goebel reported that 3-(1-α-picolinoyl)triazolopyridine reacts with 3,5-dinitrobenzoic acid providing the corresponding salt but without information on the protonation site[13]. However, the reaction with iodine or bromine leads to the formation of the corresponding pyridines with loss of nitrogen[26] (**Scheme I-14**):

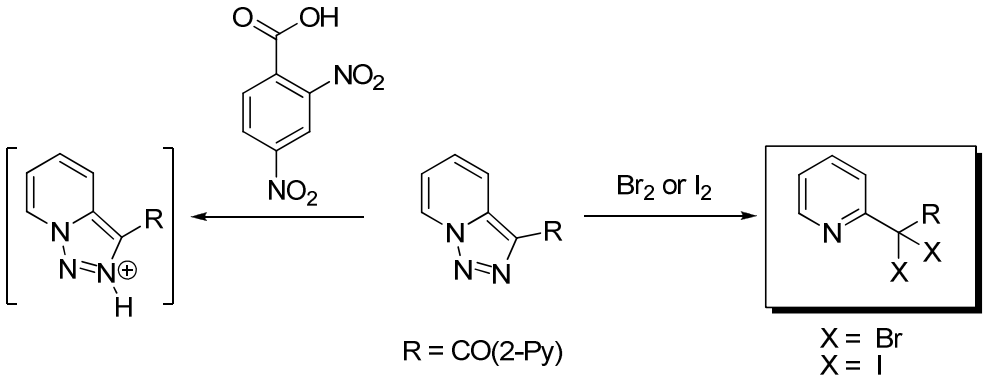

Scheme I-14: Later *et al.* works with 3-(1-α-picolinoyl)triazolopyridine.

The treatment of 3-acyltriazolopyridines with perchloric acid in dioxane to form the corresponding salts was performed by Regitz[18]. The authors assumed that the protonation of the pyridinic nitrogen atom (N^8) was the first step of the sequence (**Scheme I-15**). Then the triazole ring opens without loss of nitrogen.

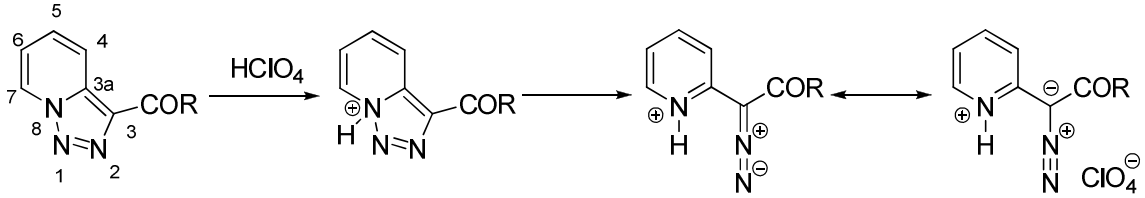

Scheme I-15: Protonation with perchloric acid.

The protonation position of [1,2,3]triazolo[1,5-*a*]pyridines has also been discussed by Armarego, suggesting that protonation takes place exclusively at N^2, upon analysis of pka

values obtained by UV spectroscopic studies.[27] This suggestion was confirmed later in two interesting papers. The first one studies the alkylation of triazolopyridines[28] showing that alkylation also takes place at the N^2 position (**Figure I-5**). Only when bulky substituents are placed in position 3 (R = *tert*-butyl) the alkylation can take place at the nitrogen atom N^1. The second paper confirms with calculations[29] that the most favorized position for alkylation is the N^2 position.

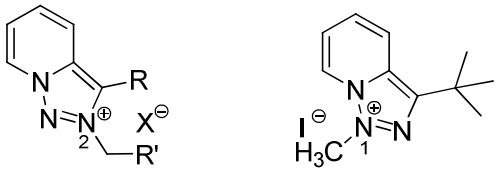

Figure I-5: Alkylation of triazolopyridines.

Jones *et al* studied the Vilsmeier formylation[30] and nitration[26] and obtained new 3-substituted triazolopyridines in low yields (**Scheme I-16**). Up to now, these compounds are the only examples of electrophilic substitution at position C^3.

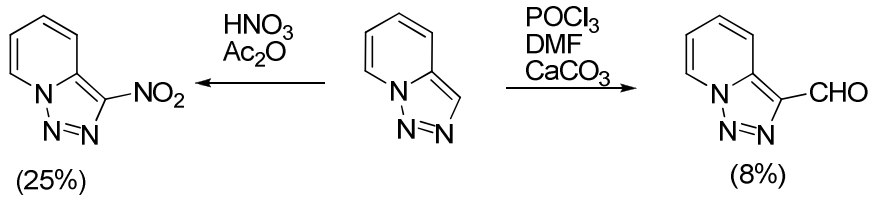

Scheme I-16: Vilsmeier formylation and nitration of [1,2,3]triazolo[1,5-*a*]pyridine.

Jones performed an exhaustive and methodological study[11] about the ring opening reaction with loss of nitrogen with electrophiles like sulfuric acid, acetic acid, halogens and selenium dioxide (**Table I-1**).

Abarca and Ballesteros also studied the ring opening reaction of dienic compounds[31] from triazolopyridine in sulfuric acid, acetic acid and selenium (IV) oxide (**Scheme I-17**).

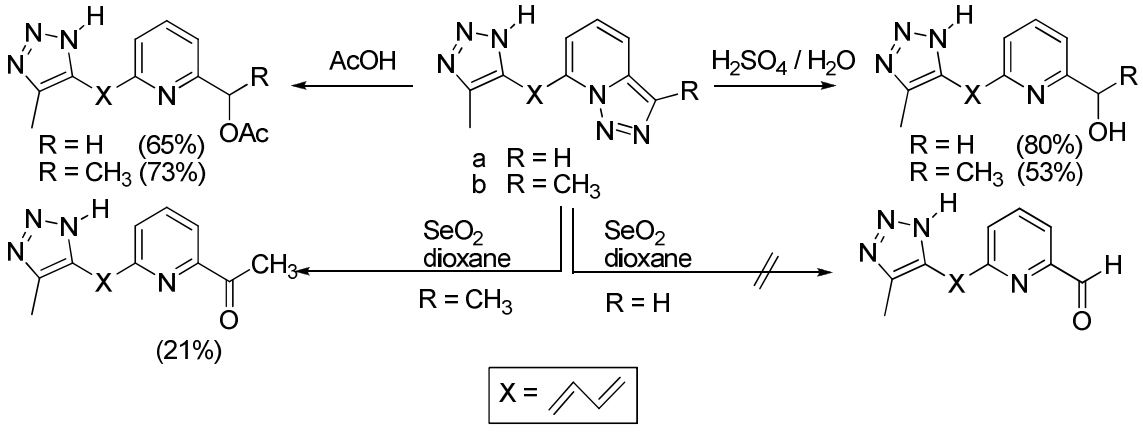

Scheme I-17: Abarca and Ballesteros studies concerning the ring opening reaction.

These results are consistent with those of Jones. The reactions performed with sulfuric and acetic acids provide the corresponding pyridines in acceptable yields. However, with selenium (IV) oxide, the reaction gives the ketone in a low yield (21%) when R = methyl, and a complex mixture which cannot be purified when R = hydrogen.

Table I-1: Methodological study of the ring opening reaction with different conditions.

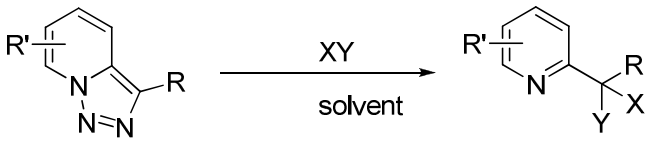

Entry	R	R’	XY	solvent	X	Y	yield
1	H	H	Cl_2	CCl_4	Cl	Cl	67%
2	H	H	Br_2	CCl_4	Br	Br	75%
3	H	H	NBS	CCl_4	Br	Br	79%
4	H	H	Hg(OAc)	AcOH	HgOAc	OAc	60%
5	H	5-OCH_3	Br_2	CH_2Cl_2	Br	Br	30%
6	H	5-OCH_3	H_2SO_4	H_2O	H	OH	78%
7	H	7-(*p*-$MeOC_6H_4CHOH$)	Br_2	CH_2Cl_2	Br	Br	98%
8	H	7-$(C_6H_5)_2CHOH$	Br_2	CH_2Cl_2	Br	Br	76%
9	H	H	H_2SO_4	H_2O	H	OH	78%
10	H	H	AcOH	AcOH	H	OAc	70%
11	H	H	SeO_2	Dioxane	O	O	89%
12	CH_3	H	H_2SO_4	H_2O	H	OH	69%
13	CH_3	H	AcOH	AcOH	H	OAc	98%
14	CH_3	H	SeO_2	Chlorobenzene	O	O	84%
15	H	4-CH_3	Br_2	CCl_4	Br	Br	58%
16	H	5-CH_3	Br_2	CH_2Cl_2	Br	Br	30%
17	H	5-CH_3	H_2SO_4	H_2O	H	OH	80%
18	H	6-CH_3	AcOH	AcOH	H	OAc	98%
19	H	7-CH_3	SeO_2	Dioxane	O	O	<10%
20	H	7-CH_3	SeO_2	xylene	O	O	100%
21	$CONEt_2$	H	H_2SO_4	H_2O	H	OH	70%
22	$CONEt_2$	H	AcOH	AcOH	H	OAc	73%
23	$CONEt_2$	H	SeO_2	xylene	O	O	80%
24	H	7-CH_2OH	SeO_2	xylene	O	O	50%
25	H	7-O CH_3	H_2SO_4	H_2O	H	OH	80%
26	H	7-O CH_3	SeO_2	chlorobenzene	O	O	60%
27	Me	7-(*p*-anysol)	SeO_2	chlorobencene	O	O	70%
28	Me	7-piperidinyl	AcOH	AcOH	H	OAc	75%

1.3.1.1 Reaction mechanism of the ring opening reaction in [1,2,3]triazolo[1,5-*a*]pyridine

Two alternative explanations can be found in the literature concerning the reaction of the [1,2,3]triazolo[1,5-*a*]pyridine ring with non alkylating electrophiles. The first one, proposed by Jones, is based on an ionic process. It explains the reaction with non alkylating electrophiles[26] (sulfuric acid, acetic acid...) and also nitration and formylation at C^3. This mechanism is based on the equilibrium between the open form of the triazole and the closed one (**Scheme I-18**) (A), and the corresponding equilibrium of the intermediated C^3 substituted compound before loss of nitrogen (B). With electron accepting electrophiles the deprotonation of the C^3 hydrogen can take place instead of the loss of nitrogen if the electrophile does not stabilise the diazonic compound (D and E). Irreversible modification occurs if the nucleophilic attack can take place with loss of molecular nitrogen (C).

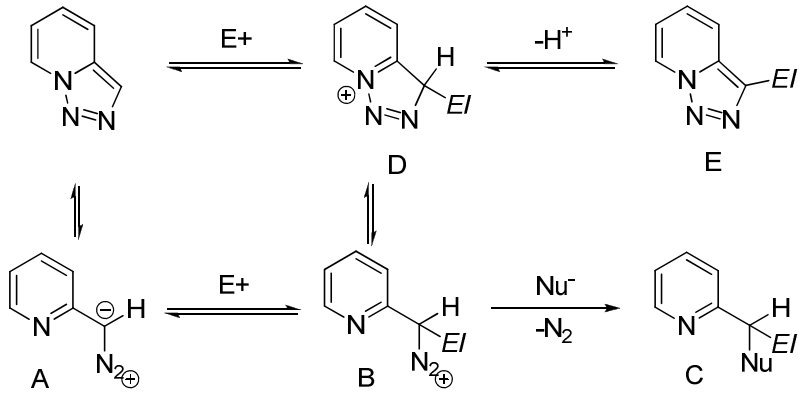

Scheme I-18: Ionic mechanism.

In 1978, Wentrup[32] published the hydrogen-deuterium exchange at C^3 by heating [1,2,3]triazolo[1,5-*a*]pyridine in deuterated water (**Scheme I-19**). This reaction was catalysed by bases like NaOD.

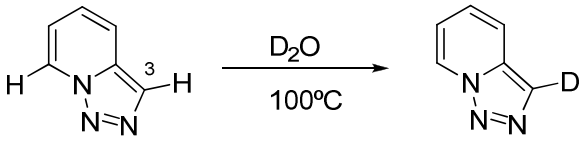

Scheme I-19: Regioselective deuteration at C^3.

Abarca and Ballesteros[33] also published the C^3 functionalization of [1,2,3]triazolo[1,5-*a*]pyridine in presence of molecular iodine or bromine in a DMF/KOH system. The mechanism proposed to explain these results also involved triazol-ring opened species (**Scheme I-20**).

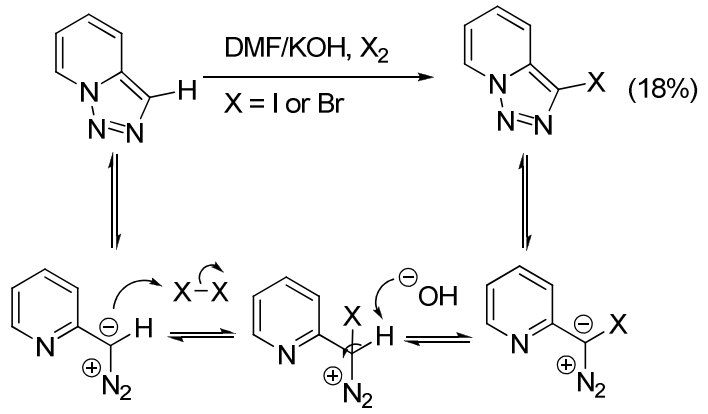

Scheme I-20: Regioselective halogenation at C^3.

The formation of carbenes from triazolopyridines was reported by Wentrup in the 60's-70's.[32, 34, 35] Abarca and Ballesteros also reported on the generation of carbene in the course of their study[36] on the thermal decomposition of 7-bromotriazolopyridines. The carbene intermediate can be generated by loss of nitrogen in the corresponding diazo compound before electrophile attack. As a result of these reactions, cyclopropanes were observed as well as vinyl pyridines (**Scheme I-21**).

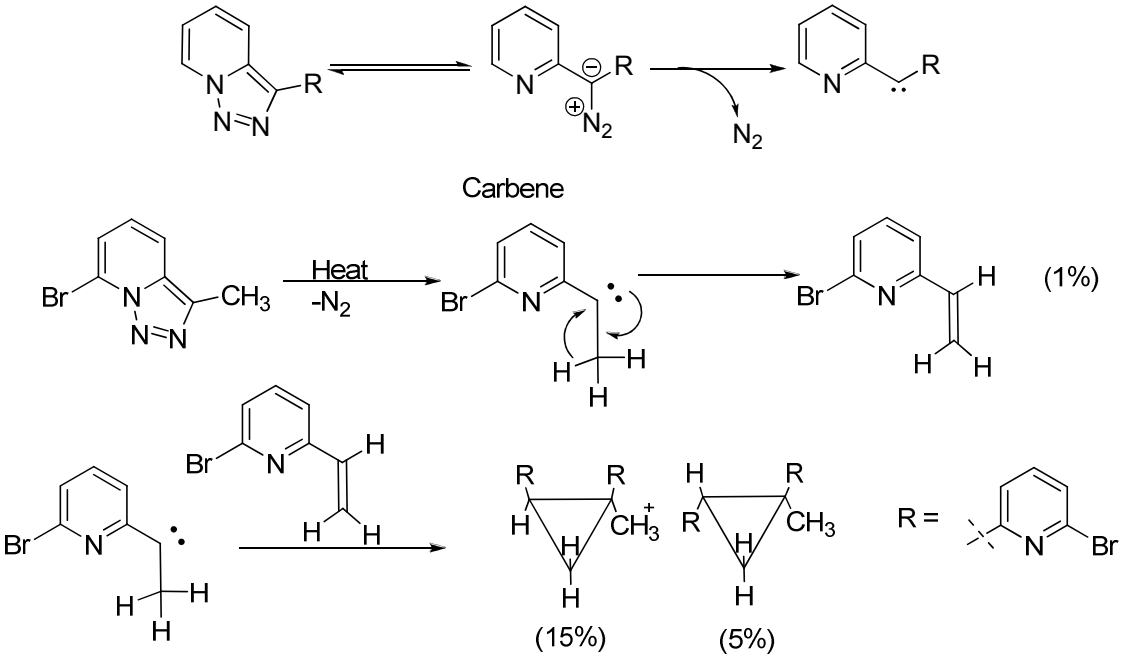

Scheme I-21: Carbene generation, Synthesis of cyclopropanes.

Very recently Gevorgyan[37, 38] has reported on the reaction of 7-chlorotriazolopyridines with rhodium acetate and alkynes or nitriles to afford indolizines and imidazopyridines (**Scheme I-22**).

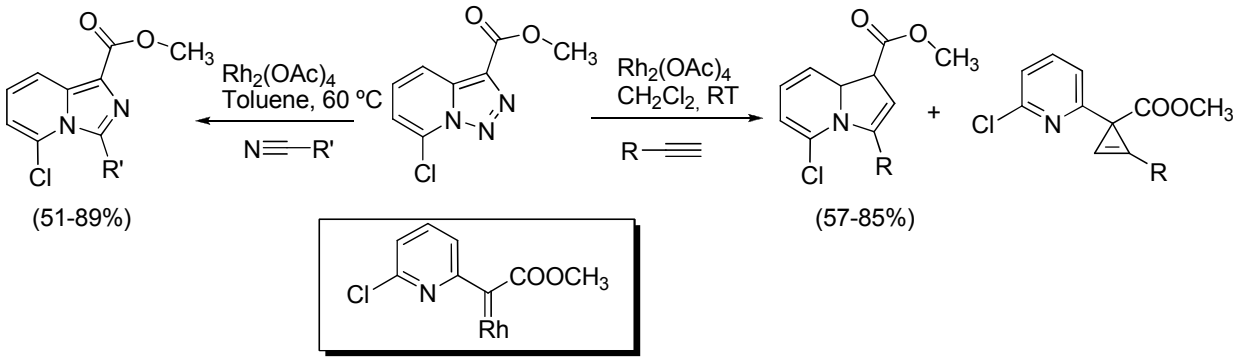

Scheme I-22: Gevorgyan's results concerning the carbene formation.

In 1998 a mechanistic study was carried out by Abarca and Ballesteros.[39] The reaction of triazolopyridine with alkylating agents gave a complex mixture of products and their formation was explained by radical intermediates. The first step of the proposed mechanism is the coordination of the electrophile on the nitrogen atom N^2, then the nucleophile attacks the carbon C^3 which leads to an open form which decomposes. Then, nitrogen is released and two radicals are formed. Their combination provides the corresponding 2-subtituted pyridine (**Scheme I-23**). The presence of a pyridinic radical was coherent with the side products observed.

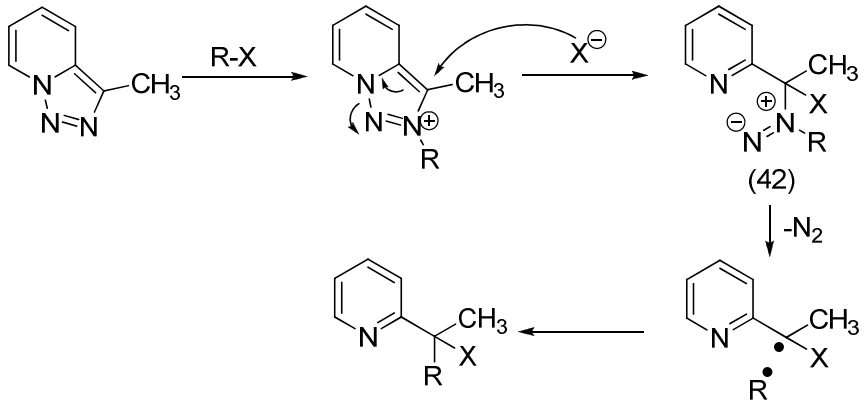

Scheme I-22: Radical mechanism proposed by Abarca and Ballesteros.

To find evidences for the presence of radicals the reactions were carried out in the presence of DDPH (2,2-di-(4-ter-octifenyl)-1-pricriyhidrazylo) as radical scavenger(**Figure I-6**).

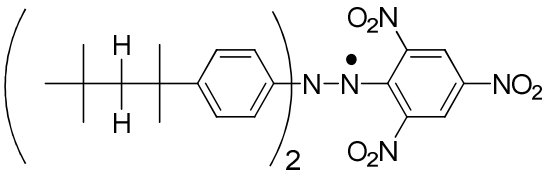

Figure I-6: 2,2-di-(4-ter-octifenyl)-1-picrylhidrazylo.

A DDPH solution in acetonitrile has a violet colour. When the decomposition reaction of the triazolopyridine was carried out in acetonitrile in presence of DDPH, the violet coloration became yellow. This colour change demonstrates the interaction between DDPH and free radicals present in the reaction medium. Furthermore, the radicals were trapped with

nitrosobenzene and different radicals were detected by EPR. These observations confirm the formation of radicals in the course of the reaction and the proposed mechanism.

1.3.2 Regioselective metalations of [1,2,3]triazolo[1,5-*a*]pyridines

In 1982, Jones and Sliskovic[10] reported for the first time observations on reaction of triazolopyridines and strong lithium bases, like LDA (lithium di-*iso*-propylamide) or butyllithium. They screened different reaction conditions in order to optimize the metalation at C^7 (**Table I-2**).

Table I-2: Metalation of triazolopyridine.

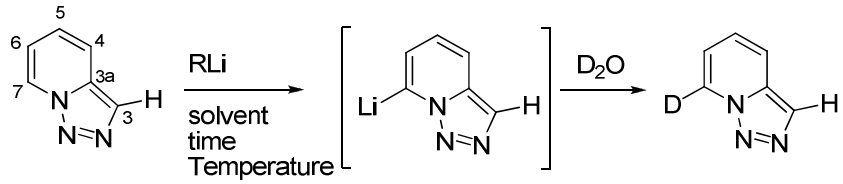

Entry	Base	Solvent	Temperature	Time	Conversion (%)
1	BuLi	ether	-10 °C	3 h	50
2	BuLi	ether	-40 °C	6 h	70
3	BuLi	ether	-50 °C	2 h	66
4	BuLi	ether	-70 °C	0.5 h	50
5	BuLi	THF	-40 °C	6 h	50
6	BuLi	THF	-40 °C	24 h	50
7	BuLi /TMEDA	THF	-40 °C	6 h	10
8	BuLi /TMEDA	THF	-40 °C	24 h	20
9	LDA	ether	-40 °C	6h	85
10	LDA	THF	-60 °C	6h	60

These results show that whatever the reaction conditions, the metalation is highly regioselective as no traces of other lithiated side products were observed.

The conditions LDA/Ether/-40 °C/ 6h (**Table I-2**, entry 9) were found to be the best ones in terms of conversion. Later these conditions were optimiced by Abarca and Ballesteros[40, 41]. By treating [1,2,3]triazolo[1,5-*a*]pyridine at -40 °C in toluene with 1.05 equivalents of butyllithium, the metalation was completed in 30 minutes (**Scheme I-23**) instead of 6 hours and the conversion was increased to 95%.

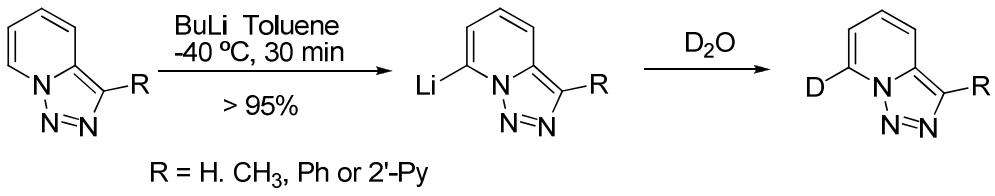

Scheme I-23: Abarca and Ballesteros metalation conditions.

The regioselectivity observed in the metalation of [1,2,3]triazolo[1,5-*a*]pyridine, furnishes an essential information about the role of the nitrogen atoms. As mentioned previously (**Scheme I-19**), the hydrogen atom at C^3 can be exchanged by deuterium when [1,2,3]triazolo[1,5-*a*]pyridine is treated with NaOD in D_2O, which means that this hydrogen atom is the most acidic one. But surprisingly, when [1,2,3]triazolo[1,5-*a*]pyridine is metalated with BuLi at -40 °C no traces of C3 metalated products were found. Furthermore, metalation occurs selectively at C^7.

This observation allowed us to assume that the metalation should be directed by the nitrogen atom at N^1, in the "*peri*" postion to H^7, which would act like an *ortho*-directing group.

Very recently and in collaboration with Elguero, Alkorta and Blanco,[42] this regioselective metalation was studied from a theoretical point of view by means of DFT and AIM analysis. These calculations highlight that the C^7-lithiated triazolopyridine is the most stable one due to the presence of the N^1 electron pair which coordinates the lithium specie (**Scheme I-24**).

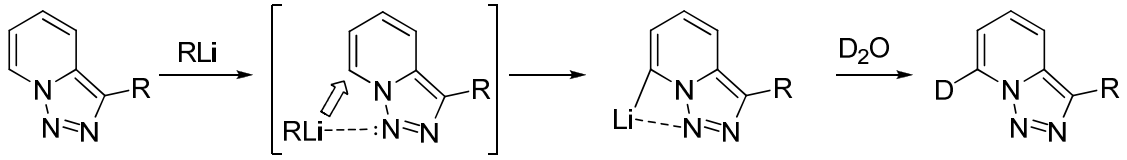

Scheme I-24: N^1 lone-pair effect on the metalation.

Finally, several authors took advantages from this regioselectivity to create a new substituted [1,2,3]triazolo[1,5-*a*]pyridine family. For example, Jones[10, 43] trapped the lithiated triazole with aldehydes and ketones as electrophiles to synthesice secondary or tertiary alcohols, respectively (**Scheme I-25**).

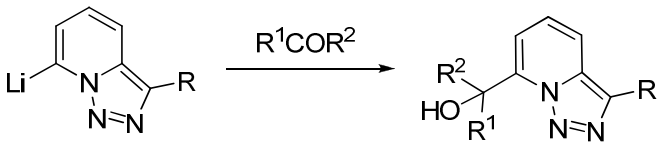

	a	b	c	d	e	f	g
R^1	H	H	H	H	CH_3	$(CH_2)_4$	Ph
R^2	C_7H_{12}	Ph	4-$H_3COC_6H_4$	4-$O_2NC_6H_4$	4-Py	$(CH_2)_4$	Ph
Yield	30%	30%	69%	20%	40%	25%	52%

Scheme I-25: Synthesis of secondary or tertiary alcohols.

This regioselectivity , allowing the functionalization with electrophiles at C^7 combined with the ring opening reaction described previously (**Table I-1**), provides one of the most important aspects of [1,2,3]triazolo[1,5-*a*]pyridine chemistry: the synthesis[11] of 2,6-difunctionalized pyridines (**Scheme I-26**).

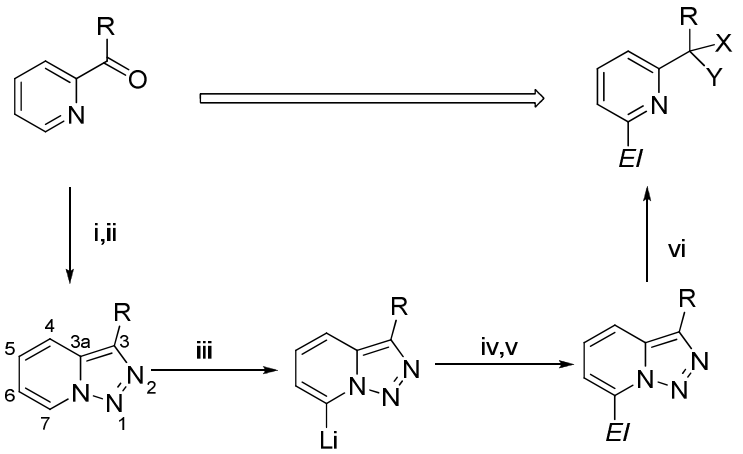

Scheme I-26: Synthesis of 2,6-difunctionalized pyridines i) H_2NNH_2 ii) MnO_2,$CHCl_3$ iii) BuLi,Toluene,-40 ºC iv) Electrophile v) NH_4Cl, H_2O vi) AcOH (X = H, Y = OAc), H_2SO_4 3M (X = H, Y = OH)....

The directing effect of the nitrogen atom N^1 was also observed by Jones[10] in 1982 in the deprotonation of 7-methyl[1,2,3]triazolo[1,5-*a*]pyridine affording the benzylic organolithium intermediate. This property was employed by Daines[44] *et al.* in the synthesis of a Leukotriene B4 receptor antagonist in 1993 (**Scheme I-27**).

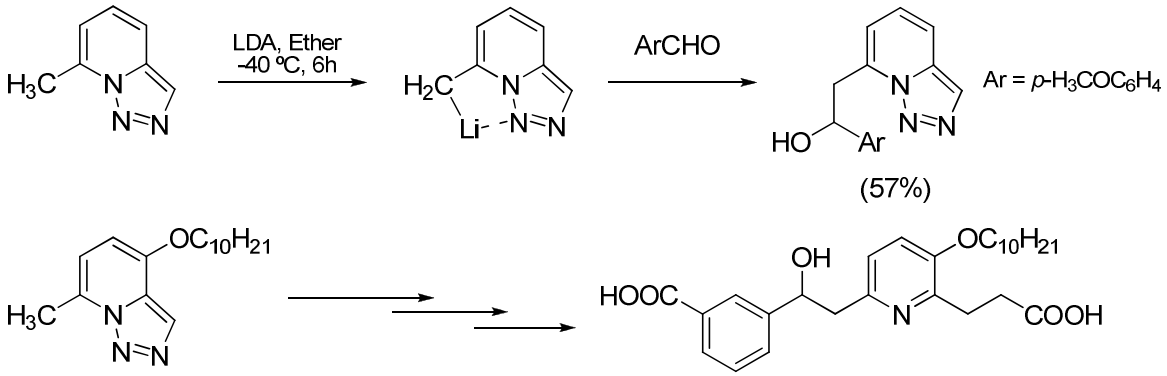

Scheme I-27: N^1 *ortho* directing effect.

When this reaction was carried out in presence of oxygen, different products were obtained, like 7-hydroxymethyl[1,2,3]triazolo[1,5-*a*]pyridine and a dimer (**Scheme I-28**). As it will be discussed later, dimerization of triazopyridines allows the preparation of disubstituted bipyridines.

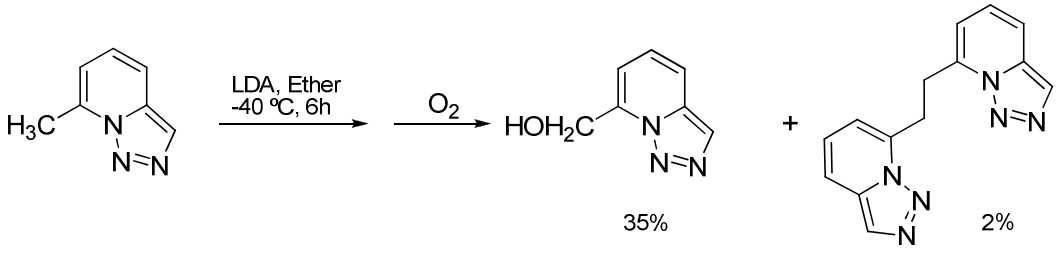

Scheme I-28: *Ortho* effect with 7-CH_3 triazolopyridine. Oxygen dimerization.

The *ortho* directing effect of the triazole ring towards *peri*-metalation remains an important aspect in the chemistry of these molecules. Some studies have been performed[15] by introducing other *ortho*-directing groups on the triazolopyridine ring and the metalation with LDA provided exclusively 7-substitued triazolopyridines (**Scheme I-29**).

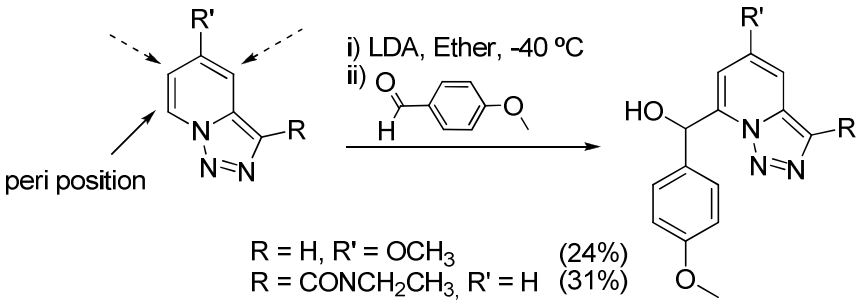

Scheme I-29: *Ortho* effect with different triazolopyridines.

So far, only few examples of metalation at other positions are described in literature. Nevertheless, in 1995, Jones reported the metalation of 3-cyano[1,2,3]triazolo[1,5-*a*]pyridine with LDA. Although this reaction provides a complex mixture of product, after metalation and trapping with trimethylsilyl chloride, 4-substituted triazolopyridine was identified (**Scheme I-30**). However, the low yield remained an important drawback from a synthetic point of view.

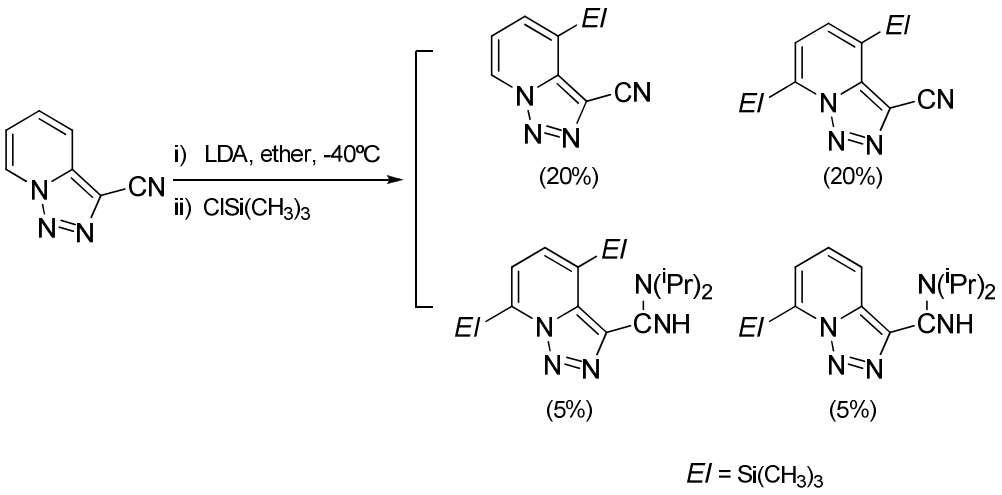

Scheme I-30: Exceptions concerning the regioselective metalation.

As reported by Jones, 4-substitution[45] could also be achieved with 7-trimethylsilyl-3-carboxamide [1,2,3]triazolo[1,5-*a*]pyridine but in a low yield (5%) (**Scheme I-31**).

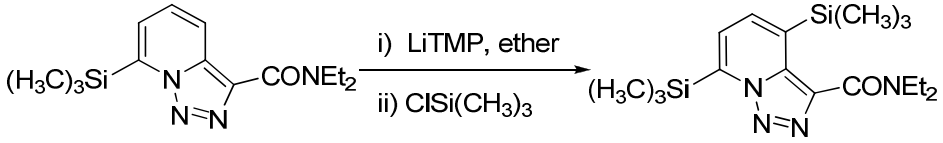

Scheme I-31: 4-substitution with 7-protected compounds.

Recently, Abarca, Ballesteros, Quéguiner and Mogin[46] performed different metalations at C^7 with the Bu_3MgLi complexes, providing excellent yields. Also double and triple metalations were reported using (TMP_3CdLi·TMEDA) as a base (**Scheme I-32**).

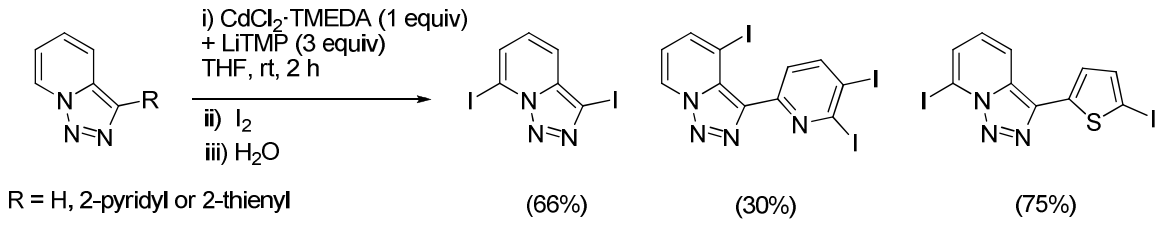

Scheme I-32: Double and triple metalation.

In spite of these recent results, no direct metalation at the C^4-, C^5- or C^6-position has been achieved.

1.3.3 Reactions with nucleophiles

The [1,2,3]triazolo[1,5-*a*]pyridines do not react directly[2] with nucleophiles. However, some S_NAr reactions with the corresponding 7-bromo-3-substituted-[1,2,3]triazolo[1,5-*a*]pyridines and 5-bromo-3-substituted[1,2,3]triazolo[1,5-*a*]pyridines are described. 7-Bromo-3-substituted-[1,2,3]triazolo[1,5-*a*]pyridine reacts with nucleophiles like sodium methoxide, sodium 4-methoxyphenolate or sodium benzenethiolate in DMF at 90 °C to give substituted compounds in high yields (**Scheme I-32**). In ethanol at 80 °C , sodium hydrazinide and sodium piperidide derivatives were used and afforded substitution products in respectively 60 and 65% yield. No reaction occurs with sodium azide and potassium isocyanate.[47]

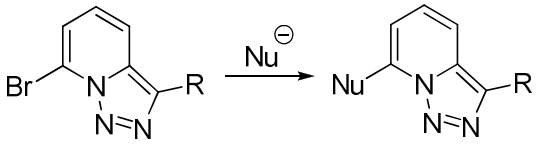

R	H	CH_3	CH_3	CH_3	CH_3	CH_3	$CONCH_2CH_3$
Nu	OCH_3	OCH_3	4-OC_6H_4O CH_3	SPh	Piperidine	$NHNH_2$	OCH_3
Yield	95%	90%	90%	95%	60%	65%	92%

Scheme I-32: S_NAr reactions with 7-bromo-3-substituted-[1,2,3]triazolo[1,5-*a*]pyridines.

Nucleophilic substitutions can also be performed on 5-bromotriazolopyridines. However, as no regioselective metalation can be accomplished at C^5, these compounds must be prepared starting with commercial bromopyridines[16, 48] as starting material (**Scheme I-33**).

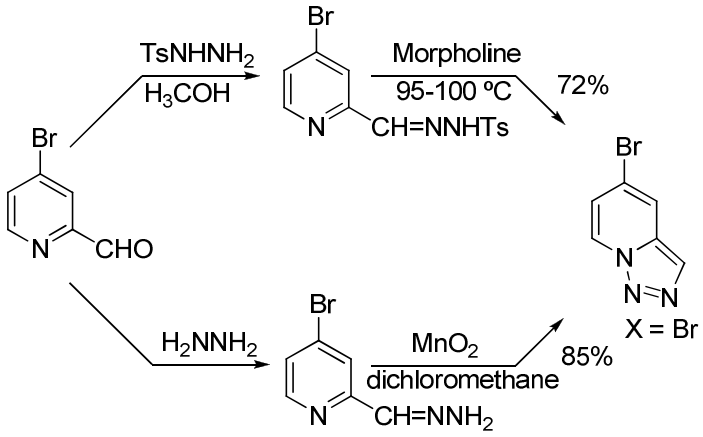

Scheme I-33: synthesis of 5-bromotriazolopyridine.

This substrate reacts with nucleophiles (**Scheme I-34**) allowing the functionalization at the C^5 position.[49] No reaction occurs when the reaction is carried out with the chlorinated derivative or with 6-bromo[1,2,3]triazolo[1,5-*a*]pyridine.

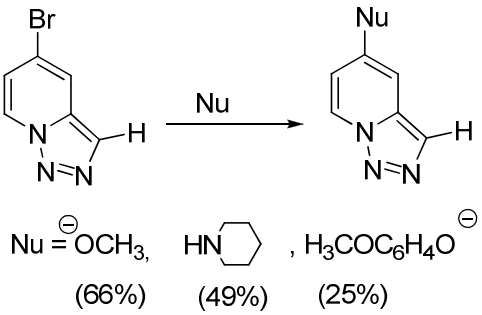

Scheme I-34: S_NAr reactions with 5-bromo-[1,2,3]triazolo[1,5-*a*]pyridine.

1.3.4 Dimerization reaction with triazolopyridine towards functional bipyridines

1.3.4.1 Dimerization reaction in triazolopyridines

Under specific metalation conditions, heterocyclic π-deficient compounds can undergo dimerization. This kind of aryl-aryl coupling is known, but it was not intensively investigated. Some data about dimerization of pyridine[50] can be found. The reaction of dimerization of [1,2,3]triazolo[1,5-*a*]pyridines was observed by Abarca and Ballesteros for the first time in 1997. When 3-methyl[1,2,3]triazolo[1,5-*a*]pyridine was treated with LDA at -40 °C in THF followed by trapping with 2-pyridylcarboxaldehyde, the corresponding dimer was obtained as a side product[51] (**Scheme I-35**).

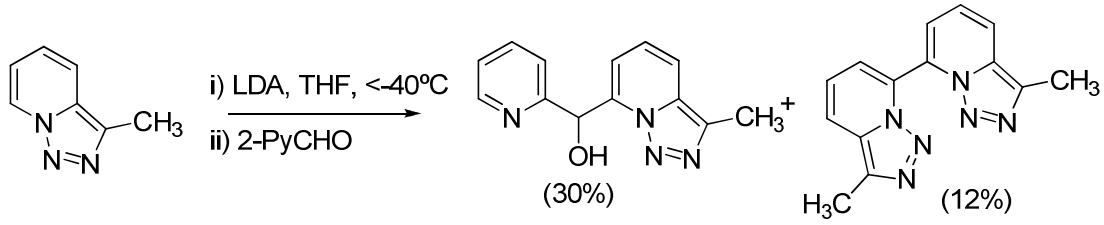

Scheme I-35 First evidence of the dimmerization of triazolopyridines.

Due to the interesting structure of this dimer, the authors modified the reaction conditions in order to favour dimerization.[16] They found out that the optimal conditions were LDA (1 eq)/THF/-70 °C. After 9 hours, the dimer was obtained in a 50% yield but surprisingly, another side product (1-(3-methyl[1,2,3]triazolo[1,5-*a*]pyridin-7-yl)-4-(5-methyl-1*H*-1,2,3-triazol-4-yl)-1,3-butadienyl)appeared and was formed in a non-negligeable amount (25%) (**Scheme I-36**).

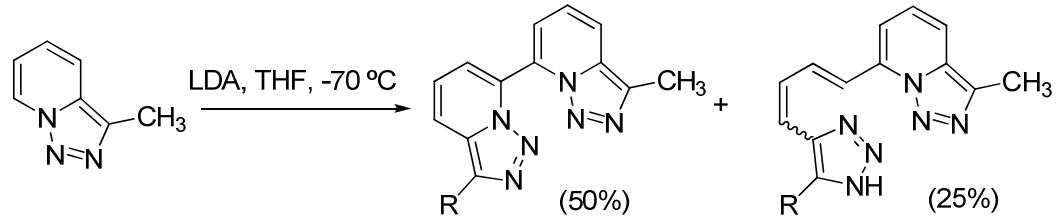

Scheme I-36: Dimer and diene formation.

To explain this unusual reactivity, one has to consider that one equivalent of 7-triazolopyridinyl lithium attacks the C^7 nucleophilic position (See part 1.3.3) of a non-lithiated triazolopyridine. This leads to the formation of a pseudo-dimer which was isolated after protonation with D_2O. This pseudo-dimer can be converted in the dimer by loss of LiH, or air oxidation. Finally the unexpected diene is formed after a ring opening reaction without loss of nitrogen.[51](**Scheme I-37**)

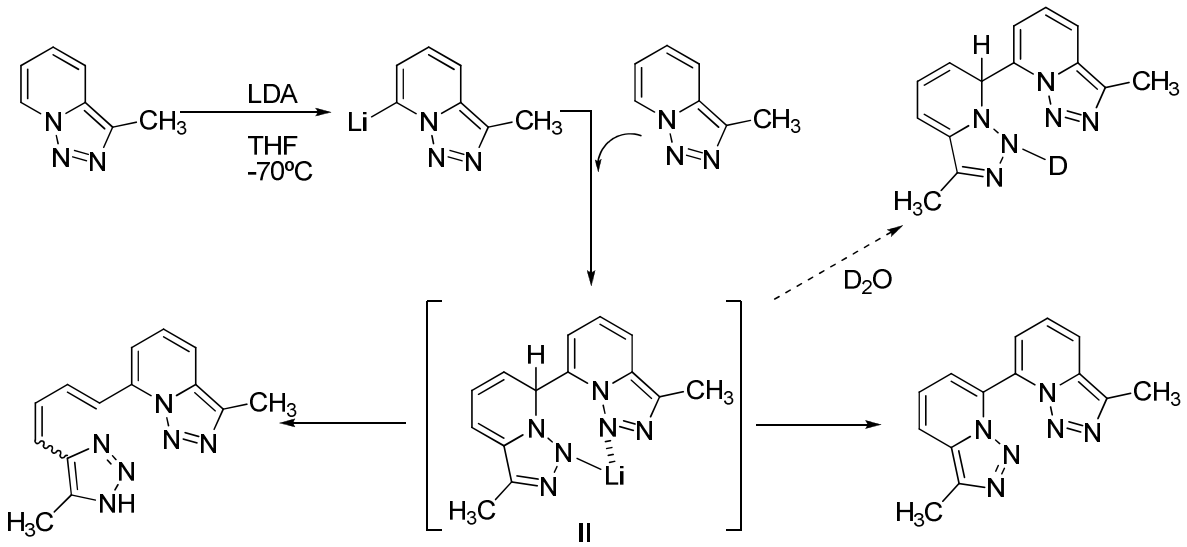

Scheme I-37: Mechanism for the dimer and diene formation.

The preparation of other dimers has also been described for other triazolopyridines (R = H, Ph and 2-Py). The corresponding dienes were also observed. The presence of dimers can be easily detected thanks to their fluorescent properties (λ_{exc} = 380 nm, λ_{em} = 455 nm).[52] All of them are solid and highly fluorescent compounds with melting points superior to 350 °C.

Furthermore, their solubility in organic solvents is very limited in particular in chloroform and dichloromethane.

1.3.4.2 Synthesis of disubstituted pyridines and 2,2'- bipyridines

As shown in scheme I-26, the metalation/ring opening approach [10, 43, 53] allows an easy and straightforward access to 2,6 disubstituted pyridines. If the nucleophilic substitution at C^7 on the bromo-derivative is taken into account, triazolopyridines can be considered as an excellent precursor of 2,6-disubstituted pyridines. In addition, as bromine can be introduced as an electrophile and can be replaced by another group *via* a S_NAr reaction, this strategy seems to be extremely versatile (**Scheme I-38**).

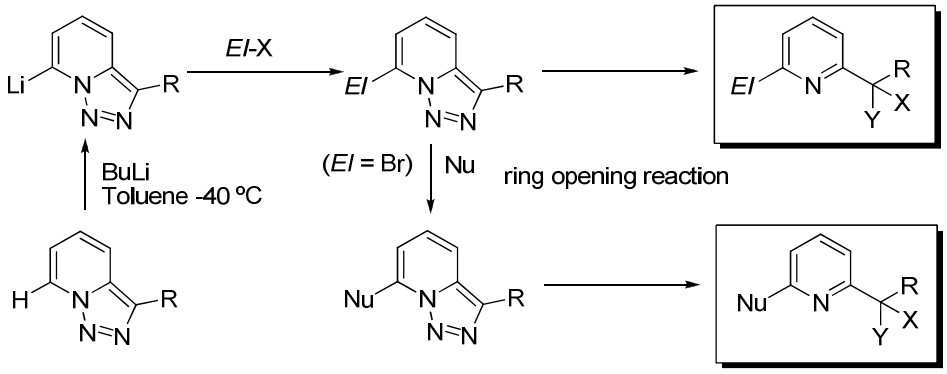

Scheme I-38: Obtention of different 2,6-disubstituted pyridines.

After the isolation of the corresponding dimers from triazolopyridines, the ring opening reactions were directly performed[14] on these new structures. Triazolopyridine dimers can be considered as masked 6,6'-disubstituted-2,2'-bypyridines. The synthesis of bipyridines has been recently revised by Newkome *et al*[54] . The following scheme shows the classical ring opening reactions performed on the dimers with sulfuric acid, acetic acid and selenium(IV)oxide (**Scheme I-39**).

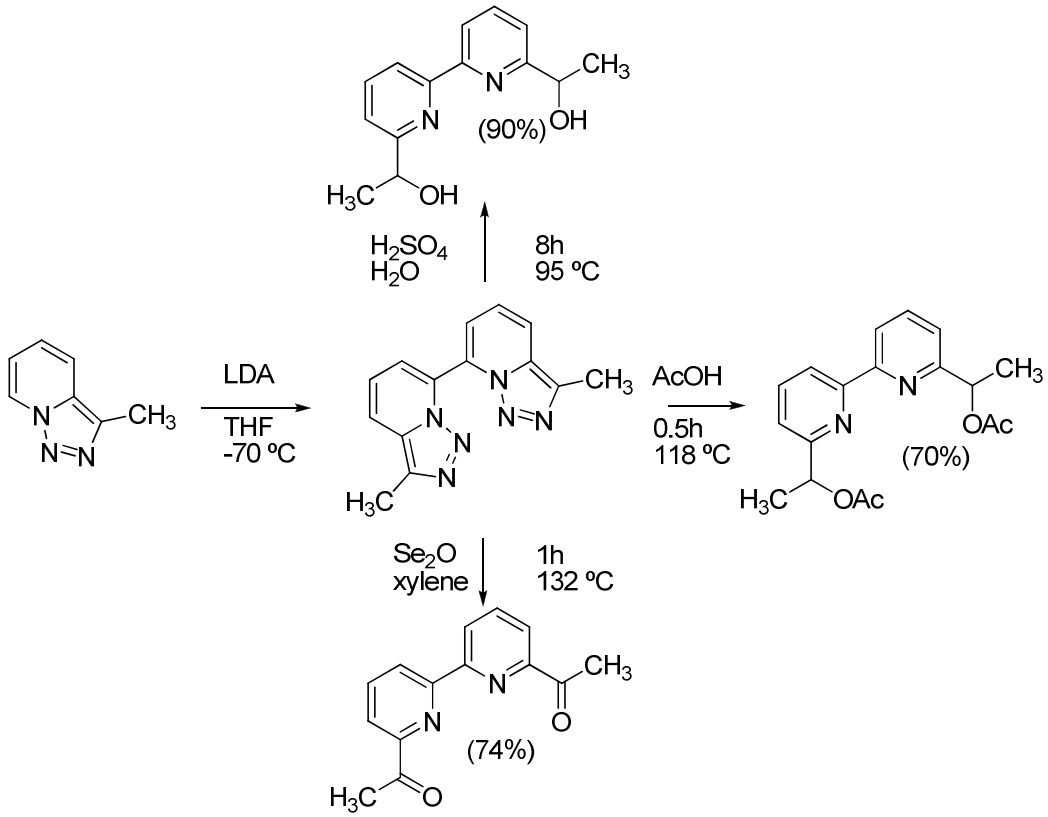

Scheme I-39: Synthesis of different 6,6'-disubstituted-2,2'-bypyridines.

1.3.5 Hydrogenation reactions of triazolopyridines

In 1999, Abarca *et al* published a complete study on the hydrogenation [55] by means of heterogeneous catalysis under mild conditions (Pd/C, methanol, 25 °C, atmospheric pressure) and obtained the following compounds (**Scheme I-40**):

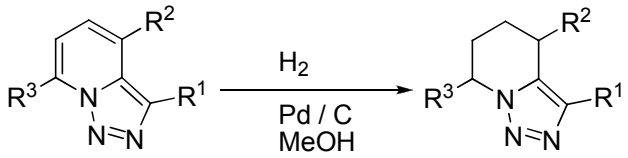

$R^1 = R^2 = R^3 = H$	$R^1 = R^2 = R^3 = H$, (90%)
$R^1 = CH_3$, $R^2 = R^3 = H$	$R^1 = CH_3$, $R^2 = R^3 = H$, (100%)
R^1 = 2-Py, $R^2 = R^3 = H$	R^1 = 2-Py, $R^2 = R^3 = H$, (46%)
R^1 = 2-Th, $R^2 = R^3 = H$	R^1 = 2-Th, $R^2 = R^3 = H$, (46%)
$R^1 = H$, $R^2 = CH_3$, $R^3 = H$	$R^1 = H$, $R^2 = CH_3$, $R^3 = H$, No reaction
$R^1 = R^2 = H$, $R^3 = CH_3$	$R^1 = R^2 = H$, $R^3 = CH_3$, No reaction
$R^1 = COOC_2H_5$, $R^2 = R^3 = H$	$R^1 = COOC_2H_5$, $R^2 = R^3 = H$, (50%)
$R^1 = CN$, $R^2 = R^3 = H$	$R^1 = CH_2NH_2$, $R^2 = R^3 = H$, (30%)

Scheme I-40: Hydrogenation reactions performed on triazolopyridines.

Under these conditions [1,2,3]triazolo[1,5-*a*]pyridines afford readily 4,5,6,7-tetrahydro-[1,2,3]triazolo[1,5-*a*]pyridines. When the triazolopyridine is substituted by a methyl group in position 3, the reactions leads to the formation of the tetrahydro derivate in good

yield. However, if the methyl group is on the pyridinic ring (**Scheme I-40**), no hydrogenation product was observed and the starting material was recovered. When the pyridine is substituted with a thiophene at position 3, the product was obtained in low yield even with increased catalyst charge. This can be explained by the poisoning effect of sulfur towards palladium.

On the other hand, the authors highlighted that the presence of electron-withdrawing substituents at the 3-position decreases the reactivity towards hydrogenation.

When 3-cyanotriazolopyridine was hydrogenated, a side product was also isolated and characterized as 3-((4-(pyridin-2-yl)-1*H*-1,2,3-triazol-1-yl)methyl)-4,5,6,7-tetrahydro-[1,2,3]triazolo[1,5-*a*]pyridine. Its formation can be explained by the following mechanism (**Scheme I-41**).

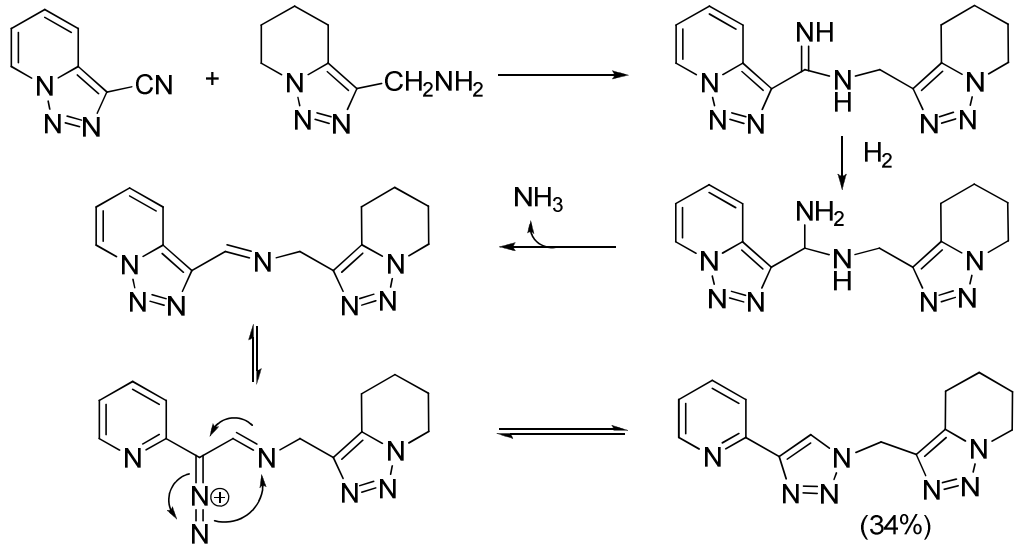

Scheme I-41: Hydrogenation of 3-cyanotriazolopyridine.

Under these reduction conditions 3-cyanotriazolopyridine is also hydrogenated on the cyanide group, affording the corresponding tetrahydrotriazolopyridine methyl amine. The amine reacts with another cyanide group of the starting reagent to provide the corresponding imine. This imine is reduced to provide the amine. By loss of ammonia, another imine is generated. The new formed imine provides then the final compound by electronic restructuration of the triazole ring. This result was relevant because it was the first evidence of a triazolo-ring isomerisation process, property that will be discussed later more in detail.

1.3.6 Reactivity towards alkylating electrophiles

The reactivity of triazolopyridines towards different alkylating agents has been investigated. In all cases, the alkylation position remains unchanged: the alkylation always occurs on N^2. This position has been identified by DIFNOE analysis. Then, strongly yellow

coloured triazolopyridinium ylides[56, 57], are formed *in situ* after a basic treatment with potassium carbonate and triethylamine in toluene or potassium carbonate in acetonitrile (**Scheme I-42**).

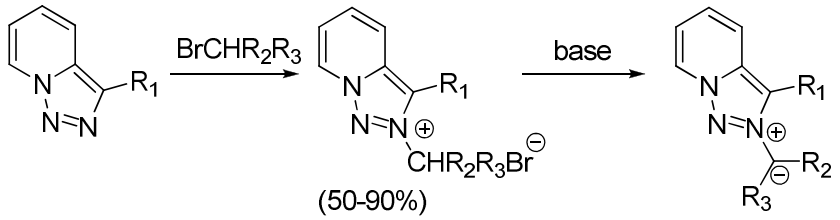

Scheme I-42: Preparation of triazolopyridinium ylides.

1.3.7 Reactivity of triazolopyridinium ylides towards dipolarophiles

Initially, these experiences were performed with [1,2,3]triazolo[1,5-*a*]pyridinium ylide and acetylenic esters.[58-61] The authors found out that these reactions are extremely solvent polarity dependent and the results can vary according to the acetylenic ester. When acetonitrile was used as solvent, the reaction of the ylides with methyl propynoate gives in each case two products characterized as 1:1 and 1:2 adducts (**Scheme I-43**). Both compounds have the ylide structure and a deep red/orange coloration depending on the structure. Thesy revealed pronounced solvatochromism.[62]

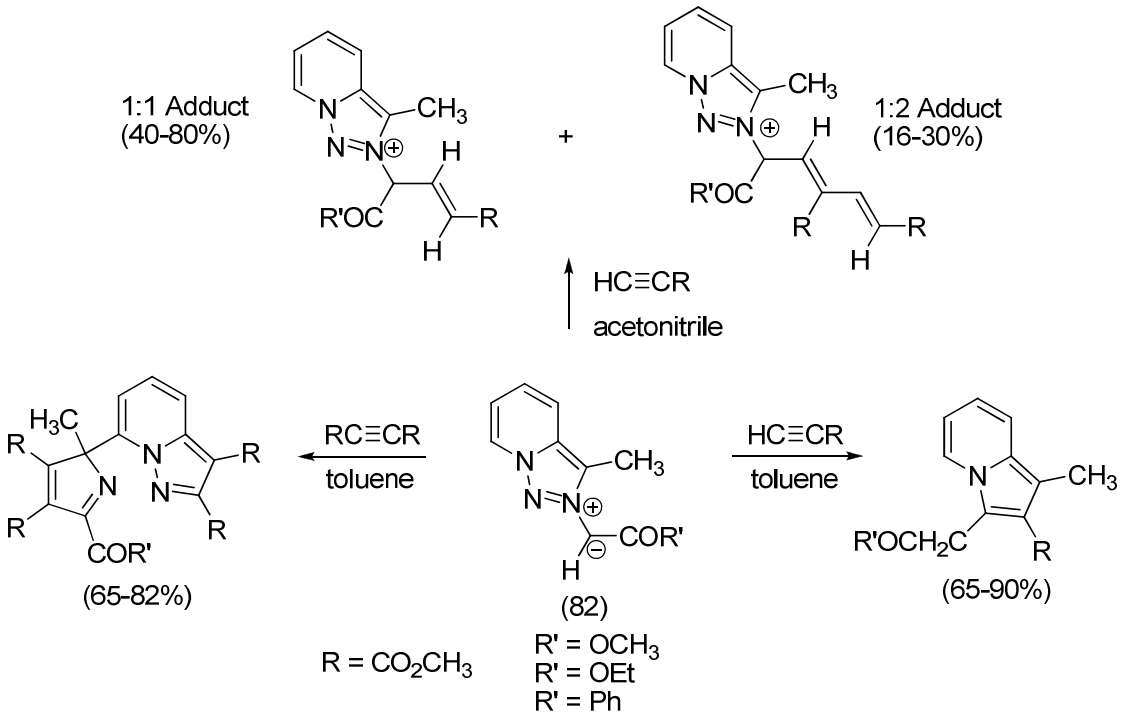

Scheme I-43: Ylide reactivity towards different acetylenic esters and different solvents.

When the synthesis was performed in toluene with acetylenic esters, indolicines were obtained, providing a new way to synthesize this heterocycle.[60] However, when dimethyl acetylenedicarboxylate (DMAD) was used as dipolarophile in toluene, pyrazolo[1,5-*a*]pyridines

were obtained after addition of two molecules of DMAD, and cleavage of the N^2-N^3 bond, leading to the triazole ring opening. In each case 1,3-dipolar cyclo addition was observed. The structure of these compounds was confirmed by single X-Ray. Two alternative mechanisms[59] had been proposed to explain the formation of these compounds.

The reaction of ylides with different acrylates[60] allowed the formation of 3-(2-pyridyl)acrylates, 2-pyridylcyclobutanes, pyridylpent-1-ene and the zwiterion as major products (**Scheme I-44**).

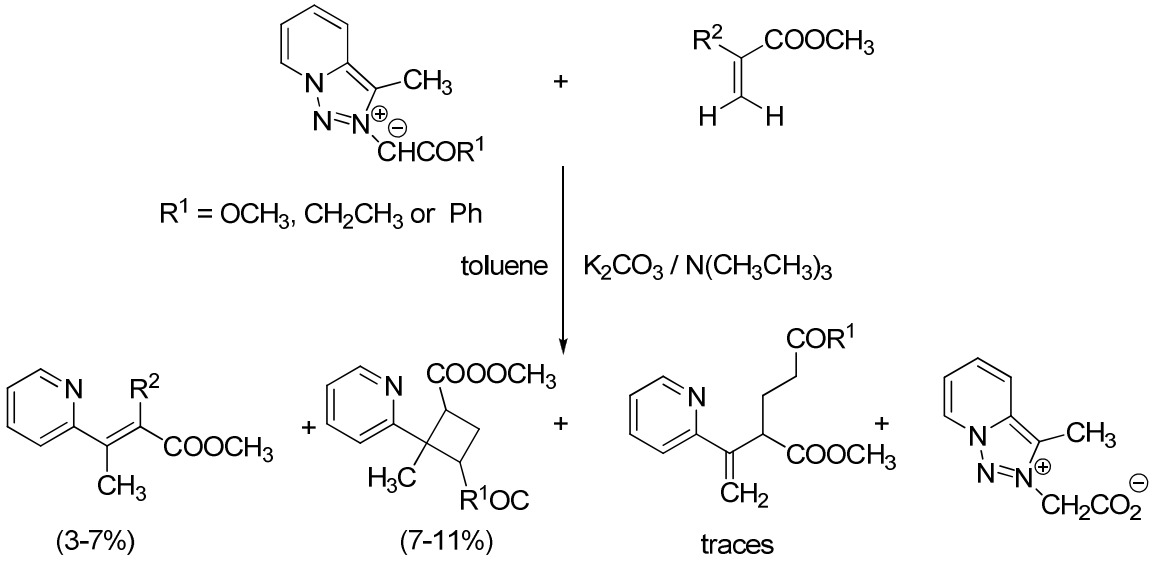

Scheme I-44: Ylide reactivity towards different acrylates.

The formation of these compounds can be explained by the mechanism depicted in scheme I-45. The first step is a kind of Michael addition between the ylide and the dipolarophile. When a polar solvent is used, a proton migration gives a 1:1 adduct, which undergoes a second addition with the dipolarophile to provide a 1:2 adduct. When the solvent is toluene the hydrogen migration is less favoured then and a diazene intermediate is formed. This intermediate generates a diradical by loss of nitrogen. The stabilization of this diradical explains the formation of cyclobutane and indolizines (**Scheme I-45**).

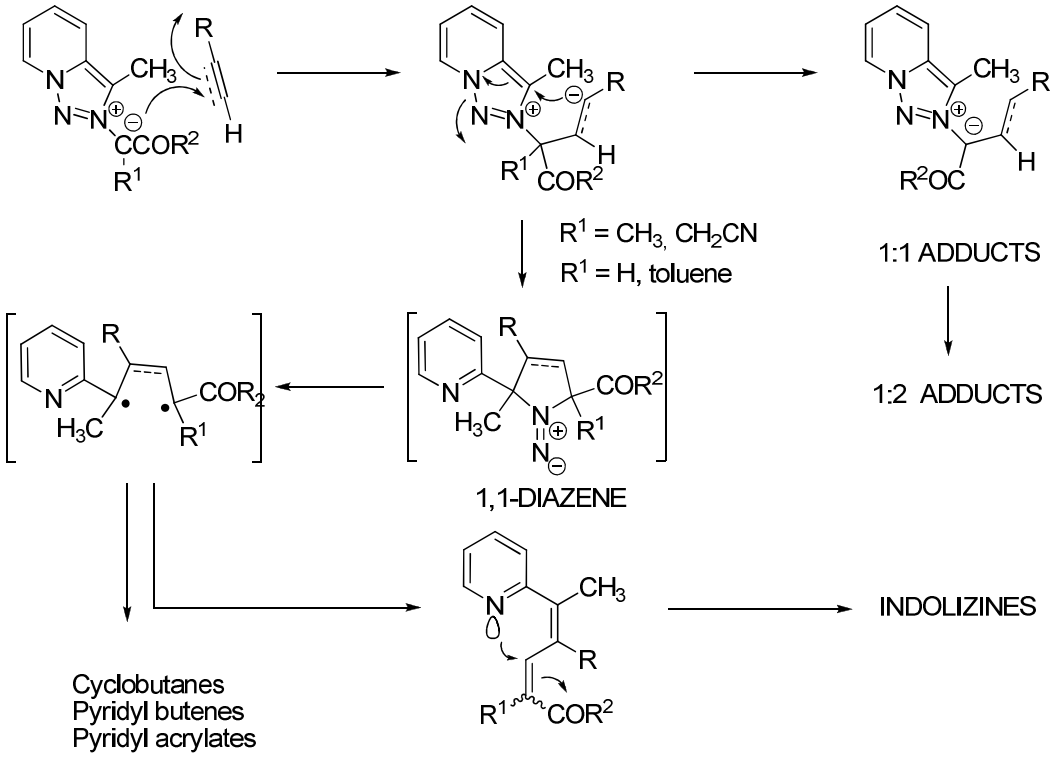

Scheme I-45: Mechanism proposed for the obtention of adducts, indolizines and cyclobutanes.

2-Dicyanomethyl-3-methyl-[1,2,3]triazolo[1,5-*a*]pyridinium ylide and 2-dicyanomethyl-7-methyl-[1,2,3]triazolo[1,5-*a*]pyridinium ylide were also easily prepared[63] by reaction of the corresponding triazolopyridines with tetracyanoethylene oxide (TCNEO, **Scheme I-46**) by the method developed by Linn *et al*.[64-66]

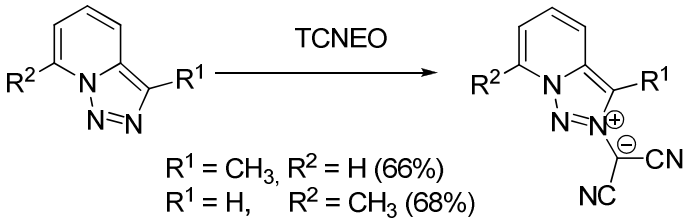

Scheme I-46: Preparation of TCNEO ylide derivatives.

The reactivity of these compound towards acetylenic esters is different, depending on the choice of the dipolarophile[63]. 3-Methylated (R^1 = CH_3, R^2 = H) ylides react with methyl propynoate in acetonitrile as solvent to provide indolizines and cyclazines (**Scheme I-47**). These cydazines are formed by [8+2] cycloaddition between the indolizine and methyl propyonate and was already described in the literature. The reaction performed with the 7-methylated (R^1 = H, R^2 = CH_3) ylides provided exclusively the indolizine. 7-Methylated ylides reacted with DMAD to afford 4*H*-4,4-dicyan-2,3-dimethoxycarbonyl-6-methylquinolizine[63] (**Scheme I-47**).

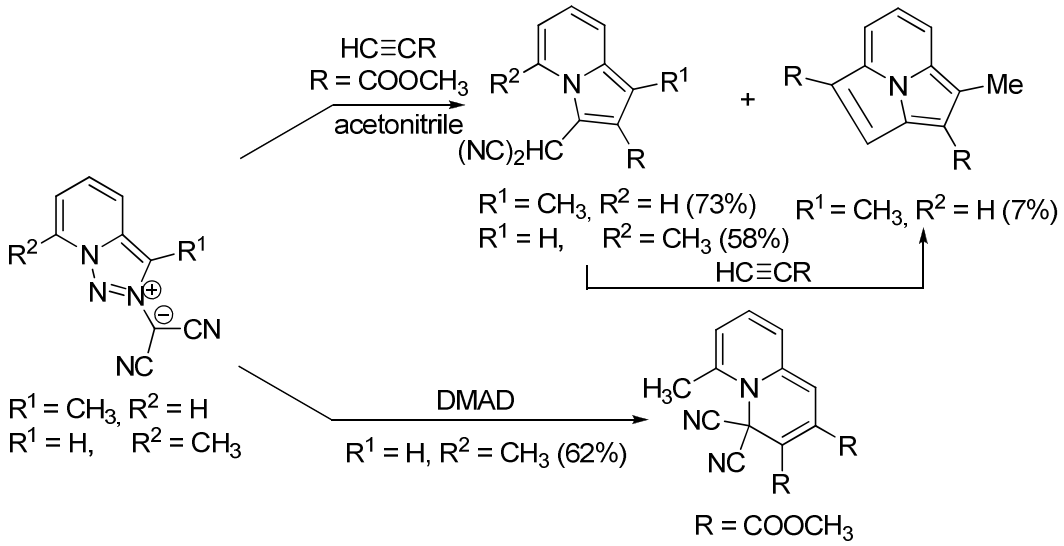

Scheme I-47: Reactivity of TCNEO ylide derivatives.

1.3.8 Photochemistry of triazolopyridinium ylides

As described in literature, methoxyethyl and ethoxethyl ylides can provide azines by irradiation[67] with an Hg lamp under argon atmosphere (**Scheme I-48**). The formation of these azines can only be explained by an electrocyclic ring closure of the ylide. Then, diazyridine is formed and subsequently rearranged to give the expected azines.

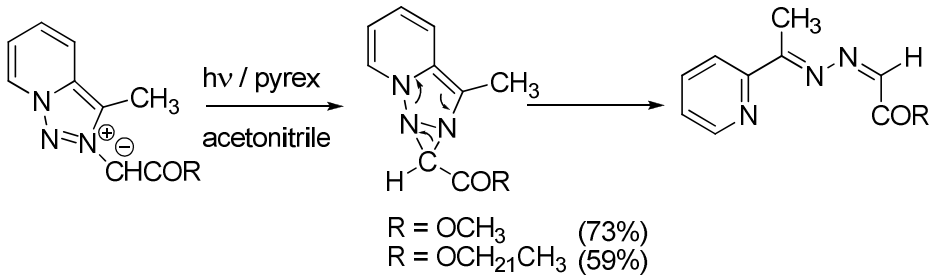

Scheme I-48: Photochemical synthesis of azines.

However, when this reaction was performed with other ylides described before, like 2-benzoylmethyl-3-methyl[1,2,3]triazolo[1,5-*a*]pyridinium ylide, only the starting triazolopyridine was obtained as major product. The same reactivity was observed with dicyanomethyl derivatives (**Scheme I-49**).

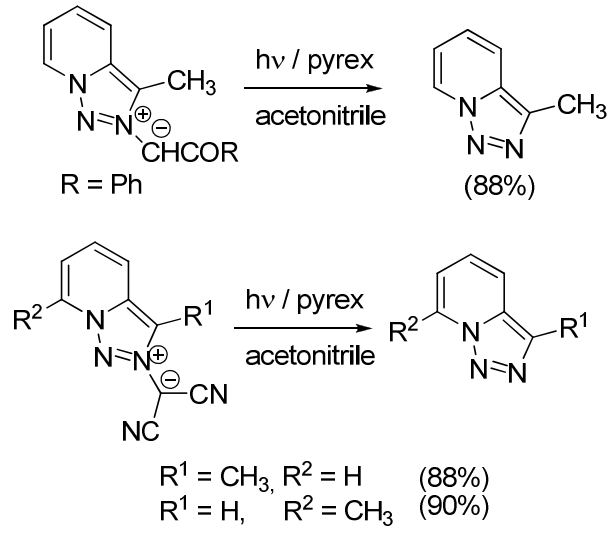

Scheme I-49: Photochemistry of triazolopyridinium ylides.

.

1.5 Experimental analysis and theoretical calculations of the triazolopyridine-pyridine ring-chain isomerisation

As previously described, the position of the triazole ring in [1,2,3]triazolo[1,5-*a*]pyridines allows the existence of an open state *via* a ring-chain isomerisation. This kind of process is an important property of many heterocyclic systems[68, 69] and is often the first step of various chemical transformations. In particular, it is related to several fundamental properties of heterocyclic systems, such as aromaticity [70, 71]. The closed state of the triazole must be stabilized by the formation of the second aromatic ring. Although no open intermediates have ever been isolated and characterized, the reactivity of [1,2,3]triazolo[1,5-*a*]pyridines, like the cyclopropane formation under thermal condition[36] or the rhodium[37] insertion, can only be explained by this particular behaviour (**Scheme I-50**).

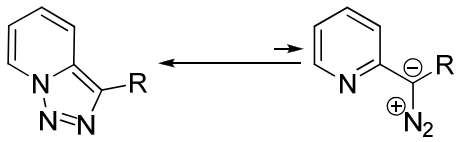

Scheme I-50: Open and closed form for 3-substituted-[1,2,3]triazolo[1,5-*a*]pyridine.

Actually, Abarca and Ballesteros were the first to propose the existence of this ring-chain isomerisation in the course of their studies on 3-substituted triazolopyridine derivatives.[14] They performed the metalation of 3-substituted triazolopyridines with BuLi in toluene at -40 °C and trapped the aryllithium intermediate with ethyl picolinate. However, the ^{1}H-NMR analysis revealed significant differences between the pyridyl derivate (R = 2'-Py) and the other compounds synthesized in the course of this study (R= H, Me, Ph) (**Scheme I-51**).

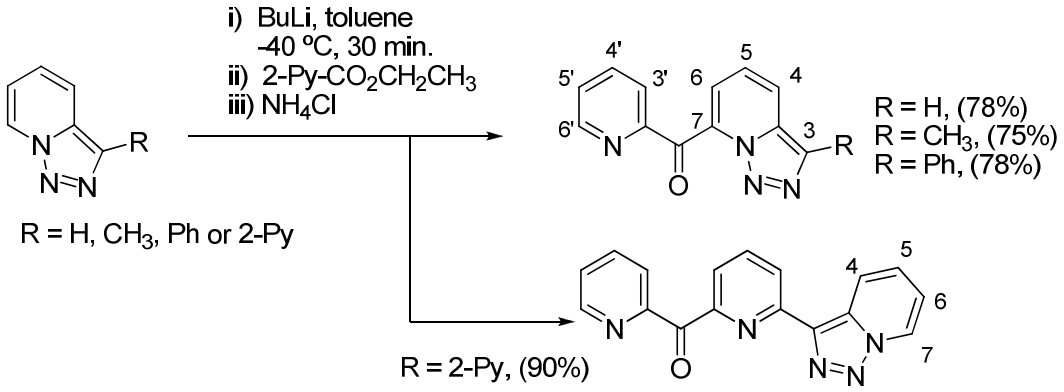

Scheme I-51: Synthesis of pyridyl-triazolopyridyl ketones.

When R = 2-pyridyl, a coupling constant of 6.9 Hz was observed but not when R = H, CH_3 or Ph. HRMS analysis confirmed the presence of five nitrogen atoms for R = 2-pyridil, and the ^{1}H-NMR spectrum presented a free triazolopyridinic H^7 with ^3J = 6.9 Hz. Actually, in all triazolopyridines, $^3J_{H7\text{-}H6}$ is around 6.9-7.0 Hz. Whereas in pyridines the corresponding coupling constant $H^{5'}$-$H^{6'}$ is around 4.7-5.1 Hz. To explain these findings, the authors proposed[72] for the first time the following ring-chain isomerisation which occurs in solution (**Scheme I-52**):

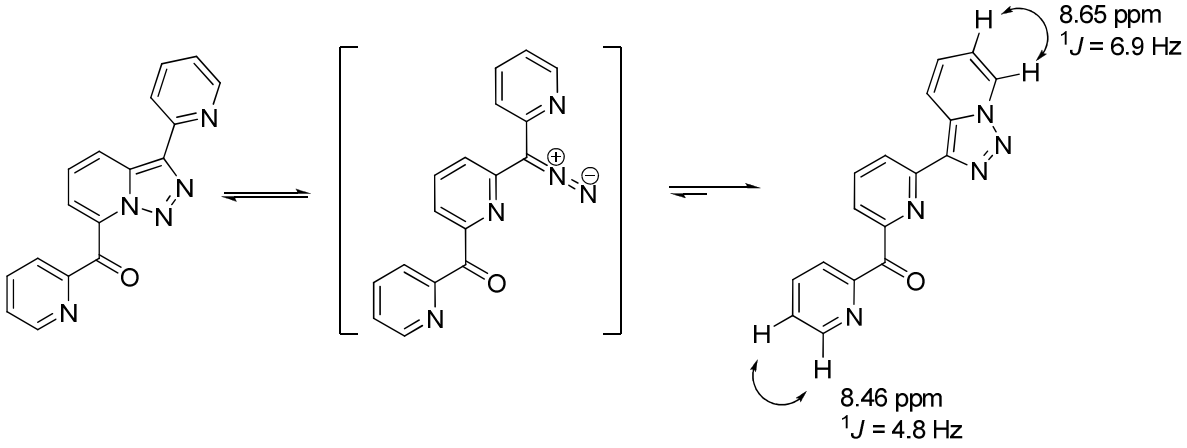

Scheme I-52: Triazolopyridine isomerisation.

The existence of this phenomenon was also confirmed, when lithiated triazolopyridines were trapped for example with iodine or bromine. In these cases, a coupling constant of 7 Hz was systematically found in the ^{1}H-NMR spectrum.

By means of regioselective metalation and trapping the 7-lithiated intermediate with different electrophiles (**Scheme I-53**), many other 3-(2'-pyridy)[1,2,3]triazolo[1,5-*a*]pyridine derivatives or their corresponding isomers were obtained. For example, in order to introduce a *p*-methoxyphenyl group at position 7, a Suzuki cross coupling was performed between the iodo derivate and the corresponding *para*-methoxyphenylboronic acid in presence of palladium *tetrakis*-triphenylphosphine, sodium carbonate in dioxane providing this compound in 80% yield.

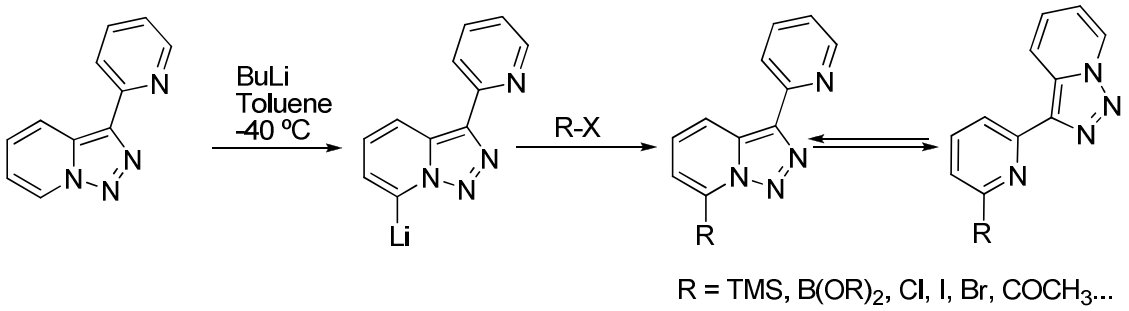

Scheme I-53: Synthesis of triazolopyridine-pyridine derivatives.

When R = CH_3CO or an halogen (scheme I-54), the isomerizated structure (**B structure**), having a ^{1}H-NMR signal with *J* = 7 Hz, was the only one to be isolated. With R= $Si(CH_3)_3$, only the non isomerizated structure (**A structure**) was observed. Other compounds were also synthesized[72] and their structure is reported in **Scheme I-54**:

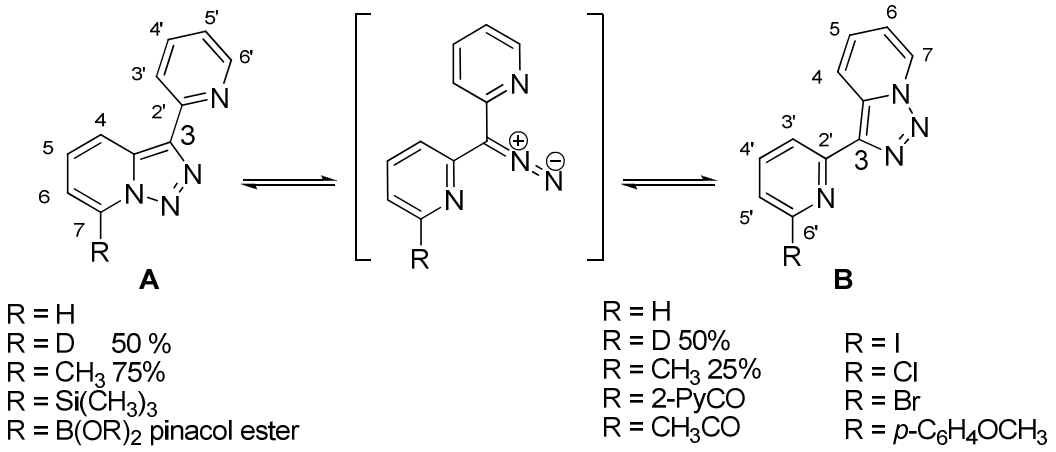

Scheme I-54: Structure of the synthesized triazolopyridine-pyridine derivatives.

In fact, the identification of each species was performed by careful analysis of the ^{1}H-NMR spectrum (**Table I-3**).

Table I-3: ^{1}H-NMR spectra data for triazolopyridine-pyridine derivatives.

R	H^4	H^5	H^6	H^7	$H^{3'}$	$H^{4'}$	$H^{5'}$	$H^{6'}$	Others
H	**8.69m**	**7.28dd**	**6.96dd**	**8.69m**	**8.27d**	**7.71dd**	**7.13dd**	**8.69m**	**---**
		J = 9.0	J = 6.6		J = 8.0	J = 8.0	J = 5.1		
		J = 6.6	J = 7.3			J = 7.5	J = 7.5		
CH_3 75%	**8.61d**	**7.32dd**	**6.89d**	**---**	**8.37d**	**7.78dd**	**7.56ddd**	**8.66d**	**2.92s,CH_3**
	J = 9.0	J = 9.0	J = 6.9		J = 8.1	J = 7.8	J = 7.5	J = 4.8	
		J = 6.9				J = 7.8	J = 4.8		
							J = 0.9		
CH_3 25%	**8.74m**	**7.50m**	**7.04dd**	**8.74m**	**8.13d**	**7.67dd**	**7.07ddd**	**---**	**2.62s,CH_3**
			J = 7.2		J = 7.8	J = 7.5	J = 7.8		
			J = 6.9			J = 7.8			
Si $(CH_3)_3$	**8.61d**	**7.20dd**	**7.01d**	**---**	**8.27d**	**7.69dd**	**7.10dd**	**8.57d**	**---**
	J = 9.1	J = 9.1	J = 6.6		J = 8.0	J = 8.0	J = 5.1	J = 5.1	
		J = 6.6				J =7.6	J = 7.6		
$B(OR)_2$	**8.76d**	**7.26dd**	**7.46d**	**---**	**8.32d**	**7.72dd**	**7.14dd**	**8.59d**	**1.38s,4CH_3**
	J = 8.9	J = 8.9	J = 6.6		J = 7.9	J = 7.7	J = 4.9	J = 4.9	
		J = 6.6				J =7.7	J = 7.5		
2-PyCO	**8.01d**	**7.10 dd**	**6.95dd**	**8.65dd**	**8.40d**	**7.92dd**	**7.98**	**---**	**8.73d,$H^{6''}$**
	J = 9.0	J = 9.0	J = 6.9	J = 6.9	J = 7.6	J = 7.6	J = 7.7		**8.01d,$H^{3''}$**
		J = 6.0	J = 6.0			J = 7.7			**7.85dd,$H^{4''}$**
									7.47dd,$H^{5''}$
CH_3CO	**8.71d**	**7.46dd**	**7.10ddd**	**8.80d**	**8.55dd**	**7.95m**	**7.95m**	**---**	**2.87s,CH_3**
	J = 9.0	J = 9.0	J = 6.9	J = 6.9	J = 6.9 J = 2.4				
		J = 6.9	J = 6.9						
			J = 1.2						
I	**8.61d**	**7.43dd**	**7.07dd**	**8.76d**	**8.29d**	**7.38dd**	**7.61d**	**---**	**---**
	J = 9.0	J = 9.0	J = 6.9	J = 6.9	J = 7.8	J = 7.8	J = 7.8		
		J = 6.9	J = 6.9			J = 7.8			
Cl	**8.66d**	**7.40ddd**	**7.04dd**	**8.72d**	**8.22d**	**7.70dd**	**7.19dd**	**---**	**---**
	J = 9.0	J = 8.7	J = 6.9	J = 6.9	J = 7.8	J = 7.8	J = 7.8		
		J = 6.9	J = 6.9			J = 7.8	J = 0.6		
		J = 0.9	J = 1.2						
Br	**8.65d**	**7.43dd**	**7.07dd**	**8.75d**	**8.28d**	**7.63dd**	**7.37d**	**---**	**---**
	J = 9.0	J = 9.0	J = 7.2	J = 6.9	J = 7.8	J = 7.8	J = 8.1		
		J = 6.9	J = 6.6			J =7.8			
***p*-H_3COPh**	**8.61d**	**7.43dd**	**7.34dd**	**8.70d**	**8.19d**	**7.76dd**	**7.56d**	**---**	**7.98d,2H**
	J = 9.0	J = 9.0	J = 6.9	J = 6.9	J = 7.8	J = 7.8	J = 7.8		**6.99d,2H**
		J = 6.9	J = 6.9			J = 7.8			**3.9,OCH_3**

From a more deep analysis of NMR structure and coupling constants compared to the triazolopyridines and the pyridines, not only $J_{H6\text{-}H7}$ vs $J_{H5'\text{-}H6'}$ became characteristic but also $J_{H4\text{-}H5}$ vs $J_{H3'\text{-}H4'}$ and the chemical shift position can be used to determine whether the system is presented as an **A structure**, a **B structure** or a mixture of both (**Figure I-7**).

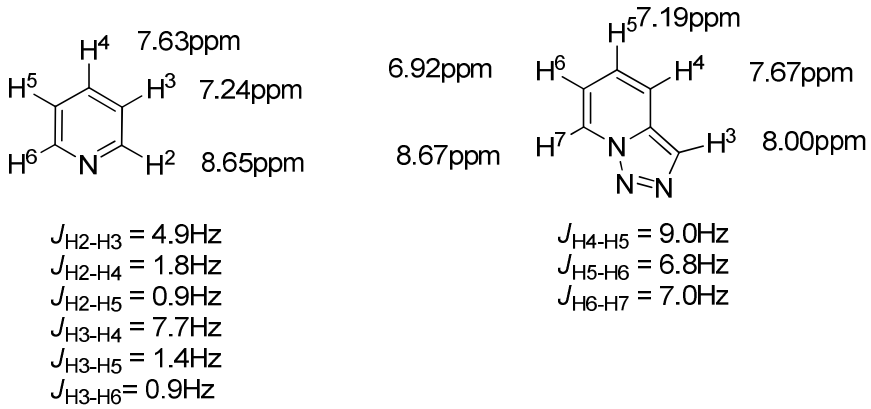

Figure I-7: ^{1}H-NMR analysis.

With the deuterated compound, the ^{1}H-NMR was exactly the same as the starting triazolopyridine-pyridine. The differences were observed in the integration of the corresponding signal. The H^{7} and $H^{6'}$ signals had a relative integration of 0.5 hydrogen atoms each one, which means a 50% **A** and 50% **B** mixture if we consider the metalation as a quantitative process. Finally, the ratio between structures **A** and **B** seemed to be dependent on the nature of the R substituent. The **A** structure being the favorized one with electron-donor systems, like TMS or $B(OR)_2$, and the **B** structure is favorized with halogens, ketones and aldehydes (typical electron-accepting substituents). Mixtures were observed only with deuterium and methyl substituents.

In parallel, Elguero and Alkorta[72] investigated this process from a theoretical point of view and performed DFT calculations. First of all, they analysed the possible intermediate states and established the isomerisation mechanism. They explained why one structure (**A** or **B**) can be favoured when R is not a deuterium or hydrogen atom. Non-substituted triazolopyridine-pyridine (R = H) was first studied. This system is degenerated as structure **A** is exactly the same as structure **B**. The starting state M corresponds to the *anti* (N^{2}-Npy) structure which opens towards state R14 without previous rotation of the triazolopyridine-pyridine bond, or applying a 180° rotation to obtain intermediate R12 and the ring-opening to provide a symmetric intermediate R13. The rotation of R14 can provide R13 or the most energetic intermediate state R15 (**Scheme I-55**).

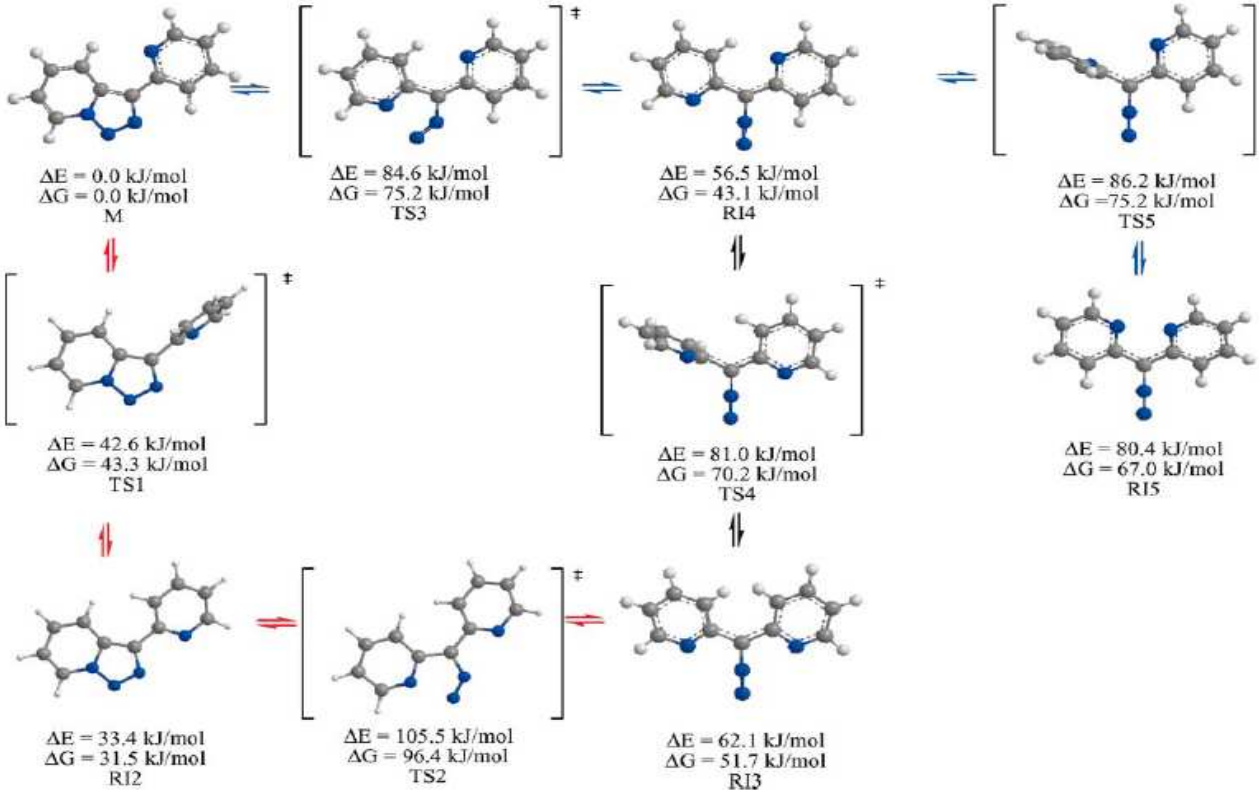

Scheme I-55: Isomerization mechanism.

Energies of these intermediates (R_X) and transition states (TS_X) are represented in the following graphic (**Figure I-8**).

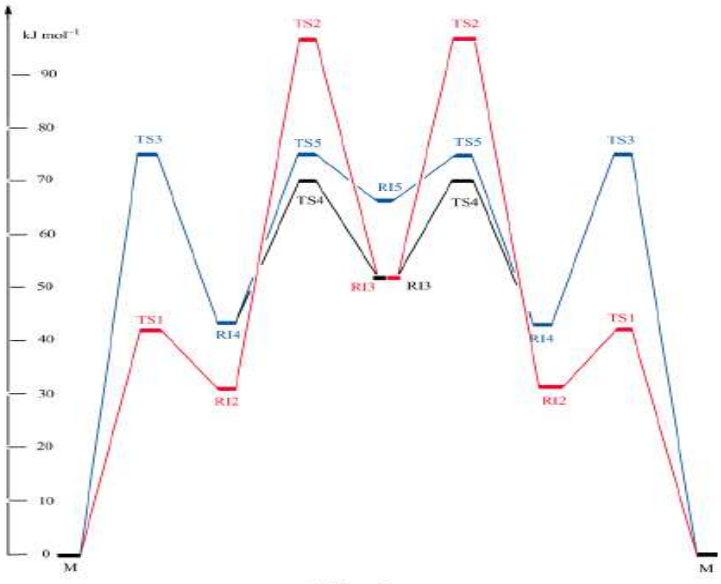

Figure I-8: Electronic profile of the isomerisation.

Actually, three different routes (red, blue and black lines) can be proposed for the isomerisation from A to B. However, they are different from an energetic point of view: TS2 is the most energetic transition state, corresponding to a ring(M)-ring(R12)-chain(R13)-ring(R12)-

ring(M) pathway (red lines). On the other hand, the black and blue pathways correspond to a ring(M)-chain(R14)-chain(R14 or R13)-chain(R14)-ring(M) isomerisation where the highest energy associated to a transition state is around 75 kjmol^{-1}. This low barrier can explain the mixture obtained in solution with deuterium and with a methyl group. In order to study the distribution of the **A**/**B** structures, other calculations with different R-substituted triazolopyridine-pyridines were performed (**Table I-4**).

Table I-4: Calculated energetic differences between A and B structures for different R.

Entry	R =	DE (kjmol^{-1})	Predicted Structure	Experimental Structure
1	NO_2	-53.8	B	
2	F	-40.7	B	
3	Cl	-30.5	B	B
4	Br	-30.5	B	B
5	OCH_3	-22.0	B	
6	CN	-18.8	B	
7	OH	-17.9	B	
8	$N(CH_3)_2$	-17.8	B	
9	$COCH_3$	-14.0	B	B
10	NH_2	-4.9	A and B	
11	^{t}Bu	-4.3	A and B	
12	H	0	A and B	A and B
13	CH_3	6.4	A and B	A and B
14	SiH_3	15.1	A	
15	$Si(CH_3)_3$	20.7	A	A
16	$B(OH)_2$	29.2	A	A

These results were compared with the experimental observations. All synthesized compounds having a negative calculated energy isomerised towards structure **B**. On the other hand, all compounds (R = TMS and R= $B(OH)_2$) with positive calculated energy exist exclusively as structure **A**. According to calculations, when R = CH_3, the corresponding structure should exist as both forms with a ratio **A**/**B** = 93:7. Experimentally, this ratio was found to be 75:25. Therefore, calculated values give an acceptable approximation of experimental results and predict that structure **A** is the major isomer for R= CH_3. On the other hand, the analysis of these values showed that the electronic properties of the R substituents mainly contribute to the modification of the equilibrium.

This can be clearly seen if we observe intermediate R13. In this case the most electron-rich nitrogen atom (*i.e.* most nucleophilic one) will undergo the triazol ring formation (**Figure I-9**):

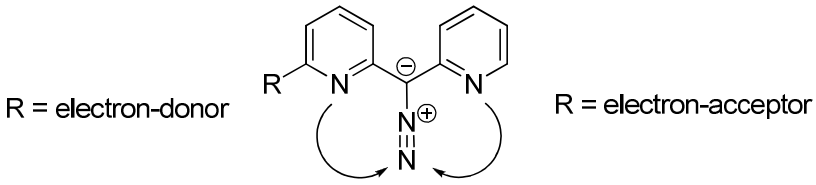

Figure I-9: R13 intermediate state.

Very recently, a new theoretical study on the ring chain isomerism has been performed[42] by Blanco *et al.* in [1,2,3]triazolo[1.5-*a*]pyridine, and revealed how this ring chain isomerisation also affects metalation, ring opening reactions and protonations.

1.6 Applications of triazolopyridines

For many years, research was directed towards the understanding of the reactivity of [1,2,3]triazolo[1,5-*a*]pyridine derivatives. The chemistry of these compounds was intensively studied and it allows now to design complex structures with many applications in several fields which are still under investigation.

1.6.1 Coordination chemistry

Although the coordination chemistry of triazolopyridines used as polynitrogenated ligands is quite young, some examples of metallic complexes of these compounds are already described. They exhibited interesting properties, for example in fluorescence. In addition, spin crossover materials or molecular magnetism are just some promising applications resulting from the properties of triazolopyridines.

In 1996 , 2-(3-methyl-[1,2,3]triazolo[1,5-*a*]pyridinium) acetate (mpta) was crystallized in presence of copper (II)[73]. The resulting complex, $[Cu(mtpa)_2(NO_3)_2]$ has a copper in an octahedral geometry without coordination with the N^1 atom from the triazolo ring (**Figure I-10**):

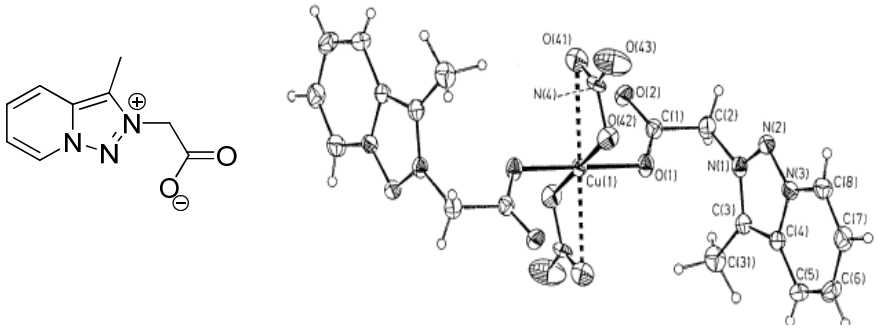

Figure I-10: 2-(3-methyl-[1,2,3]triazolo[1,5-*a*]pyridinium) acetate (mtpa) copper complex

In 1999 , Abarca *et al* obtained another Cu(II) complex but with participation of the triazolopyridine N^2 nitrogen atom, using 3-methyltriazolopyridine[74] as ligand (**Figure I-11**).

Recently, ruthenium complexes with bipyridines and triazolopyridines have been reported by Fithcetl *et al.*[75]

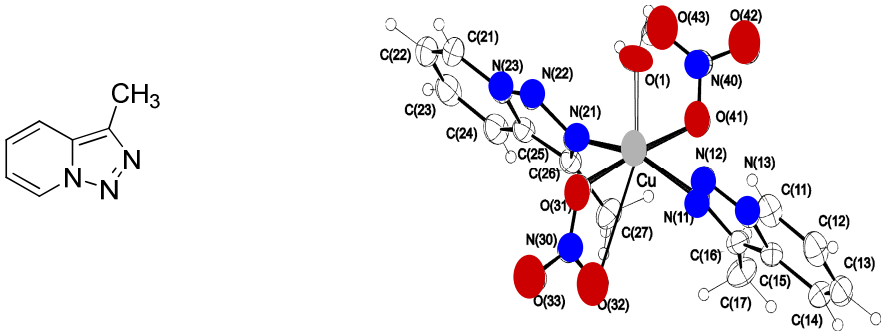

Figure I-11: 3-methyl-[1,2,3]triazolo[1,5-*a*]pyridine copper complex.

Bataglya *et al.* reported on the preparation of triazolopyridine-pyridine complexes with Cu(II) and Co(II).[12]. Abarca *et al.* crystallized different iron complexes (**Figure I-12**) that showed interesting magnetic properties[76] like spin-crossover and quantitative light-induced excited spin-state trapping (CLIESST effect). Very recently, this system has been restudied[77] by Sheu *et al*.

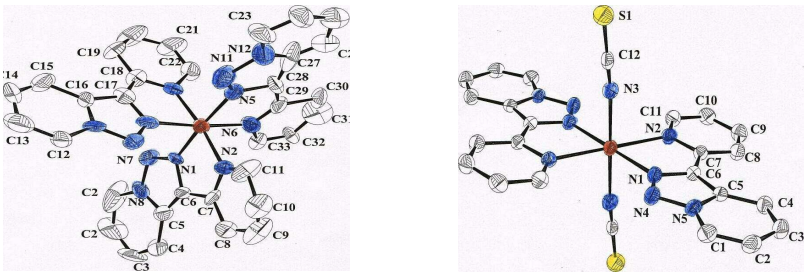

Figure I-12: 3-Pyridyl-[1,2,3]triazolo[1,5-*a*]pyridine iron complexes.

They also reported on the synthesis and magnetic properties of tetranuclear copper[78] cubane (**Figure I-13**).

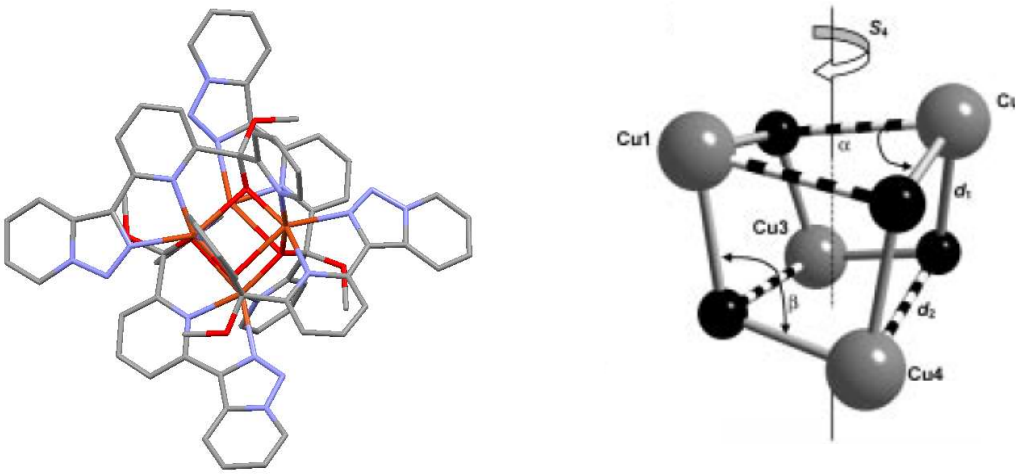

Figure I-13:Tetranuclear copper cubane.

1.6.2 Fluorescent properties

Recently, *Abarca et al.* published a new zinc/anion sensor based on the electronic and fluorescent properties of triazolopyridines. This system [79, 80] used the triazolopyridine ring as a fluorophore (**Figure I-14**).

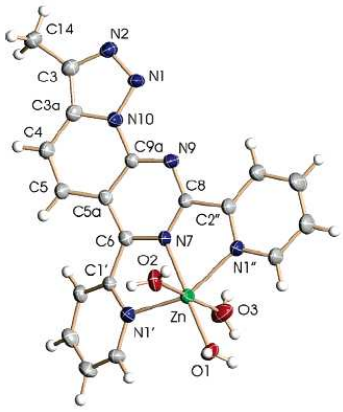

Figure I-14: Fluorescent sensor containing a triazolopyridine as fluorophore

The system is able to detect nitrites in presence of nitrates and dicarboxylic amino acids. The electron density of the triazolopyridine is responsible for the fluorescent properties; when the triazole ring was opened all fluorescent properties disappear.

The fluorescent properties of triazolopyridines was studied in detail by Abarca, Ballesteros and García-España.[81] By means of Suzuki reactions, different triazolopyridine-heterocycles were prepared in order to evaluate the quantum yields of these compounds without metal coordination. They were prepared by means of Suzuki-Miyaura cross coupling with halotriazolopyridines (**Scheme I-56**).

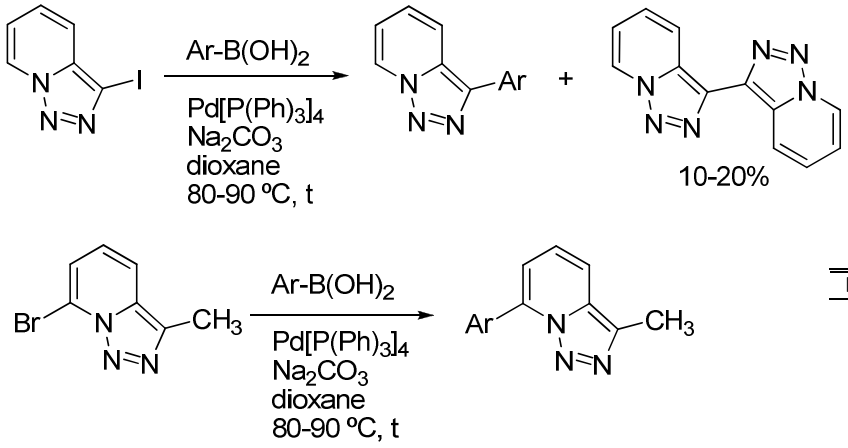

Entry	3-Ar	Time	Yield
1	C_6H_5	24h	54%
2	*p*-$H_3COC_6H_4$	20h	76%
3	*p*-$H_3CC_6H_4$	24h	62%
4	*m*-$H_3CC_6H_4$	20h	81%
5	*o*-$H_3CC_6H_4$	24h	62%
6	*p*-BrC_6H_4	18h	68%
7	3-pyridyl	24h	46%
8	6-fluor-3-pyridyl	24h	61%
9	6-chloro-3-pyridyl	24h	26%
10	2-furyl	26h	27%

Entry	7-Ar	Time	Yield
1	C_6H_5	24h	96%
2	*p*-$H_3COC_6H_4$	20h	66%
3	*p*-$H_3CC_6H_4$	24h	76%
4	*m*-$H_3CC_6H_4$	20h	80%
5	*o*-$H_3CC_6H_4$	24h	60%
6	*p*-BrC_6H_4	18h	70%
7	3-pyridyl	24h	52%

Scheme I-56: Preparation of fluorescent derivatives,

1.6.3 Synthesis of potential polynitrogenated ligands

Abarca and Ballesteros also developed a "lego methodology"[14] to obtain poly-pyridyl-ketone ligands using the chemistry of triazolopyridines. After metalation and trapping with ethyl picolinate, 2-pyridyl ketones were obtained. These compounds were again transformed in new triazolopyridines with tosylhydrazine/NaOH, providing a new triazolopyridine ready to be metalated. Finally, after successive metalation/trapping/triazol formation, all triazole rings were opened with selenium (IV) oxide to provide the corresponding oligocarbonylpyridines (**Scheme I-57**).

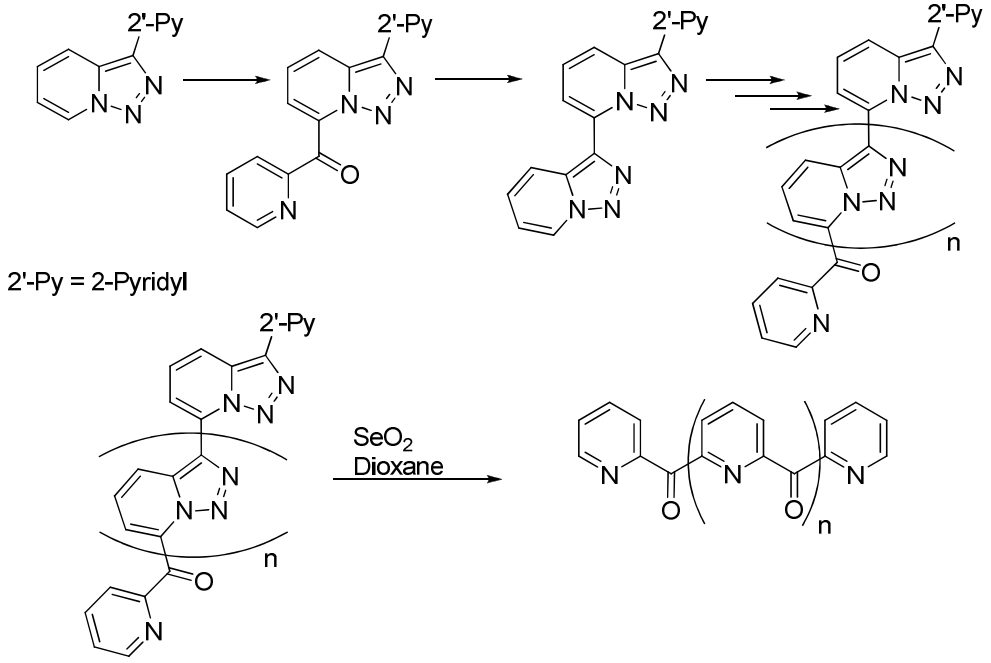

Scheme I-57: Preparation of polynitrogenated ligands.

In a similar way, triazolopyridines were metalated and trapped with diethyl pyridine-2,6-dicarboxylate and then submitted to a ring opening reaction with selenium(IV)oxide, to provide similar structures (**Scheme I-58**):

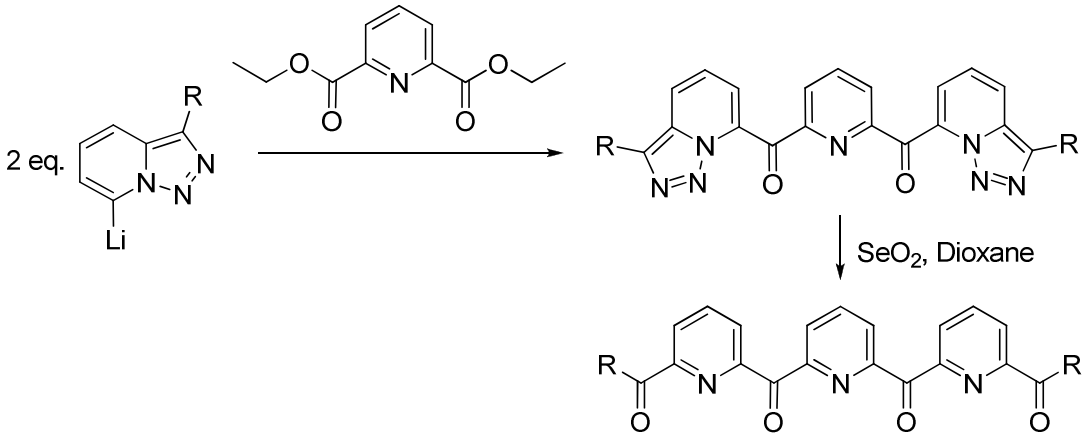

Scheme I-58: Preparation of polynitrogenated ligands using diethyl pyridine-2,6-dicarboxylate.

Abarca and Boodalis used these structures to obtain metallic clusters with interesting magnetic properties[82-85]. For example, they prepared the second biggest Co cluster ever synthesized using Py(CO)Py(CO)Py as ligand [82] (**Figure I-15**).

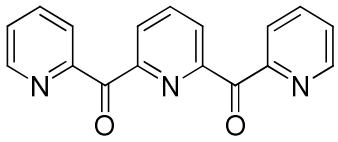

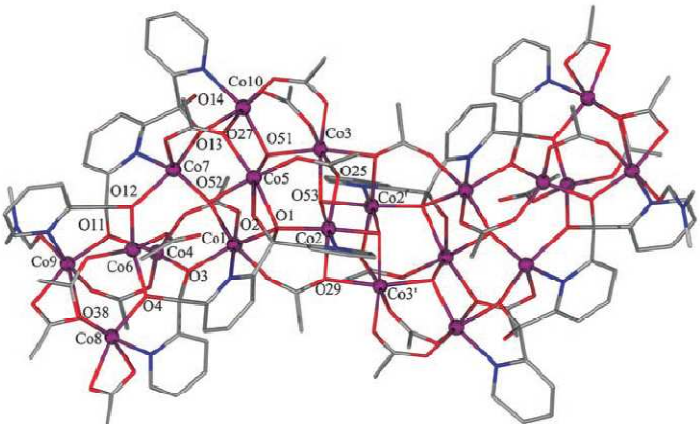

Figure I-15: Cluster including 20 cobalt atoms.

Or a nickel cluster[84], presenting a helical disposition of the Ni atoms (**Figure I-16**).

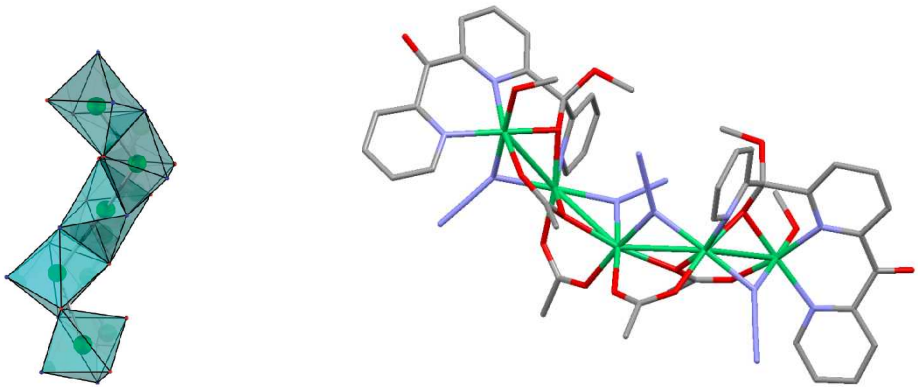

Figure I-16: Cluster including 5 nickel atoms in a pseudo-helical disposition.

1.7 References

[1] W. L. Mosby, *Chem. Heterocycl. Compd.* **1961**, 1411.
[2] G. Jones, D. R. Sliskovic, *Adv. Heterocyclic. Chem.* **1983**, 79.
[3] S. W. Schneller, *Comp. Heterocycl. Chem. 1st edn.* **1984**, *5*, 887.
[4] D. R. Sliskovic, *Comp. Heterocycl. Chem. 2nd edn.* **1996**, *8*, 383.
[5] G. Jones, *Adv. Heterocyclic. Chem.* **2002**, 1.
[6] B. Abarca-González, *J. Enzyme Inhib. Med. Chem.* **2002**, *17*, 359.
[7] J. H. Boyer, R. Borgers, L. T. Wolford, *J. Am. Chem. Soc.* **1957**, *79*, 678.
[8] C. Mayor, C. Wentrup, *J. Am. Chem. Soc.* **1975**, *97*, 7467.
[9] J. D. Bower, G. R. Ramage, *J. Chem. Soc.* **1957**, 4506.
[10] G. Jones, D. R. Sliskovic, *J. Chem. Soc., Perkin Trans. 1* **1982**, 967.
[11] G. Jones, D. J. Mouat, D. J. Tonkinson, *J. Chem. Soc., Perkin Trans. 1* **1985**, 2719.
[12] L. P. Bataglia, M. Carcelli, F. Ferraro, L. Mavilla, C. Pilizzi, G. Pilizzi, *Dalton Trans.* **1994**, 2615.
[13] J. H. Boyer, N. Goebel, *J. Org. Chem.* **1960**, 304.
[14] B. Abarca, R. Ballesteros, M. Elmasnaouy, *Tetrahedron* **1998**, *54*, 15287.
[15] B. Abarca, D. J. Hayles, G. Jones, D. R. Sliskovic, *J. Chem. Res. (S)* **1983**, 1341.
[16] G. Jones, M. A. Pitman, E. Lunt, D. J. Lythgoe, B. Abarca, R. Ballesteros, M. Elmasnaouy, *Tetrahedron* **1997**, *53*, 8257.
[17] H. Reimlinger, F. Billian, M. Peiren, *Chem. Ber.* **1964**, 339.
[18] M. Regitz, A. Liedhegener, *Chem. Ber.* **1966**, 2918.
[19] M. Regitz, A. Liedhegener, *Angew. Chem.* **1965**, 428.
[20] G. Jones, D. J. Mouat, M. A. Pitman, E. Lunt, D. J. Lythgoe, *Tetrahedron* **1995**, *51*, 10969.
[21] H. Balli, R. Loew, V. Mueller, H. Rempfler, A. Sezen-Gezgin, *Helv. Chim. Acta* **1978**, *61*, 97.
[22] H. J. Monteiro, *Synth. Commun* **1987**, 983.
[23] M. Regitz, W. Anschütz, *Chem. Ber.* **1969**, *12*, 481.
[24] Y. Tamura, J. H. Kim, Y. Miki, H. Hayashi, M. Ikeda, *J. Heterocycl. Chem.* **1975**, 481.
[25] J. H. Boyer, L. T. Wolford, *J. Am. Chem. Soc.* **1958**, 2741.
[26] G. Jones, D. R. Sliskovic, B. Foster, J. Rogers, A. K. Smith, M. Y. Wong, A. C. Yarham, *J. Chem. Soc., Perkin Trans. 1* **1981**, 78
[27] W. L. F. Armarego, *J. Chem. Soc.* **1965**, 2778.
[28] A. Asensio, B. Abarca, G. Jones, M. B. Hursthouse, K. M. Abdul Malik, *Tetrahedron* **1993**, *49*, 703.
[29] G. Jones, C. M. Richardson, P. C. Yates, G. Hajós, G. Timari, *Tetrahedron* **1993**, *49*, 4307.
[30] L. S. Davies, G. Jones, *J. Chem. Res.* **1970**, 688.
[31] B. Abarca, R. Ballesteros, M. Elmasnaouy, *Arkivoc* **2002**, *v*, 146.
[32] C. Wentrup, *Helv. Chim. Acta* **1978**, *61*, 1755.
[33] B. Abarca, R. Aucejo, R. Ballesteros, F. Blanco, E. Garcia-Espana, *Tetrahedron Lett.* **2006**, *47*, 8101.
[34] W. D. Crow, C. Wentrup, *Tetrahedron Lett.* **1968**, *9*, 6149.
[35] C. Wentrup, *Tetrahedron* **1974**, *30*, 1301.
[36] B. Abarca, R. Ballesteros, F. Blanco, *Arkivoc* **2007**, *iv*, 297.
[37] S. Chuprakov, F. W. Hwang, V. Gevorgyan, *Angew. Chem., Int. Ed.* **2007**, *46*, 4757.
[38] S. Chuprakov, V. Gevorgyan, *Org. Lett.* **2007**, *9*, 4463.
[39] B. Abarca, R. Ballesteros, G. Rodrigo, G. Jones, J. Veciana, J. Vidal-Gancedo, *Tetrahedron* **1998**, *54*, 9785.
[40] B. Abarca, R. Ballesteros, F. Mojarred, G. Jones, D. J. Mouat, *J. Chem. Soc., Perkin Trans. 1* **1987**, 1865.
[41] B. Abarca, F. Mojarred, G. Jones, C. Phillips, N. Ng, J. Wastling, *Tetrahedron* **1988**, *44*, 3005.
[42] F. Blanco, I. Alkorta, J. Elguero, V. Cruz, B. Abarca, R. Ballesteros, *Tetrahedron* **2008**, *64*, 11150.
[43] G. Jones, D. R. Sliskovic, *Tetrahedron Lett.* **1980**, *21*, 4529.
[44] R. A. Daines, P. A. Chambers, I. Pendrak, D. R. Jakas, H. M. Sarau, J. J. Foley, D. B. Schmidt, W. D. Kingsbury, *J. Med. Chem.* **1993**, *36*, 3321.
[45] G. Jones, D. J. Mouat, M. A. Pitman, *Tetrahedron* **1995**, *51*, 10969.
[46] G. Bentabed-Ababsa, F. Blanco, A. Derdour, F. Mongin, F. Trecourt, G. Queguiner, R. Ballesteros, B. Abarca, *J. Org. Chem.* **2009**, *74*, 163.
[47] B. Abarca, R. Ballesteros, G. Jones, F. Mojarrad, *Tetrahedron Lett.* **1986**, *27*, 3543.
[48] F. Blanco, *Ph.D. Thesis, University of Valencia* **2006**.
[49] G. Jones, M. A. Pitman, E. Lunt, D. J. Lythgoe, B. Abarca, R. Ballesteros, M. Elmasnaouy, *Tetrahedron* **1997**, *53*, 8257.
[50] A. J. Clarke, S. McNamara, O. Meth-Cohn, *Tetrahedron Lett.* **1974**, *15*, 2373.
[51] B. Abarca, R. Ballesteros, M. Elmasnaouy, *ARKIVOC* **2002**, v, 146.
[52] M. Elmasnaouy, *PhD Thesis, University of Valencia* **1999**.
[53] B. Abarca, E. Gomez-Aldaravi, G. Jones, *J. Chem. Res., (S)* **1984**, 140.
[54] G. R. Newkome, A. K. Patri, E. Holder, U. S. Schubert, *Eur. J. Org. Chem.* **2004**, 235.
[55] B. Abarca, R. Ballesteros, M. Elmasnouy, *Tetrahedron* **1999**, *55*, 12881.

[56] B. Abarca, A. Asensio, R. Ballesteros, J. Bosch, G. Jones, F. Mojarrad, M. R. Metni, C. M. Richardson, *J. Chem. Res., Synop.* **1990**, 9.

[57] B. Abarca, R. Ballesteros, F. Mojarrad, M. R. Metni, S. Garcia-Granda, E. Perez-Carreño, G. Jones, *Tetrahedron* **1991**, *47*, 5277.

[58] M. R. Metni, *Ph.D. Thesis, University of Valencia* **1991.**

[59] B. Abarca, R. Ballesteros, M. R. Metni, G. Jones, D. J. Ando, M. B. Hursthouse, *Tetrahedron Lett.* **1991**, *32*, 4977.

[60] B. Abarca, R. Ballesteros, M. R. Metni, G. Jones, *Heterocycles* **1992**, *33*, 203.

[61] B. Abarca, R. Ballesteros, G. Jones, *Heterocycles* **1993**, *35*, 851.

[62] N. Houari, *Ph.D. Thesis, Valencia University* **2000**.

[63] B. Abarca, R. Ballesteros, A. Muñoz, G. Jones, *Tetrahedron* **1996**, *52*, 10519.

[64] W. J. Linn, E. Ciganek, *J. Org. Chem.* **1969**, *34*, 2146.

[65] W. J. Linn, O. W. Webster, R. E. Benson, *J. Am. Chem. Soc.* **1965**, *87*, 3651.

[66] W. J. Linn, O. W. Webster, R. E. Benson, *J. Am. Chem. Soc.* **1963**, *85*, 2032.

[67] B. Abarca, R. Ballesteros, N. Houari, *Arkivoc* **2000**, *i*, 281.

[68] H. Plas, *Ring Transformation of Heterocycles*, Academic, London **1973**.

[69] R. Valters, *Ring-Chain Tautomerism,* Plenum, New York, NY*,* **1985**.

[70] K. N. Zelenin, V. V. Alekseev, *Khim. Geterotsikl. Soedin.* **1988**, 3.

[71] K. N. Zelenin, V. V. Alekseev, *Khim. Geterotsikl. Soedin.* **1992**, 851.

[72] B. Abarca, I. Alkorta, R. Ballesteros, F. Blanco, M. Chadlaoui, J. Elguero, F. Mojarrad, *Org. Biomol. Chem.* **2005**, *3*, 3905.

[73] J. Garcia-Lozano, M. Sanau, J.-V. Folgado, E. Escriva, S. Garcia-Granda, B. Abarca, R. Ballesteros, *Polyhedron* **1996**, *15*, 3481.

[74] R. Ballesteros, B. Abarca, A. Samadi, J. Server-Carrio, E. Escriva, *Polyhedron* **1999**, *18*, 3129.

[75] C. M. Fitchetl, F. R. Keene, C. Richardson, P. J. Steel, *Inorg. Chem. Comm.* **2008**, *11*, 595.

[76] V. Niel, A. B. Gaspar, M. C. Munoz, B. Abarca, R. Ballesteros, J. A. Real, *Inorg. Chem.* **2003**, *42*, 4782.

[77] C.-F. Sheu, K. Chen, S.-M. Chen, Y.-S. Wen, G.-H. Lee, J.-M. Chen, J.-F. Lee, B.-M. Cheng, H.-S. Sheu, N. Yasuda, Y. Ozawa, K. Toriumi, Y. Wang, *Chem. Eur. J.* **2009**, *15*, 2384.

[78] B. Abarca, R. Ballesteros, M. Chadlaoui, C. Ramirez de Arellano, J. A. Real, *Eur. J. Inorg. Chem.* **2007**, 4574.

[79] B. Abarca, R. Aucejo, R. Ballesteros, M. Chadlaoui, E. Garcia-Espana, C. Ramirez de Arellano, *ARKIVOC.* **2005**, *xiv*, 71.

[80] M. Chadlaoui, B. Abarca, R. Ballesteros, C. RamirezdeArellano, J. Aguilar, R. Aucejo, E. Garcia-Espana, *J. Org. Chem.* **2006**, *71*, 9030.

[81] B. Abarca, R. Aucejo, R. Ballesteros, F. Blanco, E. García-España, *Tetrahedron Lett.* **2006**, *47*, 8101.

[82] A. K. Boudalis, C. P. Raptopoulou, B. Abarca, R. Ballesteros, M. Chadlaoui, J.-P. Tuchagues, A. Terzis, *Angew. Chem., Int. Ed.* **2006**, *45*, 432.

[83] A. K. Boudalis, C. P. Raptopoulou, V. Psycharis, Y. Sanakis, B. Abarca, R. Ballesteros, M. Chadlaoui, *Dalton Trans.* **2007**, 3582.

[84] K. Boudalis Athanassios, M. Pissas, P. Raptopoulou Catherine, V. Psycharis, B. Abarca, R. Ballesteros, *Inorg. Chem.* **2008**, *47*, 10674.

[85] A. N. Georgopoulou, C. P. Raptopoulou, V. Psycharis, R. Ballesteros, B. Abarca, A. K. Boudalis, *Inorg. Chem.* **2009**, *48*, 3167.

II: Chiral Triazolopyridines: Towards chiral 2,6-disubstituted pyridines

2.1 Introduction and objectives

The pyridine ring can be found as structural motif in a large number of chiral ligands used in asymmetric catalysis[1] or in molecular recognition chemistry.[2] Many of these structures are 2,6-disubstituted or 2-substituted pyridines. It had been already showed that [1,2,3]triazolo[1,5-*a*]pyridines can be regioselectively metalated[3] at C^7 (*See Chapter 1, Part 1.3.2*) and can undergo a ring opening reaction to form polysubstituted pyridines[4, 5] (*See Chapter 1, Part 1.3.4*). In this way, triazolopyridines can be considered as a turntable towards these structures. However, no chiral [1,2,3]triazolo[1,5-*a*]pyridine has been reported until now. Their preparation should be possible by trapping the 7-lithiumtriazolopyridine intermediates with a chiral electrophile (**Figure II-1**).

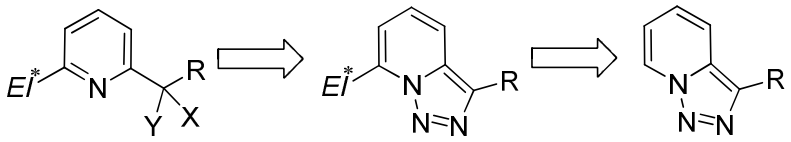

Figure II-1: Towards chiral 2,6-disubstituted pyridines

Furthermore, it would be interesting to study if a chiral induction could be reached after performing the triazole ring opening reaction. Depending on the chosen conditions, the ring opening could lead to a mixture of diastereoisomers, (for example, by heating a chiral triazolopyridine in acetic acid (**Figure II-1**, X = H, Y = $OCOCH_3$) or sulfuric acid (**Figure II-1**, X = H, Y = OH). Our studies focused on:

- The preparation of the first chiral-triazolopyridine family by means of metalation and trapping with chiral electrophiles.
- The preparation of chiral 2,6-disubstituted pyridines and the study of the possible chiral induction on the triazole ring opening.
- The study of the **A**/**B**-isomerism through the preparation of chiral triazolopyridine-pyridine ligands due to its interesting coordinating properties.

2.2 Selection of the starting compounds

The generation of an asymmetric carbon atom by ring opening reaction of a non chiral triazolopyridine was already known.[4] We focused our attention on two triazolopyridine **1a** and **1b** as starting molecules (**Figure II-2**) for three important reasons. First, both compounds provide chiral compounds (as a racemic mixture) when the triazolo-ring is opened with sulfuric acid for example. Secondly, as shown in chapter 1 (section 1.4) compound **1b** can provide different structures depending on the electronic properties of the attached substituent. Third, compound **1b** has interesting fluorescent[6] behaviour; its derivatives (especially under the **B** form) could lead to tridentate fluorescent ligands. In our particular case, the introduction of a chiral substituent will provided suitable molecules for the enantio-discrimination by means of fluorescence spectroscopy.

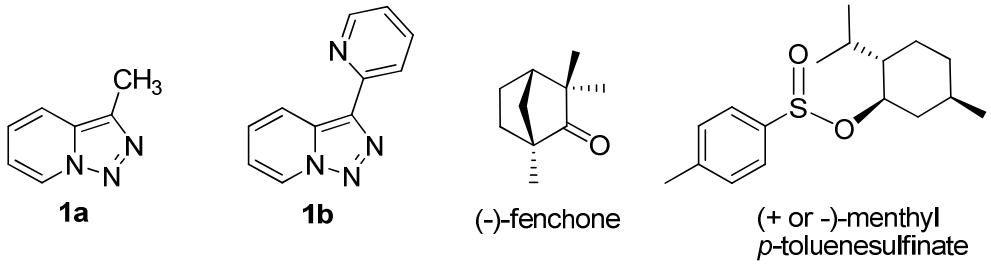

Figure II-2: Starting triazolopyridines **1a** and **1b** and chiral compounds.

In order to introduce a chiral centre into the triazolopyridine moiety, we needed to find two commercially available chiral compounds able to react with the 7-lithium derivate from **1a** and **1b**. With the aim to prepare two different chiral families we selected a terpenoic ketone, (-)-fenchone, and (+ or -) menthyl *p*-toluenesulfinate. In the literature many pyridine derivatives from terpenic ketones (camphor, menthone, fenchone...) have been proposed as chiral ligands for catalysis by Chelucci[1], Genov[7] *et al.* and Kwong[8, 9] *et al.* (**Figure II-3**).

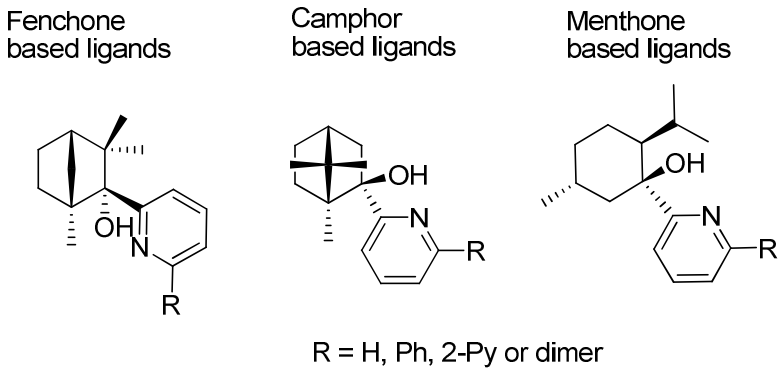

Figure II-3: Chiral compounds from terpenoic ketones.

We selected (-)-fenchone as chiral compound in order to avoid possible enolization side reactions. As second chiral compound we were interested in (+ or -) menthyl *p*-toluenesulfinate. Sulfoxides from heterocyclic aromatic compounds are present in many

important drugs.[10, 11] *Omeprazole*[12] derivatives (**Figure II-3**) like *Nexium*© (S_s enantiomer of *omeprazole*) is one of the most important commercial drugs containing sulfoxides. Furthermore, sulfoxides have a double synthetic interest, Its use as chiral inductor in asymmetric synthesis has been reported,[13-15]and, although the use of chiral S-based ligand in catalysis seems to be underdeveloped, its applications had been recently reviewed.[15, 16] In addition there is a growing interest in this kind of ligands, for example the White ligand for C-H activation[17, 18] is a very recent example of a successful sulfoxide-based commercial compound(**Figure II-4**).

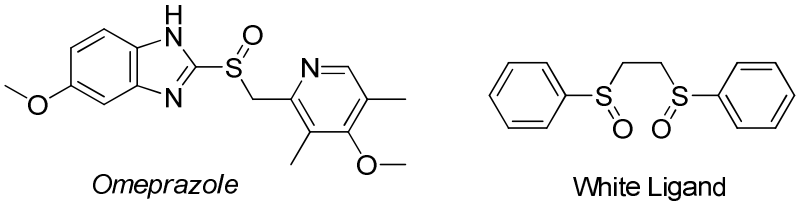

Figure II-4: Important sulfoxide-based compounds.

2.3 Preparation of the first chiral triazolopyridines

3-Methyl[1,2,3]triazolo[1,5-*a*]pyridine (**1a**) was metalated at -40 °C in toluene with butyllithium during 2 hours before (-)-fenchone was added, providing the corresponding alcohol **2** in a yield of 88% (**Scheme II-1**). This reaction can be performed on gram scale.

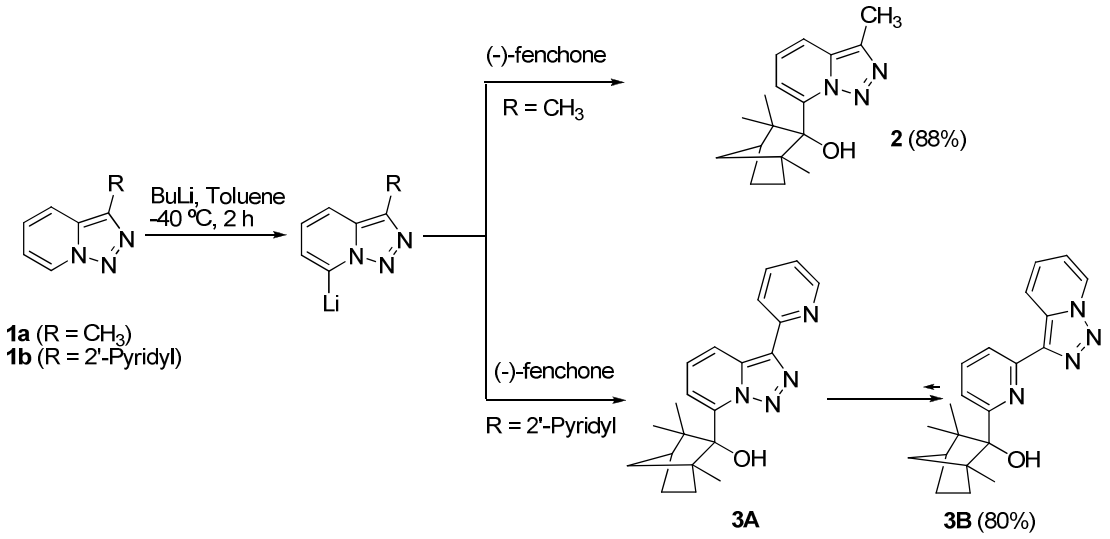

Scheme II-1: Preparation of chiral alcohols **2** and **3B.**

Similarly, starting from 3-(2'-pyridyl)[1,2,3]triazolo[1,5-*a*]pyridine (**1b**), compound **3A** was obtained but isolated under its isomer form **B** enantiomeric pure. The enantioselectivity of this reaction can be explained by the steric hindrance of fenchone. According to Herrman[19] *et al.*, nucleophilic attack is favorized only on one side of the ketone (**Figure II-5**).

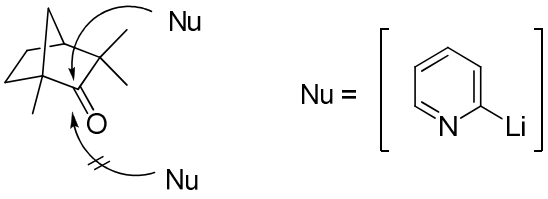

Figure II-5: Enantioselectivity of the nucleophile addition to fenchone.

We already highlighted that 7-substituted triazolopyridine pyridine can undergo a ring-chain isomerisation[20] (*See Chapter 1, Part 1.4*) according to the electron properties of the substituent. In this case, considering the electron-acceptor ability of the β-alcohol **3A,** isomerisation takes place to give **3B** in an excellent yield of 80%. The ^{1}H-NMR and H,H-COSY analysis of compound **3**, showed an aromatic four hydrogen system with typical triazolopyridine coupling constants (See chapter one, part 1.4, **figure I-7**). This indicated the presence of a **B** structure. Although no DFT calculations were performed for this compound, two main reasons could be proposed to explain the pure **B** structure.

1. The inductive effect of the alcohol combined with the other two substituents bonded to the carbon atom.

2. A possible bifurcated hydrogen bond between the pyridine nitrogen atom, the N^{2} from the triazolopyridine and the hydrogen from the alcohol (**Figure II-6**).

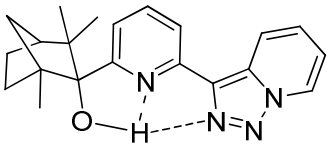

3B

Figure II-6: Possible intramolecular hydrogen bond in **3B**.

Both arguments were compatible and the conformation of the first one required DFT calculations. However if the second argument (hydrogen bond) was the most important effect, the methylation of the alcohol should provide a mixture of **A** and **B** structures or maybe pure **A** structure.

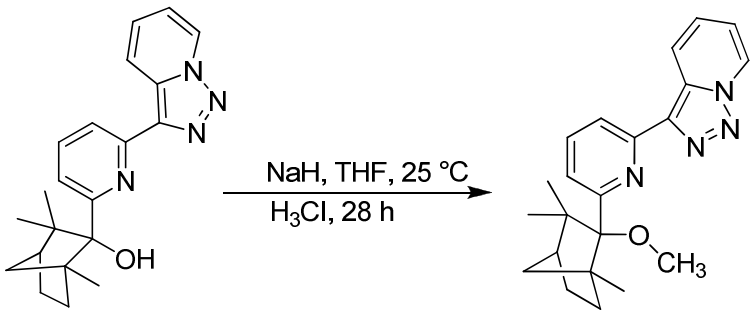

3B **4B** (95%)

Scheme II-2: Protection of compound **3**.

3-(6-(2-methoxy-1,3,3-trimethylbicyclo[2.2.1]heptan-2-yl)pyridin-2-yl)-[1,2,3]triazolo [1,5-a]pyridine (**4B**) was obtained in good yield after treatment with sodium hydride and iodomethane in tetrahydrofuran during 28 hours (**Scheme II-2**). ^{1}H-NMR analysis revaled a similar pattern to compound **3B**. The presence of a pure B structure indicated that the second argument was wrong and that inductive effects were entirely responsible for the B structure in compounds **3B** and **4B**.

The synthesis of the sulfoxide derivatives **5** and **6B** was performed using the Andersen's method.[21] Quéguiner[22] reported on the synthesis of heterocyclic sulfoxides (pyridines, diazines et pyrimidines) in acceptable yields and with excellent enantiomeric excess by trapping lithium- or magnesium-derivatives with menthyl *p*-toluenesulfinate. But under these conditions, and after trapping with the corresponding enantiopure sulfinate, (*R*)-3-methyl-7-(toluene-4-sulfinyl)-[1,2,3]triazolo-[1,5-*a*]pyridine (**5**) and (*R*)-3-[6-(toluene-4-sulfinyl)-pyridin-2-yl]-[1,2,3]-triazolo[1,5-*a*]pyridine (**6**) were unfortunately only obtained in low yields (20 % and 15%, respectively) (**Scheme II-3**). Formation of dimmers **7a** (56%) and **7b** (26%) were responsible for this result (**Figure II-4**).

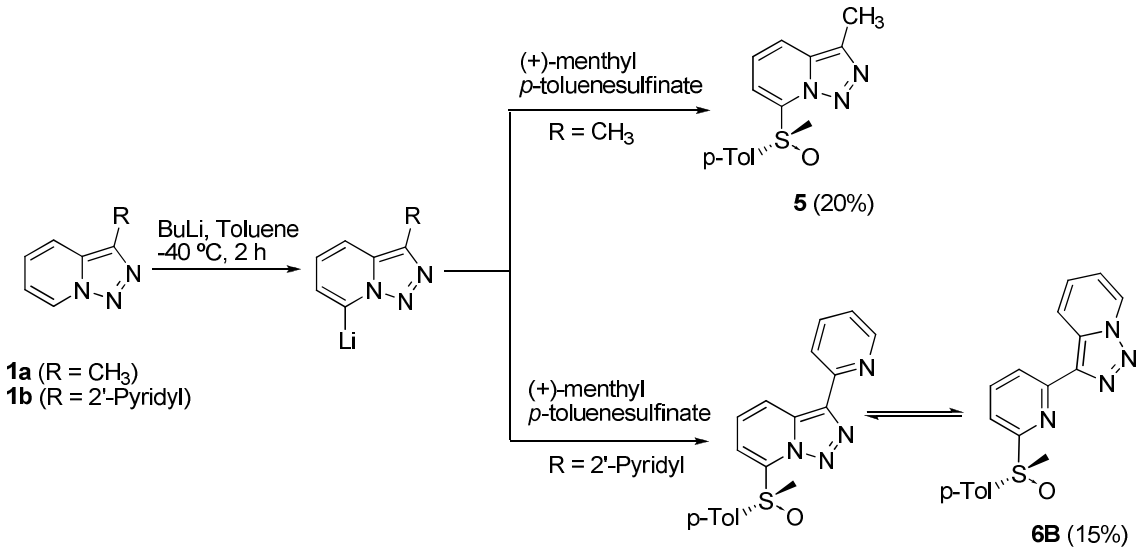

Scheme II-3: Preparation of chiral sulfoxides **5** and **6B.**

Actually, the lithiated triazolopyridine was canulated on a solution of the sulfinate, (*R*)-(+)-menthyl-*p*-toluenesulfinate. When instead inverse addition was performed, *i.e.* the electrophile was directly added into the solution of triazolopyridine at -40 °C, dimers **7a** and **7b** were obtained instead of the expected sulfoxides **5** and **6B**.

In fact, sulfoxides can be considered as a good leaving group. Moreover, the *in situ* formed triazolopyridines **5** or **6** can undergo an S_NAr reaction at C^7 by reacting with the aryllithium intermediate to give the dimers **7a** or **7b**, respectively (**Scheme II-4)**. This kind of

reactivity was already observed on pyridines in 1984 by Oae and Fukuraba[23-25] when they tried to obtain the corresponding sulfoxide from 2-bromopyridine by a similar strategy.

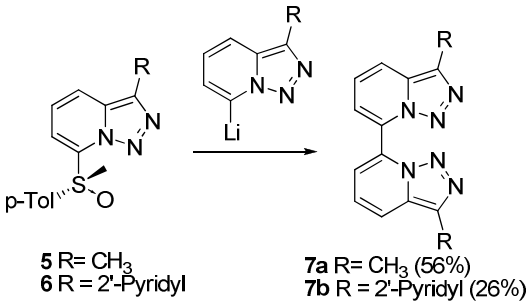

Scheme II-4: Formation of dimmers **7a** and **7b**.

Although other organometallic reagents, like magnesium ate complexes, were tested, no efficient synthesis of sulfoxides was established. Compound **6** was found to present a B structure after ^{1}H-NMR analysis. The strong electron-acceptor character of the sulfoxide are responsible of the pure **B** structure.

2.4 Catalytic sulfenation, a new methodology to prepare aromatic sulfoxides

As a consequence of the low yields obtained with chiral sulfoxides, another synthetic pathway had to be envisaged in order to prepare compounds **5** and **6** in an efficient manner and we thought that the sulfoxide moiety could be introduce *via* metal catalysed reaction. In 2006, Poli *et al.* reported on the palladium catalyzed synthesis of aryl sulfoxides.[26] These authors showed that *in situ* formed sulfenate anions[27] from β-sulfinyl esters can provide under biphasic conditions several aryl sulfoxides (**Scheme II-5**). The sulfoxides were obtained in good yields from the corresponding aryl iodides. However, the use of arylbromides was unsuccessful. On the other hand, only one heterocyclic compound (a thiophene derivative) was synthesized.

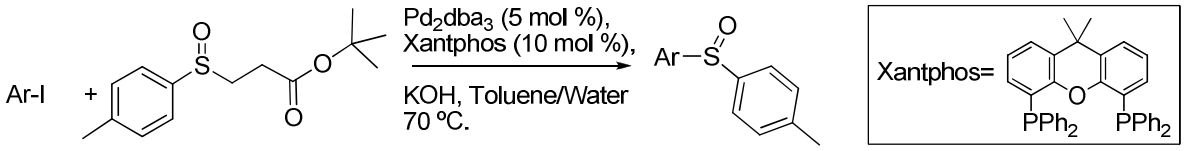

Scheme II-5: Palladium catalysed synthesis of aryl sulfoxides.

With the objective to synthesize compounds **5** and **6** in good yields, we performed a methodological study on the synthesis of heterocyclic sulfoxides by palladium-catalyzed reactions. However due to the availability and the price of iodinated heterocycles, we focused on bromo-heterocycles. Nevertheless, arylbromides are in general less reactive than their iodo analogues. Therefore, the temperature was increased from 70 °C to reflux (85 °C Toluene/Water azeotrope b.p.). Under these conditions the desired sulfoxides were obtained in good yields (**Table II-1**).

Table II-1: Preparation of heterocyclic sulfoxides.

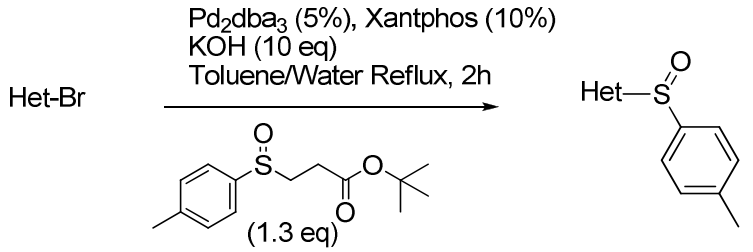

Entry	Halo-heterocycle	Product		Yield (%)
1	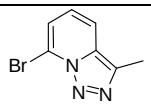	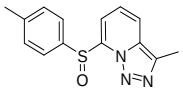	**5**	82%
2	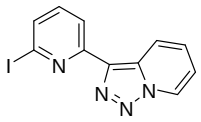	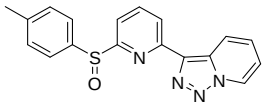	**6B**	95%
3		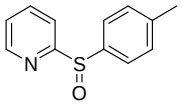	**8a**	63%
4		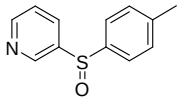	**8b**	82%
5		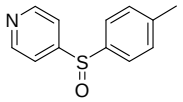	**8c**	75%
6		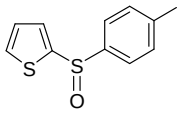	**9a**	69%
7		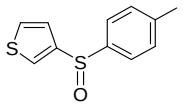	**9b**	50%
8		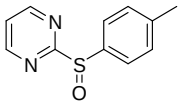	**10a**	41%
9		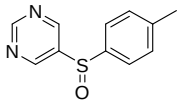	**10b**	31%
10	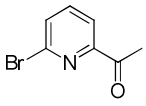	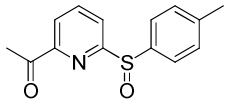	**11**	52%

Under these conditions compounds **5** and **6B** were prepared in excellent yields without traces of dimers **7a** or **7b**. Pyridine derivatives **8a**, **8b** and **8c** were obtained in good yield (**Table II-1, Entries 3-5**). In a similar way, thiophene derivatives **9a** and **9b** were prepared as well as pyrimidine derivatives **10a** and **10b**. We also noticed that the lower yields were obtained with the most π-electron deficient heterocycles (pyrimidines). Especially important was the

preparation of compound **11**, without protection of the ketone, required for the Andersen's method due to the incompatibility of classical Grignard reagents with ketones. In order to study the limitation of this C-S coupling, we performed the reaction on a family of dihalogenated pyridines (**Table II-2**).

Table II-2: Preparation of heterocyclic disulfoxides

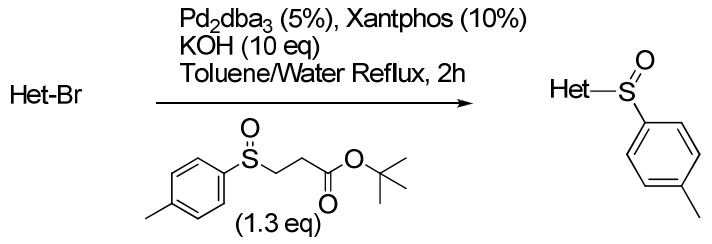

Entry	Halo-heterocycle	Product		Yield (%)
1	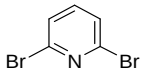	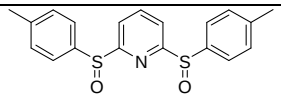	**12**	74%
2	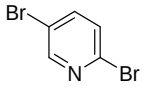	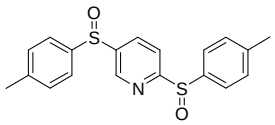	**13**	84%
3	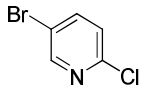	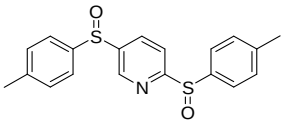	**13**	30%

The reaction provided in all cases the disulfoxides. No traces of mono-substituted pyridines were observed. 2,6-Dibromopyridine provided **12** in 74% yield and **13** in 84% yield as a mixture of dl/meso compounds in a ratio of 66:33 for **12**, and 55:45 for **13** (measured by ^{1}H-NMR). Even when one bromine atom was substituted by a chlorine atom, pyridine **13** was isolated in lower yield but without traces of mono substituted compound. However, when the reaction was performed with 3-chloropyridine, no traces of **8b** were found. This indicated that electron withdrawing groups (the first sulfoxide) favorize the insertion of the second sulfoxide. Although all compounds were obtained as a mixture of enantiomers (**5**, **6B** and **8-11**) or diastereomers (**12** and **13**) Poli[28] reported in 2007 the catalytic enantioselective synthesis by employing chiral diphosphines, with moderate enantiomeric excess (40-83%) and yield (70-80%).

2.5 Preparation of the sulfoxide-triazolopyridine family

The excellent yields obtained with the catalyzed sulfenation of triazolopyridines encouraged us to synthesize the corresponding sulfoxides on all free positions of the

triazolopyridine ring as depicted in **scheme II-6**, in order to see how the position can affect the coupling reaction.

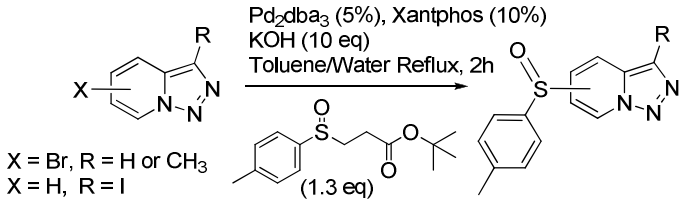

Scheme II-6: Preparation of the sulfoxide derivatives from triazolopyridines.

However, although the preparation of most of the halo-derivatives of 3-methyl[1,2,3]triazolo[1,5-*a*]pyridine (**1a**) has been previously reported (5- and 7-bromo derivatives),[20, 29-31] two of them have never been prepared (4- and 6-bromo derivatives). Two synthetic routes were then developed to obtain these new compounds in order to complete the family of halo-triazolopyridines (**Scheme II-6**). 3-Bromopyridine reacted with lithium di-*iso*-propylamide (LDA) at -78 °C in tetrahydrofuran, to provide compound **14** in a 70 % yield after trapping with trimethylsilyl chloride.[32] Compound **14** was transformed into ketone **15** by reaction with lithium tetramethylpiperidid (LiTMP) at -78 °C and trapping with *N*,*N*-dimethylacetamide in good yield (96 %). 2-Acetylpyridine **15** was directly involved in the next step without purification and was treated with hydrazine[33] and MnO_2 to give triazolopyridines **16** (20 %) and **17** (78%). These products could be separated by columm chromatography on silica gel. Desilylation of **16** to give **17** was performed in a heterogeneous system with Al_2O_3, KF in aqueous THF at reflux.[34]

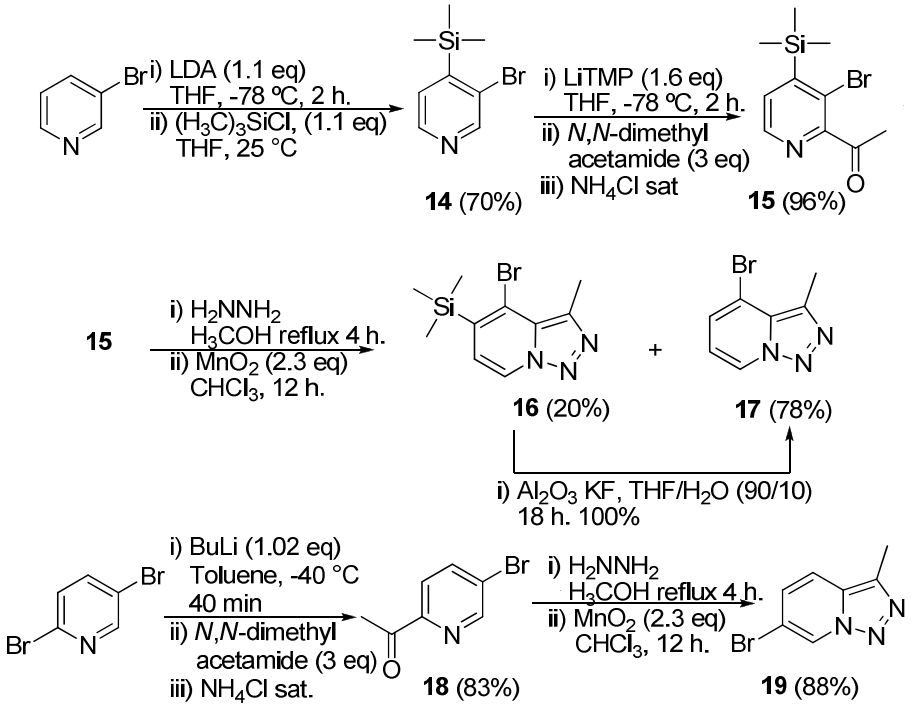

Scheme II-6: Preparation of compounds **16** and **18.**

In this way, **17** was obtained in quantitative yield. Finally, 4-bromo-3-methyl-[1,2,3]triazolo[1,5-*a*]pyridine (**17**) was obtained in eight steps on gram scale with an overall yield of 52%. In order to obtain the last 6-halotriazolopyridine, a regioselective halogen/metal exchange was performed on 2,5-dibromopyridine. As described in the literature, the bromine atom in position 2 of the pyridine reacts faster at -40 °C in toluene with butyllithium.[35] By trapping the 2-lithio derivative with *N*,*N*-dimethylacetamide, we obtained 1-(5-bromopyridin-2-yl)ethanone (**18**). After reaction with hydrazine and MnO_2, 6-bromo-3-methyl-[1,2,3]triazolo[1,5-*a*]pyridine (**19**) was formed in an excellent yield and also on multi gram scale (**Scheme II-6**). The same reaction conditions, as described before for the introducition of the sulfoxide, were applied to the new triazolopyridines (**Table II-3**).

Table II-3: Preparation of triazolopyridine sulfoxides.

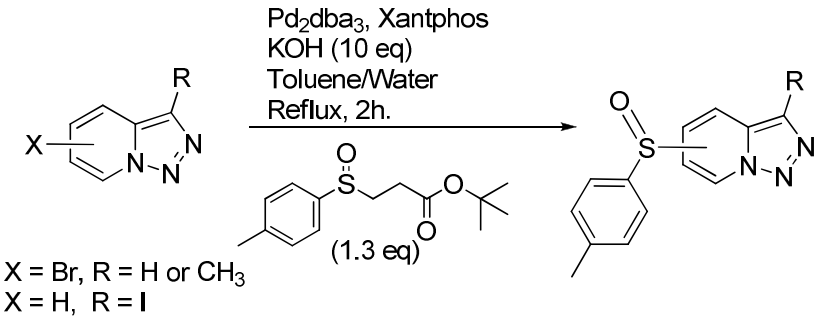

Entry	Halo-heterocycle	Product	Yield (%)
1	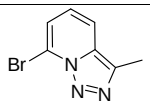	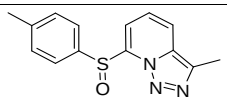 **5**	82%
2	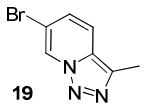 **19**	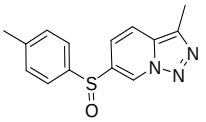 **20a**	32%
3	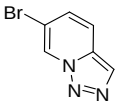	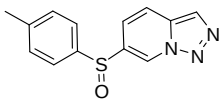 **21a**	–
4	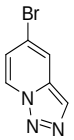	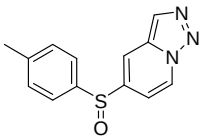 **22**	84%
5	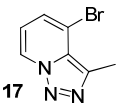 **17**	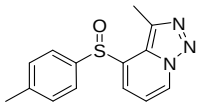 **23a**	80%
6	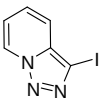	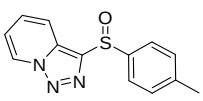 **24**	20%

The sulfoxides **5** and **22** were prepared using halotriazololopyridines where the halogen atom is located on a nucleophilic position (see chapter 1; part 1.3.3) (C^7 and C^5, **Table II-3**, entries 1 and 4) and were obtained in excellent yield. Surprisingly, 6-bromo-3-methyl-[1,2,3]triazolo[1,5-*a*]pyridine (**19**) (**Table II-3** entry 2) and 6-bromo[1,2,3]triazolo[1,5-*a*]pyridine (**Table II-3**, entry 3) do not have the same reactivity.

Sulfoxide **20a** was obtained in a low yield of 32%, mainly reduced compounds 6-(*p*-tolylthio)-3-methyl-[1,2,3]triazolo[1,5-*a*]pyridine (**20b**) and 6-(*p*-tolylthio)[1,2,3]triazolo[1,5-*a*]pyridine (**21b**) were obtained (**Figure II-7**). However, when 4-bromo-3-methyl-[1,2,3]triazolo[1,5-*a*]pyridine (**17**) was submitted to the catalityc reaction, sulfoxide **23a** was obtained in good yield of 80%. Traces of reduced product **23b** were also detected.

3-Iodo[1,2,3]triazolo[1,5-*a*]pyridine provided the sulfoxide **24** in low yield (**Table II-3**, entry 6) because of a dimerization which affords 3,3'-di[1,2,3]triazolo[1,5-*a*]pyridine (**25**) in 40% yield (**Figure II-6**). This behavior of 3-iodo-[1,2,3]triazolo[1,5-*a*]pyridine had already been observed by Abarca *et al*. in previous works concerning the preparation of fluorescent molecules.[29]

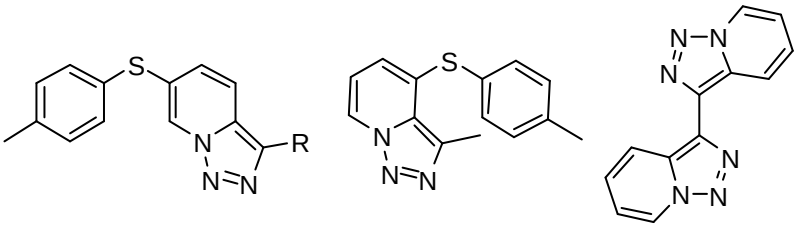

20b R = CH_3 (31%)
21b R = H (33%)

23b (traces)

25 (40%)

Figure II-7. Side products observed.

The traces of **23b** observed besides sulfoxide **23a** could be explained by considering that palladium oxidation, or phosphines (from Xantphos) oxidation could occurs and transform sulfoxide **23a** in compound **23b**. However the formation of compounds **20b** and **21b** in high quantity required other explanation. First, the reduction of sulfoxides was explained by the formation of a carbene[36, 37] and by transfer of oxygen from the sulfoxide.[38] The substitution at C^6 position by an electron-withdrawing group as sulfoxide could stabilize the diazo[39, 40] form (**Scheme II-7**).

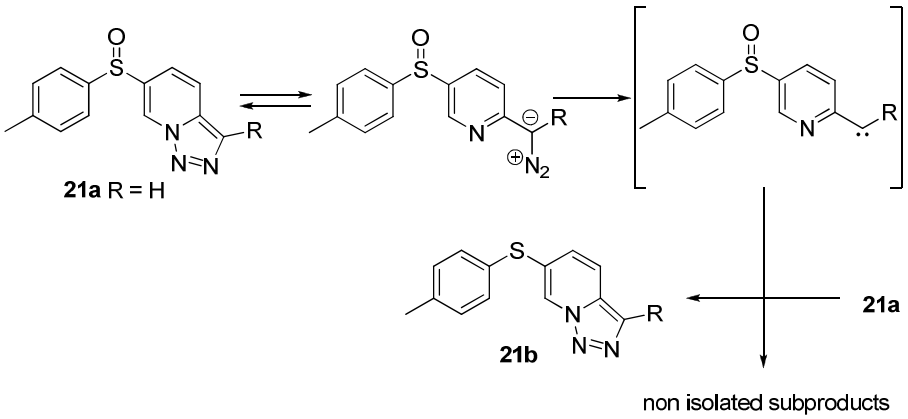

Scheme II-7: Formation of thioethers by carbenoid intermediate.

This mechanism involves an intermolecular collision between the carbene of **21a** and a second molecule of **21a**. The second mechanism involves palladium into the carbene formation and also sulfenate anion. In this mechanism, the carbene from **21a** (**Scheme II-8**) is coordinated to the palladium. Then, *in situ* sulfenate anion is transformed by the carbene into the corresponding thiolate. This thiolate undergoes the catalytic cycle providing the corresponding compounds **20b**, **21b**.

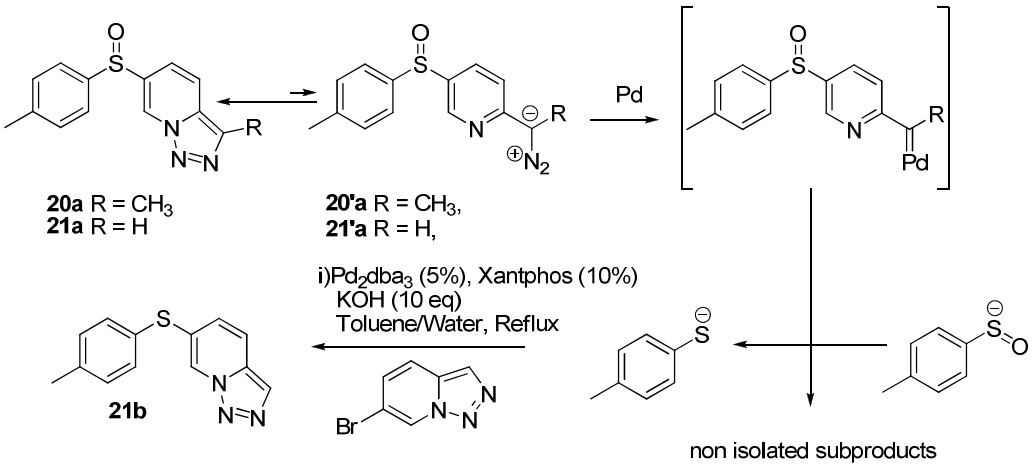

Scheme II-8: Formation of thioethers by palladium catalyzed reduction of sulfenates and catalytic sulfuration.

The catalytic sulfuration reaction was already proposed by Poli[26] as a way to obtain thioethers under exactly the same conditions as the catalytic sulfinylation (**Scheme II-8**). The thiolate could be provided by a non-catalyzed intermolecular collision between sulfenate and a carbene. All mechanisms are depicted in **Scheme II-9**.

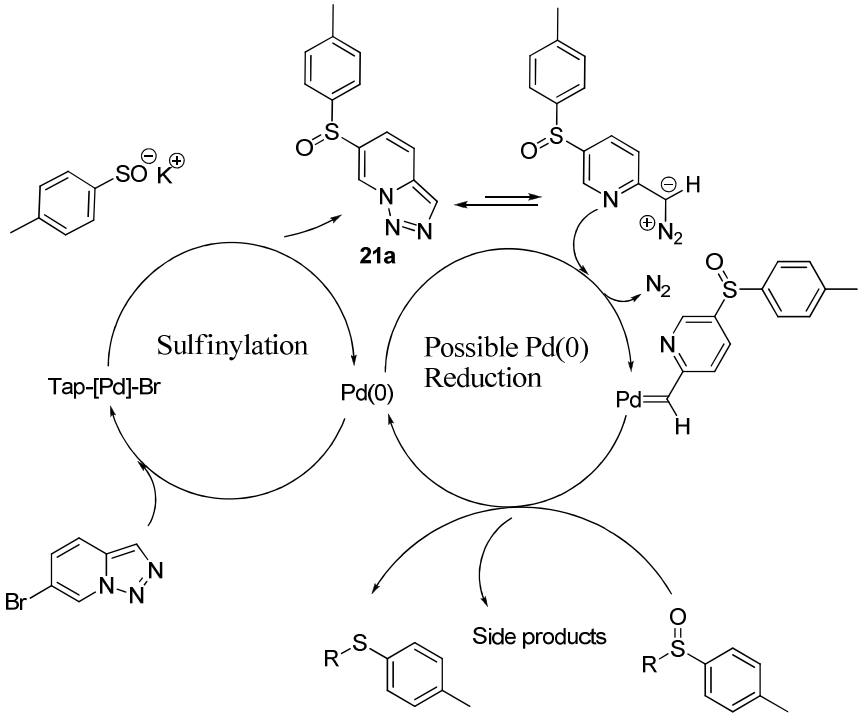

Scheme II-9: Possible mechanisms for the transformation of **21a** in **21b**. Tap = Triazolopyridine

2.6 ^{1}H-NMR table of the sulfoxide-triazolopyridine family

The ^{1}H-NMR analysis of all triazolopyridines has been performed systematically by Abarca *et al.* and it was found as a useful tool in the **A**/**B** assignation, as well as for the NMR prediction of new compounds. In order to corroborate spectral properties (chapter 1, part 1.4), we describe now ^{1}H-NMR spectra for the sulfoxides and the halogen families. Caracteristical coupling constant for the triazolopyridine ring can be found for all compounds (J_{H6-H7} near 7.0 Hz and J_{H4-H5} near 9.0 Hz).

Table II-4: ^{1}H-NMR fort the triazolopyridine-sulfoxide family and halo-triazolopyridine family

Compound	H^3	H^4	H^5	H^6	H^7	CH_3	Other signals
3CH_3 1a	**-**	**7.65 d**	**7.20 d**	**6.95 d**	**8.67 d**	**2.30**	
		J = 8.8	J = 8.8	J = 7.3	J = 7.3		
			J = 6.9	J = 6.9			
3Br	**-**	**7.60 d**	**7.27 dd**	**6.99 dd**	**8.64**	**-**	
		J = 8.9	J = 8.9	J = 7.0	J = 7.0 d		
			J = 6.7	J = 6.7			
4Br3CH_3 17	**-**	**-**	**7.33**	**6.75**	**8.59**	**2.83**	
			J = 7.0 d	J = 7.0	J = 7.0 d		
				J = 7.0			
4Br3$CH_3$5TMS 16	**-**	**-**	**-**	**6.82 d**	**8.51 d**	**2.82**	**0.42**
				J = 7.0	J = 7.0		
5Br	**8.01 s**	**7.92 s**	**-**	**7.05 d**	**8.61 d**	**-**	
				J = 7.2	J = 7.2	-	
6Br	**8.07 s**	**7.63 d**	**7.32 d**	**-**	**8.91 s**		
		J = 9.3	J = 9.3				
6Br3CH_3 19	**-**	**7.51 d**	**7.22 d**	**-**	**8.79 s**	**2.60**	
		J = 9.3	J = 9.3				
7Br3CH_3	**-**	**7.57**	**7.02 dd**	**7.14 d**	**-**	**2.58**	
		J = 8.7	J = 8.7	J = 7.2			
			J = 7.2				
7Br	**8.16 s**	**7.69 d**	**7.11 dd**	**7.20 d**	**-**	**-**	
		J = 8.6	J = 8.6	J = 7.1			
			J = 7.1				
3SO*p*Tol 24	**-**	**7.8 d**	**7.33 dd**	**7.09 t**	**8.77**		**7.69 d, 7.33 d *J* = 8.0, 2.39 s**
		J = 8.4	J = 8.4	J = 7.0	J = 7.0		
			J = 7.0	J = 7.0			
4SO*p*Tol3CH_3 23a	**-**	**-**	**7.90 d**	**7.10 t**	**8.70 d**	**2.60**	**7.50d, 7.27d, *J* = 8.0, 2.38s**
			J = 7.0	J = 7.0	J = 7.0		
				J = 7.0			
5SO*p*Tol 22	**8.2 s**	**8.23 s**	**-**	**6.88 d**	**8.67 d**	**-**	**7.56d, 7.30d, *J* = 8.0, 2.38s**
				J = 7.3	J = 7.3		
6SO*p*Tol3CH_3 20a	**-**	**7.59 d**	**7.06 d**	**-**	**9.05**	**2.58**	**7.59d, 7.31d, *J* = 8.0, 2.39s**
		J = 9.3	J = 9.3				
7SO*p*Tol3CH_3 4	**-**	**7.65 d**	**7.38 dd**	**7.71 d**	**-**	**2.58**	**7.89d, 7.22d, *J* = 8.2, 2.30s**
		J = 8.8	J = 8.8	J = 6.9			
			J = 6.9				
6S*p*Tol 21b	**8.00 s**	**7.60 d**	**7.12 d**	**-**	**8.48**	**-**	**7.38d, 7.21d, *J* = 8.0, 2.38s**
		J = 9.2	J = 9.2				
6S*p*Tol3CH_3 20b	**-**	**7.44 d**	**7.00 d**	**-**	**8.36 s**	**2.54**	**7.32d, 7.15d, *J* = 8.0, 2.33s**
		J = 9.1	J = 9.1				
4S*p*Tol3 CH_3 23b	**-**	**-**	**6.55 d**	**6.66 t**	**8.39 d**	**2.60**	**7.30d, 7.18d, *J* = 8.0, 2.38s**
			J = 7.0 d	J = 7.0	J = 7.0		

2.7 Chiral 2,6-disubstituted pyridines

As it has been mentioned before, 2,6-disubstituted pyridine based ligands have widespread applications in catalysis[1] and supramolecular[2] chemistry. 3,7-Disubstituted-[1,2,3]triazolo[1,5-*a*]pyridines react with electrophiles *via* a triazole ring opening reaction with loss of nitrogen yielding 2,6-disubstituted pyridines.[4, 5] We studied the triazole ring opening reaction of the chiral alcohols **2** and **3** with the aim to obtain chiral 2,6-disubstituted pyridines. The reactions were performed with acetic acid, 2.5 M sulfuric acid and selenium dioxide as electrophiles (**Scheme II-10**).

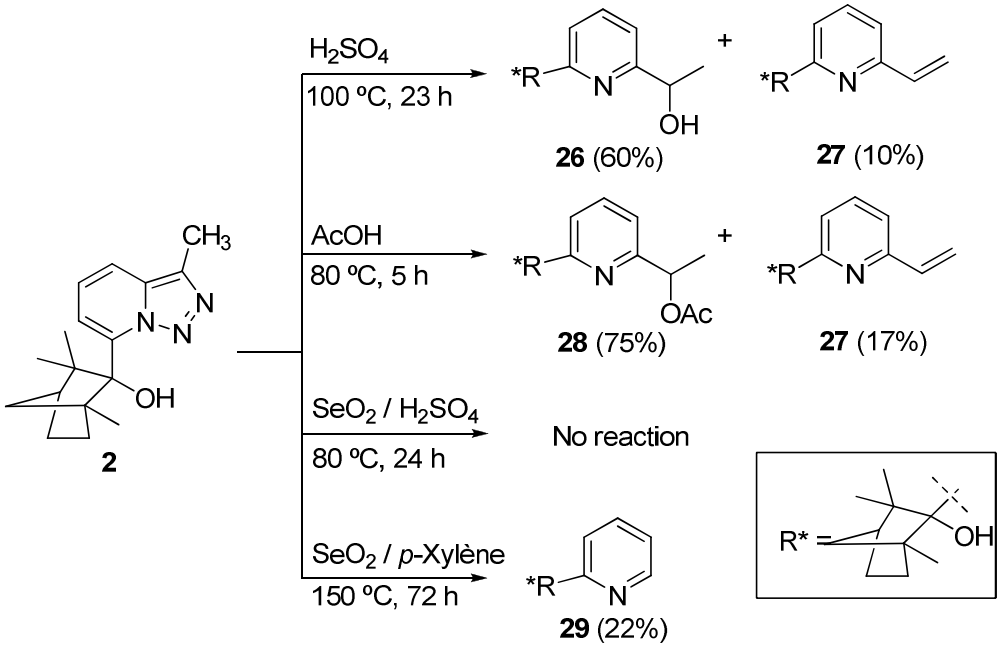

Scheme II-10: Ring opening reactions of **2**.

Treatment of compound **2** with aqueous sulfuric acid gave the alcohol **26** (60%) as a diastereoisomeric mixture (d.e. 5% was determined by ^{1}H-NMR). Small quantities of the elimination product, the vinylpyridine **27** were also obtained in 10 % yield. Whereas with acetic acid the acetate **28** (75%, d.e. 5%) was obtained and **27** in 17% yield. Therefore, the chiral fenchyl group is too far from the triazolopyridine 3-position to induce chirality in a significant manner. Under the classical treatment with selenium dioxide (*i.e.*, 2.5 M sulfuric acid, 80 °C, 24 h) no reaction was observed. However, in *p*-xylene at reflux, the known pyridine **29** was obtained.[7]

However, with 2-(6-([1,2,3]triazolo[1,5-*a*]pyridin-3-yl)pyridin-2-yl)-1,3,3-trimethylbicyclo[2.2.1]heptan-2-ol **(3)**, the ring-opening reactions were not successful: the high stability of this molecule was unexpected (**Scheme II-11**).

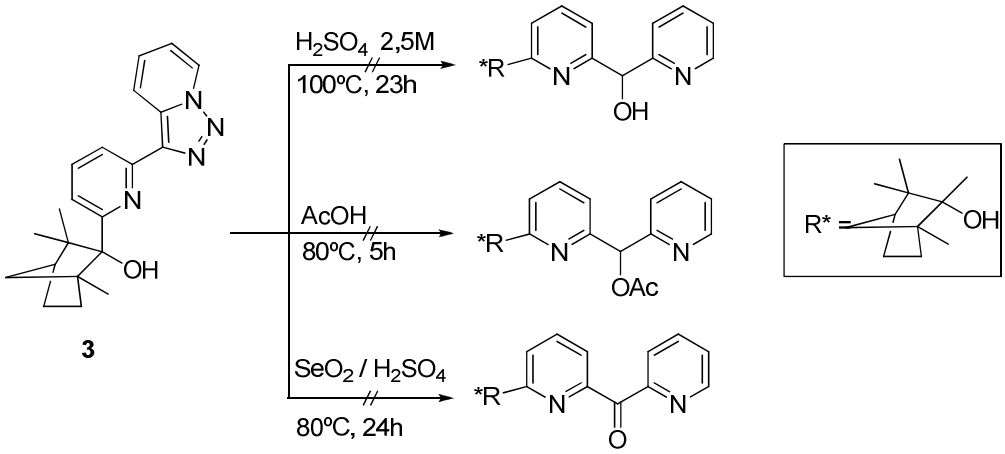

Scheme II-11: Stability of **3** towards acid conditions.

When the reaction was performed with molecule **3** and acetic acid at higher temperature, compound **30** was obtained (d.e. 3.5 % determined by ^{1}H-NMR) (**Scheme II-12**). No other ring opening reaction was successful, even by increasing the temperature.

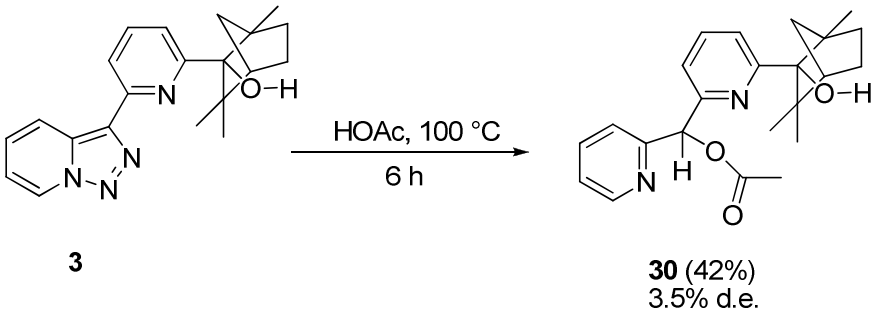

Scheme II-12: Ring opening reaction of **3**.

We investigated then the opening reaction of protected compound **4** as a methyl ether under various conditions (**Scheme II-13**). The following side products were obtained depending on the electrophiles used.

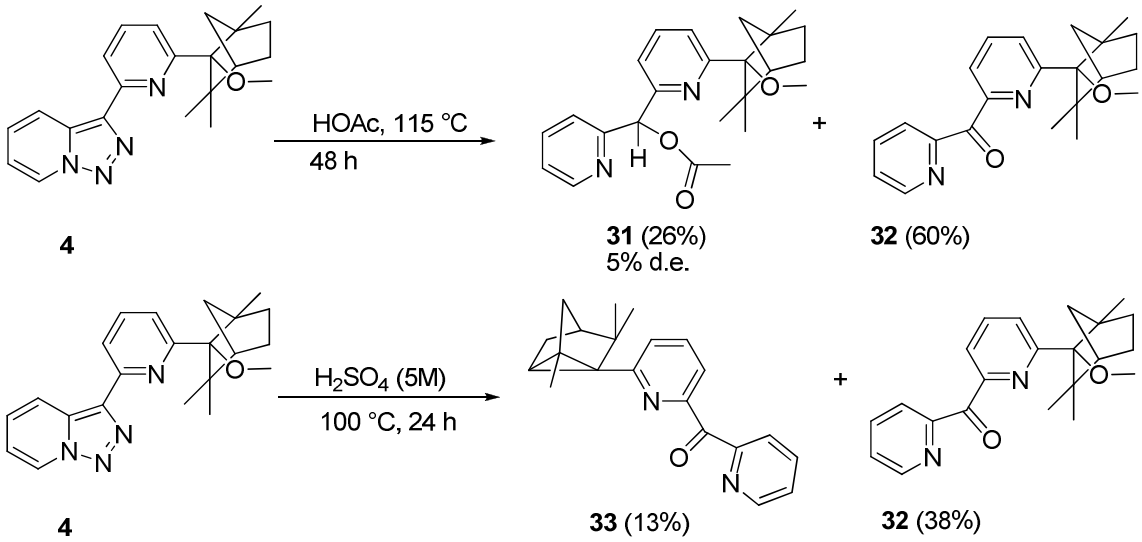

Scheme II-13: Ring opening reactions for compound **4**.

Compound **31** was obtained in low yield, however ketone **32** was obtained as the major product and results from the radical degradation of **31** (**Scheme II-14**). This reaction had also been proposed by Serafinowsky and Garland[41] as a way to obtain diaryl ketones.

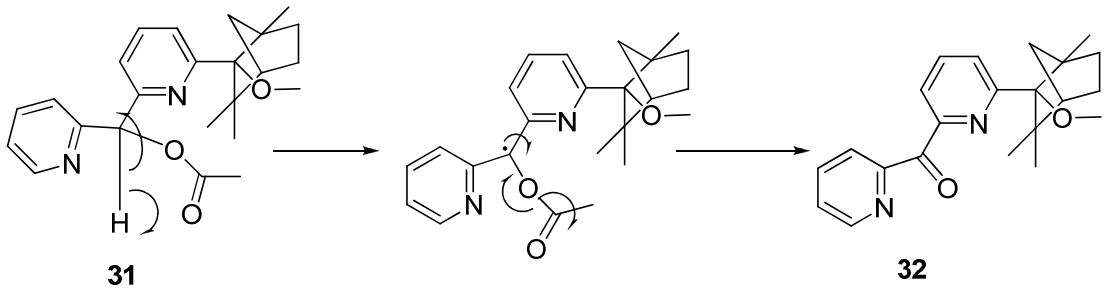

Scheme II-14. Degradation of 30.

The sulfuric acid treatment gave a complex mixture of products. After purification, products **32** and **33** were isolated, but not the expected alcohol.

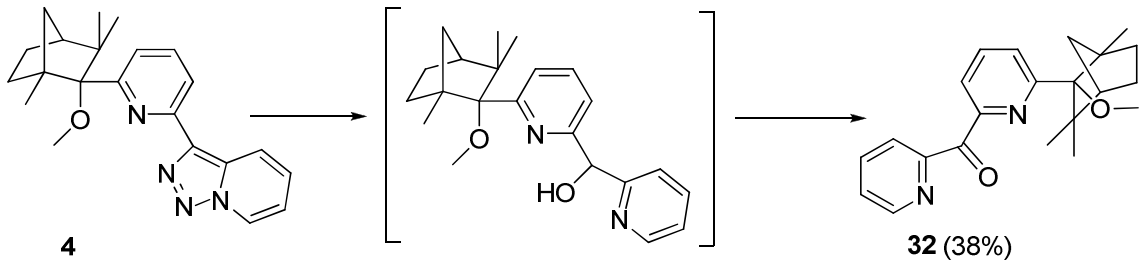

Scheme II-15: Formation of the ketone **32.**

The formation of ketone **32** in sulfuric media implies necessarily the passage by the intermediate formation of the corresponding alcohol (**Scheme II-15**). The explanation of this result is similar to the previous comments. The oxidation of these alcohols (dipyridyl-derivated

alcohols) undergoes easy, with an oxidation potential near -1.18 eV, according to Olea-Azar, Abarca *et al*.[42]

On the other hand, compound **33** was formed in low yield (13%). It can be obtained by a rearrangement induced by the generation of a norbornyl cation with loss of methanol starting from **4** (**Scheme II-16**).

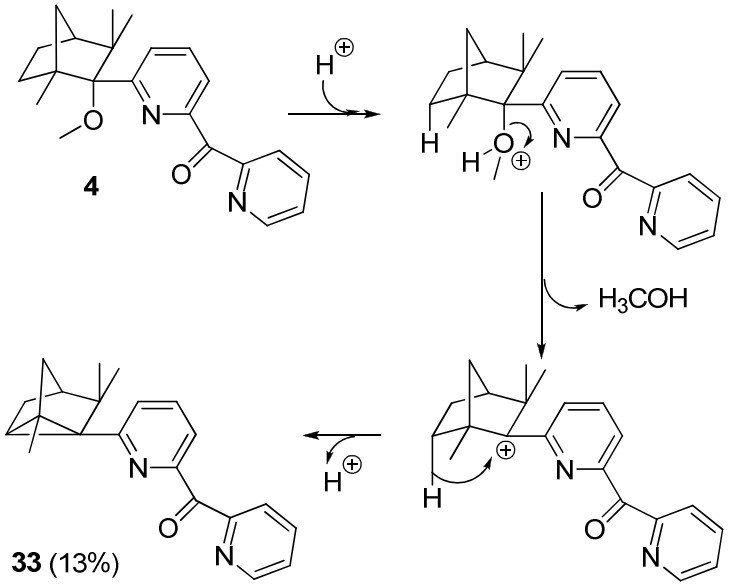

Scheme II-16: Rearrangement induced by the generation of a norbornyl cation.

This process was already reported by Vonwiller[43] (**Scheme II-17**), and is as well known for fenchone derivatives to produce cyclo[6.2.0]fenchen systems.

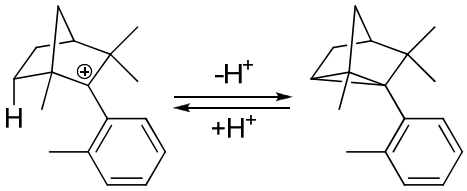

Scheme II-17: Rearrangement described by Vonwiller.

Ring opening reactions were also performed on the sulfoxide derivatives **5**, **6** and **23** with acetic acid or 2.5 M sulfuric acid as electrophiles.

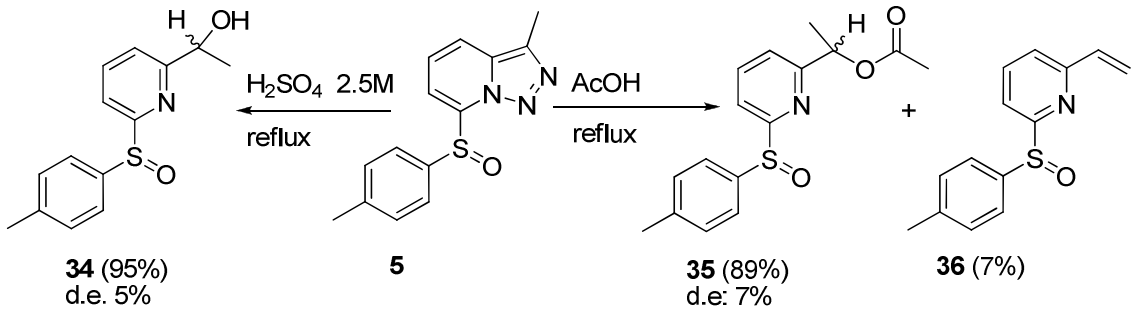

Scheme II-18: Ring opening reactions for sulfoxide **5**.

Treatment of compound **5** (racemic) with aqueous sulfuric acid gave the alcohol **34** (95%) as a diastereoisomeric mixture, 5% d.e. (determined by ^{1}H-NMR). With acetic acid the acetate **35** (89%, 7% d.e.) was obtained. Small quantities of the elimination product, vinylpyridine **36**, were also formed (**Scheme II-18**). Treatment of compound **23** with glacial acetic acid gave the acetate **36**, also as a diastereomeric mixture (10% d.e.). The higher chiral induction can be associated to the proximity of the chiral sulfoxide to the triazolopyridine prochiral carbon (C^{3}) (**scheme II-19**).

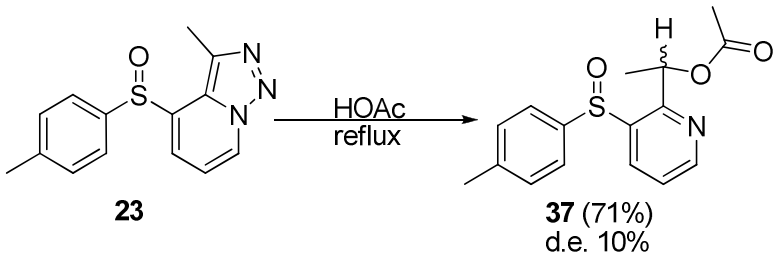

Scheme II-19: Treatment of compound **23** with glacial acetic.

Reaction of compound **6** with glacial acetic acid provided the acetate **38** in a 56% yield (5% d.e.). When the reaction was performed with sulfuric acid, the alcohol **39** and its oxidation product **40** were isolated. In fact, alcohol **39** is spontaneously oxidized by air to provide compound **40** (**Scheme II-20**).

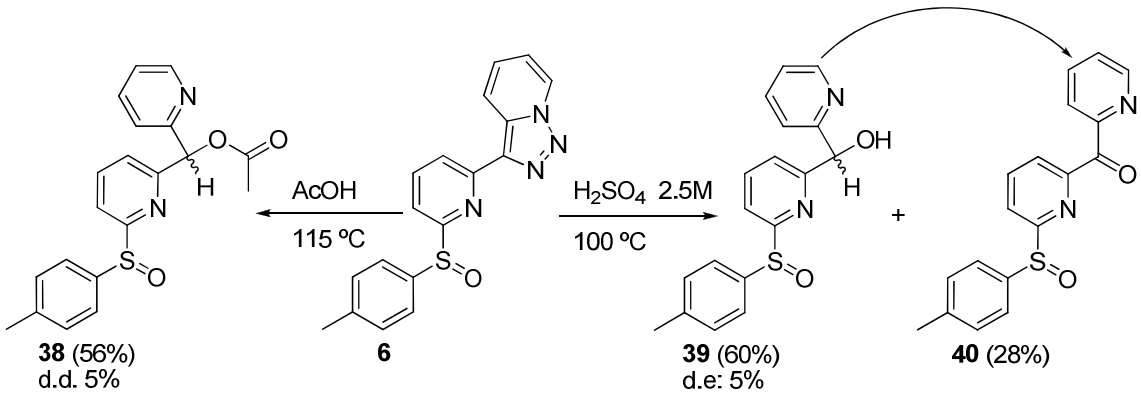

Scheme II-20: Ring opening reactions of compound **6**.

2.8 Long distance chiral sulfoxides

By making good use of the methodologies developed in our laboratory during the last years, two different sulfoxides were synthesized.[44] First, we wanted to study the ring opening reaction on these new structures. But we also wanted to design new bidentate S(O)-N structures (**Figure II-7**).

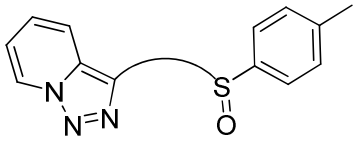

Figure II-7: Bidentate S(O)-N structures.

To obtain these compounds the sulfoxide needed to be introduced before the triazole ring formation. Thus, two equivalents of *para*-toluenemethylsulfinate reacted with LDA and was condensed over ethyl [1,2,3]triazolo[1,5-*a*]pyridine-3-carboxylate, providing compound **41** as shown in **scheme II-21**.

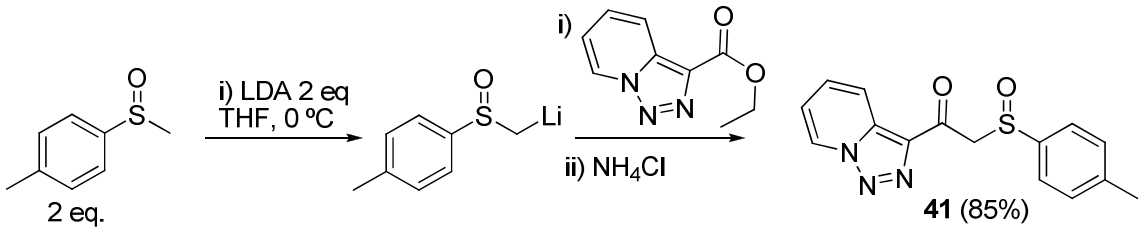

Scheme II-21: Synthesis of compound **41**.

In a similar way, following the Solladie[44] protocol, compound **42** was also obtained in good yield (93%) by trapping with methyl picolinate (**Scheme II-22**). Compound **42** was then transformed into triazolopyridine **43** using the hydrazine/MnO_2 method.

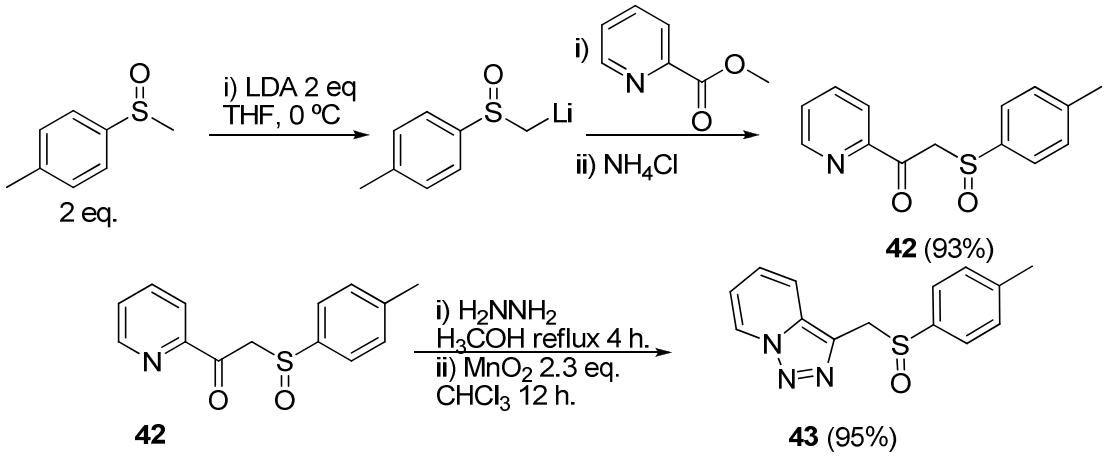

Scheme II-22: Preparation of compound **43**.

However, ring opening reactions were performed on compounds **41** and **43** using acetic acid, complex mixtures were observed and no successful purification could be achieved.

2.9 Conclusions

- By means of regioselective metalation we have been able to prepare our chiral target compounds **2**, **3**, **5** and **6B**. Due to the dimerization problem we have applied the catalytic sulfenation to provide compounds **5** and **6B** in high yield. Furthermore we have extended this methodology to other heterocyclic compounds.

- Concerning the regioisomeric **A**/**B** structures, we have proved how structure **3B** is really dependent on the inductive effect of the fenchone system. Compound **4B** helped us to discard the possible stabilization by a bifurcated hydrogen bond.

- The analysis of the d.e. for pyridines **26**, **28**, **30**, **31**, **34**, **35**, **38** and **39** indicates that there is an irrelevant chiral induction (d.e. < 5 %) when the chiral group is at C^7. However when the chiral group is near to C^3 (compound **37**, sulfoxide C^4) this induction is higher (d.e. 10 %).

- Compounds **3** and **6B** present a tridentate structure (**Figure II-8**) and they seem to have fluorescent properties. They will be tested as ligands for fluorescence recognition.

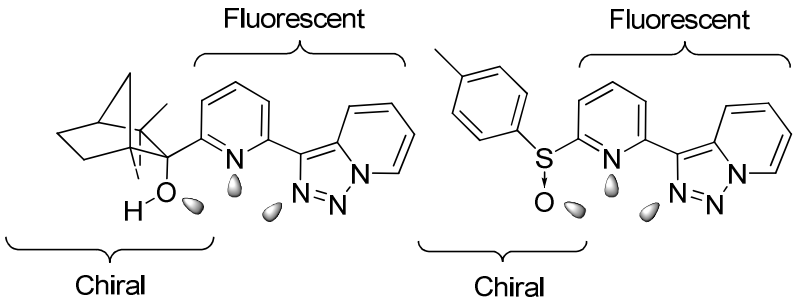

Figure II-8: Tridentate chiral fluorescent structure of compounds **3** and **6**.

- Due to the interest of heterocyclic sulfoxides in biological and pharmaceutical research, some of these compounds (**5**, **6**, **41** and **43**) will be evaluated as inhibitors for zinc based enzymes. This current study will be presented in the outlook .

2.10 References.

[1] G. Chelucci, *Chem. Soc. Rev.* **2006**, *35*, 1230.
[2] J. M. Lehn, *Supramolecular Chemistry, Concepts and Perspecties.*, VCH, Weinheim, **1995**.
[3] B. Abarca, R. Ballesteros, F. Mojarred, G. Jones, D. J. Mouat, *J. Chem. Soc., Perkin Trans. 1* **1987**, 1865.
[4] G. Jones, D. J. Mouat, D. J. Tonkinson, *J. Chem. Soc., Perkin Trans. 1* **1985**, 2719.
[5] B. Abarca, R. Ballesteros, M. Elmasnaouy, *ARKIVOC* **2002**, *vi*, 145.
[6] B. Abarca, R. Aucejo, R. Ballesteros, F. Blanco, E. Garcia-Espana, *Tetrahedron Lett.* **2006**, *47*, 8101.
[7] M. Genov, K. Kostova, V. Dimitrov, *Tetrahedron: Asymmetry* **1997**, *8*, 1869.
[8] H.-L. Kwong, W.-S. Lee, *Tetrahedron: Asymmetry* **1999**, *10*, 3791.
[9] W.-S. Lee, H.-L. Kwong, H.-L. Chan, W.-W. Choi, L.-Y. Ng, *Tetrahedron: Asymmetry* **2001**, *12*, 1007.
[10] R. Bentley, *Chem. Soc. Rev.* **2005**, *34*, 609.
[11] J. Legros, J. R. Dehli, C. Bolm, *Adv. Synth. Catal.* **2005**, *347*, 19.
[12] U. F. Junggren, S. E. Sjostrand, Eur. Patent 0005129, **1981**.
[13] M. C. Carreno, *Chem. Rev.* **1995**, *95*, 1717.
[14] G. Hanquet, F. Colobert, S. Lanners, G. Solladié, *Arkivoc* **2003**, *vii*, 328.
[15] I. Fernandez, N. Khiar, *Chem. Rev.* **2003**, *103*, 3651.
[16] H. Pellissier, *Tetrahedron* **2006**, *63*, 1297.
[17] M. S. Chen, N. Prabagaran, N. A. Labenz, M. C. White, *J. Am. Chem. Soc.* **2005**, *127*, 6970.
[18] J. H. Delcamp, A. P. Brucks, M. C. White, *J. Am. Chem. Soc.* **2008**, *130*, 11270.
[19] W. A. Herrmann, J. J. Haider, J. Fridgen, G. M. Lobmaier, M. Spieegler, *J. Organomet. Chem.* **2000**, *603*, 69.
[20] B. Abarca, I. Alkorta, R. Ballesteros, F. Blanco, M. Chadlaoui, J. Elguero, F. Mojarrad, *Org. Biomol. Chem.* **2005**, *3*, 3905.
[21] K. K. Andersen, W. Gaffield, N. E. Papanikolaou, J. W. Foley, R. I. Perkins, *J. Am. Chem. Soc.* **1964**, *86*, 5637.
[22] P. Pollet, A. Turck, N. Ple, G. Queguiner, *J. Org. Chem.* **1999**, *64*, 4512.
[23] T. Kawai, N. Furukawa, S. Oae, *Tetrahedron Lett.* **1984**, *25*, 2549.
[24] N. Furukawa, S. Ogawa, K. Matsumura, H. Fujihara, *J. Org. Chem.* **1991**, *56*, 6341.
[25] J. Uenishi, T. Tanaka, S. Wakabayashi, S. Oae, H. Tsukube, *Tetrahedron Lett.* **1990**, *31*, 4625.
[26] G. Maitro, S. Vogel, G. Prestat, D. Madec, G. Poli, *Org. Lett.* **2006**, *8*, 5951.
[27] C. Caupene, C. Boudou, S. Perrio, P. Metzner, *J. Org. Chem.* **2005**, *70*, 2812.
[28] G. Maitro, S. Vogel, M. Sadaoui, G. Prestat, D. Madec, G. Poli, *Org. Lett.* **2007**, *9*, 5493.
[29] B. Abarca, R. Aucejo, R. Ballesteros, F. Blanco, E. García-España, *Tetrahedron Lett.* **2006**, *47*, 8101.
[30] G. Jones, M. A. Pitman, E. Lunt, D. J. Lythgoe, B. Abarca, R. Ballesteros, M. Elmasnaouy, *Tetrahedron* **1997**, *53*, 8257.
[31] B. Abarca, R. Ballesteros, G. Jones, F. Mojarrad, *Tetrahedron Lett.* **1986**, *27*, 3543.
[32] J. Le Notre, J. J. Firet, L. A. J. M. Sliedregt, B. J. Van Steen, G. Van Koten, R. J. M. K. Gebbink, *Org. Lett.* **2005**, *7*, 363.
[33] B. Abarca, R. Ballesteros, M. Elmasnaouy, *Tetrahedron* **1998**, *54*, 15287.
[34] G. W. Kabalka, L. Wang, R. M. Pagni, *Arkivoc* **2001**, *iv*, 5
[35] X. Wang, P. Rabbat, P. O'Shea, R. Tillyer, E. J. J. Grabowski, P. J. Reider, *Tetrahedron Lett.* **2000**, *41*, 4335.
[36] B. Abarca, R. Ballesteros, F. Blanco, *Arkivoc* **2007**, *iv*, 297.
[37] W. D. Crow, C. Wentrup, *Tetrahedron Lett.* **1968**, *9*, 6149.
[38] R. Oda, M. Mieno, Y. Hayashi, *Tetrahedron Lett.* **1967**, *8*, 2363.
[39] F. Blanco, I. Alkorta, J. Elguero, V. Cruz, B. Abarca, R. Ballesteros, *Tetrahedron* **2008**, *64*, 11150.
[40] J. H. Boyer, R. Borgers, L. T. Wolford, *J. Am. Chem. Soc.* **1957**, *79*, 678.
[41] P. J. Serafinowski, P. B. Garland, *J. Am. Chem. Soc.* **2003**, *125*, 962.
[42] C. Olea-Azara, B. Abarca, E. Norambuena, L. Opazo, C. Rigol, R. Ballesteros, M. Chadlaoui, *Spectrochim. Acta, Part A* **2005**, *61*, 2261.
[43] M. Scott, S. Starling, C. Vonwiller, N. Joost, H. Reek, *J. Org. Chem.* **1998**, *63*, 2262.
[44] M. C. Carreño, J. L. Garcia Ruano, A. M. Martin, C. Pedregal, J. H. Rodriguez, A. Rubio, J. Sanchez, G. Solladie, *J. Org. Chem.* **1990**, *55*, 2120.

III: [1,2,3]Triazolo[1,5-*a*]quinoline

3.1 Toward 2,8-disubstituted quinolines

3.1.1 Introduction and objectives

[1,2,3]Triazolo[1,5-*a*]quinoline (**44**) can be considered as a benzoderivate from the [1,2,3]Triazolo[1,5-*a*]pyridine (**1c**), having a similar reactivity patern in many aspects (**Figure III-1**).

Figure III-1: Triazoloquinoline and triazolopyridine.

Triazoloquinoline (**44**) was synthesized for the first time by Abramovitch and Takaya[1] in 1972 by reacting quinaldine with tosylazide. Abarca and Jones[2] also proposed a different synthesis based on the methodologies developed for triazolopyridines. Analogously, as compound **1c** was prepared using 2-pyridinecarboxaldehyde with hydrazine/MnO_2,[3] triazoloquinoline **44** can be synthesized employing quinoline-2-carbaldehyde. This compound is commercially available, but can also be obtained by oxidation of quinaldine (**Scheme III-1**) with selenium(IV) oxide in dioxane water (96/4 v:v).[4]

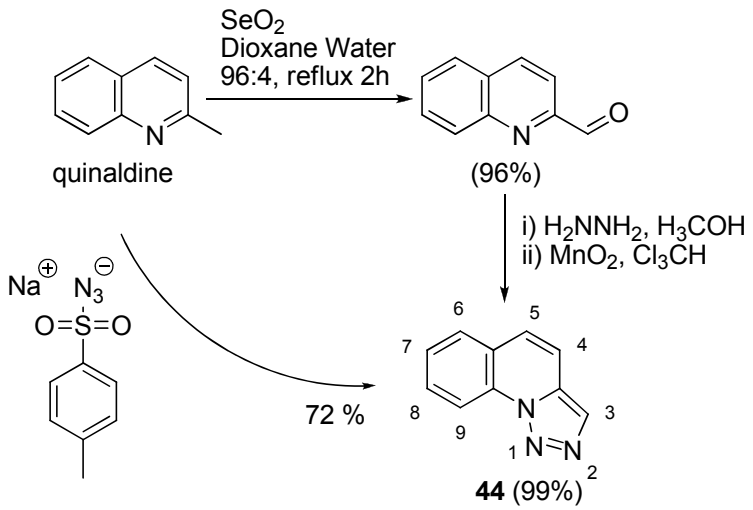

Scheme III-1: Synthesis of [1,2,3]Triazolo[1,5-*a*]quinoline (**44**)

When triazoloquinoline **44** is compared to triazolopyridine **1c**, remarkable similarities can be found in the chemistry of both compounds. Indeed, the extra aromatic ring in **44** seems not to modify the chemical properties. Analogous compounds, to those obtained with **1c**, are obtained by nitration, hydrogenation, alkylation or ring openin reactions (**Scheme II-2**):

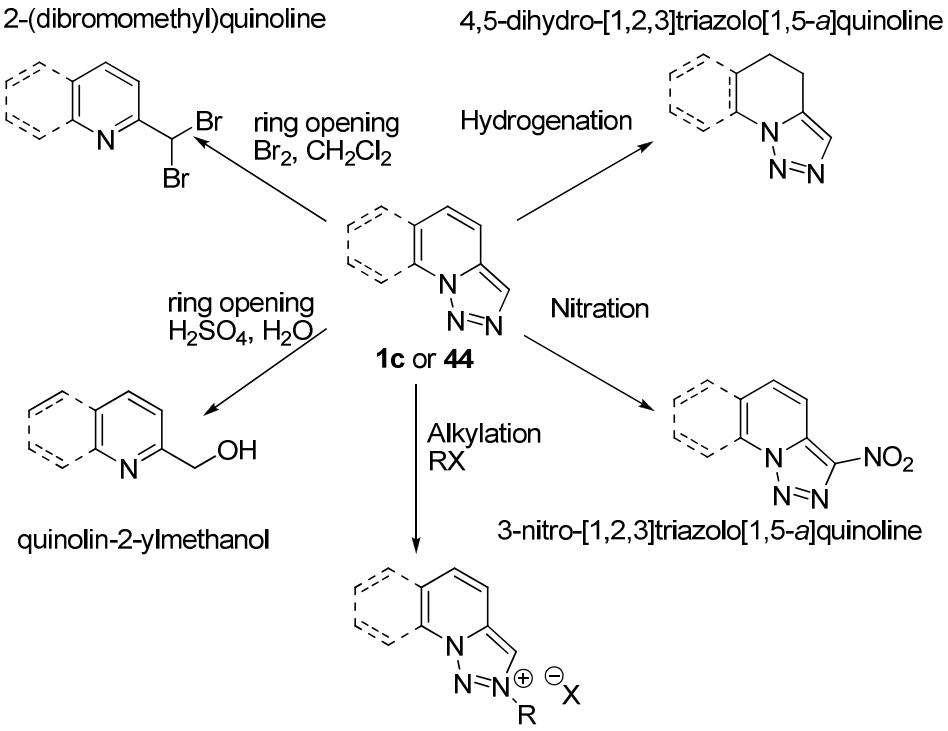

Scheme III-2: Comparison between **1c** and **44.**

The hydrogenation of **44** or **1c** under mild conditions (Pd/C, H_2, H_3COH) provides the regioselective hydrogenation of the pyridine ring in both structures.[5] Nitration takes place at the 3 position affording nitrotriazolopyridines[6] and nitrotriazoloquinolines.[2] In both cases no other position is functionalized. Alkylation of compound **44** takes place at N^2, as its the case for compound **1c** under same conditions.[7, 8] The ring opening reaction of triazoloquinoline **44** provides the corresponding quinolines[2] in the same way as **1c** provides pyridines.[9] For example, after heating in sulfuric acid, both systems (**44** and **1c**) leads to similar alcohols.[2, 9] Treatment with bromine also provides 2-dibromomethyl substituted quinoline or pyridine.[2, 9] Although these similarities, the metalation with lithium di-*iso*-propylamide (LDA) provides completely different results (**Scheme III-3**):

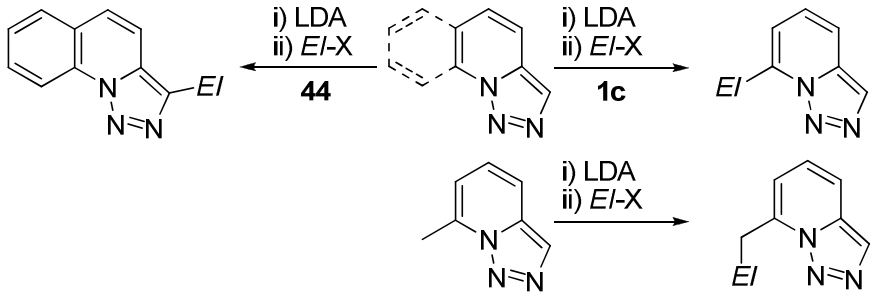

Scheme III-3: Comparison towards metalation reaction.

A striking difference in regioselectivity can be observed with compounds **1c** and **44**. Whereas [1,2,3]triazolo[1,5-*a*]pyridine is selectively deprotonated at the 7-position,[10] the corresponding 9-position in [1,2,3]triazolo[1,5-*a*]quinoline seems to be much less reactive,

favouring deprotonative metalation at the 3-position (which has never been observed with **1c**). Furthermore, even with 7-methyl-[1,2,3]triazolo[1,5-*a*]pyridine the metalation takes place at the methyl group at C^7 (see chapter 1).[10] This regiolectivity was employed by Abarca *et al*. to obtain *N*,*N*-diethyl-[1,2,3]triazolo[1,5-*a*]quinoline-3-carboxamide which after subsequent remote-lithiation allowed the preparation of 3,4-disubstituted triazoloquinoline.[11] The opening of the triazole ring in the presence of acetic acid gave rise to dihydrofuro[3,4-*b*]quinoline, formally a 2,3-disubstituted quinoline (**Figure III-2**

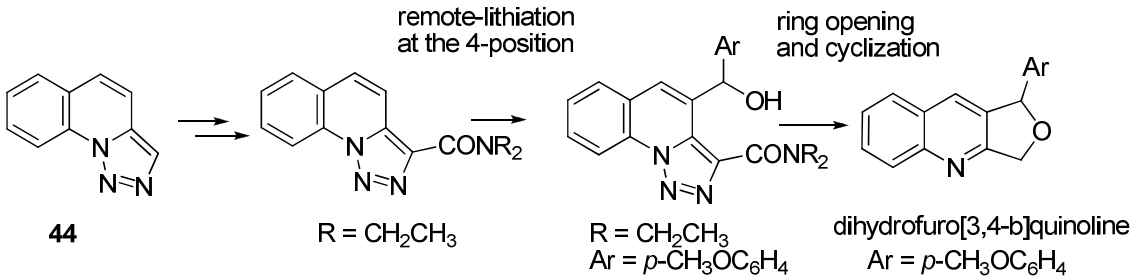

Figure III-2: From triazoloquinoline 41 to dihydrofuro[3,4-*b*]quinolines.

We have already shown the utility of the metalation/ring opening reaction strategy in triazolopyridines[9, 12] (See chapter 1, and chapter 2) for the preparation of 2,6-disubstitued pyridines. Although no examples of H^9 activation by metalation had ever been reported in **44,** the activation of the 9-position would lead to a masked 8-susbtituted quinoline, by means of a ring opening reaction (**Figure III-3**).[2]

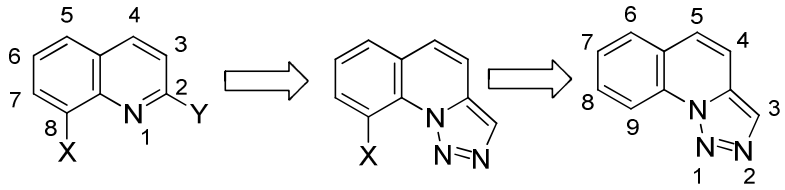

Figure III-3: From triazoloquinoline **44** to 2,8-disubstituted quinolines.

8-Substituted quinolines can be found in many pharmaceutical compounds. For example *Mefloquine* contains the 8-trifluoromethylquinoline motive and is known as an antimalarian drug.[13] Another example is *Styrylquinoline*,[14] a new highly active drug preventing HIV-1 replication, the also contains a 8-substituted quinoline (**Figure III-4**).

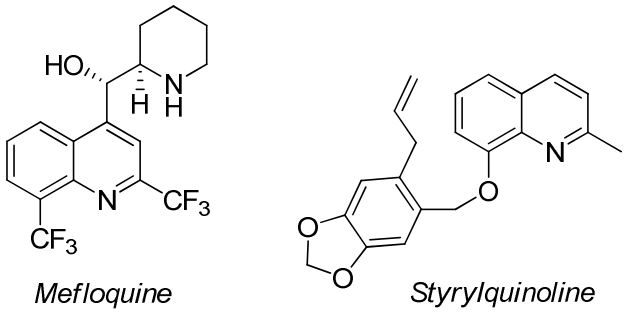

Mefloquine *Styrylquinoline*

Figure III-4: 8-Substituted quinolines in drug development.

Albeit the functionalization of quinolines at the 8-position by metalation and/or bromine/lithium exchange has been reported,[15-26] a lack of regioselectivity is often a major drawback. In this way Kondo *et al.*[27] reported on the regioselective metalation of quinoline at C^8 by employing (TMP)Zn^{t}Bu$_2$Li affording a mixture of 2-metalated and 8-metalated compounds. Recently, Knochel *et al.*[28] reported on the metalation at the C^8 position with TMPMgCl·LiCl of 2,3,4-trisubstituted quinolines.

The work performed by Abarca *et al.* in past with triazoloquinoline had provided interesting structures as mentioned before.[2, 11] However, in order to provide a link between 2,6-disubstituted pyridines and 2,8-disubstituted quinolines, we wanted to examine carefully the chemistry of this compound (**44**) in order to:

- Functionalize the triazoloquinoline-C^9 position by means of metalation.
- Provide an easy access to 2,8-disubstituted quinolines.

3.1.2 Metalation study on triazoloquinoline 44

All works concerning triazoloquinoline metalation performed by Abarca and Jones dated from 1984-1985.[2, 11] However, the optimal metalation conditions for triazolopyridines with butyllithium[29, 30] instead of LDA were not found until 1987. All metalation reactions on triazoloquinoline were performed before this date and employed LDA as base.[10] The more basic butyllithium had never been used with compound **44**. Thus, the first test performed . Focused on a screening of different base systems. By employing butyllithium instead of LDA and after quenching with methyl iodide a complex mixture was observed (**Scheme III-4**) associated to compounds (**45-47**)**a**.

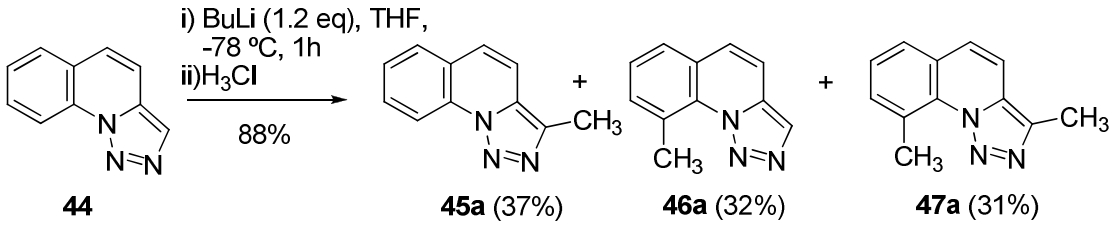

Scheme III-4:Metallation of triazoloquinoline **44** with BuLi**.**

Under these conditions, the metalation was no longer regioselective at C^3 as in the case of the LDA-promoted deprotonative metalation of triazoloquinoline **44**. A mixture of three metalation products was obtained, indicating that the metalation in position 9 is possible and that also a double metalation can be achieved.

In a similar way, with the aim of increasing the basicity but still employing amide bases, the reaction was performed with LiTMP instead of LDA. Under these conditions, no 9-susbtituted compound (**46a**) was found (**Scheme III-5**). Compound **45a** was obtained as major product (86%) and small amount of **47a** could also be isolated.

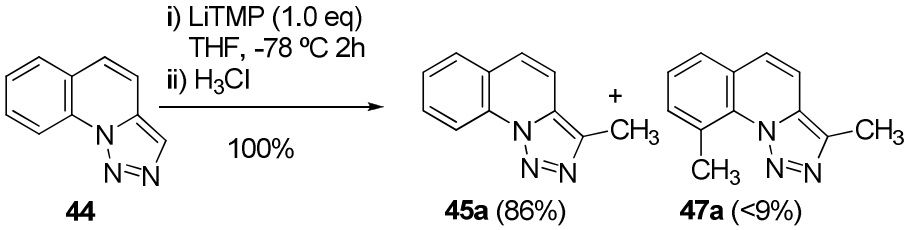

Scheme III-5: Metallation of triazoloquinoline **44** with LiTMP.

Under these new conditions, a 3-subtituted triazoloquinoline family was prepared by quenching with different electrophiles. After deuteration with CD_3OD, triazoloquinoline **45b** was obtained in 96% yield. Chlorotrimethylsilane gave the corresponding silylated derivative **45c** in quantitative yield, iodine the compound **45d** in a yield of 72% and (1*R*,2*S*,5*R*)-(-)-menthyl-(*S*)-*p*-toluenesulfinate[31] the sulfoxide **45e** in 82% yield (**Scheme III-6**). In case of trapping with iodine, trace amounts of disubstituted derivative **47d** were detected in the ^{1}H-NMR.

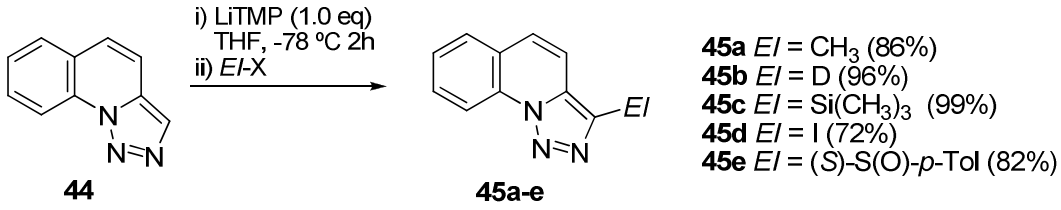

Scheme III-6: Metallation of triazoloquinoline **44** towards 3-susbtituted triazoloquinolines **45a-e.**

9-Methyltriazoloquinoline **46a** had already been identified (**Scheme III-4**). However, it was impossible to isolate it without traces of starting reagent **44**. In addition, the global yield of **46a** was poor. We could develope a secondary strategy to obtain this compound pure and with acceptable yields. The 3-trimethylsilyl-protected triazoloquinoline **45c** could be successfully deprotonated at C^9, although an excess of butyllithium (1.7 eq.) had to be used in order to achieve complete conversion. Thus 9-Methyl-3-(trimethylsilyl)-[1,2,3]triazolo[1,5-*a*]quinoline (**48a**) was obtained in excellent yield after trapping with iodomethane. Deprotection with tetrabutyl ammonium fluoride[32] in THF at room temperature afforded the triazoloquinoline **46a** after chromatography (**Scheme III-7**).

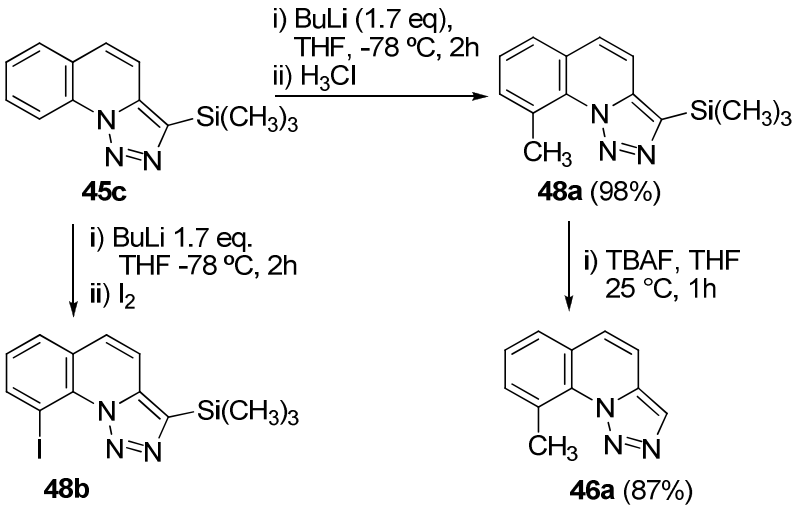

Scheme III-7: Preparation of compound **46a.**

This compound was obtained in an excellent overall yield of 84% starting from triazoloquinoline **44**. In order to obtain the 9-iodinated analogue, the organolithium intermediate was trapped with iodine. Unfortunately the iodo-derivative **48b** could not be isolated in pure form, neither by crystallization nor by column chromatography, as this compound readily decomposed on silica gel.

Next we studied more in detail the metalation of **44**, as we had now the authentic reference compounds of 3- and 9- monometalation (**45a** and **46a**,) as well as the 3,9-dimetalated compound (**47a**)(**Table III-1**).

Table III-1: Metalation study of triazoloquinoline **44**.

Entry	Base[a]	Solvent	t (h)	T (C °)	**45a**[b]	**46a**[b]	**47a**[b]	Conv.[b]
1	LiTMP	THF	2h	-78 °C	91(86)[c]	0	9	100%
2	LDA	THF	4h	-40 °C	100			84 %
3	*tert*-BuLi	THF	2h	-78 °C	88	0	12	100%
4	BuLi[d]	THF	1h	-78 °C	37	32	31	88%
5	BuLi/KO *tert*-Bu	THF	2h	-78 °C	100	0	0	59%
6	BuLi/PMDTA	THF	2h	-78 °C	100	0	0	64%
7	BuLi	THF	2min	-78 °C	41	50	9	82%
8	BuLi	THF	1h	-78 °C	50	42	8	75%
9	BuLi	THF	2h	-78 °C	54	41	5	71%
10	BuLi	THF	2h	0 °C	100	0	0	83%
11	BuLi	Tol	2h	0 °C	90	3	7	33%
12	BuLi[e]	THF	2h	-78 °C	0	0	82[c]	100%

a) 1.0 eq of base, b) Ratios determined from the integration values of the ^{1}H NMR spectra of the crude reaction mixtures, c) Isolated yield, d) 1.2 eq of BuLi e) 3.0 eq of base were employed

The metalation with LiTMP and *tert*-butyllithium afforded mainly metalation at the sterically more accessible 3-position (**Table III-1**, entries 1-3) albeit with trace amounts of dimetalation products. When the Schlosser superbase (butyllithium/potassium *tert*-butoxide) was employed (**Table III-1**, entry 5), still the 3-position was exclusively metalated however with a decreased conversion. Almost the same result was obtained using butyllithium in presence of PMDTA (*N*,*N*,*N*',*N*'',*N*''-pentamethyl diethylene triamine, **Table III-1**, entry 6). Thus, amide bases and *tert*-BuLi lead to an exclusive metalation at the 3-position, without any formation of 9-metalation product. The metalation at the 9-position cannot be performed with *tert*-butyllithium, probably for steric reasons. When a slight excess of butyllithium was employed, a mixture of 3- and 9-metalation products together with a 3,9-dimetalation product was obtained in a ratio of 37:32:31 (**Table III-1**, entry 4), indicating that 9-metalation is possible. By comparing different metalation times using butyllithium as base (now under stechiometric conditions), a slightly higher reactivity of the 9-position could be deduced (**Table III-1**, entry 7). The amount of dilithiated intermediate, as well as the ratio between 3- and 9-metalation remained more or less unchanged (**Table III-1**, entries 7 to 9) at -78 °C. At higher temperature (**Table III-1**, entry 10) only the metalation product at position 3 was observed but with smaller

conversion. So far, no base system allowed a regioselective metalation at the 9-position. Finally with a large excess of base (**Table III-1**, entry 12) double metalation was obtained in high yield.

3.1.3 Double metalation of triazoloquinoles 44, towards 2,8-disubstituted quinolines

When a small excess of base was used (1.2 eq of BuLi) the dimethylated product 4**7a** could be detected (**Table III-1**, entry 4) after trapping with iodomethane. As no regioselective metalation at C^9 could be achieved, we reached the double metalation with the aim of obtaining 3,9-disubstituted triazoloquinolines. With a big excess of BuLi (3 eq, **Table III-1**, entry 12) compound **47a** was obtained in good yield (82%). As well as compounds **47b-d** after trapping with iodine, 1,2-dibromo-tetrafluoroethane and 1,1,2-trichloro-1,2,2-trifluoroethane, respectively (**Scheme III-8**).

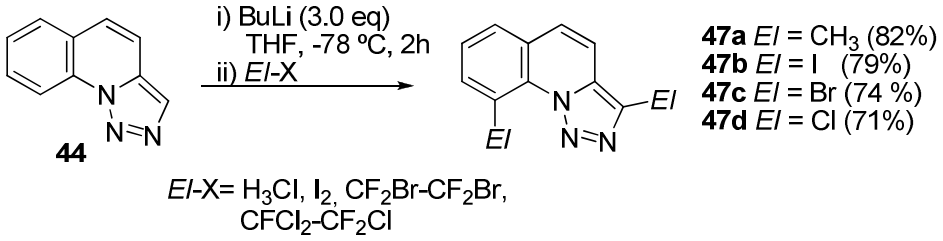

Scheme III-8:Preparation of compounds **47a-d.**

In order to complete the halogen family of **47b-d** we tried to obtain the corresponding difluorinated compound by quenching the dilithiated compound with *N*-fluorobenzenesulfonimide (NFSI). However, exclusively the monofluorinated product **49** was obtained in a yield of 60% (**Scheme III-9**). The outcome of the reaction revealed reproducible. Even when different sources of NFSI were employed, no difluorinated product could be detected. Although the double metalation could be performed, only 9-fluorotriazoloquinoline **49** was obtained. 8-Fluoroquinolines are difficult to obtain,[33, 34] however compound **49** could be easily transformed, in 70% yield, into quinoline **50** by ring opening reaction, providing a new way to obtain 8-fluoroquinolines.

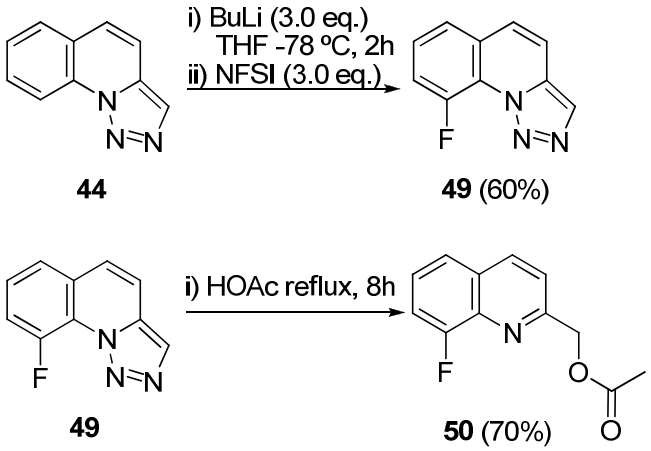

Scheme III-9: Preparation of fluorinated compounds **49** and **50.**

In order to study the scope and limitation of the use of 3,9-dihalogenated triazoloquinolines in the synthesis of 2,8-disubstituted quinolines, we studied more in detail their ring opening reaction. So far, no examples of ring opening reactions[9] on C^3-halogen-containing triazolopyridines or triazoloquinolines are described in the literature. When the triazole ring of 3,9-diiodo-[1,2,3]triazolo[1,5-*a*]quinoline (**47b**) was submitted to a ring opening reaction in a THF/water/HOAc (8:2:2) mixture at reflux, the aldehyde **51a** was obtained in a yield of 90% (**Scheme III-10**). Another possibility to undergo a triazole ring opening towards ketones or aldehydes frequently employed in triazolopyridine chemistry is the use of SeO_2 as oxidant.[9] However, 3-halogenated triazoloquinolines undergo exclusively aldehyde formation. In this context, the high acid-sensitivity of 3,9-diiodo-[1,2,3]triazolo[1,5-*a*]quinoline (**47b**) has to be pointed out. Similarly, when **47b** was kept in an NMR tube, traces of HCl present in deuterium chloroform were sufficient to induce the ring opening affording the acid **52** in an excellent yield (**Scheme III-10**).

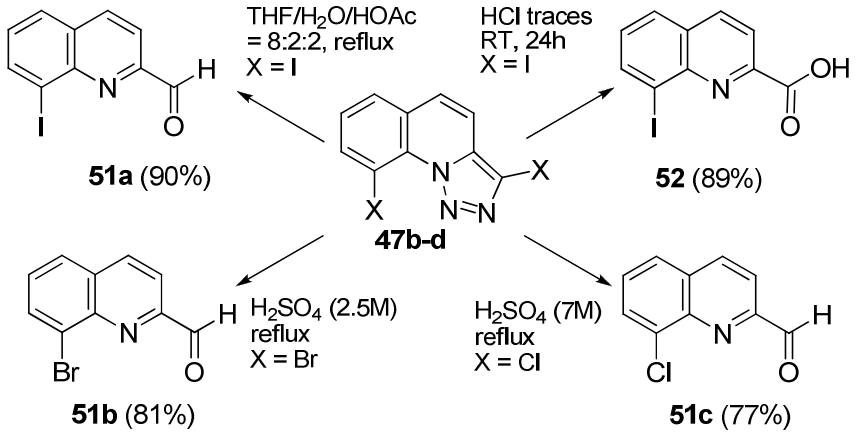

Scheme III-10: 2,8-disubstited quinolines.

In contrast, the corresponding dibromo and dichloro derivatives **47c** and **47d** underwent the ring opening only under more drastic reaction conditions. For 3,9-dibromo-[1,2,3]triazolo[1,5-*a*]quinoline (**47c**), heating under reflux in 2.5 M sulfuric acid was required to

obtain the analogous quinoline **51b.** In case of 3,9-dichloro-[1,2,3]triazolo[1,5-*a*]quinoline (**47d**) the ring opening only occurred when 7 M sulfuric acid was employed affording quinoline **51c**. The presumable mechanism for the ring opening reaction is similar to the one published before, and is depicted in **scheme III-11**:

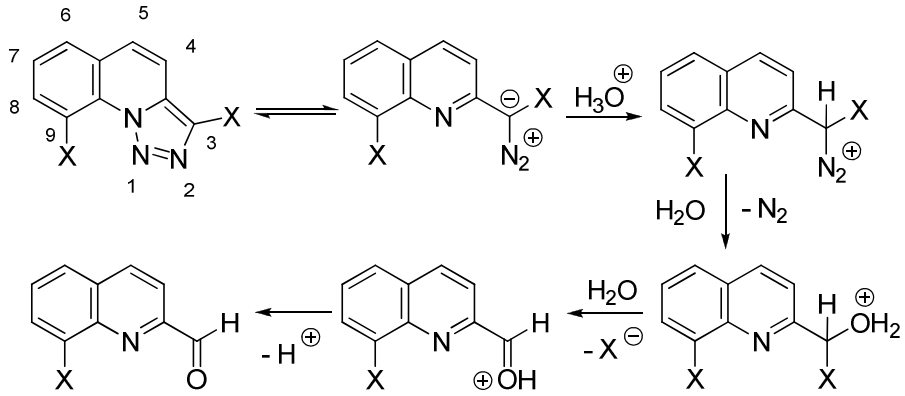

Scheme III-11: Mechanism for the obtention of compounds **51a-c**.

3.1.4 ^{1}H-NMR table of the triazoloquinoline family

In the second part of this chapter a discussion concerning the ^{1}H-NMR of triazoloquinoline-pyridine based compounds will be done. As it has been reported before, spectral properties of triazolopyridines are well know, however with triazoloquinoline derivatives this data are not available. These compounds also have a similar pattern, $J_{H4\text{-}H5}$ = 9.4 Hz. H^{9} can be found as a doublet ($J_{H8\text{-}H9}$ = 8.2 Hz) near 8.4 ppm.

Table III-2: ^{1}H-NMR for triazoloquinoline derivatives.

	H^3	H^4	H^5	H^6	H^7	H^8	H^9	OTHERS
44	**8.10 s**	**7.55 d**	**7.54 d**	**7.84 dd**	**7.60 dd**	**7.76 ddd**	**8.71 s**	
		J = 9.3	J = 9.3	J = 7.9	J = 7.9	J = 8.3	J = 8.4	
					J = 7.3	J = 7.3		
45a	**CH_3**	**7.42 app s**	**7.42 app s**	**7.80 dd**	**7.56 dd**	**7.72 ddd**	**8.74 d**	**2.64 s CH_3**
				J = 7.9	J = 7.9	J = 8.0	J = 8.0	
				J = 0.9	J = 7.8	J = 7.8		
						J = 0.9		
45b	**D**	**7.5-7.4 m**	**7.44 d**	**7.76 d**	**7.5-7.4 m**	**7.69 dd**	**8.71 d**	
			J = 9.3	J = 7.9		J = 8.3	J = 8.3	
				J = 1.0		J = 7.7		
45c	**TMS**	**7.6-7.5 m**	**7.46 d**	**7.76 dd**	**7.6-7.5 m**	**7.69 ddd**	**8.8 d**	**0.49 s $Si(CH_3)_3$**
			J = 9.3	J = 7.9		J = 8.3	J = 8.3	
				J = 1.1		J = 7.9		
						J = 1.1		
45d	**I**	**7.7-7.6 m**	**7.41 d**	**7.87 dd**	**7.7-7.6 m**	**7.74 ddd**	**8.76 d**	
			J = 9.3	J = 7.9		J = 8.3	J = 8.3	
				J = 1.0		J = 7.9		
						J = 1.0		
45e	**S(O)pTol.**	**7.7-7.6 m**	**7.6-7.5 m**	**7.87 dd**	**7.6-7.5 m**	**7.81 ddd**	**8.78 d**	**7.7-7.6 m $H^{2'}$**
				J = 7.9		J = 8.4	J = 8.4	**7.32 d $H^{3'}$**
				J = 1.0		J = 7.3		J = 8.0
						J = 1.2		**2.39 s CH_3**
46a	**8.04 s**	**7.5-7.4 m**	**7.5-7.4 m**	**7.6 d**	**7.5-7.4 m**	**7.5 d**	**CH_3**	**3.16 s CH_3**
				J = 7.7		J = 7.2		
47a	**CH_3**	**7.38 app s**	**7.38 app s**	**7.62 dd**	**7.43 dd**	**7.51 DD**	**CH_3**	**2.63 s 3- CH_3**
				J = 7.7	J = 7.7	J = 7.4		**3.18 s 9- CH_3**
				J = 0.9	J = 7.4	J = 0.9		
47b	**I**	**7.52 d**	**7.46 d**	**8.44 dd**	**7.25 dd**	**7.83 dd**	**I**	
		J = 9.3	J = 9.3	J = 7.7	J = 7.7	J = 7.8		
				J = 1.3	J = 7.8	J = 1.3		
47c	**Br**	**7.53 d**	**7.47 d**	**8.05 dd**	**7.42 dd**	**7.79 dd**	**Br**	
		J = 9.3	J = 9.3	J = 7.8	J = 7.9	J = 7.9		
				J = 1.3	J = 7.8	J = 1.3		
47e	**Cl**	**7.5-7.5 m**	**7.5-7.5 m**	**7.76 dd**	**7.5-7.5 m**	**7.71 dd**	**Cl**	
				J = 7.9		J = 7.9		
				J = 1.1		J = 1.1		
49	**8.12 d**	**7.6-7.5 m**	**7.6-7.5 m**	**7.6-7.5 m**	**7.6-7.5 m**	**7.6-7.5 m**	**F**	
	J = 0,4							
48a	**TMS**	**7.5-7.4 m**	**7.6-7.5 m**	**7.66 d**	**7.6-7.5 m**	**7.5-7.4 m**	**CH_3**	**3.21 s CH_3**
				J = 8.1				**0.49 s $Si(CH_3)_3$**

3.1.5 Conclusions

- The study performed on triazoloquinoline has completed the previous works by optimizing the regioselective metalation with LiTMP at C^3.

- No system has been found able to perform the regioselective metalation a C^9, however, a sequence of C^3-protection, C^9-fonctionalization and C^3-deprotection (employing TMS as protecting group) has been proposed as efficient alternative.

- 3,9-Dihalotriazoloquinolines **47a-c** have been prepared by means of a double metalation and have revealed their utility in the synthesis of interesting 8-halogen 2-quinolinecarboxyaldehydes (compounds **51a-c**).

- By this synthetic pathway, the triazole ring (which can be easily introduced by the hydrazine/MnO_2 method starting from quinoline aldehyde) has been used as protecting and activating group of 2-quinolinecarboxaldehydes providing highly substituted molecules with compatible substituent pattern towards subsequent functionalizations that cannot be obtained by direct metalation of quinoline aldehyde (**Scheme III-12**).

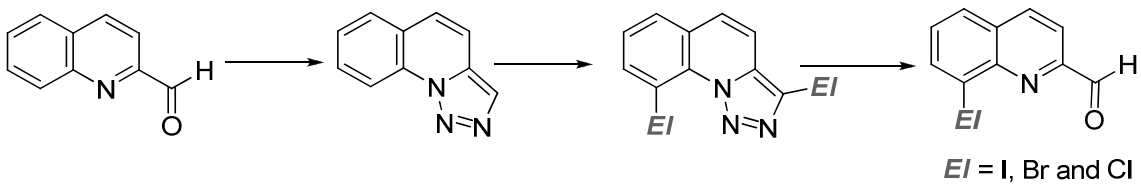

Scheme III-12: Synthesis of 8-haloquinolin-2-carboxaldehydes.

III :[1,2,3]Triazolo[1,5-*a*]quinoline

3.2 Triazoloquinoline-Pyridine Isomerisation

3.2.1 Introduction and objectives

As it outlined in chapter 1 (part 1.4) Abarca and Elguero proved, theoretically and experimentally, how, in the particular case of substituted 3-(2'-pyridyl)-[1,2,3]triazolo[1,5-*a*]pyridines (**1b**),[35] the ring-opening equilibrium can provide an isomerisation between two different isomers (**Figure III-5**).

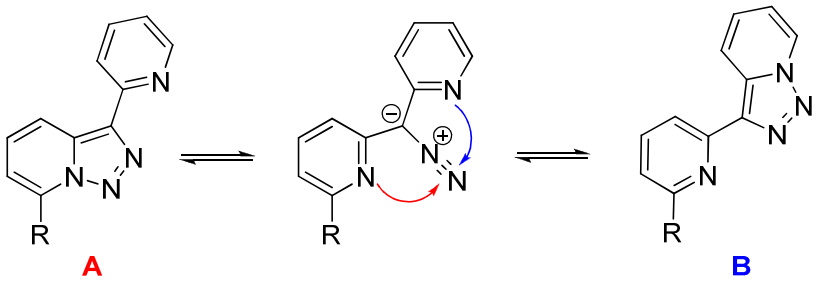

Figure III-5: The ring-chain isomerisation.

This ring-chain-ring isomerisation between structures **A** and **B** was found essentially dependant on the electronic properties of the R substituent. In general, compounds having an **A** structure are obtained with electron-donating substituents (R = TMS or $B(OR)_2$), meanwhile compounds with **B** structure are found with electron-withdrawing groups (R = I, Br, Cl...). We became interested in the possibility to provide a different isomerisation sensible to both electronic and steric properties. In this way the 9-fonctionalized triazoloquinoline revealed as a key compound in the search of this new isomerisation (**Figure III-6**). 9 Position leads the introduced substituent (R) close to the N^2 lone-pair being possible a steric interaction favouring maybe **B** structure with big R substituents.

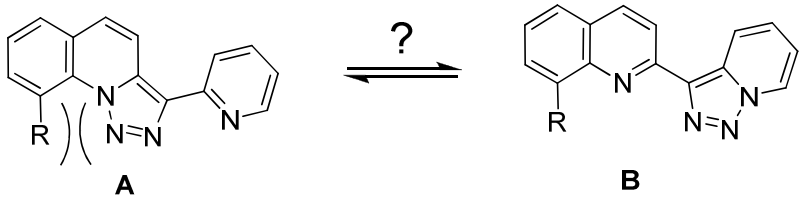

Figure III-6: The new ring-chain isomerisation.

As they are no longer two pyridines (but a quinoline and a pyridine) the rearrangement would provide different structures: Triazoloquinoline-pyridine or quinoline-triazolopyridine. Furthermore **A** and **B** isomers will no longer have the same energies providing a non degenerated equilibrium (in contrast to **1b**, see chapter 1, part 1.4). With the intention to study this new system (with an extra aromatic ring to **1b)** we pointed on:

- The synthesis of triazoloquinoline-pyridine and to perform a complete ^{1}H-NMR analysis of these structures (**A** and **B**).
- The synthesis of a family of functionalized compounds based on triazoloquinoline-pyridine and the study experimental a theoretical of the **A**/**B** isomerisation in terms of electron-density, steric hindrance or other possible effects.

This study was performed in collaboration with Dr. Fernando Blanco, Pr. Ibón Alkorta and Pr. José Elguero at the IQM (Madrid). Theoretical calculations were performed simultaneously in order to confirm/corroborate experimental results.

3.2.2 Synthesis, ^{1}H-NMR analysis and metalation of triazoloquinoline pyridine (53)

Triazoloquinoline-pyridine **53** was synthesized using a similar method as described for the synthesis of triazolopyridine-pyridine **1b** (R = H) starting from ketone **54**. However, pyridin-2-yl(quinolin-2-yl)methanone (**54**), was found to be commercial but a rare compound. In order to obtain it in large quantity 2-bromopyridine was submitted to a halogen/metal permutation with butyllithium in THF at -78 ^{o}C. Then it was added to methyl quinoline-2-carboxylate. Ketone **54** was obtained in 82% yield. Finally, **53** was synthesised according to the hydrazine/methanol method and then oxidized with MnO_2/chloroform, in excellent yield (**Scheme III-13**).[3]

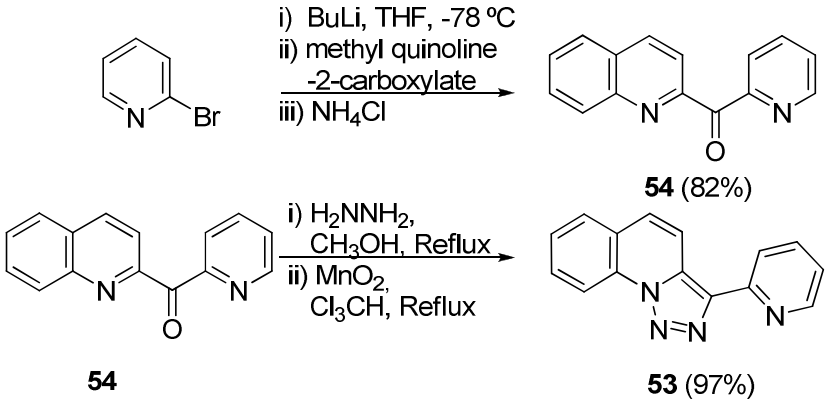

Scheme III-13: Synthesis of **53**.

With compound **1b** the isomerisation between **A** and **B** structures gave a degenerate equilibrium between two equal structures (**A** and **B, figure III-5**, R = H). In contrast, the isomerisation of the unsubstituted triazoloquinoline **53** leads to two distinctly different structures, the isomer **53A** (triazoloquinoline-pyridine), and the isomer **53B**, (quinoline-triazolopyridine) as depicted in **Figure III-6** (R = H). In this case, the ^{1}H-NMR spectra should present significantly different.

[1,2,3]Triazolo[1,5-*a*]pyridines show very typical ^{1}H-NMR spectra with characteristic coupling constants for the hydrogen at C^7, adjacent to the nitrogen bridge of the triazolopyridine ring (doublet near 8.7 ppm, $J_{H6\text{-}H7}$ = 6.9-7.1 Hz). This hydrogen can be clearly differentiated from hydrogen atoms in a pyridine system (broad doublet near 8.6 ppm, $J_{2H\text{-}3H}$ = 4.7-5.1 Hz) (**Figure III-7**). Also the triazoloquinoline structure has a characteristic coupling constant of $J_{8H\text{-}9H}$ = 8 Hz.(**Table III-2**)

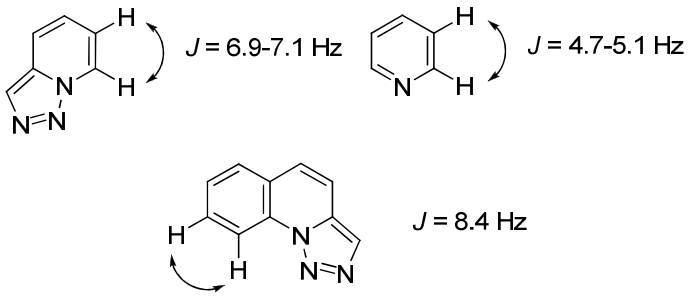

Figure III-7: Characteristic ^{1}H-NMR coupling constants.

The NMR analysis of compound **53** showed characteristic signals corresponding to pyridine and triazoloquinoline structures. No evidence for the presence of a triazolopyridine ring was found. Four significant signals (all doublets) appeared between 8.4 and 8.9 ppm (**Figure III-8**, down spectra).

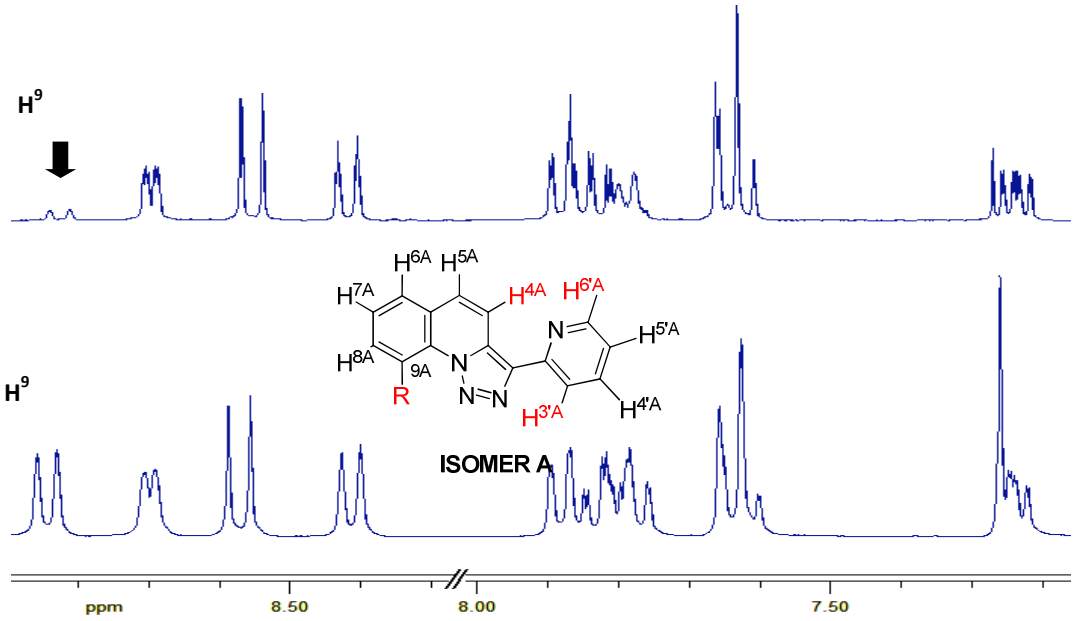

Figure III-8: ^{1}H-NMR of **53A** (down) and the corresponding 9-deuterated **50'A** compound (up).

Although the broad doublet near 8.7 ppm (J = 4.9 Hz) and the doublet at 8.4 ppm (J = 8.0 Hz) were enough to determine the **A** structure, we were also interested to attribute the other two signals. Indeed the most deshielded signal (8.86 ppm, J = 8.4 Hz) was found to be H^9 from the triazoloquinoline and the doublet near δ = 8.6 (J = 9.4 Hz) was associated to H^4. The chemical shift displacement of these signals (all between 8.3 – 8.99 ppm) was associated to the proximity of the different nitrogen atoms lone pairs.

With these observations, the conclusion was that the only isomer found was the corresponding triazoloquinoline-pyridine (**53A**), and no traces of the isomer **53B** were detected. The presence of a pure **A** structure for compound **53** provided a second question. Metalation of compound **53** can be controlled by different effects: It can rely on the ortho directing effect of the pyridine towards H^4, similar to previous works reported by Jones and

Abarca.[11] But we can also take advantage of the ortho directing effect of the triazole ring towards H^9, when the 3 position is protected (**scheme III-14**):

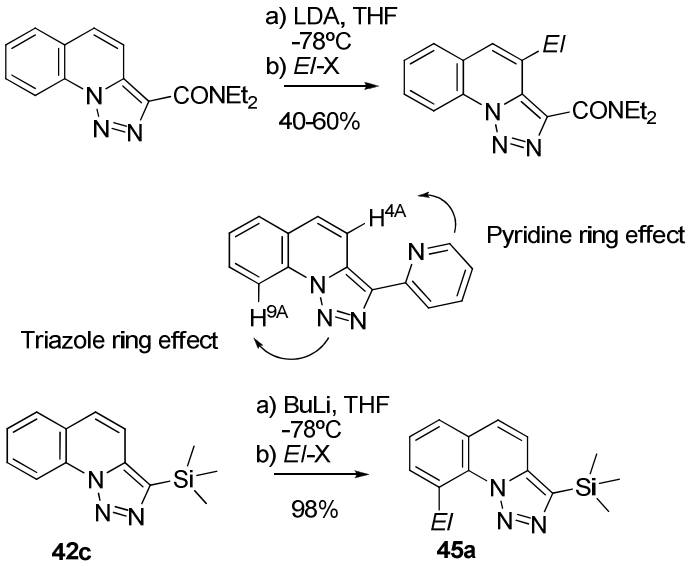

Scheme III-14: Different metalation position.

When 3-(2-pyridyl)-[1,2,3]triazolo[1,5-*a*]quinoline (**53**) was deprotonated with butyllithium in THF at -78 ºC followed by trapping with methanol-d_4 (**Scheme III-15**), the ^{1}H-NMR signal corresponding to proton H^9, the most down shielded-proton, disappeared almost completely (**Figure III-8**, up spectra). Thus, the deuteration of the benzo-part of **53A**, leads exclusively to **55A**. In contrast, 3-(2-pyridyl)-[1,2,3]triazolo[1,5-*a*]pyridine (**1b**) afforded after metalation and deuteration of the triazolopyridine ring the degenerated equilibrium **A**/**B** = 50/50 (see chapter 1, part 1.5) of the deuterated derivatives.

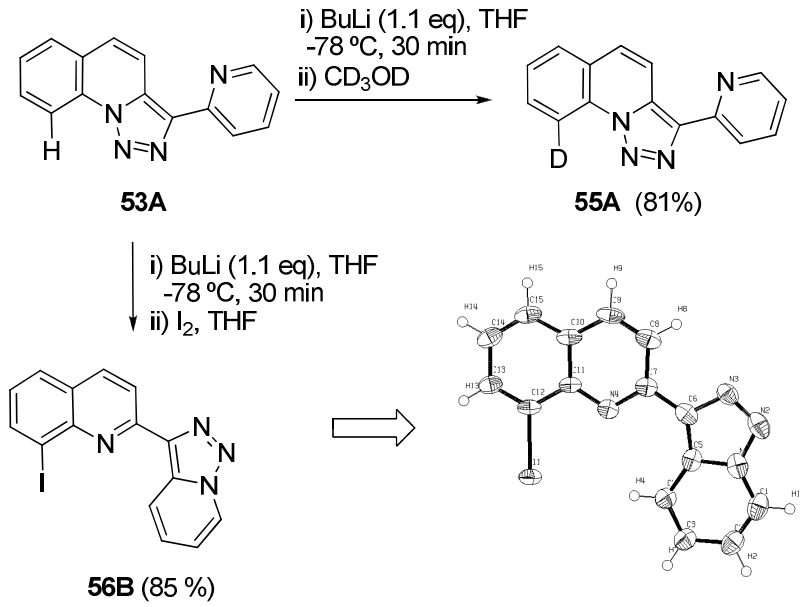

Scheme III-15: Synthesis of triazoloquinoline **55A** and triazolopyridine **56B.** X-Ray structure of **56B.**

When the same organometallic intermediate was quenched with iodine (**Scheme III-15**), a completely different pattern of the ^{1}H-NMR spectra was obtained with respect to the deuterated analogue **55A**. Now, the coupling constants indicated the exclusive presence of a quinoline-triazolopyridine ring system. These results suggest that the new iodo derivative possesses a structure of type **B** and is obtained by ring-chain isomerisation from the starting material with structure **A**. Furthermore, X-ray analysis confirmed the structure of the iodinated compound **56B**.

3.2.3 Reversibility of the isomerisation

As noticed before, we were able to obtain a **B** structure (compound **56B**) starting from a pure **A** structure (compound **53A**). In order to verify the reversibility of this isomerisation, compound **56B** was treated with butyllithium at -78 ºC and trapped with methanol in order to provide again compound **53A**. NMR analysis confirmed the transformation of **56B** in **53A** after work up (**Scheme III-16**).

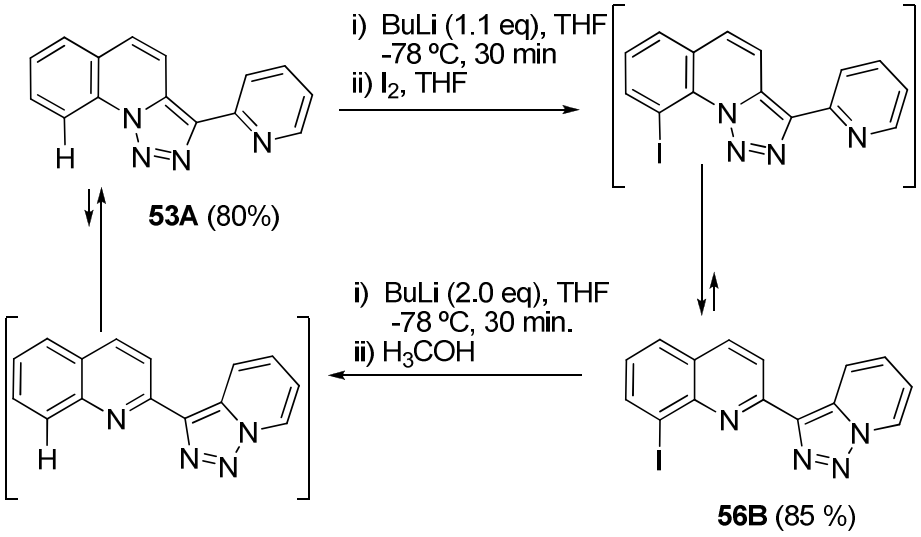

Scheme III-16: Reversibility of the isomerisation.

By this experience, we could demonstrate that although a preferential isomer can be obtained (**A** or **B**) the mechanism leading from **A** to **B** was reversible, being also valid for the interconversion of **B** into **A**.

3.2.4 Preparation triazoloquinoline-pyridines

Based on these results, we decided to prepare a series of new triazoloquinoline-pyridines by metalation of **53**, and reaction with different electrophiles. The lithiated intermediate was trapped with iodomethane affording after chromatography the methyl derivative **57** (77%). The brominated compound **58** was obtained after trapping with 1,2-dibromo-1,1,2,2-tetrafluoroethane (73%) and the chlorinated quinoline **59** (62%) by means of 1,2,2-trichlorotrifluoroethane. After trapping with NFSI **(***N*-fluorodibenzenesulfonimide) the fluorinated compound **60** was obtained in a yield of 50%. Carbinol **61** was obtained by quenching of the lithium intermediate with acetone (50%) (**Scheme III-16**).

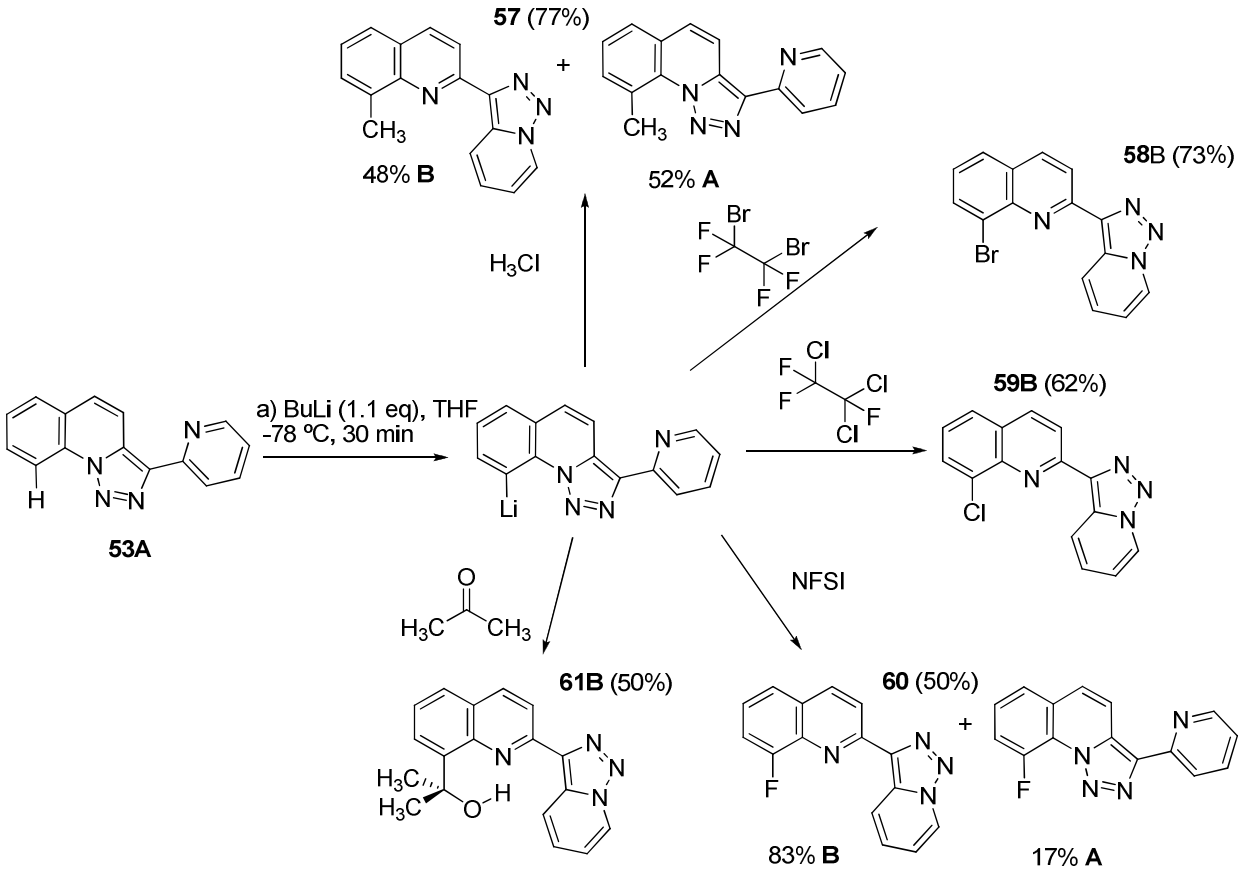

Scheme III-16: Preparation of compounds **52-56**.

Also by means of regioselective metalation at C^9 and trapping with the corresponding electrophiles compounds **62A** and **63A** were obtained in good yield. By employing fluorodimethoxyborane diethyl etherate as electrophile, alcohol **62A** was obtained in good yield (82%) after addition of alkaline hydrogen peroxide. Borane **63A** was also obtained in good yield (79%) by trapping with 2-isopropoxy-4,4,5,5-tetramethyl-1,3,2-dioxaborolane (**Scheme III-17**).

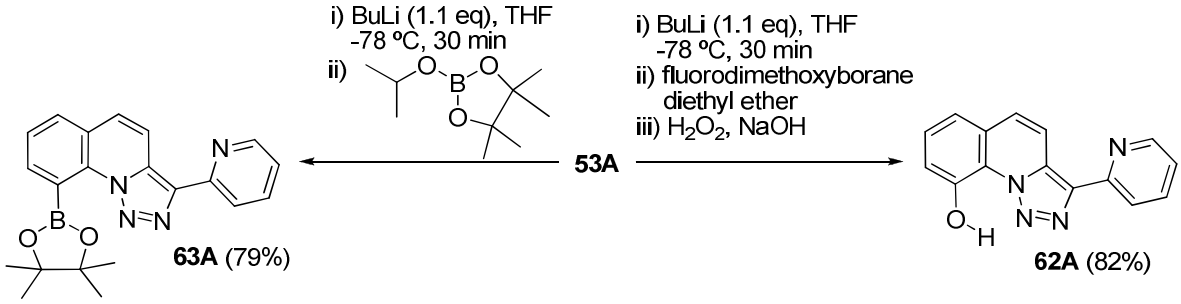

Scheme III-17: Preparation of compounds **62A** and **63A**.

The methoxy derivative **64** was synthesized by methylation of alcohol **62A** with methyl iodide and potassium carbonate in acetone (87%). Alcohol **62A** was also converted into the isopropyloxy derivate **65** using similar conditions but with an excess of 2-bromopropane in 80% yield (**Scheme III-18**). Unfortunately, all attempts to obtain a silylated derivative by trapping with different chloro trialkylsilanes were unsuccessful, probably due to steric hindrance of the C[9].

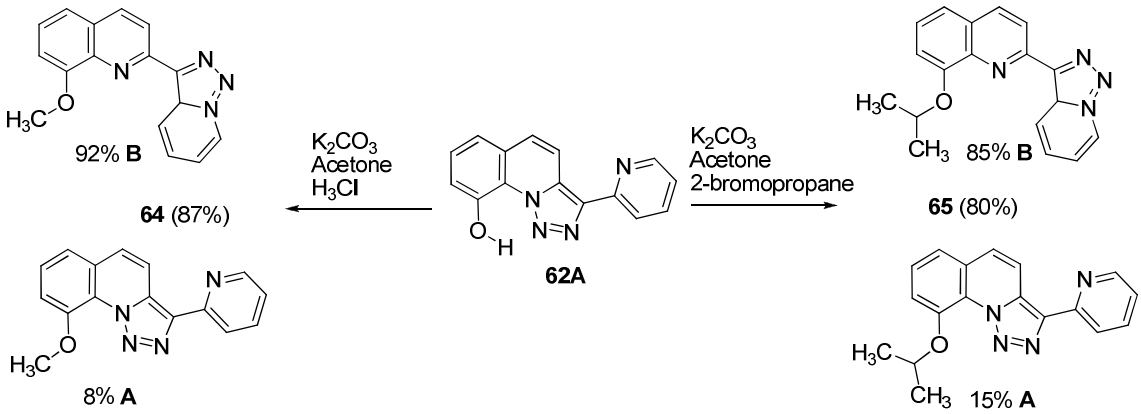

Scheme III-18: Synthesis of derivatives **64** and **65**.

Once again, the structure of the final products, **A** or **B**, depends on the electronic and steric properties of the substituent (**Scheme III-19**). Moreover, some of the synthesized derivatives (**57**, **60**, **64** and **65**) were obtained as a mixture of both isomers with a different ratio of distribution (**Tables III-3 and III-4**). These results allowed us to corroborate the existence of the isomer equilibrium.

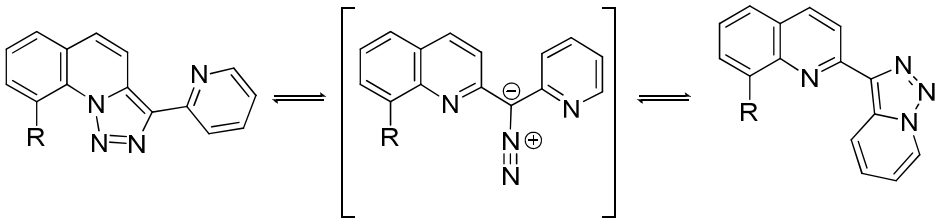

Structure A Structure B

		Ratio [%]	
53A	R = H	> 99 : 1	**53B** R = H
55A	R = D	> 99 : 1	**55B** R = D
56A	R = I	< 1 : 99	**56B** R = I
57A	R = CH_3	52 : 48	**57B** R = CH_3
58A	R = Br	< 1 : 99	**58B** R = Br
59A	R = Cl	< 1 : 99	**59B** R = Cl
60A	R = F	17 : 83	**60B** R = F
61A	R = $C(OH)(CH_3)_2$	< 1 : 99	**61B** R = $C(OH)(CH_3)_2$
62A	R = OH	> 99 : 1	**62B** R = OH
63A	R = $B(OR)_2$ pinacol ester	> 99 : 1	**63B** R = $B(OR)_2$ pinacol ester
64A	R = OCH_3	8 : 92	**64B** R = OCH_3
65A	R = O^{i}Pr	15 : 85	**65B** R = O^{i}Pr

Scheme III-19: Various triazoloquinoline derivatives obtained according to the substituent nature at C9. Ratio determined by ^{1}H-NMR in $CDCl_3$

3.2.5 ^{1}H-NMR analysis of compounds 53-65

In **Tables III-3 and III-4** the ^{1}H-NMR data of all synthesized derivatives are reported. The δ and J values of the most characteristic signals prove that compounds **A** present a triazoloquinoline-pyridine system, whereas compounds **B** present a quinoline-triazolo-pyridine structure.

A-type structures: As outlined before (**Figure III-8**), the unsubstituted derivative **50A** (R = H) shows four characteristic signals between 8 and 9 ppm corresponding to the hydrogen atoms closest to the ring nitrogen (protons in red, **Figure III-9** and **Figure III-8** down spectra). For all molecules belonging to the **A**-series, the pyridine ring-system could well be characterized as reported in **Table III-3**. All compounds of this series show similarities related to the coupling constants and chemical shifts for the signals of H^{4A} (δ = 8.5-8.6 ppm, $J_{H4A\text{-}H5A}$ = 9.3-9.4 Hz) and H^{5A} (δ = 7.5-7.6 ppm, $J_{H4A\text{-}H5A}$ = 9.3-9.4 Hz), as well as for the pyridine hydrogen atoms $H^{3'A}$ and $H^{6'A}$ (columns 3' and 6' in **Table III-3**). These characteristics remained constant for the whole **A** family, for example compound **63A** (**Figure III-10**, up spectra).

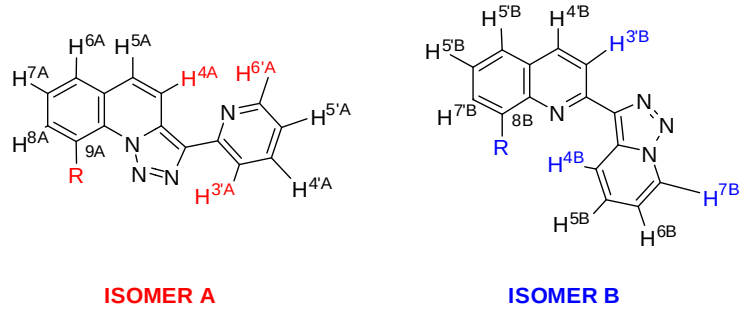

Figure III-9: . Proton assignment for **A**- and **B**-type isomers.

B-type structures: The same analysis which was applied to the **A**-series, revealed similar ^{1}H-NMR patterns for the quinoline proton $H^{3'B}$ (δ = 8.5-8.6 ppm, $J_{H3'B-H4'B}$ = 8.6-8.7). For all studied systems B the signals corresponding to the triazolopyridine-ring could be well characterized (H^{7B}, H^{6B}, H^{5B} and H^{4B}) with H^{4B} being the most down shielded signal in all cases (protons in blue, **Figure III-9** and **III-10** down spectra, and **Table III-4**).

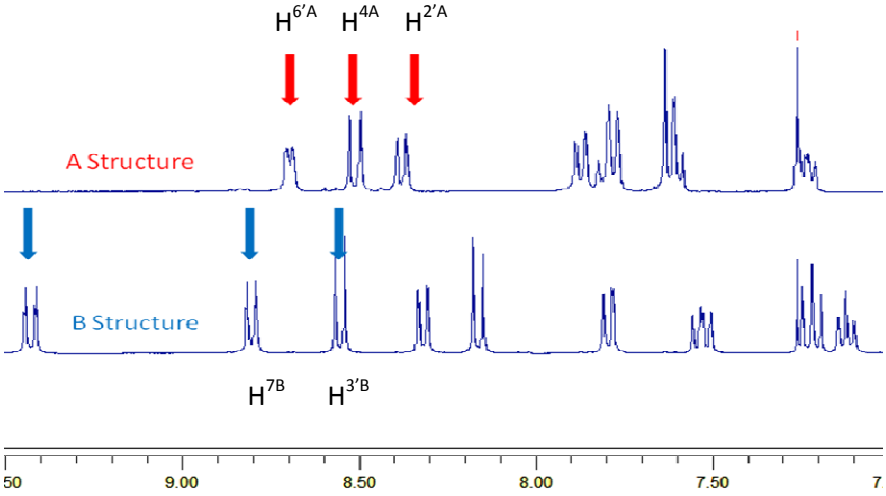

Figure III-10: Aromatic region for the ^{1}H-NMR spectra of a representative structure **A** (**63**, up) and a representative structure **B** (**56**, down).

The chemical shift of the H^{4B} proton revealed to be very sensitive towards the nature of the substituent R. This phenomenon can be associated to the geometry of the B structure where the two heterocyclic ring systems are oriented with the nitrogen atoms being opposite to each other in order to avoid unfavourable repulsion between the nitrogen lone pairs. According to this orientation, the hydrogen H^{4B} shows towards the lone pair of the quinoline ring nitrogen, and is close to the substituent R. Thus, the proximity H^{4B} and R explain the subtle influence of R onto the shielding of H^{4B}. This hypothesis was supported by analyzing the different halogenated derivatives. As we can see in **Table III-4** there is a marked decrease of the chemical shift of H^{4B} with the decrease of the size of the halogen: δ = 9.43 ppm for the iodo compound **56B**, 9.29 ppm for bromo derivative **58B** and 9.12 and 9.03 for the chloro- and fluoroquinolines **59B** and **60B**, respectively.

Table III-3. ^{1}H-NMR data for compounds that provided type **A** structures.

Product	4	5	6	7	8	9	3’	4'	5'	6'	others
53A	**8.53 d**	**7.6-7.5 m**	**7.9-7.8 m**	**7.6-7.5 m**	**7.9-7.8 m**	**8.86 d**	**8.42 d**	**7.9-7.8 m**	**7.24 dd**	**8.70 brd**	
	J_1 = 9.3					J_1 = 8.4	J_1 = 8.0		J_1 = 7.4	J_1 = 4.9	
									J_2 = 4.9		
57A	**8.61 d**	**7.62 d**	**7.6-7.4 m**	**7.6-7.4 m**	**7.6-7.4 m**	**CH_3**	**8.41 ddd**	**7.82 ddd**	**7.24 ddd**	**8.7 brd**	**3.26 s CH_3**
A/B:	J_1 = 9.3	J_1 = 9.3					J_1 = 8.0	J_1 = 8.0	J_1 = 7.6	J_1 = 4.8	
							J_2 = 1.0	J_2 = 7.8	J_2 = 4.8	J_2 = 1.0	
							J_3 = 1.0	J_3 = 1.0	J_3 = 1.0	J_3 = 1.0	
60A	**8.63 d**	**7.7-7.4 m**	**7.7-7.4 m**	**7.7-7.4 m**	**7.7-7.4 m**	**F**	**8.42 brd**	**7.81 app td**	**7.25 ddd**	**8.68 d**	
A/B:	J_1 = 9.4						J_1 = 8.0	J_1 = 7.9	J_1 = 7.7	J_1 = 4.8	
								J_2 = 7.8	J_2 = 4.8		
								J_3 = 1.8	J_3 = 1.1		
62A	**8.56 d**	**7.70 d**	**7.4-7.3 m**	**7.52 app t**	**7.4-7.3 m**	**OH**	**8.38 d**	**7.86 apptd**	**7,30 ddd**	**8.73 brd**	**10.71 s OH**
	J_1 = 9.4	J_1 = 9.4		J_1 = 7.9			J_1 = 8.0	J_1 = 7.8	J_1 = 7.5	J_1 = 4.8	
								J_2 = 7.8	J_2 = 4.8		
								J_3 = 1.1	J_3 = 1.1		
63A	**8.52 d**	**7.53 d**	**7.87 dd**	**7.6-7.5 m**	**7.6-7.5 m**	**$B(OR)_2$**	**8.38 ddd**	**7.6-7.5 m**	**7.23 ddd**	**8.70 ddd**	**1.58 s 4 CH_3**
	J_1 = 9.3	J_1 = 9.3	J_1 = 7.9			pinacol	J_1 = 8.0		J_1 = 7.5	J_1 = 4.9	
			J_2 = 1.3			borane	J_2 = 1.0		J_2 = 4.9	J_2 = 1.7	
							J_3 = 1.0		J_3 = 1.0	J_3 = 1.0	
64A	**8.55 d**	**7.6-7.4 m**	**7.30 dd**	**7.6-7.4 m**	**7.6-7.4 m**	**OCH_3**	**8.34**	**7.6-7.4 m**	**7.3-72**	**8.60 m**	**4,18 s OCH_3**
A/B:	J_1 = 9.3		J_1 = 7.9				J_1 = 7.9				
			J_2 = 1.3								
65A	**8.63 d**	**7.51 d**	**7.4-7.3 m**	**7.43 app t**	**7.4-7.3 m**	**O^{i}Pr**	**8.44 ddd**	**7.73 ddd**	**7.15 ddd**	**8.69 d**	**4.74 sp A O^{i}Pr**
A/B:	J_1 = 9.3	J_1 = 9.3		J_1 = 7.8			J_1 = 7.9	J_1 = 7.9	J_1 = 7.6	J_1 = 4.9	J_1 = 6.1
							J_2 = 0.9	J_2 = 7.8	J_2 = 4.9	J_2 = 1.7	**1.58 d (A+B) O^{i}Pr**
							J_3 = 0.9	J_3 = 1.8	J_3 = 1.0	J_3 = 0.9	J_1 = 6.1

Table III-4. ^{1}H-NMR data for compounds that provided type **B** structures.

Product	3'	4'	5'	6'	7'	8’	4	5	6	7	others
56B	**8.55 d**	**8.16 d**	**7.80 dd**	**7.22 app t**	**8.31 dd**	**I**	**9.43 td**	**7.53 ddd**	**7.12**	**8.80 td**	
	J_1 = 8.6	J_1 = 8.6	J_1 = 8.0	J_1 = 7.7	J_1 = 7.4		J_1 = 8.9	J_1 = 8.9	J_1 = 6.9	J_1 = 6.9	
			J_2 = 1.2		J_2 = 1.2		J_2 = 1.0	J_2 = 6.7	J_2 = 6.9	J_2 = 1.0	
							J_3 = 1.0	J_3 = 1.0	J_3 = 1.0	J_3 = 1.0	
57B	**8.50 d**	**8.23 d**	**7.6-7.4 m**	**7.6-7.4 m**	**7.6-7.4 m**	**CH_3**	**8.98 ddd**	**7.48 ddd**	**7.12 app**	**8.83 ddd**	**2.93 s CH_3**
A/B: 52/48	J_1 = 8.6	J_1 = 8.6					J_1 = 8.9	J_1 = 8.9	J_1 = 6.9	J_1 = 7.0	
							J_2 = 1.0	J_2 = 6.7	J_2 = 6.9	J_2 = 1.0	
							J_3 = 1.0	J_3 = 1.0	J_3 = 1.0	J_3 = 1.0	
60B	**8.56 d**	**8.24 dd**	**7.6-7.4 m**	**7.6-7.4 m**	**7.6-7.4 m**	**F**	**9.03 td**	**7.6-7.4**	**7.1 ddd**	**8.79 ddd**	
A/B: 17/83	J_1 = 8.7	J_1 = 8.7					J_1 = 8.9		J_1 = 6.9	J_1 = 7.0	
		J_2 = 1.2					J_2 = 1.0		J_2 = 6.8	J_2 = 1.0	
							J_3 = 1.0		J_3 = 1.0	J_3 = 1.0	
64B	**8.52 d**	**8.21 d**	**7,07 d**	**7.5-7.4 m**	**7,5-7.4 m**	**OCH_3**	**9.03 td**	**7.48 m**	**7.10 app**	**8.79 ddd**	**4,14 s OCH_3**
A/B: 8/92	J_1 = 8.6	J_1 = 8.6	J_1 = 6,8				J_1 = 8.9	J_1 = 8.9	J_1 = 6.9	J_1 = 7.0	
							J_2 = 1.0	J_2 = 6.7	J_2 = 6.9	J_2 = 1.0	
							J_3 = 1.0	J_3 = 1.0	J_3 = 1.0	J_3 = 1.0	
58B	**8.57 d**	**8.24 d**	**8.05 dd**	**7.36 app t**	**7.79 dd**	**Br**	**9.29 td**	**7.54 ddd**	**7.13 ddd**	**8.81 ddd**	
	J_1 = 8.6	J_1 = 8.6	J_1 = 7.5	J_1 = 7.8	J_1 = 8.0		J_1 = 8.9	J_1 = 8.9	J_1 = 6.9	J_1 = 7.0	
			J_2 = 1.2		J_2 = 1.2		J_2 = 1.0	J_2 = 6.7	J_2 = 6.8	J_2 = 1.0	
							J_3 = 1.0	J_3 = 1.0	J_3 = 1.0	J_3 = 1.0	
59B	**8.58 d**	**8.26 d**	**7.84 dd**	**7.43 app**	**7.75 dd**	**Cl**	**9.21 td**	**7.54 ddd**	**7.13 ddd**	**8.81 ddd**	
	J_1 = 8.6	J_1 = 8.6	J_1 = 7.5	J_1 = 7.8	J_1 = 8.1		J_1 = 8.9	J_1 = 8.9	J_1 = 6.9	J_1 = 7.0	
			J_2 = 1.2		J_2 = 1.2		J_2 = 1.0	J_2 = 6.7	J_2 = 6.8	J_2 = 1.0	
							J_3 = 1.0	J_3 = 1.0	J_3 = 1.0	J_3 = 1.0	
61B	**8.62 d**	**8.33 d**	**7.70 dd**	**7.5-7.4 m**	**7.75 dd**	**C(OH)(CH_3)**	**8.80 ddd**	**7.56 ddd**	**7.12 ddd**	**8.83 ddd**	**8.35 s OH**
	J_1 = 8.7	J_1 = 8.7	J_1 = 7.4		J_1 = 8.0		J_1 = 9.0	J_1 = 9.0	J_1 = 6.9	J_1 = 7.0	**1.90 2 CH_3**
			J_2 = 1.3		J_2 = 1.3		J_2 = 1.0	J_2 = 6.7	J_2 = 6.8	J_2 = 1.0	
							J_3 = 1.0	J_3 = 1.0	J_3 = 1.0	J_3 = 1.0	
65B	**8.50 d**	**8.21 d**	**7.1-7.0 m**	**7.5-7.4 m**	**7.5-7.4 m**	**O^{i}Pr**	**9.20 td**	**7.46 m**	**7.09 app**	**8.80 ddd**	**4.90 sp B O^{i}Pr**
A/B: 15/85	J_1 = 8.6	J_1 = 8.6					J_1 = 8.9	J_1 = 8.9	J_1 = 6.9	J_1 = 7.1	J_1 = 6.0
							J_2 = 1.0	J_2 = 6.7	J_2 = 6.9	J_2 = 1.0	**1.59 d (A+B) O^{i}Pr**
							J_3 = 1.0	J_3 = 1.0	J_3 = 1.0	J_3 = 1.0	J_1 = 6.1

3.2.6 General trends observed by the analysis of compounds 53-65

- As expected, electron-donating substituents favor the structures of type **A**, whereas electron-accepting groups favor **B**-type structures. This observation corresponds to the triazolopyridine-pyridine ring system **1b**.

- The ^{1}H-NMR chemical shifts H^{4A}, $H^{6'A}$, $H^{3'A}$, $H^{3'B}$, H^{4B} and H^{7B} indicate that, in chloroform, all systems present an *anti* orientation of the two heterocyclic subunits in order to avoid repulsive interactions between the nitrogen lone pairs. This observation was confirmed by X-ray structural analysis of compound **56B** as shown in **Scheme III-15**.

- If one considers only the electronic properties of substituents, the methyl derivative **57** should adopt essentially the donor-structure **57A**. For example the analogous 3-(2-pyridyl)-7-methyl[1,2,3]triazolo[1,5-*a*]pyridine systems shows a **A/B** ratio of 75:25 favouring the donor structure (**Figure III-11**).[35] In contrast, the isomeric ratio found for the methyl derivative **57A/57B** = 52:48 indicates, that in the triazoloquinoline-pyridine ring systems steric effects must play an important role influencing the isomeric distribution (**A/B**). The structure **B** is sterically more favourable than the initial structure **A.**

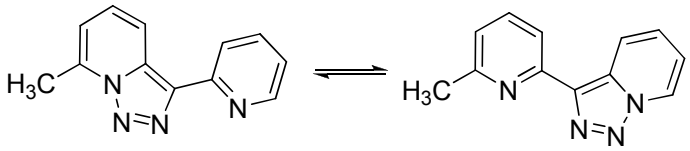

Figure III-11: Corresponding ratio for 7-methyl-3-(2-Pyridyl)-[1,2,3]triazolo[1,5-*a*]pyridine

- We studied also the equilibrium **57A/57B** in function of temperature and solvent. The initial ratio was not modified when the mixture was heated up to 65 °C (ratio **A/B** = 52:48). However, when changing the polarity of the solvent (acetone-d_6 *vs.* chloroform-d_1), an inversion of the isomeric distribution (ratio **A/B** = 41:59) can be observed (**Figure III-12**). Differences in the dipole moments of both structures (**5A** and **5B**) as confirmed by the computational studies are certainly responsible for this behaviour. The solvent effect was also evaluated with the mixture of compounds **60A/60B**, however, the small modification (< 1%) did not allow to establish a general conclusion in this case.

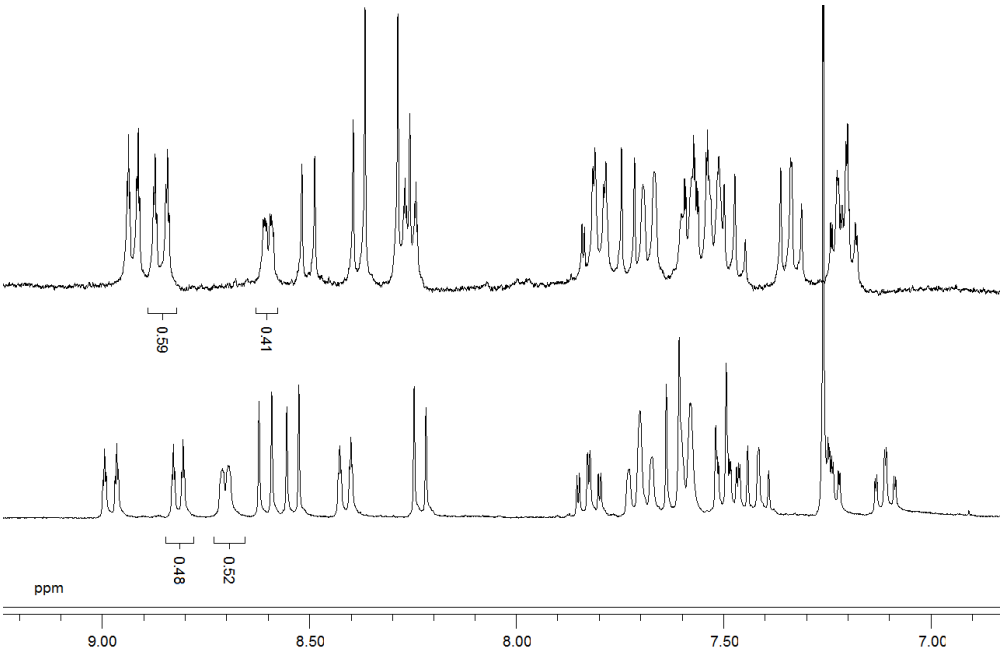

Figure III-12: ^{1}H-NMR of compound **52** in ^{6}d-acetone (up) and $CDCl_3$ (down).

- Compounds **62A** was found as a unique isomer with **A** structure. In this case other effects different to the electronic character of the substituent may have a significant influence. The possibility of an intramolecular hydrogen bond, as will be explained in the computional section, must also be accounted in the whole effect. The ^{1}H-NMR deshielding of the OH signal (δ = 10.71 ppm) could be associated to the coordination with one of the nitrogen (N^{1}) atom of the adjacent ring by a hydrogen bond.

3.2.7 Computational studies (Gaussian and AIMM)[36, 37]

Two aspects of the structural behaviour of 3-(2-pyridyl)-[1,2,3]triazolo[1,5-*a*]quinolines have been studied computationally: the energetic profile of the isomerisation process for the unsubstituted derivative, and the isomer ratio **A**/**B** in function of the substituents.

3.2.7.1 Reaction profile (53, R = H)

Figure III-13 shows the stationary points (minima and TS's) of the isomerisation reaction. The picture reveals an intricate process with several possible alternative paths combining opening and rotational steps. We have found eight local minima, four closed-ring (**M1-4**) and four open-chain (**M5-8**) isomers, and the subsequent transition states (**TSXY**). For the studied derivative (**53**, R = H), the global minimum corresponds to **M1**, the closed triazoloquinoline-pyridine isomer (**53A**) which is 14.9 kJmol^{-1} more stable than **M3**, corresponding to the quinoline-triazolopyridine system (**53B**). **M2** and **M4** minima are the rotational isomers of **M1** and **M3**, respectively, and present lower stability due to repulsive effects explained in the next section.

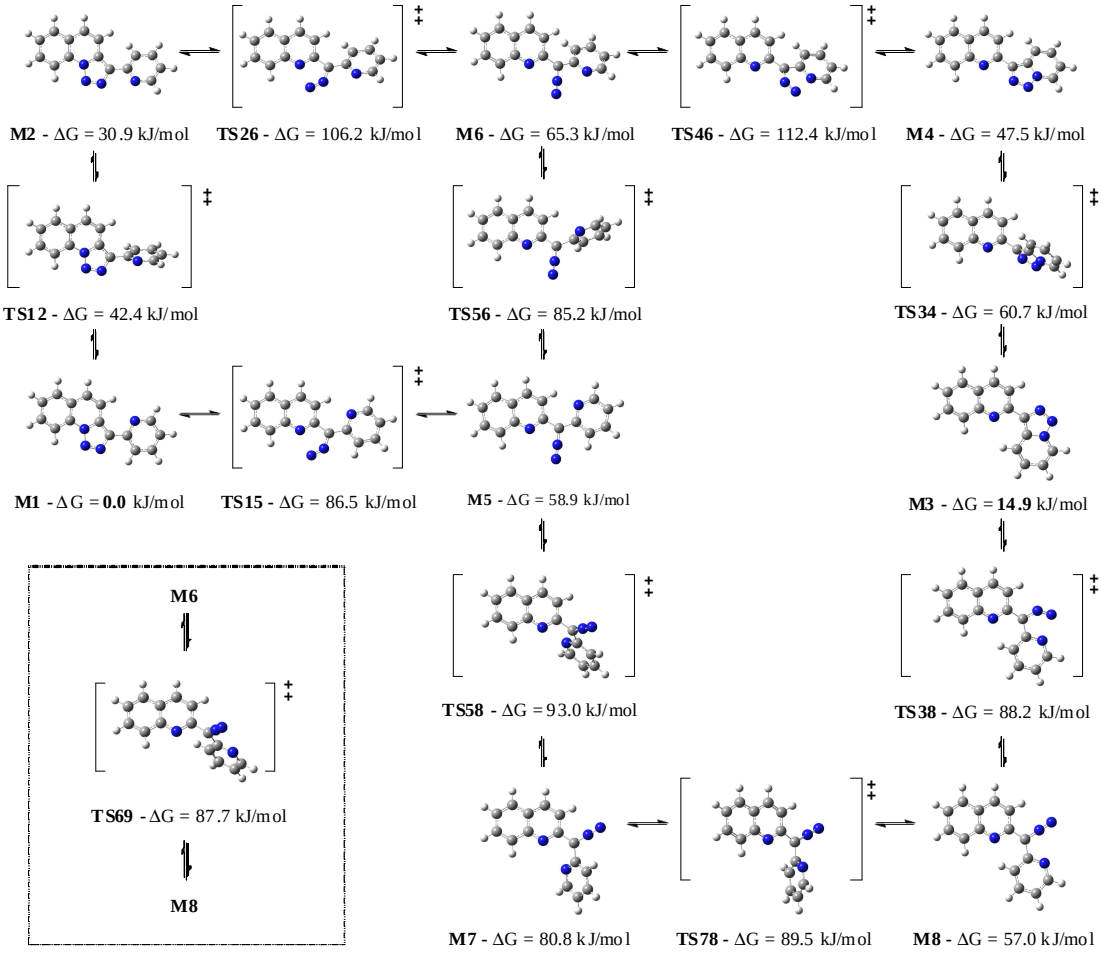

Figure III-13: Stationary points (minima and TS's) of the isomerisation reaction for **53** (R = H).

The open-chain minima (**M5-8**) show higher relative energy values. Given the complexity of the sequence, it is not easy to establish a single well-defined path to explain the equilibrium between the absolute minimum of each series (**M1** and **M3**). Therefore, we will make an explanation of the most likely situation considering the route which presents the transition states with lower energetic barriers. According to this criterion, we can see in the energetic diagram (Figure III-14, red pathway) that the most favourable way from **M1** to **M3** proceeds by a first opening step of **M1** through a planar **TS15** transition state giving the **M5** intermediate, two consecutive rotational steps of the two heterocyclic rings over the diazo group (giving the **M6** and **M8** intermediates, respectively) and a final locking ring step of **M8** to form the close isomer **M3**. From **M5** to **M8** there is a second slightly less favourable way through the intermediate **M7** (Figure III-14, yellow pathway). Other possible sequences starting with a rotation of the ring from **M1** to **M2** pass through a second opening step with a significant higher energetic barrier transition state **TS26** (Figure III-14, blue pathway).

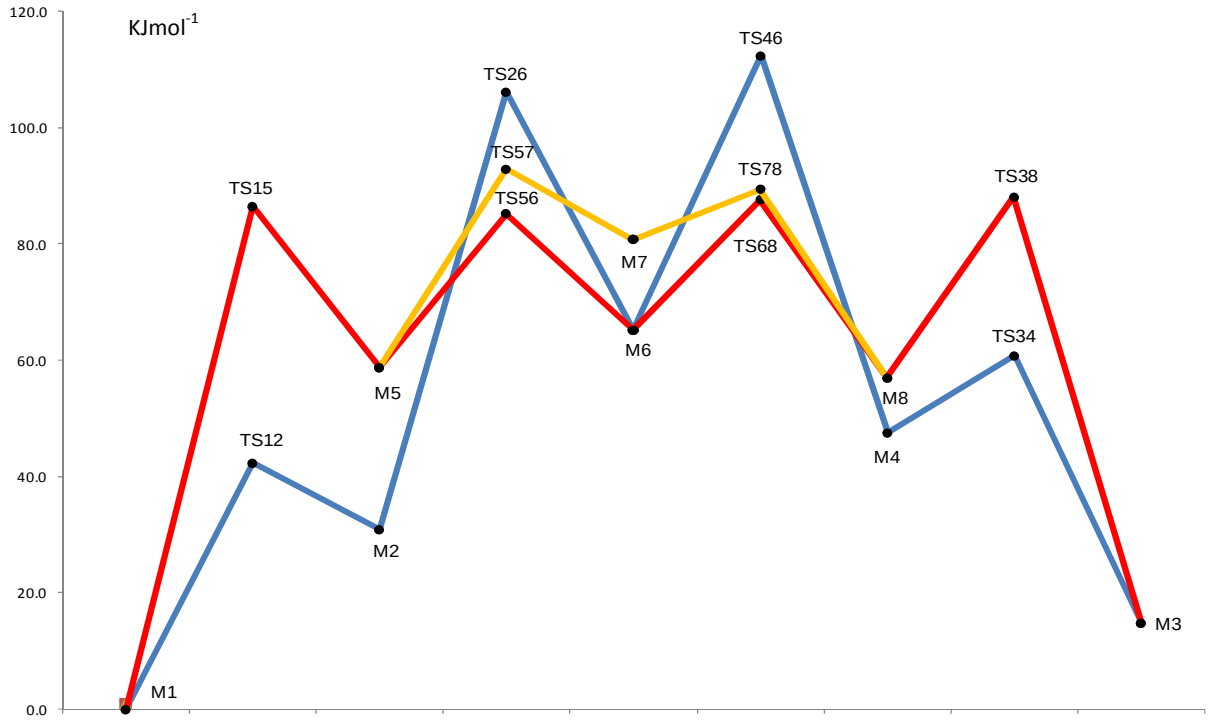

Figure III-14: Energy diagram of the isomerisation reaction for compound **53** (R=H).

3.2.7.2 A/B ratio (computational aspects)

In order to see the effect of the substituent on the **A/B** ratio, different R groups have been chosen to be studied, some of them corresponding to those obtained experimentally. For all substituents the four closed isomers (**Figure III-15**) were calculated.

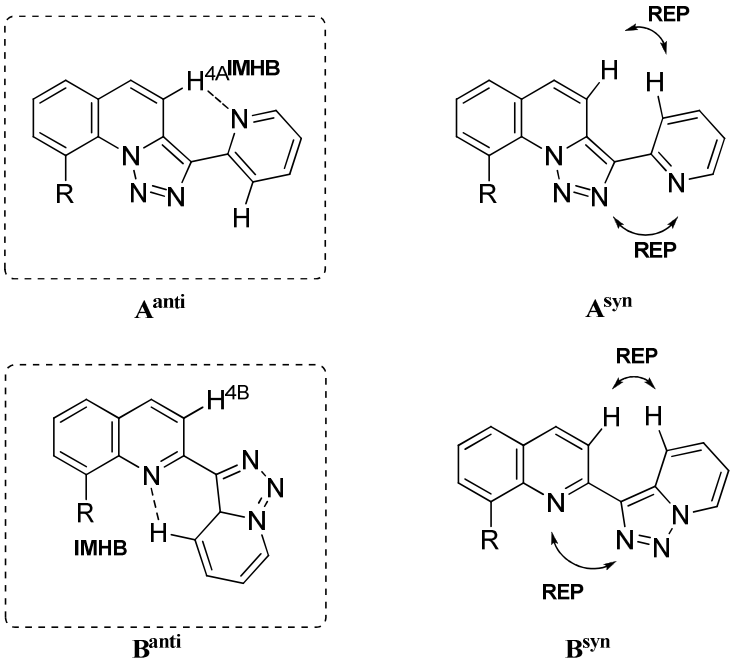

Figure III-15: Structure of the isomers studied theoretically.

Except in the case of R = Li, $\mathbf{A}^{anti}$ and $\mathbf{B}^{anti}$ are more stable than the respective rotamers $\mathbf{A}^{syn}$ and $\mathbf{B}^{syn}$. The geometry of them is more favourable as the repulsive effect between the nitrogen lone pairs and the proximal hydrogen atoms are avoided. In addition, these structures allow an extra stabilization due to intramolecular hydrogen bonding (**IMHB**) between H^{4A} and the pyridine nitrogen (structure $\mathbf{A}^{anti}$) or H^{4B} and the quinoline nitrogen in structure $\mathbf{B}^{anti}$, respectively (**Figure III-16**). These factors explain, in the same way, the geometrical preference between the two heterocyclic ring systems. In general, **A** and **B** structures adopt a planar *anti* orientation, whereas the $\mathbf{A}^{syn}$ and $\mathbf{B}^{syn}$ structures should adopt torsional arrangement.

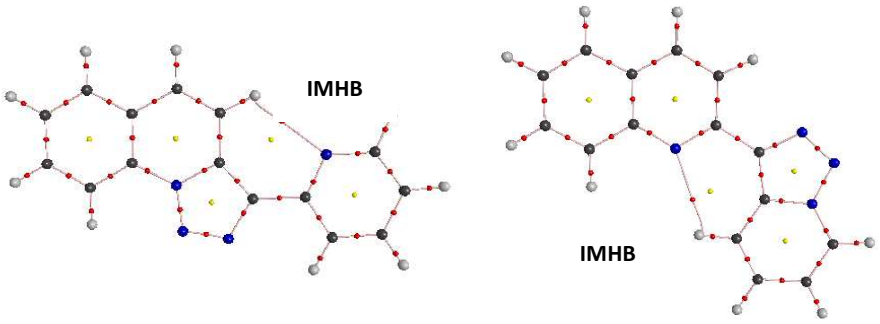

Figure III-16. Molecular graph of the electron density analysis of the structures **53A** (left) and **53B** (right). Bond and ring critical points are indicated with red and yellow dots and the lines connecting the atoms show the bond paths.

For certain cases (R = OH, CHO, OCH_3, NH_2, $N(CH_3)_2$), we have evaluated a large number of structures considering the relative orientation of the substituent, since it could have an important influence on the final stability of the molecule, due to the possibility of creating attractive interactions by hydrogen bonding or repulsive ones between neighbouring atoms (**Figure III-17**).

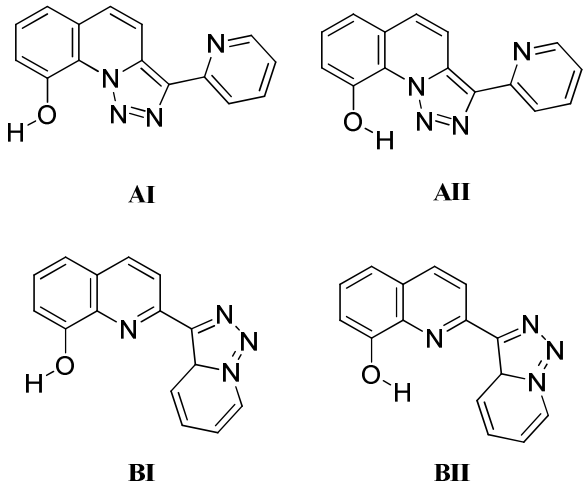

Figure III-17. Structures studied in function of the substituent orientation

Table III-5 shows the relative energies between the most stable configurations of each substituent considered. Negative values reflect that, for the corresponding compound, the isomer **A** is favoured with respect to form **B** and positive values the opposite situation. We can observe that the predictions deduced from the theoretical calculations are in agreement with the experimental results.

Table III-5: Calculated **A/B** ratios of the derivatives ($kJmol^{-1}$). Compounds synthesized are indicated with their corresponding numeration.

Entry	Compound	R	ΔE (Kjmol-1)	Theoretical A/B-ratio	Experimental A/B-ratio
1		Li	-66.11	A	---
2		BH_2	-60.58	A	---
3	**62**	OH	-19.87	A	> 99 : 1
4	**63**	$B(OH)_2$	-16.25	A	> 99 : 1
5	**53**	H	-15.56	A	> 99 : 1
6		NH_2	-15.54	A	---
7		SiH_3	-9.66	A	---
8		$Si(CH_3)_3$	-6.34	A	---
9	**57**	CH_3	-4.68	A/B Mixture	52 : 48
10		CHO	2.84	A/B Mixture	---
11	**60**	F	3.70	A/B Mixture	17 : 83
12	**65**	$OCH(CH_3)_2$	3.78	A/B Mixture	15 : 85
13	**64**	OCH_3	5.02	A/B Mixture	9 : 92
14		$N(CH_3)_2$	7.06	B	---
15	**61**	$C(OH)(CH_3)_2$	14.90	B	< 1 : 99
16	**59**	Cl	16.98	B	< 1 : 99
17		CN	17.96	B	---
18	**56**	I	19.95	B	< 1 : 99
19		$C(CH_3)_3$	20.61	B	---
20	**58**	Br	21.28	B	< 1 : 99
21		NO_2	21.84	B	---
22		CF_3	22.08	B	---

3.2.7.3 General Trends

The electronic properties of the substituent play an essential role in the equilibrium. The general trend is that electron-donating substituents stabilize the isomers of type **A** (R = Li (carbanion), BH_2, $B(OH)_2$, H, SiH_3, $Si(CH_3)_3$) (**Table III-5**, entries 1, 2, 4, 5, 7 and 8), whereas electron-accepting substituents stabilize the isomers type **B** (R = CF_3, NO_2, Br, I, CN, Cl, NMe_2, OCH_3) (**Table III-5** entries 14-18 and 20-22). This observation is in accordance with the experimental results obtained in this work for the derivatives (R = $B(OH)_2$, H, Cl, Br, I) and is in analogy to the isomerisation equilibrium of 3-(2-pyridyl)-[1,2,3]triazolo[1,5-*a*]pyridines.

In those cases where the calculated energy difference between the two isomers was lower than 5 $kJmol^{-1}$, CH_3 (**57**), CHO, F (**60**), $OCH(CH_3)_2$ (**65**) and OCH_3 (**64**) (**Table III-5**, entries 9-13) the experimental results show a mixture of both isomers. Furthermore, the experimental ratios were coherent with the sign of the value for the calculated energies. The energetic ratio calculated for the methyl derivative **57** (R = CH_3) is very low if we only take electronic criteria

into consideration. Moreover, the parent compound **53** (R = H) clearly favours the form **A**. This fact could be explained by the influence of steric effects as outlined above.

The structures bearing a halogen atom follow the general criteria, *i.e.* structure type **B** being more favourable due to their electronegativity (**Table III-5**, entries 11, 16, 18 and 20. However, their stability (Br > I > Cl >> F) is not directly related to the electronegative character of the halogen (F > Cl > Br> I). The ratio **A/B** is considerably more favourable for the isomer **B** in case of the bromo and iodo derivatives than for the fluorinated one. The formation of intramolecular hydrogen bonds together with possible steric factors may justify this order of stability. As it is shown in the graphical AIM analysis, in the case of bromine and iodine, due to the geometry of the molecule and the electronic properties of the halogens, we can observe an interaction between the halogen and the neighbouring hydrogen atom creating a bifurcated hydrogen bond.[38] In the case of chlorine and fluorine, this interaction is less pronounced, insufficient to reflect a bifurcated hydrogen bond in the AIM analysis (**Figure III-18**).

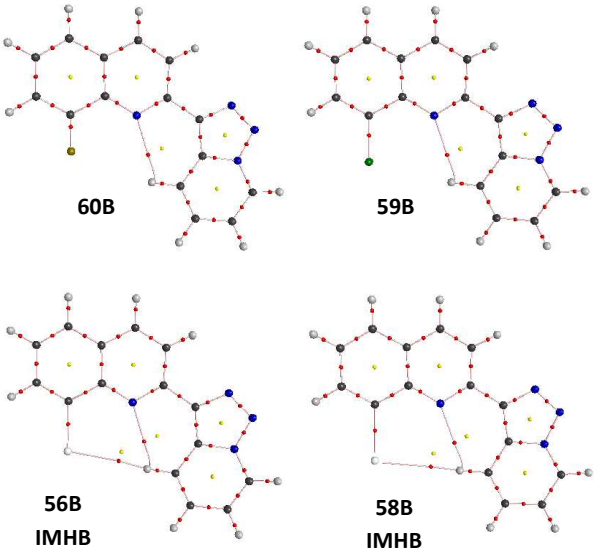

Figure III-18: Molecular graph of the electron density analysis of the halogenated derivatives.

This **IMHB** interaction between the halogens and the proton H^{4B} is reflected in the ^{1}H-NMR spectra. **Figure III-19** shows how the signal corresponding to H^{4B} is significantly shifted downfield from the fluoro derivative **60B**, to the chloro- **59B**, bromo- **58B** and iodo-analogue **56B**. Given the geometry of the molecules, the most likely explanation is that the influence of the halogen on H^{4B} occurs by spatial proximity, leaving out a possible connectivity effect due to the large distance that separates the two nuclei through the bonds. It is known that the interaction by hydrogen bond produces a deshielding of the hydrogen involved. As we can see in **Figure III-19**, for the series of halogenated compounds there is an increasing deshielding of the signal H^{4B} from fluorine to iodine.

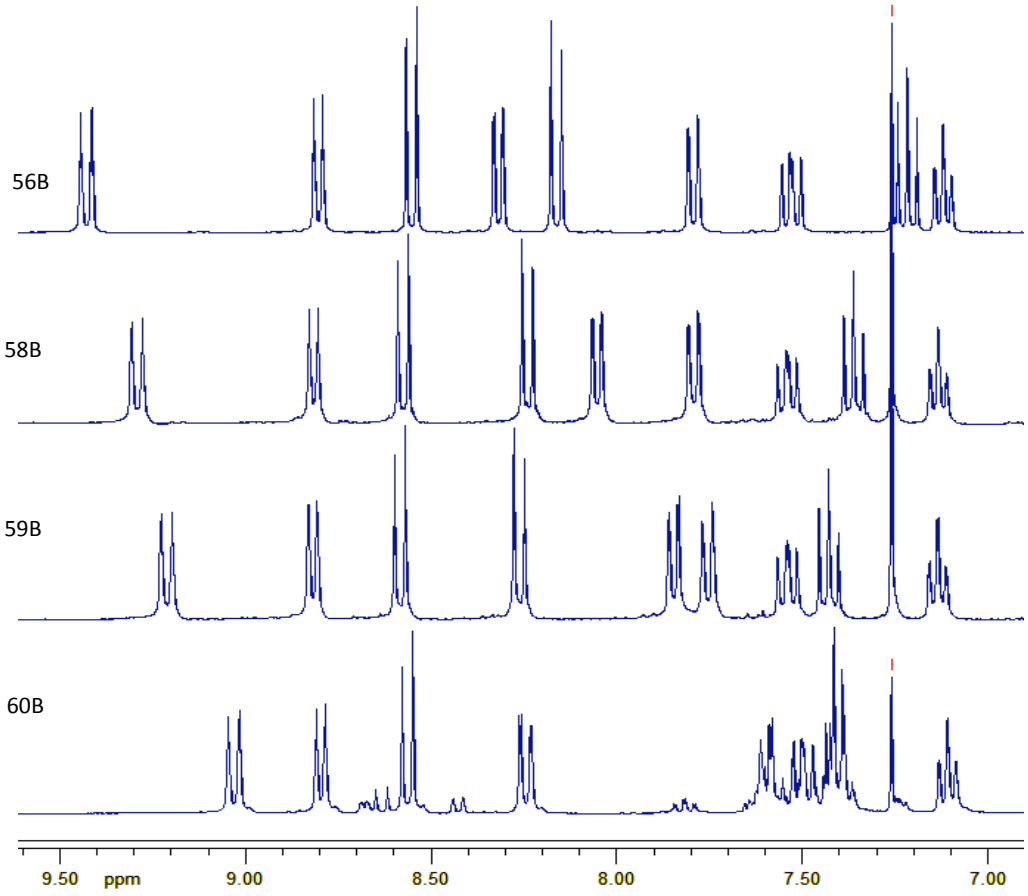

Figure III-19: Comparison of the ^{1}H-NMR spectra of the halogenated derivatives. From up to down, iodide **51B**, bromide **53B**, chloride **54B** and fluoride **55B**. The most downfield shifted signal corresponds to H4B.

3.2.7.4 Exceptions

The hydroxy derivative **62** shows a clear preference for the structure type **A**, although, due to the electronegativity of oxygen one should expect a preference for structure **B**. In fact, for this compound the relative orientation of the hydroxy substituent plays a crucial role. Structure **AII** in **Figures III-20** and **III-17** reveals to be more stable than any of the **B**-forms, due to the possibility of intramolecular hydrogen bonding (**IMHB**) between the OH group and the nitrogen atom N^1 of the triazole ring. In contrast, the methoxy derivative **9**, having similar electronic effects than OH, but without the possibility of hydrogen bonding, favours the isomer type **B**.

The computation studies predict a similar situation in case of R = NH_2). The AIM analysis illustrates the presence of an **IMHB** for these derivatives (**Figure III-20**).

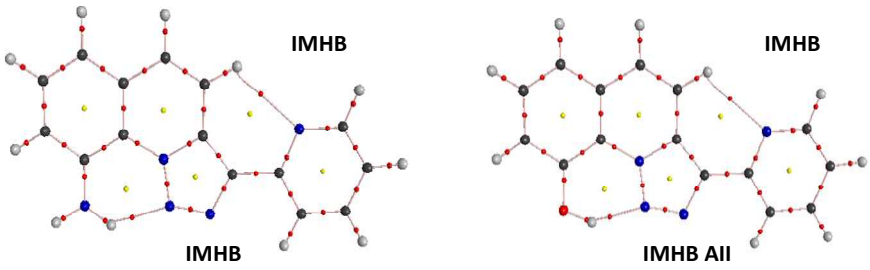

Figure III-20. Molecular graph of the electron density analysis of the isomers **AII** for **60** (R = OH, right molecule) and NH_2 (left molecule).

In case of the carbinol **61** (R = $CHOH(CH_3)_2$), being moderately electron-attracting, the only isomer obtained experimentally is isomer **B**, which is in accordance with the computational studies. The AIM representation shows that the isomer **B** can undergo stabilizing interactions between the OH of the substituent, the nitrogen of the quinoline ring and the nearest H of the adjacent heterocycles (**Figure III-20**).

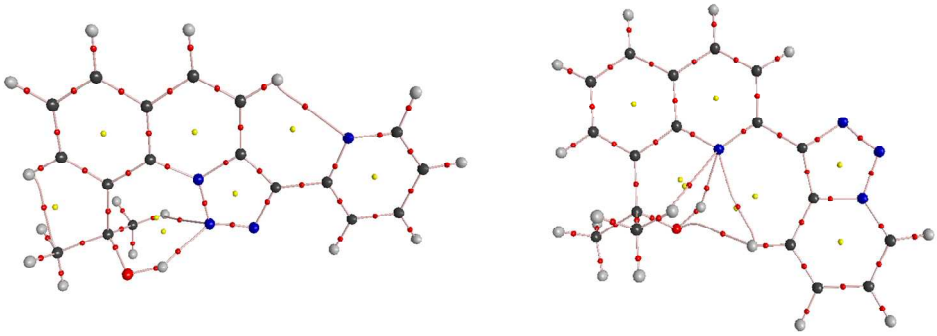

Figure III-20: Molecular graph of the electron density analysis of compound **56** for **A** (left) and **B** isomers (right).

According to the computational studies, the *tert*-butyl substituted (**Tablle III-5**, entry 19) derivative shows a clear preference for the form **B**, for steric reasons, although the form **A** should be more favourable due to its electron-donating properties (+I).

The absolute minimum of the lithiated intermediate due to the carbanion corresponds to the isomer type **A** (**Table III-5**, entry 1), with the greatest energetic difference of all substituents studied (66.11 $kJmol^{-1}$). Nevertheless, if we compare the relative stabilities of the isomer form **B**, this is the unique case were the isomer **B'**, with the nitrogen atoms of the two heterocycles situated on the same side, is more stable than the isomer **B** (7.69 $kJmol^{-1}$). This specific case can be explained by the repulsion effect of the lithium atom over the nearly hydrogen of the **B** structure (**Figure III-17**) forcing a loss of planarity of the system. In contrast,

form **B'** has less significant repulsions, only between close hydrogen atoms, and becomes therefore the more favourable structure (**Figure III-21**).

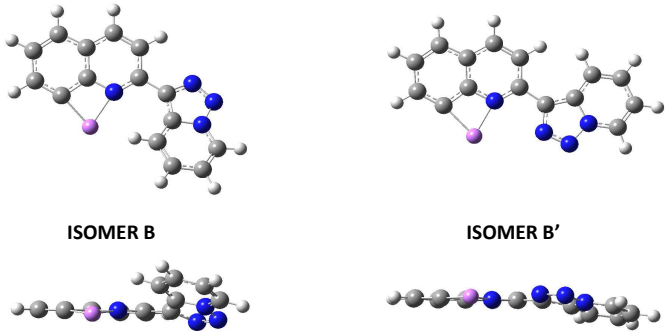

R = Li

Figure III-21: Structures B and B' for the corresponding lithium-derivate compound.

3.2.8 Triazolopyridine-quinoline vs Triazoloquinoline-pyridine

If we compare now the different triazolopyridine structures (**1b**), we can modify the isomeric ratio of triazolopyridine-pyridines[35] by introduction of a substituent onto the 7 position (**Scheme III-20**, 1st row) and the rearrangement affords a 2,6-disubstituted pyridine. Triazoloquinoline-pyridines (**53**) undergo a similar rearrangement after introduction of substituents at the 9 position (**Scheme III-20**, 2nd row) affording analogously 2,8-disubstituted quinolines.[2,3] However, so far we could not modify the substitution pattern of the pyridine ring in triazoloquinoline-pyridines in order to study which ring system dictates the ring-chain isomerisation (**Scheme III-20**, 3rd row).

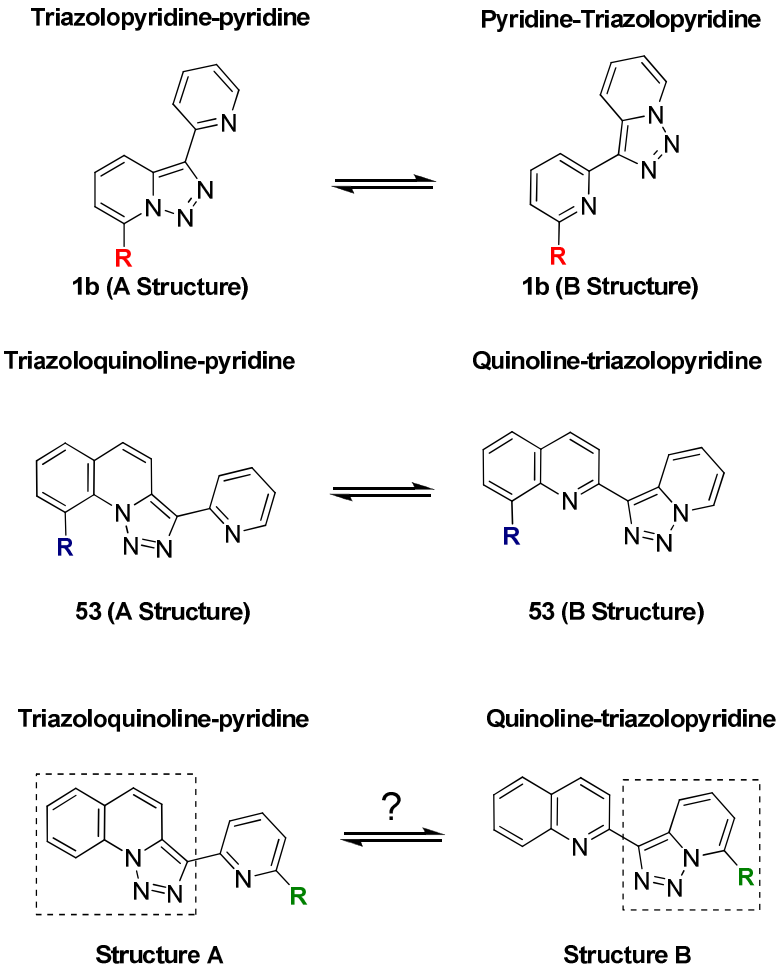

Scheme III-20. Triazoloquinoline *vs.* triazolopyridine.

Therefore, we decided to prepare the derivatives **66** and **67** as depicted in **Scheme III-21**, now possessing a $C^{6'}$-brominated **66** and $C^{6'}$-methylated pyridine **67** part in the triazoloquinoline-pyridine structure. The introduction of substituents in triazoloquinoline **53A** has been described by means of regioselective metalation in position C^{9}, followed by trapping with various electrophiles. Here, a new synthetic strategy was required. 2,6-Dibromopyridine was converted into ketone **68** in 70% yield after trapping of the monolithiated intermediate

with methyl quinoline-2-carboxylate. Hydrazone-formation and consecutive oxidation with MnO_2, afforded the bromo derivative **66**. Halogen/metal permutation and trapping with iodomethane gave the methylated derivative **67** in 50% yield (**Scheme III-21**). As well as 3-(6-bromopyridin-2-yl)-[1,2,3]triazolo[1,5-*a*]quinoline (**66**) 3-(6-methylpyridin-2-yl)-[1,2,3]triazolo[1,5-*a*]quinoline the (**67**) was exclusively obtained as form **A**.

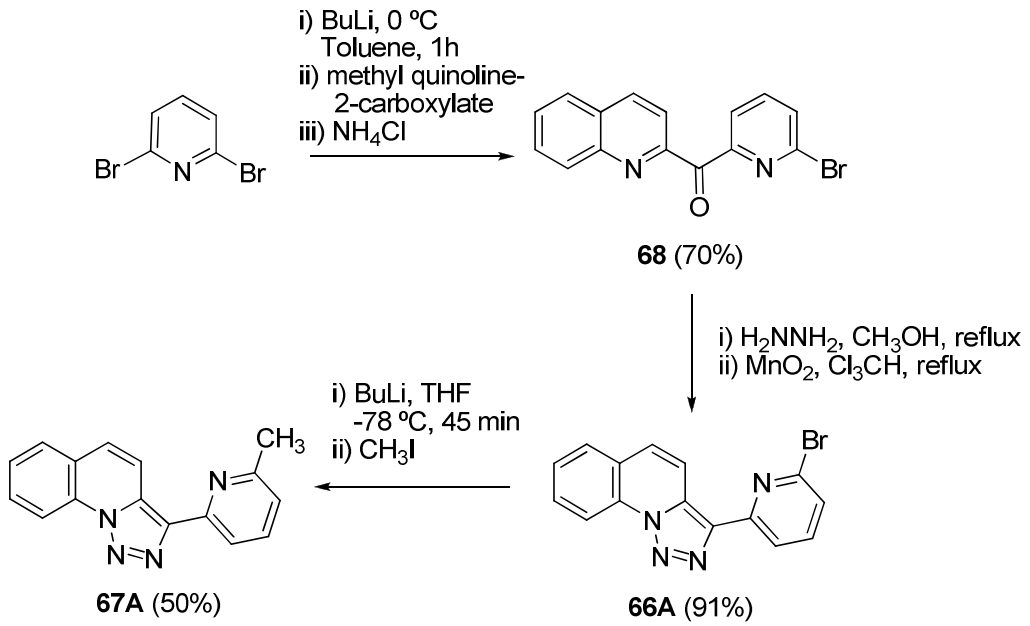

Scheme III-21. Synthesis of pyridine substituted compounds **66-68.**

These results can be interpreted in two ways: either from the effect of the triazoloquinoline ring or from the effect of the triazolopyridine ring. The brominated derivative **66A** is obtained in the form expected from both interpretations, *i.e.* the pyridine ring being the most electron-deficient heterocyclic subunit.

In contrast, the methylated derivative **67** gave a quite interesting result. If the triazoloquinoline-pyridine system is considered (**Scheme III-20**, 3rd row, Structure **A**), the introduction of the methyl group on the pyridine ring should not have a significant influence onto the equilibrium. In fact, according to the computational studies, the unsubstituted triazoloquinoline-pyridine structure **53** under form **A** is more stable than form **B** (**Table III-5**, entry 5). However, if we consider the quinoline-triazolopyridine system (**Scheme III-20**, 3rd row, structure **B**), the substitution of the triazolopyridine ring by an electron-donating methyl group should lead to the preferential form **B** having the more electron-rich triazolopyridine subunit. Surprisingly, the only isomer obtained was **67A**, without any traces of **67B**. This experimental result indicates that a) the contribution of the quinoline is more important in the overall electronic situation of triazoloquinoline-pyridines than the one of the pyridine part, and b) stabilization of the **A** isomer, with a system of three condensated rings (triazoloquinoline), is stronger than the electron-donor effect of the methyl group in the triazolopyridine ring system

of structure **B**. Calculations for compound **66** and **67** were in agreement with the experimental results (**Figure III-22**), showing the higher stabilization of the **A** isomer in the two studied cases with significantly differences of 41.90 and 9.27 kJmol^{-1}, respectively.

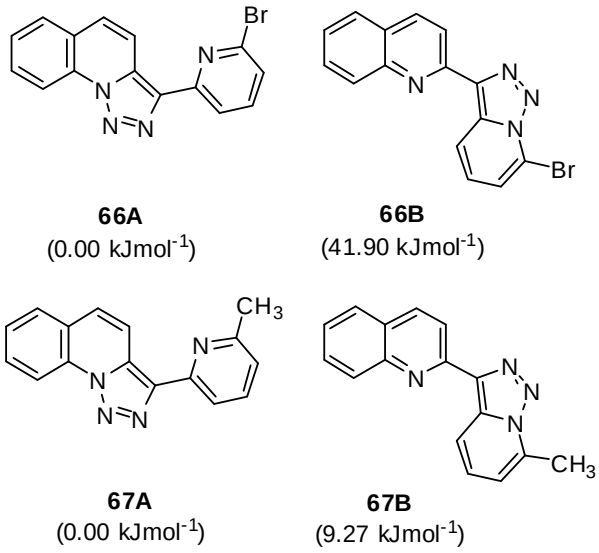

Figure III-22. Relative energies of the two isomers of **66** and **67.**

3.2.9. Conclusions

The theoretical and experimental study of the ring-chain isomerisation of new triazoloquinoline-pyridine systems, allowed us to explain the observed equilibrium ratios of two possible ring-chain isomers **A/B** by means of several effects appointing that:

- The present system triazoloquinoline-pyridine (**50**) provides a non-degenerated system, being **A** structure the more stable.

- The electronic properties of the R substituents influence the ratio **A**/**B**. However, due to the spatial disposition of the R substitutent (C^9 in **A** structures and/or C^8 in B structures), the steric effects are also contributing to the final **A**/**B** ratio.

- In some cases intramolecular hydrogen bond has been also found as responsible of the stabilization of one particular isomer. Hydrogen bonding has also been found as the explanation of H^4 shielding in the halogen family.

- The stabilization of **A** structure has been compared to the donor effect of methyl group by the preparation of compound **66** and **67**. These compounds represent the link between the previous works (with **1b**) and the present non degenerated isomerization with compound **53**.

- Although it has not been mentioned in the text, triazoloquinoline-pyridine scaffold has an interesting fluorescent behavior and will be employed later to prepare fluorescent sensors.

3.10 References

[1] R. A. Abramovitch, T. Takaya, *J. Org. Chem.* **1972**, *37*, 2022.

[2] B. Abarca, E. Gomez-Aldaravi, G. Jones, *J. Chem. Res., (S)* **1984**, 140.

[3] B. Abarca, R. Ballesteros, M. Elmasnaouy, *Tetrahedron* **1998**, *54*, 15287.

[4] H. Kaplan, *J. Am. Chem. Soc.* **1941**, *63*, 2654.

[5] B. Abarca, R. Ballesteros, M. Elmasnouy, *Tetrahedron* **1999**, *55*, 12881.

[6] L. S. Davies, G. Jones, *J. Chem. Res.* **1970**, 688.

[7] A. Asensio, B. Abarca, G. Jones, M. B. Hursthouse, K. M. Abdul Malik, *Tetrahedron* **1993**, *49*, 703.

[8] B. Abarca, R. Ballesteros, N. Houari, *Tetrahedron* **1997**, *53*, 12765.

[9] G. Jones, D. J. Mouat, D. J. Tonkinson, *J. Chem. Soc., Perkin Trans. 1* **1985**, 2719.

[10] G. Jones, D. R. Sliskovic, *J. Chem. Soc., Perkin Trans. 1* **1982**, 967.

[11] B. Abarca, R. Ballesteros, E. Gomez-Aldaravi, G. Jones, *J. Chem. Soc., Perkin Trans. 1* **1985**, 1897.

[12] B. Abarca-González, *Enzyme Inhib. Med. Chem.* **2002**, *17*, 359.

[13] J. Wiesner, R. Ortmann, H. Jomaa, M. Schlitzer, *Angew. Chem., Int. Ed.* **2003**, *42*, 5274.

[14] K. Mekouar, J.-F. Mouscadet, D. Desmaele, F. Subra, H. Leh, D. Savoure, C. Auclair, J. Angelo, *J. Med. Chem.* **1998**, *41,*2846.

[15] D. L. Comins, J. M. Nolan, I. D. Bori, *Tetrahedron Lett.* **2005**, *46*, 6697.

[16] F. Mongin, G. Queguiner, *Tetrahedron* **2001**, *57*, 4059.

[17] D. L. Comins, H. Hong, J. K. Saha, G. Jianhua, *J. Org. Chem.* **1994**, *59*, 5120.

[18] E. Arzel, P. Rocca, F. Marsais, A. Godard, G. Queguiner, *Tetrahedron* **1999**, *55*, 12149.

[19] M. Schlosser, *Angew. Chem., Int. Ed.* **2005**, *44*, 376.

[20] S. Dumouchel, F. Mongin, F. Trecourt, G. Queguiner, *Tetrahedron Lett.* **2003**, *44*, 2033.

[21] K. Kitagawa, A. Inoue, H. Shinokubo, K. Oshima, *Angew. Chem., Int. Ed.* **2000**, *39*, 2481.

[22] M. Marull, M. Schlosser, *Eur. J. Org. Chem.* **2004**, 1008.

[23] M. Marull, O. Lefebvre, M. Schlosser, *Eur. J. Org. Chem.* **2004**, 54.

[24] M. Marull. M. Schlosser, Olivier Lefebvre, *Eur. J. Org. Chem.* **2003**, 2115.

[25] M. Schlosser, M. Marull, *Eur. J. Org. Chem.* **2003**, 1576.

[26] F. Cottet, M. Marull, O. Lefebvre, M. Schlosser, *Eur. J. Org. Chem.* **2003**, 1559.

[27] Y. Kondo, M. Shilai, M. Uchiyama, T. Sakamoto, *J. Am. Chem. Soc.* **1999**, *121*, 3539.

[28] N. Boudet, J. R. Lachs, P. Knochel, *Org. Lett.* **2007**, *9*, 5525.

[29] B. Abarca, R. Ballesteros, F. Mojarred, G. Jones, D. J. Mouat, *J. Chem. Soc., Perkin Trans. 1* **1987**, 1865.

[30] B. Abarca, F. Mojarred, G. Jones, C. Phillips, N. Ng, J. Wastling, *Tetrahedron* **1988**, *44*, 3005.

[31] K. K. Andersen, W. Gaffield, N. E. Papanikolaou, J. W. Foley, R. I. Perkins, *J. Am. Chem. Soc.* **1964**, *86*, 5637.

[32] S. Y. a. B. A. Keay, *Chem. Soc., Perkin Trans. 1,* **1991**, 2600

[33] R. D. Chambers, D. Holling, G. Sandford, A. S. Batsanov, J. A. K. Howard, *J. Fluorine Chem.* **2004**, *125*, 661.

[34] R. D. Chambers, D. Holling, G. Sandford, H. Puschmann, J. A. K. Howard, *J. Fluorine Chem.* **2002**, *117*, 99.

[35] B. Abarca, I. Alkorta, R. Ballesteros, F. Blanco, M. Chadlaoui, J. Elguero, F. Mojarrad, *Org. Biomol. Chem.* **2005**, *3*, 3905.

[36] M. J. Frisch, G. W. Trucks, H. B. Schlegel, G. E. Scuseria, M. A. Robb, J. R. Cheeseman, J. A. Montgomery, T. Vreven, K. N. Kudin, J. C. Burant, J. M. Millam, S. S. Iyengar, J. Tomasi, V. Barone, B. Mennucci, M. Cossi, G. Scalmani, N. Rega, G. A. Petersson, H. Nakatsuji, M. Hada, M. Ehara, K. Toyota, R. Fukuda, J. Hasegawa, M. Ishida, T. Nakajima, Y. Honda, O. Kitao, H. Nakai, M. Klene, X. Li, J. E. Knox, H. P. Hratchian, J. B. Cross, V. Bakken, C. Adamo, J. Jaramillo, R. Gomperts, R. E. Stratmann, O. Yazyev, A. J. Austin, R. Cammi, C. Pomelli, J. W. Ochterski, P. Y. Ayala, K. Morokuma, G. A. Voth, P. Salvador, J. J. Dannenberg, V. G. Zakrzewski, S. Dapprich, A. D. Daniels, M. C. Strain, O. Farkas, D. K. Malick, A. D. Rabuck, K. Raghavachari, J. B. Foresman, J. V. Ortiz, Q. Cui, A. G. Baboul, S. Clifford, J. Cioslowski, B. B. Stefanov, G. Liu, A. Liashenko, P. Piskorz, I. Komaromi, R. L. Martin, D. J. Fox, T. Keith, M. A. Al-Laham, C. Y. Peng, A. Nanayakkara, M. Challacombe, P. M. W. Gill, B. Johnson, W. Chen, M W. Wong, C. Gonzalez, J. A. Pople, Gaussian-03 ed.; Gaussian, Inc.: Wallingford CT, 2003.

[37] a) R. F. W. Bader, *Atoms in Molecules: A Quantum Theory*. Clarendon Press. Oxford, **1990**. b) F. W. Biegler-König, J. Schönbom, AIMM2000, 2.0 ed. Bielefeld, Germany, **2002**.

[38] I. Rozas, I. Alkorta, J. Elguero, *J. Phys. Chem. A* **1998**, *102,* 9925.

[39] R. Bartels-Keitanhd, R. W. Cieciuch, *Can. J. Chem.* **1968**, *46*, 2593.

IV: Triazolopyridine-phosphines

4.1 The isomerisation strategy part 1

4.1.1 Introduction and objectives

The isomerisation of triazolopyridine-pyridine[1] **1b** was first experimentally described and then completely investigated by DFT calculations as shown in chapter 1 part 1.4. This special characteristic provided a new way to reveal the electronic properties of substituents introduced at position 7 of the triazolopyridine-pyridine scaffold (**Scheme IV-1**).

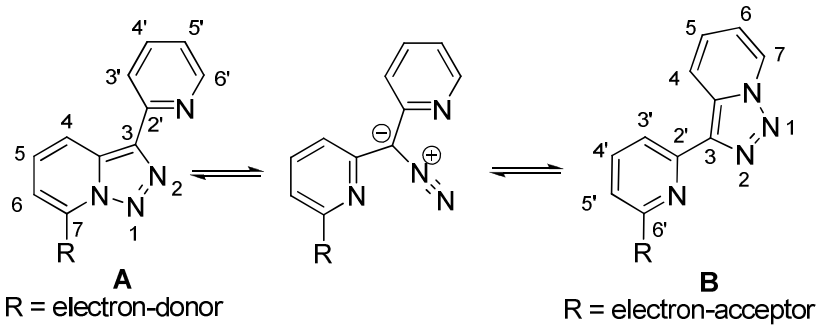

	A/B =
R = Si(CH$_3$)$_3$	1 : 0
B(OR')$_2$ R' = pinacol	1 : 0
CH$_3$	3 : 1
D or H (**1b**)	1 : 1
2-PyCO	0 : 1
CH$_3$CO	0 : 1
Br	0 : 1
I	0 : 1
p-C$_6$H$_4$OCH$_3$	0 : 1

Scheme IV-1: Triazole-ring rearrangement.

Electron-donor groups like trimethylsilyl or boronic ester provided **A** structures, whereas with electron-acceptors, **B** structures were obtained. Only with the methyl substituent, a mixture of both structures was found. Although theoretical calculations allowed establish the electronic profile of these substituents, the only affirmation that could be done experimentally was the existence of an **A** or a **B** structure, or the mixture of both. However, the **A**/**B** mixture can offer experimentally more informations (**Figure IV-1**).

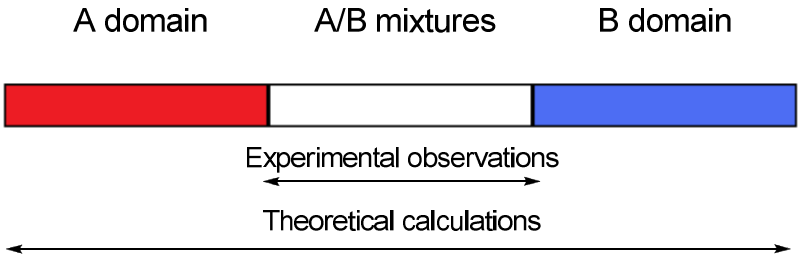

Figure IV-1: Experimental observations vs Theoretical calculations.

For example, although calculations indicated that the donor character of the boron atom in (B(OR$_2$)) is more important than silicium's one in a TMS group, this result could not be experimentally confirmed due to the fact that both compounds exist as an **A** structure.

Similarly, the methyl substituent provided a mixture of both isomers with isomer **A** as the major one (75%). One would have expected to obtain only the isomer **A**, as the methyl group if known as a inductive donor substituents. The preparation of a family of compounds that gives mixtures of isomers **A** and **B**, will afford, in an experimental way, a new entry to evaluate the properties (donor/acceptor) of them.

Particularly we focused on phosphines which are typical substituents owing an "amphoteric" electronic character as they have both σ-donor- and π-acceptor properties. Over the last 40 years, chemists made good use of this property in particular in the field of catalysis. In this context, the fundamental milestone[2-4] over the last two decades is certainly the discovery of BINAP-Ru complexes for asymmetric hydrogenations.[5] New families of chiral phosphines (DIOP,[6] ferrocene-based ligands[7] like the JOSIPHOS-family,[8-10] or TANIAPHOS,[11] as well as biaryl-based ligands[12-14] like MeO-BIPHEP,[15] SEGPHOS,[16, 17] and DIFLUORPHOS[18-20]) have been developed. Monophosphines (PAP-ligands,[21] S-PHOS,[22, 23] X-PHOS, ClickPHOS[24, 25] etc.) are highly performing for a large variety of cross coupling reactions like C-C, C-O, C-N or C-B bond formations. Phosphine-based ligands are nowadays one of the most intensively studied areas in chemistry. Many efforts are devoted to the search of new ligands for transition metals. This research led to the development of new and extremely active P-ligands which are now in many cases commercially available and used at industrial scale[26, 27] suitable for many different kinds of reaction. Systematic screening of these ligands for catalytic reactions showed without any doubts that the modification of the environment of a phosphine can affect dramatically its catalytic performance.

In fact, the modification of the substituents of the phosphine has an impact on its steric and electronic profile. These two parameters are closely interconnected and cannot be easily separated. Nevertheless, some parameters were established in order to quantify each effect. For example, Tolman[28, 29] highlighted the importance of the steric effect and introduce the cone angle θ to rank numerous phosphines. He defined it as "the apex angle of a cylindrical cone, centred 2.28 Å from the centre of the P atom, which just touches the van der Waals radii of the outermost atoms of the model" (**Figure IV-2**).

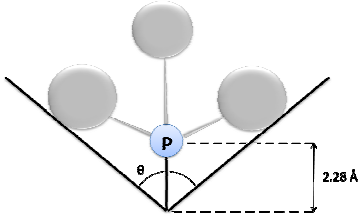

Figure IV-2: Definition of the Cone Angle θ

As mentioned previously, the electronic properties of phosphines are commonly divided into σ-donicity and π-acidity. These effects depend on the nature of the substituent atoms on phosphorus and few methods were so far established to evaluate them.

- For example, the Tolman χ_l values for $Ni(CO)_3L$ complexes represent the electron donicity of a ligand (σ- as well as π-effects).[28, 30]
- The p*K*a values of $R_3PH^{\oplus}$ were used to measure the σ-donicity.[31-34]
- ^{13}C NMR chemical shifts of the carbonyl atoms in $(CO)_5NiL$ were used to determine the donor/acceptor ratios.[35]

Nevertheless, one has to be aware that the steric and electronic properties of the phosphorus substituents have a mutual influence. Indeed, the modification of one factor will affect the other one. For example, the percentage of s-character in the phosphorus donor pair should decrease as the cone angle increases and thus the σ-donor ability should increase. The electronic properties of a phosphine are governed by its particular and unique capacity to give electron density through σ-donation from the phosphorus lone pair towards an empty orbital (of a metal for example) and accept electron-density *via* π-back donation (from a filled orbital of a metal towards an empty orbital of the phosphorus for example). In the field of ligand design for catalysis, two main methods are commonly used to determine separately the σ-donor and π-acceptor abilities of ligands.

σ-Donor Ability of Phosphines

According to Allen and Taylor,[36] the magnitude of $^1J_{P,Se}$ in the ^{77}Se isopotomer of a phosphine selenide ($R^1R^2R^3P{=}Se$) allows to evaluate the σ-donor ability of the free phosphine. An increase of this coupling constant indicates an increase in the s character of the phosphorus lone pair orbital *i.e*. that the phosphine is less basic and that it has a lower σ-donor ability.

π-Acceptor Properties

The π-acceptor ability of the empty *d*π-orbitals of phosphorus is obtained by measuring the carbonyl stretching frequency in (CO)-M-phosphine complex (M= Ni or Rh).[37-39] When the phosphine is linked to electron donor substituents, the phosphorus is electron rich and does not favour the π-back donation from the metal towards the phosphorus atom. Indeed, a more efficient back donation from the metal into the anti-bonding orbital of the CO bond takes place and its bond order decreases from 3 to 2. Therefore, ν_{CO} decreases. Analogously, a higher carbonyl stretching frequency indicates a higher π-acceptor character of the phosphine. These methods have provided a donor- and acceptor-profile of phosphines of

many important compounds used in catalysis. However all these techniques required a modification of the oxidation state/coordination of the phosphorus atom and do not reflect the real catalytic active ligand. It is also important to note that σ-donor and π-acceptor properties are measured by two different ways which don't allow to compare the relative importance of one toward the other.

As a consequence, we thought that the triazolopyridine-pyridine ring isomerisation could be a tool sensitive to measure the global electronic properties of PR_2 groups. Starting from **1b**, we prepared a triazolopyridine-phosphine family and evaluated the ratio between structures **A** and **B**. As suggested in previous calculations, steric effects were not relevant towards the presence of an **A** or **B** structure. Although this strategy will not allow the study of ligands (all of them are trisubstituted phosphines $PR^1R^2R^3$), our investigations provided informations on the influence of the substituents R^2 and R^3 on PR^2R^3. These substituents are often introduced on the ligands, attached to a scaffold R^1 which can be a biphenyl for example (*i.e*. Buchwald,[23] Beller[40] and Zhang[24, 25] monophosphines)(**Figure IV-3**).

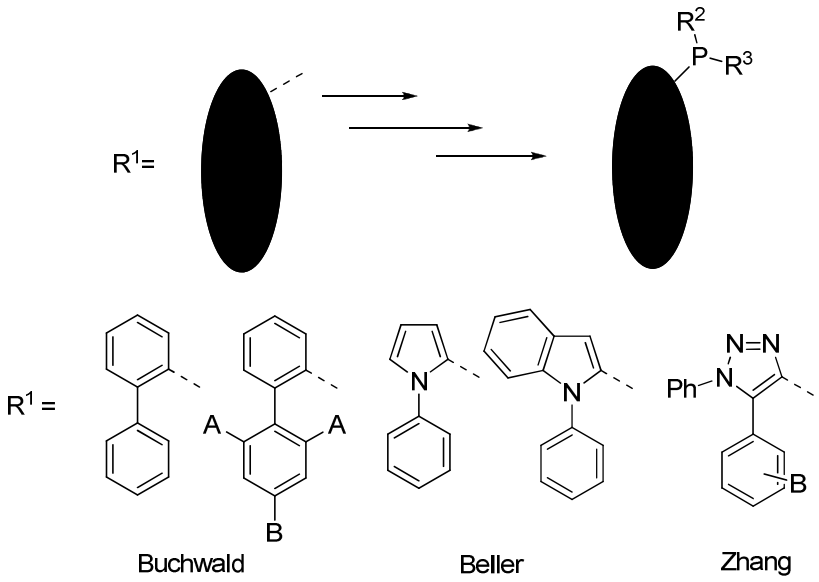

Figure IV-3: Structures of most common phosphine ligands

In order to analyse the ring chain isomerisation with substituents having donor- and acceptor properties we proposed to:

- Introduce different disubstituted phosphines on the triazolopyridine-pyridine **1b** by means of metalation and subsequent trapping with the corresponding disubstituted chlorophosphine in order to prepare a family of compounds.

- Analyse the effects of the different phosphines in terms of **A**, **B** or possible **A**/**B** ratio determined by ^{1}H-NMR.

- Evaluate the electronic properties of these new target structures by at least one of the classical methods, to analyze these results and to compare them with the results obtained from the `possible triazolopyridine isomerisation.

This work was performed with Dr. Laurence Bonnafoux in the framework of her PhD thesis with the synthesis of phosphine based ligands for catalysis (2005-2008) under the direction of Dr. Frédéric Leroux and Prof. Françoise Colobert in collaboration with LONZA AG.

4.1.2 Synthesis of the triazolopyridine-pyridine-phosphine family 69a-g

3-(2'-Pyridyl)-[1,2,3]triazolo[1,5-*a*]pyridine (**1b**) was treated with butyllithium[41, 42] in toluene at -40 °C during 30 minutes, followed by trapping of the 7-lithiated intermediate with diphenylphosphine chloride, di-*iso*-propylphosphine chloride and dicyclohexylphosphine chloride as a test to see if an equilibrium was obtained (**Scheme IV-2**).

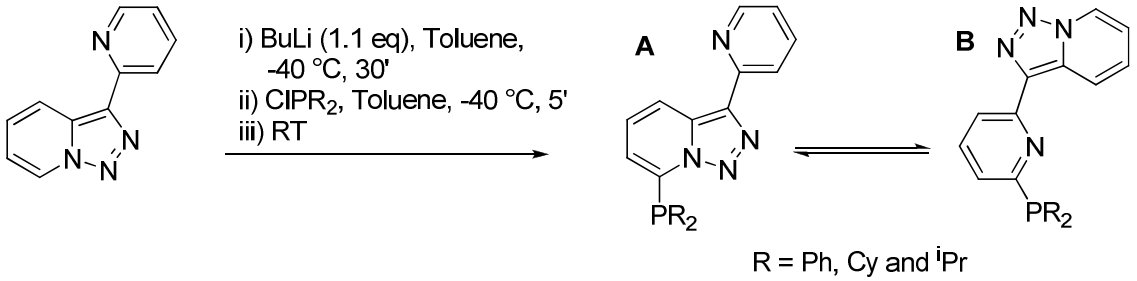

Scheme IV-2: Preparation of compounds **69a**, **69b** and **69c**.

To our great satisfaction after work up and chromatography, the different isomers could not be isolated separately, but could be identified by ^{1}H-NMR as they show very distinct signals. In a preliminary analysis phenyl phosphine **69a** provided a **B**-type isomer as major compound, the *iso*-propyl derivate **69b**, afforded an equimolecular distribution between **A** and **B** and the cyclohexyl with phosphine **69c,** an **A**-type. These results were consistent with the properties of these phosphines. Actually, it is well known that alkyl phosphines are more electron rich than phenyl phosphines. In order to include more examples this reaction was performed with other commercially available chlorophosphines affording after work-up the whole family **69a-g** as depicted in **Table IV-1**:

Table IV-1: Preparation of phosphines **69a-g**.

Entry	Compound	Cl-PR_2	Yield
1	**69c**	PCy_2	22%
2	**69d**	P(*p*-$PhOCH_3)_2$	10%
3	**69b**	P*i*-Pr_2	13%
4	**69a**	PPh_2	40%
5	**69e**	P(*p*-$PhCH_3)_2$	22%
6	**69f**	P(*p*-$PhF)_2$	66%
7	**69g**	P(*p*-$PhCF_3)_2$	46%
8	-	P(^{t}Bu)$_2$	0%

Fluorinated compounds **69f** and **69g** were obtained after purification in 66% and 46% yield, respectively (**Table IV-1**, entries 6-7). The methoxy derivate **69d** was obtained in low yield (10%, **Table IV-1**, entry 2) in a similar way as the methylated compound **69e** (**Table IV-1,** entry 5, 22%). The corresponding *tert*-butyl derivative could not be synthesized, probably due to steric hindrance, and only degradation side products of the triazolopyridine **1b** and starting reagent were recovered after purification.

Even if the isomers **A** and **B** have different R^f on the TLC plate, they cannot be separated by chromatography. Actually, when the product is in solution, the rearrangement occurs and the mixture of both structures is reformed. Even if the yields were not excellent, the conversion were for each cases between 80-90%, however in some cases the starting material **1b** had a polarity intermediate of the 2 isomers which made the isolation of them without traces of starting reagent **1b** very difficult.

Finally, in this way we prepared a family of triazolopyridine phosphines presenting for all compounds a mixture of **A**- and **B**-type structures (**Figure IV-4**).

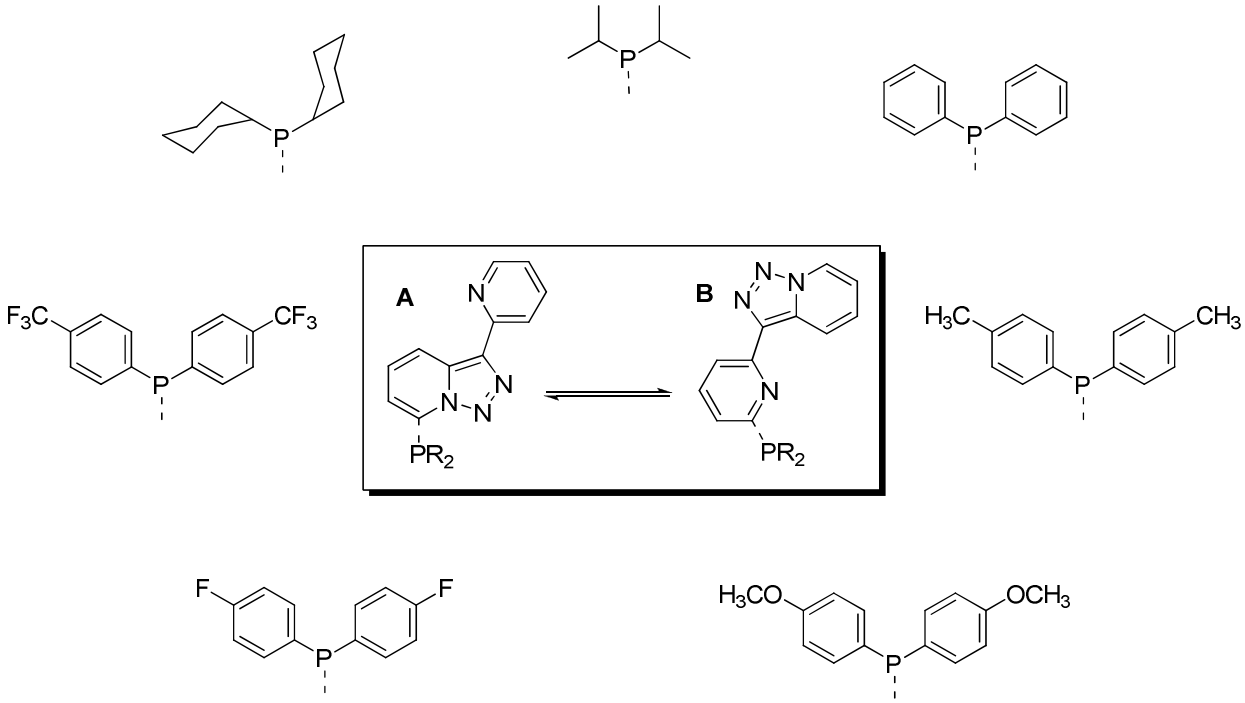

Figure IV-4: Target molecules presenting mixtures between **A** and **B** isomers.

4.1.3 Determination of the A/B Ratio with various phosphine groups

The δ and *J* values for isomers **A** were compared to other **A** isomers described in the literature indicating that they have a pyridyl-triazolopyridinephosphine structure. They contained a 3,7-disubstituted triazolopyridine moiety and a 2-substituted pyridine (See chapter I, part 1.4). The presence of a proton near 8.8 ppm with a coupling constant of *J* = 8.8–9.0 Hz was significant, corresponding to the H^{4A} triazolopyridine proton. Furthermore, another signal with the same integration could be found near 6.5 ppm with *J* = 6.7–6.9 Hz corresponding with H^{6A}. In the same way two more signals (appearing as a doublet) with the same integration were found ($H^{3'A}$ and $H^{6'A}$). Although $H^{6'A}$ has, normally, a similar chemical shift as H^{7B}, $H^{3'A}$ could be perfectly found near 8.4 ppm (*J* = 8.0 Hz). H-H COSY correlation allowed to complete the assignment of these systems (**Figure IV-5**).

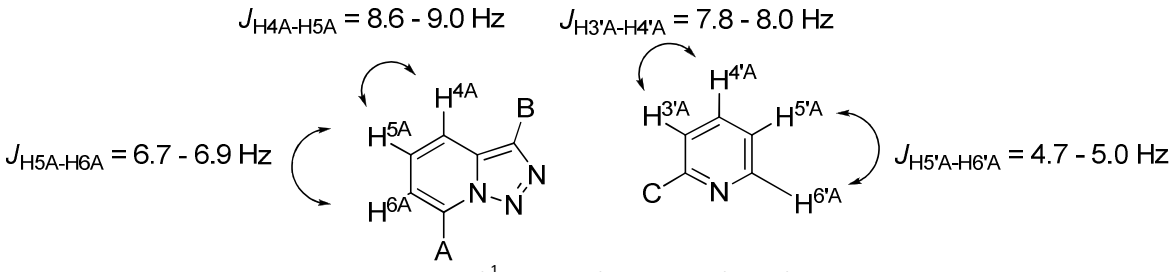

Figure IV-5: Typical ^{1}H-NMR values in triazolopyridines.

On the other hand, isomer **B** which has a 3-substituted triazolopyridine and a 2,6-disubstituted pyridine scaffold. The triazolopyridine presents its 4 hydrogen atoms (**Figure IV-5**, left). H^{7B} and H^{4B} were mixed with other signals from **A** and/or **B** structure. However H^{6B} and H^{5B} appear as two apparent triplets. Once these signals were identified by H-H COSY, the assignment of the whole 3-subtituted triazolopyridine became possible. Near 8.3 ppm a doublet with *J* = 8.0 Hz could be found with the same integration as H^{6B} and H^{5B}. As it has been shown before ($H^{3'A}$: 8.5 ppm doublet, *J* = 8.0 Hz) this signal can be assigned to $H^{3'B}$. The integration analyses corroborated this as it can be found in the ^{1}H-NMR Spectrum for compound **64a** (**Scheme IV-2**, **figure IV-6**).

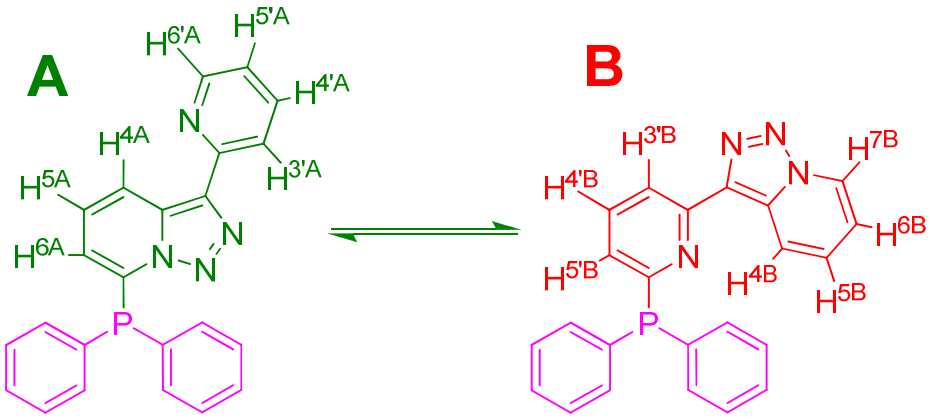

Scheme IV-2: Isomers A and B for compound **69a**

In this example, we considered that H^{A} = **0.4** and H^{B} = **0.6**. P($^{A}Ph_2$) and P($^{B}Ph_2$) are coloured in purple. Red colour corresponds to the clear signals of the major isomer (**B** in this case): $H^{3`B}$, H^{5B} and H^{6B}. Green colour corresponds to the signals of the minor isomer (**A** in this case): H^{4A}, $H^{3'A}$ $H^{5'A}$ and H^{6A}. No colour is used when more than one hydrogen appear at the same chemical shift.

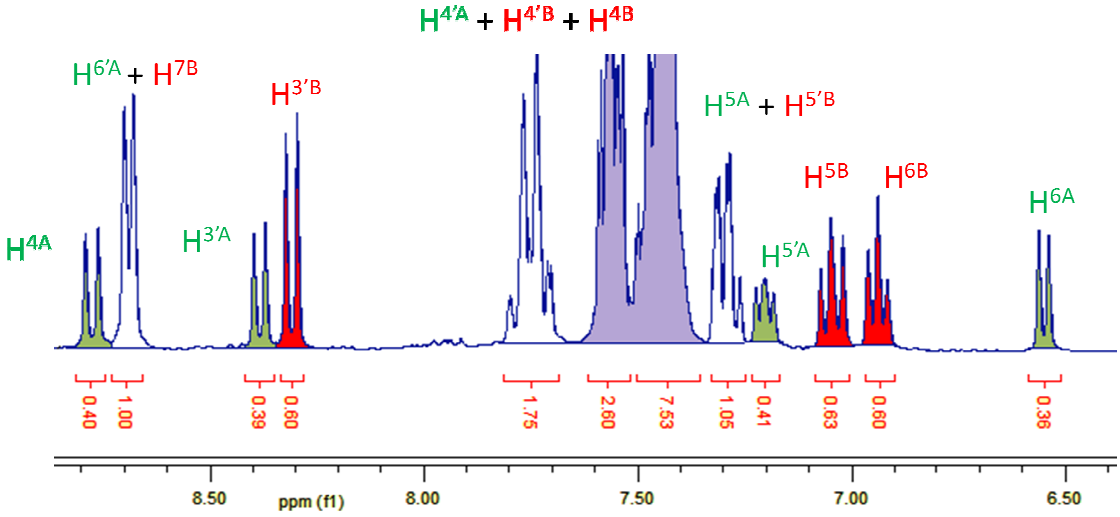

Figure IV-6: Assignment of protons for each isomer. $H^A + H^B = 1$ and $2H^A + H^B = 1.4$ and $H^A + 2H^B = 1.6$.

In a similar way, the spectra of compounds **69b-g** were analysed in order to determine the corresponding ratio between both structures as it is shown in **Table IV-2**:

Table IV-2: Values of the A/B ratio.

Entry	Compound	Cl-PR_2	A	B	A/B	A/B[a]
1	**69c**	PCy_2	1.39	1.00	1.39	1.00
2	**69d**	P(*p*-$PhOCH_3$)$_2$	1.23	1.00	1.23	0.88
3	**69b**	P*i*-Pr_2	1.05	1.00	1.04	0.75
4	**69a**	PPh_2	1.00	1.41	0.72	0.52
5	**69e**	P(*p*-$PhCH_3$)$_2$	1.00	1.41	0.71	0.51
6	**69f**	P(*p*-PhF)$_2$	1.00	2.54	0.40	0.28
7	**69g**	P(*p*-$PhCF_3$)$_2$	1.00	5.65	0.18	0.13

a. Normalized **A/B** values.

The evolution of the ratio between the different phosphines is graphically represented in **Figure IV-7** where the aromatic domain of the corresponding phosphines **69a-g** is compared. Corresponding signals from $H^{3'A}$ and $H^{3'B}$ near 8.4 ppm and H^{6A} at 6.50 ppm were employed to calculate the **A/B** ration. From up to down: R = PCy_2 (**69c**), P(*p*-OMePh)$_2$ (**69d**), P(^{i}Pr)$_2$ (**69b**), PPh_2 (**69a**), P(*p*-MePh)$_2$ (**69e**), P(*p*-FPh)$_2$ (**69f**), P(*p*-CF_3Ph)$_2$ (**69g**).

As depicted in **Table IV-3**, all compounds were characterized and the assignment provided the amount of each isomer in solution. For compound **69a** low temperature NMR studies were performed, however no significant changes of the ratio from 25 °C to -50 °C were observed.

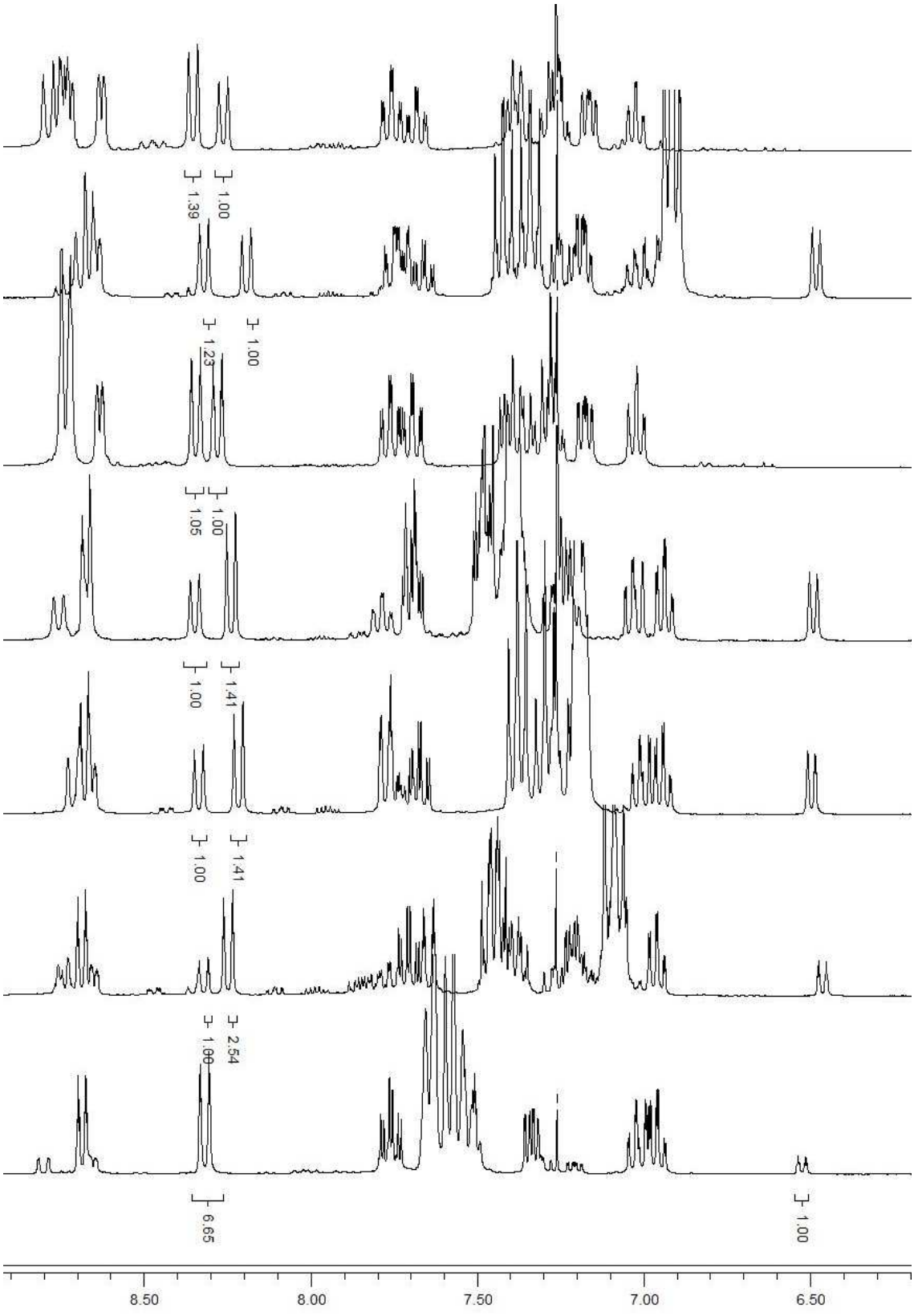

Figure IV-7: ^{1}H-NMR from compounds **69a-g**, aromatic domain.

Table IV-3: ^{1}H-NMR values for **A** and **B** isomers for compounds **69a-g**.

Compound	A B	7 6'	6 5'	5 4'	4 3'	3' 4	4' 5	5' 6	6' 7	other
69a	**PPH_2 A**	**P**	**6.55 d** $J_{6'-5'}$ = 6.8	**7.3-7.2**	**8.77 d** J_{4-5} = 8.8	**8.38 d** $J_{3'-4'}$ = 8.0	**7.8-7.6**	**7.2-7.1**	**8.69 app d** J = 6.3	**$P(Ph)_2$** 7.6-7.3
69a	**PPH_2 B**	**P**	**7.3-7.2**	**7.8-7.6**	**8.31 d** J_{4-5} = 8.0	**7.8-7.6**	**7.1-7.0 app t** J = 6.6 J = 8.6	**6.94 app t** J = 6.8 J = 6.8	**8.69 app d** J = 6.3	
69b	**P^iPr_2 A**	**P**	**8.8-8.7 m**	**7.5-7.2 m**	**8.8-8.7 m**	**8.37 br d** $J_{3'-4'}$ = 8.0	**7.78 ddd** $J_{3'-4'}$ = 7.9 $J_{4'-5'}$ = 7.6 $J_{4'-6'}$ = 1.8	**7.20 ddd** $J_{4'-5'}$ = 7.6 $J_{5'-6'}$ = 4.9 $J_{5'-3'}$ = 1.2	**8.66 br d** $J_{6'-5'}$ = 4.9	**P^iPr_2** 2.92 2.5-2.3 1.3-1.1
69b	**P^iPr_2 B**	**P**	**7.5-7.2 m**	**7.72 ddd** $J_{3'-4'}$ = 7.9 $J_{4'-5'}$= 7.7 $J_{4'-6'}$ = 1.9	**8.30 br d** $J_{3'-4'}$ = 7.9	**7.5-7.5 m**	**7.5-7.2 m**	**7.1-7.0**	**8.8-8.7 m**	0.96
69c	**PCy_2 A**	**p**	**8.8-8.7**	**7.4-7.2**	**8.78 d** J_{3-4} = 8.9	**8.35 d** $J_{3'-4'}$ = 7.9	**7.75 ddd** $J_{3'-4'}$ = 7.9 $J_{4'-5'}$= 7.6 $J_{4'-6'}$ = 1.8	**7.16 dd** $J_{4'-5'}$ = 7.6 $J_{5'-6'}$ = 4.9	**8.6 br d** $J_{5'-6'}$ = 4.9	**PCy_2** 2.8-2.6 m 2.3-2.1 m 2.0-1.8 m
69c	**PCy_2 B**	**p**	**7.4-7.2**	**7.68 ddd** $J_{3'-4'}$ = 8.0 $J_{4'-5'}$ = 7.7 $J_{4'-P}$ = 1.9	**8.26 d** $J_{3'-4'}$ = 8.0	**7.4-7.2**	**7.4-7.2**	**7.02 ddd** J_1 = 6.9 J_2 = 6.8 J_3 = 1.1	**8.8-8.7**	1.8-1.5 m 1.3-0.9 m
69d	**$P(p\text{-}OCH_3Ph)_2$ A**	**P**	**6.48 d** $J_{4'-5'}$ = 6.8	**7.3-7.1 m**	**8.7-8.6 m**	**8.32 d** $J_{3'-4'}$ = 8.0	**7.8-7.7 m**	**7.3-7.1 m**	**8.7-8.6 m**	**$P(p\text{-}OCH_3Ph)_2$** 7.4-7.3 m 7.1-6.9 m
69d	**$P(p\text{-}OCH_3Ph)_2$ B**	**P**	**7.3-7.1 m**	**7.66 ddd** $J_{3'-4'}$ = 7.9 $J_{4'-5'}$ = 7.8 $J_{4'-P}$ = 2.5	**8.19 d** $J_{3'-4'}$ = 7.9	**7.8-7.7 m**	**7.1-6.9 m**	**7.1-6.9 m**	**8.7-8.6 m**	3.82 s 3.80 s
69e	**$P(p\text{-}CH_3Ph)_2$ A**	**P**	**6.42 d** J_{6-5} = 6.8	**7.4-7.3 m**	**8.7-8.6**	**8.33 br d** J_{4-5} = 8.1	**7.8-7.7 m**	**7.4-7.3 m**	**8.7-8.6**	**$P(p\text{-}CH_3Ph)_2$** 7.4-7.3 m 7.2-7.1 m 3.38 s
69e	**$P(p\text{-}CH_3Ph)_2$ A**	**P**	**7.2-7.1 m**	**7.67 ddd** $J_{3'-4'}$ = 7.9 $J_{4'-5'}$ = 7.8 $J_{4'-P}$ = 2.4	**8.22 br d** $J_{3'-4'}$ = 7.9	**7.8-7.7 m**	**7.1-6.9 m**	**7.1-6.9 m**	**8.7-8.6**	2.36 s
69f	**$P(p\text{-}FPh)_2$ A**	**P**	**6.46 d** $J_{5'-4'}$ = 6.8	**7.3-7.2 m**	**8.74 d** J_{4-5} = 8.9	**8.32 d** $J_{3'-4'}$ = 8.0	**7.8-7.7 m**	**7.3-7.2 m**	**8.65 d** $J_{5'-6'}$ = 4.9	**$P(p\text{-}CF_3Ph)_2$** 7.42 m 7.1-7.0 m
69f	**$P(p\text{-}FPh)_2$ B**	**P**	**7.3-7.2 m**	**7.7 ddd** $J_{3'-4'}$ = 7.9 $J_{4'-5'}$ = 7.8 $J_{4'-P}$ = 2.5	**8.24 d** $J_{3'-4'}$ = 8.0	**7.64 br d** J_{4-5} = 8.9	**7.1-7.0 m**	**6.96 ddd** J_{6-7} = 6.9 J_{5-6} = 6.7 J_{4-6} = 1.4	**8.68 d** J_{6-7} = 7.0	
69g	**$P(p\text{-}CF_3Ph)_2$ A**	**P**	**6.84 d** J_{5-6} = 6.84	**7.21 dd** J_{4-5} = 8.7 J_{5-6} = 6.8	**8.80** J_{4-5} = 8.7	**8.32 app d** $J_{3'-4'}$ = 8.0	**7.76 ddd** $J_{3'-4'}$ = 7.9 $J_{4'-5'}$ = 7.7 $J_{4'-6'}$ = 2.8	**7.4-7.3 m**	**8.7-8.6 m**	**$P(p\text{-}CF_3Ph)_2$** 7.7-7.5 m
69g	**$P(p\text{-}CF_3Ph)_2$ B**	**P**	**7.4-7.3 m**	**7.767 app dd** $J_{3'-4'}$ = 7.9 $J_{4'-5'}$ = 7.7	**8.32 app d** $J_{3'-4'}$ = 8.0	**7.7-7.5 m**	**7.1-6.9 m**	**7.1-6.9 m**	**8.7-8.6 m**	

We were able to isolate a single crystal from the ring-chain isomer **69a (B)** and confirm its structure by single crystal X-ray analysis (**Figure IV-8**). In solution, the pure isomer **69a (B)** undergoes once again equilibration and affords the equilibrium ratio with isomer **A**.

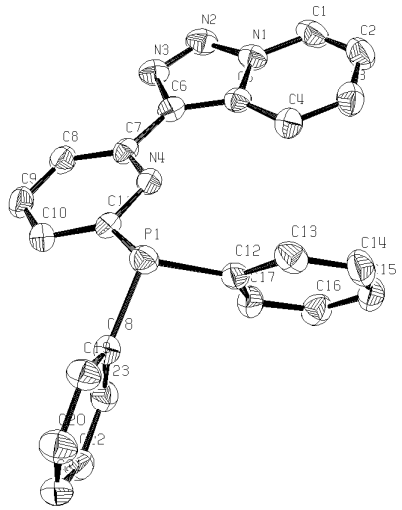

Figure IV-8: X-ray strucure of compound **69a B** isomer.

4.1.4 Analysis of the observed results

Structures **A** and **B** are the result of both accepting and donating properties of phosphines. However in order to understand how this effect takes place we have to examine the intermediate system where these properties take place *i.e*. intermediate state R13 of the equilibrium, see chapter 1, part 1.4 (**Figure IV-9**).

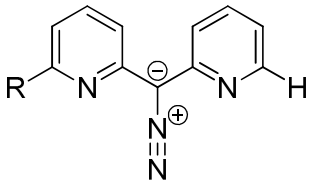

Figure IV-9: Intermediate state R13 of the isomerisation.

In previous studies when the substituent acts essentially as an electron-donor, the 2'-phosphino-pyridyl ring-nitrogen becomes more nucleophilic and attacks the diazo intermediate giving rise to the triazole structure **A**. However, with electron-withdrawing substituents at position 7, the ring-nitrogen of the unsubstituted pyridine in the diazo intermediate is the most nucleophilic one leading to triazole structure **B.** Although this argument can be applied to the phosphines there is an important difference compared to classical substituents that must be taken into account.

Actually, phosphines always act as donor and acceptor substituents at the same time. Therefore, a pure **A** structure cannot be exclusively associated to the donor properties as well as the **B** structure cannot be relied only to accepting properties, The triazolopyridine-pyridine ring reflects at the same time the electro-donation and the electro-acceptor properties of the

phosphines, both properties co-existing at the same time. The ratio **A**/**B** is a measurable value resulting from the sum of donor and acceptor properties (**Scheme IV-3**):

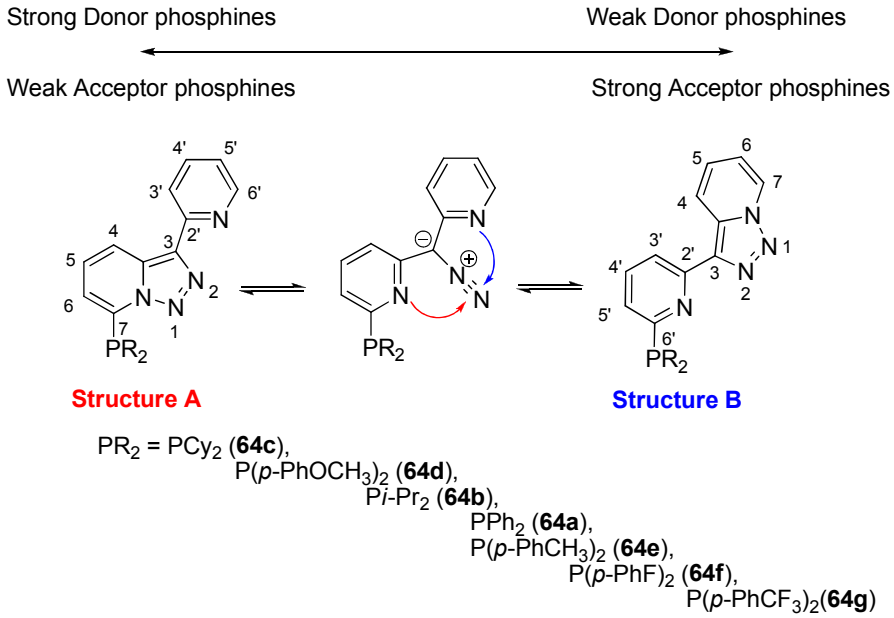

Scheme IV-3: Influence on the ring-chain isomers depending on the donor/acceptor-properties of the phosphines.

The results obtained with the dicyclohexyl-, di-*iso*-propyl- and diphenyl phosphines (entries 1, 3 and 4 in **Table IV-2**) reflect the predominant σ-donor properties of alkyl phosphines compared to aryl phosphines. However, the triazolopyridine system reflects at the same time the dual property of phosphines. For instance, in the case of di-*iso*-propyl phosphine, there is no preferential structure. **A** and **B** are in equilibrium with a ratio of 1.05:1.00 (entry 3 in **Table IV-2**). In terms of electron density, this phosphine has equal properties of an acceptor and a donor. This observation is in accordance with calculations by Pacchioni and Bagus[43] revealing that the π-acidity of PR_3 increases along the series $PMe_3 < PH_3 < P(OMe)_3 < PF_3$ with PMe_3 having a "remarkable" π-acidity. When the phenyl-ring in diphenyl phosphine is substituted in the *para* position by electron-accepting groups like F or CF_3, the triazolopyridine **B** is obtained as the major compound. The presence of a methyl group in *para* position has almost no influence on the global properties of the phosphine (entries 4 and 5 in **Table IV-2**). However, our study revealed that a *para*-methoxy diphenyl phosphine provides a higher **A**/**B** ratio than di-*iso*-propyl phosphine (entries 2 and 3 in **Table IV-2**). As it will be shown later, compound **69b** is a better donor than methoxy derivative **69d** (donor properties will be measured by the selenide derivate method). The donating properties of the methoxy group can provide electron density to the phosphorous empty d-orbital making this compound (**69d**) not a better donor than di-*iso*-propyl phosphine (**69b**) but a remarkably worse acceptor.

4.1.5 Determination of σ-donor ability of phosphines 69a-g

In order to measure the σ-donor ability of phosphines **69a-g**, and according to Allen and Taylor, selenides of these compounds were prepared (**Scheme IV-4**). The conversion of phosphines into their corresponding selenides[36] shifted completely the equilibrium towards the electron-acceptor structure **B**. This modification of the equilibrium was detected by change in the ^{1}H-NMR profile and was confirmed by single crystal X-ray analysis of the triazolopyridine phosphine selenides (**Figure IV-10**).

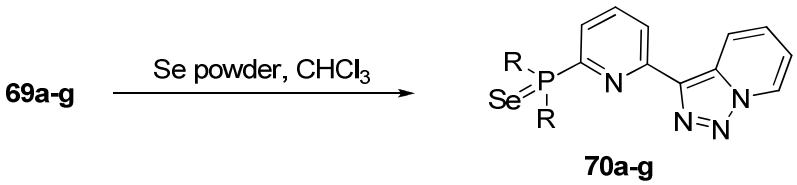

Scheme IV-4: Preparation of selenides **70a-g**. Only **B** structures were observed.

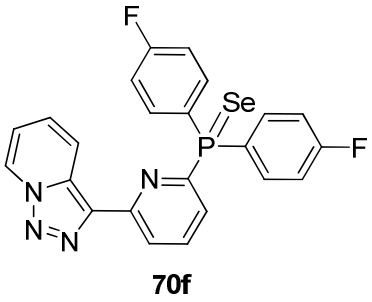

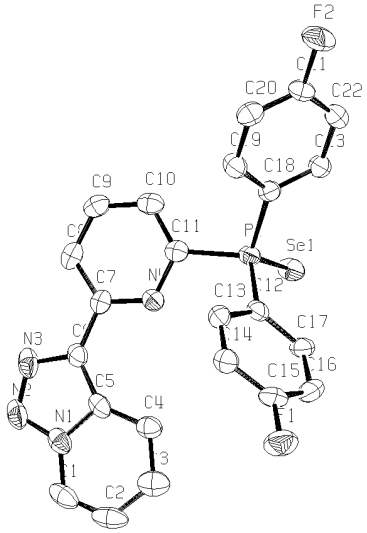

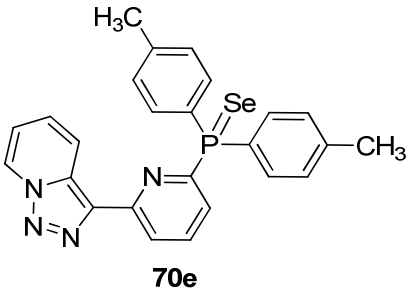

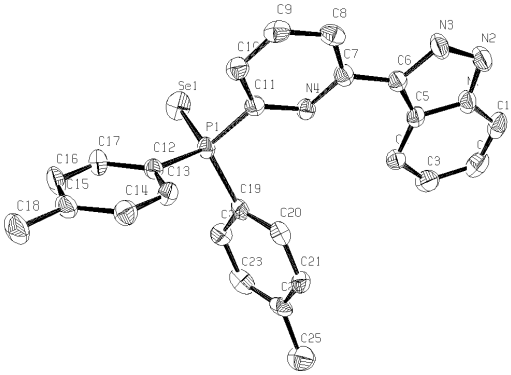

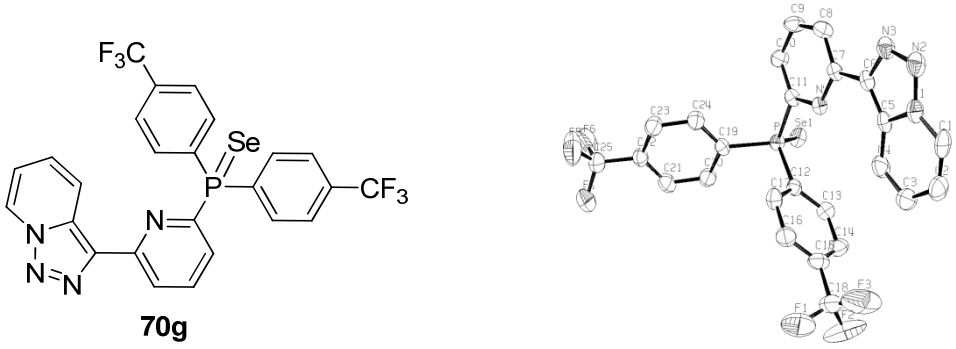

Figure IV-10: Single crystal X-Ray Analysis of compounds **70e**, **70f** and **70g.**

The coupling constants in compounds **70a-g** quantify the σ-donor properties from the most to the less σ-donor: **70c > 70b > 70d > 70e > 70a > 70f > 70g** (**Table IV-4**).

Table IV-4: $^{1}J_{P\text{-}Se}$ values of the selenides of **70a-g**.

Entry	PR_2	$^{1}J_{P,Se}$	$^{1}J_{P,Se}$ [a]
1	PCy_2 (**70c**)	705.5 Hz	0.93
2	$P(p\text{-}PhOCH_3)_2$ (**70d**)	725.4 Hz	0.95
3	P*i*-Pr_2 (**70b**)	713.5 Hz	0.94
4	PPh_2 (**70a**)	736.4 Hz	0.97
5	$P(p\text{-}PhCH_3)_2$ (**70e**)	729.6 Hz	0.96
6	$P(p\text{-}PhF)_2$ (**70f**)	744.4 Hz	0.98
7	$P(p\text{-}PhCF_3)_2$ (**70g**)	760.6 Hz	1.00

a: Normalized $^{1}J_{P,Se}$ values.

In order to compare results obtained with the selenide method and with our **A**/**B** ratio, the values were normalized. We observed a large field of **A**/**B** ratio between the highest value and the smallest one (difference of 90%).This indicates a high sensitivity of the **A**/**B** ratio, especially when compared with the selenide method (difference of 10%) (**Figure IV-11).**

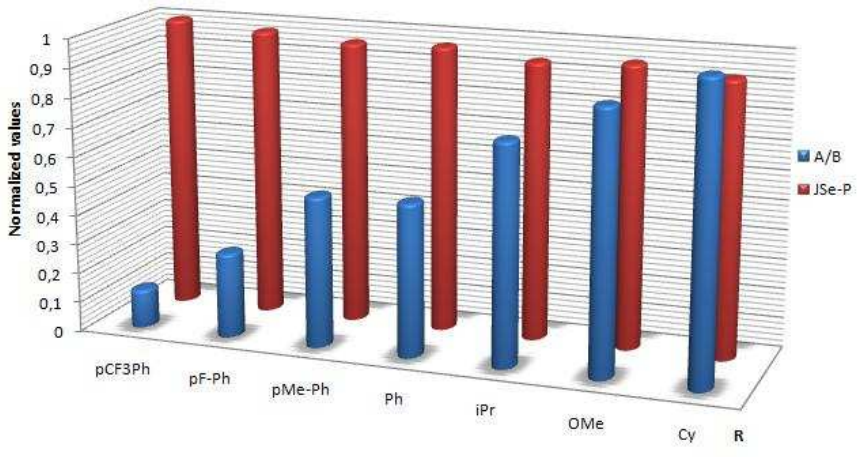

Figure IV-11: Comparison between normalized $^{1}J_{P\text{-}Se}$ (red) and normalized **A**/**B** ratio (blue) for the different couple of phosphines **69a-g**.

4.1.6 Conclusions

- The analysis of the structures obtained after introduction of a phosphine group on triazolopyridine **1b** revealed several interesting results. Although each isomer **A** or **B** could not be isolated, their mixture was fully characterized and allowed to understand how this equilibrium takes place with these substituents, affording a ranking of phosphines depending on the global electronic properties.

- We have also compared the results obtained with the isomerisation method with the σ-donor ability of these compounds determined by the selenide method. Both results are completely consistent. Furthermore, the most remarkable observations made with the methoxy derivative **69d** were explained by means of its electron-accepting properties.

- After transformation of the phosphines into their corresponding selenides **70a-g** we observed a full isomerisation towards the **B**-type structure. Single crystal x-ray analysis were performed and confirmed the structures. The presence of exclusively **B** structures in solution indicates that the lone-pair on phosphorus is involved in the donation.

- Our method allows, for the first time, to see the global electronic profile of these phosphines without modification of the oxidation state or by coordination onto a metal.

IV: Triazolopyridine-phosphines

4.2 Triazoloquinoline-pyridine-phosphines

4.2.1 Introduction and objectives

Thanks to the triazolopyridine-pyridine **1b** isomerisation, we were able to determine how the electronic profile of the phosphines can influence the isomerisation of the triazole-ring and were able to evaluate both donor and acceptor properties. Our study was based on the fact that steric effects are not involved in the rearrangement and the final **A**/**B** ratio. This was previously proven by theoretical calculations.

We found it interesting just to perform the analogous reaction on triazoloquinoline **53**, in order to see if the values of the equilibrium were found to be logical. Furthermore, as the triazoloquinoline-pyridine **53** isomerisation is influenced by steric and electronic effects (see chapter 3.2), we considered interesting to prepare some of these compounds in order to:

- Study the possible isomerisation between the non-degenerated isomer structures (**53 A** and **B** structures).

- Compare the values of the **A**/**B** ratio of this system to the previous ones (with **1b**) in order to study if steric properties provide a main difference. It would be highly intriguing if a comparison of all steric and electronic properties *via* the study of the isomerisation reaction was possible (**Figure IV-12**).

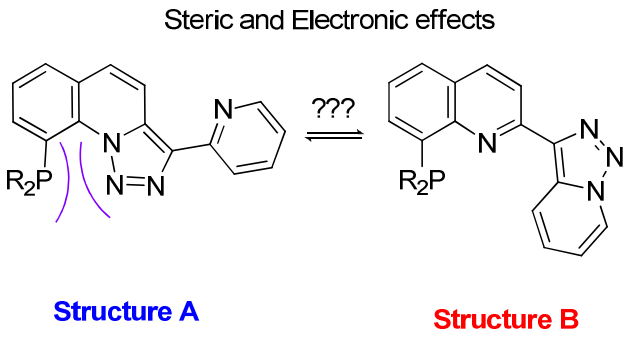

Figure IV-12: triazoloquinoline-pyridine **53** equilibrium with phosphines.

4.2.2 Preparation of triazoloquinoline-pyridine phosphine derivatives

As it has been previously reported (chapter 3, part 3.2.2), triazoloquinoline **53** undergoes regioselective metalation at C^9 with butyllithium in THF at -78 °C. By trapping the lithium intermediate with chlorodiphenylphosphine we obtained the first derivative **71.** As reported in chapter 4, part 1, the experimental values would only be useful if mixtures of **A** and **B** were observed. After the work up, no mixture of compounds **71A** and **71B** could be detected (**Scheme IV-5**).

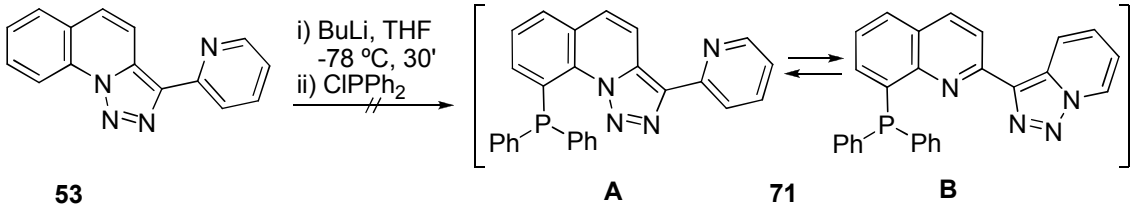

Scheme IV-5: Preparation of triazoloquinoline-pyridine phosphines.

When the crude product was treated with ethyl acetate a white powder precipitated. After NMR and HRMS analysis, we identified this compound not as the expected phosphine but the phosphine oxide **72** with structure **B** (**Scheme IV-6**). The presence of H^7, H^6, H^5 and H^4 on a triazolopyridine indicated the existence of **B** isomer. ^{31}P NMR afforded a signal near 31 ppm. This chemical shift is typical for a phosphine oxide, whereas the classical chemical shift of triaryl phosphines is usually < 0 ppm.

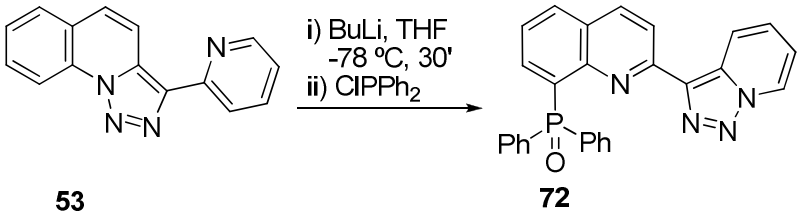

Scheme IV-6: Preparation of **72.**

This rapid oxidation is quite surprising because triaryl phosphines are usually stable and oxidize less fast than their trialkyl counterparts.[44]

We repeated this reaction in order to introduce other arylphosphines and to modify the electron density around the phosphorus center. Therefore, after lithiation, we trapped the aryllithium intermediate with $(p\text{-}CF_3Ph)_2PCl$ and $(p\text{-}H_3COPh)_2PCl$. As results, in all cases phosphine oxides were observed (compounds **73** and **74**, **Scheme IV-7**). A single crystal of compound **73** could be obtained, as reported before (chapter 3, part 2) which presented a **B** structure and an *anti* orientation between $N_{quinoline}$ and $N2_{triazolopyridine}$.

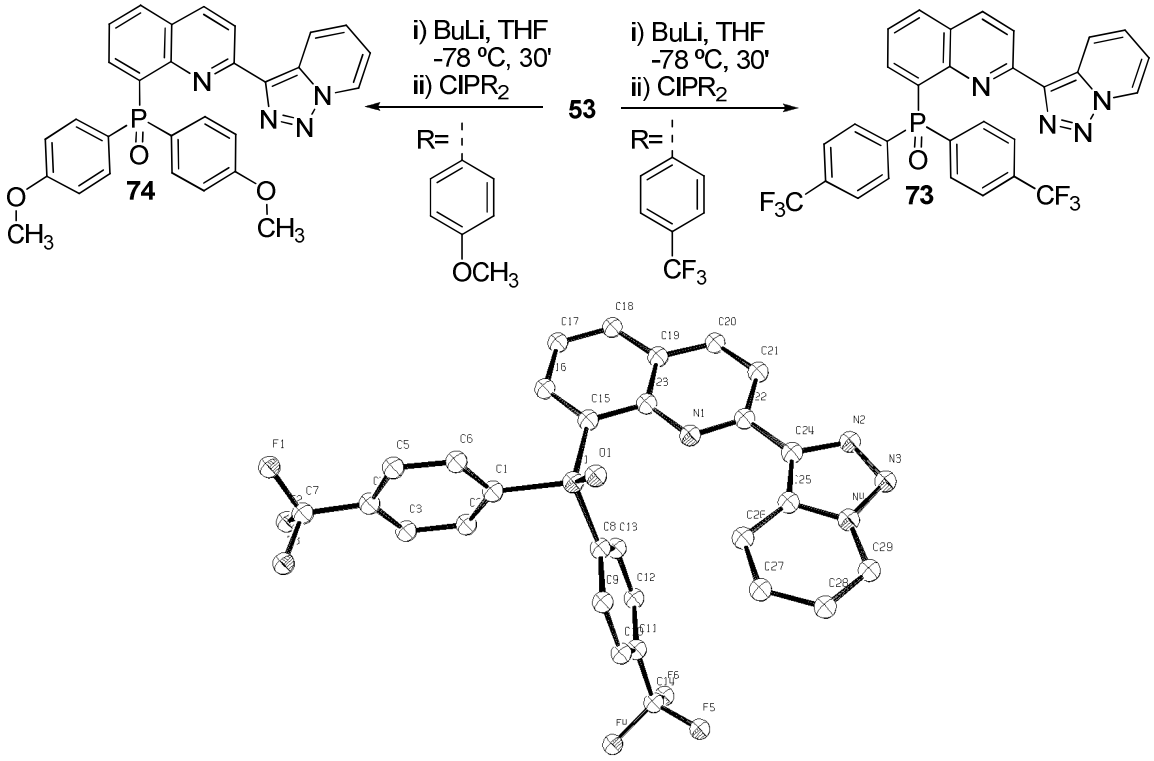

Scheme IV-7: Preparation of **73** and **74.** Single crystal X-Ray Analysis of **73**.

These three results reveal that triazoloquinoline-pyridine phosphines can not be obtained *via* a metalation/$ClPR_2$ strategy, as the exclusive formation of phosphines oxides occurs. This is surprising, as normally triarylphosphines are stable towards oxidation, especially when they are electron poor. [45] In the case of triazolopyridine phosphines we confirmed this property (compounds **69a-g**).

Our hypothesis why this rapid oxidation in the case of triazoloquinoline-pyridine phosphines happens, is based on the special triazoloquinoline geometry and the ring chain isomerisation.

After lithiation and trapping with $ClPR_2$ the isomer **71A** should be formed and equilibrate with form **71B** (**Scheme IV-8**). In order to get the phosphine oxide **68B**, oxidation of **71B** has to occur. However, as outlined above and according to the literature,[45] such an oxidation of triarylphosphines under our reaction conditions is not possible. A second approach is based on a preferential conformation of isomer **71A** in which a σ-donation of the nitrogen lone pair of N^1 towards phosphorus is possible. This leads to a higher electron-density at phosphorus and makes the oxidation to compound **71A** possible. Next, as we have now a strong electron-acceptor on the triazoloquinoline ring, isomerisation towards acceptor structure **72B** takes place.

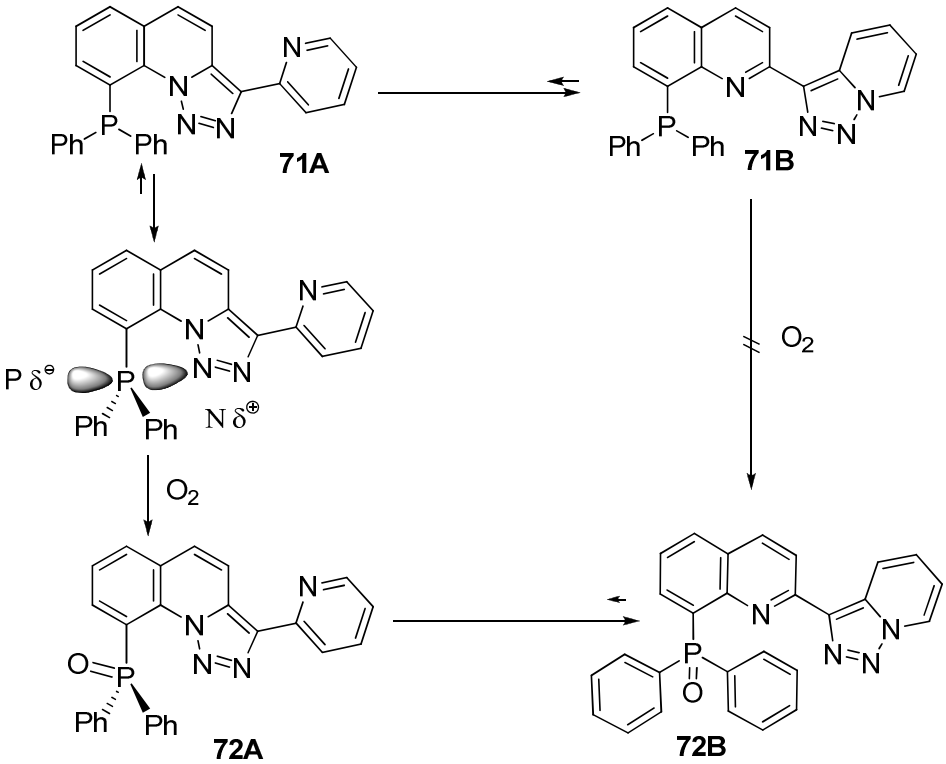

Scheme IV-8-: Oxidation mechanism.

4.2.3 Conclusions

- The oxidation process avoided any ratio studies due to the presence of pure **B** structures. However, these results also confirmed the presence of the isomerisation and enhanced the relevance of the triazoloquinoline-pyridine (**53**) equilibrium showing how, just by modifying the geometry, completly different results can be obtained.

- Although no **A**/**B** ratio study could be performed due to the oxidation, the molecules presented a remarkable fluorescence and were studied as fluorescence sensors due to their tridentate, non-symmetric structure.

IV: Triazolopyridine-phosphines

4.3 Triazolopyridine-phosphines

4.3.1 Introduction and objectives

The structural properties of 3-(2'-pyridyl)-[1,2,3]triazolo[1,5-*a*]pyridine (**1b**) revealed to be a unique sensor for the electronic properties of different phosphine substituents linked.

This property was highlighted by the analysis of the ^{1}H-NMR spectra of the isomeric mixtures of compounds **A** and **B**. On the other hand, we were surprised by the complexity of the ^{13}C NMR spectra of these mixtures. In order to understand them, we decided to focus on more simple and non-isomerizable triazolopyridines like **1a**, **1c** and **1d** which can be considered as compounds of structure type **A**. In this way, we hoped to distinguish the different effects of the phosphine groups on the heteroaromatic ring. (**Figure IV-13**).

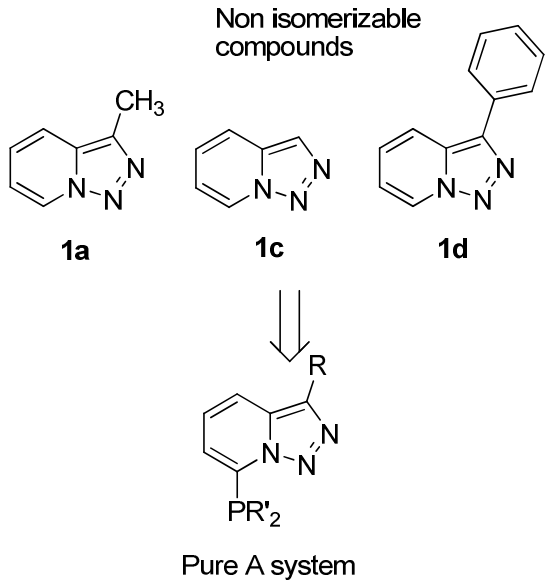

Figure IV-13: Non isomerizable phosphines.

Phosphines based on a heteroaromatic compounds are interesting from different point of view. For example, QUINAP[45] and the PAP ligand family from Beller[21] proved to be excellent ligands in Pd catalysis. On the other hand, molecular materials based on phosphines are nowadays one of the most important topics in chemistry due to their application as alternative OLED's for example.[46, 47]

The preparation of non-isomerizable triazolopyridine phosphines seems to be interesting considering the multiple coordination ways that these molecules could offer two aspects are intriguing (**Figure IV-14**):

1. The position of the phosphorus lone pair relative to the triazolopyridine aromatic plane.

2. The coordinating nitrogen atom from the triazolopyridine

The presence of two different coordinating atoms (phosphorus and nitrogen) provides also interesting properties to these compounds being for example preferential *P*-ligands with palladium or *N*-ligands with zinc.

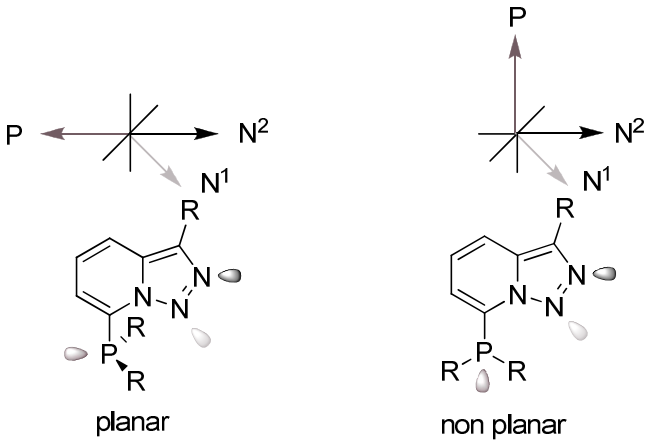

Figure IV-14: Example of possible coordination ways.

Thus, we functionalized 3-substituted[1,2,3]triazolo[1,5-*a*]pyridines (**1a**: R = CH_3, **1c**: R= H and **1d**: R = phenyl) with different kinds of phosphine groups (-PPh_2, -PCy_2 and -P^iPr_2) and evaluated the effect of the phosphorus lone pair position and tested this new class of triazole-based monophosphine ligands in coupling reactions.

This work was performed in collaboration with Dr. Laurence Bonnafoux for the experimental part and Dr. Fernando Blanco, Dr. Ibón Alkorta, and Pr. Jose Elguero for the theoretical study.

4.3.2 Preparation of phosphine-based triazolopyridines

In a similar way as compounds **69a-g**, non-isomerisable triazolopyridinephosphines **75a-c**, **76a-c** and **77a-c** were synthesized. Lithiation[41, 42] of the triazolopyridines **1a**, **1c** or **1d** in toluene at -40 °C during 30 minutes provided the lithium-intermediates which were trapped with the corresponding $ClPR_2$ (**Scheme IV-9**).

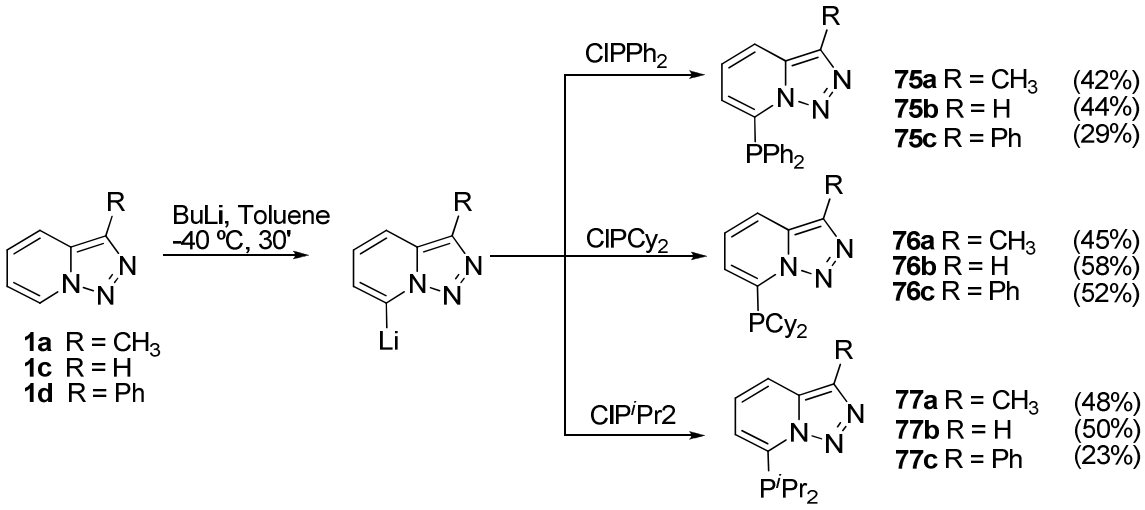

Scheme IV-9: Preparation of phosphine-based triazolopyridines.

3-Methyl[1,2,3]triazolo[1,5-*a*]pyridine (**1a**) provided after trapping with different chloro phosphines compounds **75a**, **76a** and **77a** in moderate yields. Similarly, the other members of this family were synthesized by regioselective metalation of **1b** and **1d**. All of them were purified by columm chromatography. Compounds **75a-c** and **76a-c** were obtained as colorless solids, compounds **77a-c** were presented as orange oils. No spontaneous oxidation of any of these compounds was observed.

4.3.3 ^{1}H-NMR comparison of diphenylphosphine-triazolopyridines

The ^{1}H-NMR spectra of compounds **75a-c revealed** several tendencies. Our observations particularly concerned the shielding of H^6 relative to the parent compounds **1a**, **1c** and **1d**. This phenomenon was already described for the arylphosphines **69a** and **69d-g**) as shown in **Figure IV-7**, and it was only observed with aryl phosphines (**Figure IV-15**). In contrast the alkyl derivatives like compounds **76a-c** or **77a-c** presented a completely different ^{1}H-NMR pattern.

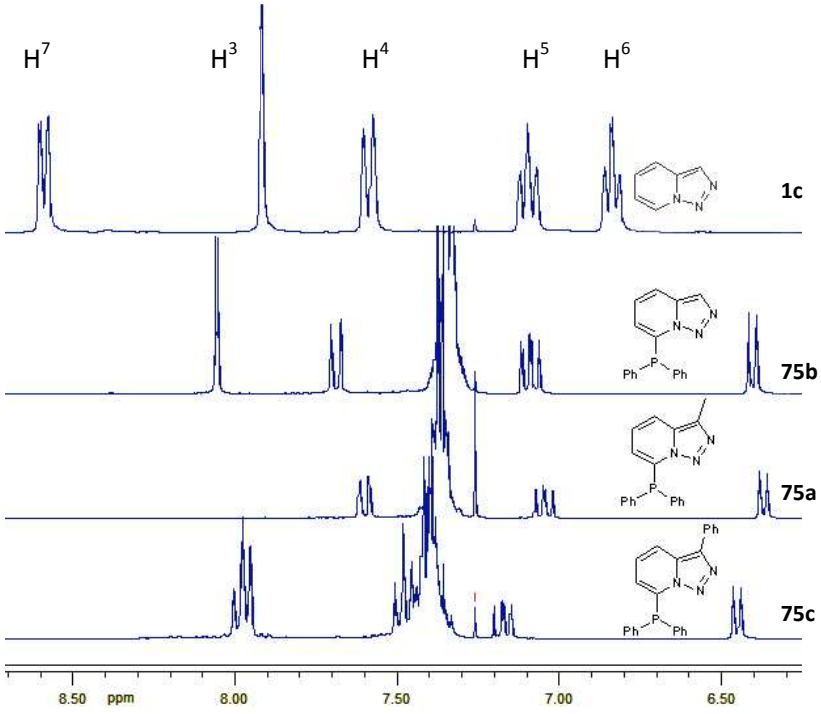

Figure IV-15: ^{1}H-NMR spectra of the different arylphosphines **75a-c** compared to **1c**.

At first, we associated this effect (shielding of H^6) to the relative position of the phosphine. If we consider that the phosphorous lone pair is perpendicular to the triazolopyridine plane, the phenyl ring of the phosphine is directly facing H^6. Thus, the signal of this hydrogen atom is shielded as shown in **Figure IV-16**:

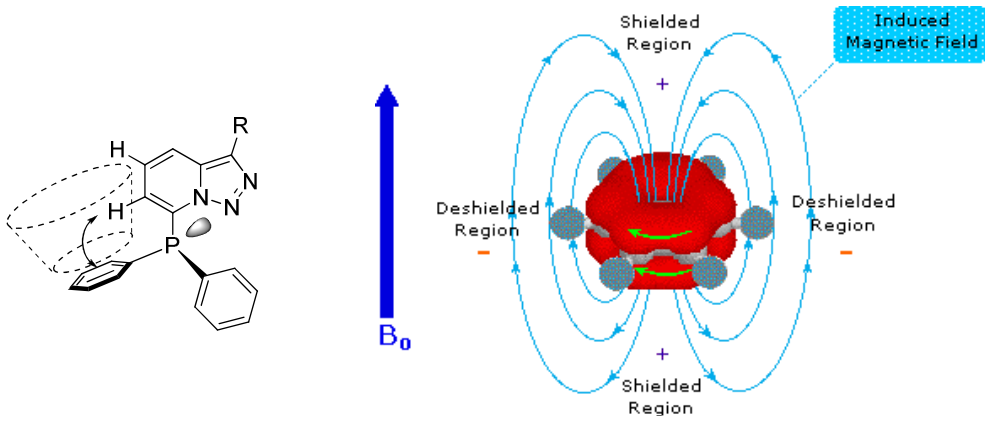

Figure IV-16: Anistropic influence of the phenyl ring on H^6.

This phenomenon has been reported in many cases but the clearest examples are paracyclophanes.[48, 49] We succeeded to obtain single crystals of compounds **75a-c** (**Figure IV-17**). Althougth the X-ray structures cannot be taken as structural model for the molecules in solution, all these structures present the right conformation to provide the shielding effect of H^6. Thus, one of the aromatic rings bond to the phosphine leads the shielding H^6.

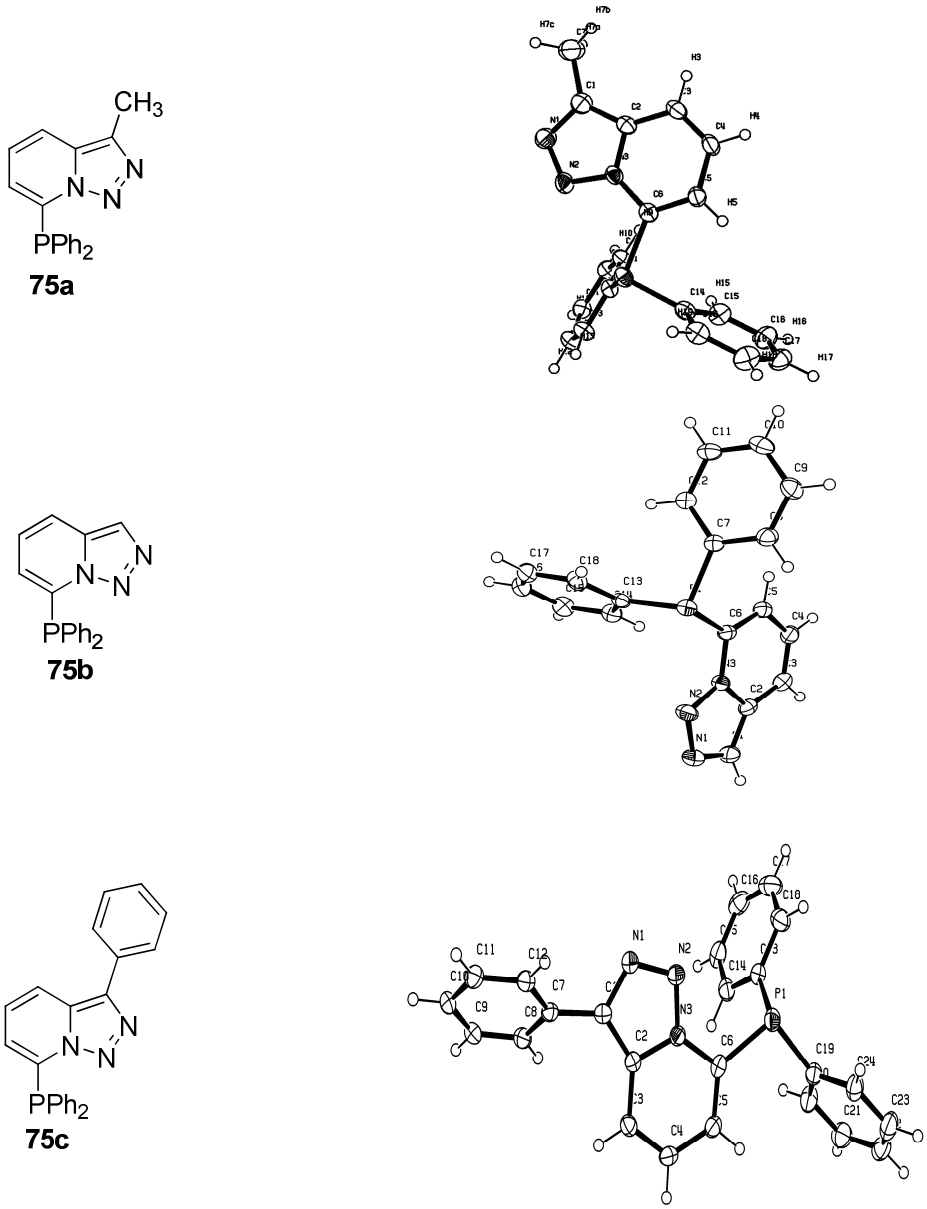

Figure IV-17: Single crystal X-ray analysis of compounds **75a-c**.

4.3.4 ^{1}H-NMR comparison of dialkylphosphines

When the ^{1}H-NMR spectra of dialkylphosphines **76a-c** (dicyclohexylphosphines) and **77a-c** (di-*iso*-propylphosphines) were compared no shielding of H^6 was observed. However, deshielding of H^6 which become a multiplet due to the coupling with H^5 can be found (a shown in **figure IV-18**).

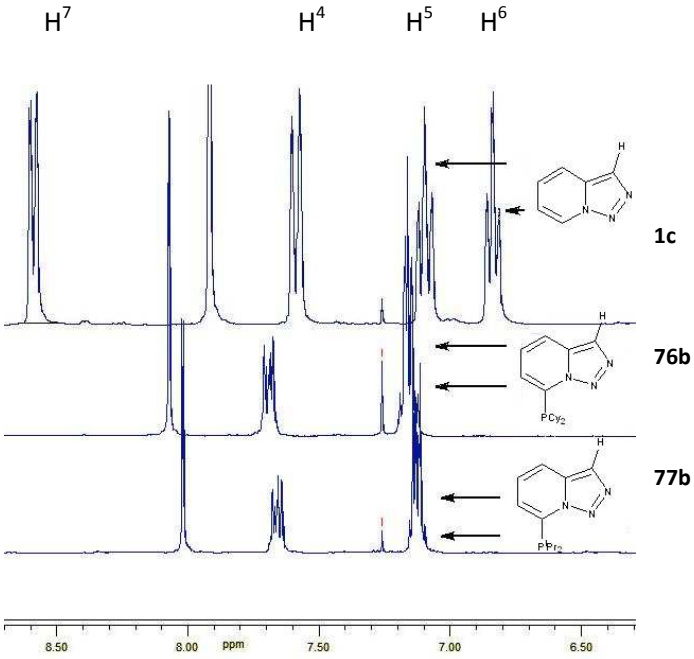

Figure IV-18: ^{1}H-NMR comparison between **1c**, **76b** and **77b** in $CDCl_3$

In order to explain this difference in the ^{1}H-NMR chemical shifts we proposed the following hypothesis. In chapter 3, part 2 we explained that hydrogen atoms on the triazoloquinoline-pyridine scaffold close to the lone pairs of nitrogen atoms N^1, N^2 and N^3 (H^{9A}, H^{4A} and $H^{3'A}$) are deshielded due to the presence of hydrogen bonding. Tentatively we attribute now the same effect to the phosphines. The basic arylphosphines should allow a hydrogen-bond like interaction with proton H^6 which became then deshielded in ^{1}H-NMR.

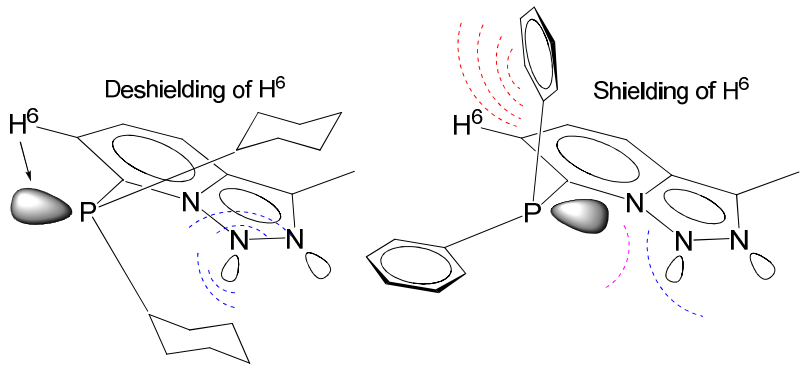

Figure IV-19: Different ^{1}H-NMR effects depending on the phosphorus lone pair position.

As **77a-c** are oils, no crystal structures could be obtained. However, we isolated monocrystals of compounds **76a** and **76b**. Both structures presented the phosphorus lone pair in front of H[6] (**Figure IV-20**):

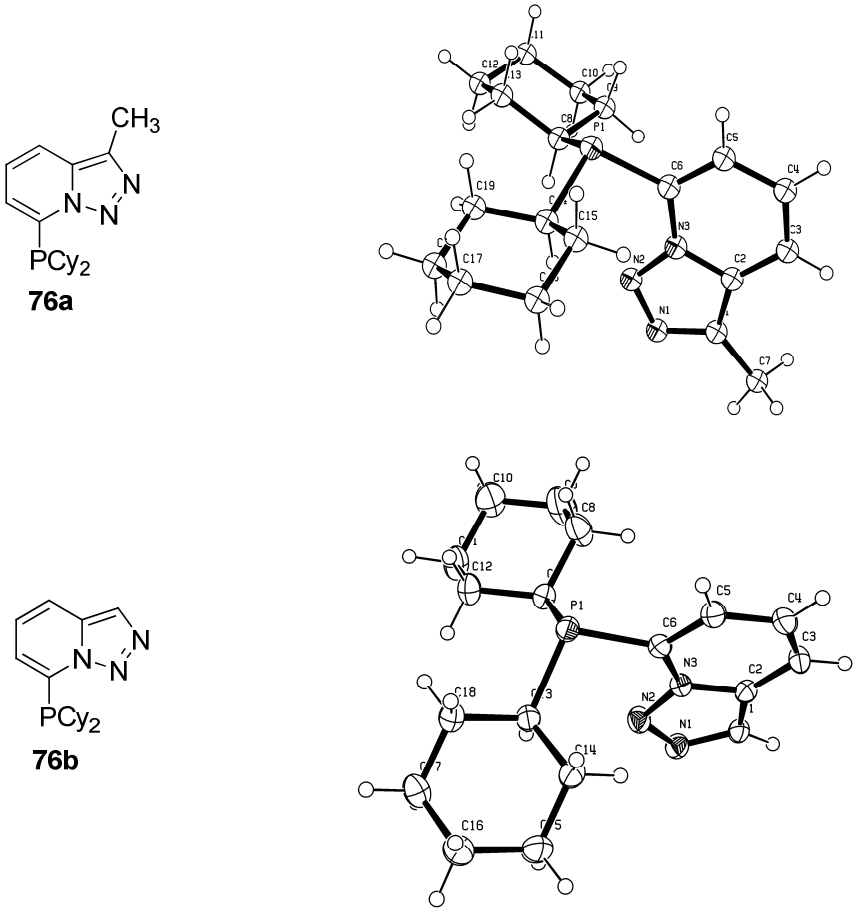

Figure IV-20: X-ray structure for compounds **76a** and **76b**.

The ^{1}H-NMR and X-ray structures suggest that the relative position of the phosphorus lone pair in the solid phase is not the same in alkyl and in arylphosphines. The different (and opposed) effects observed in the NMR-spectra suggest that for each kind of phosphine (aryl or alkyl ones) there is a preferential conformation in solution. In order to corroborate our observations with our assumptions, a theoretical rotational study was performed.

4.3.5 DFT Conformational Study on Isomerism

Geometries of the minima were fully optimised at the B3LYP theoretical level with the 6-31G** basis set as implemented in the Gaussian 03 program.[50] Harmonic frequency calculations verified the nature of the stationary points as minima (all real frequencies). The scanning of the rotation was performed using the IRC type calculation implemented in the Gaussian 03 program at the same level. ^{1}H shieldings of compounds have been calculated over

the fully optimized geometries within the GIAO[52] (Gauge-Independant Atomic Orbital) approximation.

Experimental observations suggested a preferential emplacement of phosphorus lone pair depending on the kind of phosphines. This was proposed due to the significant effects observed in the ^{1}H-NMR spectra of H^6. The possibility of a preferential configuration (between the different rotamers) can be associated to 3 reasons:

- The absence of free rotation between the triazolopyridine and the phosphine.
- The existence of one preferential structure although having free rotation.
- The existence of one privileged structure and the absence of free rotation.

Figure IV-21 shows the general formula of the studied compounds. For a better understanding, we focused only on the orientation of the phosphine substituents with respect to the triazolopyridine ring (C^7-PX_2 rotation), regardless of possible conformations resulting from the internal rotation of the phosphine substituents (X-P rotation) and, in the special case of X = Cy, other conformations as consequence of the flip motion. Besides the electronic effects through the bond, in the figure, we pointed out other (electronic or steric) factors that, could have a significant influence. The proximity of both the hydrogen H^6 of the triazole ring and the lone pair of the nitrogen N^1, may allow them to exert attractive or repulsive interactions with either the lone pair or the substituents on the phosphine group, influencing the relative stability of the different conformers.

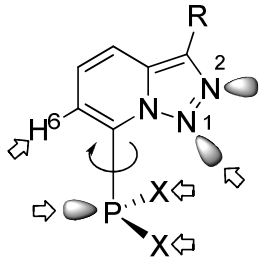

Figure IV-21: Rotational study.

As mentioned before, the ^{1}H-NMR spectra revealed two different signals patterns for the phosphines, depending on the substituents on the phosphine group. X-ray studies confirmed later two different conformations. The conformer **A**, found in the series of alkyl substituted phosphines (X = Cy: **76a-c** and ^{i}Pr: **77a-c**) has the lone pair of the phosphine group on the opposite side of the triazole nitrogen atom N^1 and oriented towards the H^6 hydrogen atom. The substituents are oriented on both sides of the ring. The conformer **B**, X = Ph (**75a-c**), has one of the phenyl substituents oriented towards the hydrogen atom H^6 of the heterocyclic ring, and the second phenyl ring and the phosphorus lone pair on both sides of the triazole ring and towards nitrogen atom N^1(**Figure IV-22**).

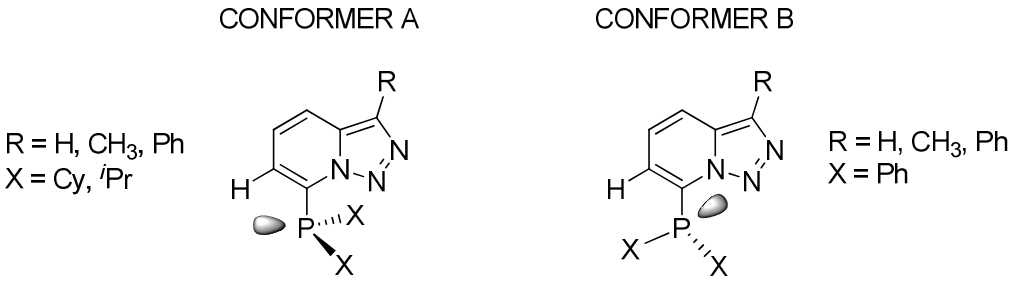

Figure IV-22: Conformers.

4.3.5.1 Reaction profile

As shown in **Figure IV-23**, the minimum corresponding to the conformer **A**, with the geometry described above, the rotation in either direction lead, through the transition states **TS AB$_1$** and **TS AB$_2$**, to the two equivalent minima **B$_1$** and **B$_2$** which have the substituents located on the opposite side of the triazole ring plane. Finally, the transition between **B$_1$** or **B$_2$** go through **TS B$_1$B$_2$**, where the lone pair of N[1] and the lone pair of phosphorous are arranged on the same plane.

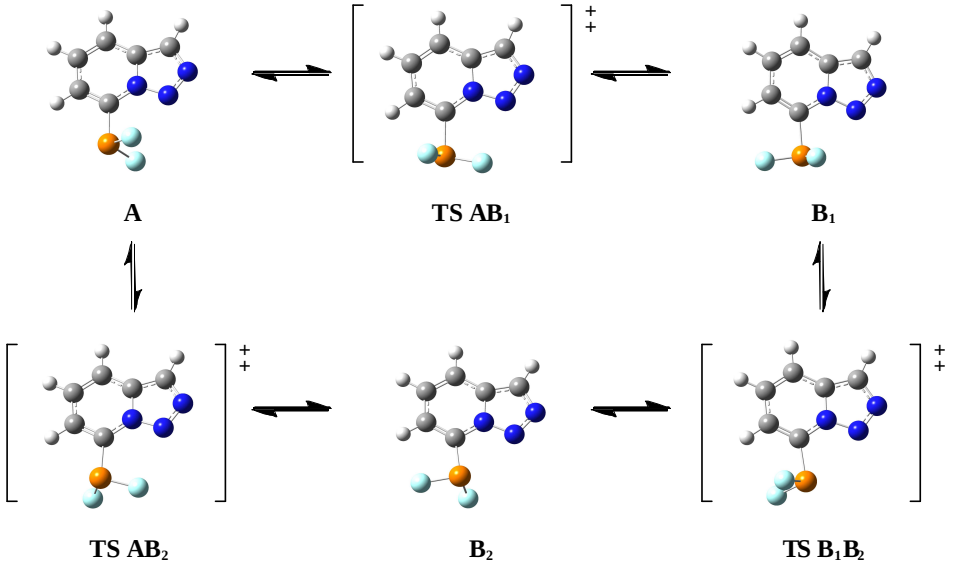

Figure IV-23: Rotational mechanism from **A** to **B**.

Given the nature of the substituents in the synthesized compounds, both steric hindrance and the electronic profile must be evaluated. In order to minimize the steric factor, firstly, we screened the rotation in phosphines substituted by small groups but with very different electronic properties (**X = H, CH$_3$** and **F**). **Figure IV-24** shows the reaction path for the studied derivatives in terms of relative energy with respect to the minimum **A**. For each case the profile is characteristic.

An initial conclusion is, that all transition barriers were found to be smaller than 30 kJmol^{-1} and that therefore it can be considered that in all cases a free rotation exists. Therefore, the conformational preference in solution can be explained based on a

thermodynamic approach. Concerning the electronic nature of the substituents, there are clear differences in the rotation profile when the phosphine is substituted by an electron-attractor group (**X = F**) or when it is substituted by an electron-donor (**X = H, CH_3**). As shown, when **X=F**, the absolute minimum corresponds to the conformer type **B**, with an energy difference close to 10 $kJmol^{-1}$.

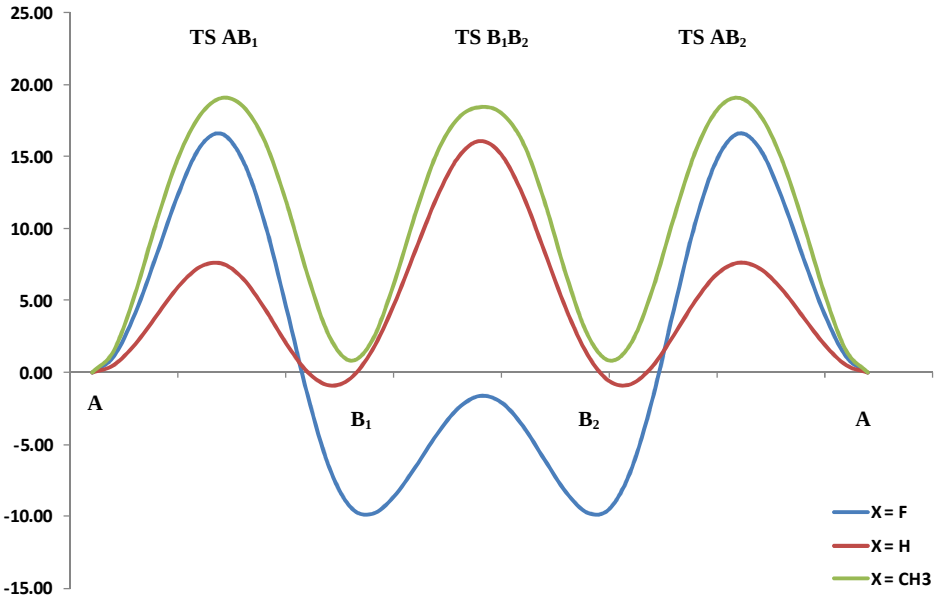

Figure IV-24: Reaction path for the studied derivatives.

The orientation of one of the fluorine atoms toward H^6 of the triazole ring, allowing a stabilization and low repulsion between the N^1 lone pair and the phosphine lone pair explain the lower energy of this conformation. Moreover, in conformation A for this case, the two fluorine atoms are located next to the N^1 lone pair. A situation which is clearly destabilizing. For **X = H** and **X = CH_3**, the energy differences between the conformers **A** and **B** are very small, although in the case of **X = CH_3** the conformer **A** is slightly favored. There are no electronic or steric factors favoring one of the two conformations.

The analysis of the transition barriers offers interesting results, in spite of the low-energy range which would not block a free rotation under normal conditions. For example the transition state **TS AB_{1-2}**, corresponding to the geometries in which the phosphine substituents (-F, -H or -CH_3) pass through the position closest to N^1. The energies of **X=F** and **CH_3** are very similar, corresponding to the repulsion between **N^1-X**, In contrast they decrease significantly for **X = H** (7.50 $kJmol^{-1}$), possibly due to a stabilizating interaction by hydrogen bonding (N^1---H). **TS B_1B_2**, however, shows similar energetic barriers for **X = H, CH_3** (15.00 - 20.00 $kJmol^{-1}$), while visibly it decreases for **X = F**. In this case, the most decisive situation is the interaction of the phosphine lone pair and N^1. One possible explanation is that for **X = F**, the effect of the electron-attracting of fluorine atom, reduces the charge on the lone pair of phosphorus, and,

as a corollary decreasing the repulsion with the lone pair of N[1]. For **X = H, CH_3**, however, this repulsive interaction would be increased due to the donor character of the substituents that could increase the electronic density of phosphorus lone pair. **Figure IV-25** shows the screening of the rotation for two of the synthesized compounds (**X = Cy 76b and Ph 75b**). As it can be seen, the graph corresponding to the rotation of **76b** shows clear discontinuities. In this compound, the substituent can adopt a large number of conformations depending on the movements of the cyclohexyl rings, complicating the analysis of results. However, from a very general point of view, we can see that: first, the transition barriers are quite high, compared to the previously studied compounds **(X = H, CH_3, F).** This can be due to steric hindrance, but always within the limits of free rotation under normal conditions. Secondly, the most stable geometry corresponds, as seen for the methylated derivative (**X = CH_3**), to the conformer **A**. This will be discussed later in the study of the ratios of the optimized minima. The rotation of compound **75b** (**X = Ph**), is much easier to interpret. The rigidity of the aromatic ring decreases the number of possible conformations. As it can be seen, the sequence has only a small discontinuity and is largely similar to that obtained for **X = F**. This result is consistent when electronic effects are considered, as the phenyl substituent group, has a smaller electron-donor effect on phosphorus compared to cyclohexyl. The transition barriers are slightly higher than for small substituents, but less than in the case of cyclohexyl groups with a more pronounced steric effect.

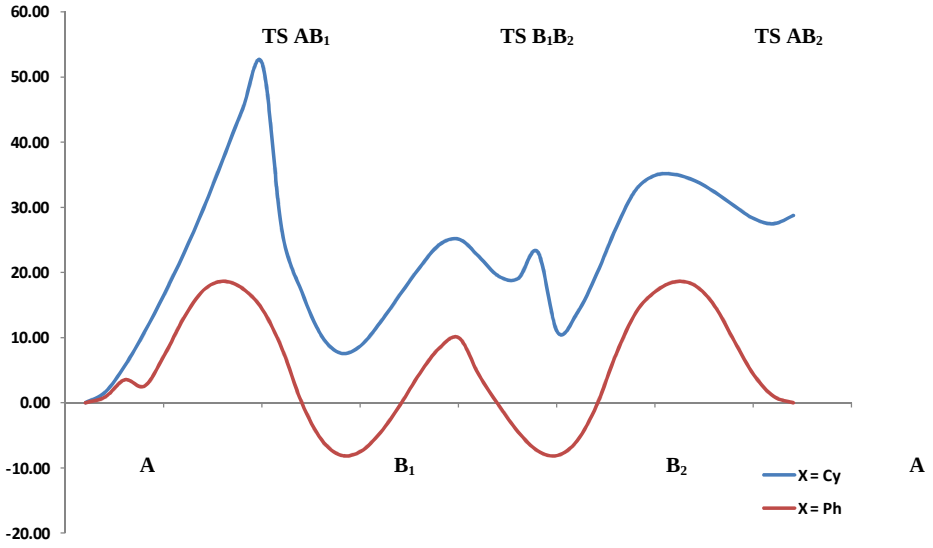

Figure IV-25: Reaction path for the studied derivatives -PCy_2 **76b** and -PPh_2 **75b**.

4.3.5.2 Theoretical calculations concerning the A-B ratios

As explained above, we have selected different groups, the experimentally studied (-PCy_2: **76b**, -PPh_2: **75b** and P^iPr_2: **77b**), and (**X = H, CH_3, F**), to optimize their geometries and to locate the energy minima. In the case of substituents with secondary conformations as a result of the internal movement of the substituent, some different geometries have been minimized. **Table IV-5** shows the relative energies between the most stable configuration of each isomer for the different substituents considered. Negative values indicate that for the corresponding compound, the conformer **A** is favored while positive values favor isomer **B**. The results obtained experimentally indicate the good prediction of the theoretical results.

Table IV-5: **A**/**B** ratio

X		ΔE (kJmol^{-1})	Theoretical	Experimental
Cy	**76b**	-7.54	A	A
^{i}Pr	**77b**	-7.38	A	A
CH_3		-0.81	A	---
H		0.91	B	---
Ph	**75b**	8.13	B	B
F		9.90	B	---
Br		11.16	B	---

It can be seen that the electronic properties of the substituent plays an essential role in the results. The trend is that the substituents with inductive effect (+I) stabilize the conformer type **A** (X = Cy, ^{i}Pr, CH_3), whereas substituents with inductive effect (-I) stabilize the conformer type **B** (X = Br, F, Ph). This observation is in accordance with the experimental results obtained in this work. Moreover, the energy differences calculated are high enough to explain, that these compounds are present as the most stable isomer in the equilibrium.

4.3.5.3 Comparison between predicted and experimental NMR chemical shifts[51]

Table IV-6 presents the comparison between experimental and calculated values of ^{1}H-NMR chemical shifts. For the dicyclohexylphosphine-substituted compound **76b,** the ^{1}H-NMR is close to the predicted one for the **A** isomer (Entries 1 and 2) and the *iso*-propyl derivate **77b**, respectively (entries 4 and 5). Especially the experimental spectra of **75b** (entry 10) and of the calculated **B** isomer (entry 12) are remarkable. When both values are compared, for example looking to the H^6 isomer, big differences appears between the **A** and **B** isomers being really close to the **B** isomer, the one who can be involved in the upshielding observed experimentally (**Figure IV-19**). The ^{1}H-NMR results, the single crystal X-ray analysis and the DFT calculations concerning the rotation between the phosphine-triazolopyridine bonds indicate without any

doubt that, depending on the kind of phosphines, a characteristically spatial orientation of phosphorus lone pair can be deduced.

Theoretical calculations revealed not only a steric, but also an electronic influence. Although these observations cannot be used as a sensor for the electronic properties (like the triazole ring isomerisation) the specific orientation of the phosphorus lone pair has a strong consequence on the ^{13}C-NMR spectra.

Table IV-6: Experimental and calculated values of the ^{1}H-NMR.

Entry	Compound	Isomer	H^3	H^4	H^5	H^6
1	**76b**	**A exp**	8.07	7.7-7.6	7.2-7.1	7.2-7.1
2	**Cy**	**A**	8.08	7.61	6.99	7.27
3	**Cy**	**B**	8.01	7.50	7.01	6.88
4	**77b**	**A exp**	8.02	7.7-7.6	7.2-7.1	7.2-7.1
5	**^{i}Pr**	**A**	8.1	7.64	7.03	7.34
6	**^{i}Pr**	**B**	8.04	7.53	7.06	6.90
7	**Me**	**A**	8.09	7.64	7.03	7.36
8	**Me**	**B**	8.04	7.54	7.07	6.76
9	**H**	**A**	8.19	7.76	7.09	7.30
10	**H**	**B**	8.06	7.58	7.04	6.96
11	**Ph**	**A**	8.03	7.67	7.12	7.61
12	**Ph**	**B**	7.99	7.53	6.92	6.20
13	**75b**	**B exp**	7.98	7.61	7.01	6.32
14	**F**	**A**	8.19	7.81	7.10	7.19
15	**F**	**B**	8.15	7.74	7.21	7.33
16	**Br**	**A**	8.29	7.83	7.07	7.14
17	**Br**	**B**	8.18	7.78	7.28	7.89

4.3.6 Phosphorus interaction in the ^{13}C-NMR

The special properties of the phosphorus atom in ^{13}C-NMR has been reported for some molecules.[52] In phosphines, the effect of the phosphorus lone pair orientation on P-C coupling is well known. Quin[53, 54] *et al.* reported on the orientational lone pair effect on the ^{2}J(P,C) couplings in 7-(phosphamethyl)-norbornene derivatives with the ring carbon atoms (**Figure IV-26**).

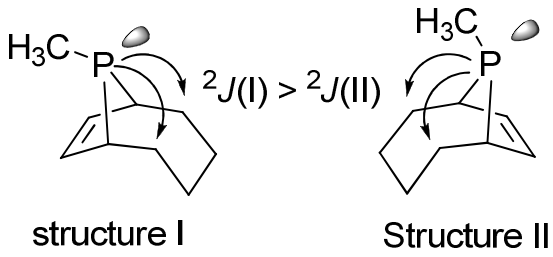

Figure IV-26: Effect orientation of the lone pair on the J(P,C)

He observed the enhancement of the *J*(P,C) value with the proximity to the lone pair. Due to the properties of these molecules (cyclic phosphine) no free rotation on phosphorus is possible. Contrary to the free C-P rotation which is thermodynamically possible for our phosphines, in the cyclic phosphines the phosphorus atom can no undergo free rotation and bigger coupling constants are observed, for structure I $^2J(P\text{-}CH_2)_{(Structure\ I)}$ = 16.5 Hz compared to $^2J(P\text{-}CH_2)_{(Structure\ II)}$ = 4.3 Hz. Recently, Peralta and Contreras[55] calculated the evolution of the ^2J(P,C) value for ethyl phosphine, observing a dependence on the C-C-P angle (φ) (**Figure IV-27**).

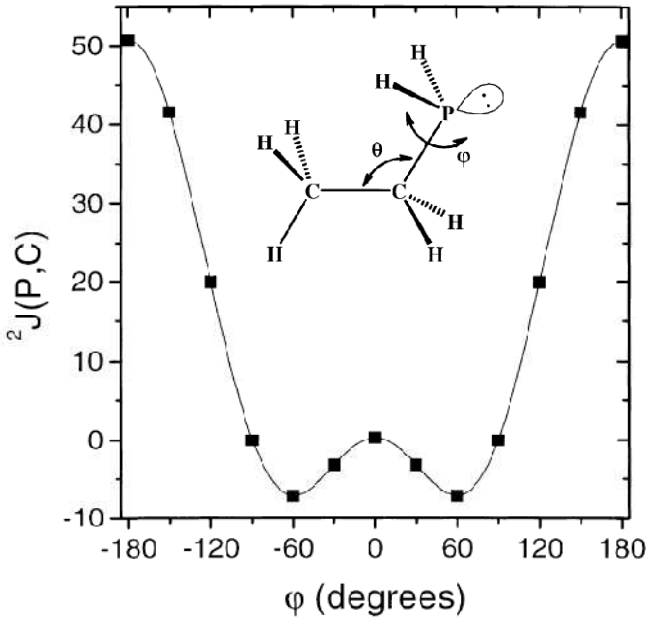

Figure IV-27: Angle (φ) dependence in *J*(P,C).

By means of DFT calculations Peralta and Contreras proposed the following equation to predict the value of the coupling constant for this compound:

$$^2J(P,C)\ (Hz) = 12{,}74 - 25{,}88\cos(\varphi) + 12{,}76\cos(2\varphi) + 0{,}61\cos(3\varphi) \qquad (1)$$

Although many phosphine-based compounds are published every year, the assignment of carbon signals and the phosphorous lone pair effect are normally not reported. Some experimental results showing the influence of the angle on the coupling constants can be found on the review article from Gil and Philipsborn.[56]

4.3.6.1 ^{13}C-NMR Analysis of compounds 75a-c, 76a-c and 77a-c

In the previous chapter, we showed how the compounds **75a-c**, **76a-c** and **77a-c** can have preferential conformations as observed by ^{1}H-NMR, despite possible free rotation around the P-C bond. The special stability of these structures was confirmed by DFT calculations and by single x-ray structure analysis for the solid state. Depending on the kind of phosphine, we observed a special orientation of the phosphorus lone pair as shown in **Figure IV-28**:

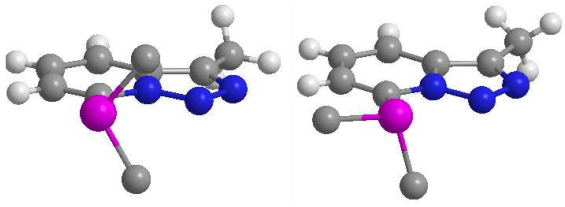

Figure IV-28: Simplified single crystal X-ray analysis for **75a** (right) and **76a** (left), comparison of relative position of the phosphorus doublet. R-Substituents of the phosphine have been omitted for clarity.

The ^{13}C-NMR carbon assignation for the triazolopyridine-phosphines **69a-g** was difficult due to the numerous P-C couplings, the number of equivalent nuclei and the presence of both isomers (**A** and **B**) due to the ring chain isomerisation. However, in the phosphines **75a-c**, **76a-c** and **77a-c** the assignment of C^7, C^6, C^5, C^4 and C^3 carbon signals can be more easily done because no isomerisation occurs (**Table IV-7**).

Table IV-7: Triazolopyridines **75a-c**, **76a-c** and **77a-c** C^7, C^6, C^5, C^4 and C^3 assignation, chemical shift (ppm) and *J*(P-C) coupling constant (Hz).

Entry	Compound	C^7	C^6	C^5	C^4	C^3	$^1J_{(C7-P)}$	$^2J_{(C6-P)}$	$^3J_{(C5-P)}$	$^4J_{(C3-P)}$
1	**1a**	124,9	115,1	125,1	117,7	133,5	0	0	0	0
2	**1c**	123,3	114,9	124,5	116,9	125.5	0	0	0	0
3	**71a**	138,4 d	120,9	124,5	117,4	134,2 d	22,4	0	0	1,2
4	**72a**	137,1 d	124,1 d	124,6 d	118,2	134.2	41,8	25,9	8,2	0
5	**73a**	137,5 d	124,2 d	124,2 d	118,1	134,4	42,2	24,2	7,6	0
6	**71b**	138,5 d	120,8	123,1	117,2	125,6 d	22	0	0	1,6
7	**72b**	136,7 d	122,5 d	124,5 d	117,8	125.7	41,8	26,7	8,5	0
8	**73b**	137,4 d	122,7 d	124,4 d	117,9	125.6	41,8	26,1	8,3	0
9	**71c**	139,3 d	120,9	124,9	117,9	137.8 d	23,3	0	0	1,9
10	**72c**	137,6 d	125,1 d	124,6 d	118,8	137,8	44,2	27,6	8,7	0
11	**73c**	138,2 d	124,6 d	124,7 d	118,8	137.9	43,6	26,2	8,3	0

[a] $CDCl_3$, ^{13}C-NMR experiences were performed on a 300 MHz Brukner NMR.

If we compare the ^{13}C-NMR chemical shifts of the parent compounds **1a** and **1c** with the corresponding phosphines, a downfield shift for the carbon atom C^7 of almost 15 ppm can be observed. For the C^6 a shift of 5 – 10 ppm and less than 5 ppm for C^5 can be deduced. There

is almost no influence on the carbon C^4. This influence is the same if we are considering alkyl- or aryl-phosphines.

However, the most intriguing is the influence on the C-P coupling constants. For example the alkyl phosphines (**76a-c** and **77a-c**) show *J*(C-P) couplings for the carbon atoms C^7, C^6 and C^5, in contrast to C^4, which shows no coupling. The situation is completely different when considering aryl phosphines (**75a-c**), where only C-P couplings for carbon C^7 and C^3 can be observed, but not with C^6 and C^5. Furthermore, for compounds **75a-c**, coupling constants (^2J and ^3J) can be found with the carbon atoms of the phenyl rings (from the diphenylphosphine) (**Figure IV-29**).

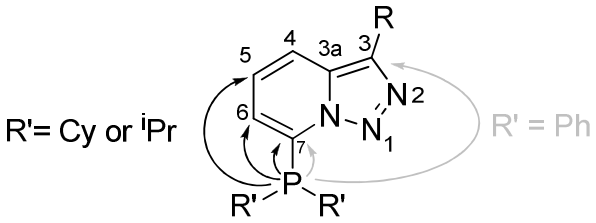

Figure IV-29: Selective coupling of different phosphines with the triazolopyridine ring.

Despite the absence of a theoretical model to predict the values of the coupling constants, we can affirm that the phosphorus lone pair plays an essential role in these values. A relation between the P-C coupling constant and the lone pair orientation is observed. This phenomenon can now undoubtfully be observed due to the relative simplicity of compounds **75a-c – 77a-c**.

4.3.7 ^{31}P-NMR study

Next we wanted to study how the triazolopyridine ring influences the ^{31}P chemical shift with respect to the classical phosphines. **Table IV-8** shows the ^{31}P-NMR chemical shift of the phosphines **75a-c – 77a-c,** as well as the corresponding selenides (from **71a-c**) and their coupling constants. These coupling constants reveals, as outlined in part 3.1, the σ-donor capacity of phosphines, which increases **75a (-PPh_2)** < **77c (-P^iPr_2)** < **76b (-pCy_2).** The chemical shift of the different phosphines (**Table IV-8**, entry 1) is similar the one observed with trisubstituted phosphines (^{31}P-NMR for PPh_3 δ = -4 ppm, PCy_3 δ = 9.8 ppm and for P^iPr_3 δ = 19.4 ppm)

Table IV-8: ^{31}P-NMR for compounds **75a-c**, **76a-c** and **77a-c**.

Entry	^{31}P	75a	76a	77a	75s	76b	77b	75c	76c	77c
1	δ P (ppm)	-15	6,5	16,1	-15	7,1	15,4	-15	6,8	17,3
2	σ P[Se-75-77a](ppm)	32,3	65,9	75,3						
3	*J*(Se-P) (Hz)	758	737	745						

4.3.8 ^{13}C-NMR study of compounds 78a-c and 79a-c

Interested by the effects associated to the phosphorus lone pair, we carefully examined the ^{13}C-NMR spectra of the selenides **78a-c** and oxides **79a-c**. The selenides were prepared by the classical method[36] starting from **75a**, **76a** and **77a** as shown in **Scheme IV-10**:

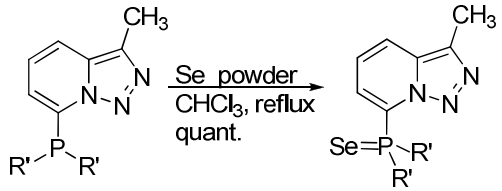

75a R' = Ph
76a R' = Cy
77a R' = ^{i}Pr

78a R' = Ph
78b R' = Cy
78c R' = ^{i}Pr

Scheme IV-10: Preparation of selenides.

The phosphines oxides **79a-c** where obtained by reaction with hydrogen peroxide in methanol as shown in **Scheme IV-11**.

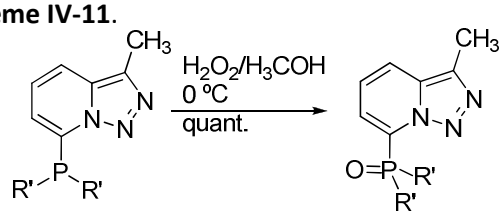

75a R' = Ph
76a R' = Cy
77a R' = ^{i}Pr

79a R' = Ph
79b R' = Cy
79c R' = ^{i}Pr

Scheme IV-10: Preparation of oxides.

The modification of the oxidation state of phosphorous induced a general deshielding of H^6 and H^5 for the oxides **79a-c** and selenides **78a-c**, more significant for the selenides. All compounds presented similar characteristics independently of the kind of phosphine. The ^{13}C-NMR revealed, contrary to the free phosphines, coupling with all pyridine ring carbon atoms, for all compounds (**Figure IV-30).**

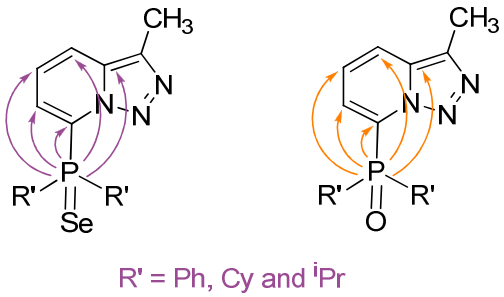

Figure IV-30: ^{13}C-NMR P-C coupling constant of compounds **78a-c** and **79a-c**.

4.3.9 Conclusions

- The ^{1}H-NMR and DFT study revealed how the phosphorus lone pair orientation influences the shielding/deshielding of H^{6}. This phenomenon was already observed with compounds **69a-g**. However due to the structural simplicity of the present compound family, calculations, X-ray and NMR studies allowed now a complete argumentation on this phenomenon. Although a free rotation between the phosphine-triazolopyridine bond is possible, some rotamers revealed to be more favourable, which is coherent with the experimental findings.

- The orientation of the phosphorus lone pair induces an uncommon ^{13}C-NMR coupling pattern. This phenomenon was clearly identified due to the simplicity of compounds **75-77a-c** (compared to **69a-g**). The lone pair has been found to favour P-C NMR coupling constants when the carbon atoms are near or coplanar or at the same side to it. When the lone pair is "removed" (oxidation or selenide formation), a general NMR coupling pattern can be found. Although no structural analogues of our molecules have been studied previously, the observed NMR coupling pattern was described for different organic molecules where a correlation between lone pair orientation and ^{13}C resonance can be done.

IV: Triazolopyridine-phosphines

4.4 Triazoloquinoline-phosphines

4.4.1 Introduction and objectives

Between 2004 and 2007, several heteroaryl-aryl ligands were developped by Beller, Singer and Kwong for coupling reactions. In 2005, Zhang *et al*. reported on the synthesis of original triazole-based monophosphine ligands, **ClickPhos**,[24] *via* an 1,3-dipolar cycloaddition of organoazides and acetylenes developed by Sharpless.[57]

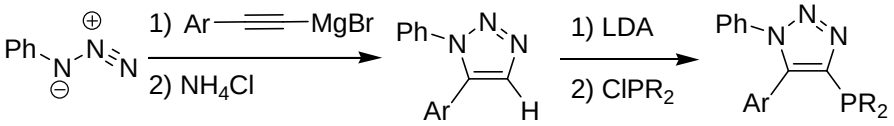

Ar= Ph	**75%**	Ar= Ph	R= Ph	**90%**
Ar= 1-Np	**58%**	Ar= Ph	R= Cy	**93%**
Ar= 2-OCH_3Ph	**83%**	Ar= Ph	R= ^{t}Bu	**91%**
Ar= 2-$N(CH_3)_2$-Ph	**61%**	Ar= 1-Np	R= Cy	**81%**
Ar= 2,6-$(OCH_3)_2$-Ph	**78%**	Ar= 1-Np	R= ^{t}Bu	**75%**
		Ar= 2-OCH_3Ph	R= Cy	**64%**
		Ar= 2-CH_3Ph	R= ^{t}Bu	**76%**
		Ar= 2-$N(CH_3)_2$-Ph	R= ^{t}Bu	**69%**
		Ar= 2,6-$(OCH_3)_2$-Ph	R= ^{t}Bu	**79%**
		Ar= 2,6-$(OCH_3)_2$-Ph	R= Cy	**76%**

Scheme IV-11: Clickphos family:

The authors highlighted their efficiency in amination and Suzuki-Miyaura couplings with aryl chlorides. Excellent yields and TONs were obtained for the coupling of sterically non-hindered substrates.[24, 25] Comparing these structures with triazoloquinoline derivatives **45a-e**, we could easily prepare analogues by regioselective metalation at C^3 as developed in chapter III. In this way, we proposed to synthesize triazoloquinoline phosphines, having the phosphine group bonded to the triazole ring.

This work was performed with Dr. Laurence Bonnafoux (who performed a PhD on the synthesis of phosphines based ligands for catalysis between 2005-2008 under the direction of Dr. Frédéric Leroux and Prof. Françoise Colobert).

4.4.2 Preparation of triazoloquinoline-based analogues to Click Phos

As reported previously there is no way to provide a regioselective metalation at C^3 of triazolopyridines. However, triazoloquinoline undergoes C^3 metalation with ^{t}BuLi or LiTMP (See Chapter 3 part 1). For example [1,2,3]triazolo[1,5-*a*]quinoline (**44**) is functionalized by regioselective lithiation at the C^3 position with *tert*-butyl lithium in THF at -78°C during 2 hours. Trapping with the chlorophosphine afforded only for chlorodiphenylphosphine the desired derivated **80a**. Di-*iso*-propyl- and dicyclohexyl phosphines were oxidized during purification, affording the corresponding phosphine oxides **81a** and **81b** as shown in **Scheme IV-12**:

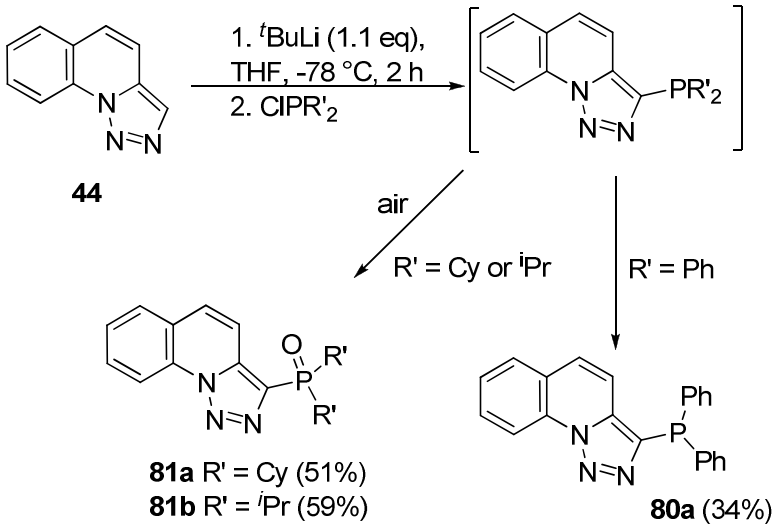

Scheme IV-12: Preparation of compounds **80a**, **81a** and **81b**.

Finally, monophosphine **80a,** those structure was confirmed by single crystal X-ray analysis (**Figure IV-22),** is the only triazoloquinoline derivative suitable for an application in catalysis. However, in the catalytic tests performed by Zhang alkyl phosphines provided the most interesting results.

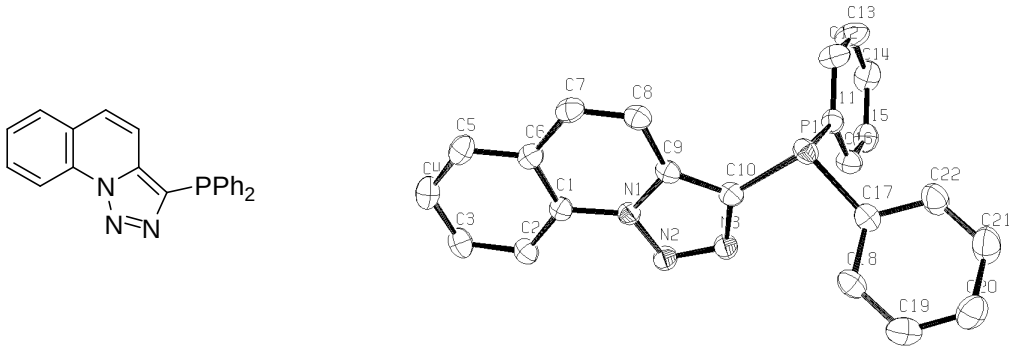

Figure IV-22: Structure and X-ray representation of compound **80a.**

Although in his previous work, Zhang never mentioned the possible oxidation of clickphos ligands, all solvents as well as brine and silica had to be previously deoxygenated.

As outlined before, the phosphines **72-74** are highly air-sensitive and amongst a family of various phosphines with different electronic profile, they are the only ones to show spontaneous air oxidation.

We outlined already in the previous chapters, that triarylphosphines are more stable towards air oxidation compared to alkylphosphines.[44] Highly electron-rich alkyl phosphines (-PCy_2 and -P^iPr_2) are easily oxidized. In our case, we can consider the triazolopyridine ring as electron-rich, after introduction of the phosphine group rather on a triazole ring than on a pyridine ring like in chapter 4 part 3. Thus, the high electron-density at phosphorous leads to rapid oxidation, the situation is completely different with respect to the triazoloquinoline-pyridine phosphines (chapter 4, part 2). They were electron-rich due to coordination of the nitrogen (N^1) lone pair.

4.4.3 Conclusions

- Although, we have been able to prepare triazoloquinoline having a phosphine at C^3, the oxidation of the most suitable phosphines for catalysis revealed an important drawback. The only stable phosphine is the most electron-poor PPh_2-subtituted **80a**. Compared to Zhang's results, **80a** is not the most suitable kind of phosphine for Suzuki-Miyaura couplings.

4.5 References

[1] B. Abarca, I. Alkorta, R. Ballesteros, F. Blanco, M. Chadlaoui, J. Elguero, F. Mojarrad, *Org. Biomol. Chem.* **2005**, *3*, 3905.
[2] W. Knowles, S. , *Angew. Chem. Int. Ed.* **2002**, *41*, 1998.
[3] R. Noyori, *Angew. Chem. Int. Ed.* **2002**, *41*, 2008.
[4] K. B. Sharpless, *Angew. Chem. Int. Ed.* **2002**, *41*, 2024.
[5] M. Berthod, G. Mignani, G. Woodward, M. Lemaire, *Chem. Rev.* **2005**, *105*, 1801.
[6] T. P. Dang, H. B. Kagan, *J. Chem. Soc., Chem. Commun.* **1971**, 481.
[7] R. G. Arrayás, J. Adrio, J. C. Carretero, *Angew. Chem., Int. Ed.* **2006**, *45*, 7674.
[8] A. Togni, N. Bieler, U. Burckhardt, C. Köllner, G. Pioda, R. Schneider, A. Schnyder, *Pure Appl. Chem.* **1999**, *71*, 1531.
[9] A. Togni, *Angew. Chem. Int. Ed.* **1996**, *35*, 1475.
[10] A. Togni, C. Breutel, A. Schnyder, F. Spindler, H. Landert, A. Tijani, *J. Am. Chem. Soc.* **1994**, *116*, 4062.
[11] T. Ireland, G. Grossheimann, C. Wieser-Jeunesse, P. Knochel, *Angew. Chem. Int. Ed.* **1999**, *38*, 3212.
[12] M. McCarthy, P. J. Guiry, *Tetrahedron* **2001**, *57*, 3809.
[13] W. Tang, X. Zhang, *Chem. Rev.* **2003**, *103*, 3029
[14] H. Shimizu, I. Nagasaki, T. Saito, *Tetrahedron* **2005**, *61*, 5405.
[15] R. Schmid, J. Foricher, M. Cereghetti, P. Schönholzer, *Helv. Chim. Acta* **1991**, *74*, 370.
[16] N. Sayo, T. Saito, T. Yokozawa, (to Takasago Int. Corp. Japan, **1999**) Eur. Pat. 945457.

[17] T. Yokozawa, N. Sayo, K. Matsumura, H. Kumobayashi, *Chem. Abstr.* **1998**, *128*, 270732.

[18] S. Jeulin, S. Duprat de Paule, V. Ratovelomanana-Vidal, J.-P. Genet, N. Champion, P. Dellis, *Angew. Chem. Int. Ed.* **2004**, *43*, 320

[19] F. Leroux, J. Gorecka, M. Schlosser, *Synthesis* **2004**, 326.

[20] H. Mettler, F. Leroux,(to Lonza AG, Switz., **2005**) Eur. Pat. 1528053.

[21] A. Zapf, R. Jackstell, F. Rataboul, T. Riermeier, A. Monsees, C. Fuhrmann, N. Shaikh, U. Dingerdissen, M. Beller, *Chem. Commun.* **2004**, 38.

[22] S. D. Walker, T. E. Barder, J. R. Martinelli, S. L. Buchwald, *Angew. Chem. Int. Ed.* **2004**, *43*, 1871.

[23] R. Martin, S. L. Buchwald, *Acc. Chem. Res.* **2008**, *41*, 1461.

[24] D. Lui, W. Gao, X. Zhang, *Org. Lett.* **2005**, *7*, 4907.

[25] Q. Dai, W. Gao, D. Liu, L. M. Kapes, X. Zhang, *J. Org. Chem.* **2006**, *71*, 3928.

[26] H. U. Blaser, F. Spindler, M. Studer, *App. Catal. A: General* **2001**, *221*, 119.

[27] H. U. Blaser, C. Malan, B. Pugin, F. Spindler, H. Steiner, M. Studer, *Adv. Synth. Cat.* **2003**, *345*, 103.

[28] C. A. Tolman, *J. Am. Chem. Soc.* **1970**, *92*, 2953.

[29] C. A. Tolman, *Chem. Rev.* **1977**, *77*, 313.

[30] K. A. Bunten, L. Chen, A. L. Fernandez, A. J. Poe, *Coord. Chem. Rev.* **2002**, *233-234*, 41.

[31] H. G. Schuster-Woldan, F. Basolo, *J. Am. Chem. Soc.* **1966**, *88*, 1657.

[32] C. A. Streuli, *Anal. Chem.* **1960**, *32*, 985.

[33] T. Allman, R. G. Goel, *Can. J. Chem.* **1982**, *60*, 716.

[34] W. A. Henderson, C. A. Sreuli, *J. Am. Chem. Soc.* **1960**, *82*, 5791.

[35] G. M. Bodner, M. P. May, L. E. McKinney, *Inorg. Chem.* **1980**, *19*, 1951.

[36] D. W. Allen, B. F. Taylor, *J. Chem. Soc., Dalton Trans.* **1982**, 51.

[37] K. Mashima, K. Kusano, N. Sato, Y. Matsumura, K. Nozaki, H. Kumobayashi, N. Sayo, Y. Hori, T. Ishizaki, S. Akutagawa, H. Takaya, *J. Org. Chem.* **1994**, *59*, 3064.

[38] A. R. Sanger, *J. Chem. Soc., Dalton Trans.* **1977**, 120.

[39] L. Vallarino, *J. Chem. Soc.* **1957**, 2287.

[40] K. Junge, G. Oehme, A. Monsees, T. Riermeier, U. Dingerdissen, M. Beller, *Tetrahedron Lett.* **2002**, *43*, 4977.

[41] B. Abarca, R. Ballesteros, F. Mojarred, G. Jones, D. J. Mouat, *J. Chem. Soc., Perkin Trans. 1* **1987**, 1865.

[42] B. Abarca, F. Mojarred, G. Jones, C. Phillips, N. Ng, J. Wastling, *Tetrahedron* **1988**, *44*, 3005.

[43] G. Pacchioni, P. S. Bagus, *Inorg. Chem.* **1992**, *31*, 4391.

[44] T. E. Barder, S. L. Buchwald, *J. Am. Chem. Soc.* **2007**, *129*, 5096.

[45] N. W. Alcock, J. M. Brown, D. I. Hulmes, *Tetrahedron: Asymmetry* **1993**, *4*, 743.

[46] D. G. Cuttell, S.-M. Kuang, P. E. Fanwick, D. R. McMillin, R. A. Walton, , *J. Am. Chem. Soc.* **2001**, *124*, 6.

[47] O. Moudam, A. Kaeser, B. Delavaux-Nicot, C. Duhayon, M. Holler, G. Accorsi, N. Armaroli, I. Séguy, J. Navarro, P. Destruel, J. F. Nierengarten, *Chem. Commun.* **2007**, 3077

[48] A. Agarwal, J. A. Barnes, J. L. Fletcher, M. C. McGlinchey, B. G. Sayer, *Can. J. Chem.* **1977**, *55*, 2575.

[49] J. S. Waugh, R. W. Fessenden, *J. Am. Chem. Soc.* **1957**, *79*, 846.

[50] M . J. Frisch, G. W. Trucks, H. B. Schlegel, G. E. Scuseria, M. A. Robb, J. R. Cheeseman, J. A. Montgomery, T. Vreven, K. N. Kudin, J. C. Burant, J. M. Millam, S. S. Iyengar, J. Tomasi, V. Barone, B. Mennucci, M. Cossi, G. Scalmani, N. Rega, G. A. Petersson, H. Nakatsuji, M. Hada, M. Ehara, K. Toyota, R. Fukuda, J. Hasegawa, M. Ishida, T. Nakajima, Y. Honda, O. Kitao, H. Nakai, M. Klene, X. Li, J. E. Knox, H. P. Hratchian, J. B. Cross, V. Bakken, C. Adamo, J. Jaramillo, R. Gomperts, R. E. Stratmann, O. Yazyev, A. J. Austin, R. Cammi, C. Pomelli, J. W. Ochterski, P. Y. Ayala, K. Morokuma, G. A. Voth, P. Salvador, J. J. Dannenberg, V. G. Zakrzewski, S. Dapprich, A. D. Daniels, M. C. Strain, O. Farkas, D. K. Malick, A. D. Rabuck, K. Raghavachari, J. B. Foresman, J. V. Ortiz, Q. Cui, A. G. Baboul, S. Clifford, J. Cioslowski, B. B. Stefanov, G. Liu, A. Liashenko, P. Piskorz, I. Komaromi, R. L. Martin, D. J. Fox, T. Keith, M. A. Al-Laham, C. Y. Peng, A. Nanayakkara, M. Challacombe, P. M. W. Gill, B. Johnson, W. Chen, M W. Wong, C. Gonzalez, J. A. Pople, Gaussian-03 ed.; Gaussian, Inc.: Wallingford CT, 2003.

[51] GIAO: a) R. Ditchfield *Mol. Phys.* **1974**, *27*, 789. b) F. J. London *Phys. Radium* 1**937,** *8*, 397.

[52] S. Berger, S. Braun, H-O. Kalinowski, *NMR-Spektroskopie von Nichtmetallen. Band 3,* ^{31}*P-NMR-Spektroskopie.*Georg Thieme Verlag, Stuttgart, **1993**.

[53] L. D. Quin, M. J. Gallagher, G. T. Cunkle, D. B. Chesnut, *J. Am. Chem. Soc.* **1980**, *102*, 3136.

[54] L. D. Quin, K. C. Caster, J. C. Kisalus, K. A. Mesch, *J. Am. Chem. Soc.* **1984**, *106*, 7021.

[55] R. H. Contreras, J. E. Peralta, *Prog. Nucl. Magn. Reson. Spectros.* **2000**, *37*, 321.

[56] V. M. S. Gil, W. V. Philipsborn, *Magn. Reson. Chem.* **1989**, *27*, 409.

[57] A. Krasinski, V. V. Fokin, K. B. Sharpless, *Org. Lett.* **2004**, *6*, 1237.

V: Fluorescence

5.1 The isomerisation strategy part II

5.1.1 Introduction and objectives.

Fluorescent sensors are nowadays a top domain of research in chemistry. Their applications can be found in many different specialities, from medical or genetic applications *i.e. in vivo* cell cleavage[1-3] to materials chemistry like LEDS.[4] Very recently O. Shimomura, M. Chalfie and R. Y. Tsien obtained the Nobel price for their research concerning green fluorescent proteins.[5]

Fluorescent detection allows numerous applications. Organic systems involving fluorescent behaviour are well known (*i.e.* anthracene, phenantrene...) and can be easily associated with coordinating structures in order to obtain fluorescent receptors. In addition, fluorescence is a very sensitive time-real technique that affords limits of detection near ppb.[6]

5.1.1.1 Luminescence

Photoluminescence is an old phenomenon having its first report in 1595 by Nomardes who reported the emission of light by an infusion of wood *Lignum Nephriticum*.[7] Indeed, luminescence is just a radiative (emission of a photon) de-excitation process.[6] Depending on the electronic configuration of the excited state (singlet or triplet) luminescence can be classified (in a simplified way) in fluorescence or phosphorescence. In solution a molecule into its ground state (S_0) can promote an electron to an excited state (S_1 or S_2) by absorbing energy from the light (**Figure V-1**). This phenomenon leads to a less stable electronic configuration. In order to recover the stability, the molecule needs to lose the absorbed energy. There are two main options.[8]

- By non radiative deactivation. The molecule is going to transform the energy into rotational and vibrational energy reaching the S_0 without emission of a photon (known as internal conversion IC).
- By a radiative mechanism. The emission of a photon leads to the ground state S_0.

To this second mechanism belongs fluorescence or phosphorescence. Emission of photons accompanying the $S_1 \rightarrow S_0$ relaxation is called fluorescence. It should be emphasized that, apart from a few exceptions, fluorescence emission occurs from S_1. This means that non radiative relaxation must take place before in order to afford the transition $S_2 \rightarrow S_1$. In fluorescence, there is no spin interconversion, providing always singlet states. However, in phosphorescence spin is not conserved, being required for a transition $S_1 \rightarrow T_1$. This transition is also named as intersystem crossing (ISC). Crossing between states of different (spin) multiplicity is in principle

forbidden; however, this phenomenon is favorized by the presence of heavy atoms (*i.e.* whose atomic number is large, for example Br, Pb). The Perrin-Jablonski diagram (**Figure V-1**) illustrates all these possible phenomena.[8]

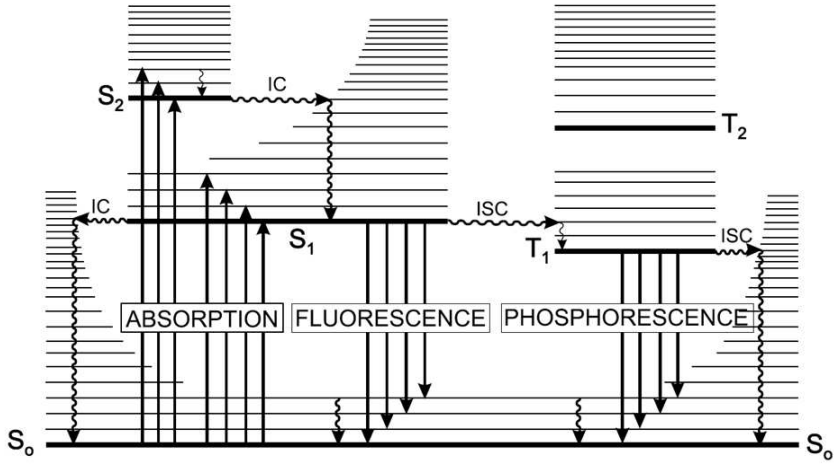

Figure V-1: Perrin-Jablonski diagram.

The energy of the corresponding excited state decreases as IC and ISC phenomena take place, providing $\lambda_{exc} > \lambda_{fluo} > \lambda_{phos}$ (**Figure V-2**). It's interesting to remark the time scale of these conversions. Figure V-2 indicates the normal time required for each kind of conversion.

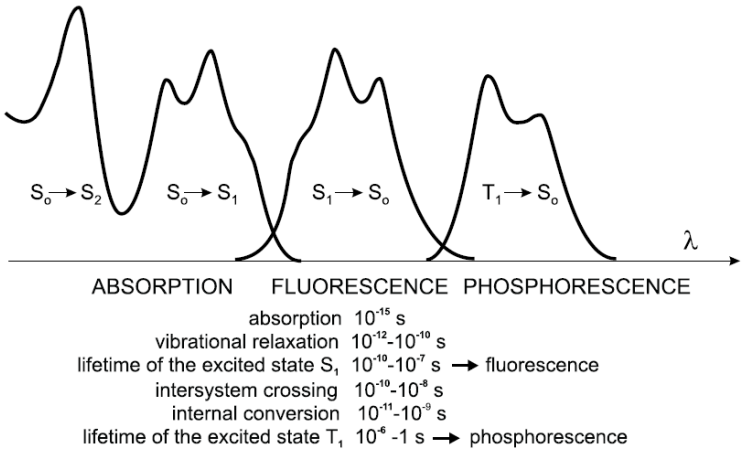

Figure V-2: Characteristic times for electronic conversions.

It's important to notice that fluorescence and phosphorescence are by far the slowest transitions (**Figure V-2**). This implicates that before the emission of a photon all possible non radiative relaxation mechanism had already taken place.

Fluorescence is a property that can be found in both organic and inorganic compounds.[6, 8] Quantum dots (CdSe/ZnS), uranyl ion ($UO_2^{\oplus}$) or some lanthanide ions like $Eu^{3\oplus}$ or $Tb^{3\oplus}$ are a few examples of inorganic fluorescent compounds. Concerning the organic compounds fluorescence can be closely associated with conjugation and rigidity. Many

examples of naphthalene or anthracene and other aromatic derivatives can be found as fluorescent molecules in the literature.

5.1.1.2 Fluorescent sensors

The preparation of fluorescent sensor is a very important area of research. Their demand in many different domains is growing due to the possibility to recognise in real time and with high selectivity many different substrates, from small ions (like metal cations or anions) to biologic active molecules (like ATP). In a general way, fluorescent sensors can be classified[8] in 3 different families (**Figure V-3**):

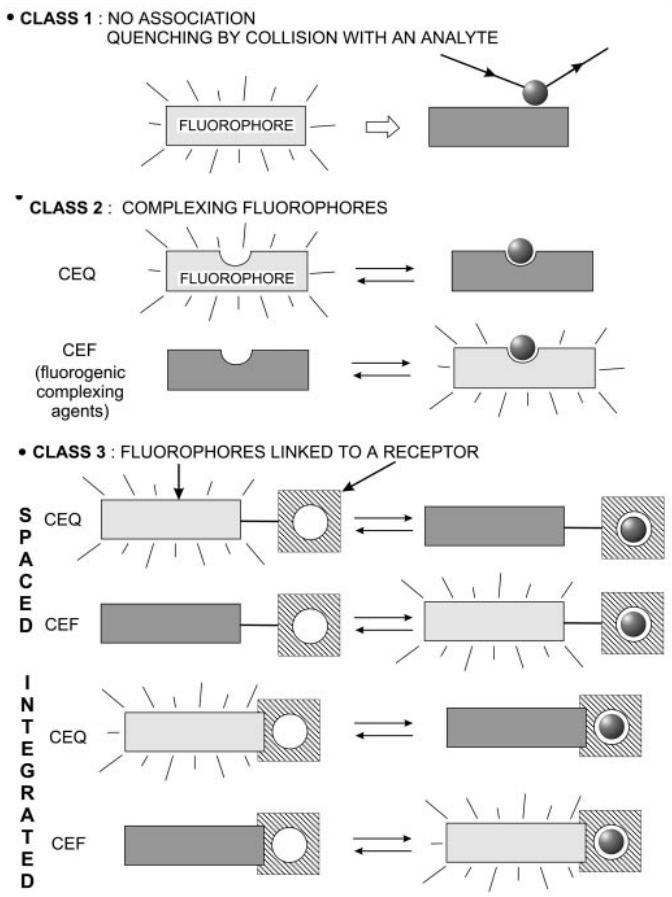

Figure V-3: Families of fluorescent compounds.

The first class involves fluorescent molecules that already undergo quenching (loss of fluorescence) by an intermolecular collision. The second class involves systems that can reversibly bind an analyte. This allows two options: quenching by coordination of the analyte (CEQ type: Chelation Enhancement of Quenching), or enhancement by coordination (CEF type: Chelation Enhancement of Fluorescence). The third family involves compounds where there is a receptor and a fluorophore; these two parts can be separated by a linker or integrated. In this class CEF and CEQ phenomena also provide two different kinds of receptors.

Although many fluorescent sensors are nowadays commercial and a large variety of them is described in the literature, the improvement of the selectivity and the limit of detection (LOD) is still required.

5.1.1.3 The isomerisation Strategy

The preparation of fluorescent sensors can be organized in many different ways. We have already discussed about the different kinds of fluorescent receptors that can be found in the literature. Until now there are only two studies concerning fluorescent applications or properties of [1,2,3]triazolo[1,5-*a*]pyridines.[9-11] As reported in chapter I (part 1.5) Abarca *et al*. reported on a fluorescent receptor for anions based on a triazolopyridine. However, this work employed the triazolopyridine ring exclusively as a fluorophore as no coordination from N^1 or N^2 was found (**Figure V-4**). In parallel, these authors reported on the fluorescent properties of the triazolopyridine system bonded to other aromatic ring.[11]

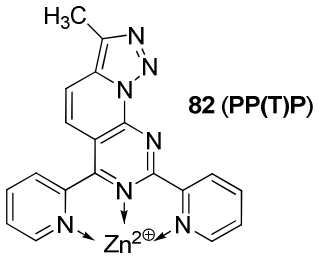

Figure V-4: First [1,2,3]triazolo[1,5-*a*]pyridine based sensor **82** (**PP(T)P**).

Although **82** (**PP(T)P**) revealed useful for the detection of anions, the coordinating properties of the triazolopyridine ring were not employed. Analyzing the fluorescent properties of aryl-derivatives of triazolopyridine, starting triazolopyridine-pyridine **1b** had interesting fluorescent properties in addition to its ring chain isomerisation. Thus, **1b** could be considered as scaffold for fluorescent bidentate ligands. The regio-selective metalation[12, 13] and trapping with electrophiles could provide, depending on the choice of the electrophile,[14] interesting fluorescent tridentate structures (**Figure V-5**):

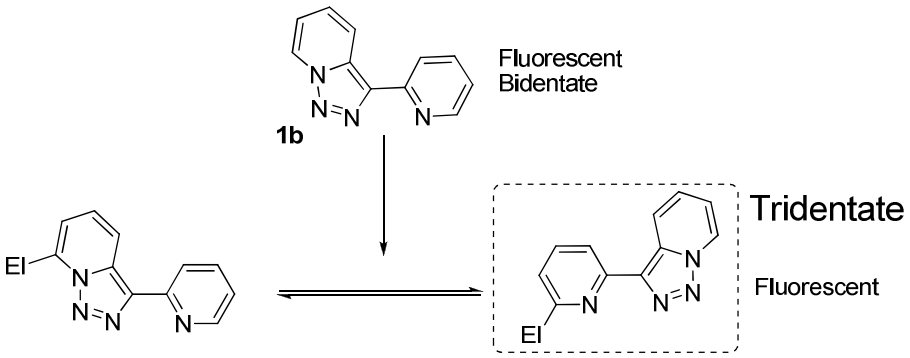

Figure V-5: Employing **1b** isomerisation to obtain fluorescent tridentate ligands.

If this isomerisation could be controlled by the choice of the right electrophile and by choosing electrophiles that have coordinating properties, we could obtain a large family of tridentate fluorescent derivatives from **1b** in a few synthetic steps. Indeed, we have already employed this strategy in the preparation of chiral triazolopyridines. The synthesis of fenchone **3B** (**TPF**) and sulfoxide **6B** (**TPS**) constituted the first examples of the isomerisation strategy. These two examples even exceeded the initial two objectives, because, despite of being fluorescent and tridentate, they were also chiral (**Figure V-6**).

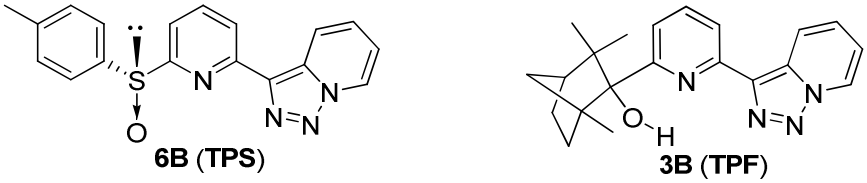

Figure V-6: First prepared ligand employing **1b** isomerisation.

Fenchone **3B** derivative could be considered as an important compound, due to the perseverance of structure **B** even when the alcohol function was methylated (see chapter 2 part 3). In a similar way, employing commercial ketones many analogues having **B** structure could be obtained like compound **83** (see Chapter 1, part (**Figure V-7**). Abarca and Ballesteros[15] also reported on the synthesis of compound **84** (**TPT**).

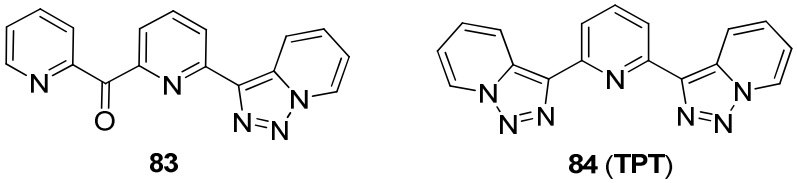

Figure V-7: **83** and triazolopyridine-Pyridine-Triazolopyridine **84** (**TPT**)

No fluorescent experience had ever been performed with **84** (**TPT**). However, the symmetric tridentate structure and the presence of coordinating electron-rich systems (triazolopyridines) and electron deficient (central pyridine) required to reconsider it study as fluorescent ligand. As soon as we performed the first fluorescent test, this hypothesis was completely confirmed by its high performance in zinc recognition. The chemistry developed in chapter 3 (part 2) already allowed us to focus on the preparation of triazoloquinolinic derivatives from **84** (**TPT**)**.** With these structures in mind we concentrated on:

- The preparation of different tridentate fluorescent sensors based on the isomerisation of **1b** by means of regioselective metalation and trapping with electrophiles.Particular interest will be given to compounds containing extra aromatic rings in order to increase the electron density (**Figure V-8**).
- The synthesis of compounds with similar structures to **84** (**TPT**) but with modification of the electron density by employing quinolines instead of pyridines (**Figure V-8**). As it

has been outlined in chapter 3 part 2, the preferential stability of triazoloquinoline-pyridine compared to quinoline-triazolopyridine should favour the preparation of triazoloquinoline-based **84** (**TPT**) tridentate analogues (**Figure V-8**, down).

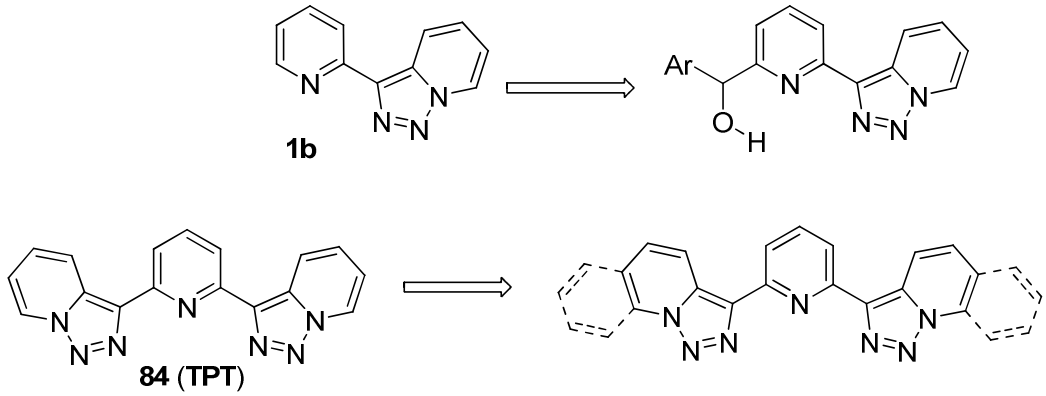

Figure V-8: Target tridentate fluorescent structures.

5.1.2 Synthesis of tridentate fluorophores by means of the isomerisation strategy

In chapter 2 we reported on the synthesis of two possible tridentate fluorophores by means of regioselective metalation and trapping with chiral electrophiles, leading to chiral tridentate **B** structures **3** and **6**. In order to provide different structures we selected 3 prochiral ketones/aldehydes as shown in **figure V-9**:

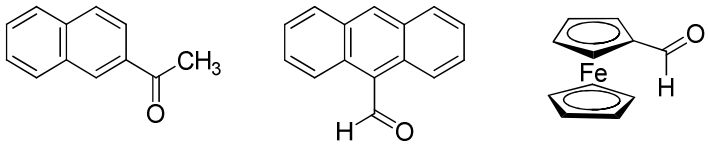

Figure V-9: Chosen ketone and aldehydes.

1-(Naphthalen-2-yl)ethanone and anthracene-9-carbaldehyde were selected due to their fluorescent properties. Many examples of fluorescent sensors based on them can be found in the literature.[16] Ferrocenaldehyde was selected for two reasons. First it was supposed to provided also a **B** structure, and second, albeit to possible fluorescent interesting applications, the presence of a tridentate system combined with a ferrocene could lead to interesting electrochemical properties.

As reported, the regioselective metalation[12, 13] of **1b** was performed in toluene at -40 °C with butyl lithium affording the lithium intermediate which was trapped with 1-(naphthalen-2-yl)ethanone to provide alcohol **85** (**TPON**) in good yield 60 %. In a similar way, alcohol **86** (**TPOA**) was also obtained as a mixture of enantiomers in 50 % yield (**Scheme V-1**).

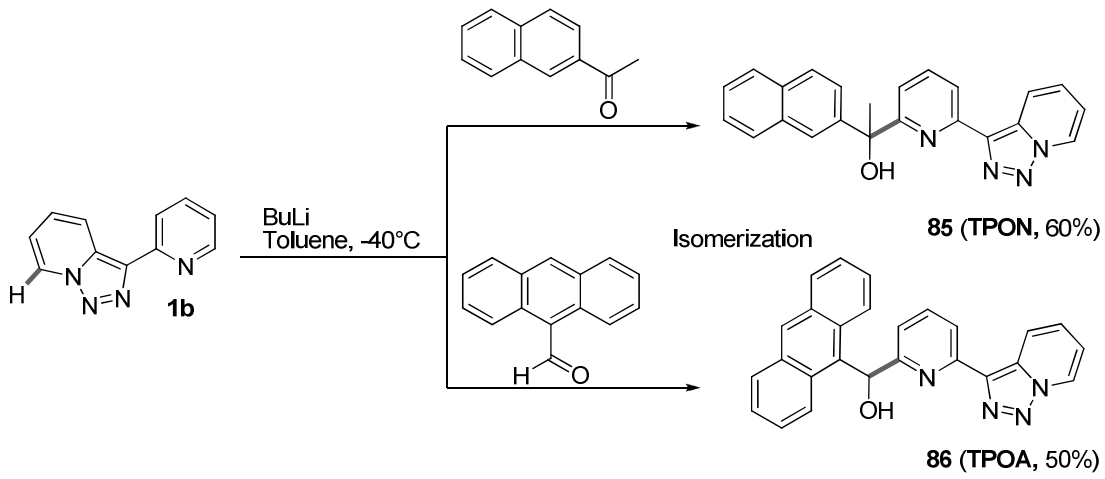

Scheme V-1: Preparation of **TPON** and **TPOA**. The newly created bond is in grey in order to highlight the isomerisation.

These compounds, obtained as a racemic mixture, were found to be fluorescent. Preparative chiral HPLC (Chiralpak IA) separation was tempted in order to obtain enantiopure compounds. Unfortunately **85** (**TPON**) could not be separated into its enantiomers. In contrast, with an acetonitrile/water (80/20) mixture we observed a retention time of 25 minutes for one enantiomer of **86** (**TPOA**) and 30 minutes for the second (5 mL/min, P= 89 bar). This allowed us to isolate 20 mg of each enantiomer, providing **(+) TPOA** and **(-) TPOA** (**Scheme V-2**).

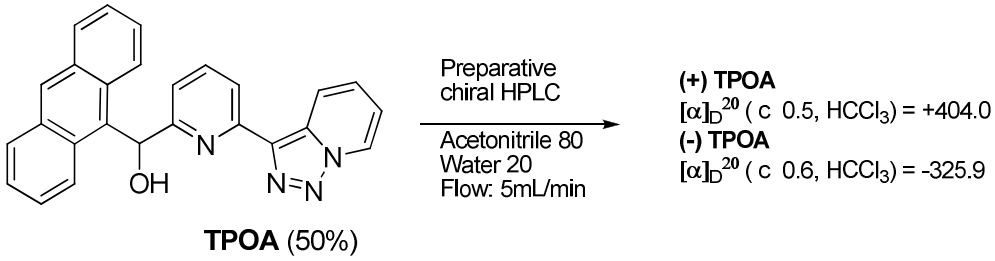

Scheme V-2: Separation of **TPOA** by HPLC.

The preparation of ferrocene derivative **87** followed a similar strategy. However after work up, a more complex mixture was observed. After chromatography, **87** (**TPFe**) was obtained in 58 % yield (**Scheme V-3**).

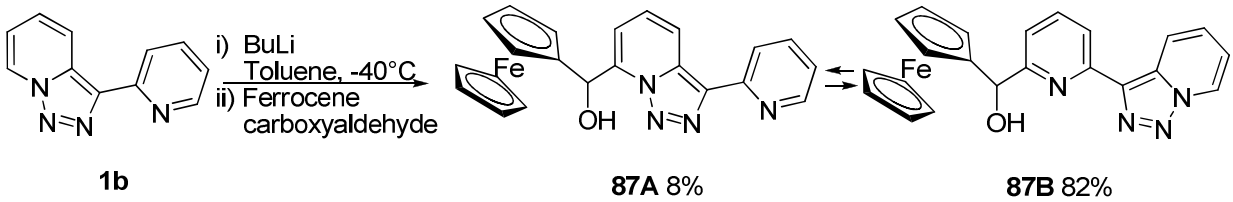

Scheme V-3: Preparation of **87** (**TPFe**), presence of A and B structures.

The ^{1}H-NMR spectra revealed a **B** structure. However, small signals were found which were attributed to an **A** structure. The ratio between **A** and **B** structures was measured employing the same hydrogen atoms as in chapter 4, part 1. $H^{3'A}$ and $H^{3'B}$ appeared as two doublets at 8.2 and 8.3 ppm with a *J* = 8.0 Hz.

5.1.3 Preparation of 84 (TPT) analogues: Larger π-systems

Abarca *et al.* reported on the synthesis of compound **84** (**TPT)** by means of regioselective metalation as reported **Scheme V-4**.[15] This methodology provided the corresponding ketone which was transformed into the bistriazol **84** (**TPT**) by the tosylhydrazine/NaOH method.[17] The hydrazine/MnO_2 method[18] did not afford **84** (**TPT**) but only reduction products.[19]

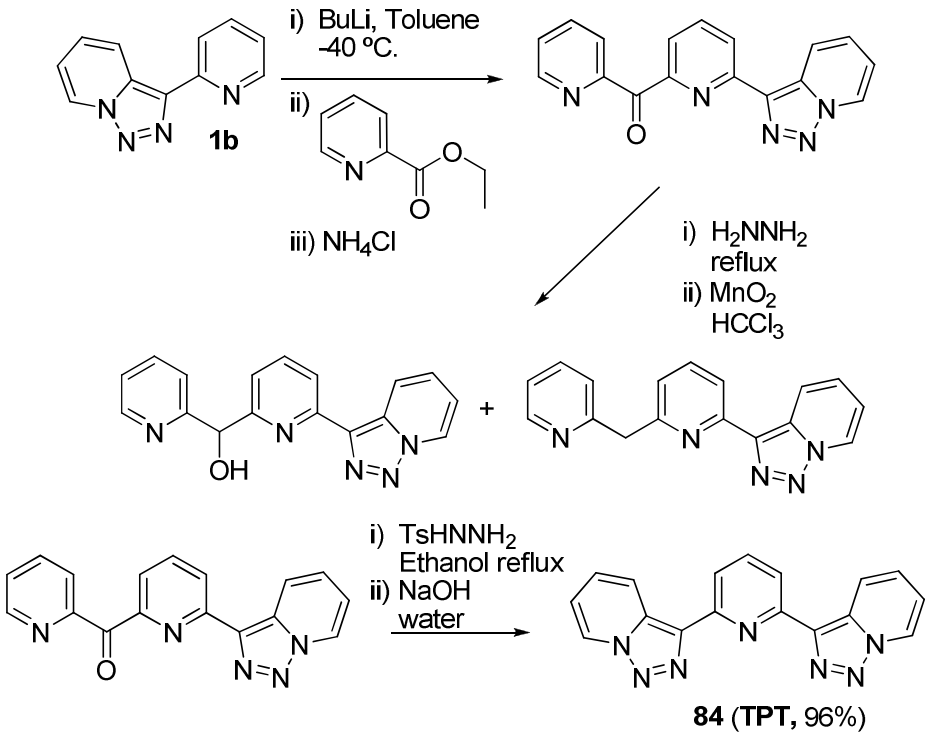

Scheme V-4: Preparation of **84** (**TPT**).

With the idea of adding one more aromatic ring, we performed the same strategy but employing methyl quinoline-2-carboxylate as electrophile in this way, compound **88** was obtained in good yield (78%). In order to form the triazolo quinoline ring, both methodologies were tested. However, only tosylhydrazine provided **89** (**TPTq**) in low yield (17%). Although the low yield, the purification of this compound was found to be easy. Abarca *et al.* reported on the low solubility of **84** (**TPT**) in ethanol.[19] Thus by treatment in hot ethanol **89** (**TPTq**) was isolated in pure form (**Scheme V-5**).

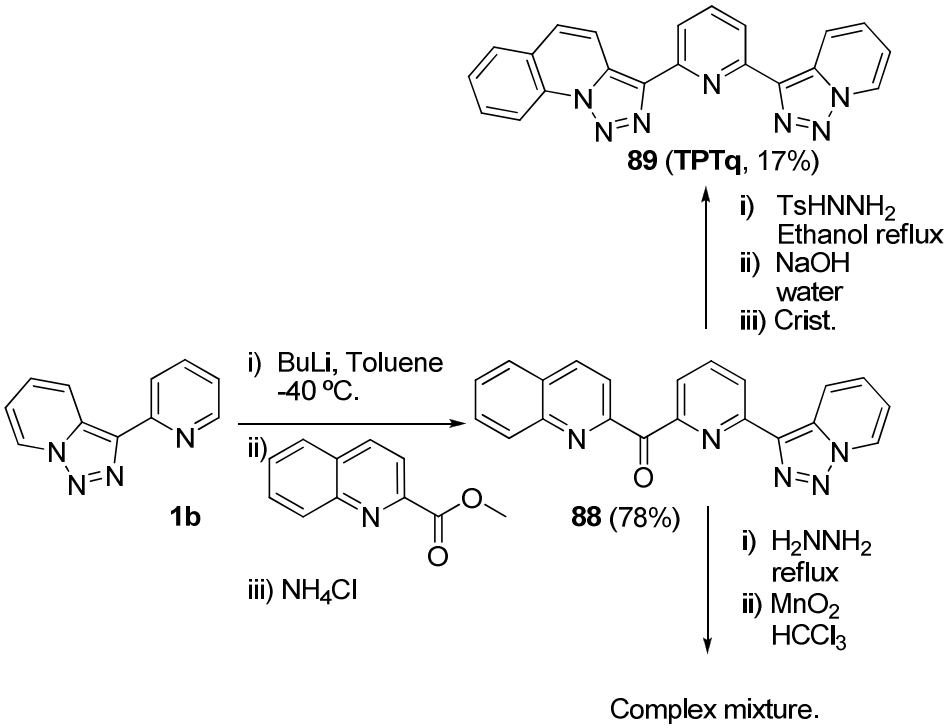

Scheme V-5: Preparation of **89** (**TPTq**).

We also revised the synthesis of **84** (**TPT**). Its symmetry suggested that another synthetic way could be employed to obtain **84** (**TPT**), without using **1b** as starting reagent. In order to prepare it, we synthesized compound **90** by means of a double addition of 2-lithiopyridine to the dimethyl pyridine-2,6-dicarboxylate (**Scheme V-6**),[20, 21]

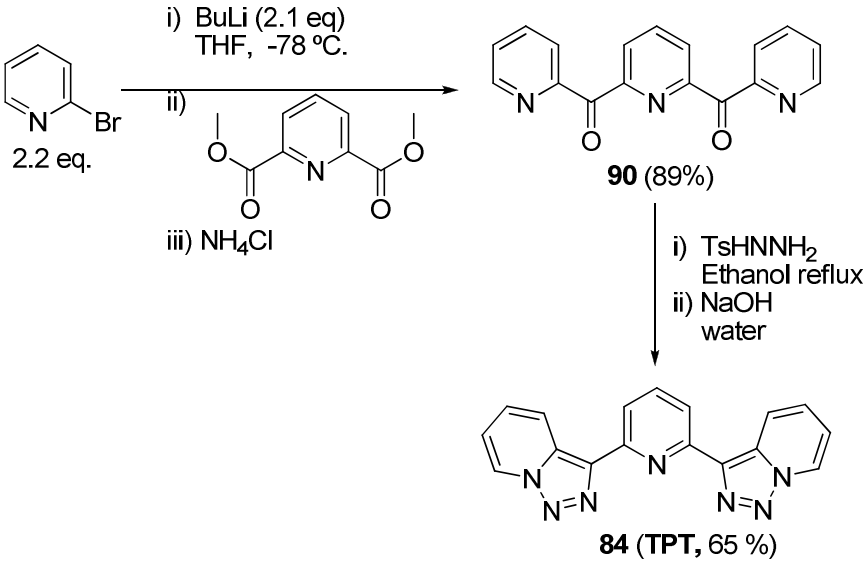

Scheme V-6: alternative preparation of **84** (**TPT**).

The solubility properties of **90** (insoluble in ethyl acetate) allowed the synthesis in 3 gram scale. Compound **90** was quantitatively precipitated by addition of ethyl acetate and application of ultrasound (excess of 2-bromopyridine provided pyridine as side product; 2-bromopyridine, and pyridine are liquids and could be separated). Diketone **90** was transformed

into **84** (**TPT**) by a double triazolo ring formation with the tosylhydrazine/NaOH method. Although **84** (**TPT**) could be obtained in good yield by Abarca's methodology, this strategy was developed also employing **84** (**TPT**) as a model substrate for future analogues like **91** (**TqPTq**). (**Figure V-10**)

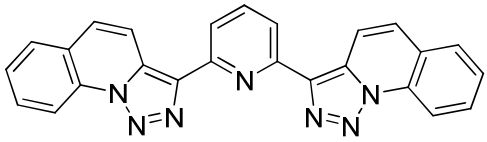

91 (**TqPTq**)

Figure V-10: Structure of **91** (**TqPTq**)**.**

Many different synthetic paths are possible to prepare compound **91.** The double addition was found as an easy way to obtain it in two steps (**Scheme V-7**).

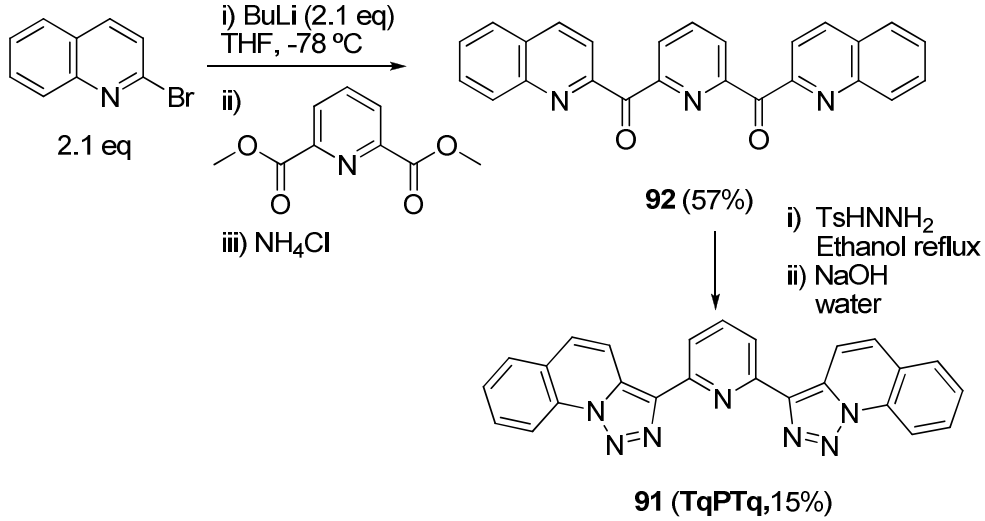

Scheme V-7: Preparation of **91** (**TqPTq**).

2-Bromoquinoline was submitted to a halogen/metal permutation with butyllithium in THF at -78 °C and added to a solution of dimethyl pyridine-2,6-dicarboxylate. Work up provided ketone **92** in moderate yield (57%) after precipitation with ethyl acetate. The double triazolo pyridine formation provided compound **91** in low yield. The high insolubility of this compound in ethanol seemed to be the cause of this poor yield. Althougth the yields of compounds **89** and **91** were low, the quantity obtained (between 30-60 mg) allowed the following fluorescence studies.

5.1.4 Preparation of 84 (TPT) analogues: Smaller π-systems

Until now, all derivatives synthesized are systems where one or two extra aromatic rings had been introduced into the **84** (**TPT**) structure. However we wanted to obtain one compound with less aromatic rings. In the literature, some of these structures (**Figure V-11**) can be found.[22, 23]

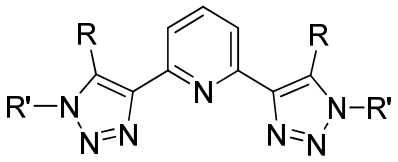

Figure V-11: Triazol-Pyridine-Triazol derivatives.

These compounds have been applied as fluorescent ligands,[22] and they are usually prepared by click chemistry. However, the properties of triazolopyridines allow an easy access to these structures. As mentioned in chapter 1 (part 1.3.5), under hydrogen atmosphere and with Pd/C catalyst, triazolopyridine hydrogenation[24] takes exclusively place on the pyridinic ring. 2,6-Bis(4,5,6,7-tetrahydro-[1,2,3]triazolo[1,5-*a*]pyridin-3-yl)pyridine **93** (**BTH-TPT**) was prepared in this way (**Scheme V-8**) with an excellent yield (92%). Thus, we could prepare a tridentate symmetric system with only 3 aromatic rings.

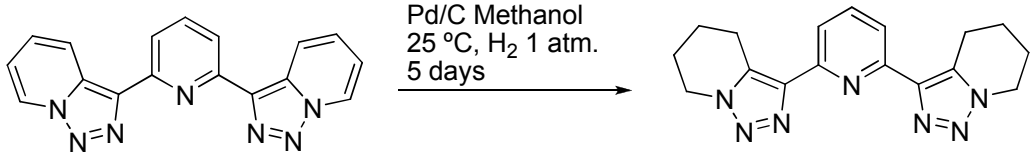

84 (**TPT**) **93** (**BTH-TPT,** 92%)

Scheme V-8: Hydrogenation of **84**, synthesis of **93** (**BTH-TPT**).

5.1.5 Conclusions

- By means of regioselective metalation we have been able to prepare different systems having a tridentate structure. **6B** (**TPS**), **3B** (**TPF**), **86** (**TPOA**), **85** (**TPON**) and **87** (**TPFe**) constitute a family of interesting tridentate compounds with different structures but a common tridentate coordination subunit.
- **87** (**TPFe**) has been the unique compound of this family that provided a mixture of **A**/**B** isomers. As ferrocene can be considered as an electron-rich system, it can provide much more electron density favouring a small amount of **A** structure.
- Although the yields of **89** (**TPTq**) and **91** (**TqPTq**) are low, we have been able to prepare these compounds as well as **93** (**BTH-TPT**). These structures have a different degree of delocalization through a more or less extended π-system, **91** (**TqPTq**, 7 rings) > **89** (**TPTq**, 6 rings) > **84** (**TPT**, 5 rings) > **93** (**BTH-TPT**, 3 rings).

V: Fluorescence

5.2 Zinc and Copper detection

5.2.1 Introduction and objectives

Zinc, copper and related d-block metals are emerging as significant players in both neurophysiology and neuropathology,[25-27] particularly concerning aging and neurodegenerative diseases such as Alzheimer. These kinds of metals are also involved in many essential functions in the human body playing different roles in proteins.[28] One of the most studied zinc/copper enzymes is the superoxide dismutase (SOD1) (**Figure V-12**) that decomposes superoxide anion ($O_2^{\ominus}$) in order to prevent possible cell degradation.

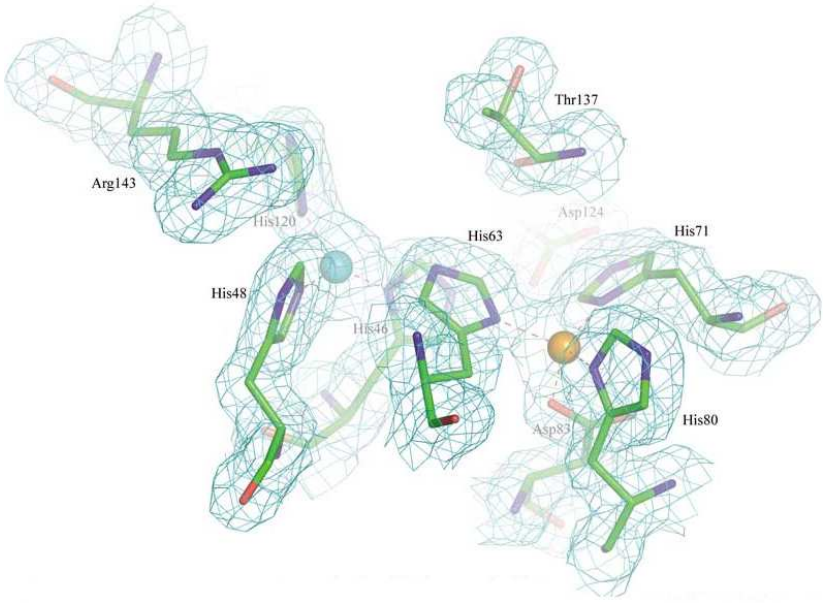

Figure V-12: Human SOD1[29] metal binding site. Cu (cyan sphere) Zn (orange sphere).

Due to the relevance of metals in biochemistry and biology, it must be developed efficient methods to detect, control, and measure these cations. Fluorescence offers this possibility, being a high sensitive real time technique. One practical example is the quick and reliable quantification of blood electrolyte levels with a family of fluorescent sensors.[30, 31] Many studies are devoted to the preparation of compounds able to detect these metals. These fluorescent sensors are small molecules like quinoline derivatives up to CdSe quantum dots, ruthenium bipyridine coordination complexes, bodipy scaffolds or even rare earth metals.[16, 32] Applications are found in biology (*i.e. in vivo* fluorescent test[25]), material chemistry or analytical chemistry (*i.e* anion recognition[33, 34]). However, in this domain of research, organic chemistry finds its place in the discovery and the development of new fluorophores, based in many cases on organic aromatic compounds.

5.2.1.1 Zinc detection

Zinc plays an essential role in the human body[25, 35] (gene transcriptions, neural signal transmission...). However $Zn^{2\oplus}$ does not show distinct spectroscopic or magnetic signals that would allow its detection by common techniques (UV-Vis spectroscopy, Mössbauer spectroscopy, NMR or EPR) due to its electronic configuration ($3d^{10}$ $4s^{0}$). This combination of biological relevance and "silent" spectroscopy has forced the development of molecules able to quantify zinc.[25, 36-44] Zinc fluorescent detection is normally based on the enhancement of the emission intensity (Turn-On strategy) by means of PET[32] (photoinduced electron transfer) (**Figure V-13**).

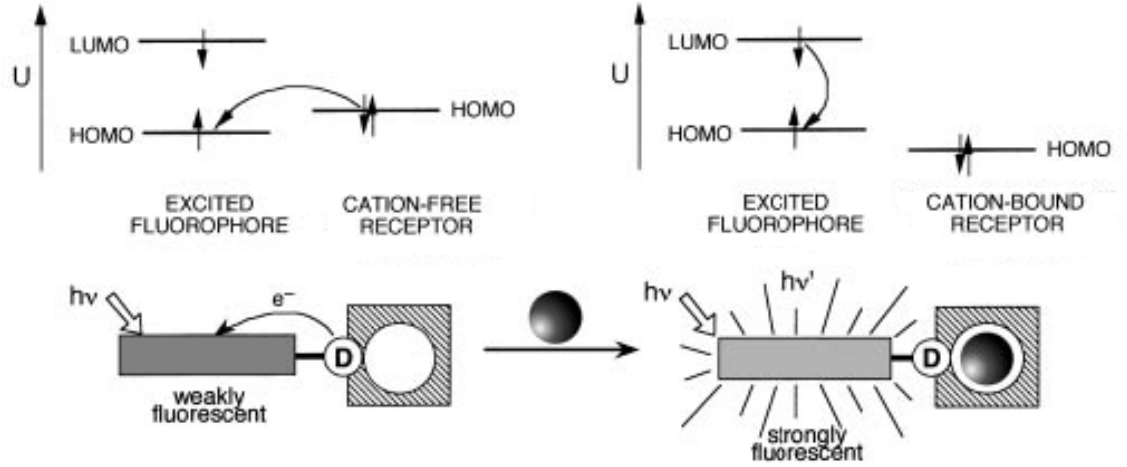

Figure V-13: PET mechanism.

PET mechanism can be explained in terms of partial electron transfer from a lone pair of a donating group to the HOMO causing the fluorophore quenching. Upon metal coordination, this HOMO (from the receptor) becomes lower in energy, not being able to quench anymore the fluorophore and thus an enhacement of the fluorescence is observed. **Figure V-14** shows two fluorophor-spacer-receptor examples.

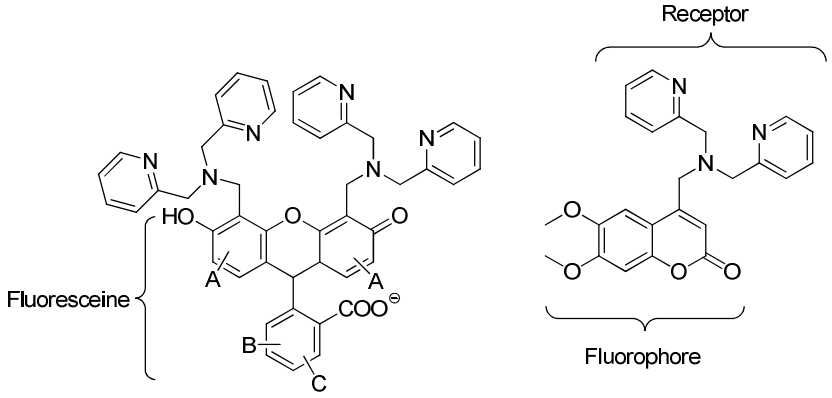

Figure V-14: PET Fluorophore-spacer-receptor systems.

These systems show an increase of the emission upon zinc coordination, stopping the quenching effect of the amine lone pair. Fluoresceine[45, 46] can be found in many sensors as

fluorophore subunit. Different systems of PCT can be found in the literature. Intramolecular Charge Transfer (ICT) has revealed as powerful technique for imaging zinc ions *in vivo*.[47, 48] ICT affords intensity differences upon coordination of the metal, but also a possible shift of the excitation or emission profile. In this situation donor groups are directly bonded to the fluorophore (**Figure V-15**):

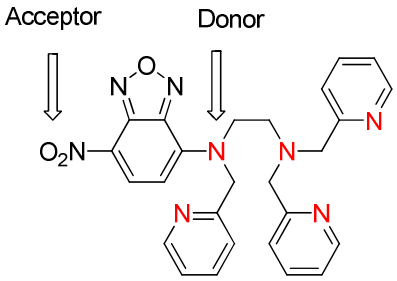

Figure V-15: ICT, red colour indicates the atoms involved in the zinc coordination.

The ICT system requires donor and acceptor groups directly bonded to the fluorescent system. Nitro, cyano and carboxyl groups are common acceptor subunits employed, as well as amines and methoxides which are used as donor groups.[49] The charge transfer between these two groups is responsible for the quenching of this system. However, when zinc is coordinated the ICT decreases affording an enhancement of the fluorescence.

5.2.1.2 Copper detection

Copper is the third-most abundant transition metal in the human body. It is an essential cofactor in numerous enzymes like cytochrome c *oxidase*, SOD1, and other enzymes related to handle oxygen metabolites (peroxide, superoxide).[26] In the human body copper can be found as cuprous ($Cu^{\oplus}$) and cupric ($Cu^{2\oplus}$) cations. However the detection of copper requires selectivity in terms of oxidation state. Furthermore $Cu^{2\oplus}$ is hard to be detected by a Turn-On strategy due to its paramagnetic configuration ($4s^0\ 3d^9$) that tends to quench emission. Despite this, some example are proposed in the literature for selective $Cu^{\oplus}$ Turn-ON sensing[50] (**Figure V-16**).

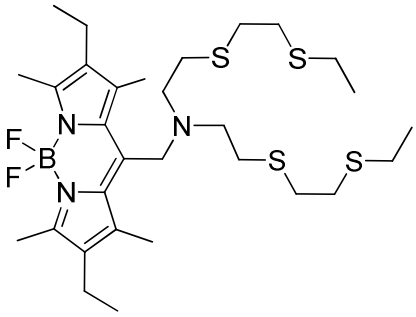

Figure V-16: BODIPY based $Cu^{\oplus}$ Turn-On sensor.

The detection of $Cu^{2\oplus}$ is normally related to a Turn-Of strategy, the majority of fluorogenic reagents that have sensitivity or selectivity for this metal report this interaction by means of loose of fluorescence (Turn Off). However a few examples of Turn-On compounds can be found, like rhodamine-based sensors[51] (**Figure V-17**):

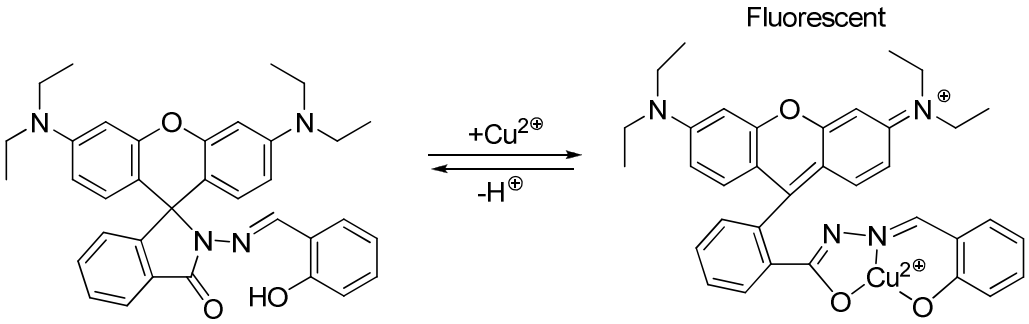

Figure V-17: Rhodamine-based Turn-On $Cu^{2\oplus}$ sensor.

Similar to zinc, Magnetic-resonance-based sensors containing rare earth metals can also be found in the literature. However, the quantity of compounds based on the Turn-On strategy proposed for copper is not comparable to those proposed to zinc detection. In this way, as it has been mentioned earlier, copper (and specially $Cu^{2\oplus}$) is based on the study of the quenching effect (Turn-Off) strategy.

Zinc and copper can be considered as a general metals that could be used to evaluate fluorophores, having normally opposite behaviour. In this way Yu *et al.* work with 1,8-naphthyridine[52] which is a really good example (**Figure V-18**), being a Turn-On sensor of zinc and a Turn-Off sensor of copper.

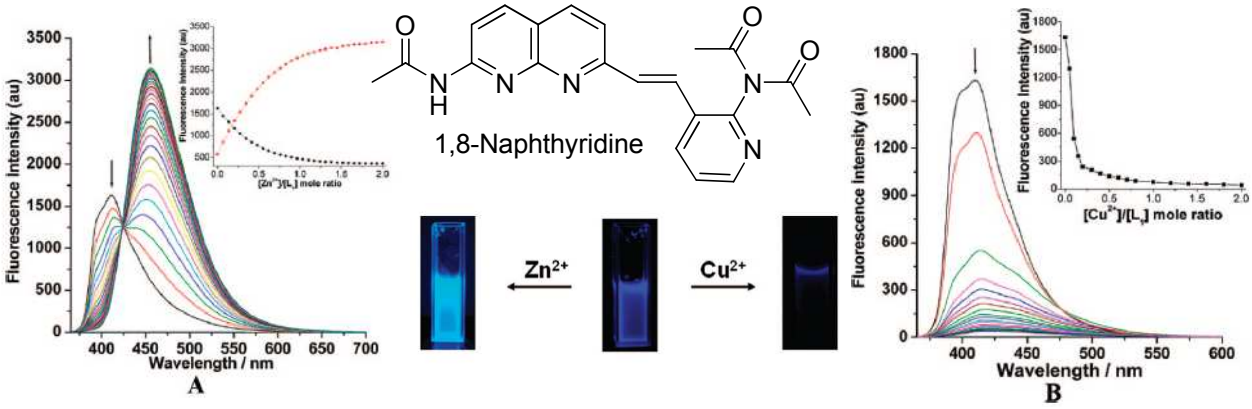

Figure V-18: 1,8-Naphthyridine-based ligand Turn On $Zn^{2\oplus}$ and Turn Off $Cu^{2\oplus}$ sensor.

This compound experiments fluorescent enhancement (A graph) with zinc, quenching is observed with copper (B graph).

5.2.1.3 Objectives

In the previous chapters we have been able to prepare different tridentate fluorescent compounds (**Figure V-19**):

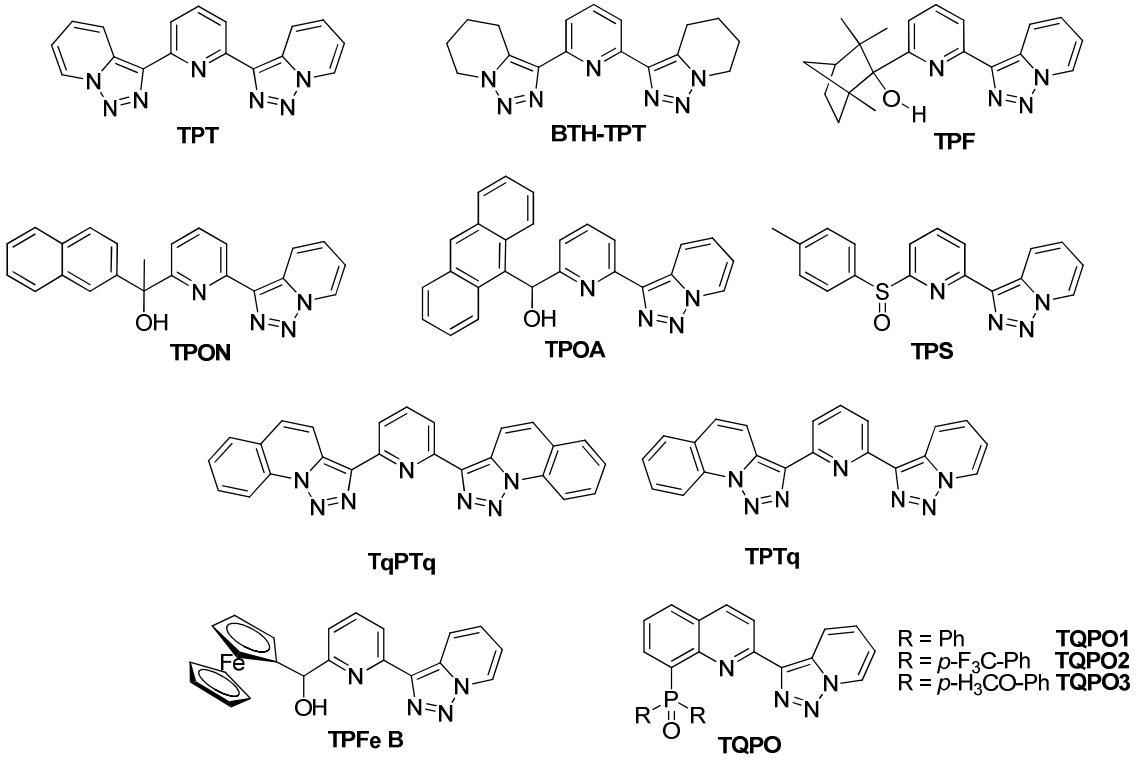

Figure V-19: Target molecules suitable for the fluorescence study.

We were then interest in the evaluation of these compounds in terms of fluorescence spectroscopy. We focused on:

- The study of the fluorescent spectra of these compounds and its modification upon the addition of zinc or copper ion solutions. We studied also the quantum yields and its possible application as zinc or copper sensors.
- The modification of the fluorescence intensity upon the addition of a metal by means of anion coordination. (**Figure V-20**).

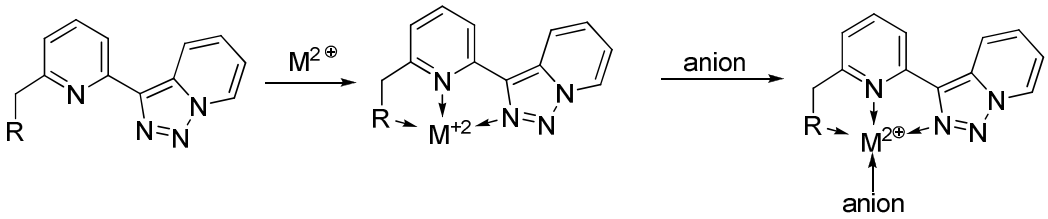

Figure V-20: Study of the fluorescent properties and its dependence towards anion coordination.

Compared to the bibliography, our system presents a condensed structure where the receptor and the fluorophore are the same molecule. All these ligands can not be considered as receptor-fluorophore ligands because both functions are present in the triazolopyridine tridentate subunit. The most interesting ligands (the ones with a large enhancement of

intensity upon zinc addition) will be tested with anions (halogens, nitrites...) to see if an anion sensor can be developed from these molecules as it was done in the past by Abarca and García-España.[10, 33]

5.2.2 Spectroscopic properties and metal coordination analysis

5.2.2.1 Sample preparation

In order to evaluate fluorescent properties of our ligands we prepared ethanol solutions of them. The domain of concentration for this technique requires normally 10^{-5} M solutions of the ligands, with our compounds (M.W. = 300-400 g/mol) this concentration corresponds to 4-7 mg in 250 mL of ethanol. The choice of ethanol was partly motivated by the complete solubility at these concentrations of the ligands and because it is totally miscible with water (**Table V-1**). Our ligands were not very soluble in water; however, the preparation of solutions in ethanol allowed the addition of aqueous metal or anion solutions affording a homogeneous phase. Zinc and copper solutions were prepared from corresponding perchlorate salts ($[Zn^{2\oplus}]$ = 0.00483 M and $[Cu^{2\oplus}]$ = 0.004945 M).

Table V-1: Molar concentration of ethanolic solution of our ligands.

Ligand		[M]
Tp	**1b**	0,00009
TPF	**3**	0,00008
TPS	**6**	0,00005
TqP	**53**	0,00008
TPT	**84**	0,00008
BTHTPT	**93**	0,00002
TPTq	**89**	0,00007
TqPTq	**91**	0,00002
TQPO1-3	**72-74**	0,00005
TPON	**85**	0,00007
TPOA	**86**	0,00001
TPFe	**87**	0,00005

Each test required 2 mL of the corresponding ligand which were introduced in a quartz cuvette with a small magnetic stirrer. To this solution metal ions were added with high precision volumetric material (calibrated micropipette). Metals and ligand were prepared at 10^{-3} M aqueous solutions in order to require 40-50 µL to reach one equivalent.

5.2.2.2 Absorption and emission spectra

Before starting the interaction with metals, maximal absorption and emission wavelength were determined for each ligand as well as for analogues **1b** and **53**. These two compounds are not tridentate but were considered as fluorophore. In this way, their study

allows us to compare results between different compounds. All ligands have different fluorescent subunits, from anthacene or naphthalene up to sulfoxides, quinolines or triazoles, and these can afford different fluorescent properties. By scanning the emission near 400 nm (all molecules are blue coloured with a laboratory UV lamp at 254 nm) we found the excitation peaks. Then by exciting at this wavelength and scanning the emission we affined the emission bands. **Figure V-21** represents the emission and excitation scans for **TQPO1**.

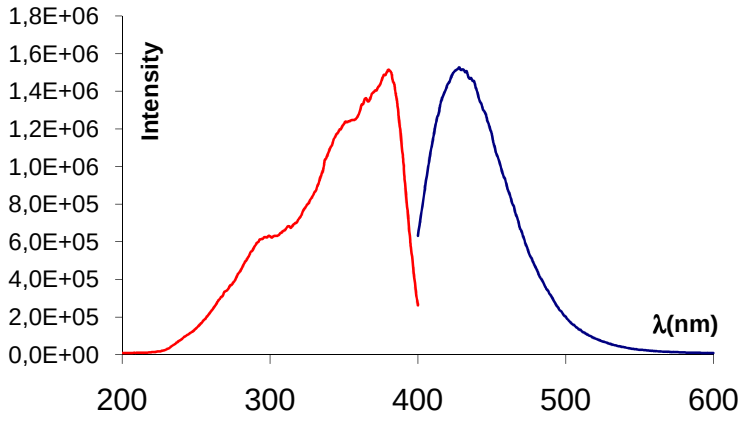

Figure V-21: Excitation (red) and emission (blue) scans for **TQPO1.**

Although the **TQPO** spectrum only presents one signal for the emission like **TPT**, **BTH-TPT**, other compounds (**TP** and **TPOA** present a 2 bands fine structure) present 2 or 3 signals. **Table V-2** shoes emission and excitation maximas.

Table V-2: λexc and λemi in nm for prepared compounds. Most intense emission wavelength is noted when more than one signal has been observed in the emission

Entry	Compound	λexc (nm)	λemi (nm)	Stokes shift[a]	Quantum yield[b] ϕ_F
1	**Tp** (**1**)	359	411	52	0.01
2	**TPF** (**3**)	360	418	58	0.02
3	**TPS** (**6**)	340	400	60	0.02
4	**TqP** (**53**)	358	397	39	0.13
5	**TPT** (**84**)	359	412	53	0.02
6	**BTH-TPT** (**93**)	323	357	34	0.08
7	**TPTq** (**89**)	355	406	51	0.19
8	**TqPTq** (**91**)	351	400	49	0.24
9	**TQPO1** (**72**, R=Ph)	376	423	47	0.54
10	**TQPO2** (**73**, R=*p*-F_3CPh)	380	427	47	0.60
11	**TQPO3** (**74**, R=*p*-H_3COPh)	375	419	46	0.48
12	**TPON** (**85**)	347	409	62	0.02
13	**TPOA** (**86**)	347	412	65	0.18
14	**TPFe** (**87**)	371	425	54	0.01

a) Stokes shift = λemi - λabs. b) Quantum yield: ratio of the number of emitted photons to the number of absorbed photons. Quantum yields were measured with a HAMAMATSU-PHA.

Comparing these results, the first observation we can do is that all compounds have an emission near 400 nm except **BTH-TPT** (357 nm). This corresponds to a partially blue coloured

emission, that already was observed with laboratory UV lamp. Secondly, although not many correlations can be established between different molecules, **TPT** (entry 5) and **BTH-TPT** (entry 6) have a significant difference in the absorption and emission wavelengths λexc(**TPT**) > λexc(**BTH-TPT**) and λemi(**TPT**) > λemis(**BTH-TPT**). As smaller wavelengths indicates higher energies, by decreasing the number of aromatic rings (in **BTH-TPT** the pyridine rings from the triazolopyridine unit are hydrogenated) we observe a higher separation between the LUMO and the HOMO (**Figure V-22)**. However, by increasing the number of aromatic rings no significant observations in absorption or emission can be done, but the quantum yields increase, (entries 7 and 8). The quantum yield (ϕ_F) indicates the efficiency of the fluorescent phenomenon. When it is near 1 all energy absorbed from the light is emitted as photons. When it is near 0, the energy absorbed from the light is emitted by a non radiative way, decreasing the fluorescence. The addition of aromatic rings decreased the non radiative deactivation from ϕ_F **TPT** (0.02), ϕ_F **TPTq** (0.19) and ϕ_F **TqPTq** (0.24). This tendency is also observed when benzene, naphthalene and anthracene[32] are compared having ϕ_F = 0.04 for benzene, 0.21 for naphthalene and 0.27 for anthracene.

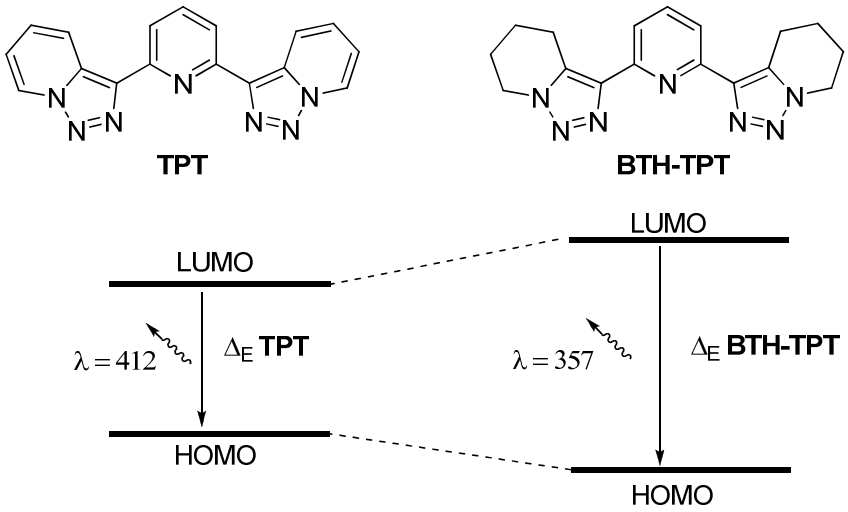

Figure V-22: **TPT** vs **BTH-TPT.**

Phosphine oxides present small differences (entries 9, 10 and 11). However, these compounds had only different substituents in the *para* position of the phenyl ring (of the phosphine oxide). Thus these substituents (-H, $-CF_3$ or $-OCH_3$) have an influence at the fluorescence. These observations will be developed later in this chapter. The presence of an anthracene moiety in our system provided a multi signal spectrum typical of this fluorophore and a big quantum yield. (Entry 13, **figure V-23**)

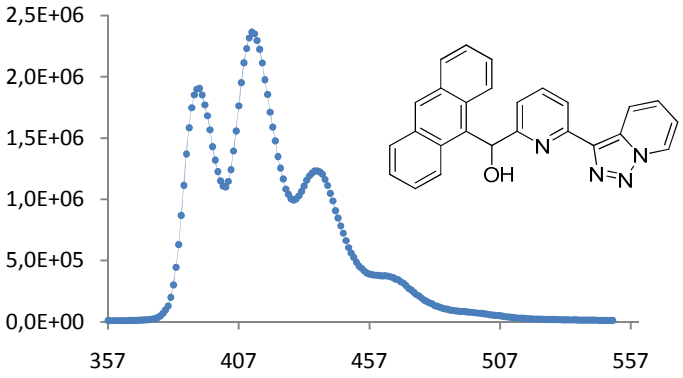

Figure V-23: **TPOA** emission spectrum (**λ**exc = 347 nm).

5.2.2.3 Zinc coordination

As it has been mentioned before, the coordination with $Zn^{2\oplus}$ can provides an enhancement of the intensity. However our tridentate system will use both (electron-rich and electron-poor) aromatic cycles for coordination and the ligands contain different fluorophore structures. A first study of the response with zinc will provide a general idea on the best structures. These tests were performed by adding small volume (5 mL) of $Zn^{2\oplus}$ solutions to the ligands and measuring the fluorescent spectra. Zinc was added until the stabilization of the signal. Normally, fluorescent enhacement was observed for all compouns (except **TPOA** that quenched upon zinc addition, and phosphines and ferrocene which had no modification of the initial spectrum Io) as it is shown in **Figure V-24**:

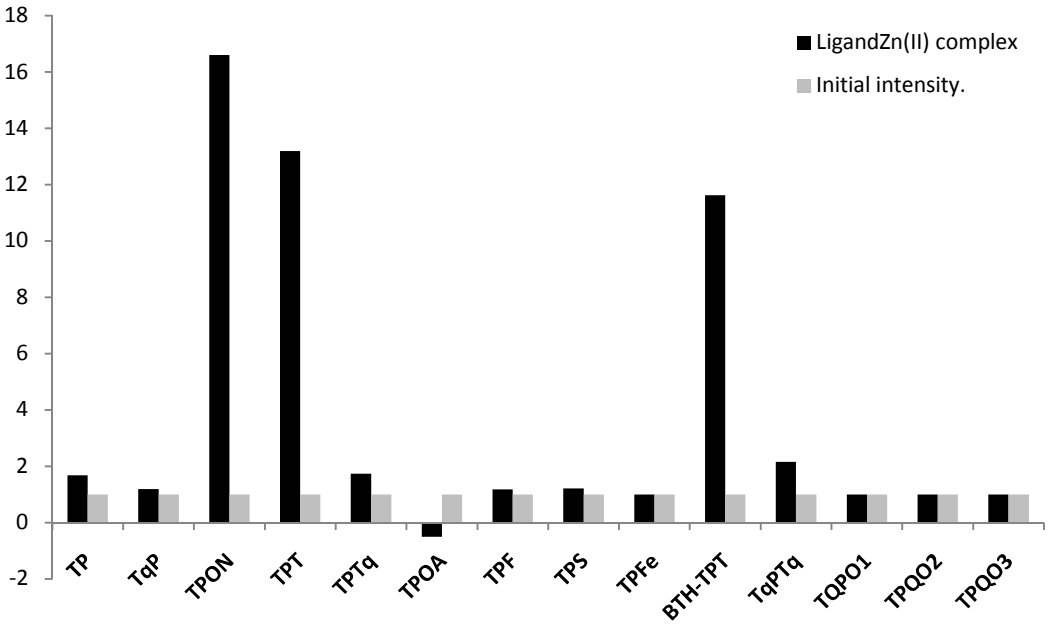

Figure V-24: Modification of the emission intensity with $Zn^{2\oplus}$ addition. Quenching is represented with negative values.

As it can be seen, most of the ligands have small variations of the emission. However, **TPON**, **TPT** and **BTH-TPT** enhanced 17, 13 and 11 times its emission intensity upon coordination of one equivalent of zinc. This enhancement could even be observed with a normal laboratory UV-Lamp for **TPT** affording a qualitative way to detect zinc in water. The ligands afforded a general blue shift and an increase of the emission. The quenching phenomenon observed for **TPOA** was near 0.5, with means a 50% decrease of the intensity.

5.2.2.4 Copper coordination

The fluorescent enhancement was observed with zinc, in order to observe the opposite effect $Cu^{2\oplus}$ solutions were added to the ligands and the fluorescence was measured. $Cu^{2\oplus}$ induces quenching phenomena in many fluorescent molecules. (**Figure V-25**).

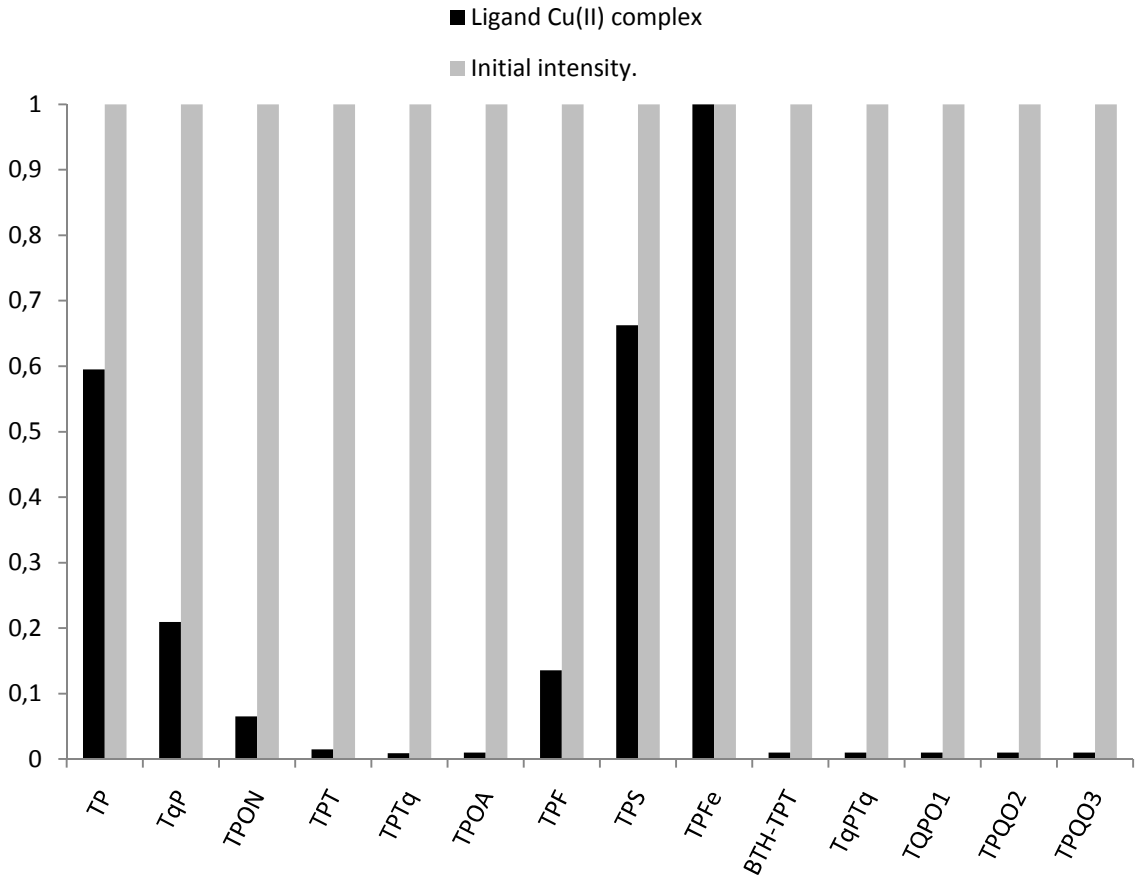

Figure V-25: Modification of the emission intensity with $Cu^{2\oplus}$ addition

Quenching was observed for many compounds except **TPFe.** Although the disappearance of the emission was evident, its relevance became higher with compounds with high quantum yields, especially **TPOA, TPTq, TqPTq** and **TPQO1-3**. These compounds could be considered as Turn-Off sensors for $Cu^{2\oplus}$ due to its important emission (big quantum yield) without copper, and its complete quenching when copper was added

5.2.2.5 TPT fluorescence study

TPT shoed an important enhancement of the emission when coordinated with zinc (**Figure V-26**). The structure of **TPT** (C_2 symmetry) is close to terpyridine, but including fluorescent properties. Terpyridine applications can be found in molecular materials, molecular magnetism or catalysis.[53-55]

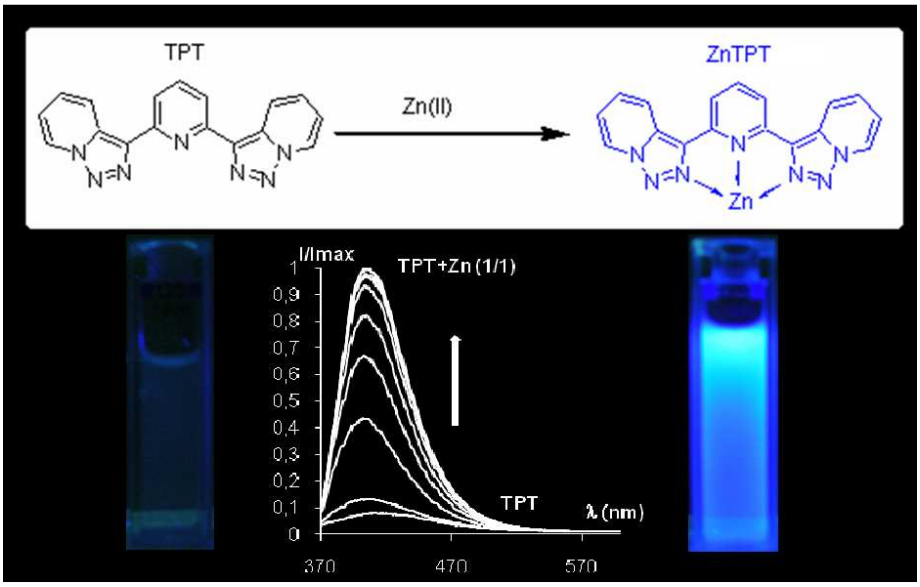

Figure V-26: Modification of the emission with **TPT**. Left **TPT** 10^{-5} M solution, right **TPT**$Zn^{2\oplus}$ 10^{-5} M solution.

TPT fluorescent properties will now be examined more deeply. However, with the applications of terpyridine in mind, it will be necessary to undergo further studies with **TPT** in order to disclose different applications.

5.2.2.5.1 TPT rotational isomery

Although we have designed all ligands with the tridentate structure, in solution in absence of metal cations, **TPT** has an *anti-anti* structure (**Figure V-27**) in order to minimize the interactions between the nitrogen lone pairs (the *anti* conformation was already observed with triazoloquinoline-pyridine derivatives in chapter 3 part 2).

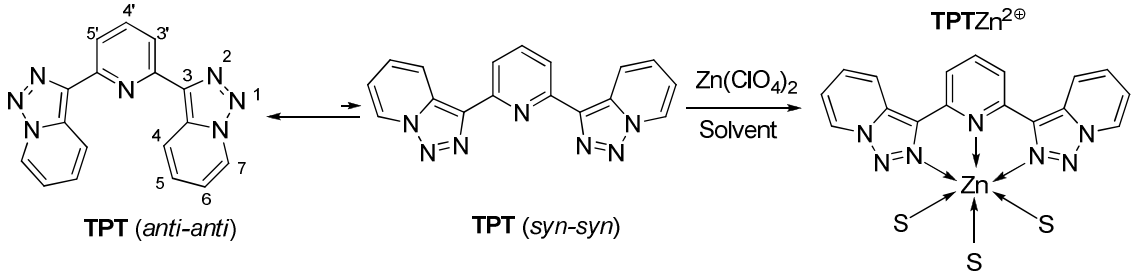

Figure V-27: Rotational isomery of **TPT**.

This behaviour has been reported recently by Meudtner *et al.* by protonation of a similar bistriazole-based structure.[22] The nitrogen lone pairs in the *anti-anti* conformation

afford a shielding in the ^{1}H-NMR signal of the hydrogen atoms close to them. In this way H^{4} and $H^{3'}$ would experiment significant changes upon coordination of zinc. In solution the *anti-anti* structure is only observed (**Figure V-28**, up spectra).

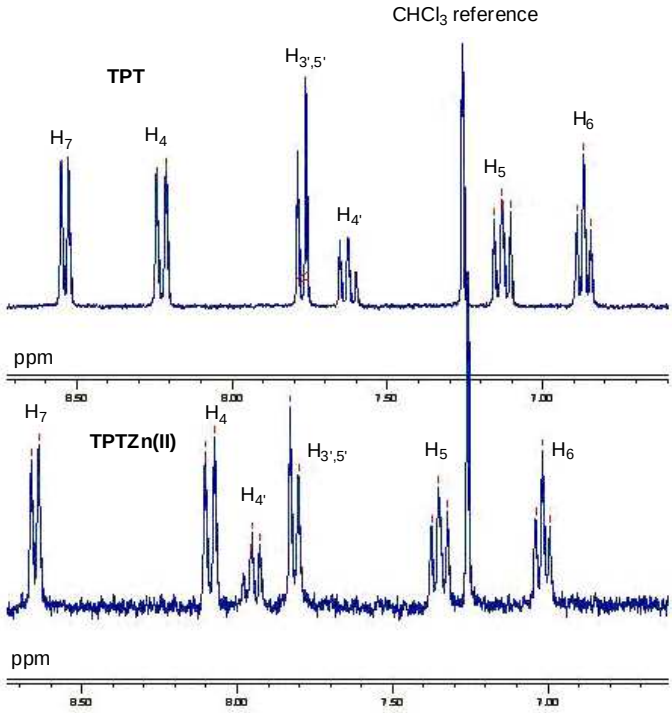

Figure V-28: ^{1}H-NMR of **TPT** (up) and **TPT**$ZnCl_2$ (down) in $CDCl_3$/CD_3OD (80/20 v:v)

In order to obtain a *syn-syn* structure, $ZnCl_2$ was added to a solution of **TPT** in deuterated chloroform/methanol (80:20) mixture. The ^{1}H-NMR of this compound (**Figure V-28** down spectrum) showed a deshielding of H^{4}, indicating the possible *syn-syn* structure. In order to provide more evidence, **TPT** was crystallized. X-ray analysis confirmed an *anti-anti* structure before coordination (**Figure V-29**)

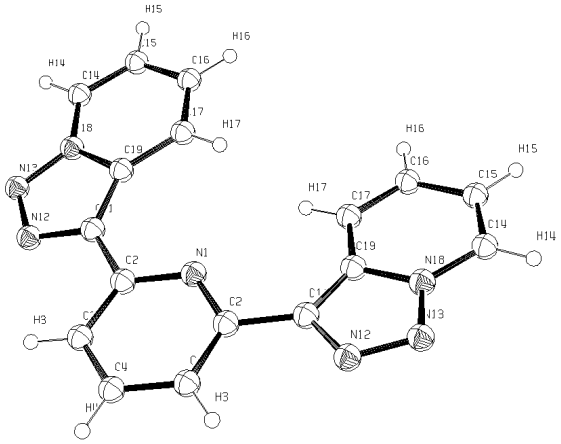

Figure V-29: **TPT** X-ray structure presenting an *anti-anti* structure.

Many efforts were devoted to obtain a single crystal from the **TPT**$Zn^{2\oplus}$ complex. Although no results were obtained, we succeeded to obtain a single crystal of the corresponding **TPT**$_2Zn^{2\oplus}$ complex (**Figure V-30**). This complex had been previously observed as a minor compound in mass spectroscopy. The **TPT**$_2Zn^{2\oplus}$ complex contains two *syn-syn* **TPT** structures.

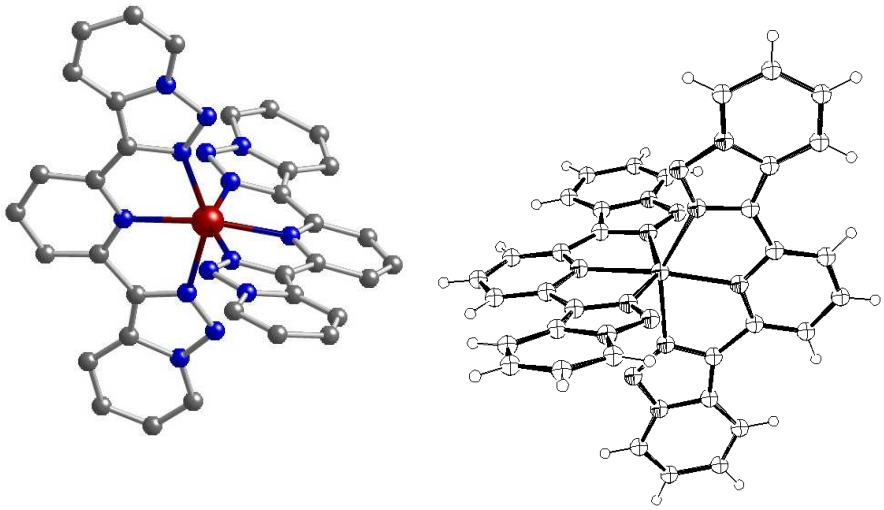

Figure V-30: **TPT**$_2$Zn X-ray structure. Labelling has been omitted for clarity as well as hydrogen atoms.

The asymmetric unit of the **TPT**$_2Zn^{2\oplus}$ complex consists of two almost equivalent $[Zn(\mathbf{TPT})_2]^{2\oplus}$ cations, the $ClO_4^{\ominus}$ counter-anion and one CH_3CN molecule (**Figure V-31**). The cationic complexe displays distorted octahedral geometry with meridional arrangement of the bis(triazolopyridino)pyridine moieties, and behave as tridentate ligands through the nitrogen donor atom of the central pyridine ring and the nitrogens placed at the 2-positions of the triazole rings.

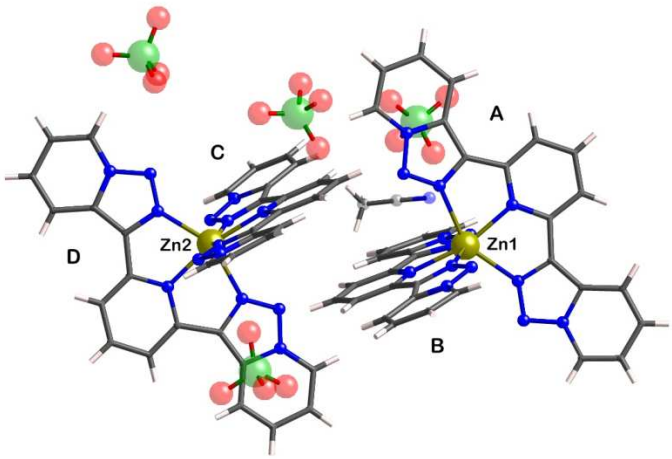

Figure V-31: Asymmetric unit of the **TPT**$_2Zn^{2\oplus}$ complex

The bond distances of the metal ion with the pyridine nitrogens (average distance 2.13 Å) are slightly shorter than those with the triazole nitrogens (average distance 2.20 Å). The ligand is slightly domed with a mean angle between the triazolopyridine unit of *ca.* 10°. The crystal packing shows π–π-stacking interactions between the cationic units which give rise to a sort of pillar-like chains.

These structures where also fully characterized by MS(ESI) showing molecular ions for [**TPT**ZnCl]$^{\oplus}$ and [**TPT**$_2$ZnCl]$^{\oplus}$ with the corresponding isotopic distribution (of zinc and chlorine isotopes) **(Figure V-32**).

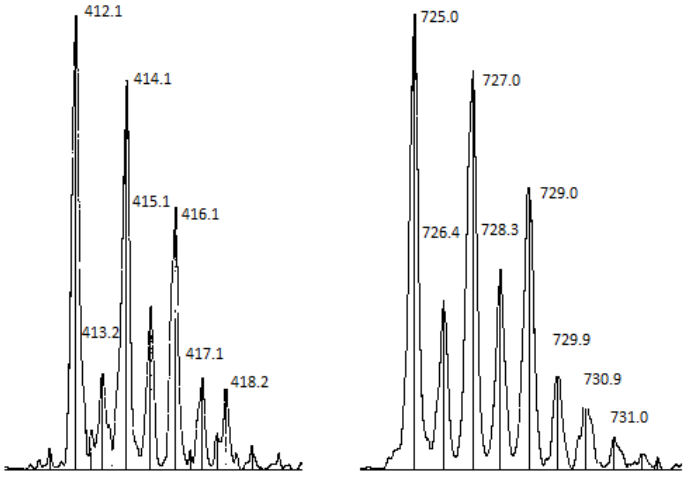

Figure V-32: MS(ESI) for [**TPT**ZnCl]$^{\oplus}$ (412.1, left) and [**TPT**$_2$ZnCl]$^{\oplus}$ (725.0, right).

5.2.2.5.2 TPT Metal coordination

TPT had an excellent response to the addition of zinc, leading to a very significant chelation enhancement of fluorescence (CHEF)[8] (**Figure V-26**). The intensity increased after addition of one equivalent of $Zn^{2\oplus}$ to **TPT** very significantly. When the quantum yield of **TPT**$Zn^{2\oplus}$ was measured, it was found to reach 0.23, which already corresponded to an enhancement of 11 times, of the **TPT** quantum yield. The fluorescence increase is accompanied by a small (8 nm) hypsochromic effect (displacement of the λ_{emi} to smaller wavelength, blue shift). These fluorescence properties fit with a Photoinduced Charge Transfer (PCT) mechanism **(Figure V-33)**. PCT[8] mechanism involves the coordination of a cation to the donor side of a fluorophore providing a blue shift. The coordination decreases the ICT, providing normally increments in intensity and or in the quantum yields. If the coordination takes place on the acceptor part, a red shift is then observed. However, in our system the metal is interacting with two donor groups (the lateral triazolopyridines by means of N^2) and one acceptor, the central pyridine. The classical considerations concerning the PCT model do not imply a double interaction with the donor and the acceptor groups. Thus, in our system

other factors can be also important like rigidity increment upon coordination (as it will be shown later).

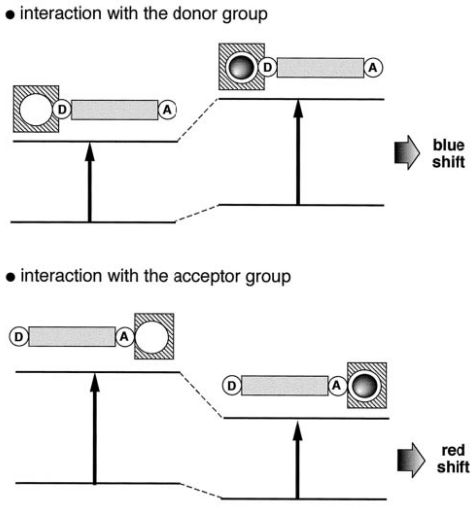

Figure V-33: Classical PCT mechanism.

We were interested in the importance of the central pyridine ring from **TPT**, Abarca *et al,* had already synthesized an analogue of **TPT** but with a central thiophene instead of the pyridine.[19] This compound, **TTT** (**Figure V-34**), has three aromatic electron-rich π-systems. When $Zn^{2\oplus}$ was added to a solution of **TTT (**10^{-5} M) no changes were observed, no intensity modification was detected, indicating that the presence of an aromatic electron-poor π-system was necessary. Thus, the donor-acceptor-donor **TPT** structure was necessary to obtain an enhancement of fluorescence. The metal coordination is also responsible of the decrease of rotational non radiative deactivation by adding rigidity to the aromatic structure and blocking **TPT** in a *syn-syn* structure (**Figure V-27**).

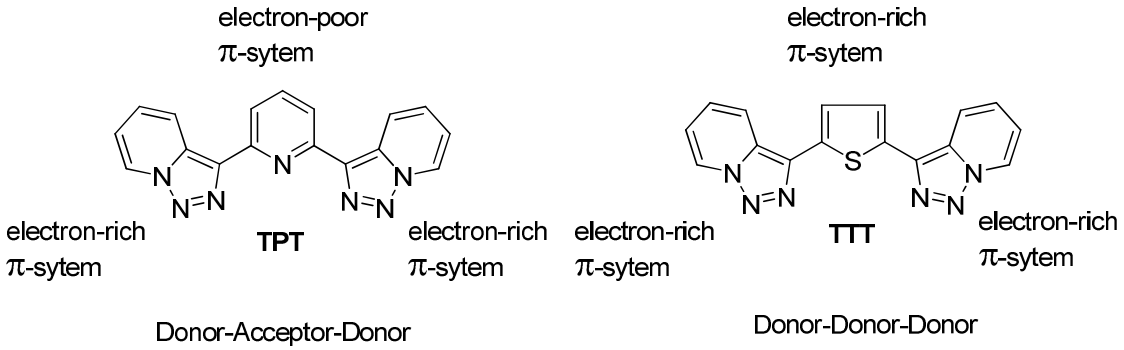

Figure V-34: **TPT** *vs* **TTT**.

The fluorescence behaviour of **TPT** was also checked in the presence of divalent transition metal ions like $Co^{2\oplus}$, $Ni^{2\oplus}$ and of the post-transition ones $Cd^{2\oplus}$ and $Pb^{2\oplus}$ (**Figure V-35**). Although not so large as in the case of $Zn^{2\oplus}$, significant CHEF effects were produced in the system $Cd^{2\oplus}$-**TPT**. Quenching phenomena were observed with $Cu^{2\oplus}$, $Ni^{2\oplus}$ and $Co^{2\oplus}$.

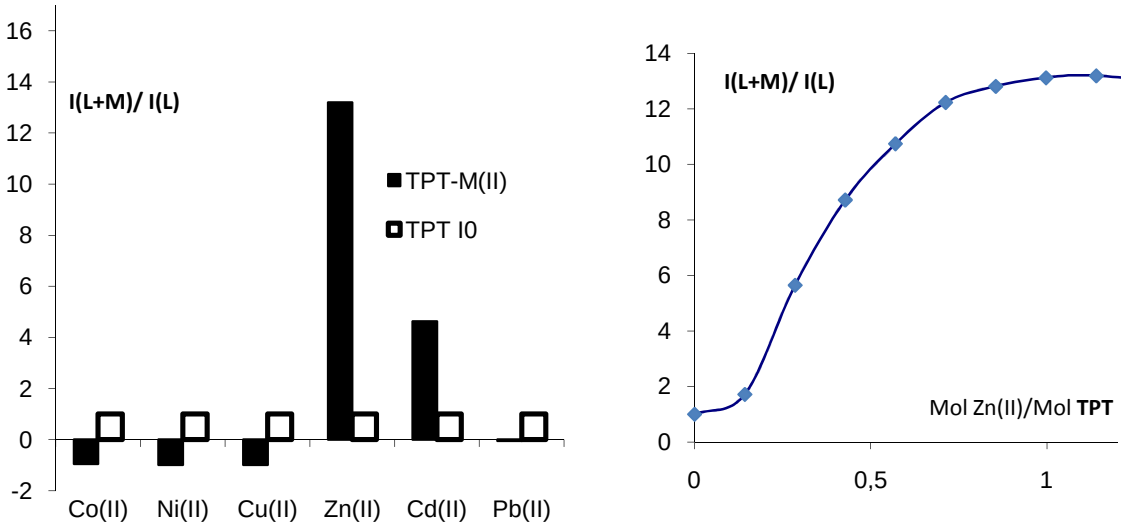

Figure V-35: Metal screening for TPT and TPT-Zn titration representation.

In **Figure V-35** it can also be observed how the intensity of **TPT** emission increases until the 1:1 complex is obtained. Further addition of zinc does not provide intensity modification pointing out that the 1:1 species is the fluorescent intermediate.

5.2.2.5.3 TPT anion recognition

Anion recognition by means of fluorescence is a general topic that has been largely developed,[16, 33, 34, 56, 57] as well for zinc as for copper detection. There are many different fluorescent ligands able to perform anion recognition. The study of the evolution of the fluorescence upon the addition of anions affords, once again, a sensitive real time technique. The different interactions between the anions with the fluorophores (hydrogen bond, π-stacking...) offers a huge family of sensor. By means of hydrogen bonding, protonated polyamines linked to a fluorophore have been proposed as good receptors for different anions or biological anionic compound (ATP, ADP, amino acids...). The first example of a fluorescent sensor for anions is due to Czarnik[58] (**Figure V-36**).

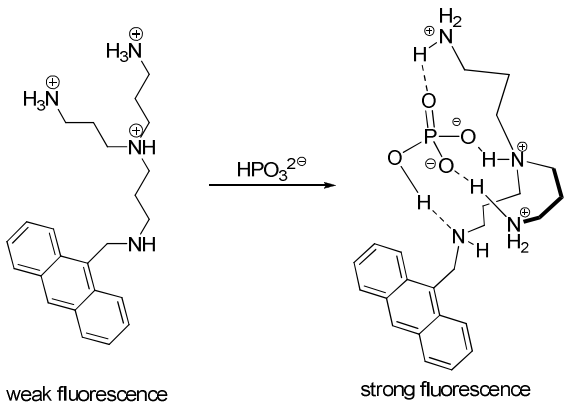

Figure V-36: Recognition and sensing of $HPO_3^{2\ominus}$.

In this way protonated polyamines have revealed as a useful scaffold in the preparation of water soluble fluorescent receptors. Many other structures like urea, thiourea, guanidine or pyridine derivatives can be found as good scaffolds in anion receptors due to the possibility of hydrogen bonding,[59] i.e. for fluoride anion (**Figure V-37**).

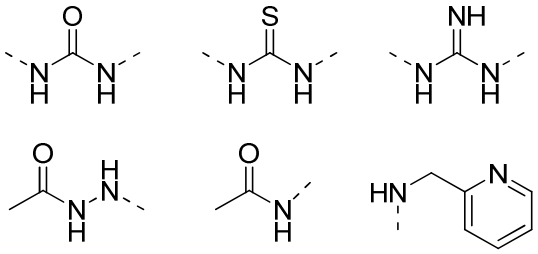

Figure V-37: Common subunits founds in anion receptor.

However, there are not many examples of fluorescent studies where a metal cation is employed as receptor (for ions), as Abarca and Garcia España have reported.[10] One of these examples was reported by Santis[60] *et al.* and is depicted in **Figure V-38:**

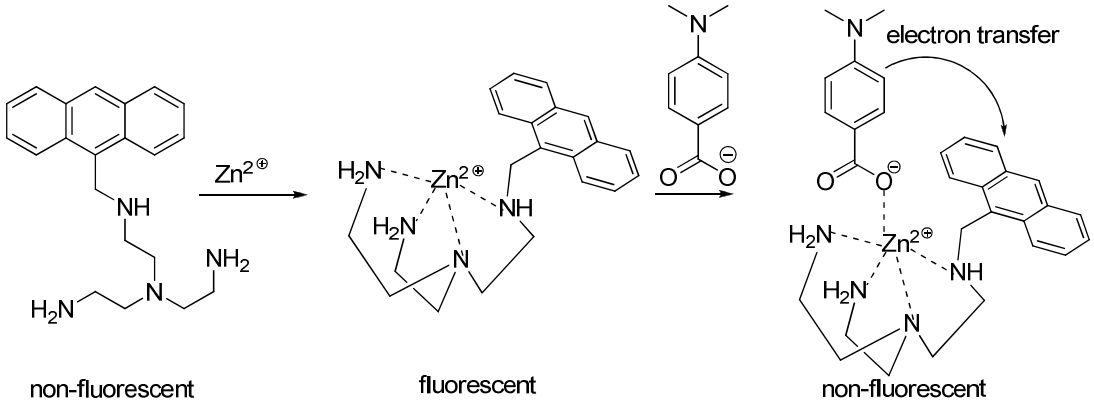

Figure V-38: Sensing carboxylates based on the metal-ligand interaction.

In this example, a fluorescence enhancement is observed when zinc is added. The coordination of an aromatic acid with a donor group (-$N(CH_3)_2$) or and acceptor (-NO_2) affords fluorescence quenching by electron transfer (from the amine to the anthracene in the first case, and from anthracene to the nitrobenzoic acid in the second case).

As reported by Abarca and Garcia España, coordination of anions to the metal centre provided fluorescence quenching of sensors where the triazolo ring was employed as fluorophore.[10] This is one of the rare examples of anion detection by means of metal coordination. In our particular case, the Zn(**TPT**)$^{2\oplus}$ complex has also a coordinatively unsaturated coordination sphere. Three positions are occupied by ancillary ligands, likely solvent molecules that can be readily replaced by anionic ligands. Such subtitutions should affect the emissive properties of the system and can thereby be used to detect anionic species.

Thus, we have checked the interaction of solutions containing $Zn^{2\oplus}$ and **TPT** in a 1:1 molar ratio for which the 1:1 complex is the predominant species in solution, with different

monovalent anions ($F^{\ominus}$, $Cl^{\ominus}$, $Br^{\ominus}$, $I^{\ominus}$, $CN^{\ominus}$, $SCN^{\ominus}$, $NO_2^{\ominus}$, $NO_3^{\ominus}$) by adding solutions of tetrabutylamonium salts of all anions (except $NaNO_2$) to Zn(**TPT**)$^{2\oplus}$ solutions. In all cases, quenching of the emission was produced (**Figure V-39**).

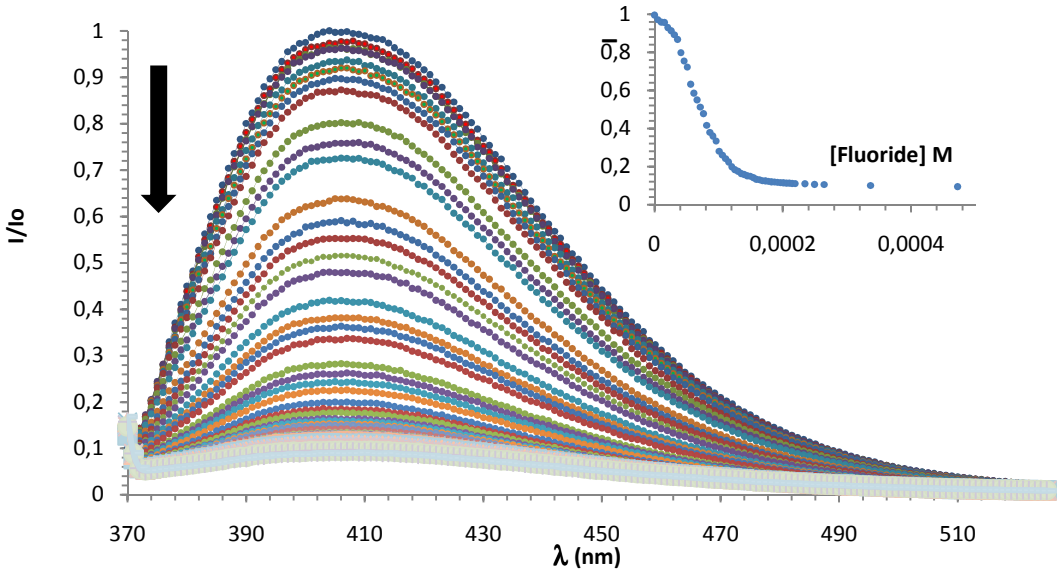

Figure V-39: Normalized fluorescence emission spectra of Zn**TPT**$^{2\oplus}$ in ethanol:water (98:2 v/v), (10^{-5} M) upon addition of fluoride in water (10^{-3} M) (λ_{exc} = 359 nm).

The analysis of the fluorescence spectra with the program SPECFIT[61-64] has allowed us to determine the stability constants shown in **Table V-3** for the formation of a mixed Zn(**TPT**)$^{2\oplus}$-anion complex. Only complexes of 1:1 stoichiometry were obtained from the analysis of the experiemental data. The constants show, for the halide anions, reveal the stability sequence $F^{\ominus} > Cl^{\ominus} \approx Br^{\ominus} < I^{\ominus}$.

The $CN^{\ominus}$ binding constant is one order of magnitude lower than $SCN^{\ominus}$ while $NO_2^{\ominus}$ anions interact much stronger than $NO_3^{\ominus}$ with Zn(**TPT**)$^{2\oplus}$.

Table V-3: Logarithms of the binding constants (log K) for the formation of Zn(**TPT**)(anion) complexes in ethanol/water (98:2 v/v).

	$F^{\ominus}$	$Cl^{\ominus}$	$Br^{\ominus}$	$I^{\ominus}$	$CN^{\ominus}$	$SCN^{\ominus}$	$NO_2^{\ominus}$	$NO_3^{\ominus}$
logK	4.85	4.08	4.23	4.58	3.87	4.88	5.07	3.50
	±0.05	± 0.04	±0.02	±0.02	±0.09	±0.04	±0.03	±0.02

However, as it is often observed,[65] the magnitudes of the binding constants do not correlate exactly with the extension of the quenching phenomena. Particularly, in spite of having lower binding constant, $CN^{\ominus}$ anions exert a much more marked quenching than $SCN^{\ominus}$ anions (**Figure V-40**). These differences become apparent by representing the I/I_0 (I = intensity of the sample, I_0 = initial intensity) against the concentration of the analyte or ratio

analyte/sensor (anions in our system). This representation is also known as Stern-Volmer plot.[6] (Io = Initial intensity, I = Intensity after the addition of the analyte)

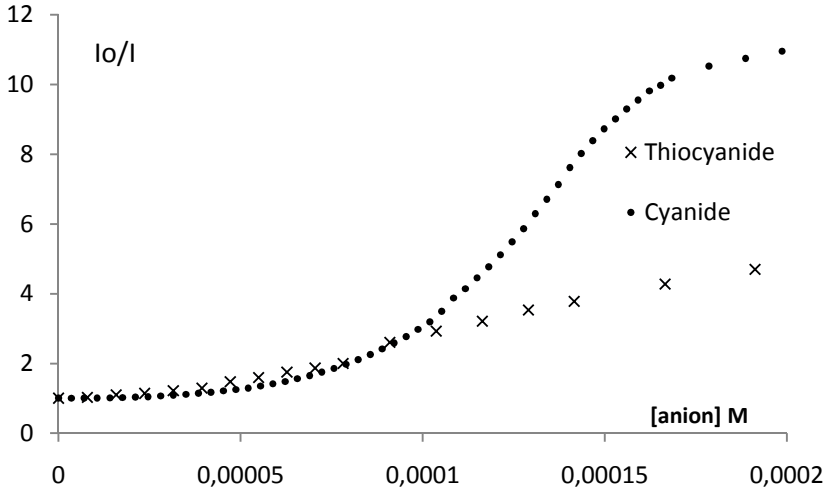

Figure V-40: Quenching observed with thiocyanide and cyanide.

In **Figure V-40** we can observe how with a concentration of 0.0001 M, a reduction of 75% of the intensity is observed. Cyanide, however, is able to quench completely the emission of the 10^{-5} M solution of **TPT**$Zn^{2\oplus}$. It is also interesting to notice the neat discrimination that our system produces between $NO_2^{\ominus}$ and $NO_3^{\ominus}$ (**Figure V-41**). The π-acceptor character of these two ligands $CN^{\ominus}$ and $NO_2^{\ominus}$ can contribute to the quenching effects. Taking into account the sensitivity of the equipment, a plot of the fluorescence intensity variation with respect to the concentration of the substrate reveals detection limits for $NO_2^{\ominus}$ of 3.2 ppb and below 1 ppb for $CN^{\ominus}$. The discrimination of nitrites from nitrates is a very important result, ($K_{nitrite}/K_{nitrate}$ = 37). That means, that the response of nitrite is 37 times the one for nitrate. In **Figure V-41** this effect is represented. With a concentration of 0.0001 M nitrates do not modify the emission while the intensity has decreased by 75% with nitrite.

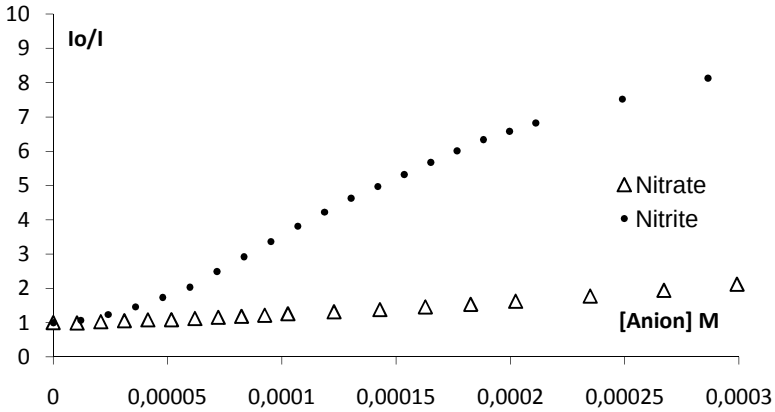

Figure V-41 Plot of I_0/I of Zn(**TPT**)$^{2\oplus}$ (8×10^{-5} M) in 98:2 v/v EtOH/H_2O upon succesive additions of nitrite (up) and nitrate (dowm)

The values $K_{nitrite}$ ($K = 1.2\times10^5\ M^{-1}$) obtained for this system compared to those obtained previously by Abarca[10] *et al.* ($K = 1.5\times10^3\ M^{-1}$) already indicate the strong ability of this system to detect nitrites. In a general way, we have observed that coordinating anions provide a quenching of the **TPT**$Zn^{2\oplus}$ system and binding constants had been calculated (**Table V-3**). As it has been mentioned, the fluorescence response is more important with some anions. In **figure V-42** all systems are compared showing this behaviour.

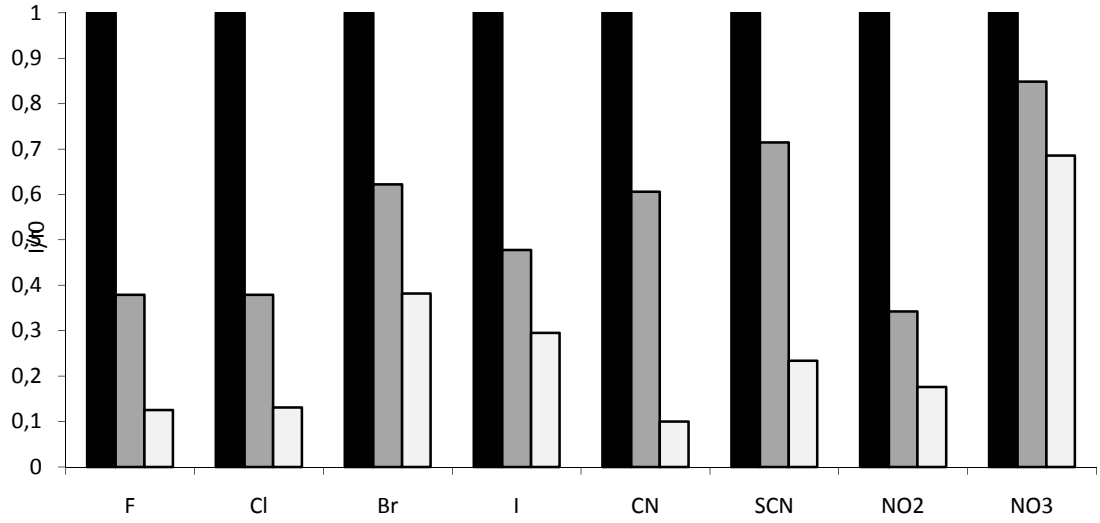

Figure V-42: Comparation between differetn anions $TPTZn^{2\oplus}$ (black), after the addition of 1 eq of anion (grey), after the addition of 2 eq. of anion (white).

Encouraged by these results, we interested on amino acids as quenchers of our system. Amino acids are essential molecules for the human body being part of enzymes and proteins. Furthermore some of them like glutamic (Glu) (mainly) or aspartic (Asp) acids play essential roles as neurotransmittors.[66, 67] A lot of research is devoted to the study and the sensing of amino acids. Their coordination with metals is omnipresent in nature as part of enzymes. The interaction between amino acids and metals can afford different coordination modes Taglietti[57, 68] and Anslyn[69] reported on the coordination of amino acids, developing different ways to quantify them. The sensor developed by Abarca and Garcia España,[10] **PP(T)P** (**Figure V-4**), was found useful to detect these two compounds (K_{Glu} = 5500, K_{Asp} = 1000). In order to compare our new system **TPT**$Zn^{2\oplus}$ with previous triazolopyridine-based sytems, we studied the evolution of the fluorescence by addition of different amino acids. Glutamic and aspartic acids were tested as well as histidine (His) and tryptophan (Trp). However, all these systems can have different coordinations modes associated to the substitution of the amino acid. Thus, we also selected alanine (Ala) and phenyl alanine (Phe) as analytes.

Although amino acids are very important for human life, its solubility in organic solvents is limited. Most of the detection techniques must be able to work in presence of aqueous solution. However, water solubility of fluorophores can be a problem, especially with anthracene or pyrene derivatives. The choice of ethanol as solvent was partly motivated by this, as it has been remarked before. These two solvents are completely miscible and the range of concentrations of 10^{-5} M avoid precipitation of ligand or analyte. In this way a **TPT**$Zn^{2\oplus}$ solution in a 98:2 v/v ethanol-water was used and amino acids were added as a 10^{-3} M water solution (like anions). By adding amino acids to the fluorescent solution, a quenching phenomenon was observed in all cases. The response of all of them provided a loss of fluorescence (**Figure V-43**).

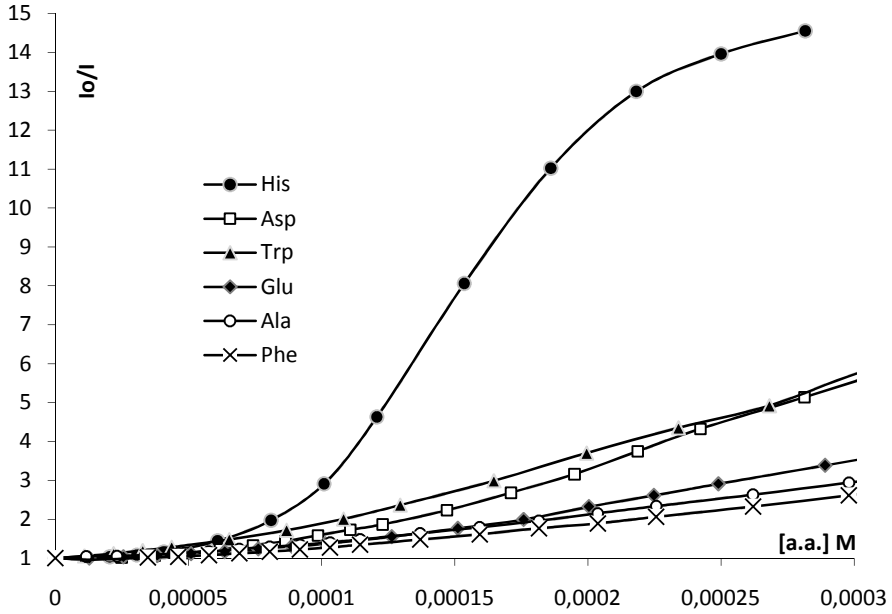

Figure V-43: Fluorescence reponse of TPTZn$^{2\oplus}$ (8×10^{-5} M) in EtOH/H_2O (98:2) to different amino acid (a.a.) concentration.

The analysis of the evolution of the fluorescence provided the corresponding binding constants (**Table V-5**), histidine (His) is the most efficient quencher, however, once again not only the K was bigger but the response was more important with His. The nature of the amino acid leads to drastic modification. With alanine (Ala) smaller quenching constant are obtained (logk = 3,60), however, with coordinating groups higher values are obtained.

Table V-4: Binding Constants for the Interaction of **TPT**$Zn^{2\oplus}$ with a.a. determined by means of the HYPERQUAD program.[70]

	L-His	**L-Glu**	**D-Asp**	**L-Try**	**L-Phe**	**L-Ala**
log(k)	4.84	3.90	4,34	4,20	3.81	3,60
	∓ 0.05	∓ 0.04	∓ 0.01	∓ 0.02	∓ 0.09	∓ 0.04

Many different coordination modes from amino acids to metals can be obtained.[71] We were particular interested on histidine due to its multiple coordination sites (**Figure V-44**) if afforded the highest logk value.

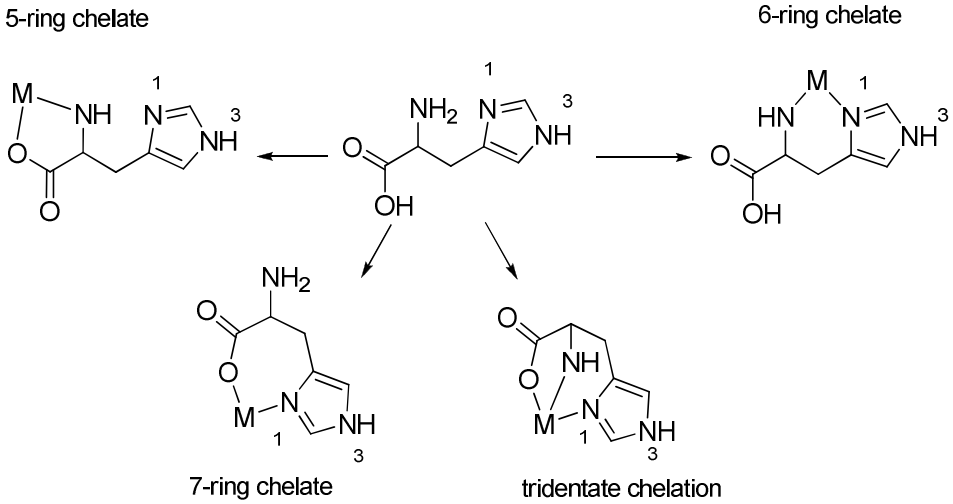

Figure V-44: Multiple coordination pattern for Histidine including at least two donor atoms.

Three possible coordinating groups can be found in the structure of histidine. The carboxylic acid, the amine and the imidazole ring. In order to study these different coordinating groups, fluorescence tests were performed with model substrates. Tetrabutyl ammonium acetate, ethylenediamine and imidazole were tested as analogs (**Figure V-45**),

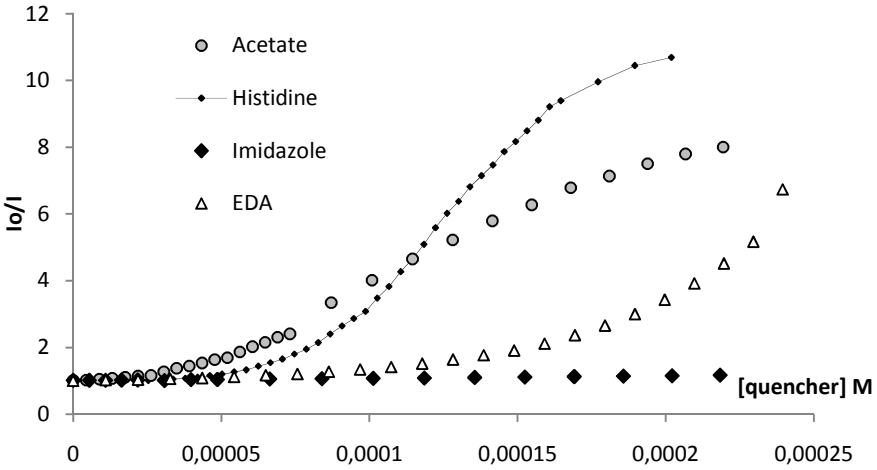

Figure V-45: Fluorescent test of model compounds, EDA: Ethylenediamine.

The quenching phenomenon was observed with acetate and ethylene diamine. However imidazole presented a smaller influence on the system. Binding constants were calculated for this system corroborating (**Table V-5**).

Table V-5: Binding constants[70] for the model compounds.

	L-His	Acetate	EDA	Imid
log(k)	4.84	4.66	4.45	3.36
	∓0.05	∓0.01	∓0.01	∓0.01

Although $k_{Acetate} > k_{EDA} >> k_{imid}$ any of these structures approached the absolute value of $k_{histidine}$. Amino acids are normally coordinated to metals by a bidentate structure involving the amino- and the acid groups. However, in the particular case of histidine, an N_{amino}-$N_{imidazole}$ 6-ring chelate, and also a O_{acide}-$N_{imidazole}$ 7-ring chelate are possible (**Figure V-44**). The study of the model compounds did not allow to establish a general statement on the coordination mode of Histidine to our system.

Then we envisaged the modification of histidine. By means of commercial protected histidines, we studied the influence of the different coordinating groups when they were interacting at the same time (**Figure V-46**).

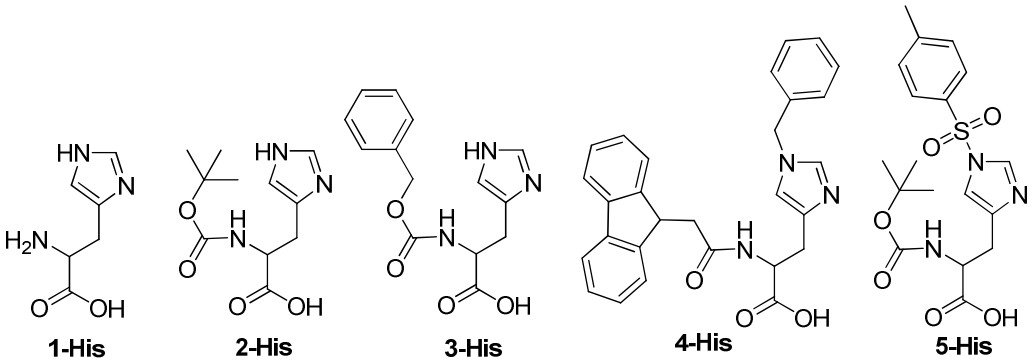

Figure V-46: Protected Histidine derivatives employed.

By studying the response of **TPT**$Zn^{2\oplus}$ towards the addition of one of these compounds we evaluated the different functions in the quenching. All compounds quenched the system, however **5-His** revealed as the worst quencher, noticing the importance of the substitution in the imidazole ring.

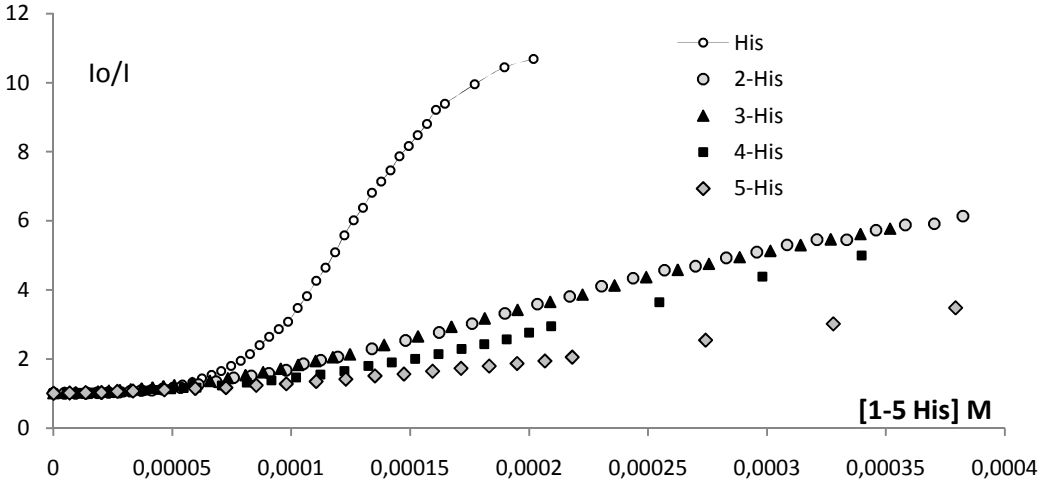

Figure V-47: Fluorescence study of protected histidines.

In all cases the reponse was smaller than with free histidine (1-His), indicating that the amine played an essential role. When this function is protected quenching is affected (**Figure V-47** and **Table V-6**).

Table V-6: Binding constants[70] for Histidines **1**-**5**.

	1-His	**2-His**	**3-His**	**4-His**	**5-His**
log(k)	4,84	4,26	4,24	4,11	3,79
	∓0,05	∓0,01	∓0,02	∓0,02	∓0,03

The protection of the amine group was found to be relevant, due to the decrease of the binding constants in all cases. However no large difference between **2-His** and **3-His** was found. In contrast the subsequent modification of the imidazole ring from **2-His** to **5-His** was significant ($K_{2\text{-His}}/K_{5\text{-His}}$ = 3) decreasing three times the strength of the binding. For the **5-His** the nitrogen N^3 is protected, but N^1 is responsible for coordination (**Figure V-44**). This reveals the influence of the tosyl group`as electron-acceptor which decreases the coordinating properties of the imidazole ring (**Figure V-48**).

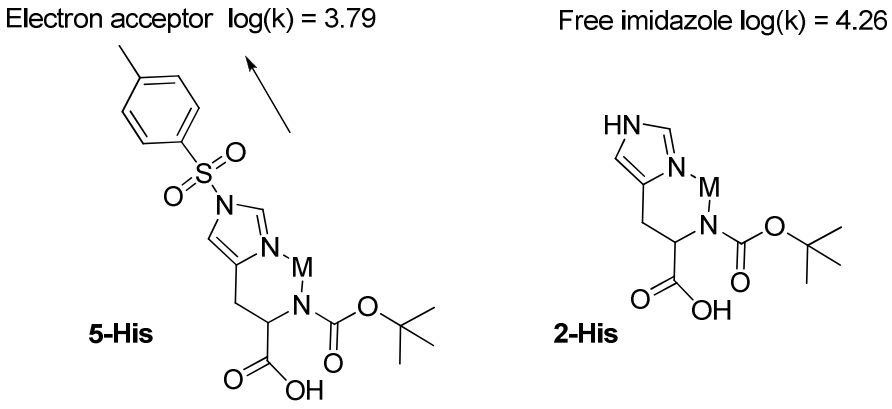

Figure V-48: Imidazole effect .

Comparing these values the first conclusion that can be drawn is that the amino group plays an essential role in the coordination because when it is protected, the k-value decreases, (**2-His** and **3-His**). Protecting groups (Boc, Cbz, and Fmoc) delocalize the electron density of the nitrogen and thus the coordination ability decreases. The protection of the imidazole ring leads to a greater decrease of k when electron-accepting protecting groups (tosyl, **5-His**) were employed. There is a direct interaction in the quenching phenomen due to the electron density of the imidazol ring (comparing **2-His** and **5-His**). The possibility of a 6-ring chelate (N_{im}-Zn-NH_2) must be more stable than the carboxylate coordination (seven-ring chelate N_{im}-Zn-OOC) providing the reponse observed with L-Histidine. This chelation (N_{im}-Zn-NH_2) has already been proposed in the literature by Anslyn.[72]

Comparing the values of the binding constants obtained with the system **TPT**$Zn^{2\oplus}$ with those obtained by Abarca in previous works (**Table V-7**), higher values have been obtained. This indicates the high sensibility of the system with **PP(T)P** (compound **82**, **Figure V-4**).

Table V-7: Comparison between binding constants.

	Chloride	Nitrite	Glu	Asp
TPTZn$^{2\oplus}$ k (M^{-1})	12000	117000	7900	21800
PP(T)P$^{2\oplus}$ k (M^{-1})	3200	1500	5500	10000

Although **TPT**Zn$^{2\oplus}$ seems to be more efficient, the combination of both systems could be more interesting, **PP(T)P** provided a recognition different from those observed with **TPT**Zn$^{2\oplus}$. Indeed, with **PP(T)P** important wavelength modifications were observed as well as modification of intensity upon coordination of anions. In our system only intensity modification were observed, affording strong LOD and binding constants. A combination of these two systems would be interesting in anion sensing, in a qualitative and quantitative way (**Figure V-49**). This idea has been employed by Anslyn in the development of families of non-selective receptors,[73, 74] and the response of all of them with different analytes to provide a selective quantification by means of mathematical analysis.

	TPTZn quantitative	**PP(T)P qualitative**
Nitrite	Strong Quenching	blue
Nitrate	Weak Quenching	green

Figure 49-V: Combination of both systems

.

5.2.2.6 TPON fluorescence study

As it has been reported, **TPON** also provided an enhancement of the fluorescence, however this time it was accompanied by an important bathochromic shift (24 nm). Furthermore two different signals could be found in the fluorescent spectra upon the coordination of zinc. The blue shift indicated also a PCT mechanism. However, this time, a second effect could also be involved in the fluorescence. Indeed rotation and charge transfer from the free alcohol to naphthalene quenches the fluorescence (**Figure V-50**).

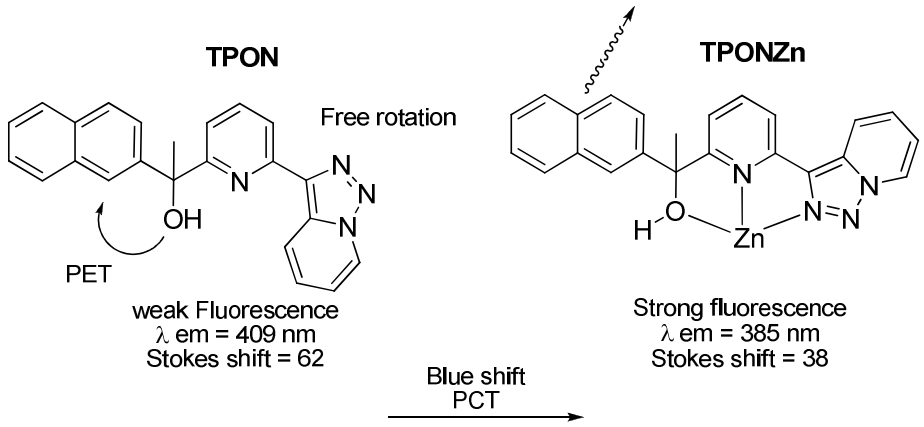

Figure V-50: **TPON** fluorescence.

The coordination of zinc avoids the PET and the rotation, providing a rigid system with a non quenched fluorophore (naphthalene) and a second (minoritary) fluorescent unit (triazolopyridine pyridine). The enhancement of the fluorescence also provided a second signal. However, the blue shift from **TPON** to **TPON**$Zn^{2\oplus}$ decreased the stokes shift and the excitation and emission wavelengths became closer (**Figure V-51**).

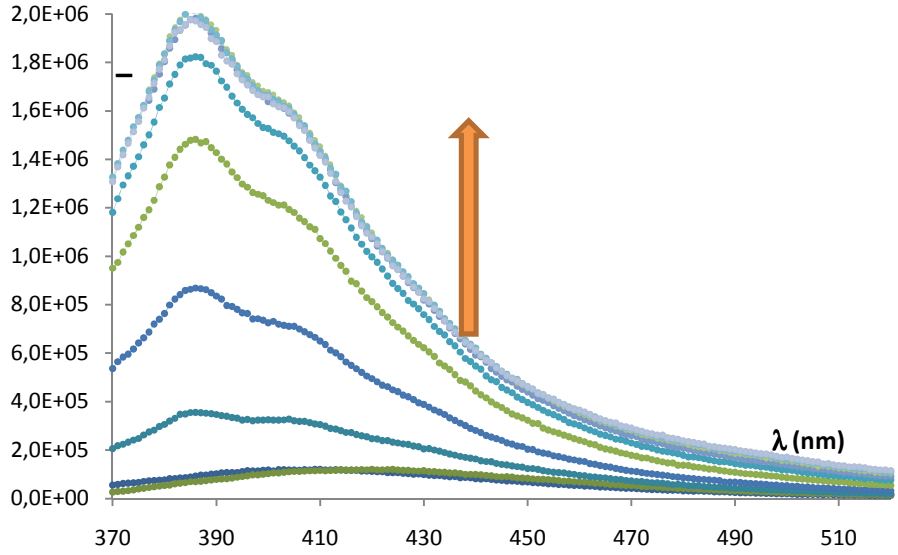

Figure V-51: **TPON** spectra upon zinc(II) addition, max was obtained wiht 1:1 ratio.

As it can be observed the first value in the graph (**figure V-51**, 370 – 380 nm) increases with the addition of zinc. This is caused by the displacement of the maximum as the excitation wavelength keeps constants. This blue shift decreases the distance and can interfere with the emission. In this case measures can still be performed, **BTH-TPT** has a stokes shift near 34 nm before coordination (**Table V-2**, entry 6), in that case no anion recognition was performed due to the proximity of excitation and emission, that makes the measurement of the quantum yield difficult.

The fluorescence enhancement of **TPON** was larger than for **TPT**. We interested then in the study of anion coordination in order to see if they could also be detected by **TPON** and compare the binding constants. The same test performed with **TPT**$Zn^{2\oplus}$ were performed with **TPON**.

Table V-8: Comparison between binding constants.[70]

	$F^{\ominus}$	$Cl^{\ominus}$	$Br^{\ominus}$	$I^{\ominus}$	$NO_2^{\ominus}$	$NO_3^{\ominus}$	$SCN^{\ominus}$	$CN^{\ominus}$	His
TPON$Zn^{2\oplus}$	4,56	4,23	4,26	4,31	5.01	3.8.	4,12	5,17	5,14
	0,04	0,04	0,03	0,03	±0.09	±0.10	0,01	0,08	0,05
TPT$Zn^{2\oplus}$	4.85	4.08	4.23	4.58	5.07	3.50	4.88	3.87	4,8
	±0.05	± 0.04	±0.02	±0.02	±0.03	±0.02	±0.04	±0.09	0,05

When the values of the binding constant were compared, **TPON** presented values but in the same magnitude as **TPT**. However, this time cyanide was stronger bound than thiocyanate. The difference could be associated to the possibility of decoordination of the alcohol function of **TPON**. **TPT** provides a symmetric tridentate, aromatic system upon zinc addition. The anion coordination increases the distance between the nitrogen atoms and zinc metal and in some cases decrease the electron density on the metal centre *i.e.* cyanide and nitrite. This modifies the rigidity of the system favoring the non-radiative deactivation (Figure V-52).

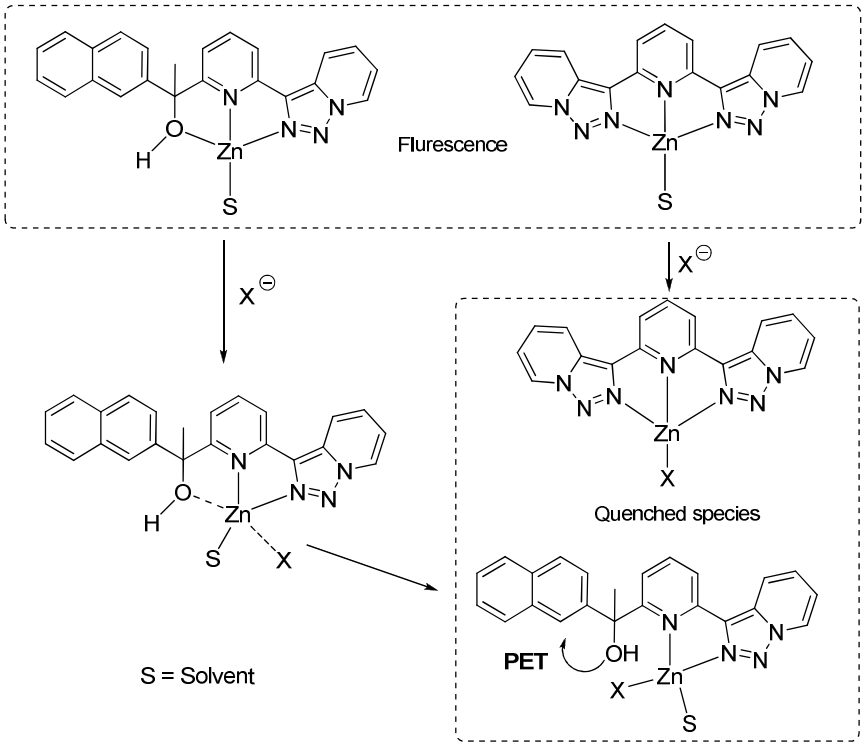

Figure V-52: Quenching of **TPT** and **TPON**. Only one of solvent molecule has been included for clarity,

However with **TPON,** the alcohol can be liberated by anion coordination, and the free alcohol can then quench naphthalene by charge transfer. This option is not applicable to **TPT** due to its rigidity and the steric hindering of the triazole ring in a possible bidentate structure (only the central pyridine and one of the triazolopyridine nitrogen atoms coordinated to zinc). All essays to crystallize an anion-**TPT**$Zn^{2\oplus}$ or anion-**TPON**$Zn^{2\oplus}$ complex were unsuccessful and no X-ray structure of the quenched species could be obtained so far.

5.2.2.7 TQPO fluorescence study

The fluorescent properties of triazolopyridine-quinoline phosphines oxides **TQPO1-3** were dependant on the substitution of the phosphines (**Table V-2**, entries 9-11). These molecules present significant differences in terms of excitation and emission wavelengths. The quantum yields have also important differences (between 0.40-0.60) because of their dependence of the substituents from the phosphine (**Figure V-53**)

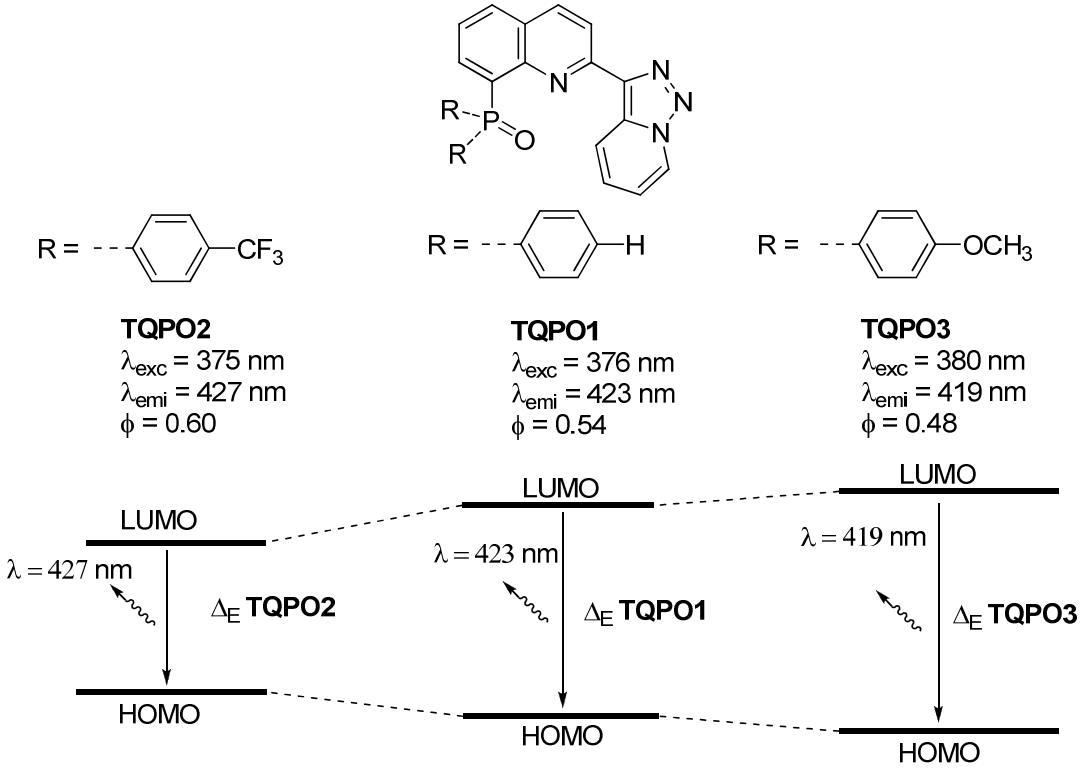

Figure V-53: Fluorescent properties of compound **TQPO1-3**.

All compounds have an aromatic phosphine oxide. However, as there are very important differences between aryl and alkyl phosphines, we prepared alkyl phosphine oxide **94** (**TQPO4**) by the same methodology that had been previously employed for **TQPO1-3** (**Scheme V-9**).

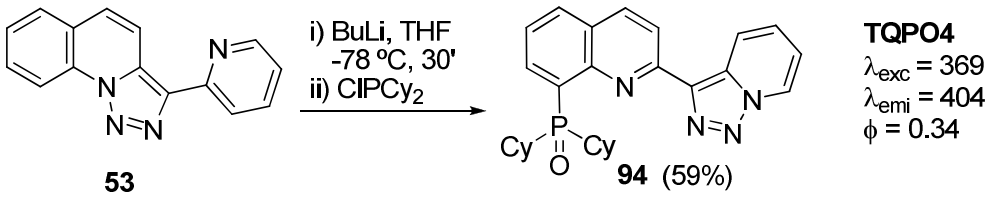

Scheme V-9: Preparation of **TQPO4**.

Triazoloquinoline-pyridine **53** was metalated with butyl lithium in THF at -78 °C and trapped with dicyclohexylchlorophosphine. After purification compound **94** was obtained as colorless solid in 59% yield. When its fluorescence properties were measured, the excitation wavelength decreased 6 nm compared to **TQPO1.** However, the emission wavelength was

found to be 404 nm, being 20 nm less than reference compound. the quantum yield also decreased to 0.34. The blue shift observed, comparing λ_{emi} of **TQPO1** and **TQPO4** ($\Delta\lambda_{emi}$ = 20 nm) reminds in some way the differences between **TPT** and **BTH-TPT** ($\Delta\lambda_{emi}$ = 45 nm). When all compounds are compared, λ_{emi} decreased as donating groups were bonded to the phosphine (**Figure V-54**).

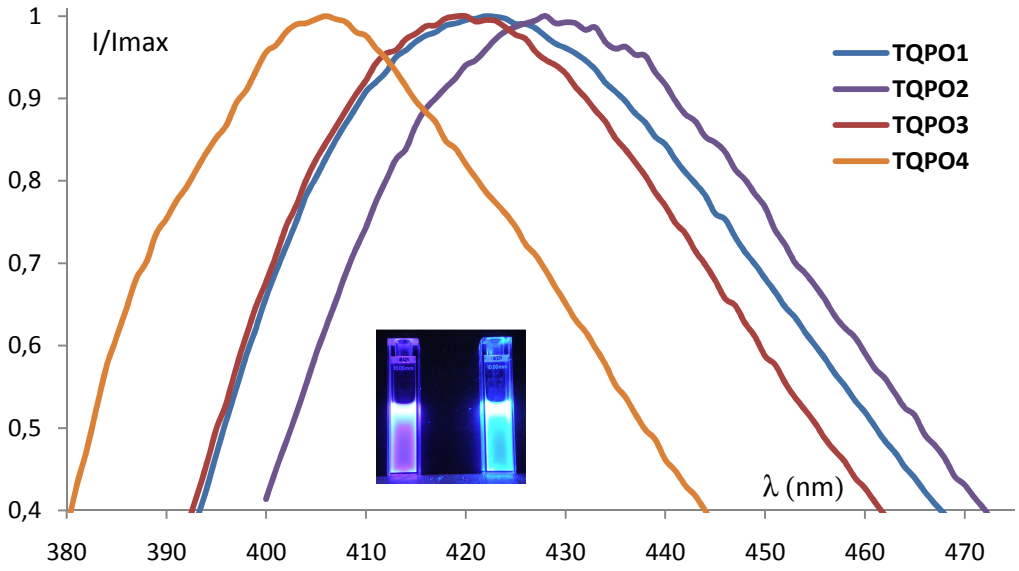

Figure V-54: Max intensity of the emission spectra for compounds **TQPO1-4**.

8-Substituted quinolines are well known compounds in coordination chemistry and fluorescence properties (for example 8-hydroxyquinoline or 5-sulfonate-8-hydroxyquinoline[8]). In our case, the structure is based on an 2,8-disubstituted quinoline (**Figure V-55**).

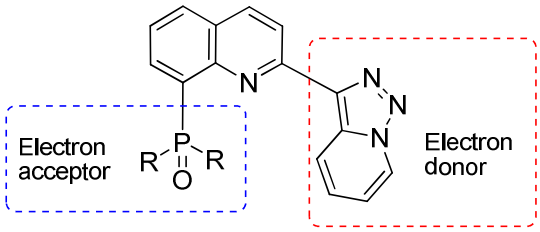

Figure V-55: **TQPO** structure.

By employing different phosphines, the electron-acceptor side had been modified, and the observed tendency indicates that electron-donating groups attached to the phosphine oxide decreases the quantum yields, and increases the energy between the LUMO and the HOMO (*i.e.* quantum yield: Cy < H_3CO-Ph < Ph < F_3C-Ph). The coordination of these compounds with zinc provides no modification of any of these parameters. But the coordination of this system is more complex than those studied before and no X-ray structures have been obtained. So far the steric hindering from the oxide can be relevant in the possibility of bidentate ($N_{quinoline}$-$N^2_{triazole}$) coordination and as zinc addition provided no modification, no

conclusion can be drawn. Copper provided some modifications, Indeed all system quenched with copper. However the quenching was not the same for all compounds (**Table V-9**).

Table V-9: Binding constants[70] with copper for the **TQPO** family.

	TQPO1	**TQPO2**	**TQPO3**	**TQPO4**
logK	5,16	4,50	6,15	6,41
	±0,06	±0,06	±0,05	±0,08

The value of the binding constants was opposite to the one of the quantum yield , the quenching phenomena was more important for compound **TQPO3** and **TQPO4** (**Figure V-56)**.

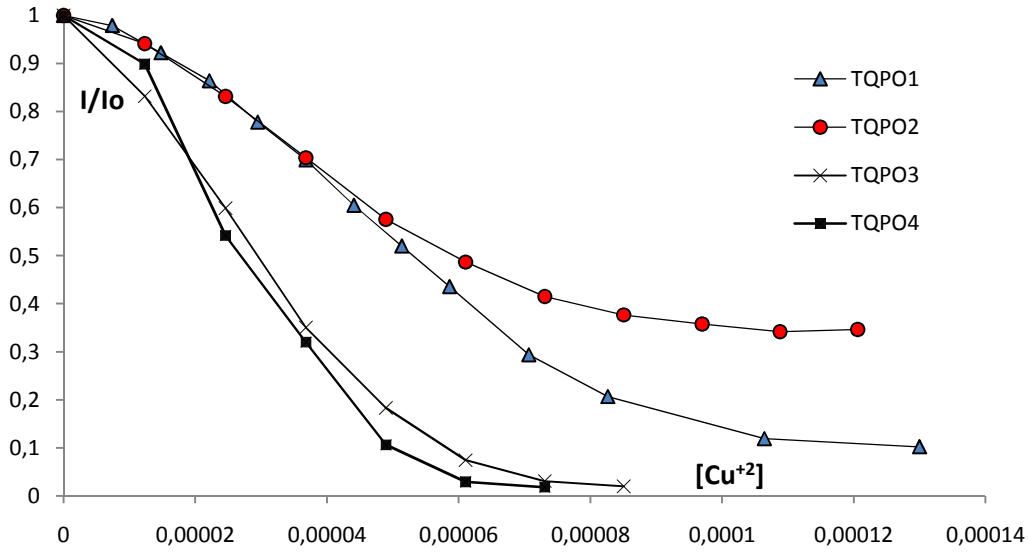

Figure V-56: Quenching of **TQPO1-4** with copper.

If we compare the values of these constants and quantum yields, the role of phosphine oxide seems relevant. When electron-donor groups are attached to phosphorus, the quantum yield decreases, but the binding constants with copper increases. Electron-donor groups favour a partial negative charge on the oxygen atom (by stabilizing the partial positive charge at phosphorus) (**Figure V-57**).

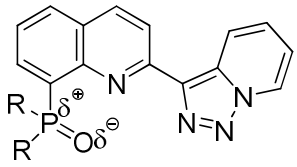

Figure V-57: Possible PET phenomena with donor R groups.

The partial negative charge could be responsible for the binding constants. A partial negative charge at oxygen atom will increase the coordination constant.

5.2.2.8 Conclusions

The study of the fluorescent properties of these compounds had afforded many important conclusions:

- The study of the fluorescent properties of **TPT** and its derivatives (*i.e.* **TqPTq**, **TPTq** or **BTH-TPT**) revealed interesting properties in terms of quantum yields, being coherent with the literature.

- The majority of compounds has revealed to be good Turn-Of sensors for copper (II), however, the **TQPO** family has been found to be the most important due to its large quantum yields.

- **TPT** has revealed as an excellent sensor of zinc and its complex (**TPT**$Zn^{2\oplus}$) has been used as a switch of sensor for anions with low limits of detection (LOD) (for cyanide and nitrite). A selective quenching between nitrites (important quenching) and nitrates has been observed. The amino acid coordination with this system has also been studied, specially coordination with histidine.

- **TPON** has revealed an excellent sensor for zinc as well as **BTH-TPT**. **TPON**$Zn^{2\oplus}$ has also been employed for the anion detection providing high binding constants.

- The **TQPO** family has been found to have very high quantum yields. The quantum yields and the emission has been found to be closely related to the substituents attached to the phosphorus atom. **TQPO2** has an intense blue emission with a high quantum yield (near 0.60).

V: Fluorescence

5.3 Chiral Amino Acid recognition

5.3.1 Introduction

Chiral luminescence recognition has been studied in the past two decades. The special features of these techniques afford fast measurements as for other targets like metals or ions. Enantiomers may have different biological activities, strict guidelines on the identification and quantification of chiral compounds have been imposed (*i.e.* U.S. FDA rules).[75-77] There are many different techniques to quantify e.e. like chiral high-performance liquid chromatography (HPLC) or HPLC coupled with circular dichroism (CD). However all these techniques require expensive equipments.[78-80] NMR spectroscopy,[81,82] liquid crystals[83,84] or molecular imprinted polymers[85] have also been used, but require expensive equipments or derivatization of target molecules. Therefore, the quantification of e.e. by means of chromogenic receptors offers several advantages, as they are the less expensive and more commonly used equipment (fluorimeter or UV-Vis spectrophotometer).

The amino acid detection and their importance in biology has already been reported previously. All amino acids (except Glycine) are chiral compounds, and only one enantiomer is present in the human body. Thus their detection and quantification of this chirality has been a real challenge for many researchers.[86, 87] Furthermore, amino acids are commonly used as chiral auxiliaries, catalysts, and chiral starting materials.[88] It is also important to point out that unnatural amino acids and D-amino acids, (being rare in nature) have to be prepared by asymmetric synthesis.[89] In this way, many methodologies have been developed to detect chirality of amino acids with high sensitivity and real time luminescent techniques (fluorescence or UV-Visible). The introduction of a chiral centre into the sensor structure leads to chiral molecules that can be employed in chirality sensing. In this way, they are a some preferential scaffolds employed to introduce chirality into the receptors.

5.3.1.1 DACH (diaminocyclohexane) based ligands

Chiral recognition based on DACH ligands had been currently developed by Anslyn[69, 72, 90] in its studies concerning the detection of amino acids (**Figure V-58**) by means of Indicator Displacement Assays (IDA).

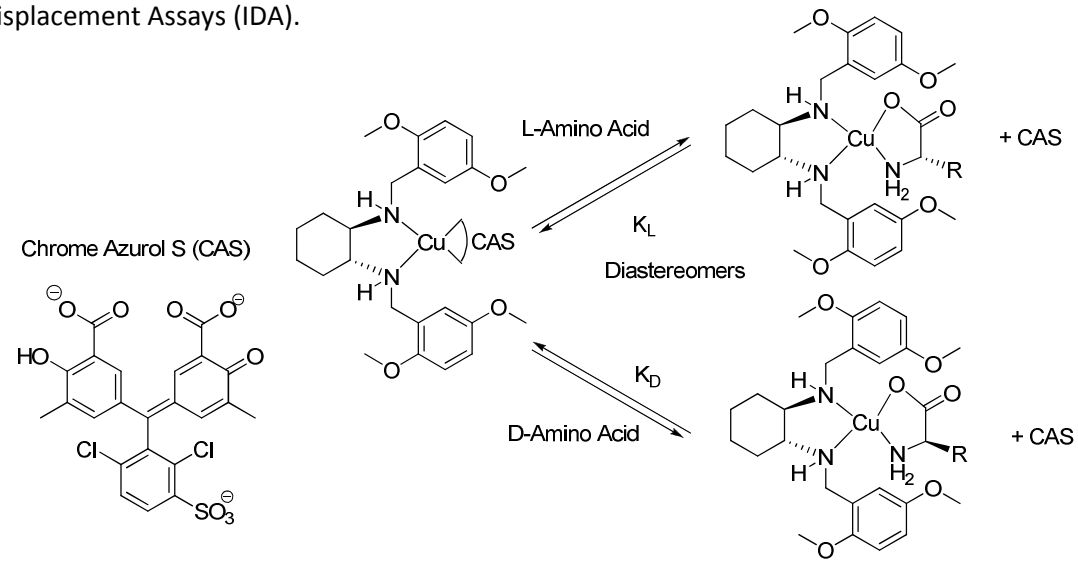

Figure V-58: Amino acid recognition by means of IDA with DACH based ligands

This methodology involves optically pure chiral ligands, prepared employing *R*,*R*-DACH (for example) structure as source of chirality in order to synthesize the ligand. When CAS is displaced from copper a colour change can be measured. The substitution of CAS by an amino acid can affords two diastereomers (*R*,*R*-DACH-*R*-(Amino acid) and *R*,*R*-DACH-*S*-(Amino acid)). The goal of this technique is the obtention of differences between K_L and K_D. All techniques employed in chiral recognition require a difference (in terms of binding constant) between two diastereomers. Employing this technique and modifying the colorant (CAS) ratios K_D/K_L between 1.7 and 2.6 have been observed. These are very good values in terms of enantio-discrimination. DACH based ligands are simple compounds, and many other chiral amines have been proposed as chirality sources (**Figure V-59**).

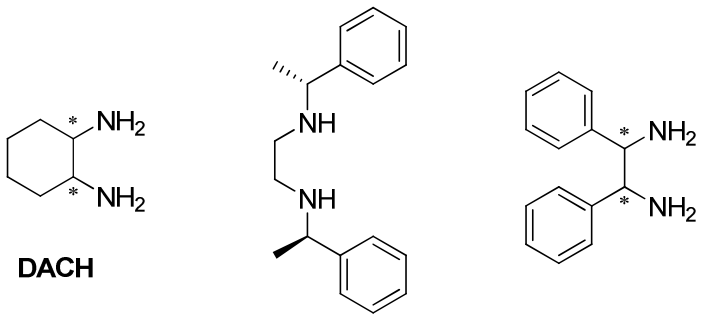

Figure V-59: Chiral diamines proposed as ligands.

5.3.1.2 Binol based ligands

The use of binol in catalysis has been oftenly reported, however its fluorescent properties due to the presence of four aromatic rings make this compound a perfect structure for fluorescent chiral ligands. Pu has reported on the preparation and fluorescence studies of many of these derivatives.[91] Employing axial chirality as source for chiral recognition binol[92, 93] derivatives (**Figure V-60**) have shown their ability in the chiral amino alcohol recognition.

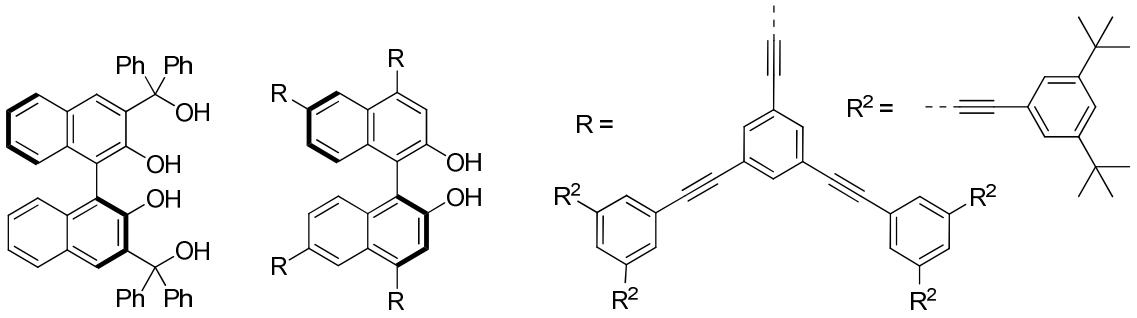

Figure V-60: Binol-based chiral fluorescence ligands.

The ratio of the corresponding binding constants for amino alcohols (K_S/K_R) were found to be 1.18 for the dendrimer[93] (**Figure V-60**) compound, and between 1.09 and 1.24 for the tetrahydroxyl 1,1'-binaphtyl compound (**Figure V-60**, left molecule). In this way Pu proposed combinations of DACH and Binol as selective sensor for mandelic acid[94, 95] (**Figure V-61**).

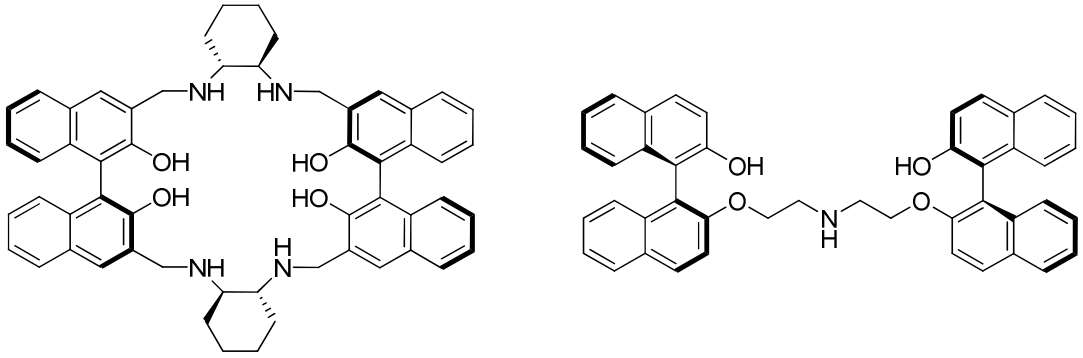

Figure V-61: Binol-DACH based sensors and acyclic binol based ligands.

Polymeric Binol based structures can also be found as well as acyclic ligands (**Figure V-61**) bonding two binol structures by an amine bridge.

5.3.1.3 Other structures

Other chiral sources have also been employed in the preparation of these ligands. Cyclodextrines for example bonded to chromophores have been proposed by Uneo[96, 97] as spectroscopic sensors for organic molecules. Pagliari *et al.* prepared β-cyclodextrine-based sensors for amino acids.[98] A very original strategy has been the development of amino acid-based (natural or not) fluorescence sensors to detect other amino acids. Copper complexes

from dansyl-amino[99] acid (DNS-AA) derivatives have also been employed in the amino acid recognition (**Figure V-62**) as well as pyrene derivatives.[100]

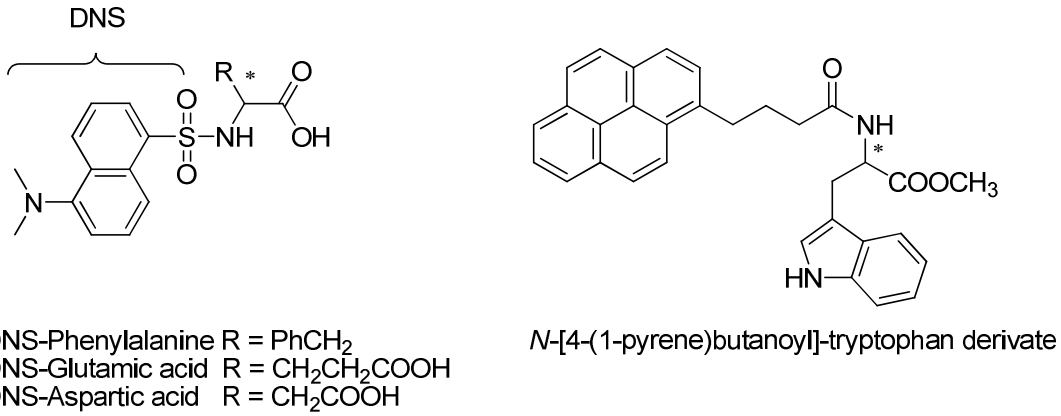

Figure V-62: DNS-AA and pyrene derivatives.

All these compounds revealed efficient to detect chirality of amino acid (or amino alcohol). Amino acids require water for solubilising them which is the major drawback of fluorophore preparation. Amino alcohols are soluble in organic solvents. By working in ethanol/water mixtures we have already avoided the problem of solubility.

5.3.1.4 Objectives

We have already developed a fluorescence family of compounds soluble in water and able to detect anions, metals and in some cases amino acids. A few of these compounds were obtained optically pure (**TPF**, **TPS**) or separated by HPLC (**TPOA**) being fluorescent chiral ligands, therefore we decided to study:

- The recognition of the chirality of glutamic and aspartic acid by direct interaction with our chiral ligands, due to their important biological role, and also as they can undergo multiple hydrogen bonding sites (**Figure V-62**).

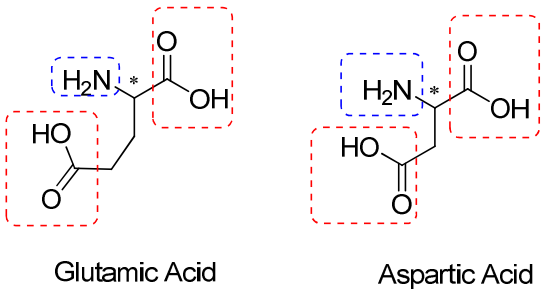

Figure V-62: Glutamic and Aspartic acids.

5.3.2 Chiral recognition with chiral ligands

As we have reported before, we succeeded to prepare three optically pure chiral compounds **TPF**, **TPS** and **TPOA** (**Figure V-63**).

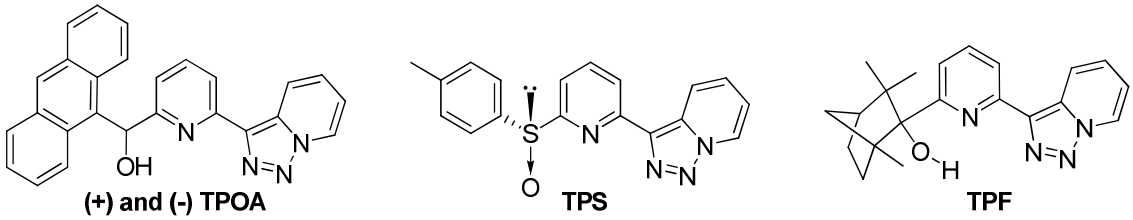

Figure V-63: Chiral ligands.

The strategy employed consisted in the study of their fluorescence spectra upon addition of different enantiomers of amino acids. Tehrefore diastereomers would be obtained and different binding constants k (of quenching or enhancement) are expected (**Figure V-64**).

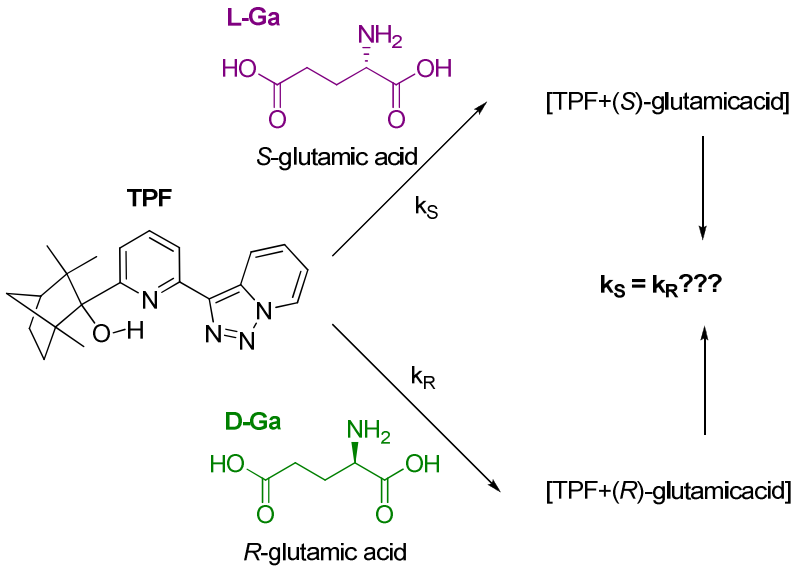

Figure V-64: Glutamic acid chiral recognition with **TPF**.

The first test performed with **TPF** revealed this ligand as extremely water insoluble. The addition of an aqueous amino acid solution (10^{-3} M) to the ethanolic solution (10^{-5} M) of **TPF** afforded quenching of fluorescence, but not due to the amino acid, but due to precipitation of **TPF**. When similar tests were performed with **TPS** or **TPOA** no solubility problems were observed. Unfortunately, no evolution of the fluorescence spectra was observed, only small quenching after adding a huge quantity of amino acid occurred. This quenching corresponded to the dilution of the sample and not to an interaction between the chiral ligand and the target amino acid. In conclusion no chiral recognition could be performed with optically pure ligands. Although **TPON**$Zn^{2\oplus}$ was an efficient fluorescence ligand, we did not succeed to separate it by chiral preparative HPLC into its enantiomers. All other compounds have not chirality. Thus, their application to the domain of chiral recognition was not possible.

5.3.3 Chiral recognition, the new strategy

The preparation of chiral fluorescence ligands for the amino acid recognition, involve in many cases chiral scaffolds like DACH or Binol. These compounds are expensive and the preparation of these ligands requires the introduction of the chirality in the synthesis, by means of chiral compounds or enantioselective synthesis. With this idea in mind we had already prepared and tested **TPF**, **TPS** and **TPOA** without result (in terms of recognition). We considered then a second strategy in order to introduce chirality into our system. The preparation of a compound able to perform chiral recognition by means of fluorescence requires: a fluorophore, a binding site (for the target molecule) and chirality (**Figure V-65**). We realized that we had already prepared one of these structures able to recognize amino acids.

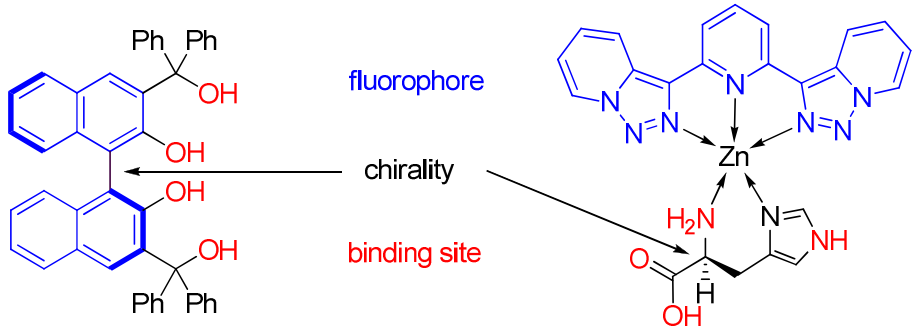

Figure V-65: Chiral fluorescence sensors.

Although **TPT**Zn$^{2\oplus}$ was not a chiral compound, upon addition of enantiopure L-Histidine it became a chiral compound. Furthermore, the fluorescence intensity of **TPT**Zn$^{2\oplus}$ was not completely quenched with one equivalent of L-histidine (**Figure V-65**).

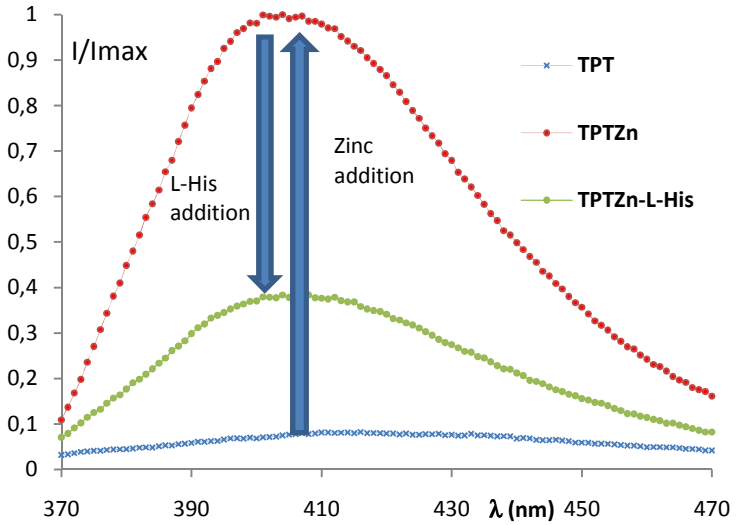

Figure V-65: Evolution of the fluorescence of **TPT** after addition of 1 eq. of Zinc and 1 eq. of L-His.

The domain between **TPT**Zn-L-His and the totally quenched system was about 1/3 of the total intensity of **TPT**Zn$^{2\oplus}$. The intensity decreased with the addition of more L-His but we

were interested to add enantiomers of other amino acids in order to see if a difference in terms of quenching could be achieved.

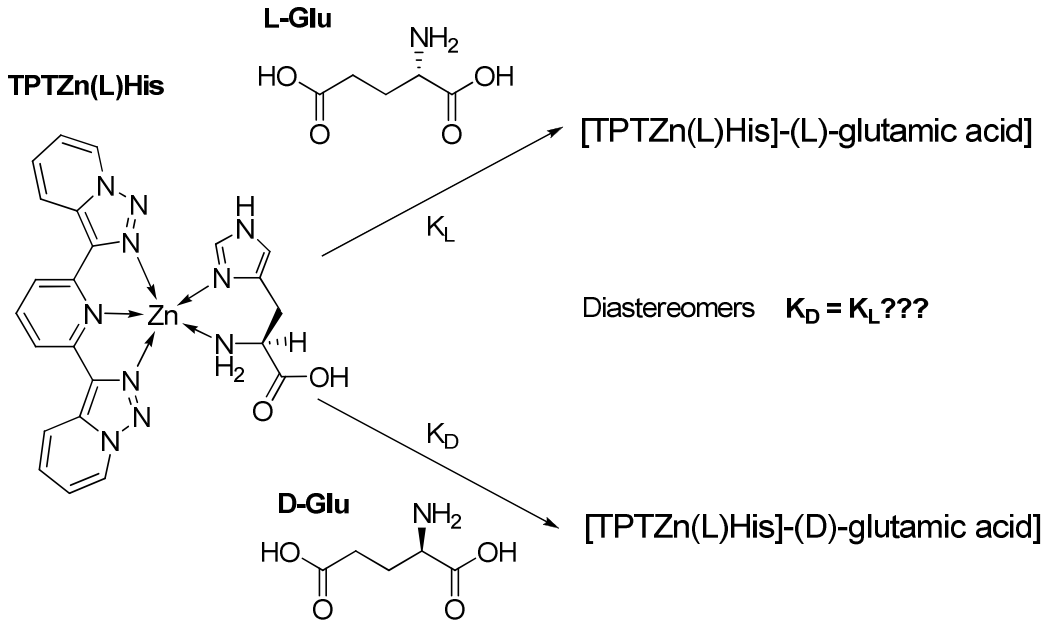

Figure V-66: Diastereomers by means of combinations of two different amino acids.

The main difference between this approach and the common ones is that the chirality is not fixed by a covalent bond to the fluorophore. However, if this strategy works, the number of modifications that can be performed (like replacing the amino acid by other chiral coordinating group) will lead to a very versatile system. The idea of adding different properties to a system by means of non covalent bonds has been reported in the literature, for example the chiral diamine induced enantioselective hydrogenation with racemic disphosphines[101] reported by Aikawa and Mikami, where the chirality is introduced by a diamine (**Figure V-67**) inducing a chirality in the starting achiral (but *atropos*) phosphine. In this case the chirality is not directly bonded to the phosphine, but introduced by a single molecule.

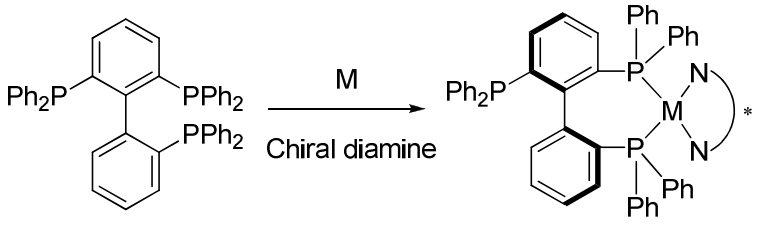

Figure V-67: Aikawa and Mikami diamine-phosphine chiral system.

Other example has been also previously showed (**Figure V-58**) by Anslyn. In his system the chirality is based in the diamine, and the chromophore (CAS) is not a chiral compound.

One of the most representative works concerning this idea can be found in the report counter ion strategy developed by Lacour.[102] By employing chiral counter ions with the active catalytic metal, chiral catalysis can be performed. In this way the preparation of ligands avoid the introduction of chirality by means of covalent bonding. In **figure V-68** an example of chiral counter ion id presented.

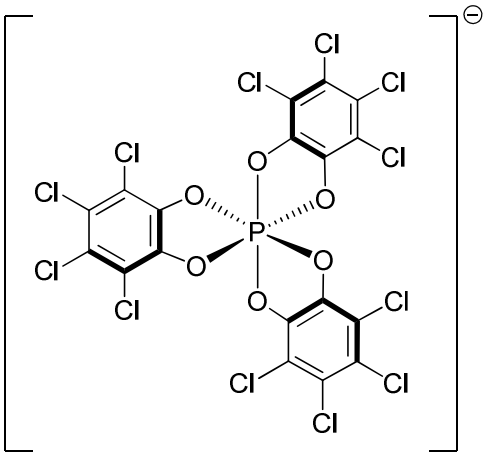

Figure v-68: Δ Trisphat ion developed by Lacour.

The system **TPT**$Zn^{2\oplus}$L-His, was prepared by adding stoichiometric quantities of zinc perchlorate and L-histidine water solutions (10^{-3} M) to a fluorescence cuvette with 2 mL of **TPT** (10^{-5} M) in ethanol. The evolution of intensity and the complexation was controlled by the fluorescence spectra (**Figure V-65**). To this solution small volumes (3 μL) of L-glutamic acid or D-glutamic acid (aqueous 10^{-3} M solutions) were added. The choice of glutamic acid was motivated by the presence of two coordinating groups (the amino-acid and the second acid) that could fix the molecule to our chiral fluorescence ligand. L-Histidine was chosen because it has the biggest binding constant. By employing L-His as chiral precursor we minimized the possibility of a substitution by L-Glutamic, which had a smaller bonding constant with respect to L-Histidine (logk = 4.84 *vs.* 3.90)

$$TPTZn^{+2} + \text{L-His} \xrightleftharpoons{\log(K) = 4.84} [\mathbf{TPT}Zn^{+2}]\text{-L-His} \qquad (1)$$

$$TPTZn^{+2} + \text{L-Glu} \xrightleftharpoons{\log(K) = 3.90} [\mathbf{TPT}Zn^{+2}]\text{-L-Glu} \qquad (2)$$

When these tests were performed, a difference between both enantiomers of glutamic acid was observed in terms of quenching (**Figure V-69**).

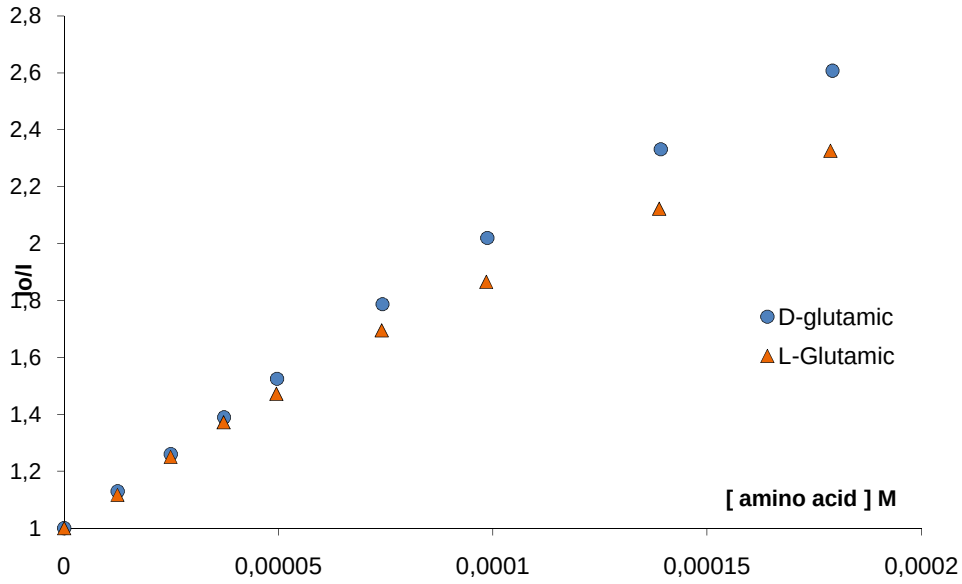

Figure V-69: Enantio sensing of glutamic acid.

The analysis of the binding constant also confirmed the preferential quenching of D-glutamic acid (**Table V-10**).

Table V-10: Binding constants[70] for Glutamic acid enantiomers, experiences were performed three times for each enantiomer.

	k	log(k)	e
D Glu	12416	4,12	±0,01
L Glu	9875	4.00	±0,03

The ratio K_D/K_L was found to be near 1.25, being acceptable compared to those obtained by Anslyn[69,72,90] and Pu[92] specially considering that the chirality has been introduced by coordination and not by covalent binding to the fluorophore. We were interested in the possibility to analyse this system with other amino acids. Aspartic acid was the most similar compound to glutamic acid. In order to compare this system, the same tests were performed as for glutamic acid. However this time no difference of quenching was observed (**Figure V-70**).

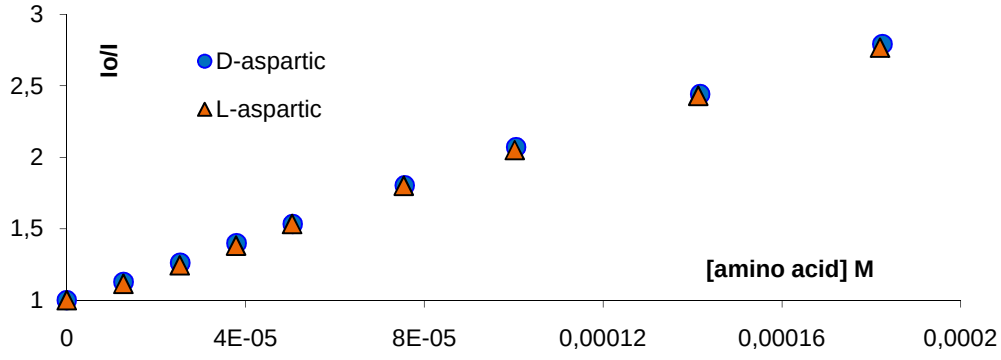

Figure V-70: Enantio sensing of aspartic acid.

Similary no difference was observed, when the binding constants were calculated (**Table V-11**).

Table V-10: Binding constants for aspartic enantiomers

	k	log(k)	e
D Asp	13677	4,14	±0,08
L Asp	13599	4,13	±0,09

The ratio between K_D/K_L = 1.005, indicates a possible preferential quenching for D Asp. The ratio was not significant enough which means not discrimination of this amino acid could be achieved. However, this result was important for two important reasons:

- Althought there was no enantio discrimination and in both cases similar binding constants were obtained, this indicates that the difference between glutamic and aspartic acid (one group CH_2) was responsible for the enantio sensing.
- In the same way the obtention of similar results (for D Asp and L Asp) validates the methodology in terms of recognition of the amino acid, but not its chirality.

The comparison of the two closest amino acids provided results which are difficult to explain. The differences between both amino acids ("size difference") was enough to avoid enantio sensing, but not sensing. The system could coordinate in many different ways, in order to elucidate this problem we studied the quenching of [**TPT**$Zn^{2\oplus}$]L-His with the worst quencher, imidazole (**Figure V-71**).

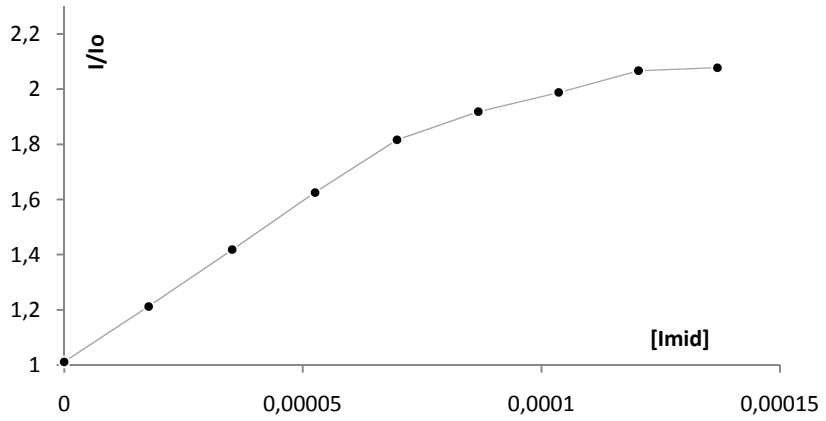

Figure V-71: Quenching of [**TPT**$Zn^{2\oplus}$]L-His with imidazole.

The value of k_{imid} was near 21000 M^{-1}, which is a larger value than previously observed between **TPT**$Zn^{2\oplus}$ imidazole. This shows that imidazole is able to quench [**TPT**$Zn^{2\oplus}$]-L-His. We propose as a possible explanation of this a hydrogen bond between imidazole and the $N_{imid}H$ (from histidine) (**Figure V-72**).

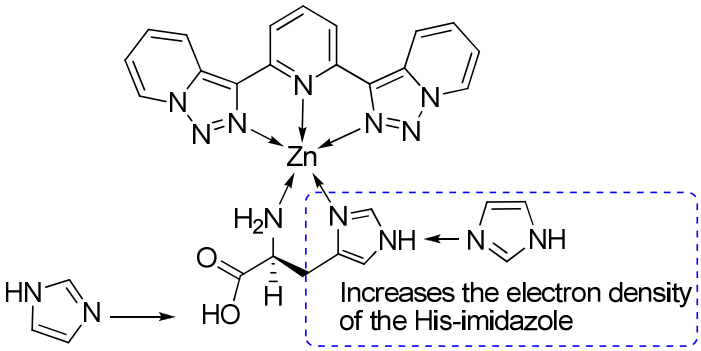

Figure V-72: Imidazole effect.

The presence of a hydrogen bond with the carboxylic acid would not be very important in terms of quenching due to the fact that, according to the proposed model, the carboxylic acid function is not directly involved in the coordination. Hydrogen bonding between the imidazole and the imidazole from the histidine would, in contrast, favour the quenching by increasing the electron density in the N1. This idea would also explains the difference between glutamic and aspartic acids (**Figure V-73**) combined with their structural difference; glutamic acid has a CH_2 group more than aspartic acid.

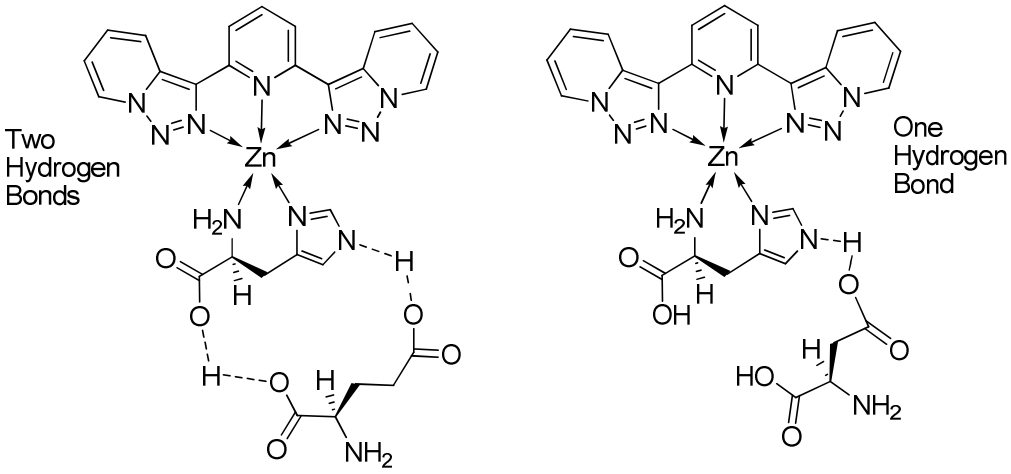

Figure V-73: Possible different coordination between Asp and Glu.

This model is coherent with the quenching values (both system coordinate the imidazole hydrogen atom). The double hydrogen bond that can be obtained with glutamic acid is more difficult to form with aspartic acid. However as no X-ray structure could be obtained, this hypothesis could not be confirmed. The role of the additional CH_2 group and the possible coordination involved in the chiral recognition remains unknown. In order to compare the efficiency of L-histidine, we substituted it by *R*,*R*-DACH. As it has been explained previously chiral DACH is a very important scaffold in chiral recognition. So we interested in its effect on our system. Before performing the chiral recognition, we calculated the corresponding binding constant of (R,R)-DACH, $\log(k_{(R,R)\text{-DACH}}) = 4.48$. The value obtained assured the stability of the [**TPT**$Zn^{2\oplus}$]-(*R*,*R*)-DACH upon the addition of glutamic acid. When the chiral recognition was

performed with this new system, also a small recognition could be observed (**Figure V-74**) and the binding constants decreased (**Table V-11**)

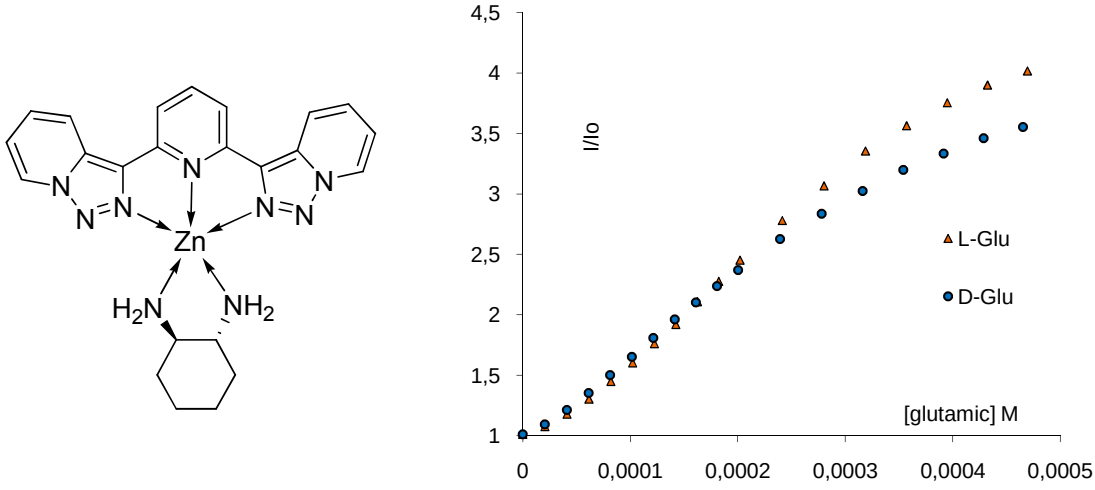

Figure V-74: Chiral recognition employing *R*,*R*-DACH

The discrimination between the two enantiomers was observed under higher concentrations. However, this range corresponded perfectly to results reported by Anslyn and Pu. In this case, L enantiomer quenched more efficaciously the system.

Table V-11: Bondong constants.[70]

	K	log(K)	e
L Glu	7847	3.89	±0,05
D Glu	6198	3.79	±0,04

In this case the ratio K_L/K_D = 1.26 was obtained, which already was also close to those reported before in the literature. The method proposed was found also useful with structures that are employed in this kind of recognition and in an acceptable way.

5.3.4 Conclusions

Although no chiral recognition has been performed with the prepared chiral ligands, we have been able to perform chiral recognition by means of fluorescence spectroscopy without chiral fluorophores. By introducing chirality (L-His) by means of coordination chemistry we have generated a chiral structure able to detect the chirality of glutaimc acid. Similar results have been obtained with *R*,*R*-DACH. The chiral recognition performed in this way has never been done before. This strategy is in analogy to the chiral diamine induced enantioselective hydrogenation with racemic disphosphines[101] and the counter ion strategy developed by Lacour.[102] In this way we have shown how chirality can play an essential role without being directly bonded to a system.

5.4 References

[1] B. N. G. Giepmans, S. R. Adams, M. H. Ellisman, R. Y. Tsien, *Science* **2006**, *312*, 217.
[2] M. Zimmer, *Chem. Rev.* **2002**, *102*, 759.
[3] M. S. T. Gonçalves, *Chem. Rev.* **2009**, *109*, 190.
[4] K. Walzer, B. Maennig, M. Pfeiffer, K. Leo, *Chem. Rev.* **2007**, *107*, 1233.
[5] O. Shimomura, M. Chalfie, R. Y. Tsien, *Nobelprice.org* **2008**.
[6] J. R. Lakowicz, *Ed. Principles of Fluorescene Spectroscopy*, Plenum Publishes Corporation, New York, **1999**.
[7] E. N. Harvey, *History of Luminiscence*, The American Philosophical Society, Philadelphia, **1957**.
[8] B. Valeur, *Molecular Fluorescence: Principles and Applications*, Wiley-VHC Verlag GmbH, Weinheim, **2001**.
[9] B. Abarca, R. Aucejo, R. Ballesteros, M. Chadlaoui, E. Garcia-Espana, C. Ramirez de Arellano, *ARKIVOC* **2005**, *xiv*, 71.
[10] M. Chadlaoui, B. Abarca, R. Ballesteros, C. RamirezdeArellano, J. Aguilar, R. Aucejo, E. Garcia-Espana, *J. Org. Chem.* **2006**, *71*, 9030.
[11] B. Abarca, R. Aucejo, R. Ballesteros, F. Blanco, E. García-España, *Tetrahedron Lett.* **2006**, *47*, 8101.
[12] B. Abarca, R. Ballesteros, F. Mojarred, G. Jones, D. J. Mouat, *J. Chem. Soc., Perkin Trans. 1* **1987**, 1865.
[13] B. Abarca, F. Mojarred, G. Jones, C. Phillips, N. Ng, J. Wastling, *Tetrahedron* **1988**, *44*, 3005.
[14] B. Abarca, I. Alkorta, R. Ballesteros, F. Blanco, M. Chadlaoui, J. Elguero, F. Mojarrad, *Org. Biomol. Chem.* **2005**, *3*, 3905.
[15] B. Abarca, R. Ballesteros, M. Chadlaoui, *Tetrahedron* **2004**, *60*, 5785.
[16] R. Martinez-Manez, F. Sancenon, *Chem. Rev.* **2003**, *103*, 4419.
[17] J. H. Boyer, N. Goebel, *J. Org. Chem.* **1960**, *25*, 304.
[18] B. Abarca, R. Ballesteros, M. Elmasnaouy, *Tetrahedron* **1998**, *54*, 15287.
[19] M. Chadlaoui, PhD Thesis, University of Valencia (Spain), **2004**.
[20] G. R. Newkome, A. Nayak, J. D. Sauer, P. K. Mattschei, S. F. Watkins, F. Fronczek, W. H. Benton, *J. Org. Chem.* **1979**, *44*, 3816.
[21] C. R. Goldsmith, T. D. P. Stack, *Inorg Chem* **2006**, *45*, 6048.
[22] R. M. Meudtner, M. Ostermeier, R. Goddard, C. Limberg, S. Hecht, *Chem. Eur. J.* **2007**, *13*, 9834.
[23] Y. Li, J. C. Huffman, A. H. Flood, *Chem. Commun.* **2007**, 2692.
[24] B. Abarca, R. Ballesteros, M. Elmasnouy, *Tetrahedron* **1999**, *55*, 12881.
[25] E. L. Que, D. W. Domaille, C. J. Chang, *Chem. Rev.* **2008**, *108*, 1517.
[26] E. Gaggelli, H. Kozlowski, D. Valensin, G. Valensin, *Chem. Rev.* **2006**, *106*, 1995.
[27] J. M. Berg, Y. Shi, *Science* **1996**, *271*, 1081.
[28] J. A. Cowan, *Inorganic Biochemistry: An Introduction 2nd ed*, Wiley-VHC, Weinheim, **1993**.
[29] R. W. Strange, S. Antonyuk, M. A. Hough, P. A. Doucette, J. A. Rodriguez, P. J. Hart, L. J. Hayward, J. S. Valentine, S. S. Hasnain, *J. Mol. Biol.* **2003**, *328*, 877.
[30] H. He, M. Mortellaro, M. J. P. Leiner, R. J. Fraazt, J. Tusa, *Anal. Chem.* **2003**, *75*, 549.
[31] H. He, M. A. Mortellaro, M. J. P. Leiner, R. J. Fraatz, J. K. Tusa, *J. Am. Chem. Soc.* **2003**, *125*, 1468.
[32] B. Valeur, I. Leray, *Coord. Chem. Rev.* **2002**, *205*, 3.
[33] A. Bianchi, K. Bowman-Jamos, E. García-España, *Supramolecular Chemistry of Anions*, Wiley-WCH, New York, **1997**.
[34] J. L. Sessler, P. A. Gale, W.-S. Cho, *Anion Receptor Chemistry*, RSC Publishing, Cambridge, **2006**.
[35] *Special issue on Zinc chemistry: BioMetals* **2001**, *14*.
[36] Y. Zhang, X. Guo, W. Si, L. Jia, X. Qian, *Org. Lett.* **2008**, *10*, 473.
[37] H.-H. Wang, Q. Gan, X.-J. Wang, L. Xue, S.-H. Liu, H. Jiang, *Org. Lett.* **2007**, *9*, 4995.
[38] S. Huang, R. J. Clark, L. Zhu, *Org. Lett.* **2007**, *9*, 4999.
[39] X.-a. Zhang, D. Hayes, S. J. Smith, S. Friedle, S. J. Lippard, *J. Am. Chem. Soc.* **2008**, *130*, 15788.
[40] R. A. Bozym, R. B. Thompson, A. K. Stoddard, C. A. Fierke, *ACS Chemical Biology* **2006**, *1*, 103.
[41] E. M. Nolan, S. J. Lippard, *Acc. Chem. Res.* **2009**, *108*, 1517.
[42] S. C. Burdette, S. J. Lippard, *Coord. Chem. Rev.* **2001**, *333*, 216.
[43] A. J. Parola, J. C. Lima, F. Pina, J. Pina, J. Seixas de Mello, C. Soriano, E. García-España, R. Aucejo, A. J., *Inorg. Chim. Acta* **2007**, *360*, 1200.
[44] J. Alarcon, M. T. Albeldba, R. Belda, P. Clares, E. Delgado-Pinar, J. C. Frias, E. García-España, J. González, C. Soriano, *Dalton Trans.* **2008**, 6530.
[45] B. A. Wong, S. Friedle, S. J. Lippard, *J. Am. Chem. Soc.* **2009**, *131*, 7142.
[46] M. A. Clark, K. Duffy, J. Tibrewala, S. J. Lippard, *Org. Lett.* **2003**, *5*, 2051.
[47] F. Qian, C. Zhang, Y. Zhang, W. He, X. Gao, P. Hu, Z. Guo, *J. Am. Chem. Soc.* **2009**, *131*, 1460.
[48] Z. Xu, G.-H. K, S. J. Han, M. J. Jou, C. Lee, J. Yoon, *Tetrahedron* **2009**, *65*, 2307.
[49] Z. R. Grabowski, K. Rotkiewicz, W. Rettig, *Chem. Rev.* **2003**, *103*, 3899.
[50] L. Zeng, E. W. Miller, A. Pralle, E. Y. Isacoff, C. J. Chang, *J. Am. Chem. Soc.* **2006**, *128*, 10.
[51] Y. Xiang, A. Tong, P. Jin, Y. Ju, *Org. Lett.* **2006**, *8*, 2863.
[52] M.-M. Yu, Z.-X. Li, L.-H. Wei, D.-H. Wei, M.-S. Tang, *Org. Lett.* **2008**, *10*, 5115.
[53] E. C. Constable, *Chem. Soc. Rev.* **2007**, *36*, 246.

[54] U. S. Schubert, H. Hofmeier, G. R. Newkome, *Modern Terpyridine Chemistry*, WILEY-E, Weinheim, **2006**.
[55] G. Chelucci, R. P. Thummel, *Chem. Rev.* **2002**, *102*, 3129.
[56] C. Suksai, T. Tuntulani, *Chem. Soc. Rev.* **2003**, *32*, 192.
[57] L. Fabbrizzi, M. Licchelli, G. Rabaioli, A. Taglietti, *Coord. Chem. Rev.* **2000**, *205*, 85.
[58] M. E. Huston, E. U. Akkaya, A. W. Czarnik, *J. Am. Chem. Soc.* **1989**, *111*, 8735.
[59] M. Cametti, K. Rissanen, *Chem. Commun.* **2009**, 2809.
[60] G. De Santis, L. Fabbrizzi, M. Licchelli, A. Poggi, A. Taglietti, *Angew. Chem. Int. Ed. Engl.* **1996**, *35*, 202.
[61] N.-U. SPECFIT Program for Global Lesat Square Fitting of Equilibrium and Kinetic Systems using Factor Analysis and Marquardt Minimization Version 1-26 4 Spectrum Software Associates Chapel Hill, **1996**. .
[62] H. Gampp, M. Maeder, C. J. Meyer, A. D. Zuberbuhler, *Talanta* **1986**, *33*, 943.
[63] H. Gampp, M. Maeder, C. J. Meyer, A. D. Zuberbuhler, *Talanta* **1985**, *32*, 95.
[64] H. Gampp, M. Maeder, C. J. Meyer, A. D. Zuberbuhler, *Talanta* **1985**, *32*, 257.
[65] P. Clares, C. Lodeiro, D. Fernandez, A. J. Parola, F. Pina, E. Garcia-Espana, C. Soriano, R. Tejero, *Chem. Commun.* **2006**, 3824.
[66] R. Dingledine, K. Borges, D. Bowie, S. F. Traynelis, *Pharmacol. Rev.* **1999**, *51*, 7.
[67] S. Ozawa, H. Kamiya, K. Tsuzuki, *Prog. Neurobiol.* **1998**, *54*, 581.
[68] M. L. Luigi Fabbrizzi, Angelo Perotti, Antonio Poggi, Giuliano Rabaioli, Donatella Sacchi and Angelo Taglietti, *J. Chem. Soc., Perkin Trans. 2* **2001**, 2108
[69] J. F. Folmer-Andersen, M. Kitamura, E. V. Anslyn, *J. Am. Chem. Soc.* **2006**, *128*, 5652.
[70] HYPEQUAD., P. Gans, A. Sabatini, A. Vacca, Talanta, 43, *Talanta* **1996**, *43*, 1739.
[71] J. Jover, R. Bosque, J. Sales, *Dalton Trans.* **2008**, 6441.
[72] D. Leung, J. F. Folmer-Andersen, V. M. Lynch, E. V. Anslyn, *J. Am. Chem. Soc.* **2008**, *130*, 12318.
[73] E. V. Anslyn, *J. Org. Chem.* **2007**, *72*, 687.
[74] M. Kitamura, S. H. Shabbir, E. V. Anslyn, *J. Org. Chem.* **2009**, *74*, 4479.
[75] FDA'S policy statement for the development of new stereoisomeric drugs, *Chirality* **1992**, *4*, 338.
[76] C. H. Kim, Y. M. Siong, S. C. Baick, *Anim. Sci. Technol.* **2004**, *46*, 91.
[77] R. Marchelli, A. Dossena, G. Palla, *Trends Food Sci. Technol.* **1996**, *7*, 113.
[78] M. T. Reetz, *Angew. Chem. Int. Ed. Engl.* **2001**, *40*, 284.
[79] V. Charbonneau, W. W. Ogilie, *Mini-Rev. Org. Chem.* **2005**, *2*, 313.
[80] M. G. Finn, *Chirality* **2002**, *14*, 534.
[81] M. T. Reetz, A. Eipper, P. Tielmann, R. Mynott, *Adv. Synth. Catal.* **2002**, *344*, 1008.
[82] M. T. Reetz, P. Tielmann, A. Eipper, A. Ross, G. Schlotterbeck, *Chem. Commun.* **2004**, 1366.
[83] R. A. Van Delden, B. L. Feringa, *Angew. Chem. Int. Ed.* **2001**, *40*, 3198.
[84] D. M. Walba, L. Eshdat, E. Korblova, R. Shao, N. A. Clark, *Angew. Chem. Int. Ed.* **2007**, *46*, 1473.
[85] Y. Chen, K. D. Shimizu, *Org. Lett.* **2002**, *4*, 2937.
[86] J. Lin, H. C. Zhang, L. Pu, *Org. Lett.* **2002**, *4*, 3297
[87] G. A. Hembury, V. V. Borovkov, Y. Inoue, *Chem. Rev.* **2008**, *108*, 1.
[88] J.-A. Ma, *Angew. Chem. Int. Ed.* **2003**, *42*, 4290.
[89] C. Najera, J. M. Sansano, *Chem. Rev.* **2007**, *107*, 4584.
[90] J. F. Folmer-Andersen, V. M. Lynch, E. V. Anslyn, *J. Am. Chem. Soc.* **2005**, *127*, 7986.
[91] L. Pu, *Chem. Rev.* **2004**, *104*, 1687.
[92] Q. Wang, X. Chen, L. Tao, L. Wang, D. Xiao, X. Q. Yu, L. Pu, *J. Org. Chem.* **2007**, *72*, 97.
[93] V. J. Pugh, Q.-S. Hu, L. Pu, *Angew. Chem. Int. Ed. Engl.* **2000**, *39*, 3638.
[94] J. Lin, Q. S. Hu, M. H. Xu, L. Pu, *J. Am. Chem. Soc.* **2002**, *124*, 2088.
[95] Z.-B. Li, L. Lin, L. Pu, *Angew. Chem. Int. Ed. Engl.* **2005**, *44*, 1690.
[96] A. Ueno, I. Suzuki, T. Osa, *J. Am. Chem. Soc.* **1989**, *111*, 6391.
[97] A. Ueno, T. Kuwaraba, A. Nakamura, F. Toda, *Nature* **1992**, *356*, 136.
[98] S. Pagliari, R. Corradini, G. Galaverna, S. Sforza, A. Dossena, R. Marchelli, *Tetrahedron Lett.* **2000**, *41*, 3691.
[99] R. Corradini, G. Sartor, R. Marchelli, A. Dossena, A. Spisni, *J. Chem. Soc., Perkin Trans. 2* **1992**, 1979.
[100] C. D. Tran, J. H. Fendler, *J. Am. Chem. Soc.* **1980**, *102*, 2923.
[101] K. Aikawa, K. Mikami, *Angew. Chem. Int. Ed. Engl.* **2003**, *42*, 5455.
[102] J. Lacour, D. Linder, *Science* **2007**, *317*, 462.

VI: General conclusion and Outlook

6.1 General conclusion

The studies performed concerning the chemistry of triazolopyridines have allowed us to prepare new families of triazolopyridines with different and interesting properties. In one way we have synthesized the first chiral triazolopyridines opening an easy access to 2,6-disubstituted chiral pyridines. We have also extended a methodology of palladium catalysed sulfenation to different heterocyclic aromatic compounds. Secondly, by restudying the chemistry of the [1,2,3]triazolo[1,5-*a*]quinoline we have proposed a new access to 2,8-disubstitued quinolines.

We have also studied the ring chain isomerisation of the triazoloquinoline-pyridine system observing how this system is controlled by steric and electronic properties of the substitutens attached to the triazoloquinoline scaffold. And we have used this isomerisation to obtain high fluorescent structures able to recognize copper.

In the course of our studies we have employed the properties of triazolopyridines to quantify the electronic profile of phosphines as well as to prepare a new generation of triazolopyridine-phosphine based ligands for catalysis. The analysis of these structures has allowed us to observe the special properties associated to the phosphorus lone pair in the electronic profile and also in the ^{13}C-NMR-spectra.

We have been able to prepare many different fluorescence receptors, and we have studied them, some of these structures have revealed as excellent zinc sensors, as well as for some anions and as for amino acids. Finally, we have been able to perform chiral recognition employing a zinc complex based on our fluorophor and L-histidine as chiral compound.

6.2 Outlook

In this paragraph, we will briefly describe some outlooks which are related to the work accomplished in the course of the PhD.

6.2.1 Biological studies with the sulfoxide family

The coordination chemistry of some of these compounds with zinc can be employed in order to avoid enzymatic catalysis. In collaboration with Prof. Tarnus (Laboratoire de Chimie Organique et Bioorganique, ENSCMU, Mulhouse) we are currently studying some of these compounds as inhibitors of different zinc-based enzymes, specially alkaline phosphatise and aminopedtidases. The sulfoxide family can be considered as the most versatile, in terms of coordinating properties. So different test are being performed to evaluate its properties (**Figure VI-1**).

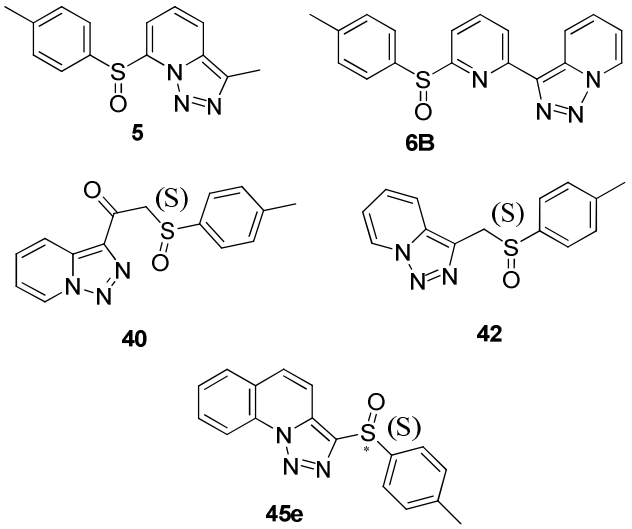

Figure VI-1: Selected compounds for the biological tests.

The colorimetric study of the enzymatic degradation of 4-nitrophenyl phosphate into 4-nitrophenol (λ_{abs} = 405 nm) in presence of these compound allows to establish the $\mathbf{IC_{50}}$ value for phosphatase enzymes. The test with amino peptidase are performed similarly, the colorimetric studies of the degradation of 2-amino-4-methyl-*N*-(4-nitrophenyl)pentanamide (**Scheme VI-1**).

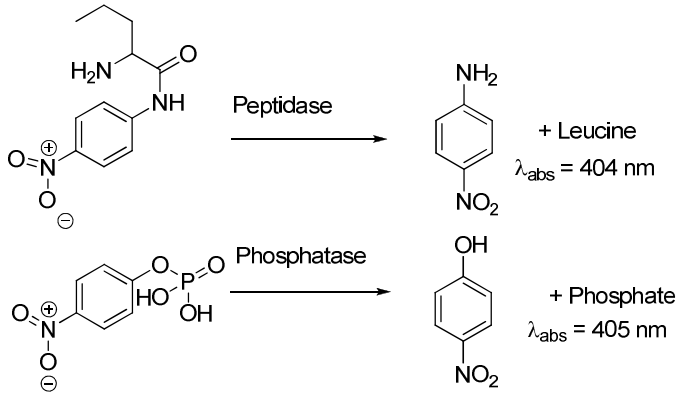

Scheme VI-1: Colorimetric enzymatic study.

Preliminary results from these test indicate that a small inhibition is afforded with some of these compounds. Coordination between the triazolopyridine sulfoxides and zinc (from the enzymes) can be responsible of this inhibition (**Table VI-1**).

Table VI-1: Preliminary results concerning the enzymatic inhibition.

Inhibiteurs	*AP-N microsomal*	*Phosphatase Alcaline from porcine kidney*	*Phosphatase Alcaline from bovine intestinal mucosa*
	[EC 3.4.11.2]	*[EC 3.1.3.1]*	*[EC 3.1.3.1]*
5	IC_{50}>>1mM	IC_{50}>>1mM	IC_{50}>>1mM
6B	IC_{50}>>1mM	IC_{50}>>1mM	IC_{50}>>1mM
40	IC_{50}>>1mM	IC_{50}>>1mM	IC_{50}>>1mM
42	IC_{50}=3.2mM	IC_{50}=5mM	IC_{50}>>1mM
	Ki=0.6mM	Ki=3mM	
45e	IC_{50}>>10µM	IC_{50}>>10µM	IC_{50}>>10µM

However, due to the low solubility of these systems in water/DMSO it is difficult to calculate the inhibition constants (Ki) as they precipitate when concentration near 1 mM.are reached

6.2.2 Catalytic tests with phosphines

Suzuki-Miyaura coupling reactions still have to be performed with the triazole-based phosphine ligands synthesized in the course of the PhD. As many of these compounds has revealed to be air sensitive, the first tests will be performed with the less air sensitive compounds (**Figure VI-2**).

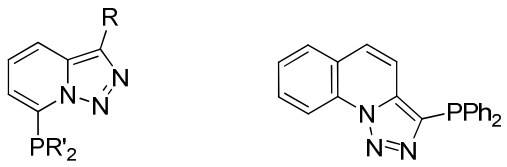

R = H, CH_3, Ph ans 2'-Py
R' = PPh_2, PCy_2, P^iPr_2

Figure VI-2: Ligands selected for catalysis.

6.2.3 Study on the [1,2,3]Triazolo[1,5-a]pyridine Rearrangement

In Chapter IV part 1, we described the ring-chain isomerization of 3-(2-pyridyl)-[1,2,3]triazolo[1,5-*a*]pyridine which helped us to evaluate the electronic influence of substituents on phosphorus. Up to now, we only determined the ratio between structures **A** and **B** in $CDCl_3$. We will perform a study in order to determine the influence of the solvent on this equilibrium. On the other hand, we only described the rearrangement with a series of PR_2 phosphines. In a second time, we would like to carry a similar investigation with mixed PR^1R^2 (with R^1 different R^2) and phosphole groups (**Scheme VI-2**).

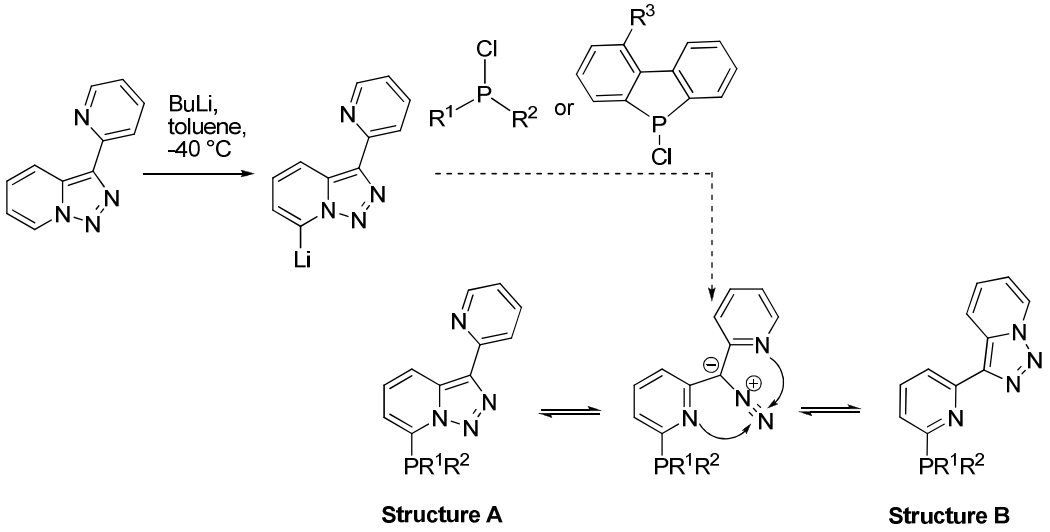

Schem VI-2: Evaluation of electronic Properties of new Phosphine Groups

Finally, the group of Elguero and Alkorta at the IQM (C.S.I.C.) in Madrid are currently performing Gaussian theoretical calculations in order to corroborate our experimental results, *i.e*. the different ratios obtained depending on the nature of the phosphine substituents.

6.2.4 Preparation of solid supported triazolopyridine based fluorophores

In collaboration with Prof. Garcia España we are interested in the preparation of fluorescence sensors based on a boehmite and a polyamine (**Figure VI-3**):

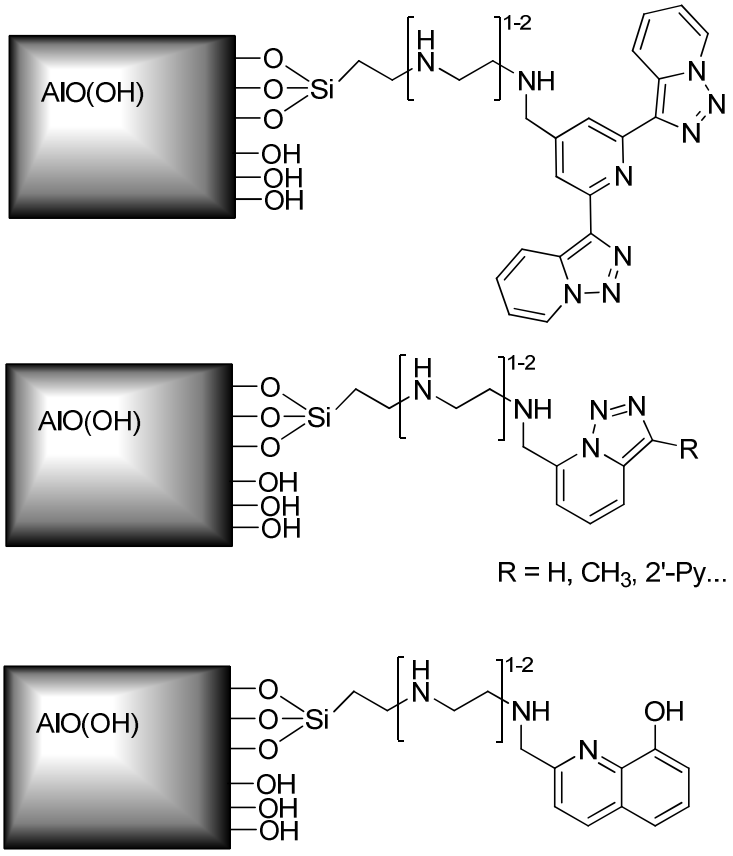

Figure VI-3: Boehmite based ligands

These kinds of compounds are water soluble and recyclable due to their weak solubility under acid pH. Combining the coordination chemistry of polyamines with those from triazolopyridines a new family of ligands will be developed.

Experimental Part

General Methods

Starting materials, if commercial, were purchased and used as such, provided that adequate checks (melting ranges, refractive indices, and gas chromatography) had confirmed the claimed purity. When known compounds had to be prepared according to literature procedures, pertinent references are given. Air- and moisture-sensitive materials were stored in Schlenk tubes. They were protected by and handled under an atmosphere of argon, using appropriate glassware. Diethyl ether and tetrahydrofuran were dried by distillation from sodium after the characteristic blue color of sodium diphenyl ketyl (benzophenone-sodium "radical-anion") had been found to persist. Ethereal or other organic extracts were dried by washing with brine and then by storage over sodium sulfate. Water was twice distilled and passed through a Millipore apparatus. Melting ranges (mp) given were found to be reproducible after recrystallization, unless stated otherwise ("decomp."), and are uncorrected. If melting points are missing, it means all attempts to crystallize the liquid at temperatures down to –75 °C failed. Thin-layer chromatography (TLC) were carried out on 0.25 mm Merck silica-gel (60-F254). The TLC plates were visualized with UV light and 7% phosphomolybdic acid. Column chromatography was carried out on a column packed with silica-gel 60N spherical neutral size 63-210 μm. The solid support was suspended in hexanes and, when all air bubbles had escaped, was washed into the column. When the level of the liquid was still 3 – 5 cm above the support layer, the dry powder, obtained by adsorption of the crude mixture to some 25 mL of silica and subsequent evaporation of the solvent, was poured on top of the column. ^{1}H and (^{1}H decoupled) ^{13}C nuclear magnetic resonance (NMR) spectra were recorded at 400 or 300 and 101 or 75 MHz, respectively. ^{31}P NMR were recorded at 162 MHz. Chemical shifts are reported in δ units, parts per million (ppm) and were measured relative to the signals for residual chloroform (7.27 ppm or 77 ppm, respectively). ^{31}P NMR relative to H_3PO_4 (external, δ = 0.0 ppm). Coupling constants *J* = are given in Hz. Coupling patterns are abbreviated as, for example, s (singlet), d (doublet), t (triplet), q (quartet), quint (quintet), td (triplet of doublets), m (multiplet), app. s (apparent singlet) and br (broad). Compounds were crystallized by slow diffusion of hexane in ethyl acetate. UV-Vis absortion spectra were recorded on Agilent 8453 spectroscopy system. The emission spectra were recorded with a PTI MO-5020 spectrofluorimeter in the 300-500 nm range. Quantum yield was determined with a Hamamatsu-PHA equipment.

7.1.1 Starting triazolopyridines

3-Methyl-[1,2,3]triazolo[1,5-*a*]piridine (1a)

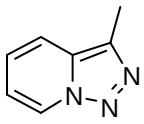

A mixture of 2-acetylpyridine (20 g, 0.16 mol, 1 eq) and hydrazine monohydrate (12 mL, 0.25 mol, 1.5 eq) in methanol (150 mL) was heated to reflux. The reaction was monitored by TLC upon completion of the reaction (3 h). The reaction mixture was quenched with an aqueous solution of NaOH (30 mL, 30%), the resulting mixture was extracted with dichloromethane (3×50 mL). The organic extracts were combined, washed with brine (3×20 mL), dried over Na_2SO_4, filtered, and concentrated providing the corresponding hydrazone. The hydrazone was directly diluted in chloroform (150 mL) then activated manganese dioxide (33 g, 0.32 mol, 2 eq) was added and the heterogeneous mixture heated to reflux over the night. The resulting mixture was cooled to 25 °C and filtrated with celite. After concentration, 3-methyl-[1,2,3]triazolo[1,5-*a*]pyridine (**1a**) was obtained as a colourless solid (18 g, 80%). mp 84 – 85 °C.[1]

^{1}H NMR (300 MHz, $CDCl_3$): δ = 8.62 (d, *J* = 7.0 Hz, 1H), 7.60 (d, *J* = 8.8 Hz, 1H), 7.15 (dd, *J* = 8.8, 6.9 Hz, 1H), 6.92 (dd, *J* = 7.0, 6.9Hz, 1H), 2.30 (s, 3H).

^{13}C NMR (75.5 MHz, $CDCl_3$): δ = 133.7 (C), 131.1 (C), 124.5 (CH), 123.3 (CH), 117.0 (CH), 114.6 (CH), 9.8 (CH_3).

3-(2-Pyridyl)-[1,2,3]triazolo[1,5-*a*]pyridine (1b)

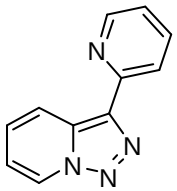

A mixture of dipyridyl ketone (10 g, 54 mmol, 1 eq) and hydrazine monohydrate (3.9 mL, 81 mmol, 1.5 eq) in methanol (120 mL) was heated to reflux. The reaction was monitored by TLC upon completion of the reaction (4 h). The reaction mixture was quenched with an aqueous solution of NaOH (25 mL, 30%), the resulting mixture was concentrated and the residual mixture was extracted with dichloromethane (3×30 mL). The organic extracts were combined, washed with brine (3×20 mL), dried over Na_2SO_4, filtered, and concentrated providing the corresponding hydrazone. The hydrazone was directly diluted in chloroform (125 mL), then activated manganese dioxide (12 g, 108 mmol, 2 eq) was added and the heterogeneous mixture heated to reflux over the night. The resulting mixture was cooled to 25 °C and filtrated with celite. After concentration, 3-methyl-[1,2,3]triazolo[1,5-*a*]pyridine (**1b**) was obtained as a colourless solid (10 g, 80%). mp 125 – 127 °C.[2]

^{1}H NMR (300 MHz, $CDCl_3$): δ = 8.69 (m, 3H), 8.27(d, *J* = 8.0 Hz,1H), 7.71 (dd , *J* = 8.0, 7.5 Hz, 1H) , 7.28 (dd , *J* = 9.0, 6.6 Hz, 1H),7.13 (dd , *J* = 7.5, 5.1 Hz, 1H), 6.96 (dd, J= 7.3, 6,6 Hz, 1H).

^{13}C NMR (75.5 MHz, $CDCl_3$): δ = 155.1 (C), 151.9 (C), 149.2 (CH), 136.53 (CH), 131.93 (C), 126.29 (CH), 125.11 (CH), 121.93 (CH), 121.20 (CH), 120.32 (CH), 115.83 (CH).

[1,2,3]Triazolo[1,5-*a*]piridine (1c)

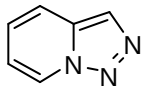

A mixture of 2-pyridine carboxaldehyde (10 g, 93 mmol, 1 eq) and hydrazine monohydrate (7 mL, 0.14 mol, 1.5 eq) in methanol (100 mL) was heated ted to reflux. The reaction was monitored by TLC upon completion of the reaction (3 h). The reaction mixture was quenched with an aqueous solution of NaOH (30 mL, 30%), the resulting mixture was extracted with dichloromethane (3×50 mL) The organic extracts were combined, washed with brine (3×20 mL), dried over Na_2SO_4, filtered, and concentrated providing the corresponding hydrazone. The hydrazone was directly diluted in chloroform (150 mL), then activated manganese dioxide (25 g, 0.19 mol, 2 eq) was added and the heterogeneous mixture was heated to reflux over the night. The resulting mixture was cooled to 25 °C and filtrated with celite. After concentration, 3-methyl-[1,2,3]triazolo[1,5-*a*]pyridine (**1c**) was obtained as a colourless solid (10 g, 94%). mp 39 – 40 °C.

^{1}H NMR (300 MHz, $CDCl_3$): δ = 8.67 (d, *J* = 7.0 Hz, 1H), 8.00 (s, 1H), 7.67 (d, *J* = 8.8Hz, 1H), 7.19 (dd, *J* = 8.8, 6.8 Hz, 1H), 6.92 (dd, *J* = 7.0, 6.8Hz, 1H).

^{13}C NMR (75.5 MHz, $CDCl_3$): δ = 133.5 (C), 125.4 (CH), 125.1 (CH), 124.9 (CH), 117.7 (CH), 115.1 (CH).[1]

3-Phenyl-[1,2,3]triazolo[1,5-*a*]pyridine (1d)

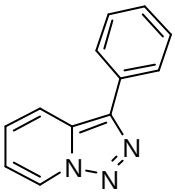

Synthesized according to the general procedure employing phenyl(pyridin-2-yl)methanone as starting reagent. The intermediate hydrazone was oxidized with activated manganese dioxide. After work up, the desired product (**1d**; 7.2 g, 90%) was obtained as colourless solid. mp 115 – 117 °C.[3]

^{1}H NMR (300 MHz, $CDCl_3$): δ = 8.69 (d, *J* = 7.0 Hz, 1H), 7.95 (d, *J* = 8.9 Hz, 1H), 7.90 (m, 2H), 7.45 (m, 2H), 7.33 (m, 1H), 7.25 (dd, *J* = 8.9, 6.8Hz, 1H), 6.95 (dd, *J* = 7.0, 6.8Hz, 1H).

^{13}C NMR (75.5 MHz, $CDCl_3$): δ = 138.4 (C), 131.9 (C), 130.9 (C), 129.4 (2×CH), 128.3 (CH), 127.1 (2×CH), 126.02 (CH), 126.0 (CH), 118.8 (CH), 115.7 (CH).

7.1.2 Chapter II : Chiral triazolopyridines: Towards 2,6-disubstituted pyridines

(1*R*,2*S*,4*S*)-1,3,3-Trimethyl-2[7'-(3'-mrthyl[1,2,3]triazolo[1,5-*a*]pyridyl)]bicyclo[2.2.1]heptan-2-ol (2)

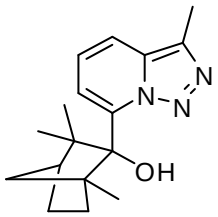

At -40 °C, butyllithium (6.6 mL, 16 mmol, 1.1 eq) in hexanes (1.54 M) was added dropwise to a stirred solution of 3-methyl-[1,2,3]triazolo[1,5-*a*]pyridine (**1a**) (2 g, 15 mmol 1 eq) in toluene (120 mL). After 15 min, an excess of (-)-fenchone (5.1 mL, 5 g, 2 eq) was added dropwise. After 1 h, the solution was allowed to reach room temperature and saturated aqueous solution of ammonium chloride (20.0 mL) was added, followed by extraction with dichloromethane (3 x 20.0 mL). The combined organic layers were dried over sodium sulfate, filtered, and evaporated providing a yellow liquid. Excess of (-)-fenchone was eliminated by distillation under reduced pressure. The crude was crystallized (AcOEt/Hex 1:7) in hexane providing (1*R*,2*S*,4*S*)-1,3,3-trimethyl-2[7'-(3'-methyl[1,2,3]triazolo[1,5-*a*]pyridyl)]bicyclo[2.2.1] heptan-2-ol (**2**) almost pure as a yellow solid (3.8 g, 88%). mp 113 – 114 °C.

^{1}H NMR (300 MHz, $CDCl_3$): δ = 7.44 (dd, *J* 7.8, 1.8 Hz, 1H), 7.14 (dd, *J* = 7.8, 7.2 Hz, 1H), 7.10 (dd, *J* = 7.2, 1.8 Hz, 1H), 6.67(s, OH), 2.5 - 2.5 (m, 1H), 2.18 (dd, *J* = 10.5, 2.1 Hz, 1H), 1.8 - 1.7 (m, 2H), 1.5 - 1.3 (m, 2H), 1.31 (s, 3H), 1.26 (s, 3H), 1.15 (ddd, *J* = 12.6, 12.6, 3.9 Hz, 1H), 0.24 (s, 3H).

^{13}C NMR (75.5 MHz, $CDCl_3$): δ = 141.2 (C), 133.8 (C), 132.7 (C), 123.6(CH), 115.0 (C), 114.3 (CH), 83.6 (C), 51.9 (C), 48.9 (CH), 45.9 (C), 42.0 (CH_2), 35.5(CH_2) 26.9(CH_2), 24.6 (CH_3), 22.8 (CH_3), 18.1 (CH_3), 10.3 (CH_3).

MS (EI): m/z(%) = 285(50), 257(58), 242(23), 229(50), 214(28), 174(41), 160(55), 105 (62), 104 (100).

HRMS for $C_{17}H_{23}N_3O$: calcd. 285.1841 found 285.1824.

(1*R*,2*S*,4*S*)-1,3,3-Trimethyl-2-(6-[1,2,3]triazolo[1,5-*a*]pyridin-3-yl-pyridin-2-yl)bicycle[2.2.1] heptan-2-ol (3)

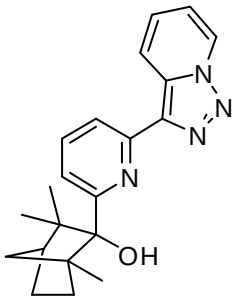

Prepared according to the procedure employed for compound **2** using 3-(2-pyridyl)-[1,2,3]triazolo [1,5-*a*]pyridine (**1b**) (1.1 g, 8.7 mmol, 0.1 M in toluene), butyllithium (4 mL, 9.3 mmol, 1.1 eq) and (-)-fenchone (3.9 mL, 4 g, 3 eq). (1*R*,2*S*,4*S*)-1,3,3-Trimrthyl-2-(6-[1,2,3]triazolo[1,5-*a*]pyridin-3-yl-pyridin-2-yl)bicycle[2.2.1] heptan-2-ol (**3**) was obtained as a colourless solid (2.5 g, 80%). mp 144 – 146 °C.

^{1}H NMR (300 MHz, $CDCl_3$): δ = 8.70 (d, *J* = 6.9 Hz, 1H), 8.34 (d, *J* = 7.9 Hz, 1H), 8.16 (d, J = 8.3 Hz, 1H) 7.72 (app t, *J* = 7.9 Hz, 1H), 7.40 (d, J= 7.9 Hz, 1H) 7.32 (dd, *J* = 6.9, 8.3 Hz, 1H), 6.99 (app t, *J* = 6.9Hz, 1H), 5.89 (brs, OH), 2.4-2.1 (m,2H), 1.9-1.7(m, 1H) 1.5-1.4 (m,1H), 1.33 (d, *J* = 10.5 Hz, 1H), 1.20-1.1 (m, 1H), 1.00 (s, 6H) 0.82 (m,1H) 0.45 (s, 3H).

^{13}C NMR (75.5 MHz, $CDCl_3$): δ = 161.5 (C), 149.1 (C), 136.9 (C), 136.2 (CH), 131.6 (C), 126.8 (CH), 125.5 (CH), 121.6 (CH), 120.1 (CH), 118.5 (CH), 115.8 (CH), 84.1 (C), 55.8 (C), 48.8 (CH), 46.0(C), 41.9 (CH_2), 32.6 (CH_2), 26.3 (CH_3), 24.3 (CH_2), 21.6 (CH_3), 17.1(CH_3).

MS (EI): m/z(%) = 348(25), 320(30), 292(100),169(80).

HRMS for $C_{21}H_{24}N_4O$: calcd. 348.1950 found 348.1915.

3-(6'-(2-Methoxy-1,3,3-trimethylbicyclo[2.2.1]heptan-2-yl)pyridin-2'-yl)-[1,2,3]triazolo[1,5-*a*]pyridine (4)

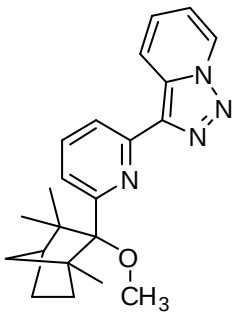

To a stirred solution of 2-(6-([1,2,3]triazolo[1,5-a]pyridin-3-yl)pyridin-2-yl)-1,3,3-trimethylbicyclo[2.2.1]heptan-2-ol **(3)** (0.3 g, 1.0 mmol, 1.0 eq.) in tetrahydrofuran (11 mL) was added NaH (0.1 mg. 4,1 mmol, 4,1 eq) at 25°C. After being stirred for 30 min, iodometane (0.6 mg, 0.6 ml, 4.0 mmol, 4.0 eq.) was added, and the resulting mixture was stirred for 16 h at 25 °C and monitored by TLC. Upon completion of the reaction sat. aq NH_4Cl (10 ml) solution was added to quench the reaction, and the resulting mixture was extracted with dichloromethane (3×10 mL). The organic extracts were combined, washed with brine (20 mL), dried over sodium sulfate filtered, and concentrated. Column chromatography (silica gel, ethyl acetate/cyclohexane gradient) provided **4** as a colourless solid (0.3 g, 95%). mp 127 – 130 °C.

^{1}H NMR (300 MHz, $CDCl_3$): δ = 8.81 (d, *J* = 9.1 Hz, 1H), 8.76 (d, *J* = 6.9 Hz, 1H), 8.26 (d, *J* = 7.8 Hz, 1H), 7.75 (t, *J* = 7.9 Hz, 1 H), 7.41 (d, *J* = 7.9 Hz, 1 H), 7.35 (dd. *J* = 6.6, 8.9 Hz, 1 H), 7.03 (t, *J* = 6.6 Hz, 1 H), 3.23 (s, 3 H), 3.05 (d, *J* = 8.61 Hz, 1 H), 2.15 (m. 1 H), 2.89 (m, 1 H), 1.7 (d, *J* = 4.2 Hz, 1 H), 1.5 (m, 2 H), 1.31 (m, 2 H) 1.04 (s, 3 H), 0.38(s, 3 H).

^{13}C NMR (75.5 MHz, $CDCl_3$): δ = 162.4 (C), 149.8 (C), 138.2 (C), 136.1 (CH), 131.5 (C), 125.9 (CH), 125.3 (CH), 121.8 (CH), 121.0 (CH), 117.8 (CH), 115.6 (CH), 90.0 (C), 54.7 (OCH_3), 52.3 (C) 48.8 (CH), 48.5 (C), 44.4 (CH_2), 32,2 (CH_2), 29.1 (CH_3), 25.1 (CH_2), 21.6 (CH_3), 20.7 (CH_3).

MS (EI): m/z(%) = 362(27), 347(64), 319(64), 281(36), 221(50), 195(24), 168(75), 167(38), 81(100), 78(65).

HRMS for $C_{22}H_{26}N_4O$: calcd. 362.2107 found 362.2096.

(*R*)-3-Methyl-7-(toluene-4-sulfinyl)-[1,2,3]triazolo-[1,5-*a*]pyridine (5)

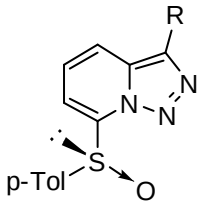

Prepared according to the procedure employed for compound **2** using 3-methyl-[1,2,3]triazolo[1,5-*a*]pyridine (**1a**) (0.1 g, 1.2 mmol, 0.1 M in toluene), and butyllithium (0.5 mL, 1.3 mmol, 1.1 eq). The lithium derivative was added to a solution of (*R*)-(+)-menthyl-*p*-toluenesulfinate (0.4 mg, 1.8 mmol, 1.5 eq) in toluene (1.5 mL). (*R*)-3-Methyl-7-(toluene-4-sulfinyl)-[1,2,3]triazolo-[1,5-*a*]pyridine (**5**) was obtained as colourless solid (0.6 mg, 20%). mp 144 – 146 °C.

^{1}H NMR (300 MHz, $CDCl_3$): δ = 7.89 (d, *J* = 8.2 Hz, 2 H), 7.71 (dd, *J* = 6.9, 1 Hz, 1.0 H), 7.65 (dd, *J* = 8.9, 1.0 Hz, 1H), 7.38 (dd, *J* = 8.9, 6.9 Hz, 1 H), 7.22 (d, *J* = 8.2 Hz, 2 H), 2.58 (s, 3 H), 2.30 (s, 3 H).

^{13}C NMR (75.5 MHz, $CDCl_3$): δ = 143.0 (C), 141.3 (C), 137.8 (C), 135.9 (C), 132.1 (CH), 129.9 (C), 126.3 (CH), 123.9 (CH), 118.9 (CH), 111.7 (CH), 21.5 (CH_3) 10.4 (CH_3).

MS (EI): m/z(%) = 273 (3), 271 (40), 243 (63), 226 (35), 195 (30), 139 (100), 120 (36), 104 (60), 91 (42),77 (67) .

HRMS for $C_{14}H_{13}N_3OS$: calcd. 271.0779 found 271.0778.

(*R*)-3-[6-(Toluene-4-sulfinyl)-pyridin-2-yl]-[1,2,3]triazolo[1,5-*a*]pyridine (6)

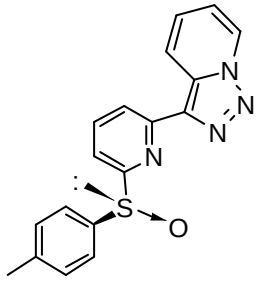

Prepared according to the procedure employed for compound **2**. 3-(2-pyridyl)-[1,2,3]triazolo [1,5-*a*]pyridine (**1b**) (0.1 g, 0.8 mmol, 0.1 M in toluene), butyllithium (0.3 mL, 0.9 mmol, 1.1 eq). The lithium derivative was added to a solution of (*R*)-(+)-menthyl-*p*-toluenesulfinate (0.3 mg, 1.2 mmol, 1.5 eq) in toluene (1.5 mL). (*R*)-3-[6-(Toluene-4-sulfinyl)-pyridin-2-yl]-[1,2,3]triazolo[1,5-*a*]pyridine (**6**) was obtained as colourless solid (0.4 15, 20%). mp 167 – 170 °C.

^{1}H NMR (300 MHz, $CDCl_3$): δ = 8.69 (d, *J* = 7.0 Hz, 1 H),8.37 (d, *J* = 8.9 Hz, 1 H), 8.27 (dd, *J* = 7.2, 1.8 Hz, 1 H), 7.91 (dd, *J* = 7.1, 7.8 Hz, 1 H) 7.88 (dd, *J* = 7.8, 1.8 Hz, 1 H), 7.65 (d, *J* = 8.1 Hz, 2 H) 7.33 (dd, *J* = 7.0, 8.9 Hz, 1 H), 7.2 (d, *J* = 8.1 Hz, 2H), 7.0 (dd, J_1 = 7.0, 6.9 Hz, 1 H), 2.30 (s, 3 H).

^{13}C NMR (75.5 MHz, $CDCl_3$): δ = **=** 165.0 (C), 152.4 (C), 141.9 (C), 141.3 (C), 138.7 (CH), 136.2 (C), 132.2 (C), 129.9 (CH), 126.9 (CH), 125.4 (CH), 125.4 (CH), 121.2 (CH), 120.8 (CH), 116.7 (CH), 116.1 (CH), 21.8 (CH_3).

MS (EI): m/z(%) = 336 (3), 334 (40), 306 (75), 258 (65), 215 (10), 199 (5), 183 (86), 167 (100), 139 (80), 113 (20), 91 (44), 78 (47).

HRMS for $C_{18}H_{14}N_4OS$: calcd. 334.0888 found 334.0904.

7,7'-Bis(3-methyl [1,2,3]triazolo[1,5-*a*]pyridine) (7a)

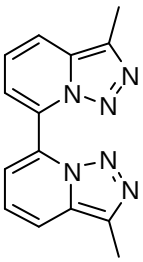

Obtained as a side product while the synthesis of **5**. 7,7'-Bis(3-methyl [1,2,3]triazolo[1,5-*a*]pyridine) (**7a**) was obtained as a yellow solid (85 mg 56%). mp 238 – 240 °C.[4]

^{1}H NMR (300 MHz, $CDCl_3$): δ = 7.80 (dd, J = 6.9, 1.1 Hz, 2H), 7.72 (dd, J = 8.8, 1.1 Hz, 2H), 7.28 (dd, J = 8.8, 6.9 Hz, 2H), 2.61(s, 6H).

^{13}C NMR (75.5 MHz, $CDCl_3$): δ = **=** 135.3 (C), 132.4 (C), 128.4 (C), 123.3 (CH), 118.9 (CH), 118.3 (CH), 10.3 (CH_3).

MS (EI): m/z(%) = 264 (17), 236 (5), 209 (7), 208 (40), 207 (100), 193 (16), 182 (22), 181 (19), 167 (5), 154 (8), 104 (9).

HRMS for $C_{14}H_{12}N_6$: calcd. 264.1123 found 264.1116.

3,3'-Di(pyridin-2-yl)-7,7'-bi[1,2,3]triazolo[1,5-*a*]pyridine (7b)

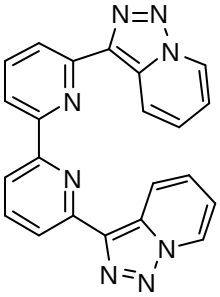

Obtained as a side product while the synthesis of **6**. 7,7'-Bis(3-methyl [1,2,3]triazolo[1,5-*a*]pyridine) (**7b**) was obtained as a highly insoluble yellow solid (85 mg 56%). mp > 350 °C.[4]

^{1}H NMR (300 MHz, CF_3COOD): δ = 9.07 (d, J = 6.9Hz, 2H), 8.63-8.45 (m, 8H), 8.00 (dd, J = 7.0, 8.0 Hz, 2H), 7.62 (app. t, 7.0Hz, 2H).

^{13}C NMR (75.5 MHz, CF_3COOD): δ = 146.2 (2×C), 145.3 (2×CH), 144.1 (2×C), 133.1 (2×C), 132.7 (2×CH), 129.5 (2×C), 126.8 (2×CH), 124.8 (2×CH), 122.7 (2×CH) 121.9 (2×CH), 118.5 (2×CH).

HRMS for $C_{22}H_{14}N_8$: calcd. 390.1341 found 390.1340.

3-*p*-Tolylsulfanyl-propionic acid *tert*-butyl ester.

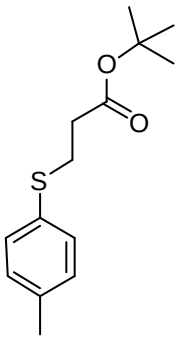

To a solution of 4-methylbenzenethiol (22 g, 0.2 mol) and potassium carbonate (5 mol%, 1.4 g) in dichloromethane (56 mL) was added rapidly *tert*-butyl acrylate (28 g, 29 mL, 0.2 mol). After stirring for 30 h at room temperature, water was added to the mixture and the organic layer was washed with successively water (3x50 mL) and brine (2x50 mL), dried over anhydrous sodium sulfate and evaporated under reduced pressure. The product was obtained as a colorless oil. (41.5 g, 92%).[5]

^{1}H NMR ($CDCl_3$, 300 MHz): δ = 7.31 (d, J = 8.1 Hz, 2 H), 7.13 (d, J = 8.1 Hz, 2 H), 3.10 (t, *J* = 7.6 Hz, 2 H), 2.53 (t, *J* = 7.6 Hz, 2 H), 2.34 (s, 3 H), 1.47 (s, 9 H).

^{13}C NMR ($CDCl_3$, 75.5 MHz): δ = 170.9 (C), 136.5 (C), 131.6 (C), 130.8 (CH), 129. (CH), 80.6 (C), 35.5 (CH_2), 29.8 (CH_2), 27.9 (3 CH_3), 20.9 (CH_3).

3-(*p*-Toluenesulfinyl)-propionic acid *tert*-butyl ester:

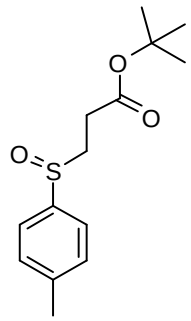

To a solution of the 3-*p*-tolylsulfanyl-propionic acid tert-butyl ester (41 g, 165 mmol) in CH_2Cl_2 (130 mL) was added dropwise *m*-CPBA (70–75% assay, 37 mg, 165 mmol) in CH_2Cl_2 (50 mL) over 30 min at 0 °C. The reaction was monitored by TLC. Upon completion of the reaction (4 h) the reaction mixture was quenched with saturated thiosulfate aqueous solution (50 mL). To the resulting mixture a saturated solution of $NaHCO_3$ (50 mL) was added. Then, the resulting mixture was extracted with dichloromethane (3×50 mL). The organic extracts were combined, washed with brine (20 mL), dried over sodium sulphate, filtered, and concentrated affording a colourless solid. After crystallization from hexane 3-(*p*-toluenesulfinyl)-propionic acid *tert*-butyl ester was obtained as a colourless solid. (40 g, 90%).[5]

^{1}H NMR ($CDCl_3$, 300 MHz): δ = 7.52 (d, *J* = 8.1 Hz, 2 H), 7.35 (d, *J* = 8.1 Hz, 2 H), 3.16 (ddd, *J* = 15.4, 8.6, 6.6 Hz, 1 H), 2.94 (ddd, *J* = 15.4, 8.6, 5.6 Hz, 1 H), 2.75 (ddd, *J* = 17.2, 8.6, 6.8 Hz, 1 H), 2.46 (ddd, *J* = 17.2, 8.6, 5.6 Hz, 1 H), 2.45 (s, 3H), 1.44 (s, 9 H).

^{13}C NMR ($CDCl_3$, 75.5 MHz): δ = 170.3 (C), 141.5 (C), 139.9 (C), 129.1 (CH), 124.0 (CH), 81.4 (C), 51.5 (CH_2), 27.9 (3 CH_3), 27.4 (CH_2), 21.3 (C).

The original protocol employed Oxone and wet alumina as oxidant observing similar yields; the use of *m*-CPBA to obtain sulfoxides is a well known methodology in our laboratory.

General procedure the for palladium-catalyzed arylation of sulfenate anions under biphasic conditions:

To a solution of tris(dibenzylideneacetone)dipalladium (5 mol%) in toluene (500 µL) was added Xantphos (10 mol%). The solution was stirred at room temperature for 5 min. Then, a solution of aryl bromide (0.5 mmol in 1.5 mL of toluene), β-sulfinylester (0.7 mmol in 1.5 mL of toluene), 3.5 mL of distilled water and 50% aqueous KOH solution (10 mmol) were successively added. The resulting biphasic system was stirred and heated to reflux. The reaction was monitored by TLC upon completion of the reaction (2-4 h). Then, after cooling to room temperature, the aqueous phase was extracted with dichloromethane (3×50 mL), the collected organic layers were dried over anhydrous sodium sulfate and the solvent was removed under reduced pressure. The crude product was purified by flash chromatography.

3-Methyl-7-(toluene-4-sulfinyl)-[1,2,3]triazolo[1,5-*a*]pyridine (5)

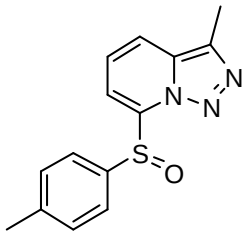

3-Methyl-7-bromo[1,2,3]triazolo[1,5-*a*]pyridine was used as starting material**.** Purification by silica gel flash chromatography (ethyl acetate/cyclohexane, 1:7) to afford the product as a colourless solid. (97.5 mg, 82% yield). The reaction was also performed in 0.5 g scale obtaining similar yields. mp 145 – 147 °C.

3-[6'-(Toluene-4-sulfinyl)-pyridin-2'-yl]-[1,2,3]triazolo[1,5-a]pyridine (6B)

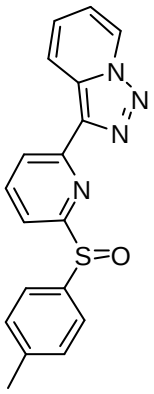

3-(6'-Iodo-pyridin-2'-yl)-[1,2,3]triazolo[1,5-a]pyridine was used as starting material**.** Purification by silica gel flash chromatography (ethyl acetate/cyclohexane, 1:7) to afford **6B** as a colourless solid. (157 mg, 95%). The reaction was also performed in 1 g scale obtaining similar yields. mp 167 – 170 °C.

2-(*p*-Tolylsulfinyl)pyridine (8a)

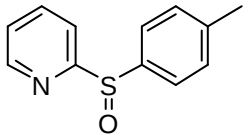

2-Bromopyridine was used as starting material. Purification by silica gel flash chromatography (ethyl acetate/cyclohexane, 1:4 → 2:1) to afford **8a** as a pale yellow oil (67 mg, 63%). [6]

^{1}H NMR ($CDCl_3$, 300 MHz): δ = 8.54 (dd, *J* = 4.9, 1.0 Hz, 1 H), 8.05 (dd, *J* = 1.0, 7.8 Hz, 1H) 7.87 (ddd, *J* = 1.0, 7.6, 7.8 Hz, 1 H), 7.67 (d, *J* = 8.0 Hz, 2 H), 7.25 (m, 3H) 2.34 (s, 3 H).

^{13}C NMR ($CDCl_3$, 75.5 MHz): δ = 166.0 (C), 149.7 (CH), 141.6 (C), 140.2 (C), 137.8 (CH), 129.8(CH), 125.0 (CH), 124.4 (CH), 118.3 (CH), 21.3 (CH_3).

3-(*p*-Tolylsulfinyl)pyridine (8b)

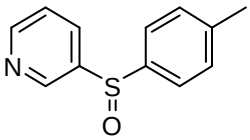

3-Bromopyridine was used as starting material. Purification by silica gel flash chromatography (ethyl acetate/cyclohexane, 1:4 → 2:1) to afford **8b** as a slightly brown oil (81 mg, 82%).[6]

^{1}H NMR ($CDCl_3$, 300 MHz): δ = 8.66 (d, *J* = 1.8 Hz, 1 H), 8.55 (dd, *J* = 1.4, 4.8 Hz, 1 H), 7.87 (td, *J* = 1.8, 1.8, 8.0 Hz, 1 H), 7.45 (d, *J* = 8.11 Hz, 2 H), 7.29 (dd, *J* = 4.8, 8.0 Hz, 1 H), 7.19 (d, *J* = 8.1 Hz, 2 H), 2.27 (s, 3 H).

^{13}C NMR ($CDCl_3$, 75.5 MHz): δ = 167.6 (C), 151.7 (CH), 146.3 (CH), 142.6 (C), 142.3 (C), 141.4 (C), 132.3 (CH), 130.3 (CH), 124.8 (CH), 124.1 (CH), 21.4 (CH_3).

4-(*p*-Tolylsulfinyl)pyridine (8c)

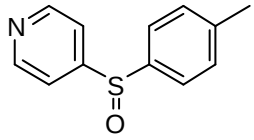

4-Bromopyridine was used as starting material. Purification by silica gel flash chromatography (ethyl acetate/cyclohexane, 1:4 → 2:1) to afford **8d** as a colourless oil (80 mg, 75%). 11 eq. of KOH were used in this reaction to neutralize the starting reagent (4-bromopyridine hydrochloride).[6]

^{1}H NMR ($CDCl_3$, 300 MHz): δ = 8.62 (d, *J* = 6.1 Hz, 2 H), 7.48 (d, *J* = 8.1 Hz, 2 H), 7.44 (d, *J* = 6.1 Hz, 2 H), 7.21 (d, *J* = 8.0.Hz, 2 H), 2.30 (s, 3 H).

^{13}C NMR ($CDCl_3$, 75.5 MHz): δ = 56.0 (C), 150.3 (CH), 142.8 (C), 141.1 (C), 130.4 (CH), 125.3 (CH), 118.3 (CH), 21.4 (CH_3).

2-(*p*-Tolylsulfinyl)thiophene (9a)

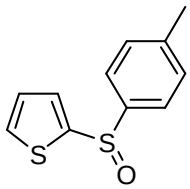

2-Bromothiophene was used as starting material. Purification by silica gel flash chromatography (ethyl acetate/cyclohexane, 1:3) to afford **9a** as a pale orange oil (77 mg, 69%).[7]

^{1}H NMR ($CDCl_3$, 300 MHz): δ = 7.6-7.5 (m, 4H), 7.32 (d, *J* = 8.1 Hz, 2H), 7.06 (dd, *J* = 5.1, 3.8 Hz, 1H), 2.42 (s, 3H).

^{13}C NMR ($CDCl_3$, 75.5 MHz): δ = 148.5 (C), 142.0 (C), 141.9 (C), 132.3 (CH), 131.2 (CH), 130.0 (CH), 127.4 (CH), 124.5 (CH), 21.6 (CH_3).

3-(*p*-Tolylsulfinyl)thiophene (9b)

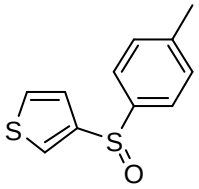

3-Bromothiophene was used as starting material. Purification by silica gel flash chromatography (ethyl acetate/cyclohexane, 1:3) to afford **9b** as a pale brown oil (55 mg, 50% yield).

^{1}H NMR ($CDCl_3$, 300 MHz): δ = 7.75 (dd, *J* = 1.3, 3.0 Hz, 1 H), 7.54 (d, *J* = 8.2 Hz, 2 H), 7.37 (dd, *J* = 3.0, 5.2 Hz, 1 H), 7.29 (d, *J* = 8.0 Hz, 1 H), 7.05 (dd, *J* = 1.3, 5.2 Hz, 1 H), 2.39 (s, 1 H).

^{13}C NMR ($CDCl_3$, 75.5 MHz): δ = 145.1 (C), 141.2 (C), 129.9 (CH), 128.2 (CH), 126.8 (CH), 124.8 (C) 124.1 (CH), 21.4 (CH_3).

2-(*p*-Tolylsulfinyl)pyrimidine (10a)

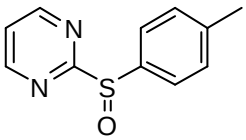

2-Bromopyrimidine was used as starting material. Purification by silica 2 mm preparative chromatography (ethyl acetate/cyclohexane, 1:3) to afford **10a** as a pale yellow oil (45 mg, 41% yield).

^{1}H NMR ($CDCl_3$, 300 MHz): δ = 8.48 (d, *J* = 4.9 Hz, 1 H), 7.52 (d, *J* = 8.1 Hz, 2 H), 7.25 (d, *J* = 8.1 Hz, 2 H), 6.94 (t, *J* = 4.9, 4.9 Hz, 1 H), 2.40 (s, 3 H).

^{13}C NMR ($CDCl_3$, 75.5 MHz): δ = 173.3 (C) 157.5 (CH), 139.3 (C), 135.3 (CH), 130.1 (CH), 125.8 (C), 116.8 (CH), 21.4 (CH_3).[8]

5-(*p*-Tolylsulfinyl)pyrimidine (10b)

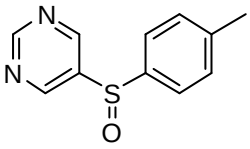

5-Bromopyrimidine was used as strating material Purification by silica 2 mm preparative chromatography (ethyl acetate/cyclohexane, 1:3) to afford **10b** as a colourless solid. (34 mg, 31%). mp 135-136 °C.[9]

^{1}H NMR ($CDCl_3$, 300 MHz): δ = 8.98 (s, 1 H), 8.52 (s, 2 H), 7.37 (d, *J* = 8.0 Hz, 2 H), 7.20 (d, *J* = 7.9 Hz, 2 H), 2.37 (s, 3 H).

^{13}C NMR ($CDCl_3$, 75.5 MHz): δ = 156.1 (CH), 155.7 (CH), 139.5 (C), 134.5 (C), 133.4 (CH), 130.7 (CH), 127.3 (C), 21.2 (CH_3).

1-[6-(Toluene-4-sulfinyl)-pyridin-2-yl]-ethanone (11)

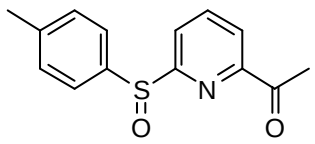

1-(6-Bromo-pyridin-2-yl)-ethanone was used as starting material. Purification by silica gel flash chromatography (ethyl acetate/cyclohexane, 1:4 → 2:1) to afford the product as a pale yellow solid (68.7 mg, 53% yield). mp 140 – 144 °C.

^{1}H NMR ($CDCl_3$, 300 MHz): δ = 8.12 (dd, *J* = 6.3, 2.7 Hz, 1H), 7.90 (m, 2H), 7.60 (d, *J* = 8.1 Hz, 2H), 7.17 (d, *J* = 8.1 Hz, 2H), 2.55 (s, 3H), 2.26 (s, 3H).

^{13}C NMR ($CDCl_3$, 75.5 MHz): δ = 198.5 (C=O), 165.8 (C), 153.1 (C), 141.8 (C), 140.5 (C), 139.0 (CH), 129.8 (CH), 124.6 (CH), 122.1 (CH), 121.5 (CH), 25.5 (CH_3), 21.3 (CH_3). **HRMS** for $C_{14}H_{13}NO_2S$: calcd. 259.0667 found 259.0669.

2,6-Bis(*p*-tolylsulfinyl)pyridine (12)

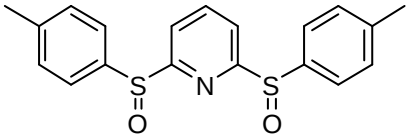

2,6-Dibromopyridine was used as starting material. Purification by silica 2 mm preparative chromatography (ethyl acetate/cyclohexane, 1:3) to afford **12** as a yellow solid (mixture of meso and enantiomeres 33/66). (128 mg, 64% yield).

^{1}H NMR ($CDCl_3$, 300 MHz): δ = 8.03 (m, 3 H), 7.63/7.43 (d, *J* = 8.1 Hz, 2 H), 7.28/7.10 (d, *J* = 8.0 Hz, 2 H), 2.39/2.36 (s, 6 H).

^{13}C NMR ($CDCl_3$, 75.5 MHz): δ = 166.8 (C), 141.9/141.4 (C), 140.4/140.2 (C), 140.0 (CH), 130.0/129.7 (CH), 124.8/124.7 (CH), 119.3/118.9 (CH), 21.4/21.3 (CH_3).

HRMS for $C_{19}H_{17}NO_2S_2$: calcd. 355.0701 found 355.0700.

2,5-Bis(*p*-tolylsulfinyl)pyridine (13)

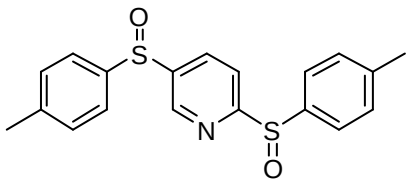

2,5-Dibromopyridine was used as starting material. Purification by silica 2 mm preparative chromatography (ethyl acetate/cyclohexane, 1:3) to afford **13** as a yellow solid (mixture of diastereomers 56/44). (148 mg, 84%).

^{1}H NMR ($CDCl_3$, 300 MHz): δ = 8.68/8.66 (m, 1 H), 8.12 (m, 2 H), 7.63/7.52 (d, *J* = 8.1 Hz, 2 H), 7.29/7.23 (d, *J* = 8.1 Hz, 2H), 2.38/2.37 (s, 3 H).

^{13}C NMR ($CDCl_3$, 75.5 MHz): δ = 168.8/168.7 (C), 146.3,(CH) 144.0/143.8 (C), 142.8/142.7 (C), 142.1/142.0 (C), 140.8/149.7 (C), 140.2/140.1 (C), 134.5/134.4 (CH), 130.5/130.0 (CH), 125.5 (CH), 125.0/124.9 (CH), 119.0/118.9 (CH), 21.5 (CH_3), 21.4 (CH_3).

HRMS for $C_{19}H_{17}NO_2S_2$: calcd. 355.0701 found 355.0703.

5-Bromo-2-chloropyridine was also used as starting material. Purification by silica 2 mm preparative chromatography (ethyl acetate/cyclohexane, 1:3) to afford the product as a yellow solid (mixture of diastereomers 56/44). (53 mg, 30% yield).

3-Bromo-4-(trimethylsilyl)pyridine (14)

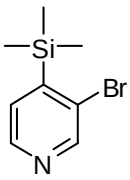

At 0 °C, butyllithium (14 mL, 22 mmol, 1.1 eq) in hexanes (1.5M) was added to a solution of diisopropylamine (2.9 mL, 21 mmol, 1.1 eq) in tetrahydrofuran (15 mL). After 15 min, the mixture was cooled to -78 °C and 3-bromopyridine (2.0 ml, 3.2 g, 20 mmol, 1.0 eq.) was added dropwise . The mixture was kept for 2 h at -78 °C before a solution of chlorotrimethyl silane (2.7 mL, 22. mmol, 1.1 eq) in tetrahydrofuran (11 mL) was added and allowed to reach to 20 °C (1 h). The reaction mixture was directly concentrated, chromatography (silica gel, ethyl acetate/cyclohexane gradient) provided **14** as brown oil, 3.29 g (70%).[10]

^{1}H NMR (300 MHz, $CDCl_3$): δ = 8.59 (s, 1 H), 8.42 (d, *J* = 4.7 Hz, 1 H), 7.26 (d, *J* = 4.7 Hz, 1 H), 0.36 (s, 3 H).

^{13}C NMR (75.5 MHz, $CDCl_3$): δ = 151.0 (CH), 150.3 (C), 146.8 (CH), 129.9 (CH), 128.4 (C), -1.5 (s, 9H).

1-(3-Bromo-4-(trimethylsilyl)pyridin-2-yl)ethanone (15)

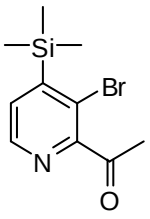

At 0 °C, butyllithium (13 mL, 21 mmol, 1.65 eq) in hexanes (1.6M) was added to a solution of tetramethylpiperidine (2.9 mL, 2.4 g, 21 mmol, 1.7 eq) in tetrahydrofuran (15 mL). After 15 min, the mixture was cooled to -78 °C and 3-bromo-4-(trimethylsilyl)pyridine (2.9 g, 13 mmol, 1.0 eq.) in tetrahydrofurane (8 mL) was added dropwise. The mixture was kept for 40 min at -78 °C before *N,N*-dimethylacetamide (3 mL, 2.8 g, 32. mmol, 2.5 eq) was added and allowed to reach to 20 °C (1 h). The reaction mixture was quenched with saturated aqueous solution of ammonium chloride (10 mL). Then the resulting mixture was extracted with dichloromethane (3×30 mL). The organic extracts were combined, washed with brine (10 mL), dried over sodium sulphate, filtered, and concentrated. Chromatography (silica gel, ethyl acetate/cyclohexane gradient) provided 1-(3-bromo-4-(trimethylsilyl)pyridin-2-yl)ethanone (**15**) as brown oil (3.4 g, 96%).

^{1}H NMR (300 MHz, $CDCl_3$): δ = 8.34 (d, *J* = 4.6 Hz, 1 H), 7.26 (d, *J* = 4.6 Hz, 1 H), 2.52 (s, 3 H), 0.30 (s, 9 H).

^{13}C NMR ($CDCl_3$, 75.5 MHz): δ = 201.0 (C), 154.1 (C), 146.1 (CH), 139.0 (C), 131.7 (CH), 123.3 (C), 28.8 (CH_3), 0.9 ($3CH_3$).

EM(E.I)m/z(%): 273(80), 271(85), 259(100), 257(96), 245(29), 243(30), 228(23), 230 (33), 216(30), 214(37), 193(45), 73(45).

HRMS for $C_{10}H_{14}NOSi_2Br$: calcd. 271.0028 found 271.0041.

4-Bromo-3-methyl-[1,2,3]triazolo[1,5-a]pyridine (17)

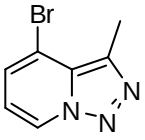

A mixture of 1-(3-bromo-4-(trimethylsilyl)pyridin-2-yl)-ethanone (**15**) (1.4 g, 4.9 mmol, 1 equiv) and hydrazine monohydrate (5 mL, 5.2 g, 103 mmol) was heated at 50 ºC for 20 min. Then methanol was added (17 mL) and the mixture was heated to reflux. The reaction was monitored by TLC upon completion of the reaction (3 h). The reaction mixture was quenched with an aqueous solution of sodium hydroxide (20 mL, 30%), and the resulting mixture was extracted with dichloromethane (3×50 mL). The organic extracts were combined, washed with brine (20 mL), dried over sodium sulfate, filtered and concentrated providing the corresponding hydrazone. The hydrazone was directly diluted in chloroform (13 mL) then activated manganese dioxide (1.5 g, 17 mmol) was added and the heterogeneous mixture was heated to reflux overnight. The resulting mixture was cooled to rt and filtered over Celite and concentrated. Chromatotron purification (silica gel, ethyl acetate/cyclohexane gradient) provided 4-bromo-3-methyl-[1,2,3]triazolo[1,5-a]pyridine (**17**) as a colourless solid (0.8 g, 78%). mp 160 – 161 °C.

^{1}H NMR (300 MHz, $CDCl_3$): δ = 8.59 (d, *J* = 7.0 Hz, 1 H), 7.33 (d, *J* = 7.0 Hz, 1 H), 6.75 (t, *J* = 7.0, 7.1 Hz, 1 H), 2.83 (s, 3 H).

^{13}C NMR ($CDCl_3$, 75.5 MHz): δ = 138.7 (C), 130.3 (C) 127.1 (CH), 124.5 (CH), 115.1 (CH), 112.3 (C) 12.7 (CH_3).

MS (EI): m/z(%) = 285(48), 283(46), 257(30), 256(42), 255(30), 254(38), 242(72), 241(35), 240(67), 239(27), 176(100), 160(91), 139(58), 137(55), 118(35), 73(20).

HRMS for $C_7H_6N_3Br$: calcd. 210.9745 found 210.9747.

4-Bromo-3-methyl-5-trimethylsilyl-[1,2,3]triazolo[1,5-a]pyridine (16)

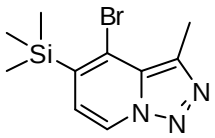

4-bromo-3-methyl-5-trimethylsilanyl-[1,2,3]triazolo[1,5-*a*]pyridine (**16**) was also obtained while the triazolo-ring formation (270 mg, 20%). mp 111 – 114 °C**.**

^{1}H NMR (300 MHz, $CDCl_3$): δ = 8.51 (d, *J* = 7.0 Hz, 1H), 6.82 (d, *J* = 7.0 Hz, 1H), 2.82 (s, 3H), 0.42 (s, 9H).

^{13}C NMR ($CDCl_3$, 75.5 MHz): δ = 137.2 (C), 136.0 (C) 129.9 (C), 124.5 (CH), 120.1 (C), 119.6 (CH), 13.6 (CH_3), 0.7 (3 CH_3).

MS (EI): m/z(%) = 285(48), 283(46), 257(30), 256(42), 255(30), 254(38), 242(72),241(35), 240(67), 239(27), 176(100), 160(91), 139(58), 137(55), 118(35), 73(20).

HRMS for $C_{10}H_{14}N_3BrSi$: calcd. 283.0140 found 283.0152.

4-Bromo-3-methyl-[1,2,3]triazolo[1,5-*a*]pyridine (17)

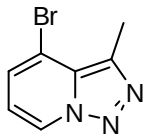

To a stirred solution of **16** (100 mg, 0.35 mmol, 1 eq.) in tetrahydrofurane (43 mL) and water (7 mL), potassium fluoride on alumina (40%) (211 mg) was added at 25 °C. The resulting mixture was heated at 66 °C and stirred for 16 h. The resulting mixture was filtrated, diluted with CH_2Cl_2 (50 mL), dried over sodium sulfate, filtered, and concentrated giving **17** as a colourless solid (74 mg, 99%). mp 160 – 161 °C**.**

1-(5-Bromopyridin-2-yl)ethanone (18)

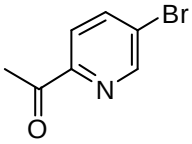

At -40 °C, butyllithium (13 mL, 21 mmol, 1 eq) in hexanes (1.6M) was added to a solution of 2,5-dibromopyridine (4.9 g, 21 mmol, 1.7 eq) in toluene (210 mL). The mixture was kept for 40 min at -40 °C before *N*,*N*-dimethylacetamide (3.5 mL, 3.6 g, 37. mmol, 1.7 eq) was added and allowed to reach 20 °C (1 h). The reaction mixture was quenched with a saturated aqueous solution of ammonium chloride (20 mL). Then the resulting mixture was extracted with dichloromethane (3×50 mL). The organic extracts were combined, washed with brine (20 mL), dried over sodium sulfate, filtered, and concentrated providing 1-(5-bromopyridin-2-yl)ethanone (**18**) as brown solid (3.5 g, 83%). mp 109 – 111 °C**.**

^{1}H NMR (300 MHz, $CDCl_3$): δ = 8.71 (d, *J* = 1.9 Hz, 1H), 7.90 (dd, J= 7.0, 1.9 Hz, 1H), 7.86 (d, J=7.0Hz,,1H), 2.67 (s, 3H).

^{13}C NMR ($CDCl_3$, 75.5 MHz): δ = 199.2 (C), 151.8 (C), 150.1 (CH), 139.5 (CH), 125.3 (C), 122.9 (CH), 25.7 (CH_3).

MS (EI): m/z(%) = 201(98), 199(100), 186(45), 184(45), 173(48), 171(50), 159(67), 158(75), 157(69), 156(73).

HRMS for $C_7H_6N_3Br$: calcd. 198.9632 found 198.9634.

6-Bromo-3-methyl-[1,2,3]triazolo[1,5-*a*]pyridine (19)

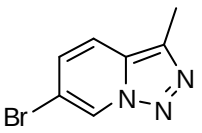

A mixture of 1-(5-bromopyridin-2-yl)ethanone (**18**) (3.5 g, 17.5 mmol, 1 eq) and hydrazine monohydrate (10 mL, 10.4 g, 206 mmol) in methanol (50 mL) was heated to reflux. The reaction was monitored by TLC upon completion of the reaction (3 h). The reaction mixture was quenched with an aqueous solution of sodium hydroxide (20 mL, 30%). The resulting mixture was extracted with dichloromethane (3×50 mL). The organic extracts were combined, washed with brine (20 mL), dried over sodium sulfate, filtered, and concentrated providing the corresponding hydrazone. The hydrazone was directly diluted in chloroform (13 ml), then activated manganese dioxide (3.7 g, 42 mmol) was added and the heterogeneous mixture was heated to reflux over the night. The resulting mixture was cooled to 25 °C and filtered over celite. After concentration, 6-bromo-3-methyl-[1,2,3]triazolo[1,5-*a*]pyridine (**19**) was obtained as a yellow solid (3.3 g, 88%). mp 116 – 119 °C.

^{1}H NMR (300 MHz, $CDCl_3$): δ = 8.79 (dd, *J* = 1.5, 0.8 Hz, 1 H), 7.51 (dd, *J* = 9.3, 0.8 Hz, 1 H), 7.22 (dd, *J* = 9.3, 1.4 Hz, 1 H), 2.60 (s, 3 H).

^{13}C NMR ($CDCl_3$, 75.5 MHz): δ = 138.7 (C), 130.3 (C) 127.1 (CH), 124.5 (CH), 115.1 (CH), 112.3 (C) 12.7 (CH_3).

MS (EI): m/z(%) = 135.2 (C), 130.2 (C), 127.4 (CH), 125.3 (CH), 117.8 (CH), 110.5(C), 10.5 (CH_3).

HRMS for $C_7H_6N_3Br$: calcd. 210.9745 found 210.9748.

General procedure for palladium-catalyzed arylation of sulfenate anions under biphasic conditions: To a solution of $Pd_2(dba)_3$ (5 mol %) in toluene (0.500 mL) was added Xantphos (10 mol %). The solution was stirred at room temperature for 5 min. Then, a solution of triazolopyridine (0.5 mmol in 1.5 mL of toluene), β-sulfinylester (0.7 mmol in 1.5 mL of toluene), distilled water (3.5 mL) and 50% aqueous KOH solution (10 mmol) were successively added. The resulting biphasic system was stirred and heated to reflux. The reaction was monitored by TLC. Upon completion of the reaction (2–4 h) and cooling to 25 °C, the aqueous phase was extracted with dichloromethane (3×10 mL). The combined organic layers were dried over anhydrous Na_2SO_4 and the solvent was removed under reduced pressure.

3-Methyl-6-(*p*-tolylsulfinyl)-[1,2,3]triazolo[1,5-*a*]pyridine (20a)

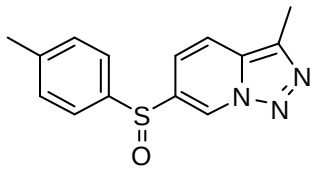

Prepared from 6-bromo-3-methyl-[1,2,3]triazolo[1,5-*a*]pyridine (0.5 g, 2.5 mmol) (**18**). The crude product was purified by flash chromatography (ethyl acetate/cyclohexane, 1:5→3:1) affording 3-methyl-6-(*p*-tolylsulfinyl)-[1,2,3]triazolo[1,5-*a*] pyridine (**20a**) as a yellow solid (213 mg, 32%). mp 152 – 154 °C**.**

^{1}H NMR (300 MHz, $CDCl_3$): δ = 9.05 (d, J= 1.3 Hz, 1 H), 7.59 (m, 3H), 7.31 (d, *J* = 8.3 Hz, 2 H), 7.06 (dd, *J* = 9.3, 1.4 Hz, 1 H), 2.58 (s, 3 H), 2.39 (s, 3 H).

^{13}C NMR ($CDCl_3$, 75.5 MHz): δ = 142.9 (C), 140.1 (C), 137.3 (C), 133.3 (C) 132.1 (C), 130.4 (CH), 125.0 (CH), 123.4 (CH), 119.1 (CH), 118.6 (CH), 21.5 (CH_3), 10.3 (CH_3).

MS (EI): m/z(%) = 271(26), 243(27), 226(30), 195(64), 139(100), 123(62), 91(40), 65(50)

HRMS for $C_{14}H_{13}N_3OS$: calcd. 271.0779 found 271.0778.

3-Methyl-6-(*p*-tolylthio)-[1,2,3]triazolo[1,5-*a*]pyridine (20b)

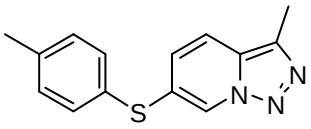

3-Methyl-6-(*p*-tolylthio)-[1,2,3]triazolo[1,5-*a*]pyridine (**20b**) was also obtained after purification as a yellow solid (0.2 g 31 %). mp 87 – 90 °C**.**

^{1}H NMR (300 MHz, $CDCl_3$): δ = 8.36 (brs, 1 H), 7.44 (dd, *J* = 9.1, 0.9 Hz, 1 H), 7.32 (d, *J* = 8.1 Hz, 2 H), 7.15 (d, *J* = 8.1 Hz, 2 H), 7.00 (dd, *J* = 9.1, 1.4 Hz, 1 H), 2.54 (s, 3 H), 2.33 (s, 3 H).

^{13}C NMR ($CDCl_3$, 75.5 MHz): δ = 139.0 (C), 134.7 (C), 132.8 (CH), 130.5 (CH), 130.2 (C), 128.5 (C), 126.6 (C), 126.3 (CH), 123.7 (CH), 117.0 (CH), 21.1 (CH_3), 10.3 (CH_3).

MS (EI): m/z(%) = 255(10), 227(100), 226(67), 123(15), 91(25), 65(20).

HRMS for $C_{14}H_{13}N_3S$: calcd. 255.0830 found 255.0833.

6-(*p*-Tolylthio)-[1,2,3]triazolo[1,5-*a*]pyridine (21b)

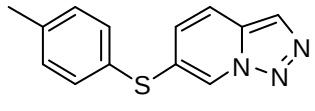

The crude product was purified by a chromatotron (silica, ethyl acetate/cyclohexane, gradient) affording 6-(*p*-tolylthio)-[1,2,3]triazolo[1,5-*a*]pyridine (**21b**) as a yellow solid, (40 mg, 36%) mp 80 – 83 °C**.**

^{1}H NMR (300 MHz, $CDCl_3$): δ = 8.48 (s, 1 H), 8.00 (s, 1 H), 7.60 (d, *J* = 9.2 Hz, 1 H), 7.38 (d, *J* = 8.1 Hz, 2 H), 7.21 (d, *J* = 8.0 Hz, 2 H), 7.12 (d, *J* = 9.2 Hz, 1 H), 2.38 (s, 3 H).

^{13}C NMR ($CDCl_3$, 75.5 MHz): δ = 139.3 (C), 133.1 (CH), 132.2 (C), 130.7 (CH), 128.1 (C), 127.7 (CH), 127.3 (C), 125.8 (CH), 123.4 (CH), 117.4 (CH), 21.2 (CH_3).

MS (EI): m/z(%) = 243(3), 241(57), 213(100), 212(58), 198(20), 171(21), 123(15), 91(10).

HRMS for $C_{13}H_{11}N_3S$: calcd. 241.0674 found 241.0680.

5-(*p*-Tolylsulfinyl)-[1,2,3]triazolo[1,5-*a*]pyridine (22)

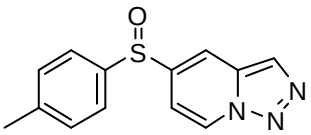

The crude product was purified by a chromatotron (silica, ethyl acetate/cyclohexane, 1:4 → 2:1) affording 5-(*p*-tolylsulfinyl)-[1,2,3]triazolo[1,5-*a*]pyridine (**22**) as a yellow solid (0.1 g, 84%). mp 134 – 135 °C**.**

^{1}H NMR (300 MHz, $CDCl_3$): δ = 8.67 (d, *J* = 7.3 Hz, 1 H), 8.23 (m, 1 H), 8.18 (d, *J* = 0.95 Hz, 1 H), 7.56 (d , *J* = 8.0 Hz, 2 H), 7.3 (d, *J* = 8.0 Hz, 2 H), 6.88 (dd, *J* = 7.3, 1.7 Hz, 1 H), 2.38 (s, 3 H).

^{13}C NMR ($CDCl_3$, 75.5 MHz): δ = 144.1 (C), 143.1 (C), 140.3 (C), 132.8 (C), 130.5 (CH), 127.3 (CH), 126.0 (CH), 125.2 (CH), 114.8(CH), 110.2(CH), 21.44 (CH_3).

MS (EI): m/z(%) = 259(4), 257(89), 229(3), 181(70), 139(15), 123(45), 90(100).

HRMS for $C_{13}H_{11}N_3OS$: calcd. 257.0623 found 257.0622.

3-Methyl-4-(*p*-tolylsulfinyl)-[1,2,3]triazolo[1,5-*a*]pyridine (23a)

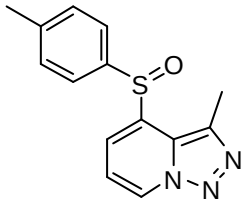

The crude product was purified by flash chromatography (silica, ethyl acetate/cyclohexane, 1:4 → 2:1) affording 3-methyl-4-(*p*-tolylsulfinyl)-[1,2,3]triazolo[1,5-*a*]pyridine (**23a**) as a yellow solid, (107 mg, 80%). mp 157 – 160 °C**.**

^{1}H NMR (300 MHz, $CDCl_3$): δ = 8.70 (d, *J* = 7.0 Hz, 1 H), 7.90 (d, *J* = 7.0 Hz, 1H), 7.50 (d, *J* = 8.1 Hz, 2H), 7.27 (d, *J* = 8.1 Hz, 2H), 7.10 (t, *J* = 7.0, Hz, 1H), 2.60 (s, 3 H), 2.38 (s, 3H).

^{13}C NMR ($CDCl_3$, 75.5 MHz): δ = 143.3 (C), 140.2 (C), 137.3 (C), 134.4 (C), 133.5 (C) 132.0 (C), 130.5 (CH), 127.3 (CH), 126.6 (CH), 122.2 (CH), 114.1 (CH), 21.5 (CH_3), 13.1 (CH_3).

MS (EI): m/z(%) = 271(0.5), 243(83), 228(32), 226(49), 200(100), 123(7).

HRMS for $C_{14}H_{13}N_3OS$: calcd. 271.0779 found 271.0786.

3-Methyl-4-(*p*-tolylthio)-[1,2,3]triazolo[1,5-*a*]pyridine (23b)

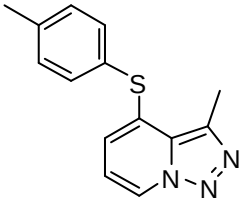

Traces of **23b** were found after purification of **32a.**

^{1}H NMR (300 MHz, $CDCl_3$): δ = 8.39 (d, *J* = 6.9 Hz, 1 H), 7.30 (d, *J* = 8.0 Hz, 2 H), 7.18 (d, *J* = 8.0 Hz, 2 H), 6.66 (t, *J* = 7.0. Hz, 1 H), 6.55 (d, *J* = 7.0 Hz, 1 H), 2.78 (s, 3 H), 2.36 (s, 3H).

^{13}C NMR ($CDCl_3$, 75.5 MHz): δ = 139.2 (C), 136.9 (C), 135.6 (C), 133.9 (C), 133.2 (CH), 130.6 (CH), 127.1 (C), 122.4 (CH), 118.3 (CH), 114.8 (CH), 21.1 (CH_3), 12.8 (CH_3)

MS (EI): m/z(%) = 255(15), 227(27), 226(95), 212(100), 194(32).

HRMS for $C_{14}H_{13}N_3S$: calcd. 255.0830 found 255.0832.

3-(*p*-Tolylsulfinyl)-[1,2,3]triazolo[1,5-*a*]pyridine (24)

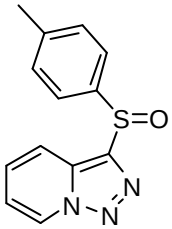

3-Iodo-[1,2,3]triazolo[1,5-*a*]pyridine, 0.43 mmol, was used. The crude product was purified by a chromatotron (silica, ethyl acetate/cyclohexane) affording 5-(*p*-tolylsulfinyl)-[1,2,3]triazolo[1,5-*a*]pyridine (**24**) as a yellow solid (25 mg, 20%) mp 119 – 123 °C**.**

^{1}H NMR (300 MHz, $CDCl_3$): δ = 8.77 (d, *J* = 7.0 Hz, 1 H), 7.80 (d, *J* = 8.9 Hz, 1 H), 7.69 (d, *J* = 8.1 Hz, 2 H), 7.33 (m, 3 H), 7.09 (dt, *J* =7.0, 1.1 Hz, 1 H), 2.39 (s, 3 H).

^{13}C NMR ($CDCl_3$, 75.5 MHz): δ = 141.6 (C), 139.9 (C), 133.3 (C), 132.4 (C), 130.0 (CH), 127.8 (CH), 125.9 (CH), 124.5 (CH), 118.2 (CH), 116.5 (CH), 21.4 (CH_3).

MS (EI): m/z(%) = 257(2), 229(13), 213(21), 212(100), 181(83), 180(51), 91(12), 78(21).

HRMS for $C_{14}H_{13}N_3S$: calcd. 255.0830 found 255.0832.

3,3'-Bis[1,2,3]triazolo[1,5-*a*]pyridine (25)

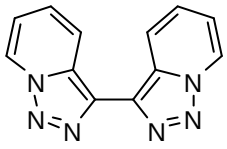

Traces of **25** were found after purification of **24.**

^{1}H NMR (300 MHz, $CDCl_3$): δ = 8.71 (dd, *J* = 7.0, 0.9 Hz, 2 H), 8.62 (dd, *J* = 9.0, 1.1 Hz, 2 H), 7.32 (ddd, *J* = 9.0, 7.0, 0.9 Hz, 2 H), 7.01 (td, *J* = 7.0, 1.1 Hz, 2H)

^{13}C NMR ($CDCl_3$, 75.5 MHz): δ = 134.2 (2C), 131.0 (2C), 125.7 (2CH), 125.0 (2CH), 120.5 (2CH), 116.1 (2CH).

HRMS for $C_{12}H_8N_6$: calcd. 236.0810 found 236.0806.

Methode A: General procedure for the ring opening reaction with sulfuric acid.

A solution of the corresponding triazolopyridine (100mg) in aqueous sulfuric acid (10 mL, 2.5 M) was heated .The solution was neutralized with a saturated aqueous solution of sodium bicarbonate and extracted with dichloromethane. The organic solvent was dried, and evaporated. The residue was purified by silica column chromatography or chromatotron. The products, yield and conditions of purification are given for each compound.

Methode B: General procedure for the ring opening reactions of triazolopyridines with AcOH.

A solution of the corresponding triazolopyridine (100 mg) in glacial acetic acid (10 mL) was heated. The solution was neutralized with a saturated aqueous solution of sodium bicarbonate and extracted with dichloromethane. The organic solvent was dried, and evaporated. The residue was purified by silica column chromatography or chromatotron. The products, yields and conditions of purification are given for each compound.

2-[6-(1-Hydroxy-ethyl)-pyridin-2-yl]-1,3,3-trimethyl-bicyclo[2.2.1]hept-2-ol (26)

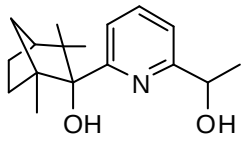

Methode A [(diastereomeric mixture, 5% d.e.) (1*R*, 2*S*, 4*S*, 1'*S*) and (1*R*, 2*S*, 4*S*, 1'*R*)]-2-[6-(1-Hydroxy-ethyl)-pyridin-2-yl]-1,3,3-trimethyl-bicyclo[2.2.1]hept-2-ol (**26**). (23h/100 °C) Purified by chromatotron with ethyl acetate/hexane (52 mg, 60% colourless oil). In the first fraction **27** (10 mg, 10%) was obtained.

^{1}H NMR (300 MHz, $CDCl_3$): δ = 7.65 (dd, *J* = 7.8, 7.5 Hz, 2 H), 7.43 (d, *J* = 7.8 Hz, 2 H), 7.18 (d, *J* = 7.5 Hz, 2 H), 4.88 (d, *J* = 6.6 Hz, 2 H), 3.2 (brs, 2 OH), 2.28 (m, 4 H), 1.87-1.78 (m, 4 H), 1.5 (d, *J* = 6.6 Hz, 3 H), 1.49 (d, *J* = 6.6 Hz, 3 H), 1.51-1.48 (m, 2 H), 1.35 (d, *J* = 9.3 Hz, 2 H), 1.17 (td, *J* = 12.9, 4.8 Hz, 2 H), 1.00 (s, 3 H), 0.99 (s, 3 H), 0.98 (s, 6 H), 0.40 (s, 3 H), 0.39 (s, 3 H).

^{13}C NMR ($CDCl_3$, 75.5 MHz): δ = 162.11 (C), 161.19 (C), 136.62 (CH), 121.90 / 121.84 (CH), 117.71 (CH), 84.24 (C), 70.09 / 69.93 (CH), 52.45 / 52.36 (C), 49.24 (CH), 46.47 (C), 42.39 (CH_2), 32.92 (CH_2), 29.55 / 29.52 (CH), 24.80 / 24.68 (CH_2), 24.41 (CH_3), 22.55 (CH_3), 17.58 (CH_3).

MS (EI): m/z(%) = 275 (8), 260 (12), 194 (100), 178 (71).

HRMS for $C_{17}H_{25}NO_2$: calcd. 275.1885 found 275.1889.

(1*R*, 2*S*, 4*S*)-1,3,3-Trimethyl-2-(6-vinylpyridin-2-yl)-bicyclo[2.2.1]hept-2-ol (27)

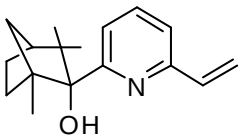

(1*R*, 2*S*, 4*S*)-1,3,3-Trimethyl-2-(6-vinylpyridin-2-yl)-bicyclo[2.2.1]hept-2-ol **27**. Purified by chromatotron with ethyl acetate/hexane (15mg, 17 % colorless oil).

^{1}H NMR (300 MHz, $CDCl_3$): δ = 7.60 (dd, *J* = 7.8, 7.5 Hz, 1 H), 7.39 (d, *J* = 7.8 Hz, 1 H), 7.16 (d, *J* = 7.5 Hz, 1 H), 6.76 (dd, J_1 = 17.4 Hz, J_2 = 12 Hz, 1H), 6.20 (dd, *J* = 17.4, 1.5 Hz, 1 H), 5.45 (dd, *J* = 12.0, 14.5 Hz, 1 H), 2.3-2.1 (m, 2 H), 1.9-1.7(m, 2 H), 1.5-1.4 (m, 1 H), 1.29 (dd, *J* = 1.5, 12.0 Hz, 1 H), 1.18 (brs, 1 OH), 1.06 (app td, *J* = 12.6, 4.8 Hz, 2 H), 0.92 (s, 3 H), 0.90 (s, 6 H), 0.39 (s, 3 H)

^{13}C NMR ($CDCl_3$, 75.5 MHz): δ = 152.56 (C), 152.41 (C), 136.30 (CH), 135.64 (CH), 122.01 (CH), 119.07 (CH), 118.00 (CH_2), 83.528 (C), 48.80 (CH), 45.96 (C), 42.01 (CH_2), 32.52 (CH_2), 29.69 (C), 29.29 (CH), 24.38 (CH_2), 24.41 (CH_3), 22.28 (CH_3), 17.17 (CH_3).

MS (EI): m/z(%) = 257 (15), 242 (15), 229 (35), 176 (100), 160 (82), 153 (12), 104 (45), 81 (60), 77 (18).

HRMS for $C_{17}H_{23}NO_2$: calcd. 257.1779 found 257.1779.

1-[6-(2-Hydroxy-1,3,3-trimethyl-bicyclo[2.2.1]hept-2-yl)-pyridin-2-yl]-ethylacetate (28)

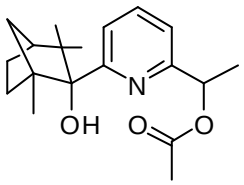

Method B: [(diastereomeric mixture, 5% d.e.) (1*R*, 2*S*, 4*S*, 1'*S*) and (1*R*, 2*S*, 4*S*, 1'*R*)]-1-[6-(2-Hydroxy-1,3,3-trimethyl-bicyclo[2.2.1]hept-2-yl)-pyridin-2-yl]-ethylacetate (**28**). (5h/80°C) Purified by chromatotron with ethyl acetate/hexane (132mg, 75%, colourless oil). In the first fraction **28** (17 mg, 17%) was obtained.

^{1}H NMR (300 MHz, $CDCl_3$): δ = 7.62 (dd, J_1 = 7.8, 7.5 Hz, 2 H), 7.40 (d, *J* = 7.8 Hz, 1 H), 7.41 (d, *J* = 7.8 Hz, 1 H), 7.17 (d, *J* = 7.5 Hz, 1 H), 7.16 (d, *J* = 7.5 Hz, 1 H), 5.92-5.84 (m, 2 H), 2.35-2.20 (brm, 2 H), 2.11 (s, 3 H), 2.10 (s, 3 H), 1.90-1.7 (m, 4 H), 1.55 (d, *J* = 6.6 Hz, 6 H), 1.51-1.41 (m, 2 H), 1.33 (d, *J*= 10.2 Hz, 2 H), 1.13 (td, *J* = 12.3, 4.5 Hz, 2 H), 0.99 (s, 3 H), 0.98 (s, 3 H), 0.97 (s, 3 H), 0.95 (s, 3 H), 0.38 (s, 3 H), 0.35 (s, 3 H).

^{13}C NMR ($CDCl_3$, 75.5 MHz): δ = 170.22 / 170.14 (C), 161.84 / 161.82 (C), 157.34 / 157.25 (C), 135.88 / 135.57 (CH), 121.75 / 121.63 (CH), 117.73 / 117.63 (CH), 83.56 (C), 72.55 / 72.49 (C), 51.62 / 51.57 (CH), 48.76 (CH), 45.92 (C), 41.84 / 41.73 (CH_3), 32.43 / 32.31 (CH_2), 29.09 (CH_2), 24.36 / 24.22 (CH_2), 22.13 (CH), 21.19 / 21.15 (CH_3), 20.84 / 20.48 (CH_3), 20.36 / 20.22 (CH_3), 17.11 / 17.08 (CH_3).

MS(E.I.) m/z(%):317 (10), 236 (85), 176 (20), 81 (100).

HRMS for $C_{19}H_{27}N_3O$: calcd. 317.1990 found 317.1986.

(1*S*,2*R*,*4S*)-1,3,3-trimethyl-2-(pyridin-2-yl)bicyclo[2.2.1]heptan-2-ol (29)

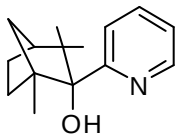

A suspension of triazolopyridine **2** (0.1 g, 0.4 mmol, 1eq) and selenium dioxide (0.9 g, 0.8 mmol, 2 eq.) *p*-xylene (10 mL) was heated to reflux during 72 h then allowed to reach room temperature. The mixture was filtered and the filtrate neutralized with a saturated aqueous solution of sodium hydrogencarbonate, and extracted with dichloromethane. The organic solvent was dried, and evaporated. The residue was purified by chromatotron affording (1*S*,2*R*,4*S*)-1,3,3-trimethyl-2-(pyridin-2-yl)bicyclo[2.2.1]heptan-2-ol (**29**) as a colourless solid (0.2 mg, 22%). mp 57 – 60 °C**.**[11]

^{1}H NMR (300 MHz, $CDCl_3$): δ = 8.4-8.5 (m, 1H), 7.60-7.67 (m, 1H), 7.52 (d, *J* = 8.0 Hz, 1H), 7.1-7.0 (m, 1H), 5.80 (s, 1 H,), 2.4-2.2 (m, 2H), 1.9-1.7 (m, 2H), 1.5-1.4 (m, 1H), 1.36 (dd, *J* = 10.5, 1.4 Hz, 1H,), 1.2-1.1 (m, 1H), 0.99 (s, 3H), 0.98 (s, 3H), 0.43 (s, 3H).

(6-(2-hydroxy-1,3,3-trimethylbicyclo[2.2.1]heptan-2-yl)pyridin-2-yl)(pyridin-2-yl)methyl acetate (30)

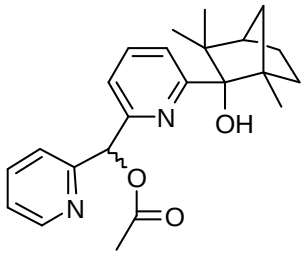

Methode B: (diastereomeric mixture, 3.5% d.e.) 150 g of starting triazolopyridine were employed at 50h/115 °C. Silica column chromatography eluted with ethyl acetate/ cyclohexane afforded (1*R*,2*S*,4*S*,1'*S*) and (1*R*,2*S*,4*S*,1'*R*)]-(6-(2-hydroxy-1,3,3-trimethylbicyclo[2.2.1]heptan-2-yl)pyridin-2-yl) (pyridin-2-yl)methyl acetate (**30**) as a colorless oil (91 mg, 42%).

^{1}H NMR (300 MHz, $CDCl_3$): δ = 7.53 (m, 2H), 7.67 (m, 4H), 7.51 (app t, *J* = 8.0 Hz, 2H), 7.40 (m, 4H), 7.18 (m, 2H), 6.87 (s, 1H), 6.85 (S, 1H), 2.21 (s, 3H), 2.20 (s, 3H),1.82-1.72 (m, 4H), 1.43 (m, 2H), 1.28 (m, 2H), 1.10 (m, 2H), 0.95 (s, 3H). 0.93 (s, 3H), 0.85 (s, 3H), 0.82 (s, 3H), 0.26 (s, 3H), 0,23 (s, 3H)

^{13}C NMR ($CDCl_3$, 75.5 MHz): δ = 169.9/169.9 (C), 157.9 (C), 155.0/154.9 (C), 149.3/149.2 (CH), 136.6 (CH), 136.1 (CH), 122.9/122.8 (CH), 122.5/122.2 (CH), 121.9/121.7 (CH), 119.8/119.2 (CH), 83.7 (C), 78.2 (CH), 48.1(CH), 46.0/45.9 (C), 41.8 (CH_3), 32.5/32.4 (CH_2), 28.8/28.7 (CH_3), 24.3 (CH_2), 22.0/21.9 (CH_3), 21.1/21.0 (CH_3) 17.1/17.0 (CH).

MS (EI): m/z(%) = 380 (7), 321 (27), 320 (100), 299 (30), 292 (31), 283 (30).

HRMS for $C_{23}H_{28}N_2O$: calcd. 380.2100 found 380.2108.

(6-(2-methoxy-1,3,3-trimethylbicyclo[2.2.1]heptan-2-yl)pyridin-2-yl)(pyridin-2-yl)methyl acetate (31)

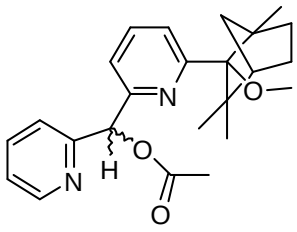

Methode B: (1*R*,2*S*,4*S*,1'*S*) and (1*R*,2*S*,4*S*,1'*R*)] diastereomeric mixture, 5% d.e.) 150 g of starting triazolopyridine were employed) (24h/100°C) (Silica column chromatography eluted with ethyl acetate/ cyclohexane afforded (1*R*,2*S*,4*S*,1'*S*) and (1*R*,2*S*,4*S*,1'*R*) (6-(2-methoxy-1,3,3-trimethylbicyclo[2.2.1]heptan-2-yl)pyridin-2-yl)(pyridin-2-yl)methyl acetate (**31**) as a yellow oil (40 mg, 26%). Compound **32** was found as side product.

^{1}H NMR (300 MHz, $CDCl_3$): δ = 8.54 (m, 2H), 7.69 (ddd, , *J* = 7.7, 7.6, 1.7 Hz, 2H), 7.61 (t, *J* 7.57 Hz, 2H), 7.57 (t, *J* = 8.8 Hz 2H), 7.32 (dd, *J* = 7.64, 2.98 Hz, 2H), 7.28 (d, *J* = 7.98 Hz, 2H), 7.17 (m, 2H), 6.91/6.89 (s, 2H), 3.12/3.11 (s, 6H), 2.51 (m, 2H), 2.21 (s, 6H), 2.0-1.9 (m, 2H), 1.8-1.7 (m, 2H), 1.54-1.36 (m, 4H), 1.18 (s, 3H), 1.15 (s, 3H), 1.1-1.0 (m, 2H), 1.00 (m, 2H). 0.92 (s, 6H), 0.08 (s, 3H), 0.05 (s, 3H).

^{13}C NMR ($CDCl_3$, 75.5 MHz): δ = 170/169 (C), 162.3/162.2 (C), 158.5 (C), 155.6/155.5 (C), 149.9/149.0 (CH), 136.4 (CH), 136.0 (CH), 122.8/122.7 (CH), 122.7/122.5 (CH), 122.0/121.9 (CH), 118.9/118.7 (CH), 89.9 (C), 78.7/78.6 (CH), 54.6 (CH_3), 52.4/52.3 (C), 48.4/48.3 (C), 48.4 (CH_3), 44.3/44.2 (CH_2), 31.7 (CH_2), 28.8/28.7 (CH_3), 25.3 (CH_2), 21.2/21.1 (CH_3), 20.0/19.8 (CH_3) 14.1 (CH).

MS (EI): m/z(%) = 394 (16), 380 (30), 379 (100), 319 (31), 314, (20), 313 (96).

HRMS for $C_{24}H_{30}N_2O_3$: calcd. 394.2256 found 394.2254.

(1*R*,2*S*,4*S*)-(6-(2-Methoxy-1,3,3-trimethylbicyclo[2.2.1]heptan-2-yl)pyridin-2-yl)(pyridin-2-yl)methanone (32)

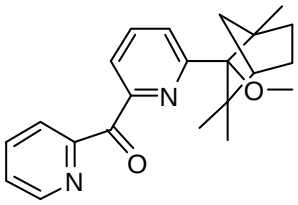

Colorless oil (83 mg, 60%).

^{1}H NMR (300 MHz, $CDCl_3$): δ = 8.68 (m, 1H), 7.95 (dd, *J* = 7.6, 1.0 Hz, 1H), 7.9-7.7 (m, 3H), 7.06 (dd, *J* = 7.9, 1.1 Hz, 1H), 7.5-7.4 (m, 1H), 3.15 (s, 3H), 2.31 (m, 1H), 2.01 (m, 1H), 1.8-1.7 (m, 1H), 1.5-1.3 (m, 3H), 1.18 (s, 3H), 1.1-1.0 (m, 1H), 0.98 (s, 3H), 0.30 (s, 3H).

^{13}C NMR ($CDCl_3$, 75.5 MHz): δ = 194.4(C=O), 162.2 (C), 155.8 (C), 152.5 (C), 148.9 (CH), 136.2 (CH), 136.1 (CH), 126.0 (CH), 125.3 (CH), 123.9 (CH), 121.6 (CH), 90.0 (C), 54.6 (CH_3), 52.2 (C), 48.5 (C), 48.4 (CH_3), 44.4 (CH_2), 31.6 (CH_2), 29.1 (CH_3), 24.4 (CH_2), 21.6 (CH_3), 19.9 (CH_3), 14.1 (CH).

MS (EI): m/z(%) = 350 (13), 335 (50), 269 (100), 78 (18).

HRMS for $C_{22}H_{26}N_2O_2$: calcd. 350.1994 found 350.1995.

(1*R*,2*S*,4*S*)-(6-(1,3,3-trimethylcyclo[6.2.0]fenchen-2-yl)pyridin-2-yl)(pyridin-2-yl)methanone (33)

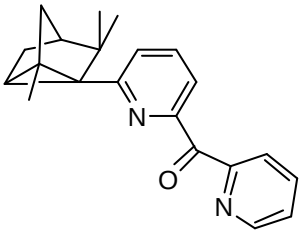

Methode B: (Silica column chromatography eluted with ethyl acetate/ cyclohexane afforded (1*R*,2*S*,4*S*)- (6-(1,3,3-trimethylcyclo[6.2.0]fenchen-2-yl)pyridin-2-yl)(pyridin-2-yl) methanone (**33**) as a brown oil (17 mg, 13%). Compound **32** was found as side product (55 mg, 38%).

^{1}H NMR (300 MHz, $CDCl_3$): δ = 8.73 (d, *J*= 4.34 Hz, 1H), 8.06 (d, *J*=*7.*82 Hz, 1H), 7.90 (dd, *J* = 7.6, 0.9 Hz, 1H), 7.83 (app td, *J* = 7.7, 7.7, 1.7 Hz, 1H) 7.74 (app t, *J* = 7.8 Hz, 1H) 7.43 (m, 1H) 7.35 (dd, *J* = 7.8, 1.0 Hz, 1H), 1.82 (m, 2H), 1.53 (m, 1H), 1.40 (s, 1H), 1.32 (m, 1H), 1.22 (m, 1H), 1.07 (s, 3H), 1.00 (s, 3H), 0.86 (s, 3H).

^{13}C NMR (75.5 MHz, $CDCl_3$): δ = 193.4 (C=O), 159.0 (C), 154.7 (C), 153.5 (C), 149.1 (CH), 136.0 (CH), 127.3 (CH), 127.2 (CH), 125.7 (CH), 125.6 (CH), 121.3 (CH), 46.8 (C), 44.1 (CH), 42.0 (C), 38.6 (CH_2), 32.2 (CH_2), 29.4 (C), 27.1 (CH_3), 22.6 (CH_3), 21.7 (CH_3), 14.0 (CH).

MS (EI): m/z(%) = 318 (100), 303 (60), 277 (34), 212 (20), 78 (20).

HRMS for $C_{21}H_{22}N_2O$: calcd. 318.1732 found 318.1733.

1-(6-(*p*-Tolylsulfinyl)pyridin-2-yl)ethanol (34)

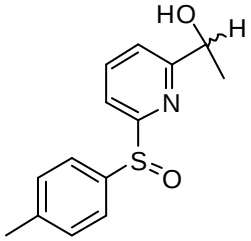

7-(*p*-Tolylsulfinyl)-3-methyl-[1,2,3]triazolo[1,5-*a*]pyridine (**5**) (0.1 g, 0.4 mmol, 1.0 eq.) was diluted in an aqueous solution of sulfuric acid (10 mL, 2.5 M) and heated to 100 °C. The reaction was monitored by TLC. Upon completion of the reaction (6 h) the reaction mixture was quenched with saturated aqueous solution of $NaHCO_3$ (11 mL) until pH = 8. Then the resulting mixture was extracted with dichloromethane (3×50 mL). The organic extracts were combined, washed with brine (20 mL), dried over sodium sulfate, filtered, and concentrated.

Column chromatography (silica gel, ethyl acetate/cyclohexane gradient) provided 1-(6-(*p*-tolylsulfinyl)pyridin-2-yl)ethanol (**34**) as a yellow oil, (91 mg, 95 %, d.e. 5%).

^{1}H NMR (300 MHz, $CDCl_3$): δ = 7.84 (m, 2 H), 7.63/7.62 (d, *J* = 8.2 Hz, 2 H), 7.32/7.31 (d, *J* = 7.5 Hz, 1 H), 7.21/7.20 (d, *J* = 8.0 Hz, 2 H), 4.85 (m, 1 H), 3.79/3.77 (s, 1 OH), 2.32 (s, 3 H), 1.43/1.42 (d, *J* = 6.6 Hz, 3 H).

^{13}C NMR (75.5 MHz, $CDCl_3$): δ = 164.5/164.4 (C), 164.3/164.2 (C), 141.6/141.5 (C), 140.6 (C), 138.8 (CH), 129.8 (CH), 124.8 (CH), 120.9/120.8 (CH), 116.9./116.8 (CH), 69.2/69.1 (CH), 24.0/23.9 (CH_3), 21.4/21.3 (CH_3).

MS (EI): m/z(%) = 261(100), 228(30),123 (40), 91(15).

HRMS for $C_{14}H_{15}NO_2S$: calcd. 261.0823 found 261.0820.

1-(6-(*p*-Tolylsulfinyl)pyridin-2-yl)ethyl acetate (36) 2-(*p*-tolylsulfinyl)-6-vinyl-pyridine (35)

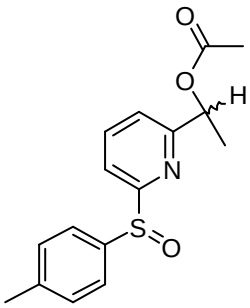

7-(*p*-Tolylsulfinyl)-3-methyl-[1,2,3]triazolo[1,5-*a*]pyridine (**5**) (0.1 g, 0.4 mmol, 1.0 eq.) was diluted in acetic acid (10 mL) and heated to 100 °C. The reaction was monitored by TLC. Upon completion of the reaction (4 h) acetic acid was separated by distillation and the reaction mixture was quenched with saturated aqueous solution of $NaHCO_3$ (5.0 mL) until pH = 8. Then the resulting mixture was extracted with dichloromethane (3×10 mL). The organic extracts were combined, washed with brine (20 mL), dried over sodium sulfate, filtered, and concentrated. Column chromatography (silica gel, ethyl acetate/cyclohexane, 1:5 → 2:1) provided 1-(6-(*p*-tolylsulfinyl)pyridin-2-yl)ethyl acetate (**35**) as a yellow-brown oil (0.1 g, 89%, 7% de). 2-(*p*-Tolylsulfinyl)-6-vinylpyridine (**36**) (6.2 mg, 7%) was obtained as side product.

^{1}H NMR (300 MHz, $CDCl_3$): δ = 7.91/7.89 (d, *J* = 7.8 Hz, 1 H), 7.81/7.80 (t, *J* = 7.8 Hz, 1 H), 7.65 (d, *J* = 8.1 Hz, 2 H), 7.32/7.29 (d, *J* = 8.0 Hz, 1 H), 7.21 (d, *J* = 7.1 Hz, 2 H), 5.86/5.85 (m, 1H), 2.32 (s, 3H), 2.08/2.06 (s, 3 H), 1.53/1.46 (d, *J* = 6.6 Hz, 3 H).

^{13}C NMR (75.5 MHz, $CDCl_3$): δ = 170.0/169.9 (C), 164.5/164.4 (C), 160.7/160.5 (C), 141.3/141.2 (C), 140.9/140.8 (C), 138.6/138.5 (CH), 129.6/129.5 (CH), 124.6/124.5 (CH), 121.3/120.8 (CH), 117.1/116.9 (CH), 72.2 (CH), 21.2 (CH_3), 21.1/20.9 (CH_3), 20.4/20.1 (CH_3).

MS (EI): m/z(%) = 303(50), 243(100), 226(40), 123(50), 91(23).

HRMS for $C_{16}H_{17}NO_3S$: calcd. 303.0929 found 303.0927.

2-(*p*-Tolylsulfinyl)-6-vinyl-pyridine (36)

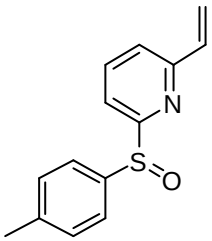

Yellow oil (6.2 mg, 7%).

^{1}H NMR (300 MHz, $CDCl_3$): δ = 7.89 (dd, *J* = 7.8, 1.0 Hz, 1 H), 7.80 (t, *J* = 7.8 Hz, 1 H), 7.70 (d, *J* = 8.2 Hz, 2 H), 7.26 (m, 3 H), 6.75 (dd, *J* = 17.4, 10.7 Hz, 1 H), 6.24 (dd, *J* = 17.4, 1.3 Hz, 1 H), 5.52 (dd, *J* = 10.7, 1.3 Hz, 1H), 2.35 (s, 3 H).

^{13}C NMR (75.5 MHz, $CDCl_3$): δ = 155.9 (C), 141.4 (C), 141.0 (C),138.4 (CH), 135.6 (CH), 129.7 (CH), 124.8 (CH), 124.7 (C) 122.0 (CH),119.9 (CH_2), 116.7 (CH), 21.3 (CH_3).

MS (EI): m/z(%) = 243(66), 242(30), 228(65), 210(33), 123(100), 104(35), 91(30).

HRMS for $C_{14}H_{13}NOS$: calcd. 243.0717 found 243.0720.

1-(3-(*p*-Tolylsulfinyl)pyridin-2-yl)ethyl acetate (37)

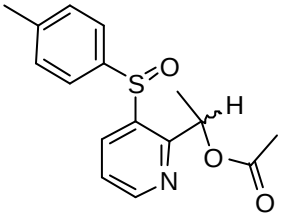

4-(*p*-Tolylsulfinyl)-3-methyl-[1,2,3]triazolo[1,5-*a*]pyridine (**23**) (0.1 g, 0.4 mmol, 1.0 eq.) was diluted in acetic acid (10 mL) and heated to 100 °C. The reaction was monitored by TLC. Upon completion of the reaction (6 h) acetic acid was separated by distillation and the reaction mixture was quenched with a saturated aqueous solution of $NaHCO_3$ (5.0 mL) until pH = 8. Then the resulting mixture was extracted with dichloromethane (3×10 mL). The organic extracts were combined, washed with brine (20 mL), dried over sodium sulfate, filtered, and concentrated. Chromatotron (silica gel, ethyl acetate/cyclohexane, 1:9 → 2:1) provided 1-(3-(*p*-tolylsulfinyl)pyridin-2-yl)ethyl acetate (**37**) as a yellow oil. (79 mg, 70%, d.e. 10 %).

^{1}H NMR (300 MHz, $CDCl_3$): δ = 8.70/8.68 (m, 1H), 8.42/8.14 (dd, *J* = 8.0, 1.6 Hz, 1 H), 8.26 (d, *J* = 7.9 Hz, 1 H), 7.55/7.48 (d, *J* = 8.2, 2 H), 7.45/7.38 (dd, *J* = 8.0, 4.6 Hz, 1 H), 7.28-7.24 (m, 2 H), 6.26/5.95 (q, *J* = 6.6 Hz, 1 H), 2.34 (s, 3 H), 2.02/1.99 (s, 3 H), 1.59/1.21 (d, *J* = 6.6 Hz, 3 H).

^{13}C NMR (75.5 MHz, $CDCl_3$): δ = 170 (C), 156.5/155.5 (C),151.7/151.2 (CH) 142.6/142.4 (C), 142.1/141.3 (C), 140.7/139.9 (C), 134.0/132.7 (CH), 130.3/130.0 (CH), 126.4/125.7 (CH), 124.2/124.1 (CH), 69.8/69.7 (CH), 21.4/21.3 (CH_3), 21.1/20.9 (CH_3), 19.9/18.6 (CH_3).

MS (EI): m/z(%) = 303(3), 286(10), 260(70), 244(100), 243(17), 226(25), 136(25), 84(45).

HRMS for $C_{16}H_{17}NO_3S$: calcd. 303.0929 found 303.0922.

(6'-(*p*-Tolylsulfinyl)pyridin-2'-yl)(pyridin-2-yl)methyl acetate (38)

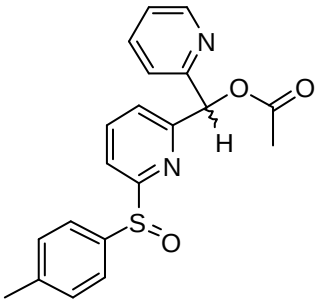

3-(6'-(*p*-Tolylsulfinyl)pyridin-2'-yl)-[1,2,3]triazolo[1,5-*a*]pyridine (**6**) (0.1 g, 0.3 mmol, 1.0 eq.) was diluted in acetic acid (10 mL) and heated to 100 °C. The reaction was monitored by TLC. Upon completion of the reaction (4 h) acetic acid was separated by distillation and the reaction mixture was quenched with a saturated aqueous solution of $NaHCO_3$ (5.0 mL) until pH = 8. Then the resulting mixture was extracted with dichloromethane (3×10 mL). The organic extracts were combined, washed with brine (20 mL), dried over sodium sulfate, filtered, and concentrated. Column chromatography (silica gel, ethyl acetate/cyclohexane, 1:5 → 2:1) provided **38** as a yellow oil (61 mg, 56%, d.e. 5%).

^{1}H NMR (300 MHz, $CDCl_3$): δ = 8.51 (m, 1 H), 7.89 (m, 2 H), 7.68 (m, 1 H), 7.48 (m, 4H), 7.21 (m, 1 H), 7.16/7.12 (d, *J* = 8.1 Hz, 2 H), 6.85/6.84 (s, 1H), 2.33/2.32 (s, 3 H), 2.20/2.18 (s, 3H).

^{13}C NMR (75.5 MHz, $CDCl_3$): δ = 169.7/169.6 (C), 165.8/165.6 (C), 158.3/158.2 (C), 157.3 (C), 149.4/149.3 (CH), 141.2/141.1 (C), 140.9/140.8 (C), 138.8/138.7 (CH), 136.7/136.6 (CH), 129.6/129.5 (CH), 124.7/124.6 (CH), 123.3/123.0 (CH), 122.9/122.7 (CH), 122.4/122.2 (CH), 117.5/117.3 (CH), 78.0/77.9 (CH), 21.4/21.3 (CH_3), 21.0/20.9 (CH_3).

MS (EI): m/z(%) = 366(100), 323(10), 291(15), 201(25), 167(23), 123(10), 78(10).

HRMS for $C_{20}H_{11}N_3O_3S$: calcd. 366.1038 found 366.1032.

(6'-(*p*-Tolylsulfinyl)pyridin-2'-yl)(pyridin-2-yl)methanol (39)

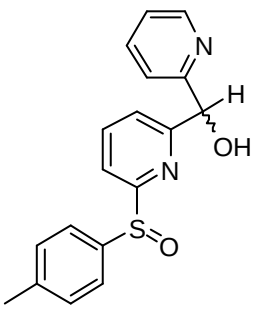

3-(6'-(*p*-Tolylsulfinyl)pyridin-2'-yl)-[1,2,3]triazolo[1,5-*a*]pyridine (**6**) (0.1 g, 0.3 mmol, 1.0 eq.) was diluted in an aqueous solution of sulfuric acid (10 mL, 2.5 M) and heated to 100 °C. The reaction was monitored by TLC. Upon completion of the reaction (6 h) the reaction mixture was quenched with a saturated aqueous solution of $NaHCO_3$ (11 mL) until pH = 8. Then the resulting mixture was extracted with dichloromethane (3×10 mL). The organic extracts were combined, washed with brine (20 mL), dried over sodium

sulfate, filtered, and concentrated. Two chromatography columns (silica gel, ethyl acetate/cyclohexane gradient) provided 6'-(*p*-tolylsulfinyl)pyridin-2'-yl)(pyridin-2-yl)methanol (**39)** as a brown oil (59 mg, 60%, d.e. 5%). Compound **39** decomposed providing (6'-(*p*-tolylsulfinyl)pyridin-2'-yl)(pyridin-2-yl)methanone (**40**) as a colorless oil (27 mg, 28%) .

^{1}H NMR (300 MHz, $CDCl_3$) δ = 8.53/8.48 (d, *J* = 4.9 Hz, 1 H), 7.88 (m, 2 H), 7.62 (m 3 H), 7.53 (m 1 H), 7.44 (m 1 H), 7.22 (m, 3 H), 5.83 (s, 1 H), 5.49 (s_{br}, 1 H), 2.38/2.37 (s, 3 H)

^{13}C NMR (75.5 MHz, $CDCl_3$) δ = 169.7/169.6 (C), 1640.8/164.7 (C), 158.3/158.2 (C), 157.3 (C), 149.4/149.3 (CH), 141.2/141.1 (C), 141.6/141.5 (C), 138.8/138.7 (CH), 136.9/136.6 (CH), 129.7/129.6 (CH), 124.8/124.7 (CH), 122.8/122.7 (CH), 121.8/121.5 (CH), 121.3/120.7 (CH), 117.3/117.1 (CH), 74.6/74.5 (CH), 21.4/21.3 (CH_3).

(6'-(*p*-Tolylsulfinyl)pyridin-2'-yl)(pyridin-2-yl)methanone (40)

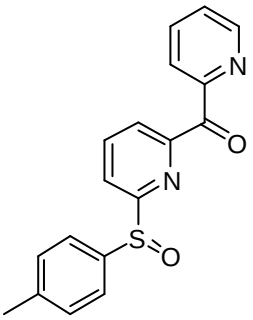

Colorless oil (27 mg, 28%) .

^{1}H NMR (300 MHz, $CDCl_3$): δ = 8.71 (d, *J* = 4.7 Hz, 1 H), 8.24 (m, 1 H), 8.06 (m, 2 H), 7.96 (d, *J* = 7.8 Hz, 1 H), 7.87 (dt, *J* = 7.7, 1.6 Hz, 1 H), 7.63 (d, *J* = 8.2 Hz, 2 H), 7.52 (m, 1 H), 7.23 (d, *J* = 8.3 Hz, 2 H), 2.39 (s, 3 H).

^{13}C NMR (75.5 MHz, $CDCl_3$): δ = 191.6 (C), 166.0 (C), 154.1 (C), 153.7 (C), 149.1 (CH), 141.6 (C), 140.5 (C), 138.8 (CH), 136.6 (CH), 129.8 (CH), 126.5 (CH), 125.7 (CH), 125.3 (CH), 124.8 (CH), 122.4/122.2 (CH), 120.8 (CH), 21.4 (CH_3).

MS (EI): m/z(%) = 322(100), 305(15), 261(20), 216(20), 199(25), 149(25), 123(40), 106(25), 78(80).

HRMS for $C_{18}H_{14}N_2O_2S$: calcd. 322.0776 found 322.0764.

(+)-[(*S*)-*R*]-1-([1,2,3]Triazolo[1,5-*a*]pyridin-3-yl)-2-(*p*-tolylsulfinyl) ethanone (41)

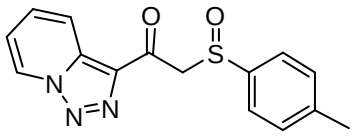

At 0 °C, butyllithium (11 mL, 16 mmol, 2 eq) in hexanes (1.5M) was added to a solution of di-*iso*-propylamine (2.2 mL, 16 mmol, 2 eq) in tetrahydrofuran (40 mL). After 15 min, the mixture was canulated into a solution of (+)-(*R*)-methyl-*p*-tolylsulfoxide (2.4 g, 16 mmol, 2.0 eq.) in tetrahydrofuran (40 mL) dropwise . The mixture was kept for 2 h at 0 °C before a solution of ethyl [1,2,3]triazolo[1,5-*a*]pyridine-3-carboxylate (1.5 g, 8 mmol, 1 eq) in tetrahydrofuran (40 mL) was added and allowed to reach 20 °C (1 h). The reaction mixture was quenched with a saturated aqueous solution of ammonium chloride (30 mL). Then the resulting mixture was extracted with dichloromethane (3×20 mL). The organic extracts were combined, washed with brine (300 mL), dried over sodium sulfate, filtered, and concentrated. Chromatography (silica gel, ethyl acetate/cyclohexane gradient) provided (+)-[(S)-*R*]-1-([1,2,3]triazolo[1,5-*a*]pyridin-3-yl)-2-(*p*-tolylsulfinyl) ethanone (**41**) as yellow solid, (2.0 g, 85%). mp 163 – 164 °C**.** $[\alpha]_D^{22}$ = +192.2 (c = 1 in acetone).

^{1}H NMR (300 MHz, $CDCl_3$): δ = ppm 8.83 (td, *J* = 7.0, 1.0, 1.0 Hz, 1H), 8.38 (td, *J* = 8.8, 1.1, 1.0 Hz, 1H), 7.67-7.60 (m, 3H), 7.28 (d, *J* = 8.5 Hz, 2H), 7.23 (dt, *J* = 6.9, 6.9, 1.1 Hz, 1H), 4.66 (AB, *J* = 13.3 Hz, Δv = 53.4 Hz, 2H), 2.37 (s, 3H).

^{13}C NMR (75.5 MHz, $CDCl_3$): δ = 185.0 (CO), 141.9 (C), 140.4 (C), 136.7 (C), 134.2 (C), 131.0 (CH), 129.9 (2×CH), 125.9 (CH), 124.3 (2×CH), 119.9 (CH), 117.3 (CH), 66.1 (CH_2), 21.4 (CH_3).

MS (EI): m/z(%) = 299(15), 148(60), 139(31), 104(35), 86(60), 84(100), 78(40).

HRMS for $C_{15}H_{13}N_3O_2S$ calcd [M+Na]: 322.0626 found: 322.0620

(+)-[(*S*)-*R*]-1-(Pyridin-2-yl)-2-(*p*-tolylsulfinyl)ethanone (42)

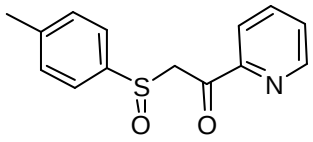

At 0 °C, butyllithium (11 mL, 16 mmol, 2 eq) in hexanes (1.5M) was added to a solution of di-*iso*-propylamine (2.2 mL, 16 mmol, 2 eq) in tetrahydrofuran (40 mL). After 15 min, the mixture was canulated to a solution of (+)-(*R*)-methyl-*p*-tolylsulfoxide (2.4 g, 16 mmol, 2.0 eq.) in tetrahydrofuran (40 mL) dropwise. The mixture was kept for 2 h at 0 °C before a solution of methyl picolinate (1.1 g, 8 mmol, 1 eq) in tetrahydrofuran (40 mL) was added and allowed to arrive to 20 °C (1 h). The reaction mixture was quenched with a saturated aqueous solution of ammonium chloride (30 mL). Then the resulting mixture was extracted with dichloromethane (3×20 mL). The organic extracts were combined, washed with brine (300 mL), dried over sodium sulfate, filtered, and concentrated. Chromatography (silica gel, ethyl

acetate/cyclohexane 1:3) provided (+)-[(*S*)-*R*]-1-(pyridin-2-yl)-2-(*p*-tolylsulfinyl)ethanone (**42**) as colourless solid, (1.9 g, 93%). mp 89-90 °C; $[\alpha]_D^{22}$ = +149 (c = 0.6 in acetone).

^{1}H NMR (300 MHz, $CDCl_3$): δ = 8.65 (dt, *J* = 1.1, 7.8 Hz, 1H), 8.03 (dt, *J* = 9.3, 1.3 Hz,1H),
7.85 (td, *J* = 9.3, 1.1 Hz, 1 H), 7.50 (ddd, *J* = 7.6, 4.8, 1.7 Hz, 1 H), 7.59 and 7.28 (AA'BB' system, 4 H), 4.82 and 4.60 (AB system, *J* = 13.6 Hz,2 H), 2.39 (s, 3 H).

(+)-[(*S*)-*R*]-3-(*p*-Tolylsulfinylmethyl)-[1,2,3]triazolo[1,5-*a*]pyridine (43)

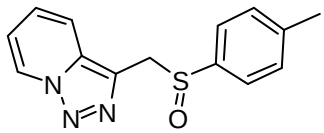

A mixture of (+)-[(*S*)-*R*]-1-(pyridin-2-yl)-2-(p-tolylsulfinyl) ethanone (**42**) (0.8 g, 2.9 mmol, 1 eq) and hydrazine monohydrate (0.2 g, 3.8 mmol, 1.3 eq) in methanol (50 mL) was heated to reflux. The reaction was monitored by TLC upon completion of the reaction (3 h). The reaction mixture was quenched with an aqueous solution of sodium hydroxide (10 mL, 30%), concentrated until complete evaporation of methanol. The resulting mixture was extracted with dichloromethane (3×20 mL). The organic extracts were combined, washed with brine (20 mL), dried over sodium sulfate, filtered, and concentrated providing the corresponding hydrazone. The hydrazone was directly diluted in chloroform (50 ml) then activated manganese dioxide (0.6 g, 6 mmol, 2 eq) was added and the heterogeneous mixture was heated to reflux over the night. The resulting mixture was cooled to 25 °C and filtrated with celite. After concentration (+)-[(S)-*R*]-3-(p-tolylsulfinylmethyl)-[1,2,3]triazolo[1,5-*a*]pyridine (**43**) was obtained as a brown solid. (0.7 g, 95%). mp 148 – 150 °C**.** $[\alpha]_D^{22}$ = + 247.9 (c = 1 in acetone).

^{1}H NMR (300 MHz, $CDCl_3$): δ = 8.65 (td, *J* = 7.0, 1.0, 1.0 Hz, 1H), 7.66 (td, *J* = 8.9, 1.1, 1.0 Hz, 1H), 7.35 (d, *J* = 8.1 Hz, 2H), 7.23 (d, *J* = 8.1 Hz, 1H), 7.19 (ddd, *J* = 8.9, 6.7, 0.9 Hz, 1H), 6.96 (dt, *J* = 7.0, 6.7, 1.1 Hz, 1H), 4.45 (AB, *J* = 13.7 Hz, , Δν = 20.9 Hz, 2H), 2.37 (s, 1H).

^{13}C NMR (75.5 MHz, $CDCl_3$): δ = 141.9 (C), 139.6 (C), 133.8 (C), 129.8 (2×CH), 128.5 (C), 125.5 (CH), 125.2 (CH), 124.0 (2×CH), 118.3 (CH), 115.5 (CH), 54.7 (CH_2), 21.4 (CH_3). MS **(EI) m/z(%)** 246(100) [M – N_2 + H], 123(70), 104(41).

HRMS for $C_{14}H_{13}N_3OS$ calcd [M+Na] : 294.0677 found: 294.0670.

7.1.3 Chapter III : [1,2,3]Triazolo[1,5-*a*]quinolines

[1,2,3]triazolo[1,5-*a*]quinoline (44)

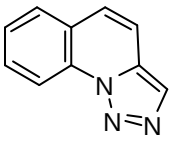

A mixture of quinoline-2-carbaldehyde (8.1 g, 52 mmol, 1 eq) and hydrazine monohydrate (4.5 mL, 80 mol, 1.5 eq) in methanol (150 mL) was heated ted to reflux. The reaction was monitored by TLC upon completion of the reaction (3 h). The reaction mixture was quenched with an aqueous solution of sodium hydroxide (30 mL, 30%) and the resulting mixture was extracted with dichloromethane (3×50 mL) The organic extracts were combined, washed with brine (3×20 mL), dried over sodium sulfate, filtered, and concentrated providing the corresponding hydrazone. The hydrazone was directly diluted in chloroform (150 mL), then activated manganese dioxide (11 g, 0.1 mol, 2 eq) was added and the heterogeneous mixture was heated to reflux over the night. The resulting mixture was cooled to 25 °C and filtered over celite. After concentration [1,2,3]triazolo[1,5-*a*]quinoline (**44**) was obtained as a colourless solid (8 g, 90%). mp 80 – 81 °C**.**[12]

^{1}H NMR (300 MHz, $CDCl_3$): δ = 8.71 (d, *J* = 8.4 Hz, 1H), 8.06 (s, 1H), 7.76 (dd, *J* = 7.9, 1.1 Hz, 1H), 7.68 (ddd, *J* = 8.5, 7.3, 1.4 Hz, 1H), 7.53 (t, *J* = = 7.6, 7.6 Hz, 1H), 7.48 (d, *J* = 9.3 Hz, 1H), 7.44 (d, *J* = 9.4 Hz, 1H)

^{13}C NMR (75.5 MHz, $CDCl_3$): δ = 131.7 (C), 131.7 (C), 130.0 (CH), 128.5 (CH), 127.5(C), 127.0 (CH), 126.6 (CH), 123.8 (C), 116.2 (CH), 114.6 (CH).

Methyl-[1,2,3]triazolo[1,5-*a*]quinoline (45a)

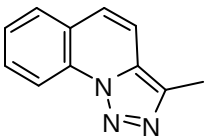

At 0 °C, butyllithium (3.94 mL, 5.92 mmol, 1.0 eq) in hexanes (1.5 M) was added to a solution of 2,2,6,6-tetramethylpiperidine (0.99 mL, 0.83 g, 5.92 mmol, 1.0 eq) in tetrahydrofuran (50.0 mL). After 15 min, the mixture was cooled to -78 °C and canulated into a solution of [1,2,3]triazolo[1,5-*a*]quinoline (**44**) (0.99 g, 5.91 mmol, 1.0 eq) in tetrahydrofuran (75.0 mL). The mixture was kept for 2 h at -78 °C before iodomethane (0.62 mL, 1.42 g, 10.0 mmol, 1.7 eq) was added and allowed to reach 20 °C in the course of 1 h. A saturated aqueous solution of ammonium chloride (20.0 mL) was added and the product extracted into dichloromethane (3×50.0 mL), washed with brine (10.0 mL) and dried over Na_2SO_4. The product was purified by flash chromatography on silica gel using a gradient of ethyl acetate/cyclohexane to give 3-methyl-[1,2,3]triazolo[1,5-*a*]quinoline (**2a**) as a yellow solid (0.93 g, 86%). mp 114–115 °C**.**

^{1}H NMR (300 MHz, $CDCl_3$): δ = 8.74 (d, *J* = 8.0 Hz, 1H), 7.80 (dd, *J* = 7.9 , 0.9 Hz, 1 H), 7.72 (ddd, *J* = 8.0, 7,8 , 0.9 Hz, 1H), 7.56 (dd, *J* = 7.9 , 7.8 Hz,1H), 7.42(app. s, 2H) , 2.64 (s, 3H).

^{13}C NMR (75 MHz, $CDCl_3$): δ = 136 (C), 132 (C), 129.8 (CH), 129.3 (C), 127.7 (CH), 126.5 (CH), 124.8 (CH), 123.8 (C), 115.7 (CH), 114.1 (CH), 10.0 (CH_3);

HRMS (EI) calcd. for $C_{11}H_9N_3$: 183.0796, found: 183.0800.

Anal. calcd. for $C_{11}H_9N_3$ (183.21): C 71.11; H 4.95; N 22.94. found: C 71.54; H 5.04; N 23.04.

3-(Deuterio)-[1,2,3]triazolo[1,5-*a*]quinoline (45b)

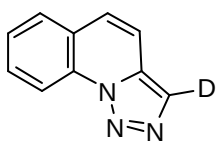

Prepared analogously as compound **45a** starting from [1,2,3]triazolo[1,5-*a*]quinoline (**44**) (0.49 g, 2.9 mmol, 1 eq) and trapping of the lithiated intermediate with excess methanol-d_4 (1.0 mL) affording 3-(deuterio)-[1,2,3]triazolo[1,5-*a*]quinoline (**45b**) as an orange solid (0.48 g, 96%). mp 81–83 °C**.**

^{1}H NMR (300 MHz, $CDCl_3$): δ = 8.71 (d, *J* = 8.3 Hz, 1H), 7.76 (dd, *J* = 7.9, 1.0 Hz, 1H), 7.69 (dd, *J* = 8.3, 7.7 Hz, 1H), 7.5-7.4 (m, 2H), 7.44 (d, *J* = 9.3 Hz, 1H).

^{13}C NMR (75 MHz, $CDCl_3$): δ = 131.8 (C), 131.6 (C), 130.0 (CH), 128.5 (CH), 127.3 (C, t, $J_{C\text{-}D}$ = 29.9 Hz, CD), 127.0 (CH), 126.6 (CH), 123.8 (C), 116.2 (CH), 114.7 (CH).

3-(Trimethylsilyl)-[1,2,3]triazolo[1,5-*a*]quinoline (45c)

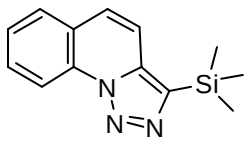

Prepared analogously as compound **45a** and trapping of the lithiated intermediate with chlorotrimethylsilane (1.26 mL, 1.09 g, 10 mmol, 1.7 eq) affording 3-(trimethylsilyl)-[1,2,3]triazolo[1,5-*a*]quinoline (**45c**) as an orange solid (1.37 g, 96%). mp 99–101 °C**.**

^{1}H NMR (300 MHz, $CDCl_3$): δ = 8.80 (d, *J* = 8.3 Hz, 1H), 7.76 (dd, *J* = 7.9, 1.1 Hz, 1H), 7.69 (ddd, *J* = 8.3, 7.9, 1.1 Hz, 1H), 7.6-7.5 (m, 2H), 7.46 (d, *J* = 9.3, 1H), 0.49 (s, $Si(CH_3)_3$).

^{13}C NMR (75 MHz, $CDCl_3$): δ 139.4 (C), 136.8 (C), 132.2 (C), 129.8 (CH), 128.3 (CH), 126.8 (CH), 126.3 (CH), 123.7 (C), 116.7 (CH), 115.0 (CH), -0.76 (3×CH_3).

HRMS (EI) calcd. for $C_{13}H_{15}N_3Si$: 241.1035, found: 241.1032.

3-Iodo-[1,2,3]triazolo[1,5-*a*]quinoline (45d)

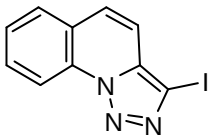

Prepared analogously as compound **45a** and trapping of the lithiated intermediate with a solution of iodine (2.41 g, 9.5 mmol, 1.6 eq) in tetrahydrofuran (15.0 mL) affording 3-iodo-[1,2,3]triazolo[1,5-*a*]quinoline (**45d**) as a colourless solid (1.22 g, 70%). mp 136–138 °C**.**

^{1}H NMR (300 MHz, $CDCl_3$): δ = 8.76 (d, *J* = 8.3 Hz, 1H), 7.87 (dd, *J* = 7.9, 1.0 Hz, 1H), 7.74 (ddd, *J* = 8.3, 7.9, 1.0 Hz, 1H), 7.67–7.57 (m, 2H), 7.41 (d, *J* = 9.3 Hz, 1H).

^{13}C NMR (75 MHz, $CDCl_3$): δ 134.2 (C), 131.6 (C), 130.2 (CH), 128.5 (CH), 127.6 (CH), 127.4 (CH), 123.9 (C), 115.9 (CH), 114.2 (CH), 81.7 (C).

HRMS (ESI-TOF) calcd. for $C_{10}H_6IN_3[M+Na]^+$: 317.9499, found: 317.9458.

(+)-[(*S*)-*R*]-3-(*p*-Tolylsulfinyl)-[1,2,3]triazolo[1,5-*a*]quinoline (45e)

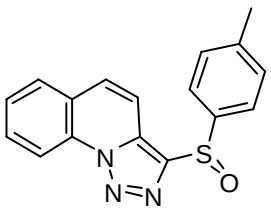

Prepared analogously as compound **45a** and trapping of the lithiated intermediate by addition into a solution of (1*R*,2*S*,5*R*)-(-)-menthyl-(*S*)-*p*-toluenesulfinate (2.21 g, 7.40 mmol, 1.3 eq) in tetrahydrofuran (50.0 mL) at -45 °C. Usual workup and purification by flash chromatography on silica gel using a gradient of ethyl acetate/cyclohexane (from 1:3 to 1:1) afforded (+)-[(*S*)-*R*]-3-(*p*-tolylsulfinyl)-[1,2,3]triazolo[1,5-*a*]quinoline (**45e**) as a colourless solid (1.49 g, 82%). mp 145–147 °C; $[\alpha]_D^{22}$ = +104.2 (c = 1 in acetone).

^{1}H NMR (300 MHz, $CDCl_3$): δ 8.78 (d, *J* = 8.4 Hz, 1H), 7.87 (dd, *J* = 7.9 , 1.0 Hz, 1H), 7.81 (ddd, *J* = 8.4, 7.3, 1.2 Hz, 1H), 7.71 (m, 3H), 7.63 (m, 2H), 7.32 (d, *J* = 8.0 Hz, 2H) , 2.39 (s, CH_3).

^{13}C NMR (75 MHz, $CDCl_3$): δ 142.4 (C), 141.7 (C), 140.3 (C), 131.7 (C), 131.1 (C), 130.7 (CH), 130.1 (2×CH), 129.1 (CH), 128.7 (CH), 127.9 (CH), 124.6 (2×CH), 124.0 (C), 116.4 (CH), 114.4 (CH), 21.4 (CH_3).

HRMS (EI) calcd. for $C_{17}H_{13}N_3OS$: 307.0779, found: 307.0784.

9-Methyl-[1,2,3]triazolo[1,5-*a*]quinoline (46)

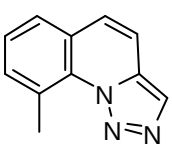

At 25 °C, tetrabutylamonium fluoride (1.20 mL, 1.20 mmol, 1.9 eq) in tetrahydrofuran (1 M) was added to a solution of 9-methyl-3-(trimethylsilyl)-[1,2,3]triazolo[1,5-*a*]quinoline (**48a**) (0.15 g, 0.60 mmol, 1.0 eq) in tetrahydrofuran (15.0 mL). After 1 h at 25 °C, a saturated aqueous solution of sodium chloride

(20.0 mL) was added. The product was extracted into dichloromethane (3×50 mL), washed with brine (10.0 mL) and dried over sodium sulfate. Flash chromatography on silica gel using a mixture of ethyl acetate/cyclohexane (2:3) gave 9-methyl-[1,2,3]triazolo-[1,5-*a*]quinoline (**46a**) as a colorless solid (0.10 g, 92%). mp 102 – 103 °C**.**

^{1}H NMR (300 MHz, $CDCl_3$): δ = 8.04 (s, 1H), 7.60 (d, *J* = 7.7 Hz, 1H), 7.50 (d, *J* = 7.2 Hz, 1H), 7.5-7.4 (m, 3H), 3.16 (s, CH_3).

^{13}C NMR (75 MHz, $CDCl_3$): δ = 132.9 (CH), 132.7 (C), 131.6 (C), 129.5 (C), 127.6 (CH), 126.3 (CH), 126.2 (CH), 126.0 (CH), 125.2 (C), 114.2 (CH), 24.3 (CH_3).

HRMS (EI) calcd. for $C_{11}H_9N_3$: 183.0796, found: 183.0791.

3,9-Dimethyl-[1,2,3]triazolo[1,5-*a*]quinoline (47a)

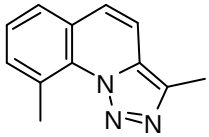

At -78 °C, butyllithium (2.36 mL, 3.54 mmol, 3.0 eq) in hexanes (1.5M) was added to a solution of [1,2,3]triazolo[1,5-*a*]quinoline (**44**) (0.19 g, 1.18 mmol, 1.0 eq) in tetrahydrofuran (15.0 mL). After 2 h at -78 °C, iodomethane (0.24 mL, 0.54 g, 3.8 mmol, 3.2 eq) was added and allowed to reach 20 °C in the course of 1h. A saturated aqueous solution of ammonium chloride (20.0 mL) was added and the product extracted into dichloromethane (3×10 mL), washed with brine (10.0 mL) and dried over Na_2SO_4. The product was purified by flash chromatography on silica gel using a 1:1 mixture of ethyl acetate/cyclohexane as eluent which provided 3,9-dimethyl-[1,2,3]triazolo[1,5-*a*]quinoline **47a** as a yellow solid (0.19 g, 82%). mp 84–85 °C**.**

^{1}H NMR (300 MHz, $CDCl_3$): δ = 7.62 (dd, *J* = 7.7, 0.9 Hz, 9H), 7.51 (dd, *J* = 7.4 , 0.9 Hz, 9H), 7.43 (dd, *J* = 7.7, 7.4 Hz, 1H), 7.38 (app. s, 2H), 3.18 (s, CH_3), 2.63 (s, CH_3).

^{13}C NMR (75 MHz, $CDCl_3$): δ = 134.7 (C), 132.8 (CH), 131.9 (C), 130.4 (C), 129.6 (C), 126.4 (CH), 126.3 (CH), 126.2 (CH), 125.5 (C), 114.1 (CH), 24.4 (9-CH_3), 10.2 (3-CH_3).

HRMS (EI) calcd. for $C_{12}H_{11}N_3$: 197.0952, found: 197.0949.

Anal. calcd. for $C_{12}H_{11}N_3$ (197.24): C 73.07; H 5.62; N 21.30. found: C 72.65; H 5.71; N 21.48.

3,9-Diiodo-[1,2,3]triazolo[1,5-*a*]quinoline (47b)

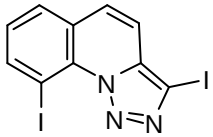

Prepared analogously as compound **47a** starting from [1,2,3]triazolo[1,5-*a*]quinoline (**44**) (0.99 g, 5.9 mmol, 1.0 eq) and trapping of the lithiated intermediate with a solution of iodine (6.09 g, 24 mmol, 4.0 eq).

Crystallization from dichloromethane gave 3,9-diiodo-[1,2,3]triazolo[1,5-*a*]quinoline (**47b**) as pale yellow needles (2.06 g, 82%). mp 144 °C decomp.

^{1}H NMR (300 MHz, $CDCl_3$): δ = 8.44 (dd, *J* = 7.7 , 1.3 Hz, 1H), 7.83 (dd, *J* = 7.8, 1.3 Hz, 1H), 7.52 (d, *J* = 9.3 Hz, 1H), 7.46 (d, *J* = 9.3 Hz, 1H), 7.25 (dd, *J* = 7.7, 7.8 Hz, 1H).

^{13}C NMR (75 MHz, $CDCl_3$): δ = 145.0 (CH), 134.8 (C), 133.4 (C), 129.2 (CH), 128.3 (CH), 127.9 (CH), 126.7 (2×C), 115.2 (CH), 83.2 (C).

HRMS (EI) calcd. for $C_{10}H_5I_2N_3$: 420.8573, found: 420.8567.

Anal. calcd. for $C_{10}H_5I_2N_3$ (426.02): C 28.53; H 1.23; N 9.98. found: C 28.00; H 1.26; N 9.98.

3,9-Dibromo-[1,2,3]triazolo[1,5-*a*]quinoline (47c)

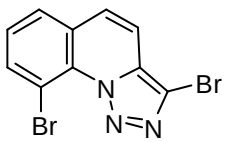

Prepared analogously as compound **47a** starting from [1,2,3]triazolo[1,5-*a*]quinoline (**44**) (0.44 g, 2.6 mmol, 1.0 eq) followed by addition of 1,2-dibromo-1,1,2,2-tetrafluoroethane (2.70 g, 10.4 mmol, 4.0 eq) affording after crystallization from dichloromethane/hexanes 3,9-dibromo-[1,2,3]triazolo[1,5-*a*]quinoline (**47c**) as pale brown needles (0.62 g, 74%). mp 166 – 168 °C**.**

^{1}H NMR (300 MHz, $CDCl_3$): δ = 8.05 (dd, *J* = 7.8, 1.3 Hz, 1H), 7.79 (dd, *J* = 7.9, 1.3 Hz, 1H), 7.53 (d, *J* = 9.3 Hz, 1H), 7.47 (d, *J* = 9.3 Hz, 1H), 7.42 (dd, *J* = 7.9, 7.8 Hz, 1H).

^{13}C NMR (75 MHz, $CDCl_3$): δ = 137.3 (CH), 131.4 (C), 130.8 (C), 128.4 (CH), 128.0 (CH), 127.7 (CH), 127.2 (C), 114.5 (CH), 114.4 (C), 110.3 (C).

HRMS (ESI-TOF) calcd. for $C_{10}H_5{}^{79}Br_2N_3$ $[M+Na]^+$: 347.8742, found: 347.8719. calcd. for $C_{10}H_5{}^{79}Br^{81}BrN_3$ $[M+Na]^+$: 349.8722, found: 349.8296. calcd. for $C_{10}H_5{}^{81}Br_2N_3$ $[M+Na]^+$: 351.8703, found: 351.8684.

Anal. calcd. for $C_{10}H_5Br_2N_3$ (326.97): C 36.73; H 1.54; N 12.85. found: C 36.24; H 1.67; N 12.64.

3,9-Dichloro-[1,2,3]triazolo[1,5-*a*]quinoline (47d)

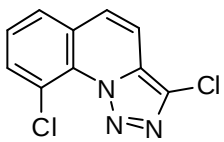

Prepared analogously as compound **47a** starting from [1,2,3]triazolo[1,5-*a*]quinoline (**44**) (0.43 g, 2.6 mmol, 1.0 eq) and trapping of the lithiated intermediate with 1,1,2-trichloro-1,2,2-trifluoroethane (1.24 mL, 1.94 g, 10.4 mmol, 4.0 eq). After crystallization from cold dichloromethane/hexanes, 3,9-chloro-[1,2,3]triazolo[1,5-*a*]quinoline (**47d**) was obtained as pale brown needles (0.43 g, 71%). mp 169 – 171 °C**.**

^{1}H NMR (300 MHz, $CDCl_3$): δ = 7.76 (d, *J* = 7.9, 1.1 Hz, 1H), 7.71 (dd, *J* = 7.9, 1.1 Hz, 1H), 7.5-7.4 (m, 3H).

^{13}C NMR (75 MHz, $CDCl_3$): δ = 133.3 (CH), 129.4 (C), 129.1 (C), 127.8 (C), 127.7 (CH), 127.6 (CH), 127.3 (CH), 126.9 (C), 123.9 (C), 113.9 (CH).

HRMS (ESI-TOF) calcd. for $C_{10}H_5{}^{35}Cl_2N_3$ $[M+Na]^+$: 259.9753, found: 259.9774. calcd. for $C_{10}H_5{}^{35}Cl{}^{37}ClN_3$ $[M+Na]^+$: 261.9724, found: 261.9748. calcd. for $C_{10}H_5{}^{37}Cl_2N_3$ $[M+Na]^+$: 263.9697, found: 263.9736.

Anal. calcd. for $C_{10}H_5Cl_2N_3$ (238.07): C 50.45; H 2.12; N 17.63. found: C 50.20; H 2.37; N 17.22.

9-Methyl-3-(trimethylsilyl)-[1,2,3]triazolo[1,5-*a*] quinoline (48a)

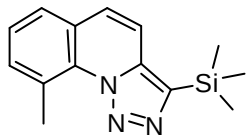

At -78 °C, butyllithium (0.90 mL, 1.40 mmol, 1.7 eq) in hexanes (1.5 M) was added to a solution of 3-(trimethylsilyl)-[1,2,3]triazolo[1,5-*a*]quinoline (**45c**) (0.19 g, 0.80 mmol, 1.0 eq) in tetrahydrofuran (15.0 mL). After 2 h at -78 °C, iodomethane (0.11 mL, 1.76 g, 1.7 mmol, 1.2 eq) was added and the mixture allowed to reach 20 °C. The reaction was quenched with a saturated aqueous solution of ammonium chloride (20.0 mL) followed by extraction into dichloromethane (3×10 mL). The combined organic extracts were washed with brine (10.0 mL), dried over sodium sulfate affording 9-methyl-3-(trimethylsilyl)-[1,2,3]triazolo[1,5-*a*]quinoline (**48a**) as yellow solid (0.2 g, 99%). mp 106 – 108 °C**.**

^{1}H NMR (300 MHz, $CDCl_3$): δ = 7.66 (d, *J* = 8.1 Hz, 1H), 7.6-7.5 (m, 2H), 7.5-7.4 (m, 2H), 3.21 (s, CH_3), 0.49 (s, $Si(CH_3)_3$).

^{13}C NMR (75 MHz, $CDCl_3$): δ = 137.9 (C), 137.7 (C), 132.9 (CH), 132.1 (C), 129.8 (C), 127.6 (CH), 126.3 (CH), 126.2 (CH), 125 .3 (C), 115.5 (CH), 24.6 (CH_3), -0.81 (3×CH_3).

HRMS (EI) calcd. for $C_{14}H_{17}N_3Si$: 255.1191, found: 255.1201.

9-Iodo-3-(trimethylsilyl)-[1,2,3]triazolo[1,5-*a*] quinoline (48b)

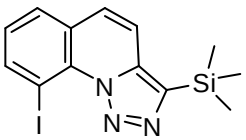

At -78 °C, butyllithium (0.90 mL, 1.40 mmol, 1.7 eq) in hexanes (1.5 M) was added to a solution of 3-(trimethylsilyl)-[1,2,3]triazolo[1,5-*a*]quinoline (**45c**) (0.19 g, 0.80 mmol, 1.0 eq) in tetrahydrofuran (15.0 mL). After 2 h at -78 °C, iodine (0.24 g, 0.96 mmol, 1.2 eq.) in THF (5.0 mL) was added and the mixture allowed to reach 20 °C. The product was characterized by HRMS as the product decomposed during purification.

HRMS (EI) calcd. for $C_{13}H_{14}IN_3Si$: 367.0001, found: 366.9999.

9-Fluoro-[1,2,3]triazolo[1,5-*a*]quinoline (49)

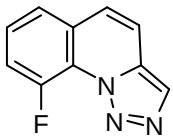

At -78 °C, butyllithium (2.33 mL, 3.50 mmol, 3.0 eq) in hexanes (1.5 M) was added to a solution of [1,2,3]triazolo[1,5-*a*]quinoline (**44**) (0.20 g, 1.20 mmol, 1.0 eq) in tetrahydrofuran (15.0 mL). After 2 h at -78 °C, a solution of *N*-fluorodibenzenesulfonimide (1.01 g, 3.50 mmol, 3.0 eq) in tetrahydrofuran (20.0 mL) was added and allowed to reach 20 °C during 1 h. After addition of a saturated aqueous solution of ammonium chloride (50.0 mL), the product was extracted into ethyl acetate (3×50.0 mL), washed with brine (10.0 mL) and dried over sodium sulfate. Flash chromatography over silica gel using a 1:1 mixture of ethyl acetate/cyclohexane afforded 9-fluoro-[1,2,3]triazolo[1,5-*a*]quinoline (**49**) as a brown solid (0.14 g, 60%). mp 109 – 111 °C**.**

^{1}H NMR (300 MHz, $CDCl_3$): δ = 8.12 (d, $J_{F\text{-}H}$ = 0.4 Hz, 1H), 7.6-7.4 (m, 5H).

^{13}C NMR (75 MHz, $CDCl_3$): δ = 152.8 (d, $J_{F\text{-}C}$ = 259.5 Hz, 9-C), 132.4 (s, 2×C), 127.1 (d, $J_{F\text{-}C}$ = 7.6 Hz, CH), 126.8 (d, $J_{F\text{-}C}$ = 1.5 Hz, C), 126.6 (d, $J_{F\text{-}C}$ = 1.3 Hz, CH), 126.5 (d, $J_{F\text{-}C}$ = 2.2 Hz, CH), 124.0 (d, $J_{F\text{-}C}$ = 4.2 Hz, CH), 117.1 (d, $J_{F\text{-}C}$ = 19.5 Hz, CH), 115.8 (d, $J_{F\text{-}C}$ = 1.5 Hz, CH);

HRMS (ESI-TOF) calcd. for $C_{10}H_6FN_3$ $[M+Na]^+$: 210.0438, found: 210.0440.

(8-Fluoroquinolin-2-yl)methyl acetate (50)

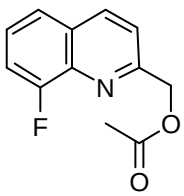

A solution of 9-fluoro-[1,2,3]triazolo[1,5-*a*]quinoline (**49**) (18.7 mg, 0.100 mmol, 1 eq) in acetic acid (15.0 mL) was heated under reflux during 8 h. After cooling to room temperature, excess acetic acid was distilled off and the residue neutralized with a saturated aqueous solution of sodium hydrogen carbonate (5.00 mL). The aqueous phase was extracted with dichloromethane (3×10.0 mL), washed with brine (10.0 mL) and dried over sodium sulfate. The product was purified by flash

chromatography on silica gel using a 1:1 mixture of ethyl acetate/cyclohexane as eluent which provided 8-fluoroquinolin-2-yl)methyl acetate (**50**) as a colorless oil (15.3 mg, 70%).

^{1}H NMR (300 MHz, $CDCl_3$): δ = 8.14 (dd, *J* = 8.6, 1.5 Hz, 1H), 7.54 (d, *J* = 8.0, 1H), 7.41 (d, *J* = 8.6, 1H) 7.4-7.3 (m, 2H), 5.38 (s, CH_2), 2.13 (d, *J* = 3.5 Hz, CH_3).

^{13}C NMR (75 MHz, $CDCl_3$): δ = 170.6 (COO), 157.9 (d, J_{F-C} = 256.9 Hz, C), 156.7 (d, J_{F-C} = 1.5 Hz, C), 137.9 (d, J_{F-C} = 11.7 Hz, C), 136.7 (d, J_{F-C} = 3.1 Hz, CH), 129.4 (d, J_{F-C} = 2.2 Hz, C), 126.5 (d, J_{F-C} = 8.0 Hz, CH), 123.3 (d, J_{F-C} = 4.7 Hz, CH), 120.3 (CH), 113.9 (d, J_{F-C} = 19.0 Hz, CH), 67.3 (CH_2), 20.9 (CH_3).

HRMS (ESI-TOF) calcd. for $C_{12}H_{10}FNO_2$ $[M+Na]^+$: 242.0588, found: 242.0554.

8-Iodoquinoline-2-carbaldehyde (51a)

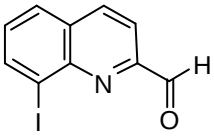

3,9-Diiodo-[1,2,3]triazolo[1,5-*a*]quinoline (**47b**) (0.13 g, 0.30 mmol, 1.0 eq.) was diluted in a mixture of water (8.00 mL), tetrahydrofuran (2.00 mL) and acetic acid (2.00 mL) and heated to reflux. The reaction, becoming deep red when the reagent was completely consumed, was monitored by TLC. Upon completion of the reaction (4 h), acetic acid was separated by distillation and the reaction mixture was quenched with a saturated aqueous solution of sodium thiosulphate (20.0 mL), observing the disappearance of the red coloration. The mixture was treated with a saturated aqueous solution of sodium hydrogen carbonate (5.0 mL) until pH 8 and the product extracted into dichloromethane (3×10 mL). The organic layers were combined, washed with brine (20.0 mL) and dried over sodium sulfate. Flash column chromatography on silica gel using a gradient ethyl acetate/cyclohexane (1:5 to 2:1) gave 8-iodoquinoline-2-carbaldehyde (**51a**) as a yellow solid (76.4 mg, 90%). mp 149 – 151 °C**.**

^{1}H NMR (300 MHz, $CDCl_3$): δ = 10.30 (s, CHO), 8.44 (dd, *J* = 7.4, 1.2 Hz, 1H), 8.25 (d, *J* = 8.4 Hz, 1H), 8.05 (d, *J* = 8.4 Hz, 1H), 7.89 (dd, *J* = 8.2, 1.2 Hz, 1H), 7.39 (dd, *J* = 8.2, 7.4 Hz, 1H).

^{13}C NMR (75 MHz, $CDCl_3$): δ = 193.4 (CH), 153.4 (C), 146.8 (C), 141.2 (CH), 138.3 (CH), 130.7 (C), 130.1 (CH), 128.7 (CH), 118.1 (CH), 104.8 (C).

HRMS (ESI-TOF) calcd. for $C_{10}H_6INO$ $[M+Li]^+$: 289.9649, found: 289.9640.

Anal. calcd. for $C_{10}H_6INO$ (283.07): C 42.30; H 2.14; N 4.830. found: C 42.30; H 2.43; N 4.83.

8-Bromoquinoline-2-carbaldehyde (51b)

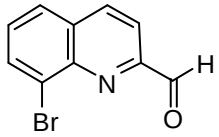

3,9-Dibromo-[1,2,3]triazolo[1,5-*a*]quinoline (**47c**) (98.1 mg, 0.30 mmol, 1.0 eq.) was diluted in aqueous sulfuric acid (10.0 mL, 2.5 M) and heated to reflux. The reaction was monitored by TLC. Upon completion of the reaction (6 h) a saturated aqueous solution of sodium hydrogen carbonate (5.0 mL) was added until pH 8. The resulting mixture was extracted with dichloromethane (3×10 mL), washed with brine (20.0 mL) and dried over sodium sulfate. Flash column chromatography on silica gel using a gradient ethyl acetate/cyclohexane (1:5 to 2:1) gave 8-bromoquinoline-2-carbaldehyde (**51b**) as a yellow solid (57.4 mg, 81%). mp 135 – 137 °C**.**

^{1}H NMR (300 MHz, $CDCl_3$): δ = 10.30 (s, CHO), 8.32 (d, *J* = 8.3 Hz, 1H), 8.15 (d, *J* = 7.5 Hz, 1H), 8.08 (d, *J* = 8.3 Hz, 1H), 7.87 (d, *J* = 8.3 Hz, 1H), 7.53 (dd, *J* = 8.3, 7.5 Hz, 1H).

^{13}C NMR (75 MHz, $CDCl_3$): δ = 193.4 (CH), 153.1 (C), 145.0 (C), 138.1 (CH), 134.2 (CH), 131.3 (C), 129.4 (CH), 127.7 (CH), 126.1 (C), 118.0 (CH).

HRMS (ESI-TOF) calcd. for $C_{10}H_6{}^{79}BrNO$ $[M+Li]^+$: 241.9788, found: 241.9756. calcd. for $C_{10}H_6{}^{81}BrNO$ $[M+Li]^+$: 243.9768, found: 243.9736.

8-Chloroquinoline-2-carbaldehyde (51c)

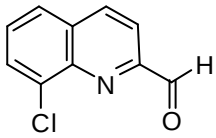

3,9-Dichloro-[1,2,3]triazolo[1,5-*a*]quinoline (**47d**) (0.14 g, 0.6 mmol, 1.0 eq.) was diluted in aqueous sulfuric acid (15.0 mL, 7 M) and heated to reflux. The reaction was monitored by TLC. Upon completion of the reaction (24 h), a saturated aqueous solution of sodium hydrogen carbonate (5.0 mL) was added until pH 8. The resulting mixture was extracted with dichloromethane (3×10 mL), the organic extracts washed with brine (20.0 mL) and dried over sodium sulfate. Flash column chromatography on silica gel using a gradient ethyl acetate/cyclohexane (1:5 to 2:1) gave 8-chloroquinoline-2-carbaldehyde (**51c**) as a yellow solid (88 mg, 77%). mp 129 – 131 °C**.**

^{1}H NMR (300 MHz, $CDCl_3$): δ = 10.32 (s, CHO), 8.35 (d, *J* = 8.4 Hz, 1H), 8.11 (d, *J* = 8.4 Hz, 1H), 7.95 (dd, *J* = 7.5, 1.3 Hz, 1H), 7.84 (dd, *J* = 8.2, 1.3 Hz, 1H), 7.62 (dd, *J* = 8.2, 7.5 Hz, 1H).

^{13}C NMR (75 MHz, $CDCl_3$): δ = 193.4 (CHO), 152.9 (C), 144.3 (C), 137.9 (CH), 134.9 (C), 131.4 (C), 130.6 (CH), 129.1 (CH), 126.9 (CH), 118.1 (CH).

HRMS (ESI-TOF) calcd. for $C_{10}H_6{}^{35}ClNO$ $[M+Li]^+$: 198.0293, found: 198.0297. calcd. for $C_{10}H_6{}^{37}ClNO$ $[M+Li]^+$: 200.0276, found: 200.0265.

8-Iodoquinoline-2-carboxylic acid (52)

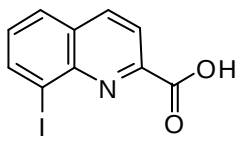

In a NMR tube, 3,9-diiodo-[1,2,3]triazolo[1,5-*a*]quinoline (**47b**) (13 mg, 0.03 mmol, 1.0 eq.) was dissolved in [^{2}H]chloroform (0.7 mL) affording a pink coloration becoming deep purple after 24h.

^{1}H NMR (300 MHz, $CDCl_3$): δ = 11.34 (b s, COOH), 8.46 (dd, *J* = 7.4, 1.2 Hz, 1H), 8.40 (d, *J* = 8.4 Hz, 1H), 8.32 (d, *J* = 8.4 Hz, 1H), 7.95 (dd, *J* = 8.2, 1.2 Hz, 1H), 7.45 (dd, *J* = 8.2, 7.4 Hz, 1H).

^{13}C NMR (75 MHz, $CDCl_3$): δ = 163.4 (C), 146.6 (C), 144.8 (C), 142.5 (CH), 139.9 (CH), 130.3 (CH,C), 128.6 (CH), 120.1 (CH) , 103.0 (C).

HRMS (ESI-TOF) calcd. for $C_{10}H_6INO_2$ $[M+Na]^+$: 321.9335, found: 321.9312.

Pyridin-2-yl(quinolin-2-yl)methanone (54)

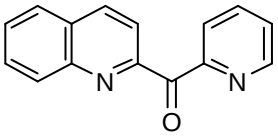

At -78 °C, butyllithium (10.8 mL, 16.7 mmol, 1.1 eq) in hexanes (1.5M) was added dropwise to a solution 2-bromopyridine (2.4 g, 15.2 mmol, 1.1 eq) in tetrahydrofuran (150 mL). The mixture was kept for 20 min at 0 °C before being canulated into a solution of methyl quinoline-2-carboxylate (2.8 g, 14.9 mmol, 1.0 eq) in tetrahydrofuran (100 mL) at -78 °C. The mixture was allowed to reach 25 °C in the course of 1 h and hydrolyzed with a saturated aqueous solution of ammonium chloride (20 mL). The resulting mixture was extracted with dichloromethane (3×30 mL). The organic extracts were combined, washed with brine (3×10 mL), dried over sodium sulphate, filtered, and concentrated. Chromatography (silica gel, ethyl acetate/cyclohexane 1:2) provided 6-bromopyridin-2-ylquinolin-2-yl methanone (**54**) as a yellow oil (3.7 g, 99%).[13]

^{1}H NMR (300 MHz, $CDCl_3$): δ = 8.77(br d, *J* = 4.8 Hz, 1H), 8.32 (d, *J* = 8.5 Hz, 1H), 8.23 (d, *J* = 7.8 Hz, 1H), 8.18 (t, *J* = 6.3, 6.3 Hz, 1H), 8.12 (t, *J* = 6.0, 6.0 Hz, 1H), 7.94-7.85 (m, 2H), 7.75 (ddd, *J* = 8.5, 6.9, 1.5 Hz, 1H), 7.63 (ddd, *J* = 8.1, 6.9, 1.2 Hz, 1H), 7.49 (ddd, *J* = 7.6, 4.8, 1.2 Hz, 1H).

^{13}C NMR (75.5 MHz, $CDCl_3$): δ = 193.2 (CO), 154.4 (C), 154.1 (C), 149.3 (CH), 147.2 (C), 136.7 (CH), 136.5 (CH), 130.6 (CH), 130.0 (CH), 129.0 (C), 128.4 (CH), 127.6 (CH), 126.4 (CH), 125.7 (CH), 121.0 (CH).

3-(Pyridin-2-yl)-[1,2,3]triazolo[1,5-*a*]quinoline (53A)

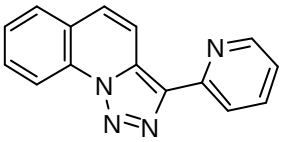

A mixture of pyridin-2-yl(quinolin-2-yl)methanone (**54**) (3.5 g, 15 mmol, 1 eq) and hydrazine monohydrate (1.4 mL, 1.1 g, 22 mmol, 1.5 eq) in methanol (150 mL) was heated to reflux. The reaction was monitored by TLC upon completion (3 h) and quenched with an aqueous solution of sodium hydroxide (20 mL, 30%). The resulting mixture was concentrated and extracted with dichloromethane (3×30 mL) The organic extracts were combined, washed with brine (20 mL), dried over sodium sulphate, filtered, and concentrated providing the corresponding hydrazone. The hydrazone was directly diluted in chloroform (150 ml). Activated manganese dioxide (3.7 g, 42 mmol, 2.8 eq) was added and the heterogeneous mixture heated to reflux overnight. The resulting mixture was cooled to 25 °C and filtered over celite. After concentration, 3-(pyridin-2-yl)-[1,2,3]triazolo[1,5-*a*]quinoline (**53A**) was obtained as a yellow solid (3.6 g, 97%). mp: 157 – 158 °C**.**

^{1}H NMR (300 MHz, $CDCl_3$): δ = 8.86 (d, *J* = 8.4 Hz, 1H), 8.70 (d, *J* = 4.9 Hz, 1H), 8.53 (d, *J* = 9.3 Hz, 1H), 8.42 (d, *J* = 8.0 Hz, 1H), 7.9-7.8 (m, 3H), 7.6-7.5 (m, 2H), 7.24 (dd, *J* = 7.6, 4.9, 1H).

^{13}C NMR (75.5 MHz, $CDCl_3$): δ = 151.9 (C), 149.2 (CH), 139.0 (C), 136.5 (CH), 131.7 (C), 129.9 (C), 129.8 (CH), 128.3 (CH), 127.3 (CH), 127.0 (CH), 124.2 (C), 122.0 (CH), 120.6 (CH), 117.7 (CH), 116.2 (CH).

MS (EI): m/z(%) = 246(11) 219(15) 218(100).

HRMS (EI) for $C_{15}H_{10}N_4$: calcd. 246.0905; found. 246.0899.

Anal. calcd. for $C_{15}H_{10}N_4$ (246.27): C 73.16; H 4.09; N 22.75; found: C 72.89; H 4.30; N 22.89.

3-(Pyridin-2-yl)-9-deuterio-[1,2,3]triazolo[1,5-*a*]quinoline (55A)

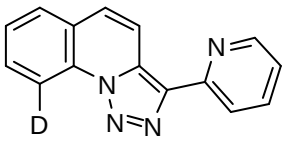

At -78 °C, butyllithium (0.5 mL, 0.5 mmol, 1.2 eq) in hexanes (1.5M) was added dropwise to a solution 3-(pyridin-2-yl)-[1,2,3]triazolo[1,5-*a*]quinoline (**2**) (0.1 g, 0.4 mmol, 1.0 eq) in tetrahydrofuran (10 mL). The mixture was kept for 30 min at -78 °C before methanol-d_4 (1.00 mL) was added and allowed to reach 25 °C (1 h). The reaction mixture was hydrolyzed with a saturated aqueous solution of ammonium chloride (20 mL). The resulting mixture was extracted with dichloromethane (3×10 mL). The organic extracts were combined, washed with brine (10 mL), dried over sodium sulphate, filtered, and concentrated providing 3-(Pyridin-2-yl)-9-deuterio-

[1,2,3]triazolo[1,5-*a*]quinoline (**55A**) as a colourless yellow solid (82 mg, 81%). mp: 155 – 158 °C**.**

^{1}H NMR (300 MHz, $CDCl_3$): δ = 8.86 (d, *J* = 8.4 Hz, 0.2 H, 0.8 D), 8.70 (d, *J* = 4.9 Hz, 1H), 8.53 (d, *J* = 9.3 Hz, 1H), 8.42 (d, *J* = 8.0 Hz, 1H), 7.9-7.8 (m, 3H), 7.6-7.5 (m, 2H), 7.24 (dd, *J* = 7.6, 4.9, 1H).

^{13}C NMR (75.5 MHz, $CDCl_3$): δ = 151.9 (C), 149.2 (CH), 139.0 (C), 136.5 (CH), 131.7 (C), 129.9 (C), 129.8 (CH), 128.3 (CH), 127.3 (CH and CD), 127.0 (CH), 124.2 (C), 122.0 (CH), 120.6 (CH), 117.7 (CH), 116.2 (CH).

2-([1,2,3]Triazolo[1,5-*a*]pyridin-3-yl)-8-iodoquinoline (56B)

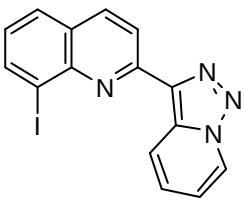

At -78 °C, butyllithium (0.5 mL, 0.5 mmol, 1.2 eq) in hexanes (1.5M) was added dropwise to a solution 3-(pyridin-2-yl)-[1,2,3]triazolo[1,5-*a*]quinoline (**53**) (0.1 g, 0.4 mmol, 1.0 eq) in tetrahydrofuran (10 mL). The mixture was kept for 30 min at -78 °C before a solution of iodine (0.2 g, 0.5 mmol, 1.3 eq) in tetrahydrofuran (15 mL) was added and allowed to reach 25 °C (1 h). The reaction mixture was hydrolyzed with a saturated aqueous solution of sodium thiosulphate (20 mL). The resulting mixture was extracted with dichloromethane (3×10 mL). The organic extracts were combined, washed with brine (10 mL), dried over sodium sulphate, filtered, and concentrated. Chromatography (silica gel, ethyl acetate/cyclohexane gradient) provided 2-([1,2,3]triazolo[1,5-*a*]pyridin-3-yl)-8-iodoquinoline (**56B**) as a colourless yellow solid (0.12 g, 85%). mp 193 – 195 °C**.**

^{1}H NMR (300 MHz, $CDCl_3$): δ = 9.43 (td, *J* = 8.9, 1.0, 1.0 Hz, 1H), 8.80 (td, *J* = 6.9, 1.0, 1.0 Hz, 1H), 8.55 (d, *J* = 8.6 Hz, 1H), 8.31 (dd, *J* = 7.4, 1.2 Hz, 1H), 8.16 (d, *J* = 8.6 Hz, 1H), 7.80 (dd, *J* = 8.0, 1.0 Hz, 1H), 7.53 (ddd, *J* = 8.9, 6.7, 1.0 Hz, 1H), 7.22 (app t, *J* = 7.7, Hz, 1H), 7.12 (app td, *J* = 6.9, 6.9, 1.0 Hz, 1H).

^{13}C NMR (75.5 MHz, $CDCl_3$): δ = 152.9 (C), 146.9 (C), 139.9 (CH), 137.3 (CH), 137.2 (C), 132.7 (C), 128.6 (CH), 127.9 (C), 127.4 (CH), 127.1 (CH), 125.2 (CH), 122.5 (CH), 119.6 (CH), 116.3 (CH), 103.3 (C).

MS (EI): m/z(%) = 372(24) 343(83) 217(100) 216 (42) 190 (25).

HRMS (EI) for $C_{15}H_9IN_4$: calcd. 371.9872; found. 371.9873.

2-([1,2,3]Triazolo[1,5-*a*]pyridin-3-yl)-8-methylquinoline (57B) and 9-methyl-3-(pyridin-2-yl)-[1,2,3]triazolo[1,5-*a*]quinoline (57A)

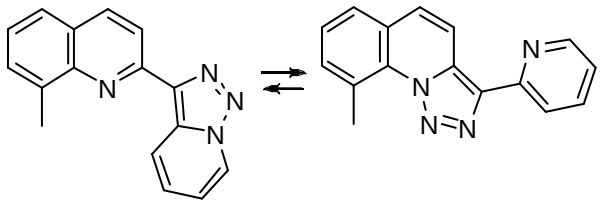

At -78 °C, butyllithium (0.3 mL, 0.5 mmol, 1.2 eq) in hexanes (1.5M) was added dropwise to a solution of 3-(pyridin-2-yl)-[1,2,3]triazolo[1,5-*a*]quinoline (**53**) (0.1 g, 0.4 mmol, 1.0 eq) in tetrahydrofuran (10 mL). The mixture was kept for 30 min at -78 °C before a solution of iodomethane (68 mg, 0.5 mmol, 1.2 eq) in tetrahydrofuran (0.5 mL) was added and allowed to reach 25 °C (1 h). A saturated aqueous solution of ammonium chloride (20 mL) was added. The resulting mixture was extracted with dichloromethane (3×10 mL). The organic extracts were combined, washed with brine (10 mL), dried over sodium sulphate, filtered, and concentrated. Chromatography (silica gel, ethyl acetate/cyclohexane 3:2) allowed the isolation of two products. However, when NMR analysis was performed, both products revealed the same spectra as they rapidly equilibrated between 9-methyl-3-(pyridin-2-yl)-[1,2,3]triazolo[1,5-*a*]quinoline (**57A**) (52%) and 2-([1,2,3] triazolo[1,5-*a*]pyridin-3-yl)-8-methylquinoline (**57B**) (48%) with a ratio A/B = 1.0:0.9 (81 mg, 77 %).

^{1}H NMR (300 MHz, $CDCl_3$): δ = 8.98 (td, *J* = 8.9, 1.2, 1.2 Hz, 1H B), 8.82 (td, *J* = 7.0, 1.0, 1.0 Hz, 1H B), 8.70 (td, *J* = 4.8, 1.0, 1.0 Hz, 1H A), 8.61 (d, *J* = 9.3 Hz, 1H A), 8.54 (d, *J* = 8.6 Hz, 1H B), 8.42 (td, *J* = 8.0, 1.0, 1.0 Hz, 1H A), 8.23 (d, *J* = 8.6 Hz, 1H B), 7.83 (dt, *J* = 7.9, 7.8, 1.8 Hz, 1H), 7.70 (app t, *J* = 8.2, 8.2 Hz, 2 H), 7.65-7.56 (m, 2H), 7.48 (ddd, *J* = 8 .9, 6.7, 1.0 Hz, 1H), 7.53-7.39 (m, 3H), 7.25-7.23 (m, 1H B), 7.11 (dt, *J* = 6.9, 6.9, 1.3 Hz, 1H A), 3.25 (s, 3H A), 2.93 (s, 3H B).

^{13}C NMR (75.5 MHz, $CDCl_3$): δ = 152.1 (C), 150.7 (C), 149.3 (CH), 148.7 (C), 147.0 (C), 138.1 (C), 137.5 (C), 136.7 (CH), 136.5 (CH), 136.4 (C), 133.1 (CH), 132.4 (C), 131.7 (C), 131.1 (C), 129.7 (CH), 128.6 (CH), 127.2 (C), 126.8 (CH), 126.4 (2×CH), 125.9 (C), 125.8 (2×CH), 125.3 (CH) , 122.0 (CH), 121.5 (CH), 120.7 (CH), 118.5 (CH), 117.4 (CH), 115.9 (CH), 24.6 (CH_3), 18.467 (CH_3).

MS (EI): m/z(%) = 260(21) 232(100) 231(94).

HRMS (EI) for $C_{16}H_{12}N_4$: calcd. 260.1062; found. 260.1073.

2-([1,2,3]Triazolo[1,5-*a*]pyridin-3-yl)-8-bromoquinoline (58B)

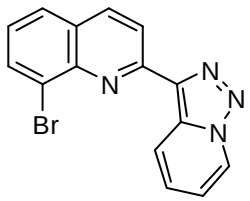

At -78 °C, butyllithium (0.3 mL, 0.5 mmol, 1.2 eq) in hexanes (1.5M) was added dropwise to a solution 3-(pyridin-2-yl)-[1,2,3]triazolo[1,5-*a*]quinoline (**53**) (0.1 g, 0.4 mmol, 1.0 eq) in tetrehydrofurane (10 mL). The mixture was kept for 30 min at -78 °C before a solution of 1,2-dibromo-1,1,2,2-tetrafluoroethane (0.2 g, 0.5 mmol, 1.3 eq) in tetrahydrofuran (1 mL) was added and allowed to reach 20 °C (1 h). A saturated aqueous solution of ammonium chloride (20 mL) was added. The resulting mixture was extracted with dichloromethane (3×10 mL) and the organic extracts were combined, washed with brine (10 mL), dried over sodium sulfate, filtered, and concentrated. Chromatography (silica gel, ethyl acetate/cyclohexane gradient) provided 2-([1,2,3]triazolo[1,5-*a*]pyridin-3-yl)-8-bromoquinoline (**58B**) as a slightly yellow solid (95 mg, 73%). Mp 231 – 233 °C**.**

^{1}H NMR (300 MHz, $CDCl_3$): δ = 9.29 (td, *J* = 8.9, 1.0, 1.0 Hz, 1H), 8.81 (td, *J* = 7.0, 1.0, 1.0 Hz, 1H), 8.57 (d, *J* = 8.6 Hz, 1H), 8.24 (d, *J* = 8.6 Hz, 1H), 8.05 (dd, *J* = 7.5, 1.2 Hz, 1H), 7.79 (dd, *J* = 8.0, 1.2 Hz, 1H), 7.54 (ddd, *J* = 8.9, 6.7, 1.0 Hz, 1H), 7.36 (app t, *J* = 7.8 Hz, 1H), 7.13 (ddd, *J* = 6.9, 6.8, 1.0 Hz, 1H).

^{13}C NMR (75.5 MHz, $CDCl_3$): δ = 152.8 (C), 145.0 (C), 137.4 (C), 137.0 (CH), 133.1 (CH), 132.9 (C), 128.5 (C), 127.6 (CH), 127.5 (CH), 126.4 (CH), 125.3 (CH), 124.9 (C), 122.1 (CH), 119.5 (CH), 116.3 (CH).

MS(EI): m/z(%) 326(16) 324(15) 298(85) 295(82) 217(100) 216(81) 190 (41).

HRMS (EI) for $C_{15}H_9{}^{79}BrN_4$: calcd. 324.0011; found. 323.9971, $C_{15}H_9{}^{81}BrN_4$: calcd. 326.0011; found. 325.9985.

2-([1,2,3]Triazolo[1,5-*a*]pyridin-3-yl)-8-chloroquinoline (59B)

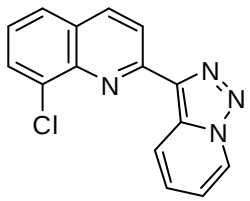

At -78 °C, butyllithium (0.3 mL, 0.5 mmol, 1.2 eq) in hexanes (1.5M) was added dropwise to a solution 3-(pyridin-2-yl)-[1,2,3]triazolo[1,5-*a*]quinoline (**53**) (0.1 g, 0.4 mmol, 1.0 eq.) in tetrahydrofuran (10 mL). The mixture was kept for 30 min at -78 °C before a solution of 1,2,2-trichlorotrifluoroethane (0.07 mL, 0.1 g, 0.5 mmol, 1.3 eq) in tetrahydrofuran (1 mL) was added and allowed to reach 25 °C (1 h). A saturated aqueous solution of ammonium chloride (20 mL) was added. The resulting mixture was extracted with dichloromethane (3×10 mL). The organic extracts were combined, washed with brine (10 mL), dried over sodium sulphate, filtered, and concentrated. Chromatography (silica gel, ethyl acetate/cyclohexane 3:2)

provided 2-([1,2,3]triazolo[1,5-*a*]pyridin-3-yl)-8-chloroquinoline (**59B**) as a light brown solid (70 mg, 62%). mp 228 – 230 °C**.**

^{1}H NMR (300 MHz, $CDCl_3$): δ = 9.21 (td, *J* = 8.9, 1.0, 1.0 Hz, 1H), 8.81 (td, *J* = 7.0, 1.0, 1.0 Hz, 1H), 8.58 (d, *J* = 8.6 Hz, 1H), 8.26 (d, *J* = 8.6 Hz, 1H), 7.84 (dd, *J* = 7.5, 1.2 Hz, 1H), 7.75 (dd, *J* = 8.1, 1.2 Hz, 1H), 7.54 (ddd, *J* = 8.9, 6.7, 1.0 Hz, 1H), 7.43 (t, *J* = 7.8 Hz, 1H), 7.13 (ddd, *J* = 6.9, 6.8, 1.0 Hz, 1H).

^{13}C NMR (75.5 MHz, $CDCl_3$): δ = 152.5 (C), 144.2 (C), 137.5 (C), 136.9 (CH), 133.4 (C), 133.0 (C), 129.6 (CH), 128.5 (C), 127.5 (CH), 126.8 (CH), 125.9 (CH), 125.3 (CH), 122.0 (CH), 119.5 (CH), 116.3 (CH).

MS (EI): m/z(%) = 282(4) 280(15) 254(31) 252(100) 217(35), 216(31) 190 (16).

HRMS (EI) for $C_{15}H_9{}^{35}ClN_4$: calcd. 280.0516; found. 280.0508, $C_{15}H_9{}^{37}ClN_4$: calcd.282,0516; found. 282.0510.

2-([1,2,3]Triazolo[1,5-*a*]pyridin-3-yl)-8-fluoroquinoline (60B)

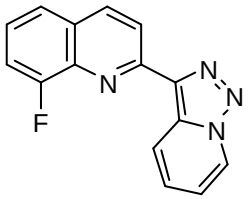

At -78 °C, butyllithium (0.3 mL, 0.5 mmol, 1.2 eq) in hexanes (1.5M) was added dropwise to a solution of 3-(pyridin-2-yl)-[1,2,3]triazolo[1,5-*a*]quinoline (**53**) (0.1 g, 0.4 mmol, 1.0 eq) in tetrahydrofuran (10 mL). The mixture was kept for 30 min at -78 °C before a solution of *N*-fluorodibenzenesulfonimide (0.16 g, 0.5 mmol, 1.3 eq) in tetrahydrofuran (20 mL) was added and allowed to reach 25 °C (1 h). A saturated aqueous solution of ammonium chloride was added (20 mL) and the resulting mixture was extracted with dichloromethane (3×10 mL). The organic extracts were combined, washed with brine (10 mL), dried over sodium sulphate, filtered, and concentrated. Preparative chromatography (silica 2 mm, ethyl acetate/cyclohexane 1:3) provided 2-([1,2,3]triazolo[1,5-*a*]pyridin-3-yl)-8-fluoroquinoline (**60B**) as the major isomer as a slightly brown solid (70 mg, 50%).

^{1}H NMR (300 MHz, $CDCl_3$): δ = 9.03 (td, *J* = 8.9, 1.1, 1.1 Hz, 1H), 8.79 (td, *J* = 7.0, 0.9, 0.9 Hz, 1H), 8.56 (d, *J* = 8.7 Hz, 1H), 8.24 (dd, *J* = 8.7, 1.2 Hz, 1H), 7.6-7.4 (m, 4H), 7.10 (dt, *J* = 6.9, 6.8, 1.0 Hz, 1H).

^{13}C NMR (75.5 MHz, $CDCl_3$): δ = 158.1 (d, J_{CF} = 256.3 Hz, C), 152.0 (d, J_{CF} = 1.4 Hz, C), 149.3 (C), 137.0 (d, J_{CF} = 51.0 Hz, C), 136.1 (d, J_{CF} = 3.1 Hz, CH), 132.8 (C), 128.8 (d, J_{CF} = 2.3 Hz, C), 127.3 (CH), 125.6 (d, J_{CF} = 7.9 Hz, CH), 125.2 (CH), 123.3 (d, J_{CF} = 4.6 Hz, CH), 121.8 (CH), 119.6 (CH), 116.3 (CH), 113.7 (d, J_{CF} =18.8 Hz, CH).

MS (EI): m/z(%) = 264(17) 236(100) 216(10) 190(2).

HRMS (EI) for $C_{15}H_9FN_4$: calcd. 264.0811; found. 264.0816.

2-(2-([1,2,3]Triazolo[1,5-*a*]pyridin-3-yl)quinolin-8-yl)propan-2-ol (61B)

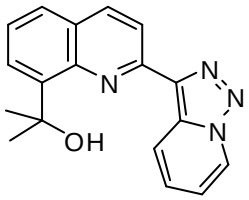

At -78 °C, butyllithium (0.3 mL, 0.5 mmol, 1.2 eq) in hexanes (1.5M) was added dropwise to a solution 3-(pyridin-2-yl)-[1,2,3]triazolo[1,5-*a*]quinoline (**53**) (0.1 g, 0.4 mmol, 1.0 eq) in tetrahydrofuran (10 mL). The mixture was kept for 30 min at -78 °C before acetone (1 mL, excess) was added and allowed to reach 25 °C (1 h). A saturated aqueous solution of ammonium chloride (20 mL) was added. The resulting mixture was extracted with dichloromethane (3×10 mL). The organic extracts were combined, washed with brine (10 mL), dried over sodium sulphate, filtered, and concentrated. Chromatography (silica gel, ethyl acetate/cyclohexane 1:3) provided 2-(2-([1,2,3]triazolo[1,5-*a*]pyridin-3-yl)quinolin-8-yl)propan-2-ol (**61B**) as a colourless solid (60 mg, 50%). mp 131 – 133 °C**.**

^{1}H NMR (300 MHz, $CDCl_3$): δ = 8.83 (ddd, *J* = 7.0, 1.0, 1.0 Hz, 1H), 8.80 (ddd, *J* = 9.0, 1.0, 1.0 Hz, 1H), 8.62 (d, *J* = 8.7 Hz, 1H), 8.35 (bs, OH), 8.33 (d, *J* = 8.7 Hz, 1H) 7.75 (dd, *J* = 8.0, 1.4 Hz, 1H), 7.70 (dd, *J* = 7.4, 1.4 Hz, 1H), 7.56 (ddd, *J* = 8.9, 6.7, 1.0 Hz, 1H), 7.5-7.4 (m,1H), 7.12 (ddd, *J* = 6.9, 6.8, 1.2 Hz, 1H), 1.90 (s, 6 H).

^{13}C NMR (75.5 MHz, $CDCl_3$): δ = 149.6 (C), 145.8 (C), 143.7 (C), 138.3 (CH), 137.0 (C), 131.9 (C), 128.2 (C), 128.0 (CH), 127.3 (CH), 126.1 (CH), 126.1 (CH), 125.8 (CH), 119.8 (CH), 119.3 (CH), 116.1 (CH), 74.3 (C), 31.2 (2 CH_3).

MS (EI): m/z(%) = 304(2) 290(12) 289(60) 276(36) 262(19) 261(100) 257(35) 243(58) 242(26) 233(16) 219(24) 190(11).

HRMS (EI) for $C_{18}H_{16}N_4O$: calcd. 304.1324; found. 304.1321.

3-(Pyridin-2-yl)-[1,2,3]triazolo[1,5-*a*]quinolin-9-ol (62)

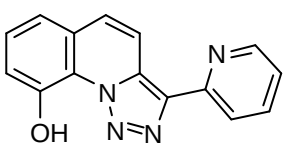

At -78 °C**,** butyllithium (1.4 mL, 2.2 mmol, 1.1 eq) was added to a solution of 3-(pyridin-2-yl)-[1,2,3]triazolo[1,5-*a*]quinoline (**53**) (0.5 g, 2.0 mmol. 1.0 eq) in tetrahydrofuran (50 mL). The mixture was kept for 30 min at -78 °C before fluorodimethoxyborane diethyletherate (0.6 mL, 2.7 mmol, 1.4 eq) was added and allowed to reach 0 °C (1 h). After 30 min, a 3.0 M aqueous solution of sodium hydroxide (0.8 mL) and a 30 % aqueous hydrogen peroxide (0.2 mL) were added dropwise. The reaction mixture was kept at 25 °C during the night. After addition of saturated aqueous solution of ammonium chloride (30 mL), the resulting mixture

was extracted with dichloromethane (3×20 mL). The organic extracts were combined, washed with brine (10 mL), dried over sodium sulphate, filtered, and concentrated. Chromatography (silica gel, ethyl acetate/cyclohexane 1:3) provided 3-(pyridin-2-yl)-[1,2,3]triazolo[1,5-*a*]quinolin-9-ol (**62**) (430 mg, 82%). mp 158 – 159 °C**.**

^{1}H NMR (300 MHz, $CDCl_3$): δ = 10.71 (s, 1H), 8.73 (br d, *J* = 4.8 Hz, 1H), 8.56 (d, *J* = 9.4 Hz, 1H), 8.38 (d, *J* = 8.0 Hz, 1H), 7.86 (app td, *J* = 7.8, 7.8, 1.1 Hz, 1H), 7.70 (d, *J* = 9.4 Hz, 1H), 7.52 (app t, *J* = 7.9, 7.9 Hz, 1H), 7.4-7.3 (m, 2H), 7.30 (ddd, *J* = 7.5, 4.8, 1.0 Hz, 1H).
^{13}C NMR (75.5 MHz, $CDCl_3$): δ = 151.4 (C), 149.5 (CH), 148.8 (C), 138.2 (C), 136.7 (CH), 129.9 (C), 128.9 (CH), 128.2 (CH), 126.2 (C), 122.6 (CH), 120.8 (CH), 120.3 (C), 118.7 (CH), 117.4 (CH), 116.9 (CH).
MS (EI): m/z(%) = 262(33) 234(100) 218(19) 206(48) 205(65).
HRMS (EI) for $C_{15}H_{10}N_4O$: calcd. 262.0855; found. 262.0853.
Anal. calcd. for $C_{15}H_{10}N_4O$ (262.27): C 68.69; H 3.84; N 21.31; found: C 68.51; H 4.02; N 21.47.

3-(Pyridin-2-yl)-9-(4,4,5,5-tetramethyl-1,3,2-dioxaborolan-2-yl)-[1,2,3]triazolo[1,5-*a*]quinoline (63A)

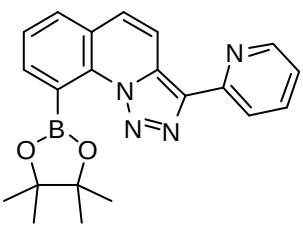

At -78 °C, butyllithium (0.6 mL, 1.0 mmol, 1.2 eq) in hexanes (1.5M) was added dropwise to a solution 3-(pyridin-2-yl)-[1,2,3]triazolo[1,5-*a*]quinoline (**53**) (0.2 g, 0.8 mmol, 1.0 eq) in tetrahydrofuran (20 mL). The mixture was kept for 30 min at -78 °C before 2-isopropoxy-4,4,5,5-tetramethyl-1,3,2-dioxaborolane (0.2 mL, 0.2 g, 1.4 mmol, 1.3 eq) was added and allowed to reach 25 °C (1 h). A saturated aqueous solution of ammonium chloride (20 mL) was added. The resulting mixture was extracted with dichloromethane (3×10 mL). The organic extracts were combined, washed with brine (10 mL), dried over sodium sulphate, filtered, and concentrated. Chromatography (silica gel, ethyl acetate/cyclohexane 1:1) provided 3-(pyridin-2-yl)-9-(4,4,5,5-tetramethyl-1,3,2-dioxaborolan-2-yl)-[1,2,3]triazolo[1,5-*a*]quinoline (**63A**) as a colourless solid (0.2 g, 79%). mp 142 – 143 °C**.**

^{1}H NMR (300 MHz, $CDCl_3$): δ = 8.70 (ddd, *J* = 4.9, 1.7, 1.0 Hz, 1H), 8.52 (d, *J* = 9.3 Hz, 1H), 8.38 (td, *J* = 8.0, 1.0, 1.0 Hz, 1H), 7.87 (dd, *J* = 7.9, 1.3 Hz, 1H),), 7.53 (d, *J* = 9.3 Hz, 1H), 7.6-7.5 (m, 3H), 7.23 (ddd, *J* = 7.5, 4.9, 1.0 Hz, 1H), 1.58 (s, 12H).

^{13}C NMR (75.5 MHz, $CDCl_3$): δ = 151.9 (C), 149.2 (CH+C), 139.0 (C), 136.7 (CH), 134.0 (CH), 133.2 (C), 130.0 (C), 129.2 (CH), 127.9 (CH), 126.7 (CH), 123.9 (C), 122.1 (CH), 120.9 (CH), 117.5 (CH), 84.810 (2×C), 25.012 (4×CH_3).

MS (EI): m/z(%) = 371(6), 345(23), 344(100),343(25) 314(23), 285(28), 245(77), 244(58), 218(47).

HRMS (EI) for $C_{21}H_{21}BN_4O_2$: calcd. 371.1794.; found. 371.1789.

Anal. calcd. for $C_{21}H_{21}BN_4O_2$ (372.23): C 67.76; H 5.69; N 15.05; found: C 67.60; H 5.69; N 15.55.

2-([1,2,3]Triazolo[1,5-*a*]pyridin-3-yl)-8-methoxyquinoline (64B)

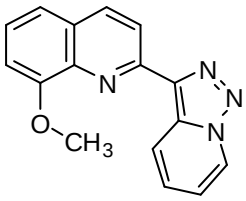

A mixture of 3-(pyridin-2-yl)-[1,2,3]triazolo[1,5-*a*]quinolin-9-ol (**62**) (60 mg, 0.23 mmol, 1 eq), iodomethane (42 mg, 0.3 mmol, 1.2 eq) and potassium carbonate (39 mg, 0.3 mmol, 1.3 eq) in acetone (20 mL) was heated to reflux. The reaction was monitored by TLC upon completion (5 h). The reaction mixture was quenched with water (10 ml), the resulting mixture concentrated and then extracted with dichloromethane (3×10 mL). The organic extracts were combined, washed with brine (20 mL), dried over sodium sulfate, filtered, and concentrated providing 2-([1,2,3]triazolo[1,5-*a*]pyridin-3-yl)-8-methoxyquinoline (**64B**) as major isomer (54 mg, 87%).

^{1}H NMR (300 MHz, $CDCl_3$): δ = 9.03 (td, *J* = 8.9, 1.2, 1.2 Hz, 1H), 8.79 (ddd, *J* = 7.0, 1.0, 1.0 Hz, 1H), 8.52 (d, *J* = 8.6 Hz, 1H), 8.21 (d, *J* = 8.6 Hz, 1H), 7.48 (ddd, *J* = 8.9, 6.7, 1.0 Hz, 1H), 7.5-7.4 (m, 2 H), 7.10 (app td, *J* = 6.9, 6.9, 1.o Hz, 1H) 7.07 (d, *J* = 6.8 Hz, 1H), 4.14 (s, 3H).

^{13}C NMR (75.5 MHz, $CDCl_3$): δ = 155.4 (C), 150.8 (C), 149.2 (C), 139.9 (C), 136.6 (C), 136.5 (CH), 128.4 (C), 127.0 (CH), 126.2 (CH), 125.2 (CH), 121.8 (CH), 119.7 (CH), 119.3 (CH), 116.1 (CH), 108.2 (CH), 56.2 (CH_3).

MS (EI): m/z(%) = 276.1(30), 248.1(50), 218.1(70), 218(100), 141.9(85).

HRMS (EI) for $C_{16}H_{12}N_4O$: calcd. [M+H] 277,1084; found. 277.1050. [M+Li] 283,1166; found. 283.1130.

2-([1,2,3]Triazolo[1,5-*a*]pyridin-3-yl)-8-isopropoxyquinoline (65B)

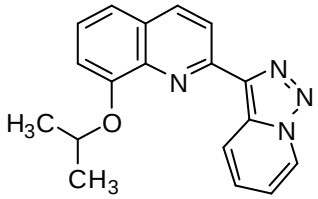

A mixture of 3-(pyridin-2-yl)-[1,2,3]triazolo[1,5-*a*]quinolin-9-ol (**62**) (60 mg, 0.23 mmol, 1 eq), 2-bromopropane (0.3 g, 2.3 mmol, 10 eq) and potassium carbonate (39 mg, 0.3 mmol, 1.3 eq) in acetone (20 mL) was heated to reflux. The reaction was monitored by TLC upon completion (24 h). The reaction mixture was quenched with water (10 ml), concentrated and extracted with dichloromethane (3×10 mL). The organic extracts were combined, washed with brine (20 mL), dried over sodium sulphate, filtered, and concentrated providing 2-([1,2,3]triazolo[1,5-*a*]pyridin-3-yl)-8-isopropoxy-quinoline **(65B)** as major isomer (59 mg, 85%).

^{1}H NMR (300 MHz, $CDCl_3$): δ = 9.20 (td, *J* = 8.9, 1.0, 1.0 Hz. 1H), 8.80 (ddd, *J* = 7.1, 1.0, 1.0 Hz, 1H), 8.50 (d, *J* = 8.6 Hz, 1H), 8.21 (d, *J* = 8.6 Hz, 1H), 7.5–7.4 (m, 2H) 7.46 (ddd, *J* = 8.9, 6.7, 1.0 Hz, 1H) 7.09 (app td, *J* = 6.9, 6.9, 1.0 Hz, 1H), 7.1–7.0 (m, 1H), 4.90 (sp, *J* = 6.0 Hz, 1H), 1.59 (d, *J* = 6.0, 6H).

^{13}C NMR (75.5 MHz, $CDCl_3$): δ = 153.7 (C), 140.69 (C), 138.2 (C), 139.9 (C), 136.4 (CH), 132.8 (C) 128.6 (C), 126.7 (CH), 126.2 (CH), 125.2 (CH), 122.1 (CH), 119.7 (CH), 118.8 (CH), 116.1 (CH), 111.8 (CH), 71.1 (CH), 22.3 (2 CH_3).

MS (EI): m/z(%) = 304(17), 289(16), 276(69), 235(22), 234(100), 218(30) 206(36), 205(62), 78(10).

HRMS (EI) for $C_{18}H_{16}N_4O$: calcd. 304.1324; found. 304.1316,

6-Bromopyridin-2-ylquinolin-2-yl methanone (68)

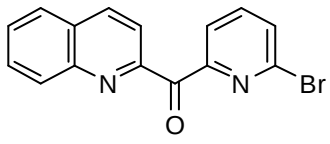

At 0 °C, butyllithium (10.8 mL, 16.7 mmol, 1.1 eq) in hexanes (1.5M) was added dropwise to a solution 2,6-dibromopyridine (3.6 g, 15.2 mmol, 1.1 eq) in toluene (75 mL). The mixture was kept for 20 min at 0 °C before being canulated into a solution of methyl quinoline-2-carboxylate (2.8 g, 14.9 mmol, 1.0 eq) in tetrahydrofuran (100 mL) at 0 °C**.** The mixture was allowed to reach 25 °C in the course of 1 h and hydrolyzed with a saturated aqueous solution of ammonium chloride (20 mL). The resulting mixture was extracted with dichloromethane (3×10 mL). The organic extracts were combined, washed with brine (3×10 mL), dried over sodium sulphate, filtered, and concentrated. Chromatography (silica gel, ethyl acetate/cyclohexane 1:2) provided 6-bromopyridin-2-ylquinolin-2-yl methanone (**68**) as a yellow oil (3.3 g, 70%).

^{1}H NMR (300 MHz, $CDCl_3$): δ = 8.32 (d, *J* = 8.5 1H), 8.2-8.1 (m, 3H), 7.88 (dd, *J* = 8.1, 1.2 Hz, 1H), 7.8-7.7 (m, 2H), 7.7-7.60 (m, 1H).

^{13}C NMR (75.5 MHz, $CDCl_3$): δ = 191.2 (C), 154.9 (C), 153.3 (C), 147.1 (C), 141.8 (C), 138.6 (CH), 136.8 (CH), 130.9 (CH), 130.6 (CH), 130.1 (CH), 129.1 (C), 128.7 (CH), 127.6 (CH), 124.7 (CH), 120.8 (CH).

MS (EI): m/z(%) = 314(63) 312(65) 286(34) 285(55) 284(31) 283(51) 205(71) 128(100) 101(29).

HRMS (EI) for $C_{15}H_9{}^{79}BrN_2$: calcd. 311.9898; found. 311.9892, $C_{15}H_9{}^{81}BrN_2$: calcd. 313.9898; found. 313.9882.

3-(6-Bromopyridin-2-yl)-[1,2,3]triazolo[1,5-*a*]quinoline (66A)

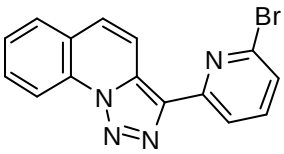

A mixture of 6-bromopyridin-2-yl quinolin-2-yl methanone (**68**) (1.0 g, 3.3 mmol, 1 eq) and hydrazine monohydrate (0.3 mL, 0.2 g, 4 mmol, 1.3 eq) in methanol (50 mL) was heated to reflux. The reaction was monitored by TLC upon completion (3 h). An aqueous solution of sodium hydroxide (20 mL, 30%) was added and the resulting mixture concentrated and extracted with dichloromethane (3×20 mL). The organic extracts were combined, washed with brine (20 mL), dried over sodium sulphate, filtered, and concentrated providing the corresponding hydrazone. The hydrazone was directly dissolved in chloroform (100 ml) before activated manganese dioxide (0.8 g, 9.1 mmol, 2.8 eq) was added. The heterogeneous mixture was heated to reflux over night. The resulting mixture was cooled to 25 °C and filtrated over celite. After concentration 3-(6-bromopyridin-2-yl)-[1,2,3]triazolo[1,5-*a*]quinoline (**66A**) was obtained as a brown solid (1 g, 91%). mp 180 – 182 °C**.**

^{1}H NMR (300 MHz, $CDCl_3$): δ = 8.82 (d, *J* = 8.4 Hz, 1H), 8.49 (d, *J* = 9.3 Hz, 1H), 8.35 (dd, *J* = 7.8, 0.8 Hz, 1H), 7.89 (dd, *J* = 7.9, 1.1 Hz, 1H), 7.79 (ddd, *J* = 8.5, 7.3, 1.4 Hz, 1H), 7.7-7.6 (m, 3H), 7.41 (dd, *J* = 7.8, 0.8 Hz, 1H).

^{13}C NMR (75.5 MHz, $CDCl_3$): δ = 152.7 (C), 141.5 (C), 139.0 (CH), 1376 (C), 131.8 (C), 130.3 (C), 130.2 (CH), 128.6 (CH), 128.1 (CH), 127.4 (CH), 126.1 (CH), 124.4 (C), 119.2 (CH), 117.5 (CH), 116.4 (CH).

MS (EI): m/z(%) = 326(14) 324(15) 298(80) 296(79) 217(100) 216(50) 190(33) 128(18).

HRMS (EI) for $C_{15}H_9{}^{79}BrN_4$: calcd. 324.0011; found. 324.0012, $C_{15}H_9{}^{81}BrN_4$: calcd. 326.0011; found. 326.0000.

Anal. Calcd. for $C_{15}H_9BrN_4$ (326.00): C, 55.40; H, 2.79; N, 17.23; found: C, 55.34; H, 3.24; N, 17.05.

3-(6-Methylpyridin-2-yl)-[1,2,3]triazolo[1,5-*a*]quinoline (67A)

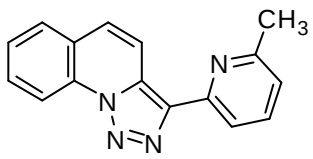

At -78 °C, butyllithium (0.4 mL, 0.7 mmol, 1.1 eq) in hexanes (1.5M) was added to a solution 3-(6-bromopyridin-2-yl)-[1,2,3]triazolo[1,5-*a*]quinoline (**66A**) (0.2 g, 0.6 mmol, 1.0 eq) in tetrahydrofuran (20 mL). The mixture was kept for 30 min at -78 °C before iodomethane (0.1 g, 0.8 mmol, 1.2 eq) was added. The mixture was warmed up to room temperature in the course of 1 h. A saturated aqueous solution of ammonium chloride (20 mL) was added. The resulting mixture was extracted with dichloromethane (3×10 mL). The organic extracts were combined, washed with brine (10 mL), dried over sodium sulphate, filtered, and concentrated. Chromatography (silica gel, ethyl acetate/ cyclohexane 1:4) provided 3-(6-methylpyridin-2-yl)-[1,2,3]triazolo[1,5-*a*]quinoline (**67A**) (81 mg, 50%). mp 116 – 117 °C**.**

^{1}H NMR (300 MHz, $CDCl_3$): δ = 8.83 (d, *J* = 8.4 Hz, 1H), 8.59 (d, *J* = 9.3 Hz, 1H), 8.20 (d, *J* = 7.9 Hz, 1H), 7.87 (dd, *J* = 7.9, 1.1 Hz, 1H), 7.77 (ddd, *J* = 8.5, 7.4, 1.4 Hz, 1H), 7.70 (t, *J* = 7.8, 7.8 Hz, 1H), 7.6-7.5 (m, 2H), 7.10 (d, *J* = 7.6 Hz, 1H), 2.66 (s, 3H).

^{13}C NMR (75.5 MHz, $CDCl_3$): δ = 158.0 (C), 151.3 (C), 139.3 (C), 136.9 (CH), 131.9 (C), 130.0 (C), 129.9 (CH), 128.4 (CH), 127.2 (CH), 127.1 (CH), 124.4 (C), 121.6 (CH), 118.1 (CH), 117.7 (CH), 116.4 (CH), 29.7 (CH_3).

MS (EI): m/z(%) = 260(16) 232(100) 231(58).

HRMS (EI) for $C_{16}H_{12}N_4$: calcd. 260.1062; found. 260.1064

7.1.4 Chapter IV: Triazolopyridine-phosphines

Typical Experimental procedure for the preparation of [1,2,3]triazolo[1,5-*a*]pyridine phosphines:

At -40 °C, butyllithium (3.6 mL, 5.6 mmol, 1.1 eq) in hexanes (1.5M) was added to a solution of 3-(pyridin-2'-yl)-[1,2,3]triazolo[1,5-*a*]pyridine (1.0 g, 5.1 mmol, 1.0 eq) in toluene (60 mL). The mixture was kept for 30 min at -40 °C before a solution of the corresponding chlorophosphine (5.9 mmol, 1.15 eq) in toluene (6.0 mL) was added and allowed to reach 20 °C (2 h). The reaction mixture was quenched with water (20 mL). The resulting mixture was extracted with dichloromethane (3×10 mL) and the combined organic extracts were washed with brine (10 mL), dried over Na_2SO_4, filtered, and concentrated. Chromatography (silica gel, ethyl acetate/cyclohexane = 3:7) provided the corresponding isomeric A/B mixture of phosphines. The corresponding selenides were prepared according to standard procedure: the phosphines were allowed to react with selenium powder in refluxing chloroform during 5 hours.

7-(Diphenylphosphino)-3-(pyridin-2'-yl)-[1,2,3]triazolo[1,5-*a*]pyridine and **3-(6'-(diphenylphosphino)pyridin-2'-yl)-[1,2,3]triazolo[1,5-*a*]pyridine** (**69a**)

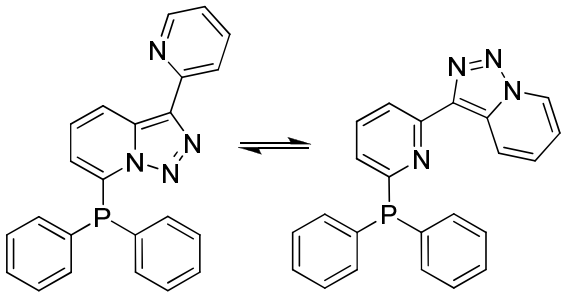

When diphenylphosphine chloride was used 0.79 g (40%) of **69a** were obtained as a yellow oil after chromatography. A/B ratio = 0.72.

^{1}H NMR (300 MHz, $CDCl_3$): δ = 8.77 (d, *J* = 8.75 Hz, H^{4A}), 8.69 (d, *J* = 6.33 Hz, $H^{6'A}$+H^{7B}), 8.38 (d, *J* = 8.00 Hz, $H^{3'A}$), 8.31 (d, *J* = 7.96 Hz, $H^{3'B}$), 7.77-7.64 (m, $H^{4'A}$ + $H^{4'B}$ + H^{4B}), 7.55-7.34 (m, $(PPh_2)^A$ + $(PPh_2)^B$), 7.33-7.28 (m, H^{5A} + $H^{5'B}$), 7.23-7.17 (m, $H^{5'A}$), 7.09-7.01 (t, *J* = 8.61, Hz, H^{5B}), 6.94 (t, *J* = 6.77, Hz, H^{6B}), 6.55 (d, *J* = 6.83 Hz, H^{6A}).

^{13}C NMR (75.5 MHz, $CDCl_3$): δ = 162.74 (s,2 C), 152.12 (d, *J* = 8.61 Hz, C), 151.91 (C), 149.02 (CH^A), 138.66 (d, J_{C-P} = 23.20 Hz, C), 137.20 (d, J_{C-P} = 1.84 Hz, C), 136.98 (C), 136.31 (CH^A), 136.30 (d, J_{C-P} = 9.69 Hz, C(PPh_2), 135.96 (d, J_{C-P} = 5.81 Hz, CH^A), 134.29 (d, *J* = 19.71 Hz, CH (PPh_2)), 134.03 (d, *J* = 20.48 Hz, CH^B), 132.31 (d, J_{C-P} = 8.31 Hz, C), 131.96 (C), 131.66 (C), 129.66 (CH^B), 128.79 (CH(PPh_2)), 128.74 (d, J_{C-P} = 7.78 Hz, CH^B), 128.39 (d, J_{C-P} = 7.34 Hz, CH(PPh_2)), 126.54 (d, J_{C-P} = *2*7.79 Hz, CH$(PPh_2)^A$), 125.96

(CH^B),125.72 (CH^A),124.63 (CH^A), 121.55 (d, J_{C-P} = 22.59 Hz, CH^A), 121.37 (CH^B), 120.68 (CH^A),120.30 (CH^A), 118.52 (CH^B), 115.63 (CH^B).

^{31}P NMR (161 MHz, $CDCl_3$): δ= -0.30 (P^B), -14.77 (P^A).

MS(EI): m/z (%) = 380 (66) [M^+], 352 (67) [M^+- N_2], 275.1(8) [M^+- Ph - N_2], 183.1 (100).

HRMS ESI-[TOF] for $C_{23}H_{17}N_4P$ [M^++O+Li]: calcd. 403.1300; found. 403.1230.

7-(Dicyclohexylphosphino)-3-(pyridin-2'-yl)-[1,2,3]triazolo[1,5-*a*]pyridine and 3-(6'-(dicyclohexylphosphino)pyridin-2'-yl)-[1,2,3]triazolo[1,5-*a*]pyridine (69b)

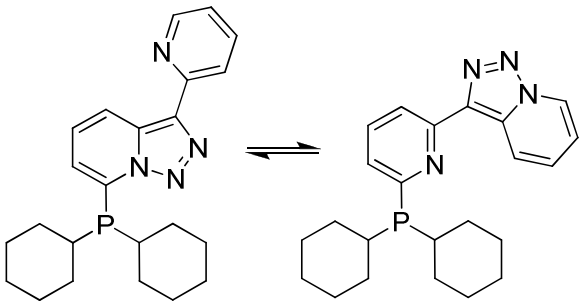

When dicyclohexylphosphine chloride was used, 0.43 g (22%) of **69b** were obtained as a yellow oil after chromatography; A/B ratio = 1.39.

^{1}H NMR (300 MHz, $CDCl_3$): δ = 8.78 (d, *J* = 8.94 Hz, H^{4A}), 8.76-8.69 (m, H^{6A}+H^{7B}), 8.65-8.60 (d, *J* = 4.88 Hz, $H^{6'A}$), 8.35 (d, *J* = 8.01 Hz, $H^{3'A}$), 8.26 (d, *J* = 7.97 Hz, $H^{3'B}$), 7.75 (dt, *J* = 7.78, 7.71, 1.78 Hz, $H^{4'A}$), 7.68 (ddd, *J* = 7.75, 7.69, 1.94 Hz, $H^{4'B}$), 7.43-7.22 (m, H^{5A}+$H^{5'B}$+H^{5B}+H^{4B}), 7.16 (ddd, *J* = 7.45, 4.90, 1.01 Hz, $H^{5'A}$), 7.02 (ddd, *J* = 6.82, 6.80, 1.13 Hz, H^{6B}), 2.77-2.64 (m, 1H), 2.26-2.09 (m, 1H), 2.03-1.85 (m, 2H), 1.80-1.55 (m, 7H), 1.34-0.95 (m, 11H).

^{13}C NMR (75.5 MHz, $CDCl_3$): δ = 160.82 (C), 160.66 (C), 152.11 (CH^A), 151.92 (d, J_{C-P} = 5.62 Hz, C), 149.20 (CH^A), 137.79 (C), 137.35 (C), 137.14 (C), 136.77 (C), 136.49 (CH^A), 135.25 (d, J_{C-P} = 8.92 Hz, CH^B), 132.13 (d, J_{C-P} = 16.02 Hz, C), 129.25 (d, J_{C-P} = 33.79 Hz, CH), 126.14 (CH), 125.71 (d, J_{C-P} = 27.09 Hz, CH), 125.40 (d, J_{C-P} = 8.78 Hz, CH), 125.18 (CH), 121.81 (CH), 121.57 (CH), 121.38 (CH), 120.36 (CH), 119.18 (CH), 115.75 (CH), 32.75 (d, J_{C-P} = 11.11 Hz, CH), 32.60 (d, J_{C-P} = 11.29 Hz, CH), 31.06 (d, J_{C-P} = 19.49 Hz, CH_2), 30.06 (d, J_{C-P} = 8.74 Hz, CH_2), 29.74 (d, J_{C-P} = 14.97 Hz, CH_2), 29.16 (d, J_{C-P} = 7.70 Hz, CH_2), 27.44 (CH_2), 27.28 (CH_2), 27.12 (CH_2), 27.01 (CH_2), 26.81 (CH_2), 26.75 (CH_2), 26.63 (CH_2), 26.36 (CH_2), 26.12 (CH_2).

^{31}P NMR ($CDCl_3$, 161 MHz): δ = 8.92 (P^B), 8.01 (P^A)

MS (EI): m/z(%) = 392.2 (24) [M^+], 364.2 (18) [M^+- N_2], 309.2 (74) [M^+- C_6H_{11}], 282.1 (74) [M^+- C_6H_{11} -N_2], 199.1 (100) [HM^+- N_2 - 2×C_6H_{11}], 168.1 (58) [HM^+- N_2 – $P(C_6H_{11})_2$].

HRMS ESI-[TOF] for $C_{23}H_{29}N_4P$ [M+H$^+$]: calc 393.2203; found 393.2145, [M+O+Li]: calcd. 415.2245; found. 415.2161.

7-(Diisopropylphosphino)-3-(pyridin-2'-yl)-[1,2,3]triazolo[1,5-*a*]pyridine and 3-(6'-(diisopropylphosphino)pyridin-2'-yl)-[1,2,3]triazolo[1,5-*a*]pyridine (69c)

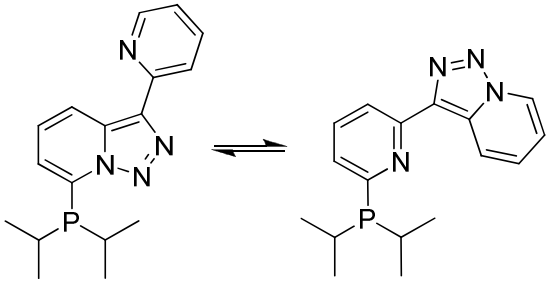

When diisopropylphosphine chloride was used 0.21 g (13%) of **69c** were obtained as a yellow oil after chromatography; A/B ratio = 1.04.

^{1}H NMR (300 MHz, $CDCl_3$): δ = 8.78-8.73 (m, H^{4A} +H^{6A}+H^{7B}), 8.66 (d, *J* = 4.88 Hz, $H^{6'A}$), 8.37 (td, *J* = 8.03, 1.03 Hz, $H^{3'A}$), 8.30 (td, *J* = 7.99, 1.19 Hz, $H^{3'B}$), 7.78 (dt, *J* = 7.62, 1.81 $H^{4'A}$), 7.72 (ddd, *J* = 7.89, 7.77, 1.95 Hz, $H^{4'B}$), 7.46-7.25 (m, H^{5A}+$H^{5'B}$+H^{5B}+H^{4B}), 7.20 (ddd, *J* = 7.49, 4.89, 1.17 Hz, $H^{5'A}$), 7.07-7.01 (m, H^{6B}), 2.92 (qd, *J* = 13.93, 6.96 Hz, 1H), 2.46-2.29 (m, 1H), 1.29-1.14 (m, 6H), 0.96 (ddd, *J* = 20.32, 12.53, 6.93 Hz, 6 H).

^{13}C NMR (75.5 MHz, $CDCl_3$): δ = 160.88 (C), 160.72 (C), 152.04 (d, J_{C-P} = 6.13 Hz, C),152.0 (CH) 149.15 (CH), 137.96 (C), 137.66 (C), 137.38 (C), 137.19 (C), 136.51 (CH), 135.27 (d, J_{C-P} = 8.54 Hz,CH), 132.07 (d, J_{C-P} = 15.42 Hz, C), 129.01 (d, J_{C-P} = 32.52 Hz,CH), 126.31 (CH), 125.45 (d, J_{C-P} = 8.17 Hz, CH), 125.27 (d, J_{C-P} = 26.08 Hz,CH), 125.15 (CH), 121.83 (CH), 121.62 (CH), 121.14 (CH), 120.34 (CH), 119.32 (CH), 115.73 (CH), 23.06 (d, J_{C-P} = 11.26 Hz, CH), 22.85 (d, J_{C-P} = 10.75 Hz,CH), 20.65 (d, J_{C-P} = 15.43 Hz, CH_3), 20.43 (d, J_{C-P} = 5.22 Hz, CH_3), 19.68 (d, J_{C-P} = 16.83 Hz, CH_3), 19.20 (d, J_{C-P} = 9.14 Hz, CH_3).

^{31}P NMR (161 MHz, $CDCl_3$): δ= 17.07 (P^B), 16.92 (P^A).

MS(EI): m/z (%) = 312.2 (23) [M$^+$], 284.2 (8) [M$^+$- N_2], 269.2 (95) [M$^+$- C_3H_7], 241.1 (49) [M$^+$- C_3H_7 -N_2], 199.1 (100) [HM$^+$- N_2 - 2×C_6H_{11}], 168.1 (29) [HM$^+$- N_2 – P(C_6H_{11})$_2$].

HRMS ESI-[TOF] for $C_{17}H_{21}N_4P$ [M+Li-N_2]: calc 305.1552; found 307.1542, $C_{17}H_{21}N_4P$ [M+O+Li]: calcd. 335.1613; found 335.1581.

7-(Di(*p*-methoxyphenyl)phosphino)-3-(pyridin-2'-yl)-[1,2,3]triazolo[1,5-*a*]pyridine and **3-(6'-(di(*p*-methoxyphenyl)phosphino)pyridin-2'-yl)-[1,2,3]triazolo[1,5-*a*]pyridine** (**69d**)

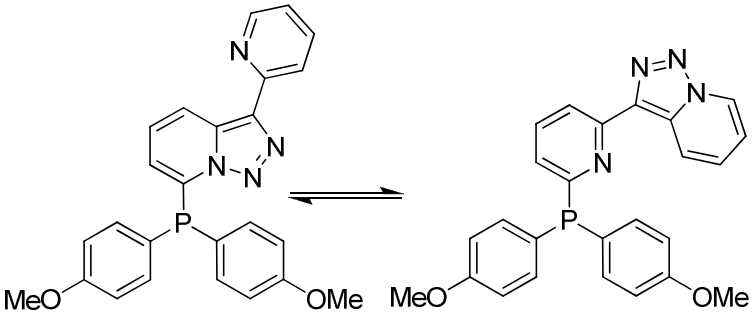

3-(Pyridine-2'-yl)-[1,2,3]triazolo[1,5-*a*]pyridine (0.30 g, 1.5 mmol) and diphenylphosphine chloride were used affording 0.13 g (10%) of **69d** as a yellow oil after chromatography; A/B ratio = 1.23.

^{1}H NMR (300 MHz, $CDCl_3$): δ = 8.73-8.63 (m, $H^{6'A}$+H^{7B} +H^{4A}), 8.32 (d, *J* = 8.02 Hz, $H^{3'A}$), 8.19 (d, *J* = 7.91 Hz, $H^{3'B}$), 7.79-7.70 (m, H^{4A} + $H^{5'B}$), 7.66 (ddd, *J* = 7.84, 7.80, 2.53 Hz, $H^{4'B}$), 7.45-7.31 (m, (Ph)+H^{4B}+ H^{5B}), 7.28-7.15 (m, $H^{5'B}$+H^{5A}+$H^{5'A}$), 7.06-6.88 (m, H^{6B}+ Ph), 6.48 (d, *J* = 6.79 Hz, H^{6A}), 3.82 (s, $3H^{B}$), 3.80 (s, $3H^{A}$).

^{13}C NMR (75.5 MHz, $CDCl_3$): δ = 164.06 (C), 160.96 (C-OMe), 160.46 (C-OMe), 152.14 (C), 152.03 (d, J_{C-P} = 8.54 Hz, C), 149.11 (CH), 140.19 (C), 139.88 (C), 137.34 (C), 137.14 (d, J_{C-P} = 1.95 Hz,1C), 136.59 (C), 136.55 (CH), 136.18-135.78 (m), 135.54 (C), 134.09 (d, *J* = 10.99 Hz, C), 132.14 (C), 131.83 (C), 127.67 (d, J_{C-P} = 6.50 Hz, C), 126.25 (d, *J* = 27.01 Hz, CH), 125.85 (CH), 124.80 (CH), 123.47 (d, *J* = 5.02 Hz, C), 122.00-121.71 (m), 121.14 (CH), 120.56 (CH), 120.44 (CH), 118.32 (CH), 115.79 (CH), 114.70-113.86 (m), 55.38 (OMe), 55.25 (OMe).

^{31}P NMR (161 MHz, $CDCl_3$): δ= -0.35 (P^{B}), -17.62 (P^{A})

MS(EI): m/z (%) = 440.1 (87) [M^+], 412.1 (64) [M^+- N_2], 411.1 (100) [M^+ -H - N_2], 305.1 (48) [M^+- MeOPh - N_2], 245.1 (98) [P(*p*-MeOPh)$_2$].

HRMS ESI-[TOF] for $C_{25}H_{21}N_4O_2P$ [M+H]: calcd. 441.1480; found. 441.1421. $C_{25}H_{21}N_4O_2P$ [M+Li+O]: calcd. 463.1511; found. 463.1446.

7-(Di(*p*-methylphenyl)phosphino)-3-(pyridin-2'-yl)-[1,2,3]triazolo[1,5-*a*]pyridine and **3-(6'-(di(*p*-methylphenyl)phosphino)pyridin-2'-yl)-[1,2,3]triazolo[1,5-*a*]pyridine** (**69e**)

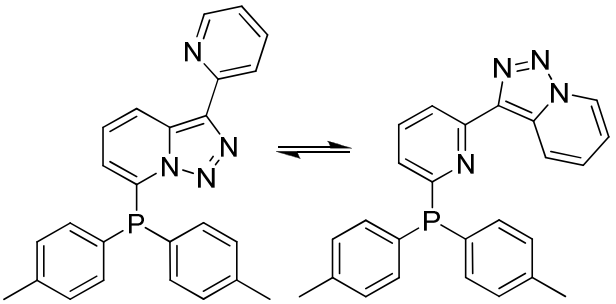

3-(Pyridine-2'-yl)-[1,2,3]triazolo[1,5*a*] pyridine (0.30 g, 1.5 mmol) and diphenylphosphine chloride were used affording 0.14 g (22%) of **69e** as a yellow oil after chromatography; A/B ratio = 0.71.

^{1}H NMR (300 MHz, $CDCl_3$): δ = 8.73-8.62 (m, H^{4A}+$H^{6'A}$+ H^{7B}), 8.33 (td, *J* = 8.06, 1.03 Hz, $H^{3'A}$), 8.22 (td, *J* = 7.94, 0.88 Hz, $H^{3'B}$), 7.79-7.72 (m, H^{4B}+$H^{4'A}$), 7.67 (ddd, *J* = 7.83, 7.80, 2.47 Hz, $H^{4'B}$), 7.43-7.26 (m, $H^{5'A}$+ H^{5A} +(*p*-MePh)), 7.23-7.15 (m, $H^{5'B}$+(*p*-MePh)), 7.04-6.90 (m, H^{6B}+H^{5B}), 6.42 (d, *J* = 6.81 Hz, H^{6A}), 2.38 (s, $3H^{B}$), 2.36 (s, $3H^{A}$).

^{13}C NMR (75.5 MHz, $CDCl_3$): δ = 163.56 (C), 152.15 (C), 152.03 (C), 149.09 (CH), 139.87 C), 139.74 (C), 139.43 (C), 137.35 (C), 136.54 (CH), 136.01 (d, J_{C-P} = 5.36 Hz, CH), 134.45 (d, J_{C-P} = 20.16 Hz, CH), 134.17 (d, J_{C-P} = 21.50 Hz, CH), 133.12 (d, J_{C-P} = 8.19 Hz, C), 132.15 (s, C), 131.83 (C), 129.69 (d, J_{C-P} = 8.08 Hz, CH), 129.31 (d, J_{C-P} = 7.60 Hz, CH), 129.06 (d, J_{C-P} = 6.81 Hz, C), 126.46 (d, J_{C-P} = 26.41 Hz, CH), 125.86 (CH), 125.79 (CH), 124.81 (CH), 121.89-121.75 (m), 121.30 (CH), 120.61-120.48 (m), 118.46 (CH), 115.74 (CH), 21.34 (CH_3), 21.01 (CH_3).

^{31}P NMR (161 MHz, $CDCl_3$): δ= -2.06 (P^{B}), -16.34 (P^{A}).

MS(EI): m/z (%) = 408.2 (72) [M^+], 396 (100) [OM^+- N_2], 396.2 (100) [MO^+ - N_2], 380.2 (68) [M^+- N_2], 289.1(53) [M^+- *p*-MePh - N_2].

HRMS ESI-[TOF] for $C_{25}H_{21}N_4P$ [M+Li+O]: calcd. 431.1613; found. 431.1537.

7-(Di(*p*-fluorophenyl)phosphino)-3-(pyridin-2'-yl)-[1,2,3]triazolo[1,5-*a*]pyridine and **3-(6'-(di(*p*-fluorophenyl)phosphino)pyridin-2'-yl)-[1,2,3]triazolo[1,5-*a*]pyridine** (**69f**)

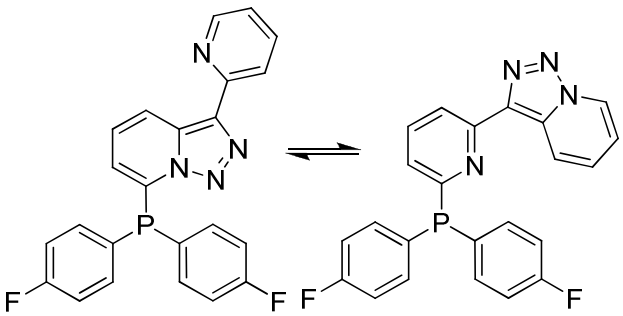

3-(Pyridine-2'-yl)-[1,2,3]triazolo[1,5-*a*] pyridine (0.30 g, 1.5 mmol) and di(*p*-fluorophenyl)phosphine chloride afforded 0.43 g (66%) of **69f** as a yellow oil after chromatography; A/B ratio = 0.40.

^{1}H NMR (300 MHz, $CDCl_3$): δ = 8.74 (d, *J* = 8.86 Hz, H^{4A}), 8.68 (d, *J* = 6.99 Hz, H^{7B}), 8.65 (d, *J* = 4.91 Hz, $H^{6'A}$), 8.32 (d, *J* = 8.02 Hz, $H^{3'A}$), 8.24 (d, *J* = 7.99 Hz, $H^{3'B}$), 7.80-7.74 (m, $H^{4'A}$), 7.70 (ddd, *J* = 7.82, 7.86, 2.56 Hz, $H^{4'B}$), 7.64 (d, *J* = 8.88 Hz, H^{4B}), 7.42 (m, (Ph-F)), 7.25-7.17 (m, H^{5A} + $H^{5'A}$ + $H^{5'B}$), 7.12-7.04 (m, H^{5B} + (Ph-F)), 6.96 (ddd, *J* = 6.83, 6.79, 1.38 Hz, H^{6B}), 6.46 (d, *J* = 6.84 Hz, H^{6A}).

^{13}C NMR (75.5 MHz, $CDCl_3$): δ = 163.99 (d, J_{C-F} = 251.04 Hz, C), 163.58 (d, J_{C-F} = 249.60 Hz, C), 162.41 (C), 152.40 (d, J_{C-P} = 8.23 Hz, C), 151.89 (C), 149.16 (CH), 137.05 (C), 136.61-135.97 (m), 132.14-131.75 (m), 126.60 (d, J_{C-P} = 29.40 Hz, CH), 126.10 (CH), 125.81 (CH), 124.96 (CH), 122.01 (CH), 121.42 (d, *J* = 1.38 Hz, CH), 121.29 (CH), 120.58 (CH), 118.92 (CH), 116.55-115.57 (m).

^{31}P NMR (161 MHz, $CDCl_3$): δ= -3.22 (t, J_{P-F} = 4.03 Hz, P^B), -17.16 (t, J_{P-F} = 4.05 Hz, P^A)

MS(EI): m/z (%) = 416.1 (39) [M^+], 404.1 (80) [M^+- N_2 + O] 388.1 (100) [M^+- N_2], 293.1(90) [M^+- *p*-F-Ph - N_2], 219.1 (65) [M^+- N_2 - *p*-F-Ph - Py].

HRMS ESI-[TOF] for $C_{23}H_{15}F_2N_4P$ [M+O+Li]: calcd. 439.1112; found. 439.1081.

7-(Di(*p*-trifluoromethylphenyl)phosphino)-3-(pyridin-2'-yl)-[1,2,3]triazolo[1,5-*a*]pyridine and **3-(6'-(di(*p*-trifluoromethylphenyl)phosphino)pyridin-2'-yl)-[1,2,3]triazolo[1,5-*a*]pyridine** (**69g**)

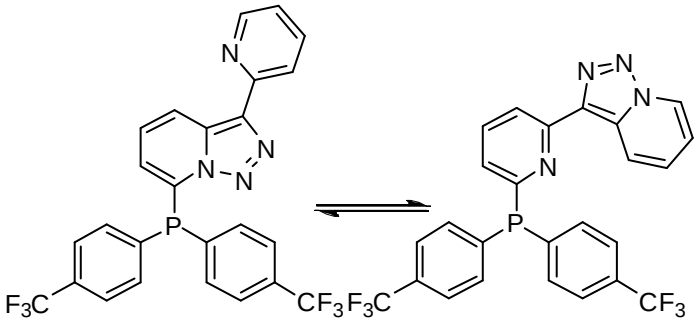

3-(Pyridine-2'-yl)-[1,2,3]triazolo[1,5-*a*]pyridine (0.30 g, 1.5 mmol) and di(*p*-trifluorophenyl)phosphine chloride were used affording 0.36 g (46%) of **69g** as a yellow oil after chromatography; A/B ratio = 0.18.

^{1}H NMR (300 MHz, $CDCl_3$): δ = 8.80 (d, *J* = 8.74 Hz, H^{4A}), 8.71-8.63 (m, H^{7B}+$H^{6'A}$), 8.32 (d, *J* = 7.99 Hz, $H^{3'A}$+$H^{3'B}$), 7.76 (ddd, *J* = 7.79, 7.75, 2.78 Hz, $H^{4'A}$+ $H^{4'B}$), 7.68-7.49 (m, (*p*-$CF_3Ph)_2$+ H^{4B}), 7.37-7.26 (m, $H^{5'A}$+ $H^{5'B}$), 7.21 (dd, *J* = 6.69, 5.04 Hz, H^{5A}), 7.06-6.91 (m, H^{5B}+ H^{6B}), 6.53 (d, *J* = 6.84 Hz, H^{6A}).

^{13}C NMR (75.5 MHz, $CDCl_3$): δ = 160.34 (C), 152.92 (d, $J_{C\text{-}P}$= 7.75 Hz, C), 151.68 (C), 149.19 (CH), 140.82 (d, $J_{C\text{-}P}$ = 13.06 Hz, C), 137.81 (C), 136.78 (C), 136.71-136.47 (C+CH), 134.54 (d, $J_{C\text{-}P}$ = 19.91 Hz, CH), 134.46 (d, *J* = 21.50 Hz, CH), 132.13 (q, $^{2}J_{C\text{-}F}$ = 33.7 Hz, C^{A}), 132.03 (C), 131,8 (C), 131.44 (C), 131.23 (q, $^{2}J_{C\text{-}F}$ = 32.6 Hz, C^{B}), 131.01 (C), 130.58 (C), 127.50 (d, $J_{C\text{-}P}$ = 33.58 Hz, CH), 126.27 (CH), 125.94-125.63 (m), 125.50-125.16 (m), 125.06 (CH), 123.91 (q, $^{1}J_{C\text{-}F}$= 272.3 Hz, C), 122.19-121.83 (m), 120.78 (CH), 120.60 (CH), 119.71 (CH), 118.50 (CH), 115.90 (CH).

^{31}P NMR (161 MHz, $CDCl_3$): δ = -1.15 (P^{B}), -15.31 (P^{A})

MS(EI): m/z(%) = 516.1 (12) [M^+], 488.1 (80) [M^+- N_2], 293.1(100) [M^+- *p*-CF_3-Ph - N_2].

HRMS ESI-[TOF] for $C_{25}H_{15}F_6N_4P$ [M+K]: calcd. 555.0576; found. 555.0513.

2-([1,2,3]triazolo[1,5-*a*]pyridin-3-yl)-8-(diphenylphosphoryl)quinoline (72, TQPO-1)

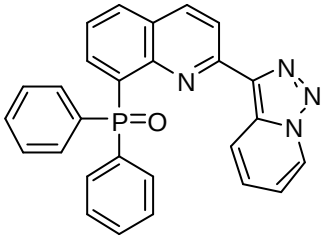

At -78 °C, butyllithium (1.6 mL, 2.2 mmol, 1.1 eq) in hexanes (1.5M) was added dropwise to a solution 3-(pyridin-2-yl)-[1,2,3]triazolo[1,5-*a*]quinoline (**50**) (0.5 g, 2.0 mmol, 1.0 eq.) in tetrahydrofuran (50 mL). The mixture was kept for 30 min at -78 °C before a solution of diphenylphosphine chloride (0.5 mL, 0.6 g, 2.3 mmol, 1.2 eq) in tetrahydrofuran (1 mL) was added and allowed to reach 25 °C (1 h). A saturated aqueous solution of ammonium chloride (20 mL) was added. The resulting mixture was extracted with dichloromethane (3×10 mL). The organic extracts were combined, washed with brine (10 mL), dried over sodium sulphate, filtered, and concentrated. Treatment with ethyl acetate provided 2-([1,2,3]triazolo[1,5-*a*]pyridin-3-yl)-8-(diphenylphosphoryl)quinoline (**72**) as a yellow powder (0.8 g, 89%). mp 401 °C decomp.

^{1}H NMR (300 MHz, $CDCl_3$): δ = 9.06 (d, *J* = 8.9 Hz, 1H), 8.68 (d, *J* = 6.9 Hz, 1H), 8.57 (d, *J* = 8.7 Hz, 1H), 8.29 (dd, *J* = 8.7, 1.1 Hz, 1H), 8.03 (d, *J* = 7.9 Hz, 1H), 7.8-7.7 (m, 4H), 7.6-7.3 (m, 9H), 7.02 (dt, *J* = 6.8, 6.8, 0.7 Hz, 1H)

^{13}C NMR (75.5 MHz, $CDCl_3$): δ = 152.1 (C), 148.8 (d, *J* = 4.4 Hz, C), 137.3 (d, *J* = 10.5 Hz, CH), 137.0 (d, *J* = 21.0 Hz,C), 136.9 (CH), 133.9 (C) 133.0 (d, *J* = 2.7 Hz, CH), 132.7 (d, *J* = 20.6 Hz, 2C), 132.0 (d, *J* = 9.9 Hz, 4CH), 131.5 (d, *J* = 2.9 Hz, 2CH), 130.8 (d, *J* = 1.4 Hz, C) 128.4 (d, *J* = 12.3 Hz, 4CH), 127.7 (d, *J* = 7.1 Hz, C), 127.1 (CH), 125.0 (d, *J* = 13.7 Hz, CH), 124.7 (CH), 122.6 (CH), 119.9 (CH), 116.3 (CH).

^{31}P NMR (161 MHz, $CDCl_3$): δ = 31.0 (PO).

MS(EI): m/z(%) = 446(10), 418(52), 417(100), 340(19).

HRMS ESI-[TOF] for $C_{27}H_{19}N_4OP$: calcd. 446.1296; found 446.1300.

2-([1,2,3]triazolo[1,5-*a*]pyridin-3-yl)-8-(bis(4-(trifluoromethyl)phenyl)phosphoryl)quinoline (73, TQPO-2)

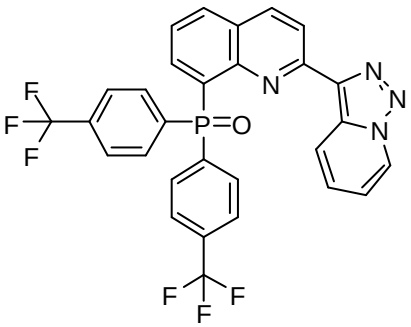

At -78 °C, butyllithium (0.8 mL, 1.1 mmol, 1.1 eq) in hexanes (1.5M) was added dropwise to a solution 3-(pyridin-2-yl)-[1,2,3]triazolo[1,5-*a*]quinoline (**53**) (0.3 g, 1.0 mmol, 1.0 eq.) in tetrahydrofuran (25 mL). The mixture was kept for 30 min at -78 °C before a solution of bis(4-(trifluoromethyl)phenyl)phosphine chloride (0.5 g, 1.2 mmol, 1.2 eq) in tetrahydrofuran (1 mL) was added and allowed to reach 25 °C (1 h). A saturated aqueous solution of ammonium chloride (20 mL)

was added. The resulting mixture was extracted with dichloromethane (3×10 mL). The organic extracts were combined, washed with brine (10 mL), dried over sodium sulphate, filtered, and concentrated. Treatment with ethyl acetate provided 2-([1,2,3]triazolo[1,5-*a*]pyridin-3-yl)-8-(bis(4-(trifluoromethyl)phenyl)phosphoryl)quinoline **(73)** as a yellow powder (0.5 g, 81%). mp 447 – 450 °C decomp.

^{1}H NMR (300 MHz, $CDCl_3$): δ = 8.75 (d, *J* = 8.9 Hz, 1H), 8.64 (d, *J* = 7.0 Hz, 1H), 8.53 (d, *J* = 8.7 Hz, 1H), 8.25 (dd, *J* = 8.7, 1.5 Hz, 1H), 8.03 (d, *J* = 7.9 Hz, 1H), 7.83 (d, *J* = 11.7 Hz, 2H), 7.80 (d, *J* = 11.8 Hz, 2H), 7.62-7.54 (m, 4H), 7.55-7.41 (m, 2H), 7.27 (dd, *J* = 8.9, 6.8 Hz, 1H), 6.97 (dt, *J* = 6.8, 6.8, 1.1 Hz, 1H).

^{13}C NMR (75.5 MHz, $CDCl_3$): δ = 152.6 (C), 148.7 (d, *J* = 4.46 Hz, C), 137.9 (C), 137.3 (d, *J* = 10.5 Hz,CH), 137.0 (d, *J* = 1.0 Hz,CH), 136.9 (d, *J* = 30.0 Hz, C),136.5 (C), 133.93 (CH), 133.9 (CH), 133.7 (qd, *J* = 30.4, 30.4 30.4,1.1 Hz,2×C), 132.7 (C), 132.4 (d, *J* = 10.2 Hz,4×CH), 127.7 (d, *J* = 7.4 Hz, 2×C), 127.6 (C), 127.3 (CH), 127.4 (q, J = 280.1 Hz, 2×C), 125.4 (dq, *J* = 11.1, 3.7, 3.7, 3.7 Hz, 4×CH), 125.1 (CH), 121.7 (CH), 120.5 (CH), 116.4 (CH).

^{31}P NMR (161 MHz, $CDCl_3$): δ = 28.0 (PO).

MS (EI): m/z(%) = 582(12), 555(43), 554(100), 553(80), 533,(47), 409(33), 355(50), 338(38).

HRMS ESI-[TOF] for $C_{29}H_{17}F_6N_4OP$: calcd. 582.1044; found 582.1048.

2-([1,2,3]triazolo[1,5-*a*]pyridin-3-yl)-8-(bis(4-methoxyphenyl)phosphoryl)quinoline (74, TQPO-3)

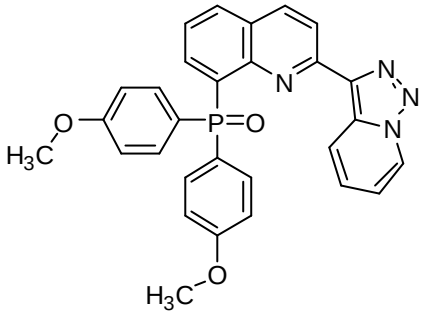

Prepared analogously as compound **72** starting from [1,2,3]triazolo[1,5-*a*]quinoline (**53**) (0.3 g, 1 mmol, 1.0 eq) and trapping of the lithiated intermediate with a solution of bis(4-methoxyphenyl)phosphine chloride (0.3 g, 1.2 mmol, 1.2 eq). Crystallization from dichloromethane gave 2-([1,2,3]triazolo[1,5-*a*]pyridin-3-yl)-8-(bis(4-methoxyphenyl)phosphoryl)quinoline (**74**) as pale colourless needles (0.4 g, 72%). mp 260 °C decomp.

^{1}H NMR (300 MHz, $CDCl_3$): δ = 9.11 (d, *J* = 8.9 Hz, 1H), 8.67 (d, *J* = 7.0 Hz, 1H), 8.54 (d, *J* = 8.7 Hz, 1H), 8.25 (dd, *J* = 8.7, 1.2 Hz, 1H), 7.99 (d, *J* = 8.0 Hz, 1H), 7.69-7.58 (m, 4H),

7.59-7.49 (m, 1H), 7.43 (dt, *J* = 7.7, 7.4, 2.3 Hz, 1H), 7.35 (dd, *J* = 8.3, 7.2 Hz, 1H), 7.00 (t, *J* = 6.8, 6.8 Hz, 1H), 6.86 (dd, *J* = 8.8, 2.0 Hz, 4H), 3.98 (s, 6H).

^{13}C NMR (75.5 MHz, $CDCl_3$): δ = 162.0 (d, *J* = 2.8 Hz,2×C), 152.1 (C), 150.0 (d, *J* = 4.4 Hz. C), 137.4 (C), 137.2 (d, *J* = 10.5 Hz, CH), 136.7 (CH), 133.8 (d, *J* = 11.3 Hz, 4×CH), 132.8 (d, *J* = 2.6 Hz,CH), 131.8 (C), 130.4 (C), 127.6 (d, *J* = 7.0 Hz, 2×C), 127.1 (CH), 125.7 (C), 125.0 (d, *J* = 13.7 Hz, CH), 124.7 (CH), 124.2 (C), 122.8 (CH), 119.7 (CH), 116.4 (CH), 113.9 (d, *J* = 13.4 Hz,4×C), 55.2 (s,2C)

^{31}P NMR (161 MHz, $CDCl_3$): δ = 30.6 (PO).

MS (EI): m/z(%) = 506(12), 478(37), 477(100), 462(22).

HRMS ESI-[TOF] for $C_{29}H_{23}N_4O_3P$: calcd. 506.1508; found 506.1504.

<u>General protocol</u>: Synthesis of [1,2,3]triazolo[1,5-*a*]pyridine based Monophosphines

At -40 °C, butyllithium (1 eq) in hexanes (1.54 M) was added dropwise to a solution of the corresponding 3-substituted[1,2,3]triazolo[1,5-*a*]pyridine (1 eq) in toluene. After 0.5 h, a solution of chlorophosphine (1 eq) in toluene (12.0 mL) was added dropwise. After 1 h, the solution was allowed to reach room temperature. Water (20.0 mL) was added, followed by extraction with dichloromethane (3 x 20.0 mL). The combined organic layers were dried over sodium sulfate, filtered, and evaporated.

7-(Diphenylphosphino)-3-methyl-[1,2,3]triazolo[1,5-*a*]pyridine (75a)

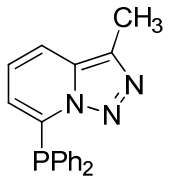

Starting from 3-methyl-[1,2,3]triazolo[1,5-*a*]pyridine (**1a**). The crude product was purified by filtration on silicagel to afford 7-(diphenylphosphino)-3-methyl-[1,2,3]triazolo[1,5-*a*]pyridine (**75a**; 42%) as a colorless solid. mp 142 – 144 °C.

^{1}H NMR (300 MHz, $CDCl_3$): δ = 7.60 (d, *J* = 8.8 Hz, 1 H), 7.45-7.30 (m, 10 H), 7.05 (dd, *J* = 8.8, 6.9 Hz, 1 H), 6.37 (d, *J* = 6.8 Hz, 1 H), 2.62 (s, 3 H).

^{13}C NMR (75 MHz, $CDCl_3$): δ = 138.5 (d, *J* = 22 Hz,) 134.5(d, *J* = 1.2 Hz, 2 C), 134.2 (d, *J* = 21 Hz, 4 C), 132.6(d, *J* = 8,3 Hz), 131.3, 129.7 (2 C), 128.84 (d, *J* = 7.7 Hz, 4 C), 123.1, 120.8, 117.2, 10.5.

^{31}P NMR (161 MHz, $CDCl_3$): δ= -15.4.

MS (EI): m/z(%) = 317.1 (63) [M^+], 288 (100) [M^+ - N_2], 212.1 (39) [M^+ - N_2 - Ph], 183.1 (93).

HRMS for $C_{19}H_{17}N_3P$**:** calcd. 318.1155; found 318.1145.

7-(Diphenylphosphine)-[1,2,3]triazolo[1,5-*a*]pyridine (75b)

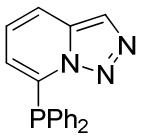

Starting from [1,2,3]triazolo[1,5-*a*]pyridine (**1c**). The crude product was purified by filtration on silicagel to afford 7-(diphenylphosphine)-[1,2,3]triazolo[1,5-*a*]pyridine (**75b**, 44%) as a colorless solid. mp 160 – 162 °C**.**

^{1}H NMR (300 MHz, $CDCl_3$): δ = 7.98 (d, *J* = 2.4 Hz, 1 H), 7.61 (d, *J* = 8.8 Hz, 1 H), 7.30-7.21 (m, 10 H), 7.01 (dd, *J* = 8.8, 6.9 Hz, 1 H), 6.32 (d, *J* = 6.8 Hz, 1 H).

^{13}C NMR (75 MHz, $CDCl_3$): δ = 138.4 (d, *J* = 22.4 Hz, 1 C) 133.9(d, *J* = 21.1 Hz, 4 C), 133.228 (s, 1 C), 132.3(d, *J* = 8.2 Hz, 2 C), 129.627 (s, 2 C) 128.7 (d, *J* = 7.8 Hz, 4 C) , 125.62 (d, *J* = 1.6 Hz, 1 C), 124.5 (s, 1 C), 120.9 (s, 1 C), 117.4 (s, 1 C).

^{31}P NMR (161 MHz, $CDCl_3$): δ= -15.0.

MS (EI): m/z(%) = 303.1 (78) [M^+], 275.1 (10) [M^+ - N_2], 274.1 (55) [M^+ - N_2 - H], 198.1 (23) [M^+ - N_2 - Ph], 183.1 (93)

HRMS for $C_{18}H_{14}N_3P$**:** [M+H^+] calcd. 304.0998; found 304.0969.

7-(Diphenylphosphino)-3-phenyl-[1,2,3]triazolo[1,5-*a*]pyridine (75c)

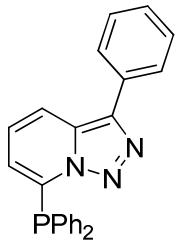

Starting from 3-phenyl-[1,2,3]triazolo[1,5-*a*]pyridine (**1d**). The crude product was purified by filtration on silicagel to afford 7-(diphenylphosphine)-[1,2,3]triazolo[1,5-*a*]pyridine (**75c**; 52%) as a yellow oil.

^{1}H NMR (300 MHz, $CDCl_3$): δ = 7.92 (d, *J* = 7.3 Hz, 3H), 7.44 (t, *J* = 7.7, 7.7 Hz, 2H), 7.31 (t, *J* = 7.4, 7.4 Hz, 1H), 7.20-7.14 (m, 2H), 2.8-2.6 (m, 2H), 2.0-1.9 (m, 2H), 1.8-1.6 (m, 3H), 1.6-1.4 (m, 5H), 1.3-1.0 (m, 10H)

^{13}C NMR (75 MHz, $CDCl_3$): δ = 139.3 (d, *J* = 23,3 Hz, 1 C), 137.8 (d, *J* = 1.9 Hz, 1 C), 134.2 (d, *J* = 21,2 Hz, 4 C), 132.4 (d, *J* = 8,3 Hz, 2 C), 131.6 (s, 1 C), 130.2 (s, 1 C), 129.8 (s, 2 C), 128.9 (d, *J* = 7,8 Hz, 4 C), 128.8 (s, 2 C), 127.7 (s, 1 C), 126.6 (s, 2 C), 124.9 (s, 1 C), 120.9 (s, 1 C), 117.9 (s, 1 C).

^{31}P NMR (161 MHz, $CDCl_3$): δ= 7.0

MS (EI): m/z(%) = 379.1 (8) [M^+], 351.1.1 (37) [M^+ - N_2], 350.1 (20) [M^+ - N_2 - H], 185.1 (72) [$P(Ph)_2$], 183.1 (100).

HRMS for $C_{24}H_{18}N_3P$: [M+O+Li^+] calcd. 402.1343; found 402.1316.

7-(Dicyclohexylphosphino)-3-methyl-[1,2,3]triazolo[1,5-*a*]pyridine (76a)

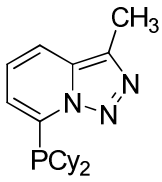

Starting from 3-methyl-[1,2,3]triazolo[1,5-*a*]pyridine (**1a**). The crude product was purified by filtration on silicagel to afford 7-(dicyclohexylphosphino)-3-methyl-[1,2,3]triazolo[1,5-*a*]pyridine (**76a**; 45%) as a colorless solid. mp 93 – 95 °C.

^{1}H NMR (300 MHz, $CDCl_3$): δ = 7.56 (d, *J* = 8.2 Hz, 1 H), 7.15-7.00 (m, 2 H), 2.73-2.57 (m, 2 H), 1.94 (dd, *J* = 16.5, 8.6 Hz, 2 H), 1.72 (d, *J* = 7.5 Hz, 2 H), 1.53 (m, 4H), 1.14 (m, 12 H).

^{13}C NMR (75 MHz, $CDCl_3$): δ = 136.5 (d, *J* = 8.2 Hz, 1C) 134.2 (s, 1 C), 131.5 (s, 1 C), 124.5 (d, *J* = 26.7 Hz, 1 C), 122.5 (d, *J* = 8.5 Hz, 1 C), 117.8 (s, 1 C), 32.4 (d, *J* = 11.0 Hz, 2 C), 30.9 (d, *J* = 19.3 Hz, 2 C), 29.9 (d, *J* = 8.9 Hz, 2 C), 26.7 (d, *J* = 3.2, 3.4 Hz, 2 C), 26.6 (bs, 2 C), 26.2-25.9 (bs, 1 C), 10.4 (s, CH_3).

^{31}P (161 MHz, $CDCl_3$): δ= 6.5

MS (EI): m/z(%) = 329.2 (35) [M^+], 301.2 (33) [M^+ - N_2], 246. (81) [M^+ - Cy], 218.2 (100) [M^+ - N_2 - Cy], 137 (66) [M^+ - N_2 - 2Cy].

HRMS for $C_{19}H_{28}N_3P$ [M+Li]: calcd. 336.2176; found 336.2215.

7-(Dicyclohexylphosphino)-[1,2,3]triazolo[1,5-*a*]pyridine (76b)

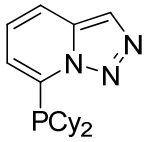

Starting from [1,2,3]triazolo[1,5-*a*]pyridine (**1c**).The crude product was purified by filtration on silicagel to afford 7-(dicyclohexylphosphino)-[1,2,3]triazolo[1,5-*a*]pyridine (**76b**; 58%) as a colorless solid. mp 124 – 126 °C.

^{1}H NMR (300 MHz, $CDCl_3$): δ = 8.07 (s, 1 H), 7.73-7.65 (m, 1 H), 7.21-7.10 (m, 2 H), 2.72-2.55 (m, 2 H), 2.02-1.90 (m, 2 H), 1.79-1.70 (m, 2 H), 1.63-1.51 (m, 4 H), 1.35.1.16 (m 10 H).

^{13}C NMR (75 MHz, $CDCl_3$): δ = 137.1 (d, *J* = 41.8 Hz, 1 C), 133.7 (s, 1 C), 125.697 (s, 1 C), 124.6 (d, *J* = 25.9 Hz, 1 C) , 124.1(d, *J* = 8.2 Hz, 1 C), 118.2 (s, 1 C), 32.6 (d, *J* = 11.3 Hz, 1 C), 30.9 (d, *J* = 19.1 Hz, 1 C), 30.0 (d, *J* = 9.0 Hz, 1 C), 26.7 (d, *J* = 3.6 Hz, 1 C), 26.6 (s, 1 C), 26.8 (d, *J* = 1.1 Hz, 1 C).

^{31}P NMR (161 MHz, $CDCl_3$): δ= 7.0

MS (EI): m/z(%) = 315.2 (42) [M^+], 287.2 (33) [M^+ - N_2], 232.1 (57) [M^+ - Cy], 204.2 (100) [M^+ - N_2 - Cy], 151,1 (45) [M^+ - 2Cy + 2H], 123 (25) [M^+ - N_2 - 2Cy + 2H].

HRMS for $C_{18}H_{26}N_3P$ [M+Li]: calcd. 322.2019; found 32.1975.

7-(Dicyclohexylphosphino)-3-methyl-[1,2,3]triazolo[1,5-*a*]pyridine (76c)

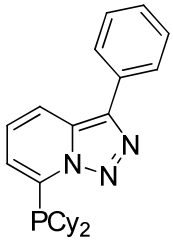

Starting from 3-methyl-[1,2,3]triazolo[1,5-*a*]pyridine (**1d**). The crude product was purified by filtration on silicagel to afford 7-(dicyclohexylphosphino)-3-methyl-[1,2,3]triazolo[1,5-*a*]pyridine (**76c**; 45%) as a colorless solid. mp 93 – 95 °C.

^{1}H NMR (300 MHz, $CDCl_3$): δ = 7.56 (d, *J* = 8.2 Hz, 1 H), 7.15-7.00 (m, 2 H), 2.73-2.57 (m, 2 H), 1.94 (dd, *J* = 16.5, 8.6 Hz, 2 H), 1.72 (d, *J* = 7.5 Hz, 2 H), 1.53 (m, 4H), 1.14 (m, 12 H).

^{13}C NMR (75 MHz, $CDCl_3$): δ = 137.8 (C), 137.6 (d, *J* = 44.5 Hz, C), 131.7 (C), 130.7 (C), 128.9 (2CH), 127.7 (CH), 126.6 (CH), 125.1 (d, *J* = 27.6 Hz, CH), 24.6 (d, *J* = 8.7 Hz, CH), 118.8 (CH), 32.7 (d, *J* = 27.6 Hz, 2×CH), 31.1 (d, *J* = 19.3 Hz, 2×CH_2), 30.2 (d, *J* = 9.0 Hz, 2×CH_2), 26.9 (2×CH_2), 26.8 (d, *J* = 3.5 Hz, 2×CH_2), 26.7 (2×CH_2), 26.2 (2×CH_2).

^{31}P NMR (161 MHz, $CDCl_3$): δ= 6.5

MS (EI): m/z(%) = 391.2 (25) [M^+], 363.2 (80) [M^+ - N_2], 280. (100) [M^+ - N_2 -Cy], 199.1 (90), 146.1 (90).

HRMS for $C_{24}H_{30}N_3P$ [M+Li]: calcd.; found.

7-(Diisopropylphosphino)-3-methyl-[1,2,3]triazolo[1,5-*a*]pyridine (77a)

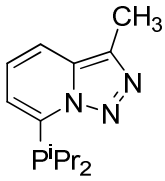

Starting from 3-methyl-[1,2,3]triazolo[1,5-*a*]pyridine (**1a**). The crude product was purified by filtration on silicagel to afford 7-(diisopropylphosphino)-3-methyl-[1,2,3]triazolo[1,5-*a*]pyridine (**77c**; 48%) as a brown oil.

^{1}H NMR (300 MHz, $CDCl_3$): δ = 7.60 (d, *J* = 8.6 Hz, 1 H), 7.21-7.06 (m, 2 H), 2.97-2.78 (m, 2 H), 2.61 (s, 3 H), 1.21 (dd, *J* = 16.1, 7.0 Hz, 1H), 0.88 (dd, *J* = 13.2, 7.0 Hz, 6 H)

^{13}C NMR (75 MHz, $CDCl_3$): δ = 137.4 (d, *J* = 41.8 Hz, C), 134.4 (s, 1 C), 131.6 (s, 1 C), 124.4 (d, *J* = 26.1 Hz, 1 C), 122.7 (d, *J* = 8.3 Hz, 1 C), 117.9 (s, 1 C), 22.6 (d, *J* = 10.4 Hz, 2 C), 20.7 5 (d, *J* = 14.5 Hz, 2 C), 20,5 (d, *J* = 4.6 Hz, 2 C), 10.4 (s, 1 C)

^{31}P NMR (161 MHz, $CDCl_3$): δ= 16.1

MS (EI): m/z(%) = 249.2 (56) [M^+], 221.2 (11) [M^+ - N_2], 206.1 (26) [M^+ - ^{i}Prop], 178.1 (100) [M^+ - N_2 - ^{i}Prop], 136.1 (64) [M^+ - N_2 - 2Cy]

HRMS for $C_{13}H_{20}N_3P$ [M+Li]: calcd. 256.1550; found 256.1519.

7-(Diisopropylphosphino)-[1,2,3]triazolo[1,5-*a*]pyridine (77b)

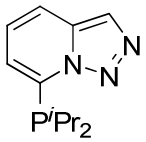

Starting from [1,2,3]triazolo[1,5-*a*]pyridine (**1c**). The crude product was purified by filtration on silicagel to afford 7-(diisopropylphosphino)-[1,2,3]triazolo[1,5-*a*]pyridine (**77b**; 50%) as a brown oil.

^{1}H NMR (300 MHz, $CDCl_3$): δ = 8.02 (d, *J* = 0.9 Hz, 1 H), 7.71-7.62 (m, 1 H), 7.17-7.09 (m, 2 H), 2.77 (pq, *J* = 12.6, 12.6, 12.6, 7.0, 7.0, 7.0, 7.0 Hz, 2 H), 1.13 (dd, *J* = 15.9, 7.0 Hz, 6 H), 0.81 (dd, *J* = 13.4, 7.0 Hz, 6 H).

^{13}C NMR (75 MHz, $CDCl_3$): δ = 137.5 (d, *J* = 42.2 Hz, 1 C) 133.6 (s, 1 C), 125.6 (s, 1 C), 124.3 (d, *J* = 24.2 Hz, 1 C), 124.2 (d, *J* = 7,6.7 Hz, 1 C), 118.1 (s, 1 C), 22.5 (d, *J* = 10.9 Hz, 2 C), 20.4 (d, *J* = 10.0 Hz, 2 C), 20.2 (s, 2 C).

^{31}P NMR (161 MHz, $CDCl_3$): δ= 15.4.

MS (EI): m/z(%) = 235.2 (49) [M^+], 207.2 (21) [$M^+ - N_2$], 192.1 (100) [$M^+ - {}^{i}$Prop], 164.1 (39) [$M^+ - N_2 - {}^{i}$Prop], 149.1 (85) [$M^+ - 2{}^{i}$Prop], 122.1 (42) [$M^+ - N_2 - 2{}^{i}$Prop + H].

HRMS for $C_{12}H_{18}N_3P$ [M+Li]: calcd. 242.1393; found 242.1371.

7-(Diisopropylphosphino)-3-phenyl-[1,2,3]triazolo[1,5-*a*]pyridine (77c)

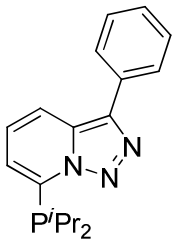

Starting from [1,2,3]triazolo[1,5-*a*]pyridine (**1d**). The crude product was purified by filtration on silicagel to afford 7-(diisopropylphosphino)-3-phenyl-[1,2,3]triazolo[1,5-*a*]pyridine (**77c**; 23%) as a brown oil.

^{1}H NMR (300 MHz, $CDCl_3$): δ =7.95-7.85 (m, 3 H), 7.46-7.39 (m, 2 H), 7.34-7.26 (m, 1 H), 7.19-7.13 (m, 2 H), 2.85 (sept.d, *J* = 13.9, 7.0, 7.0, 6.9, 6.9, 6.9, 6.9 Hz, 2 H), 1.17 (dd, *J* = 16.1, 7.0 Hz, 6 H), 0.84 (dd, *J* = 13.5, 7.0 Hz, 6 H).

^{13}C NMR (75 MHz, $CDCl_3$): δ = 138.2 (d, *J* = 43.6 Hz, 1 C), 137.9 (s, 1 C), 131.6 (s, 1 C), 130.6 (s, 1 C), 128.9 (s, 2 C), 127.8 (s, 1 C), 126.7 (s, 2 C), 124.7 (d, *J* = 26.2 Hz, 1 C), 124.6 (d, *J* = 8.3 Hz, 1 C), 118.8 (s, 1 C), 22.8 (d, *J* = 10.7 Hz, 2 C), 20.7 (d, *J* = 7. 9 Hz, 2 C), 20.5 (d, *J* = 1.7 Hz, 2 C).

^{31}P NMR (161 MHz, $CDCl_3$): δ= 17.3

MS (EI): m/z(%) = 311.2 (28) [M^+], 283.2 (58) [$M^+ - N_2$], 240.1 (55) [$M^+ - N_2 - {}^{i}$Prop], 198.1 (100) [$HM^+ - N_2 - 2{}^{i}$Prop], 167.1 (51) [$M^+ - N_2 - 2{}^{i}$Prop + H].

HRMS for $C_{18}H_{22}N_3P$ [M+Li]: calcd. 318.1716; found 318.1721.

The corresponding phosphine oxides were prepared according to standard procedure: the phosphines (80 mg) were diluted in methanol (3 mL) and hydrogen peroxide (2 mL) at 0 °C during 24 h affording the corresponding oxides in quantitative yields.

7-(Diphenylphosphoryl)-3-methyl-[1,2,3]triazolo[1,5-*a*]pyridine (78a)

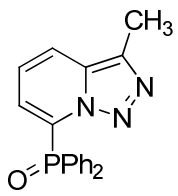

The crude product was purified by filtration on silicagel with dichloromethane affording 7-(diphenylphosphoryl)-3-methyl-[1,2,3]triazolo[1,5-*a*]pyridine (**78a**; 99%) as a colorless solid. mp 150 – 152 °C.

^{1}H NMR (300 MHz, $CDCl_3$): δ = 7.9-7.7 (m, 5H), 7.72 (d, *J* = 8.9 Hz, 1H), 7.46 (dt, *J* = 7.1, 7.1, 1.1 Hz, 2H), 7.4-7.3 (m, 4H), 7.2 (d, *J* = 7.9, 7.6 Hz, 1H), 2.50 (s, 3H)

^{13}C NMR (75 MHz, $CDCl_3$): δ = 134.9 (C), 132.7 (d, *J* = 2.5 Hz, 2CH), 132.3 (d, *J* = 11.0 Hz, 4CH), 131.6 (d, *J* = 2.6 Hz, C), 130.1 (d, *J* = 16.0 Hz, 1C), 128.4 (d, *J* = 13.2 Hz, 4CH), 124.9 (d, *J* = 8.3 Hz, CH), 123.1 (d, *J* = 8.7 Hz, CH), 121.1 (d, *J* = 2.4 Hz, CH).

^{31}P NMR (161 MHz, $CDCl_3$): δ= 21.2 (PO).

7-(Dicyclohexylphosphoryl)-3-methyl-[1,2,3]triazolo[1,5-*a*]pyridine (78b)

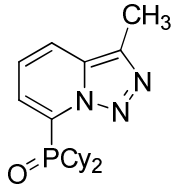

The crude product was purified by filtration on silicagel with dichloromethane affording 7-(dicyclohexylphosphoryl)-3-methyl-[1,2,3]triazolo[1,5-*a*]pyridine (**78b**; 99%) as a colorless solid. mp 174 – 176 °C.

^{1}H NMR (300 MHz, $CDCl_3$): δ = 7.8-7.6 (m, 2H), 7.3 (ddd, *J* = 8.8, 6.8, 0.8 Hz, 1H), 2.7-2.6 (m, 5H), 2.2-2.1 (m, 2H), 1.9-1.7 (m, 2H), 1.7-1.0 (m, 16H).

^{13}C NMR (75 MHz, $CDCl_3$): δ = 134.9 (s, 1 C), 131.4 (d, *J* = 2.7 Hz, C), 130.9 (d, *J* = 81.1 Hz, C), 124.8 (d, *J* = 6.1 Hz, CH), 123.1 (d, *J* = 6.1 Hz, CH), 119.9 (d, *J* = 2.2 Hz, CH), 36.0 (d, *J* = 67.5 Hz, 2CH), 26.2 (d, *J* = 4.5 Hz, $2CH_2$), 26.0 (d, *J* = 4.2 Hz, $2CH_2$), 25.6 (d, *J* = 3.9 Hz, $2CH_2$), 25.5 (d, *J* = 1.3 Hz, $2CH_2$), 25.4 (d, *J* = 3.5 Hz, $4CH_2$),

^{31}P NMR (161 MHz, $CDCl_3$): δ= 47.2 (PO)

7-(Siisopropylphosphoryl)-3-methyl-[1,2,3]triazolo[1,5-*a*]pyridine (**78c**)

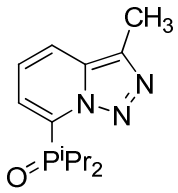

The crude product was purified by filtration on silicagel with dichloromethane affording 7-(diisopropylphosphoryl)-3-methyl-[1,2,3]triazolo[1,5-*a*]pyridine (**78c**; 48%) as a brown oil.

^{1}H NMR (300 MHz, $CDCl_3$): δ = 7.8-7.7 (m, 2H), 7.28 (dd, *J* = 9.0, 6.7 Hz, 1H), 3.0-2.7 (m, 2H), 1.36 (dd, *J* = 16.2, 7.2 Hz, 6H), 0.91 (dd, *J* = 17.3, 7.2 Hz, 6H)

^{13}C NMR (75 MHz, $CDCl_3$): δ = 134.9 (C), 131.56 (d, *J* = 0.6 Hz, C), 130.9 (d, *J* = 86.5 Hz, C), 124.8 (d, *J* = 6.0 Hz, CH), 123.3 (d, *J* = 7.4 Hz, CH), 120.2 (d, *J* = 2.3 Hz, CH), 26.3 (d, *J* = 67.5 Hz, 2CH), 16.6 (d, *J* = 3.7 Hz, $2CH_3$), 15.5 (d, *J* = 3.5 Hz, $2CH_3$),

^{31}P NMR (161 MHz, $CDCl_3$): δ= 16.1

The corresponding phosphine selenides were prepared according to standard procedure: Under argon atmosphere, the phosphines (80 mg) were diluted in chloroform (3 mL) and selenium powder was added (30 mg). Then, the mixture was heated at 60 °C during 24 h affording the corresponding selenides in quantitative yields

7-(Diphenylphosphoroselenoyl)-3-methyl-[1,2,3]triazolo[1,5-*a*]pyridine (**79a**)

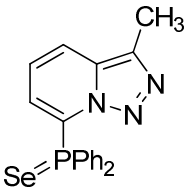

The crude product was purified by filtration on silicagel with dichloromethane affording 7-(diphenylphosphoroselenoyl)-3-methyl-[1,2,3]triazolo[1,5-*a*] pyridi (**79a**; 99%) as a colorless solid. mp 140 – 143 °C.

^{1}H NMR (300 MHz, $CDCl_3$): δ = 8.11 (ddd, *J* = 12.8, 6.8, 0.7 Hz, 1H), 7.9-7.8 (m, 4H), 7.78 (ddd, *J* = 8.8, 2.1, 1.1 Hz, 1H), 7.5-7.3 (m, 6H), 7.29 (ddd, *J* = 8.7, 7.2, 1.2 Hz, 1H), 2.56 (s, 3H).

^{13}C NMR (75 MHz, $CDCl_3$): δ = 135.0 (C), 132.6 (d, *J* = 11.8 Hz, 4CH), 132.0 (d, *J* = 3.2 Hz, 2CH), 131.7 (d, *J* = 1.9 Hz, C), 128.7 (d, *J* = 73.6 Hz, C), 128.6 (d, *J* = 83.1 Hz, 2C), 128.4 (d, *J* = 13.5 Hz, C) 127.7 (d, *J* = 14.1 Hz, CH), 123.1 (d, *J* = 10.1 Hz, CH), 121.2 (d, *J* = 2.5 Hz, CH). 10.3 (CH_3)

^{31}P NMR (161 MHz, $CDCl_3$): δ= 32.3 (d, *J* = 758 Hz, P).

7-(Dicyclohexylphosphoroselenoyl)-3-methyl-[1,2,3]triazolo[1,5-*a*]pyridine (79b)

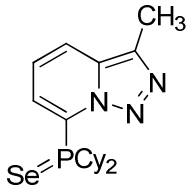

The crude product was purified by filtration on silicagel with dichloromethane affording 7-(dicyclohexylphosphoroselenoyl)-3-methyl-[1,2,3]triazolo[1,5-*a*]pyridine (**79b**; 99%) as a colorless solid. mp 95 – 97 °C.

^{1}H NMR (300 MHz, $CDCl_3$): δ = 8.17 (ddd, *J* = 11.2, 6.9, 1.2 Hz, 1H), 7.70 (ddd, *J* = 8.8, 2.2, 1.3 Hz, 1H), 7.25 (ddd, *J* = 8.8, 6.9, 0.8 Hz, 1H), 3.4-3.2 (m, 2H), 2.6-2.5 (s, 3H), 2.0-0.7 (m, 20H)

^{13}C NMR (75 MHz, $CDCl_3$): δ = 134.9 (s, 1 C), 131.5 (d, *J* = 1.8 Hz, C), 129.1 (d, *J* = 11.3 Hz, CH), 128.1 (d, *J* = 55.2 Hz, C), 123.4 (d, *J* = 9.0 Hz, CH), 120.1 (d, *J* = 2.2 Hz, CH), 36.2 (d, *J* = 41.5 Hz, 2CH), 27.9 ($2CH_2$), 26.7 (d, *J* = 3.5 Hz, $2CH_2$), 25.6 (d, *J* = 3.9 Hz, $2CH_2$), 25.9 (d, *J* = 6.6 Hz, $2CH_2$), 25.7 (d, *J* = 7.6 Hz, $2CH_2$), 25,3 (d, *J* = 1.3 Hz, $2CH_2$).

^{31}P NMR (161 MHz, $CDCl_3$): δ = 65.9 (d, *J* = 737 Hz, P).

7-(Diisopropylphosphoroselenoyl)-3-methyl-[1,2,3]triazolo[1,5-*a*]pyridine (79c)

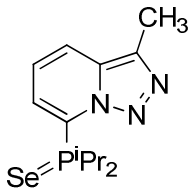

The crude product was purified by filtration on silicagel with dichloromethane affording 7-(diisopropylphosphoroyl)-3-methyl-[1,2,3]triazolo[1,5-*a*]pyridine (**79c**; 48%) as a brown oil.

^{1}H NMR (300 MHz, $CDCl_3$): δ = 8.26 (ddd, *J* = 11.2, 6.9, 1.2 Hz, 1H), 7.76 (ddd, *J* = 8.8, 2.2, 1.3 Hz, 1H), 7.31 (ddd, *J* = 8.7, 6.9, 0.8 Hz, 1H), 3.59 (qd, *J* = 13.8, 6.9, 6.9, 6.9 Hz, 1H), 2.66 (s, 1H), 1.35 (dd, *J* = 19.7, 6.8 Hz, 1H), 0.74 (dd, *J* = 19.8, 6.9 Hz, 1H)

^{13}C NMR (75 MHz, $CDCl_3$): δ = 135.1 (C), 131.6 (d, *J* = 1.8 Hz, C), 128.9 (d, *J* = 56.1 Hz, C), 128.8 (d, *J* = 11.3 Hz, CH), 123.5 (d, *J* = 9.1 Hz, CH), 120.3 (d, *J* = 2.4 Hz, CH), 26.6 (d, *J* = 42.5 Hz, 2CH), 17.9 (m, $4CH_3$).

^{31}P NMR (161 MHz, $CDCl_3$): δ = 75.3 (d, *J* = 745 Hz, P).

Synthesis of [1,2,3]triazolo[1,5-*a*]quinoline (44) based Monophosphines

At -40 °C, *tert*-butyllithium (3.6 mL, 6.2 mmol, 1.1 eq) in hexanes (1.7 M) was added dropwise to a solution of the corresponding [1,2,3]triazolo[1,5-*a*]quinoline (1.0 g, 6.1 mmol, 1 eq) in tetrahydrofuran (75%) . After 0.5 h, a solution of chlorophosphine (7 mmol,1.2 eq) in toluene (12.0 mL) was added dropwise. After 1 h, the solution was allowed to reach room temperature. Water (20.0 mL) was added, followed by extraction with dichloromethane (3 x 20.0 mL). The combined organic layers were dried over sodium sulfate, filtered, and evaporated.

3-(Diphenylphosphino)-[1,2,3]triazolo[1,5-*a*]quinoline (80a)

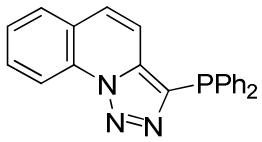

Starting from [1,2,3]triazolo[1,5-*a*]quinoline (**44**) (1g, 6 mmol, 1eq). The crude product was purified by filtration on silicagel with dichloromethane affording 3-(diphenylphosphino)-[1,2,3]triazolo[1,5-*a*]quinoline (**80a**; 34%) as a colorless solid. mp 135 – 140 °C.

^{1}H NMR (300 MHz, $CDCl_3$): δ = 8.81 (d, *J* = 8.39 Hz, 1 H), 7.82(dd, *J* = 7.8, 1.2 Hz, 1 H), 7.63 (ddd, *J* = 8.5, 7.34, 1.4, 1 H), 7.62-7.55 (m, 5 H), 7.47 (d, *J* = 9.3 Hz, 1 H), 7.34-7.39 (m, 5 H), 7.32 (d, *J* = 9.4 Hz, 1 H).

^{13}C NMR (75 MHz, $CDCl_3$): δ = 136.3 (d, *J* = 28.0 Hz, 1 C), 136.0 (d, *J* = 5.7 Hz, 1 C), 135.4 (d, *J* = 7.8 Hz, 1 C), 133.4 (d, *J* = 19.9 Hz, 4 C), 132.0 (s, 1 C), 131.5 (d, *J* = 10.4 Hz, 1 C), 130.1 (s, 1 C), 128.8 (s, 2 C), 128.55 (d, *J* = 7.4 Hz, 4 C), 128.4 (s, 1 C), 127.4 (s, 1 C), 127.1 (s, 1 C), 123.9 (s, 1 C), 116.3 (s, 1 C), 115.0 (s, 1 C), 114.9 (s, 1 C).

^{31}P NMR (161 MHz, $CDCl_3$): δ = -34.0

MS (EI): m/z(%) = 353.1 (11) [M^+], 324.9 (84) [$M^+ - N_2$], 248.1 (100) [$M^+ - N_2$ - Ph],

HRMS for $C_{22}H_{16}N_3P$: [M+Li^+] calcd. 360.1236; found 360.1189.

3-(diphenylphosphoryl)-[1,2,3]triazolo[1,5-*a*]quinoline (81a)

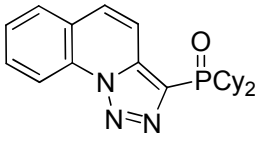

Starting from [1,2,3]triazolo[1,5-*a*]quinoline (**44**) (1g, 6 mmol, 1eq). The crude product was purified by filtration on silicagel with ethyl acetate oxidation product was isolated affording 3-(diphenylphosphoryl)-[1,2,3]triazolo[1,5-*a*]quinoline (**81a**; 51%) as a colorless solid. mp 174 – 176 °C.

^{1}H NMR (300 MHz, $CDCl_3$): δ = 8.79 (d, *J* = 8.0 Hz, 1 H), 8.16 (d, *J* = 9.3 Hz, 1 H), 7.88 (dd, *J* = 7.9, 1.0 Hz, 1 H), 7.81-7.75 (m, 1 H), 7.64 (m, 2 H), 2.34-2.22 (m, 3 H), 2.19-2.07 (m, 2 H), 1.95-1.58 (m, 8 H), 1.58-1.40 (m, 2 H), 1.32-1.02 (m, 8 H)

^{13}C NMR (75 MHz, $CDCl_3$): δ = 138.4 (d, *J* = 18.8, 1 C) 131.7 (s, 1 C), 131.0 (s, 1 C), 130.219 (s, 1 C), 128.653 (s, 1 C), 128.464 (s, 1 C), 127.484 (s, 1 C), 124.2 (s, 1 C), 116.353 (s, 1 C), 116.235 (s, 1 C), 36.0 (d, *J* = 70.4 Hz, 2 C) , 26.3 (d, *J* = 1.7 Hz, 2 C), 26.0 (d, *J* = 2.2 Hz, 2 C), 25.8 (d, *J* = 1.2 Hz, 2 C), 25.1 (d, *J* = 2.9 Hz, 2 C), 24.3 (d, *J* = 3.1 Hz, 2 C).

^{31}P NMR (161 MHz, $CDCl_3$): δ = 46.0

MS (EI): m/z(%) = 381.1 (11) [M^+], 298.0 (37) [M^+ - Cy], 270.9 (100) [M^+ - Cy - N_2], 188.0 (66) [M^+ - 2 Cy – N_2].

HRMS for $C_{22}H_{16}N_3PO$: [M+Li^+] calcd. 388.2125; found 388.2131.

3-(diisopropylphosphoryl)-[1,2,3]triazolo[1,5-*a*]quinoline (81b)

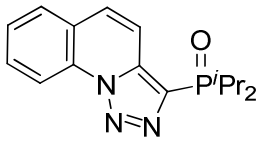

Starting from [1,2,3]triazolo[1,5-*a*]quinoline (**44**). The crude product was purified by filtration on silicagel with ethyl acetate oxidation product was isolated affording 3-(diisopropylphosphoryl)-[1,2,3]triazolo[1,5-*a*]quinoline (**81b**; 59%) as a colorless solid. mp 115 – 118 °C.

^{1}H NMR (300 MHz, $CDCl_3$): δ = 8.80 (d, *J* = 8.4 Hz, 1 H), 8.19 (d, *J* = 9.3 Hz, 1 H), 7.90 (dd, *J* = 7.9, 1.1 Hz, 1 H), 7.79 (ddd, *J* = 8.4, 7.4, 1.4, 1 H), 7.70-7.61 (m, 2H), 2.66-2.46 (m, 2 H), 1.26 (dd, *J* = 15.9, 7.1 Hz, 6 H), 1.17 (dd, *J* = 16.6, 7.1 Hz, 6 H).

^{13}C NMR (75 MHz, $CDCl_3$): δ = 138.5 (d, *J* = 18.8, 1 C), 131.7 (s, 1 C), 130.6 (s, 1 C), 130.276 (s, 1 C), 128.7 (s, 1 C), 128.601 (s, 1 C), 127.524 (s, 1 C), 124.205 (s, 1 C), 116.396 (s, 1 C), 116.143 (s, 1 C), 26.4 (d, *J* = 70.2 Hz, 2 C), 15.6 (d, *J* = 2,5 Hz, 2 C), 14.7 (d, *J* = 3,2 Hz, 2 C).

^{31}P NMR (161 MHz, $CDCl_3$): δ = 52.3

MS (EI): m/z(%) = 301.0 (20) [M^+], 258.0 (5) [M^+ - ^{i}Prop], 230.9 (83) [M^+ - ^{i}Prop - N_2], 188.0 (66) [M^+ - 2 ^{i}Prop – N_2], 128.1 (74) [M^+ - C-P(O)(^{i}Prop)$_2$ - N_2].

HRMS for $C_{16}H_{20}N_3PO$: [M+Li^+] calcd. 308.1499; found 308.1464.

7.1.5 Chapter V: Fluorescence

1-(6-([1,2,3]Triazolo[1,5-*a*]pyridin-3-yl)pyridin-2-yl)-1-(naphthalen-2-yl)ethanol (85, TPON)

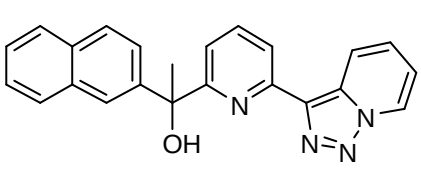

At -40 °C, butyllithium (0.8 mL, 1.1 mmol, 1.1 eq) in hexanes (1.54 M) was added dropwise to a stirred solution of 3-(2'-pyridyl)-[1,2,3]triazolo[1,5-*a*]pyridine (**1b**) (0.2 mg, 1.1 mmol 1 eq) in toluene (11 mL). After 15 min, a solution of 1-(naphthalen-2-yl)ethanone (0.2 mg, 1.1 mmol, 1.1 eq) in toluene (1.5 mL) was added dropwise. After 1 h, the solution was allowed to reach room temperature and saturated aqueous solution of ammonium chloride (20.0 mL) was added, followed by extraction with dichloromethane (3 x 20.0 mL). The combined organic layers were dried over sodium sulfate, filtered, and evaporated, chromatography (cyclohexane → ethyl acetate 1:1) provided 1-(6-([1,2,3]triazolo[1,5-*a*]pyridin-3-yl)pyridin-2-yl)-1-(naphthalen-2-yl)ethanol (**85, TPON**) as a colourless solid (0.2 mg, 60%). mp 128 – 130 °C.

^{1}H NMR (300 MHz, $CDCl_3$): δ = 8.66 (d, *J* = 7.0 Hz, 1H), 8.32 (d, *J* = 8.9 Hz, 1H), 8.17 (dd, *J* = 7.8, 0.7 Hz, 1H), 7.99 (d, *J* = 1.4 Hz, 1H), 7.8-7.7 (m, 1H), 7.7-7.6 (m, 3H), 7.50 (dd, *J* = 8.7, 1.9 Hz, 1H), 7.4-7.3 (m, 2H), 7.2-7.1 (m, 2H), 6.93 (dt, *J* = 6.9, 6.9, 1.2 Hz, 1H), 5.38 (s, OH), 2.08 (s, CH_3)

^{13}C NMR (75 MHz, $CDCl_3$): δ = 164.4 (C), 149.9 (C), 144.3 (C), 137.8 (CH), 136.9 (C), 133.0 (C), 132.4 (C), 131.8 (C), 128.1 (CH), 128.0 (CH), 127.4 (CH), 126.6 (CH), 126.0 (CH), 125.9 (CH), 125.3 (CH), 124.8 (CH), 124.1 (CH), 120.4 (CH), 119.0 (CH), 118.8 (CH), 115.7 (CH), 76.0 (C), 29.3 (CH_3).

MS (EI): m/z(%) = 366(46) 384(25) 338(71) 337(25) 323(36) 321(39) 320(100) 319(18) 259(59) 155(47) 127(29).

HRMS for $C_{23}H_{14}N_4O$: calcd. 366.1481; found 366.1489.

(6-([1,2,3]Triazolo[1,5-*a*]pyridin-3-yl)pyridin-2-yl)(anthracen-9-yl)methanol (86, TPOA)

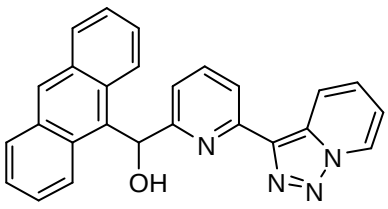

At -40 °C, butyllithium (4.2 mL, 5.6 mmol, 1.1 eq) in hexanes (1.54 M) was added dropwise to a stirred solution of 3-(2'-pyridyl)-[1,2,3]triazolo[1,5-*a*]pyridine (**1b**) (1.0 g, 5.1 mmol 1 eq) in toluene (100 mL). After 15 min, a solution of anthracene-9-carbaldehyde (1.1 g, 1.1 mmol, 1.1 eq) in toluene (10 mL) was added dropwise. After 1 h, the solution was allowed to reach room

temperature and saturated aqueous solution of ammonium chloride (20.0 mL) was added, followed by extraction with dichloromethane (3 x 20.0 mL). The combined organic layers were dried over sodium sulfate, filtered, and evaporated, crystallization from ethyl acetate provided (6-([1,2,3]triazolo[1,5-*a*]pyridin-3-yl)pyridin-2-yl)(anthracen-9-yl)methanol (**86, TPOA**) as a yellow solid (1.2 g, 58%). mp 140 – 142 °C.

^{1}H NMR (300 MHz, $CDCl_3$): δ = 8.65 (td, *J* = 7.0, 1.0, 1.0 Hz, 1H), 8.42 (s, 1H), 8.34 (d, *J* = 8.4 Hz, 2H), 8.14 (d, *J* = 7.8 Hz, 1H), 8.09 (td, *J* = 8.9, 1.1, 1.1 Hz, 1H), 8.0-7.9 (m, 2H), 7.57 (t, *J* = 7.8, 7.8 Hz, 1H), 7.4-7.3 (m, 5H), 7.11 (ddd, *J* = 8.9, 6.7, 1.0 Hz, 1H), 7.0-6.9 (m, 2H), 5.11 (s, 1H).

^{13}C NMR (75 MHz, $CDCl_3$): δ = 161.8 (C), 150.3 (C), 137.8 (CH), 136.9 (C), 132.6 (C), 131.8 (C), 131.7 (2×C), 130.5 (2×C), 129.2 (2×CH), 128.8 (CH), 126.4 (CH), 126.0 (2×CH), 125.3 (CH), 124.9 (2×CH), 124.8 (2×CH), 120.7 (CH), 118.9 (CH), 118.8 (CH), 115.7 (CH), 70.3 (CH),

MS (EI): m/z(%) = 402(62) 374(38) 373(87) 375(35) 356(28) 345(25) 278(39) 178(100) 177(22)

HRMS for $C_{26}H_{18}N_4O$: calcd. 402.1481; found 402.1477.

(6-([1,2,3]Triazolo[1,5-*a*]pyridin-3-yl)pyridin-2-yl)(ferrocenyl)methanol (87, TPFe)

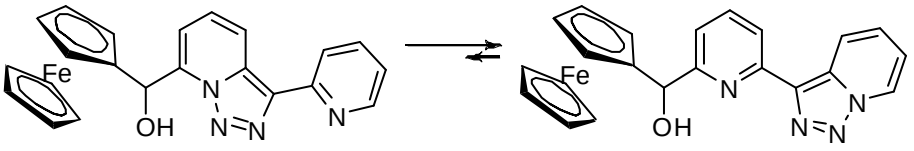

At -40 °C, butyllithium (1.0 mL, 1.7 mmol, 1.1 eq) in hexanes (1.54 M) was added dropwise to a stirred solution of 3-(2'-pyridyl)-[1,2,3]triazolo[1,5-*a*]pyridine (**1b**) (0.3 g, 1.5 mmol 1 eq) in toluene (30 mL). After 15 min, a solution of ferrocene aldehyde (1.1 g, 1.1 mmol, 1.1 eq) in toluene (50 mL) was added dropwise. After 1 h, the solution was allowed to reach room temperature and saturated aqueous solution of ammonium chloride (20.0 mL) was added, followed by extraction with dichloromethane (3 x 20.0 mL). The combined organic layers were dried over sodium sulfate, filtered, and evaporated, chromatography (ethyl acetate/cyclohexane 1:2) provided (6-([1,2,3]triazolo[1,5-*a*]pyridin-3-yl)pyridin-2-yl)(ferrocenyl)methanol (**87B**, **TPFeB**) as major isomer (92 %) and (6-(7-ferrocenyl)[1,2,3]triazolo[1,5-*a*]pyridin-3-yl)pyridin-2-yl)(ferrocenyl)methanol (**87A**, **TPFeA**) (8%), orange solid (0.4 g, 58%).

^{1}H NMR (300 MHz, $CDCl_3$): δ = 8.67 (d, *J* = 6.9 Hz, 1HB), 8.6-8.5 (m, 1HA), 8.51 (d, *J* = 8.8 Hz, 1HB + 1HA), 8.26 (d, *J* = 7.9, 1HB), 8.18 (d, *J* = 7.8 Hz, 1HB), 7.72 (t, *J* = 7.8, 7.8

Hz, 1HB + 1HA), 7.3-7.2 (m, 2HB + 1HA), 7.12 (dd, *J* = 6.7, 5.3 Hz, 1HA) 6.95 (t, *J* = 6.6, 6.6 Hz, 1HB + 1HB),6.23 (d, *J* = 4.0 Hz, 1HA), 5.51 (s, 1HB), 4.4-3.9 (m, 9HB+ 9HA, ferrocene).

^{13}C NMR (75 MHz, $CDCl_3$): δ = 160.7 (C), 150.4 (C), 137.3 (CH), 137.0 (C), 131.8 (C), 126.5 (CH), 125.3 (CH), 120.8 (CH), 119.2 (CH), 118.9 (CH), 115.7 (CH), 71.8 (CH), 68.9 (CH), 68.7(5×CH), 68.2(CH), 68.0 (CH), 67.5 (CH), 66.1 (CH), 60.3 (C),

MS (EI): m/z(%) = 410(24), 408(12), 345(100), 343(44), 329(55),317(47), 301(33), 243(44).

HRMS for $C_{22}H_{18}N_4OFe$: calcd. 408.0876; found 408.0892.

(6-([1,2,3]Triazolo[1,5-*a*]pyridin-3-yl)pyridin-2-yl)(quinolin-2-yl)methanone (88)

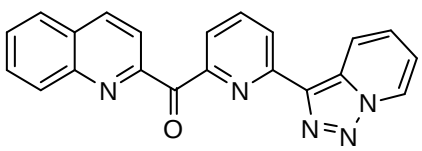

At -40 °C, butyllithium (4.2 mL, 5.6 mmol, 1.2 eq) in hexanes (1.54 M) was added dropwise to a stirred solution of 3-(2'-pyridyl)-[1,2,3]triazolo[1,5-*a*]pyridine (**1b**) (1.0 g, 5.1 mmol 1.1 eq) in toluene (60 mL). After 15 min the reaction mixture was added to a solution of methyl quinoline-2-carboxylate (0.9 g, 5 mmol, 1.0 eq) in toluene (35 mL) dropwise. After 1 h, the solution was allowed to reach room temperature and saturated aqueous solution of ammonium chloride (20 mL) was added, followed by extraction with dichloromethane (3 x 20 mL). The combined organic layers were dried over sodium sulfate, filtered, and evaporated, crystallization from ethyl acetate provided (6-([1,2,3]triazolo[1,5-*a*]pyridin-3-yl)pyridin-2-yl)(quinolin-2-yl)methanone (**88**) (1.4 g, 78%). mp 138 – 140 °C.

^{1}H NMR (300 MHz, $CDCl_3$): δ = 8.69 (d, *J* = 7.0 Hz, 1H), 8.56 (dd, *J* = 8.0, 1.0 Hz, 1H), 8.39 (d, *J* = 8.4 Hz, 1H), 8.3-8.1 (m, 3H), 7.97 (d, *J* = 8.2 Hz, 1H), 7.83 (ddd, *J* = 8.5, 6.9, 1.5 Hz, 1H), 7.8-7.7 (m, 1H), 6.91 (dt, *J* = 6.9, 6.8, 1.3 Hz, 1H), 6.78 (ddd, *J* = 8.8, 6.7, 0.9 Hz, 1H), 8.10 (d, *J* = 8.5 Hz, 1H), 8.05 (dd, *J* = 9.7, 5.9 Hz, 1H)

^{13}C NMR (75 MHz, $CDCl_3$): δ = 193.2 (CO), 155.3 (C), 153.1 (C), 151.4 (C), 147.1 (C), 137.5 (CH), 136.8 (CH), 132.3 (C), 130.4 (CH), 130.2 (CH), 128.9 (CH), 128.4 (CH), 127.8 (CH), 126.4 (CH), 125.1 (CH), 123.5 (CH), 123.3 (CH), 121.3 (CH), 121.1 (CH), 115.9 (CH).

MS (EI): m/z(%) = 351.1(20), 323.1(60), 294.2(100), 195.2(51), 128.1(66).

HRMS for $C_{21}H_{13}N_5O$: calcd. $[M+H^+]$ 352.1159; found . 352.1190.

3-(6-([1,2,3]Triazolo[1,5-*a*]pyridin-3-yl)pyridin-2-yl)-[1,2,3]triazolo[1,5-*a*]quinoline (89, TPTq)

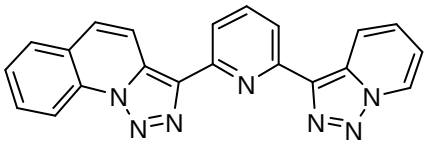

A mixture of (6-([1,2,3]triazolo[1,5-*a*]pyridin-3-yl)pyridin-2-yl)(quinolin-2-yl)methanone (**88**) (0.1 g, 0.3 mmol, 1 eq) and tosylhydrazide (70 mg, 0.4 mmol, 1.3 eq) in ethanol (100 mL) was heated to reflux during 4 h, then an aqueous solution of sodium hydroxide (30%) was added (25 mL) and the mixture was heated diring 2 h. The the mixture was allowed to reach romm temeperature followed by extraction with dichloromethane (3 x 20 mL). The combined organic layers were dried over sodium sulfate, filtered, and evaporated, trituration from hot ethanol 3-(6-([1,2,3]triazolo[1,5-*a*]pyridin-3-yl)pyridin-2-yl)-[1,2,3]triazolo[1,5-*a*]quinoline (**89**, **TPTq**)(20 mg, 17%). mp 239 – 241 °C.

^{1}H NMR (300 MHz, $CDCl_3$): δ = 8.86 (d, *J* = 8.4 Hz, 1H), 8.82 (d, *J* = 7.0 Hz, 1H), 8.66 (d, *J* = 8.9 Hz, 1H), 8.44 (d, *J* = 9.3 Hz, 1H), 8.29 (app d, *J* = 7.9 Hz, 2H), 7.96 (t, *J* = 7.9, 7.9 Hz, 1H), 7.88 (d, *J* = 7.8 Hz, 1H), 7.80 (t, *J* = 7.7, 7.7 Hz, 1H), 7.69-7.60 (m, 2H), 7.39 (dd, *J* = 8.4, 7.1 Hz, 1H), 7.08 (t, *J* = 6.8, 6.8 Hz, 1H).

^{13}C NMR (75 MHz, $CDCl_3$): δ = 151.4 (C), 151.2 (C), 139.6 (C), 137.8 (C), 137.5 (CH), 131.9 (C), 131.8 (C), 130.2 (CH), 129.8 (C), 128.4 (CH), 127.5 (CH), 127.3 (CH), 126.3 (CH), 125.5 (CH), 124.2 (C), 120.5 (CH), 119.8 (CH), 119.7 (CH), 117.0 (CH), 116.4 (CH), 115.7 (CH).

MS (EI): m/z(%) = 363(15) 308(25) 307(100) 306(62) 229(41) 179(46) 128(23) 78(20).

HRMS for $C_{21}H_{13}N_7$: calcd. 363.1232; found 363.1222.

Pyridine-2,6-diyl-bis(pyridin-2-yl-methanone) (90)

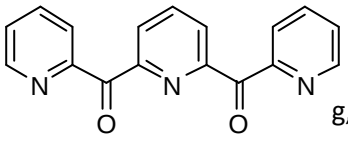

At -78 °C, butyllithium (10.8 mL, 16.7 mmol, 2.1 eq) in hexanes (1.5M) was added dropwise to a solution 2-bromopyridine (2.4 g, 15.2 mmol, 2.1 eq) in tetrahydrofuran (150 mL). The mixture was kept for 40 min at -78 °C before being canulated into a solution of dimethyl pyridine-2,6-dicarboxylate (1.4 g, 7.5 mmol, 1.0 eq) in tetrahydrofuran (100 mL). The mixture was allowed to reach 25 °C in the course of 2 h and hydrolyzed with a saturated aqueous solution of ammonium chloride (20 mL). The resulting mixture was extracted with dichloromethane (3×50 mL). The organic extracts were combined, washed with brine (3×10 mL), dried over sodium sulphate, filtered, and concentrated. Treatement with ethyl acetate provided pyridine-2,6-diylbis(pyridin-2-ylmethanone) (**90**) as a brown solid (1.9 g, 89%). mp 133 – 134 °C.

^{1}H NMR (300 MHz, $CDCl_3$): δ = 8.74 (ddd, *J* = 4.7, 1.6, 0.9 Hz, 2H), 8.30 (d, *J* = 7.7 Hz, 2H), 8.18 (td, *J* = 7.9, 0.9, 0.9 Hz, 2H), 8.10 (dd, *J* = 8.3, 7.3 Hz, 1H), 7.78 (dt, *J* = 7.8, 7.8, 1.7 Hz, 2H), 7.44 (ddd, *J* = 7.6, 4.8, 1.2 Hz, 2H)

^{13}C NMR (75.5 MHz, $CDCl_3$): δ = 191.6 (2×C), 153.5 (2×C), 153.3 (2×C), 149.1 (2×CH), 137.7 (CH), 136.4 (2×CH), 127.3 (2×CH), 126.3 (2×CH), 126.0 (2×CH).

2,6-Di([1,2,3]triazolo[1,5-*a*]pyridin-3-yl)pyridine (84, TPT)

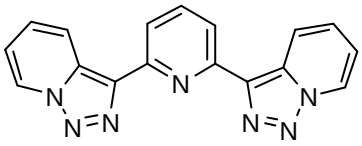

A mixture of pyridine-2,6-diyl-bis(pyridin-2-yl-methanone) (**90**) (2 g, 7.4 mmol, 1 eq) and tosylhydrazide (3.5 g, 19 mmol, 2.7 eq) in ethanol (200 mL) was heated to reflux during 4 h. Then an aqueous solution of sodium hydroxide (30%) was added (50 mL) and the mixture was heated during 2 h. The the mixture was allowed to reach 25 °C, followed by extraction with dichloromethane (3 x 20 mL). The combined organic layers were dried over sodium sulfate, filtered, and evaporated, trituration from hot ethanol gave 2,6-di([1,2,3]triazolo[1,5-*a*]pyridin-3-yl)pyridine (**84**, **TPT**) (1.5 g, 65%). mp 280 – 281 °C.

^{1}H NMR (300 MHz, $CDCl_3$): δ = 8.82 (ddd, J = 7.0, 1.0, 0.9 Hz, 1H), 8.63 (td, *J* = 9.0, 1.2, 1.2 Hz, 1H), 8.27 (d, *J* = 7.9 Hz, 1H) 7.96 (dd, *J* = 8.1, 7.6 Hz, 1H), 7.38 (ddd, *J* = 8.9, 6.6, 0.9 Hz, 1H), 7.09 (dt, *J* = 6.9, 6.8, 1.3 Hz, 1H).

^{13}C NMR (75 MHz, $CDCl_3$): δ = 151.4 (2×C), 137.0 (2×C), 137.6 (2×CH), 131.9 (2×C), 126.3 (2×CH), 125.6 (CH), 120.5 (2×CH), 119.6 (2×CH), 115.8 (2×CH).

Pyridine-2,6-diyl-bis(quinolin-2-yl-methanone)(92)

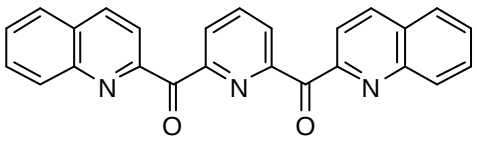

At -78 °C, butyllithium (3.2 mL, 2.4 mmol, 2.1 eq) in hexanes (1.5M) was added dropwise to a solution 2-bromoquinoline (1 g, 4.8 mmol, 2. eq) in tetrahydrofuran (100 mL). The mixture was kept for 1 h at -78 °C before being canulated into a solution of dimethyl pyridine-2,6-dicarboxylate (0.5 g, 2.4 mmol, 1.0 eq) in tetrahydrofuran (100 mL). The mixture was allowed to reach 25 °C in the course of 2 h and hydrolyzed with a saturated aqueous solution of ammonium chloride (20 mL). The resulting mixture was extracted with dichloromethane (3×50 mL). The organic extracts were combined, washed with brine (3×10 mL), dried over sodium sulphate, filtered, and concentrated. Treatement with ethyl acetate provided pyridine-2,6-diyl-bis(pyridin-2-yl-methanone) (**92**) as a brown solid (0.5 g, 57%). mp 129 – 131 °C.

^{1}H NMR (300 MHz, $CDCl_3$): δ = 8.42 (d, *J* = 7.8 Hz, 2H), 8.2-8.11 (m, 3H), 8.09 (d, *J* = 8.5 Hz, 2H), 7.88 (d, *J* = 8.5 Hz, 2H), 7.8-7.7 (m, 4H), 7.60 (dd, *J* = 8.5, 6.4 Hz, 2H).

^{13}C NMR (75.5 MHz, $CDCl_3$): δ = 192.3 (2×C), 153.9 (2×C), 153.3 (2×C), 147.2 (2×C), 137.7 (2×C), 136.1 (2×CH), 130.5 (2×CH), 130.0 (2×CH), 128.8 (CH), 128.3 (2×CH), 127.6 (2×CH), 127.5 (2×CH), 121.7 (2×CH).

MS (EI): m/z(%) = 389(100), 360(25), 332(31), 233(54), 128(87), 301(22).

HRMS for $C_{25}H_{15}N_3O_2$: calcd. 389.1164; found 389.1161.

2,6-Di([1,2,3]triazolo[1,5-*a*]quinolin-3-yl)pyridine (91, TqPTq)

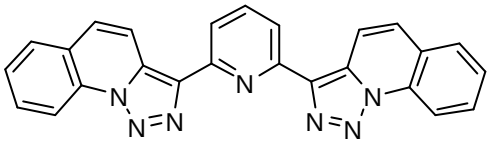

A mixture of pyridine-2,6-diyl-bis(pyridin-2-yl-methanone (**92**) (0.1 g, 0.3 mmol, 1 eq) and tosylhydrazide (0.2 g, 0.8 mmol, 2.7 eq) in ethanol (50 mL) was heated to reflux during 5 h, then an aqueous solution of sodium hydroxide (30%) was added (30 mL) and the mixture was heated diring 2 h. The mixture was allowed to reach 25 °C, where a colourless solide precipitated. The solid was filtrated and dissolved in dichloromethane (50 mL), dried over sodium sulfate, filtered, and evaporated providing 2,6-di([1,2,3]triazolo[1,5-*a*]quinolin-3-yl)pyridine **(91, TqPTq)** (1.5 g, 65%). mp > 260 °C.

^{1}H NMR (300 MHz, $CDCl_3$): δ = 8.90 (d, *J* = 8.4 Hz, 2H), 8.52 (d, *J* = 9.3 Hz, 2H), 8.35 (d, *J* = 7.8 Hz, 2H), 8.01 (dd, *J* = 8.1, 7.6 Hz, 1H), 7.92 (dd, *J* = 7.9, 1.1 Hz, 2H), 7.83 (ddd, *J* = 8.5, 7.3, 1.4 Hz, 2H), 7.7-7.6 (m, 4H)

^{13}C NMR (75 MHz, $CDCl_3$): δ = 151.4 (2×C), 139.6 (2×C), 137.6 (2×C), 132.0 (2×C), 130.2 (2×CH), 129.9 (2×C), 128.4 (2×CH), 127.6 (2×CH), 127.3 (2×CH), 124.3 (CH), 120.0 (2×CH), 117.1 (2×CH), 116.5 (2×CH),

MS (EI): m/z(%) = 413(16), 357(100), 356(46), 229(38).

HRMS for $C_{25}H_{15}N_7$: calcd. 413.1388; found 413.1394.

2,6-Bis(4,5,6,7-tetrahydro-[1,2,3]triazolo[1,5-*a*]pyridin-3-yl)pyridine (93, BTH-TPT)

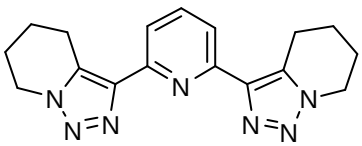

A mixture of 2,6-di([1,2,3]triazolo[1,5-*a*]pyridin-3-yl)pyridine (**84**) (0.2 g, 0.6 mmol, 1 eq) and Pd/C (100 mg, 10%) in methanol (50 mL) was stirred at room temperature for 4 days under hydrogene atmosphere (1 atmosphere). The mixture was filtered over celite, concentrated, diluted in dichloromethane (20 mL), dried over sodium sulfate, filtered, and evaporated, affording 2,6-bis(4,5,6,7-tetrahydro-[1,2,3]triazolo[1,5-*a*]pyridin-3-yl)pyridine (**93**, **BTH-TPT**) (0.2 g, 92%). mp 230 °C decomp.

^{1}H NMR (300 MHz, $CDCl_3$): δ = 8.09 (d, *J* = 7.8 Hz, 2H), 7.82 (t, *J* = 7.8 Hz, 1H), 4.45 (t, *J* = 6.0, 6.0 Hz, 4H), 3.26 (t, *J* = 6.3, 6.3 Hz, 4H), 2.2-2.1 (m, 4H), 2.0-1.9 (m, 4H)

^{13}C NMR (75 MHz, $CDCl_3$): δ = 151.4 (2×C), 137.0 (2×C), 137.6 (2×CH), 131.9 (2×C), 126.3 (2×CH), 125.6 (CH), 120.5 (2×CH), 119.6 (2×CH), 115.8 (2×CH).

MS (EI): m/z(%) = 321.2 (100),236.2 (20), 222.1 (15).

HRMS (ESI) for $C_{17}H_{19}N_7$: [M+Na] calcd. 344.1556; found 344.1594.

2-([1,2,3]Triazolo[1,5-*a*]pyridin-3-yl)-8-(dicyclohexylphosphoryl)quinoline (94, TQPO-4)

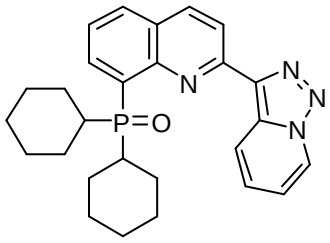

Prepared analogously as compound **72** starting from [1,2,3]triazolo[1,5-*a*]quinoline (**53**) (0.3 g, 1 mmol, 1.0 eq) and trapping of the lithiated intermediate with a solution of dicyclohexylphosphine chloride (0.3 g, 1.1 mmol, 1.1 eq). Treatment with ethyl acetate afforded 2-([1,2,3]triazolo[1,5-*a*]pyridin-3-yl)-8-(dicyclohexylphosphoryl)quinoline **(94)** as pale yellow needles (0.3 g, 59%). mp 235 °C decomp.

^{1}H NMR (300 MHz, $CDCl_3$): δ = 8.88 (app d, *J* = 7.2 Hz, 2H), 8.68 (d, *J* = 8.5 Hz, 1H), 8.46 (dd, *J* = 11.8, 6.8 Hz, 1H), 8.32 (d, *J* = 8.6 Hz, 1H), 7.99 (d, *J* = 7.9 Hz, 1H), 7.65 (t, *J* = 7.4, 7.4 Hz, 1H), 7.51 (dd, *J* = 8.6, 7.0 Hz, 1H), 7.17 (t, *J* = 6.8, 6.8 Hz, 1H), 2.9-2.7 (m, 2H), 2.4-2.2 (m, 2H), 1.9-0.8 (m, 18H).

^{13}C NMR (75.5 MHz, $CDCl_3$): δ = 151.7 (C), 147.6 (C), 137.9 7 (d, *J* = 5.6 Hz, CH), 137.7 (d, *J* = 2.2 Hz, CH), 137.6 (d, *J* = 20.1 Hz, C), 137.5 (C), 131.9 (d, *J* = 1.5 Hz, CH), 131.8 (C), 127.3 (d, *J* = 7.2 Hz, C), 126.8 (d, *J* = 0.8 Hz, CH), 125.9 (CH), 125.7 (d, *J* = 10.2 Hz, CH), 119.9 (CH), 119.9 (CH), 116.1 (CH), 38.2 (d, *J* = 67.1 Hz, 2×CH), 26.7 (d, *J* = 3.5 Hz, 2×CH_2), 26.6 (2×CH_2), 26.0 (d, *J* = 3.6 Hz, 2×CH_2), 25.7 (4×CH_2).

^{31}P NMR (161 MHz, $CDCl_3$): δ = 48.1 (PO).

MS (EI): m/z(%) = 458(39), 430(47), 376(31), 348(30), 347(30), 301(22), 267(100) 266(30), 265(45), 219(36),218(29).

HRMS ESI-[TOF] for $C_{29}H_{31}N_4OP$: calcd. 458.2235; found 458.2229.

References

[1] J. D. Bower and G. R. Ramage, *J. Chem. Soc.*, **1957**, 4506.

[2] L. P. Bataglia, M. Carcelli, F. Ferraro, L. Mavilla, C. Pilizzi and G. Pilizzi, *J. Chem. Soc. Dalton Trans*, **1994**, 2615.

[3] J. H. Boyer, R. Borgers and L. T. Wolford, *J. Am. Chem. Soc.*, **1957**, *79*, 678.

[4] B. Abarca, R. Ballesteros and M. Elmasnaouy, *Tetrahedron*, **1998**, *54*, 15287.

[5] G. Maitro, G. Prestat, D. Madec and G. Poli, *J. Org. Chem.*, **2006**, *71*, 7449.

[6] T. Kawai, N. Furukawa and S. Oae, *Tetrahedron Lett.*, **1984**, *25*, 2549.

[7] G. Maitro, S. Vogel, G. Prestat, D. Madec and G. Poli, *Org. Lett.*, **2006**, *8*, 5951.

[8] D. Broun and P. W. Ford, *J. Chem. Soc. [Section] C: Organic* **1969**, 2720.

[9] P. Pollet, A. Turck, N. Ple and G. Queguiner, *J. Org. Chem.*, **1999**, *64*, 4512.

[10] J. Le Notre, J. J. Firet, L. A. J. M. Sliedregt, B. J. Van Steen, G. Van Koten and R. J. M. K. Gebbink, *Org. Lett.*, **2005**, *7*, 363.

[11] M. Genov, K. Kostova and V. Dimitrov, *Tetrahedron: Asymmetry*, **1997**, *8*, 1869.

[12] B. Abarca, E. Gomez-Aldaravi and G. Jones, *J. Chem. Res. (S)*, **1984**, 140.

[13] E. Toshiasu, S. Seitaro and H. Masatomo, *Heterocycles*, **1975**, *3*, 19.

7.2 Fluorescence test

The solvents used were of spectroscopic or equivalent grade. Water was twice distilled and passed through a Millipore apparatus.

- UV-Vis absortion spectra were recorded on Agilent 8453 spectroscopy system.
- The emission spectra were recorded with a PTI MO-5020 spectrofluorimeter in the 300-500 nm range.
- Quantum yield was determined with a Hamamatsu-PHA equipment.

The absorbance of the excitation wavelength was maintained lower than 0.15. 10^{-5} M Solutions of ligands were prepared using 98/2 ethanol:water v/v as a solvent. M^{2+} solutions were prepared solving the correspondent perchlorate in 98/2 ethanol:water v:v 10^{-3} mol dm^{-3} concentration. Work solutions were obtained mixing 2 mL of the solution of ligands with the corresponding amounts of the solutions of the metals. 10^{-3} mol dm^{-3} aqueous solutions of the anions were prepared from $NaNO_2$, or the corresponding tetrabutyl amonium salts analytical grade salts 10^{-3} mol dm^{-3}. Amino acids aqueous solutions were prepared from commercial analytical grade amino acids (10^{-3} mol dm^{-3}). All test were performed with 2 mL of ligand solution. 2 mL of the corresponding ligand solution were introduced in a quartz cuvette with a small magnetic stirrer. To this solution metal cations or anions were added with high precision volumetric material, the mixture was mixed during ten seconds and then, the spectrum was recorded. The addition of analyte was stopped after five consecutive additions that afford no modification of the spectra.

Ligand		[M]
Tp	**1b**	0.00009
TPF	**3**	0.00008
TPS	**6**	0.00005
TqP	**53**	0.00008
TPT	**84**	0.00008
BTHTPT	**93**	0.00002
TPTq	**89**	0.00007
TqPTq	**91**	0.00002
TQPO1	**72**	0.00005
TQPO2	**73**	0.00005
TQPO3	**74**	0.00006
TQPO4	**94**	0.00005
TPON	**85**	0.00007
TPOA	**86**	0.00001
TPFe	**87**	0.00005

Spectral properties for the prepard compounds.

Entry	Compound	λexc (nm)	λemi (nm)	Stokes shift[a]	Quantum yield[b] ϕ_F
1	**Tp**	359	411	52	0.01
2	**TPF**	360	418	58	0.02
3	**TPS**	340	400	60	0.02
4	**TqP**	358	397	39	0.13
5	**TPT**	359	412	53	0.02
6	**BTH-TPT**	323	357	34	0.08
7	**TPTq**	355	406	51	0.19
8	**TqPTq**	351	400	49	0.24
9	**TQPO1** (R=Ph)	376	423	47	0.54
10	**TQPO2** (R=*p*-F_3CPh)	380	427	47	0.60
11	**TQPO3** (R=*p*-H_3COPh)	375	419	46	0.48
12	**TPQO4** (R = Cy)	369	404	35	0.34
13	**TPON**	347	409	62	0.02
14	**TPOA**	347	412	65	0.18
15	**TPFe**	371	425	54	0.01

7.2.1 Zinc(II) and Copper(II) test.

Compound	I_0	I ($LZn^{2\oplus}$)	I ($LCu^{2\oplus}$)
TP	1	1,68	0,59
TPF	1	1,18	0,14
TPS	1	1,21	0,66
TqP	1	1,19	0,21
TPT	1	13,20	0,01
BTH-TPT	1	11,62	0,01
TPTq	1	1,73	0,01
TqPTq	1	2,15	0,01
TQPO1	1	1,00	0,01
TPQO2	1	1,00	0,01
TPQO3	1	1,00	0,01
TPON	1	16,61	0,07
TPOA	1	-0,50	0,01
TPFe	1	1,00	1,00

7.2.2 TPT fluorescence study

	Co(II)	Ni(II)	Cu(II)	Zn(II)	Cd(II)	Pb(II)
TPT I_o	1.00	1.00	1.00	1.00	1.00	1.00
TPTM(II) I	0.05	0.02	0.01	13.20	4.63	0.96

$TPTZn^{2\oplus}$ anion fluorescence tests.

Fluoride:
[**TPT**] = 0.0000847 M.
$[Zn^{2\oplus}]$ = 0.00483 M.
V_{TPT} = 2.000 mL.
$V_{Zn(II)}$ = 0.0348 mL.
V_0 = 2.0348 mL.
[Fluoride] = 0.003524 M.

Entry	Volume (mL)	[analyte]	I
1	0	0,00E+00	9,95E-01
2	0,003	5,19E-06	9,71E-01
3	0,006	1,04E-05	9,59E-01
4	0,009	1,55E-05	9,57E-01
5	0,012	2,07E-05	9,30E-01
6	0,015	2,58E-05	9,13E-01
7	0,018	3,09E-05	8,92E-01
8	0,021	3,60E-05	8,68E-01
9	0,024	4,11E-05	7,98E-01
10	0,027	4,61E-05	7,54E-01
11	0,03	5,12E-05	7,22E-01
12	0,033	5,62E-05	6,32E-01
13	0,036	6,13E-05	5,86E-01
14	0,039	6,63E-05	5,50E-01
15	0,042	7,13E-05	5,12E-01
16	0,045	7,62E-05	4,77E-01
17	0,048	8,12E-05	4,17E-01
18	0,051	8,62E-05	3,79E-01
19	0,054	9,11E-05	3,60E-01
20	0,057	9,60E-05	3,34E-01
21	0,06	1,01E-04	2,80E-01
22	0,063	1,06E-04	2,60E-01
23	0,066	1,11E-04	2,42E-01
24	0,069	1,16E-04	2,25E-01
25	0,072	1,20E-04	1,99E-01
26	0,075	1,25E-04	1,84E-01
27	0,078	1,30E-04	1,76E-01
28	0,081	1,35E-04	1,64E-01
29	0,084	1,40E-04	1,59E-01
30	0,087	1,44E-04	1,52E-01
31	0,09	1,49E-04	1,49E-01
32	0,093	1,54E-04	1,41E-01
33	0,096	1,59E-04	1,34E-01
34	0,099	1,63E-04	1,31E-01
35	0,102	1,68E-04	1,26E-01
36	0,105	1,73E-04	1,26E-01
37	0,108	1,78E-04	1,22E-01
38	0,111	1,82E-04	1,20E-01
39	0,114	1,87E-04	1,19E-01
40	0,117	1,92E-04	1,18E-01
41	0,12	1,96E-04	1,16E-01
42	0,123	2,01E-04	1,15E-01
43	0,126	2,05E-04	1,13E-01
44	0,129	2,10E-04	1,13E-01
45	0,132	2,15E-04	1,12E-01
46	0,135	2,19E-04	1,11E-01
47	0,145	2,34E-04	1,10E-01
48	0,155	2,49E-04	1,07E-01
49	0,165	2,64E-04	1,06E-01
50	0,215	3,37E-04	1,00E-01
51	0,315	4,72E-04	9,47E-02
52	0,415	5,97E-04	9,22E-02
53	0,515	7,12E-04	8,98E-02

Chloride:

[**TPT**] = 0.0000847 M.

[$Zn^{2\oplus}$] = 0.00483 M.

V_{TPT} = 2.000 mL.

$V_{Zn(II)}$ = 0.0348 mL.

V_0 = 2.0348 mL.

[Chloride] = 0.003537 M.

Entry	Volume (mL)	[analyte]	I
1	0	0,00E+00	9,87E-01
2	0,003	5,21E-06	9,96E-01
3	0,006	1,04E-05	9,88E-01
4	0,009	1,56E-05	9,79E-01
5	0,012	2,07E-05	9,69E-01
6	0,015	2,59E-05	9,52E-01
7	0,018	3,10E-05	8,93E-01
8	0,021	3,61E-05	8,57E-01
9	0,024	4,12E-05	8,25E-01
10	0,027	4,63E-05	7,89E-01
11	0,03	5,14E-05	7,54E-01
12	0,033	5,64E-05	7,19E-01
13	0,036	6,15E-05	6,84E-01
14	0,039	6,65E-05	6,46E-01
15	0,042	7,15E-05	5,88E-01
16	0,045	7,65E-05	5,41E-01
17	0,048	8,15E-05	5,13E-01
18	0,051	8,65E-05	4,85E-01
19	0,054	9,14E-05	4,58E-01
20	0,057	9,64E-05	4,37E-01
21	0,06	1,01E-04	4,13E-01
22	0,063	1,06E-04	3,98E-01
23	0,066	1,11E-04	3,79E-01
24	0,069	1,16E-04	3,65E-01
25	0,072	1,21E-04	3,50E-01
26	0,075	1,26E-04	3,39E-01
27	0,078	1,31E-04	3,12E-01
28	0,081	1,35E-04	3,06E-01
29	0,084	1,40E-04	2,94E-01
30	0,087	1,45E-04	2,88E-01
31	0,09	1,50E-04	2,80E-01
32	0,093	1,55E-04	2,74E-01
33	0,096	1,59E-04	2,68E-01
34	0,099	1,64E-04	2,62E-01
35	0,102	1,69E-04	2,58E-01
36	0,105	1,74E-04	2,54E-01
37	0,108	1,78E-04	2,48E-01
38	0,111	1,83E-04	2,44E-01
39	0,114	1,88E-04	2,37E-01
40	0,117	1,92E-04	2,34E-01
41	0,12	1,97E-04	2,30E-01
42	0,123	2,02E-04	2,28E-01
43	0,126	2,06E-04	2,27E-01
44	0,129	2,11E-04	2,22E-01
45	0,132	2,15E-04	2,15E-01
46	0,135	2,20E-04	2,10E-01
47	0,145	2,35E-04	2,03E-01
48	0,155	2,50E-04	1,82E-01
49	0,165	2,65E-04	1,59E-01
50	0,215	3,38E-04	1,39E-01
51	0,315	4,74E-04	1,26E-01
52	0,415	5,99E-04	1,16E-01
53	0,515	7,14E-04	1,09E-01

Bromide:

[**TPT**] = 0.0000847 M.

[$Zn^{2\oplus}$] = 0.00483 M.

V_{TPT} = 2.000 mL.

$V_{Zn(II)}$ = 0.0348 mL.

V_0 = 2.0348 mL.

[Bromide] = 0.0031919 M.

Entry	Volume (mL)	[analyte]	I
1	0	0,00E+00	9,95E-01
2	0,003	4,70E-06	9,88E-01
3	0,006	9,38E-06	9,85E-01
4	0,009	1,41E-05	9,75E-01
5	0,012	1,87E-05	9,63E-01
6	0,015	2,34E-05	9,37E-01
7	0,018	2,80E-05	9,37E-01
8	0,021	3,26E-05	9,11E-01
9	0,024	3,72E-05	8,90E-01
10	0,027	4,18E-05	8,63E-01
11	0,03	4,64E-05	8,39E-01
12	0,033	5,09E-05	8,15E-01
13	0,036	5,55E-05	7,87E-01
14	0,039	6,00E-05	7,66E-01
15	0,042	6,46E-05	7,40E-01
16	0,045	6,91E-05	7,17E-01
17	0,048	7,36E-05	6,93E-01
18	0,051	7,80E-05	6,70E-01
19	0,054	8,25E-05	6,46E-01
20	0,057	8,70E-05	6,22E-01
21	0,06	9,14E-05	6,00E-01
22	0,063	9,59E-05	5,79E-01
23	0,066	1,00E-04	5,63E-01
24	0,069	1,05E-04	5,47E-01
25	0,072	1,09E-04	5,33E-01
26	0,075	1,13E-04	5,26E-01
27	0,078	1,18E-04	5,15E-01
28	0,081	1,22E-04	4,69E-01
29	0,084	1,27E-04	4,56E-01
30	0,087	1,31E-04	4,55E-01
31	0,09	1,35E-04	4,31E-01
32	0,093	1,40E-04	4,33E-01
33	0,096	1,44E-04	4,26E-01
34	0,099	1,48E-04	4,15E-01
35	0,102	1,52E-04	4,07E-01
36	0,105	1,57E-04	3,98E-01
37	0,108	1,61E-04	3,89E-01
38	0,111	1,65E-04	3,82E-01
39	0,114	1,69E-04	3,75E-01
40	0,117	1,74E-04	3,69E-01
41	0,12	1,78E-04	3,66E-01
42	0,123	1,82E-04	3,58E-01
43	0,126	1,86E-04	3,52E-01
44	0,136	2,00E-04	3,34E-01
45	0,146	2,14E-04	3,20E-01
46	0,156	2,27E-04	3,04E-01
47	0,206	2,93E-04	2,53E-01
48	0,306	4,17E-04	1,87E-01
49	0,406	5,31E-04	1,52E-01
50	0,506	6,36E-04	1,33E-01
51	0,606	7,32E-04	1,19E-01
52	0,706	8,22E-04	1,11E-01
53	0,806	9,06E-04	1,05E-01
54	0,906	9,83E-04	1,03E-01

Iodide:

[**TPT**] = 0.0000847 M.

[$Zn^{2\oplus}$] = 0.00483 M.

V_{TPT} = 2.000 mL.

$V_{Zn(II)}$ = 0.0348 mL.

V_0 = 2.0348 mL.

[Iodide] = 0.002959 M.

Entry	Volume (mL)	[analyte]	I
1	0	0,00E+00	9,86E-01
2	0,003	4,36E-06	9,72E-01
3	0,006	8,70E-06	9,36E-01
4	0,009	1,30E-05	9,19E-01
5	0,012	1,73E-05	8,53E-01
6	0,015	2,17E-05	8,17E-01
7	0,018	2,59E-05	7,89E-01
8	0,021	3,02E-05	7,60E-01
9	0,024	3,45E-05	7,27E-01
10	0,027	3,87E-05	6,97E-01
11	0,03	4,30E-05	6,67E-01
12	0,033	4,72E-05	6,46E-01
13	0,036	5,14E-05	6,05E-01
14	0,039	5,56E-05	5,92E-01
15	0,042	5,98E-05	5,55E-01
16	0,045	6,40E-05	5,38E-01
17	0,048	6,82E-05	5,26E-01
18	0,051	7,24E-05	5,11E-01
19	0,054	7,65E-05	5,01E-01
20	0,057	8,06E-05	4,90E-01
21	0,06	8,48E-05	4,78E-01
22	0,063	8,89E-05	4,57E-01
23	0,066	9,30E-05	4,57E-01
24	0,069	9,70E-05	4,45E-01
25	0,072	1,01E-04	4,37E-01
26	0,075	1,05E-04	4,18E-01
27	0,078	1,09E-04	4,07E-01
28	0,081	1,13E-04	4,01E-01
29	0,084	1,17E-04	3,87E-01
30	0,087	1,21E-04	3,75E-01
31	0,09	1,25E-04	3,67E-01
32	0,093	1,29E-04	3,60E-01
33	0,096	1,33E-04	3,50E-01
34	0,101	1,40E-04	3,39E-01
35	0,106	1,47E-04	3,30E-01
36	0,111	1,53E-04	3,16E-01
37	0,116	1,60E-04	3,12E-01
38	0,121	1,66E-04	2,99E-01
39	0,131	1,79E-04	2,76E-01
40	0,141	1,92E-04	2,62E-01
41	0,151	2,04E-04	2,49E-01
42	0,161	2,17E-04	2,40E-01
43	0,171	2,29E-04	2,32E-01
44	0,221	2,90E-04	1,95E-01
45	0,271	3,48E-04	1,69E-01
46	0,321	4,03E-04	1,55E-01
47	0,421	5,07E-04	1,35E-01
48	0,521	6,03E-04	1,25E-01
49	0,621	6,92E-04	1,21E-01
50	0,721	7,74E-04	1,18E-01
51	0,821	8,51E-04	1,14E-01

Cyanide:

[**TPT**] = 0.0000847 M.

[$Zn^{2\oplus}$] = 0.00483 M.

V_{TPT} = 2.000 mL.

$V_{Zn(II)}$ = 0.0348 mL.

V_0 = 2.0348 mL.

[Cyanide] = 0.0024078 M.

Entry	Volume (mL)	[analyte]	I
1	0	0,00E+00	9,87E-01
2	0,003	3,54E-06	9,89E-01
3	0,006	7,08E-06	9,88E-01
4	0,009	1,06E-05	9,85E-01
5	0,012	1,41E-05	9,83E-01
6	0,015	1,76E-05	9,72E-01
7	0,018	2,11E-05	9,60E-01
8	0,021	2,46E-05	9,57E-01
9	0,024	2,81E-05	9,32E-01
10	0,027	3,15E-05	9,16E-01
11	0,03	3,50E-05	8,90E-01
12	0,033	3,84E-05	8,73E-01
13	0,036	4,19E-05	8,52E-01
14	0,039	4,53E-05	8,22E-01
15	0,042	4,87E-05	7,93E-01
16	0,045	5,21E-05	7,71E-01
17	0,048	5,55E-05	7,31E-01
18	0,051	5,89E-05	7,07E-01
19	0,054	6,22E-05	6,73E-01
20	0,057	6,56E-05	6,37E-01
21	0,06	6,90E-05	6,07E-01
22	0,063	7,23E-05	5,73E-01
23	0,066	7,56E-05	5,38E-01
24	0,069	7,90E-05	5,04E-01
25	0,072	8,23E-05	4,74E-01
26	0,075	8,56E-05	4,47E-01
27	0,078	8,89E-05	4,13E-01
28	0,081	9,22E-05	3,88E-01
29	0,084	9,55E-05	3,60E-01
30	0,087	9,87E-05	3,37E-01
31	0,09	1,02E-04	3,12E-01
32	0,093	1,05E-04	2,86E-01
33	0,096	1,08E-04	2,58E-01
34	0,099	1,12E-04	2,42E-01
35	0,102	1,15E-04	2,23E-01
36	0,105	1,18E-04	2,10E-01
37	0,108	1,21E-04	1,95E-01
38	0,111	1,25E-04	1,82E-01
39	0,114	1,28E-04	1,71E-01
40	0,117	1,31E-04	1,59E-01
41	0,12	1,34E-04	1,50E-01
42	0,123	1,37E-04	1,41E-01
43	0,126	1,40E-04	1,30E-01
44	0,129	1,44E-04	1,24E-01
45	0,132	1,47E-04	1,20E-01
46	0,135	1,50E-04	1,14E-01
47	0,138	1,53E-04	1,12E-01
48	0,141	1,56E-04	1,07E-01
49	0,144	1,59E-04	1,05E-01
50	0,147	1,62E-04	1,02E-01
51	0,15	1,65E-04	1,00E-01
52	0,153	1,68E-04	9,91E-02
53	0,163	1,79E-04	9,44E-02
54	0,173	1,89E-04	9,34E-02
55	0,183	1,99E-04	9,08E-02

Thiocyanide:

[**TPT**] = 0.0000847 M.

[$Zn^{2\oplus}$] = 0.00483 M.

V_{TPT} = 2.000 mL.

$V_{Zn(II)}$ = 0.0348 mL.

V_0 = 2.0348 mL.

[Thiocyanide] = 0.00538 M.

Entry	Volume (mL)	[analyte]	I
1	0	0,00E+00	9,95E-01
2	0,003	7,92E-06	9,71E-01
3	0,006	1,58E-05	9,10E-01
4	0,009	2,37E-05	8,75E-01
5	0,012	3,15E-05	8,21E-01
6	0,015	3,94E-05	7,73E-01
7	0,018	4,72E-05	6,77E-01
8	0,021	5,50E-05	6,25E-01
9	0,024	6,27E-05	5,70E-01
10	0,027	7,05E-05	5,35E-01
11	0,03	7,82E-05	4,19E-01
12	0,035	9,10E-05	3,83E-01
13	0,04	1,04E-04	3,42E-01
14	0,045	1,16E-04	3,11E-01
15	0,05	1,29E-04	2,83E-01
16	0,055	1,42E-04	2,64E-01
17	0,065	1,67E-04	2,34E-01
18	0,075	1,91E-04	2,13E-01
19	0,085	2,16E-04	1,99E-01
20	0,095	2,40E-04	1,89E-01
21	0,105	2,64E-04	1,80E-01
22	0,115	2,88E-04	1,75E-01
23	0,125	3,11E-04	1,71E-01
24	0,175	4,26E-04	1,58E-01
25	0,275	6,41E-04	1,48E-01
26	0,375	8,37E-04	1,43E-01
27	0,475	1,02E-03	1,41E-01

Nitrite:

[**TPT**] = 0.0000847 M.

[$Zn^{2\oplus}$] = 0.00483 M.

V_{TPT} = 2.000 mL.

$V_{Zn(II)}$ = 0.0348 mL.

V_0 = 2.0348 mL.

[Nitrite] = 0.00802 M.

Entry	Volume (mL)	[analyte]	I
1	0	0,00E+00	9,90E-01
2	0,003	1,20E-05	9,37E-01
3	0,006	2,40E-05	8,09E-01
4	0,009	3,60E-05	6,84E-01
5	0,012	4,79E-05	5,76E-01
6	0,015	5,98E-05	4,92E-01
7	0,018	7,16E-05	4,01E-01
8	0,021	8,34E-05	3,43E-01
9	0,024	9,52E-05	2,97E-01
10	0,027	1,07E-04	2,62E-01
11	0,03	1,19E-04	2,37E-01
12	0,033	1,30E-04	2,16E-01
13	0,036	1,42E-04	2,01E-01
14	0,039	1,54E-04	1,88E-01
15	0,042	1,65E-04	1,76E-01
16	0,045	1,77E-04	1,66E-01
17	0,048	1,88E-04	1,58E-01
18	0,051	2,00E-04	1,52E-01
19	0,061	2,11E-04	1,47E-01
20	0,071	2,49E-04	1,33E-01
21	0,081	2,86E-04	1,23E-01
22	0,091	3,24E-04	1,18E-01
23	0,101	3,60E-04	1,15E-01
24	0	0,00E+00	9,90E-01

Nitrate:

[**TPT**] = 0.0000847 M.

[$Zn^{2\oplus}$] = 0.00483 M.

V_{TPT} = 2.000 mL.

$V_{Zn(II)}$ = 0.0348 mL.

V_0 = 2.0348 mL.

[Nitrate] = 0.006946 M.

Entry	Volume (mL)	[analyte]	I
1	0	0,00E+00	1,00E+00
2	0,003	1,04E-05	9,99E-01
3	0,006	2,08E-05	9,76E-01
4	0,009	3,11E-05	9,49E-01
5	0,012	4,14E-05	9,28E-01
6	0,015	5,17E-05	9,22E-01
7	0,018	6,20E-05	8,95E-01
8	0,021	7,22E-05	8,69E-01
9	0,024	8,24E-05	8,48E-01
10	0,027	9,25E-05	8,23E-01
11	0,033	1,03E-04	7,97E-01
12	0,039	1,23E-04	7,61E-01
13	0,045	1,43E-04	7,26E-01
14	0,051	1,63E-04	6,86E-01
15	0,057	1,83E-04	6,52E-01
16	0,067	2,02E-04	6,17E-01
17	0,077	2,35E-04	5,64E-01
18	0,087	2,67E-04	5,16E-01
19	0,097	2,99E-04	4,72E-01
20	0,107	3,31E-04	4,32E-01
21	0,157	3,62E-04	3,98E-01
22	0,207	5,15E-04	3,19E-01
23	0,257	6,60E-04	2,25E-01
24	0,307	7,99E-04	1,68E-01
25	0,357	9,32E-04	1,44E-01
26	0,407	1,06E-03	1,28E-01
27	0,457	1,18E-03	1,15E-01
28	0,507	1,30E-03	1,05E-01
29	0,557	1,41E-03	9,76E-02
30	0,607	1,52E-03	9,42E-02
31	0,657	1,62E-03	8,96E-02

Alanine:

[**TPT**] = 0.0000847 M.

[$Zn^{2\oplus}$] = 0.00483 M.

V_{TPT} = 2.000 mL.

$V_{Zn(II)}$ = 0.0348 mL.

V_0 = 2.0348 mL.

[Alanine] = 0.00792 M.

Entry	Volume (mL)	[analyte]	I
1	0	0	1
2	0,003	1,16E-05	9,59E-01
3	0,006	2,32E-05	9,52E-01
4	0,009	3,47E-05	9,25E-01
5	0,012	4,62E-05	8,90E-01
6	0,015	5,77E-05	8,56E-01
7	0,018	6,91E-05	8,09E-01
8	0,021	8,05E-05	7,76E-01
9	0,024	9,19E-05	7,47E-01
10	0,027	1,03E-04	7,14E-01
11	0,03	1,15E-04	6,76E-01
12	0,036	1,37E-04	6,11E-01
13	0,042	1,59E-04	5,58E-01
14	0,048	1,82E-04	5,10E-01
15	0,054	2,04E-04	4,65E-01
16	0,06	2,26E-04	4,28E-01
17	0,07	2,62E-04	3,80E-01
18	0,08	2,98E-04	3,40E-01
19	0,09	3,34E-04	3,11E-01
20	0,1	3,69E-04	2,80E-01
21	0,11	4,04E-04	2,60E-01

Phenyl alanine:

[**TPT**] = 0.0000847 M.

$[Zn^{2\oplus}]$ = 0.00483 M.

V_{TPT} = 2.000 mL.

$V_{Zn(II)}$ = 0.0348 mL.

V_0 = 2.0348 mL.

[Phenyl alanine] = 0.007748 M.

Entry	Volume (mL)	[analyte]	I	Entry	Volume (mL)	[analyte]	I
1	0	0,00E+00	1,00E+00	**15**	0,054	2,04E-04	5,29E-01
2	0,003	1,16E-05	1,04E+00	**16**	0,06	2,26E-04	4,85E-01
3	0,006	2,32E-05	1,02E+00	**17**	0,07	2,62E-04	4,30E-01
4	0,009	3,47E-05	9,80E-01	**18**	0,08	2,98E-04	3,82E-01
5	0,012	4,62E-05	9,66E-01	**19**	0,09	3,34E-04	3,40E-01
6	0,015	5,77E-05	9,27E-01	**20**	0,1	3,69E-04	3,14E-01
7	0,018	6,91E-05	8,88E-01	**21**	0,11	4,04E-04	2,90E-01
8	0,021	8,05E-05	8,59E-01	**22**	0,16	5,74E-04	2,17E-01
9	0,024	9,19E-05	8,16E-01	**23**	0,21	7,36E-04	1,93E-01
10	0,027	1,03E-04	7,85E-01	**24**	0,26	8,91E-04	1,46E-01
11	0,03	1,15E-04	7,44E-01	**25**	0,31	1,04E-03	1,30E-01
12	0,036	1,37E-04	6,78E-01	**26**	0,36	1,18E-03	1,14E-01
13	0,042	1,59E-04	6,22E-01	**27**	0,41	1,32E-03	9,85E-02
14	0,048	1,82E-04	5,66E-01	**28**	0,46	1,45E-03	9,09E-02

Tryptofan:

[**TPT**] = 0.0000847 M.

$[Zn^{2\oplus}]$ = 0.00483 M.

V_{TPT} = 2.000 mL.

$V_{Zn(II)}$ = 0.0348 mL.

V_0 = 2.0348 mL.

[Tryptofan] = 0.007325 M.

Entry	Volume (mL)	[analyte]	I	Entry	Volume (mL)	[analyte]	I
1	0	0,00E+00	1,00E+00	**10**	0,046	1,65E-04	3,35E-01
2	0,003	1,10E-05	9,47E-01	**11**	0,056	2,00E-04	2,70E-01
3	0,006	2,19E-05	8,94E-01	**12**	0,066	2,34E-04	2,30E-01
4	0,009	3,28E-05	8,37E-01	**13**	0,076	2,68E-04	2,03E-01
5	0,012	4,37E-05	7,80E-01	**14**	0,086	3,02E-04	1,73E-01
6	0,018	6,53E-05	6,76E-01	**15**	0,096	3,35E-04	1,56E-01
7	0,024	8,69E-05	5,82E-01	**16**	0,106	3,69E-04	1,43E-01
8	0,03	1,08E-04	4,98E-01	**17**	0,116	4,02E-04	1,32E-01
9	0,036	1,30E-04	4,23E-01	**18**	0,126	4,34E-04	1,23E-01
				19	0,136	4,66E-04	1,17E-01

Aspartic:

[**TPT**] = 0.0000847 M.

[$Zn^{2\oplus}$] = 0.00483 M.

V_{TPT} = 2.000 mL.

$V_{Zn(II)}$ = 0.0348 mL.

V_0 = 2.0348 mL.

[Aspartic] = 0.008324 M.

Entry	Volume (mL)	[analyte]	I	Entry	Volume (mL)	[analyte]	I
1	0	0	1	**10**	0,027	1,11E-04	5,79E-01
2	0,003	1,25E-05	1,02E+00	**11**	0,03	1,23E-04	5,36E-01
3	0,006	2,49E-05	9,86E-01	**12**	0,036	1,47E-04	4,48E-01
4	0,009	3,73E-05	9,38E-01	**13**	0,042	1,71E-04	3,73E-01
5	0,012	4,96E-05	8,84E-01	**14**	0,048	1,95E-04	3,17E-01
6	0,015	6,19E-05	8,16E-01	**15**	0,054	2,19E-04	2,67E-01
7	0,018	7,42E-05	7,53E-01	**16**	0,06	2,42E-04	2,31E-01
8	0,021	8,65E-05	6,97E-01	**17**	0,07	2,81E-04	1,95E-01
9	0,024	9,87E-05	6,33E-01	**18**	0,08	3,20E-04	1,68E-01
				19	0,09	3,58E-04	1,48E-01

Glutamic:

[**TPT**] = 0.0000847 M.

[$Zn^{2\oplus}$] = 0.00483 M.

V_{TPT} = 2.000 mL.

$V_{Zn(II)}$ = 0.0348 mL.

V_0 = 2.0348 mL.

[Glutamic] = 0.00855 M.

Entry	Volume (mL)	[analyte]	I	Entry	Volume (mL)	[analyte]	I
1	0	0	1	**14**	0,057	2,00E-04	4,31E-01
2	0,003	1,28E-05	1,00E+00	**15**	0,066	2,25E-04	3,83E-01
3	0,006	2,56E-05	9,66E-01	**16**	0,075	2,49E-04	3,44E-01
4	0,009	3,83E-05	9,35E-01	**17**	0,085	2,89E-04	2,95E-01
5	0,012	5,10E-05	8,95E-01	**18**	0,095	3,29E-04	2,59E-01
6	0,015	6,36E-05	8,58E-01	**19**	0,105	3,68E-04	2,33E-01
7	0,018	7,63E-05	8,08E-01	**20**	0,115	4,07E-04	2,10E-01
8	0,021	8,88E-05	7,68E-01	**21**	0,125	4,46E-04	1,94E-01
9	0,024	1,01E-04	7,30E-01	**22**	0,135	4,84E-04	1,79E-01
10	0,027	1,14E-04	6,86E-01	**23**	0,185	6,70E-04	1,41E-01
11	0,03	1,26E-04	6,45E-01	**24**	0,235	8,47E-04	1,20E-01
12	0,039	1,51E-04	5,66E-01	**25**	0,285	1,02E-03	1,07E-01
13	0,048	1,76E-04	5,02E-01	**26**	0,335	1,18E-03	9,82E-02

Histidine:

[**TPT**] = 0.0000827 M.

$[Zn^{2\oplus}]$ = 0.00483 M.

V_{TPT} = 2.000 mL.

$V_{Zn(II)}$ = 0.0343 mL.

V_0 = 2.0343 mL.

[Histidine] = 0.00683 M.

Entry	Volume (mL)	[analyte]	I
1	0	0	9,84E-01
2	0,003	4,25E-06	9,89E-01
3	0,006	8,49E-06	9,93E-01
4	0,009	1,27E-05	9,92E-01
5	0,012	1,69E-05	9,87E-01
6	0,015	2,11E-05	9,85E-01
7	0,018	2,53E-05	9,88E-01
8	0,021	2,95E-05	9,71E-01
9	0,024	3,37E-05	9,52E-01
10	0,027	3,78E-05	9,32E-01
11	0,03	4,20E-05	9,07E-01
12	0,033	4,61E-05	8,68E-01
13	0,036	5,02E-05	8,35E-01
14	0,039	5,43E-05	7,89E-01
15	0,042	5,84E-05	7,53E-01
16	0,045	6,25E-05	6,96E-01
17	0,048	6,65E-05	6,49E-01
18	0,051	7,06E-05	6,07E-01
19	0,054	7,46E-05	5,55E-01
20	0,057	7,87E-05	5,14E-01
21	0,06	8,27E-05	4,66E-01
22	0,063	8,67E-05	4,16E-01
23	0,066	9,07E-05	3,78E-01
24	0,069	9,47E-05	3,49E-01
25	0,072	9,87E-05	3,25E-01
26	0,075	1,03E-04	2,88E-01
27	0,078	1,07E-04	2,62E-01
28	0,081	1,11E-04	2,34E-01
29	0,084	1,14E-04	2,15E-01
30	0,087	1,18E-04	1,97E-01
31	0,09	1,22E-04	1,79E-01
32	0,093	1,26E-04	1,66E-01
33	0,096	1,30E-04	1,57E-01
34	0,099	1,34E-04	1,47E-01
35	0,102	1,38E-04	1,40E-01
36	0,105	1,42E-04	1,34E-01
37	0,108	1,46E-04	1,27E-01
38	0,111	1,49E-04	1,22E-01
39	0,114	1,53E-04	1,18E-01
40	0,117	1,57E-04	1,14E-01
41	0,12	1,61E-04	1,09E-01
42	0,123	1,65E-04	1,06E-01
43	0,133	1,77E-04	1,00E-01
44	0,143	1,90E-04	9,58E-02
45	0,153	2,02E-04	9,36E-02

Acetate:

[**TPT**] = 0.0000827 M.

$[Zn^{2\oplus}]$ = 0.00483 M.

V_{TPT} = 2.000 mL.

$V_{Zn(II)}$ = 0.0343 mL.

V_0 = 2.0343 mL.

[Acetate] = 0.00299 M.

Entry	Volume (mL)	[analyte]	I
1	0	0,00E+00	9,89E-01
2	0,003	4,41E-06	9,76E-01
3	0,006	8,80E-06	9,49E-01
4	0,009	1,32E-05	9,30E-01
5	0,012	1,75E-05	9,04E-01
6	0,015	2,19E-05	8,76E-01
7	0,018	2,62E-05	8,60E-01
8	0,021	3,06E-05	7,85E-01
9	0,024	3,49E-05	7,26E-01
10	0,027	3,92E-05	6,93E-01
11	0,03	4,35E-05	6,51E-01
12	0,033	4,78E-05	6,10E-01
13	0,036	5,20E-05	5,90E-01
14	0,039	5,63E-05	5,35E-01
15	0,042	6,05E-05	4,94E-01
16	0,045	6,47E-05	4,64E-01
17	0,048	6,90E-05	4,33E-01
18	0,051	7,32E-05	4,15E-01
19	0,061	8,71E-05	2,99E-01
20	0,071	1,01E-04	2,49E-01
21	0,081	1,15E-04	2,15E-01
22	0,091	1,28E-04	1,92E-01
23	0,101	1,41E-04	1,73E-01
24	0,111	1,55E-04	1,59E-01
25	0,121	1,68E-04	1,47E-01
26	0,131	1,81E-04	1,40E-01
27	0,141	1,94E-04	1,33E-01
28	0,151	2,07E-04	1,28E-01
29	0,161	2,19E-04	1,25E-01

Ehylenediamine (EDA):

[**TPT**] = 0.0000827 M.

$[Zn^{2\oplus}]$ = 0.00483 M.

V_{TPT} = 2.000 mL.

$V_{Zn(II)}$ = 0.0343 mL.

V_0 = 2.0343 mL.

[EDA] = 0.00447 M.

Entry	Volume (mL)	[analyte]	I
1	0	0,00E+00	9,93E-01
2	0,005	1,10E-05	9,76E-01
3	0,01	2,19E-05	9,61E-01
4	0,015	3,28E-05	9,42E-01
5	0,02	4,36E-05	9,20E-01
6	0,025	5,43E-05	8,91E-01
7	0,03	6,50E-05	8,53E-01
8	0,035	7,57E-05	8,28E-01
9	0,04	8,63E-05	7,84E-01
10	0,045	9,69E-05	7,45E-01
11	0,05	1,07E-04	7,06E-01
12	0,055	1,18E-04	6,59E-01
13	0,06	1,28E-04	6,09E-01
14	0,065	1,39E-04	5,64E-01
15	0,07	1,49E-04	5,23E-01
16	0,075	1,59E-04	4,72E-01
17	0,08	1,69E-04	4,21E-01
18	0,085	1,80E-04	3,76E-01
19	0,09	1,90E-04	3,33E-01
20	0,095	2,00E-04	2,91E-01
21	0,1	2,10E-04	2,55E-01
22	0,105	2,20E-04	2,21E-01
23	0,11	2,30E-04	1,93E-01
24	0,115	2,39E-04	1,48E-01
25	0,12	2,49E-04	1,31E-01
26	0,125	2,59E-04	1,17E-01
27	0,13	2,69E-04	1,08E-01
28	0,135	2,79E-04	1,00E-01
29	0,14	2,88E-04	9,20E-02
30	0,145	2,98E-04	8,83E-02
31	0,15	3,07E-04	8,59E-02

Imidazole:

[**TPT**] = 0.0000827 M.

[$Zn^{2\oplus}$] = 0.00483 M.

V_{TPT} = 2.000 mL.

$V_{Zn(II)}$ = 0.0343 mL.

V_0 = 2.0343 mL.

[Imidazole] = 0.00371 M.

Entry	Volume (mL)	[analyte]	I
1	0	0,00E+00	9,84E-01
2	0,003	5,47E-06	9,84E-01
3	0,006	1,09E-05	9,80E-01
4	0,009	1,64E-05	9,77E-01
5	0,012	2,18E-05	9,76E-01
6	0,017	3,08E-05	9,92E-01
7	0,022	3,98E-05	9,67E-01
8	0,027	4,87E-05	9,60E-01
9	0,037	6,64E-05	9,50E-01
10	0,047	8,39E-05	9,39E-01
11	0,057	1,01E-04	9,30E-01
12	0,067	1,18E-04	9,21E-01
13	0,077	1,36E-04	9,09E-01
14	0,087	1,52E-04	8,96E-01
15	0,097	1,69E-04	8,87E-01
16	0,107	1,86E-04	8,76E-01
17	0,117	2,02E-04	8,66E-01
18	0,127	2,18E-04	8,54E-01
19	0,177	2,97E-04	8,02E-01
20	0,227	3,73E-04	7,53E-01
21	0,277	4,45E-04	7,05E-01
22	0,327	5,15E-04	6,60E-01
23	0,377	5,81E-04	6,18E-01
24	0,477	7,06E-04	5,29E-01
25	0,577	8,21E-04	4,52E-01
26	0,677	9,28E-04	3,84E-01
27	0,777	1,03E-03	3,25E-01
28	0,877	1,12E-03	2,79E-01

N_{α}-(T*ert*-butoxycarbonyl)-L-histidine (2-His):
[**TPT**] = 0.0000827 M.
$[Zn^{2\oplus}]$ = 0.00483 M.
V_{TPT} = 2.000 mL.
$V_{Zn(II)}$ = 0.0343 mL.
V_0 = 2.0343 mL.
[2-His] = 0.0031612 M.

Entry	Volume (mL)	[analyte]	I
1	0,000	0,00E+00	9,85E-01
2	0,003	4,65E-06	9,92E-01
3	0,006	9,29E-06	9,93E-01
4	0,009	1,39E-05	9,83E-01
5	0,012	1,85E-05	9,79E-01
6	0,015	2,31E-05	9,71E-01
7	0,018	2,77E-05	9,58E-01
8	0,021	3,23E-05	9,38E-01
9	0,024	3,69E-05	9,21E-01
10	0,027	4,14E-05	9,10E-01
11	0,030	4,59E-05	8,85E-01
12	0,035	5,35E-05	8,53E-01
13	0,040	6,09E-05	7,90E-01
14	0,045	6,84E-05	7,46E-01
15	0,050	7,58E-05	6,87E-01
16	0,055	8,32E-05	6,61E-01
17	0,060	9,05E-05	6,29E-01
18	0,065	9,79E-05	5,97E-01
19	0,070	1,05E-04	5,38E-01
20	0,075	1,12E-04	5,09E-01
21	0,080	1,20E-04	4,85E-01
22	0,090	1,34E-04	4,35E-01
23	0,100	1,48E-04	3,94E-01
24	0,110	1,62E-04	3,61E-01
25	0,120	1,76E-04	3,31E-01
26	0,130	1,90E-04	3,01E-01
27	0,140	2,04E-04	2,79E-01
28	0,150	2,17E-04	2,62E-01
29	0,160	2,30E-04	2,43E-01
30	0,170	2,44E-04	2,30E-01
31	0,180	2,57E-04	2,19E-01
32	0,190	2,70E-04	2,13E-01
33	0,200	2,83E-04	2,03E-01
34	0,210	2,96E-04	1,96E-01
35	0,220	3,08E-04	1,89E-01
36	0,230	3,21E-04	1,83E-01
37	0,240	3,34E-04	1,83E-01
38	0,250	3,46E-04	1,75E-01
39	0,260	3,58E-04	1,70E-01
40	0,270	3,70E-04	1,69E-01
41	0,280	3,82E-04	1,63E-01

N_α-(Carbobenzyloxy)-L-histidine (3-His):

[**TPT**] = 0.0000827 M.

$[Zn^{2\oplus}]$ = 0.00483 M.

$V_{\mathbf{TPT}}$ = 2.000 mL.

$V_{Zn(II)}$ = 0.0343 mL.

V_0 = 2.0343 mL.

[3-His] = 0.0031802 M.

Entry	Volume (mL)	[analyte]	I
1	0	0,00E+00	9,89E-01
2	0,003	4,68E-06	9,81E-01
3	0,006	9,35E-06	9,69E-01
4	0,009	1,40E-05	9,78E-01
5	0,012	1,87E-05	9,44E-01
6	0,015	2,33E-05	9,28E-01
7	0,018	2,79E-05	9,13E-01
8	0,021	3,25E-05	8,93E-01
9	0,024	3,71E-05	8,77E-01
10	0,027	4,17E-05	8,56E-01
11	0,03	4,62E-05	8,30E-01
12	0,033	5,08E-05	8,07E-01
13	0,038	5,83E-05	7,67E-01
14	0,043	6,58E-05	7,32E-01
15	0,048	7,33E-05	6,92E-01
16	0,053	8,08E-05	6,53E-01
17	0,058	8,82E-05	6,18E-01
18	0,063	9,55E-05	5,82E-01
19	0,068	1,03E-04	5,47E-01
20	0,073	1,10E-04	5,15E-01
21	0,078	1,17E-04	4,88E-01
22	0,083	1,25E-04	4,69E-01
23	0,093	1,39E-04	4,16E-01
24	0,103	1,53E-04	3,77E-01
25	0,113	1,67E-04	3,41E-01
26	0,123	1,81E-04	3,15E-01
27	0,133	1,95E-04	2,92E-01
28	0,143	2,09E-04	2,73E-01
29	0,153	2,22E-04	2,59E-01
30	0,163	2,36E-04	2,42E-01
31	0,173	2,49E-04	2,29E-01
32	0,183	2,62E-04	2,18E-01
33	0,193	2,76E-04	2,10E-01
34	0,203	2,89E-04	2,02E-01
35	0,213	3,01E-04	1,95E-01
36	0,223	3,14E-04	1,89E-01
37	0,233	3,27E-04	1,83E-01
38	0,243	3,39E-04	1,78E-01
39	0,253	3,52E-04	1,73E-01

N_{α}-(Fluorenylmethyloxycarbonyl)-$N_{(im)}$-benzyl-L-histidine (4-His):

[**TPT**] = 0.0000827 M.

$[Zn^{2\oplus}]$ = 0.00483 M.

V_{TPT} = 2.000 mL.

$V_{Zn(II)}$ = 0.0343 mL.

V_0 = 2.0343 mL.

[4-His] = 0.0022865 M.

Entry	Volume (mL)	[analyte]	I
1	0,000	0,00E+00	9,86E-01
2	0,005	5,61E-06	9,83E-01
3	0,010	1,12E-05	9,75E-01
4	0,015	1,67E-05	9,70E-01
5	0,020	2,23E-05	9,68E-01
6	0,025	2,78E-05	9,46E-01
7	0,030	3,32E-05	9,31E-01
8	0,035	3,87E-05	9,18E-01
9	0,040	4,41E-05	9,08E-01
10	0,045	4,95E-05	8,87E-01
11	0,050	5,49E-05	8,63E-01
12	0,055	6,02E-05	8,53E-01
13	0,065	7,08E-05	8,12E-01
14	0,075	8,13E-05	7,59E-01
15	0,085	9,17E-05	7,22E-01
16	0,095	1,02E-04	6,80E-01
17	0,105	1,12E-04	6,46E-01
18	0,115	1,22E-04	6,04E-01
19	0,125	1,32E-04	5,56E-01
20	0,135	1,42E-04	5,24E-01
21	0,145	1,52E-04	5,00E-01
22	0,155	1,62E-04	4,66E-01
23	0,165	1,72E-04	4,36E-01
24	0,175	1,81E-04	4,11E-01
25	0,185	1,91E-04	3,89E-01
26	0,195	2,00E-04	3,62E-01
27	0,205	2,09E-04	3,39E-01
28	0,255	2,55E-04	2,74E-01
29	0,305	2,98E-04	2,28E-01
30	0,355	3,40E-04	2,00E-01
31	0,455	4,18E-04	1,62E-01
32	0,555	4,90E-04	1,42E-01
33	0,655	5,57E-04	1,30E-01

N_{α}-(T*ert*-butoxycarbonyl)-$N_{(im)}$-tosyl-L-histidine (5-His):

[**TPT**] = 0.0000827 M.

$[Zn^{2\oplus}]$ = 0.00483 M.

V_{TPT} = 2.000 mL.

$V_{Zn(II)}$ = 0.0343 mL.

V_0 = 2.0343 mL.

[5-His] = 0.0027531 M.

Entry	Volume (mL)	[analyte]	I
1	0,000	0,00E+00	9,88E-01
2	0,005	6,75E-06	9,78E-01
3	0,010	1,35E-05	9,68E-01
4	0,015	2,02E-05	9,66E-01
5	0,020	2,68E-05	9,38E-01
6	0,025	3,34E-05	9,26E-01
7	0,035	4,66E-05	8,99E-01
8	0,045	5,96E-05	8,69E-01
9	0,055	7,25E-05	8,50E-01
10	0,065	8,52E-05	8,05E-01
11	0,075	9,79E-05	7,77E-01
12	0,085	1,10E-04	7,36E-01
13	0,095	1,23E-04	7,02E-01
14	0,105	1,35E-04	6,59E-01
15	0,115	1,47E-04	6,38E-01
16	0,125	1,59E-04	6,06E-01
17	0,135	1,71E-04	5,77E-01
18	0,145	1,83E-04	5,55E-01
19	0,155	1,95E-04	5,33E-01
20	0,165	2,07E-04	5,14E-01
21	0,175	2,18E-04	4,86E-01
22	0,225	2,74E-04	3,92E-01
23	0,275	3,28E-04	3,31E-01
24	0,325	3,79E-04	2,87E-01
25	0,375	4,29E-04	2,53E-01
26	0,425	4,76E-04	2,26E-01
27	0,525	5,65E-04	1,86E-01
28	0,625	6,47E-04	1,62E-01
29	0,725	7,23E-04	1,44E-01
30	0,825	7,94E-04	1,36E-01
31	0,925	8,61E-04	1,23E-01

7.2.3 TPON Fluorescence study

Fluoride:

[**TPON**] = 0.0000699 M.

$[Zn^{2\oplus}]$ = 0.00483 M.

$V_{\mathbf{TPON}}$ = 2.000 mL.

$V_{Zn(II)}$ = 0.029 mL.

V_0 = 2.029 mL.

[Fluoride] = 0.003524 M.

Entry	Volume (mL)	[analyte]	I	28	0,081	1,35E-04	2,46E-01
1	0,000	0,00E+00	9,73E-01	29	0,084	1,40E-04	2,33E-01
2	0,003	5,20E-06	9,58E-01	30	0,087	1,45E-04	2,20E-01
3	0,006	1,04E-05	9,15E-01	31	0,090	1,50E-04	2,09E-01
4	0,009	1,56E-05	8,62E-01	32	0,093	1,54E-04	1,98E-01
5	0,012	2,07E-05	8,18E-01	33	0,096	1,59E-04	1,87E-01
6	0,015	2,59E-05	7,64E-01	34	0,099	1,64E-04	1,76E-01
7	0,018	3,10E-05	7,11E-01	35	0,102	1,69E-04	1,67E-01
8	0,021	3,61E-05	6,70E-01	36	0,105	1,73E-04	1,59E-01
9	0,024	4,12E-05	6,40E-01	37	0,108	1,78E-04	1,53E-01
10	0,027	4,63E-05	6,08E-01	38	0,111	1,83E-04	1,46E-01
11	0,030	5,13E-05	5,77E-01	39	0,114	1,87E-04	1,39E-01
12	0,033	5,64E-05	5,47E-01	40	0,117	1,92E-04	1,34E-01
13	0,036	6,14E-05	5,17E-01	41	0,120	1,97E-04	1,36E-01
14	0,039	6,65E-05	4,90E-01	42	0,130	2,12E-04	1,22E-01
15	0,042	7,15E-05	4,65E-01	43	0,140	2,27E-04	1,12E-01
16	0,045	7,65E-05	4,40E-01	44	0,150	2,43E-04	1,01E-01
17	0,048	8,14E-05	4,17E-01	45	0,160	2,58E-04	9,33E-02
18	0,051	8,64E-05	4,06E-01	46	0,170	2,72E-04	8,72E-02
19	0,054	9,14E-05	3,88E-01	47	0,180	2,87E-04	8,26E-02
20	0,057	9,63E-05	3,68E-01	48	0,190	3,02E-04	7,83E-02
21	0,060	1,01E-04	3,51E-01	49	0,200	3,16E-04	7,49E-02
22	0,063	1,06E-04	3,33E-01	50	0,210	3,31E-04	7,05E-02
23	0,066	1,11E-04	3,16E-01	51	0,220	3,45E-04	6,95E-02
24	0,069	1,16E-04	3,01E-01	52	0,270	4,14E-04	6,16E-02
25	0,072	1,21E-04	2,88E-01	53	0,370	5,44E-04	5,17E-02
26	0,075	1,26E-04	2,74E-01	54	0,470	6,63E-04	4,64E-02
27	0,078	1,30E-04	2,61E-01	55	0,570	7,73E-04	4,31E-02

Chloride:

[**TPON**] = 0.0000699 M.

[$Zn^{2\oplus}$] = 0.00483 M.

$V_{\mathbf{TPON}}$ = 2.000 mL.

$V_{Zn(II)}$ = 0.029 mL.

V_0 = 2.029 mL.

[Chloride] = 0.0035368 M.

Entry	Volume (mL)	[analyte]	I
1	0,000	0,00E+00	9,70E-01
2	0,003	5,22E-06	9,43E-01
3	0,006	1,04E-05	8,99E-01
4	0,009	1,56E-05	8,51E-01
5	0,012	2,08E-05	8,17E-01
6	0,015	2,60E-05	7,87E-01
7	0,018	3,11E-05	7,60E-01
8	0,021	3,62E-05	7,11E-01
9	0,024	4,13E-05	6,67E-01
10	0,027	4,64E-05	6,32E-01
11	0,030	5,15E-05	6,02E-01
12	0,033	5,66E-05	5,71E-01
13	0,036	6,17E-05	5,45E-01
14	0,039	6,67E-05	5,16E-01
15	0,042	7,17E-05	4,94E-01
16	0,045	7,67E-05	4,67E-01
17	0,048	8,17E-05	4,44E-01
18	0,051	8,67E-05	4,26E-01
19	0,054	9,17E-05	3,92E-01
20	0,057	9,66E-05	3,75E-01
21	0,060	1,02E-04	3,60E-01
22	0,065	1,10E-04	3,43E-01
23	0,070	1,18E-04	3,23E-01
24	0,075	1,26E-04	3,04E-01
25	0,080	1,34E-04	2,88E-01
26	0,085	1,42E-04	2,74E-01
27	0,090	1,50E-04	2,58E-01
28	0,095	1,58E-04	2,50E-01
29	0,100	1,66E-04	2,41E-01
30	0,105	1,74E-04	2,33E-01
31	0,110	1,82E-04	2,26E-01
32	0,120	1,97E-04	2,13E-01
33	0,130	2,13E-04	2,00E-01
34	0,140	2,28E-04	1,90E-01
35	0,150	2,43E-04	1,81E-01
36	0,160	2,59E-04	1,75E-01
37	0,210	3,32E-04	1,40E-01
38	0,260	4,02E-04	1,16E-01
39	0,360	5,33E-04	8,17E-02
40	0,460	6,54E-04	6,19E-02
41	0,560	7,65E-04	5,09E-02

Bromide:

[**TPON**] = 0.0000699 M.

[$Zn^{2\oplus}$] = 0.00483 M.

$V_{\mathbf{TPON}}$ = 2.000 mL.

$V_{Zn(II)}$ = 0.029 mL.

V_0 = 2.029 mL.

[Bromide] = 0.0031919 M.

Entry	Volume (mL)	[analyte]	I
1	0,000	0,00E+00	9,69E-01
2	0,003	4,71E-06	9,37E-01
3	0,006	9,41E-06	9,07E-01
4	0,009	1,41E-05	8,96E-01
5	0,012	1,88E-05	8,41E-01
6	0,015	2,34E-05	8,16E-01
7	0,018	2,81E-05	7,80E-01
8	0,021	3,27E-05	7,39E-01
9	0,024	3,73E-05	6,92E-01
10	0,027	4,19E-05	6,62E-01
11	0,030	4,65E-05	6,35E-01
12	0,033	5,11E-05	6,13E-01
13	0,036	5,56E-05	5,87E-01
14	0,039	6,02E-05	5,62E-01
15	0,042	6,47E-05	5,34E-01
16	0,045	6,93E-05	5,19E-01
17	0,048	7,38E-05	5,00E-01
18	0,051	7,83E-05	4,76E-01
19	0,054	8,27E-05	4,61E-01
20	0,057	8,72E-05	4,44E-01
21	0,060	9,17E-05	4,32E-01
22	0,065	9,91E-05	4,07E-01
23	0,070	1,06E-04	3,88E-01
24	0,075	1,14E-04	3,69E-01
25	0,080	1,21E-04	3,51E-01
26	0,085	1,28E-04	3,37E-01
27	0,090	1,36E-04	3,23E-01
28	0,095	1,43E-04	3,09E-01
29	0,100	1,50E-04	2,92E-01
30	0,105	1,57E-04	2,83E-01
31	0,110	1,64E-04	2,72E-01
32	0,120	1,78E-04	2,53E-01
33	0,130	1,92E-04	2,36E-01
34	0,140	2,06E-04	2,22E-01
35	0,150	2,20E-04	2,09E-01
36	0,160	2,33E-04	1,97E-01
37	0,210	2,99E-04	1,49E-01
38	0,260	3,63E-04	1,14E-01
39	0,360	4,81E-04	7,36E-02
40	0,460	5,90E-04	5,87E-02
41	0,560	6,90E-04	4,83E-02

Iodide:

[**TPON**] = 0.0000699 M.

[$Zn^{2\oplus}$] = 0.00483 M.

$V_{\mathbf{TPON}}$ = 2.000 mL.

$V_{Zn(II)}$ = 0.029 mL.

V_0 = 2.029 mL.

[Bromide] = 0.002959 M.

Entry	Volume (mL)	[analyte]	I
1	0,000	0,00E+00	9,69E-01
2	0,003	4,37E-06	9,35E-01
3	0,006	8,72E-06	9,06E-01
4	0,009	1,31E-05	8,73E-01
5	0,012	1,74E-05	8,42E-01
6	0,015	2,17E-05	8,09E-01
7	0,018	2,60E-05	7,79E-01
8	0,021	3,03E-05	7,57E-01
9	0,024	3,46E-05	7,23E-01
10	0,027	3,89E-05	7,03E-01
11	0,030	4,31E-05	6,96E-01
12	0,033	4,74E-05	6,46E-01
13	0,036	5,16E-05	6,22E-01
14	0,039	5,58E-05	6,01E-01
15	0,042	6,00E-05	5,81E-01
16	0,045	6,42E-05	5,64E-01
17	0,048	6,84E-05	5,44E-01
18	0,051	7,26E-05	5,30E-01
19	0,054	7,67E-05	5,09E-01
20	0,057	8,09E-05	4,94E-01
21	0,060	8,50E-05	4,80E-01
22	0,065	9,19E-05	4,53E-01
23	0,070	9,87E-05	4,28E-01
24	0,075	1,05E-04	4,09E-01
25	0,080	1,12E-04	3,90E-01
26	0,085	1,19E-04	3,69E-01
27	0,090	1,26E-04	3,53E-01
28	0,095	1,32E-04	3,39E-01
29	0,100	1,39E-04	3,24E-01
30	0,105	1,46E-04	3,09E-01
31	0,110	1,52E-04	2,95E-01
32	0,120	1,65E-04	2,72E-01
33	0,130	1,78E-04	2,51E-01
34	0,140	1,91E-04	2,33E-01
35	0,150	2,04E-04	2,17E-01
36	0,160	2,16E-04	2,01E-01
37	0,210	2,78E-04	1,46E-01
38	0,260	3,36E-04	1,10E-01
39	0,360	4,46E-04	7,13E-02
40	0,460	5,47E-04	5,49E-02
41	0,560	6,40E-04	4,70E-02

Cyanide:

[**TPON**] = 0.0000699 M.

$[Zn^{2\oplus}]$ = 0.00483 M.

$V_{\mathbf{TPON}}$ = 2.000 mL.

$V_{Zn(II)}$ = 0.029 mL.

V_0 = 2.029 mL.

[Cyanide] = 0.0024078 M.

Entry	Volume (mL)	[analyte]	I	17	0,080	9,13E-05	2,66E-01
1	0,000	0,00E+00	9,71E-01	18	0,085	9,68E-05	2,33E-01
2	0,005	5,92E-06	9,53E-01	19	0,090	1,02E-04	2,02E-01
3	0,010	1,18E-05	9,25E-01	20	0,095	1,08E-04	1,76E-01
4	0,015	1,77E-05	8,89E-01	21	0,100	1,13E-04	1,54E-01
5	0,020	2,35E-05	8,54E-01	22	0,105	1,18E-04	1,33E-01
6	0,025	2,93E-05	8,10E-01	23	0,110	1,24E-04	1,16E-01
7	0,030	3,51E-05	7,59E-01	24	0,115	1,29E-04	1,02E-01
8	0,035	4,08E-05	7,02E-01	25	0,120	1,34E-04	9,01E-02
9	0,040	4,66E-05	6,58E-01	26	0,125	1,40E-04	8,07E-02
10	0,045	5,22E-05	5,92E-01	27	0,130	1,45E-04	7,34E-02
11	0,050	5,79E-05	5,40E-01	28	0,135	1,50E-04	6,73E-02
12	0,055	6,35E-05	4,85E-01	29	0,145	1,61E-04	5,90E-02
13	0,060	6,92E-05	4,34E-01	30	0,195	2,11E-04	4,20E-02
14	0,065	7,47E-05	3,84E-01	31	0,295	3,06E-04	3,33E-02
15	0,070	8,03E-05	3,42E-01	32	0,395	3,92E-04	3,25E-02
16	0,075	8,58E-05	3,04E-01	33	0,495	4,72E-04	3,24E-02

Thiocyanide:

[**TPON**] = 0.0000699 M.

$[Zn^{2\oplus}]$ = 0.00483 M.

$V_{\mathbf{TPON}}$ = 2.000 mL.

$V_{Zn(II)}$ = 0.029 mL.

V_0 = 2.029 mL.

[Thiocyanide] = 0.00538 M.

Entry	Volume (mL)	[analyte]	I	12	0,055	1,42E-04	2,50E-01
1	0,000	0,00E+00	9,74E-01	13	0,065	1,67E-04	2,04E-01
2	0,005	1,32E-05	9,09E-01	14	0,075	1,92E-04	1,81E-01
3	0,010	2,64E-05	8,32E-01	15	0,085	2,16E-04	1,71E-01
4	0,015	3,95E-05	7,42E-01	16	0,095	2,41E-04	1,53E-01
5	0,020	5,25E-05	6,42E-01	17	0,105	2,65E-04	1,41E-01
6	0,025	6,55E-05	5,59E-01	18	0,155	3,82E-04	1,11E-01
7	0,030	7,84E-05	4,66E-01	19	0,255	6,01E-04	8,47E-02
8	0,035	9,12E-05	3,93E-01	20	0,355	8,01E-04	6,97E-02
9	0,040	1,04E-04	3,43E-01	21	0,455	9,85E-04	6,25E-02
10	0,045	1,17E-04	3,08E-01	22	0,555	1,16E-03	5,29E-02
11	0,050	1,29E-04	2,74E-01	23	0,655	1,31E-03	4,92E-02

Nitrite:

[**TPON**] = 0.0000694 M.

$[Zn^{2\oplus}]$ = 0.00483 M.

$V_{\mathbf{TPON}}$ = 2.000 mL

$V_{Zn(II)}$ = 0.0283 mL.

V_0 = 2.029 mL.

[Nitrite] = 0.00845 M.

Entry	Volume (mL)	[analyte]	I
1	0,000	0,00E+00	9,89E-01
2	0,003	1,25E-05	8,82E-01
3	0,006	2,49E-05	7,44E-01
4	0,009	3,73E-05	6,25E-01
5	0,012	4,97E-05	5,19E-01
6	0,015	6,20E-05	4,29E-01
7	0,018	7,43E-05	3,42E-01
8	0,021	8,66E-05	2,26E-01
9	0,024	9,88E-05	1,53E-01
10	0,029	1,19E-04	1,38E-01
11	0,034	1,39E-04	1,35E-01
12	0,044	1,79E-04	1,30E-01
13	0,054	2,19E-04	1,26E-01
14	0,064	2,58E-04	1,16E-01

Nitrate:

[**TPON**] = 0.0000694 M.

$[Zn^{2\oplus}]$ = 0.00483 M.

$V_{\mathbf{TPON}}$ = 2.000 mL

$V_{Zn(II)}$ = 0.0283 mL.

V_0 = 2.029 mL.

[Nitrate] = 0.0079 M.

Entry	Volume (mL)	[analyte]	I
1	0,000	0,00E+00	9,87E-01
2	0,005	1,94E-05	9,70E-01
3	0,010	3,88E-05	9,44E-01
4	0,015	5,80E-05	9,36E-01
5	0,020	7,71E-05	8,91E-01
6	0,025	9,62E-05	8,66E-01
7	0,030	1,15E-04	8,37E-01
8	0,035	1,34E-04	7,95E-01
9	0,040	1,53E-04	7,64E-01
10	0,045	1,71E-04	7,31E-01
11	0,050	1,90E-04	6,85E-01
12	0,060	2,27E-04	6,19E-01
13	0,070	2,64E-04	5,46E-01
14	0,080	3,00E-04	4,85E-01
15	0,090	3,36E-04	4,27E-01
16	0,100	3,71E-04	3,81E-01
17	0,110	4,06E-04	3,31E-01
18	0,120	4,41E-04	2,91E-01
19	0,130	4,76E-04	2,37E-01
20	0,140	5,10E-04	2,09E-01
21	0,150	5,44E-04	1,87E-01
22	0,160	5,78E-04	1,72E-01
23	0,170	6,11E-04	1,56E-01
24	0,180	6,44E-04	1,41E-01
25	0,190	6,77E-04	1,27E-01

Histidine:

[**TPON**] = 0.0000699 M.

[$Zn^{2\oplus}$] = 0.00483 M.

V_{TPON} = 2.000 mL

$V_{Zn(II)}$ = 0.029 mL.

V_0 = 2.029 mL.

[Histidine] = 0.00288 M.

Entry	Volume (mL)	[analyte]	I				
1	0,000	0,00E+00	9,68E-01	**13**	0,060	8,27E-05	1,71E-01
2	0,005	7,08E-06	9,27E-01	**14**	0,065	8,94E-05	1,38E-01
3	0,010	1,41E-05	8,78E-01	**15**	0,070	9,60E-05	1,14E-01
4	0,015	2,11E-05	8,14E-01	**16**	0,075	1,03E-04	9,59E-02
5	0,020	2,81E-05	7,46E-01	**17**	0,080	1,09E-04	8,05E-02
6	0,025	3,51E-05	6,64E-01	**18**	0,085	1,16E-04	6,98E-02
7	0,030	4,20E-05	5,74E-01	**19**	0,090	1,22E-04	6,12E-02
8	0,035	4,88E-05	4,93E-01	**20**	0,100	1,35E-04	5,05E-02
9	0,040	5,57E-05	4,08E-01	**21**	0,150	1,98E-04	3,68E-02
10	0,045	6,25E-05	3,28E-01	**22**	0,250	3,16E-04	3,45E-02
11	0,050	6,93E-05	2,61E-01	**23**	0,350	4,24E-04	3,41E-02
12	0,055	7,60E-05	2,10E-01	**24**	0,450	5,23E-04	3,54E-02
				25	0,550	6,14E-04	3,30E-02

7.2.4 TQPO Fluorescence study

TQPO1:

[**TQPO1**] = 0.0000536 M.

[$Cu^{2\oplus}$] = 0.00494 M.

V_{TQPO1} = 2.000 mL

Entry	Volume (mL)	[analyte]	I
1	0,000	0,00E+00	1,00E+00
2	0,003	7,41E-06	9,79E-01
3	0,006	1,48E-05	9,22E-01
4	0,009	2,22E-05	8,64E-01
5	0,012	2,95E-05	7,78E-01
6	0,015	3,68E-05	6,99E-01
7	0,018	4,41E-05	6,05E-01
8	0,021	5,14E-05	5,20E-01
9	0,024	5,86E-05	4,35E-01
10	0,029	7,07E-05	2,93E-01
11	0,034	8,27E-05	2,06E-01
12	0,044	1,06E-04	1,19E-01
13	0,054	1,30E-04	1,02E-01

TQPO2:

[**TQPO2**] = 0.0000549 M.

[$Cu^{2\oplus}$] = 0.00494 M.

V_{TQPO2} = 2.000 mL

Entry	Volume (mL)	[analyte]	I
1	0,000	0,00E+00	1,00E+00
2	0,005	1,23E-05	9,41E-01
3	0,010	2,46E-05	8,32E-01
4	0,015	3,68E-05	7,04E-01
5	0,020	4,90E-05	5,76E-01
6	0,025	6,10E-05	4,87E-01
7	0,030	7,31E-05	4,15E-01
8	0,035	8,50E-05	3,77E-01
9	0,040	9,70E-05	3,58E-01
10	0,045	1,09E-04	3,42E-01
11	0,050	1,21E-04	3,46E-01

TQPO3:

[**TQPO3**] = 0.0000559 M.

[$Cu^{2\oplus}$] = 0.00494 M.

V_{TQPO3} = 2.000 mL

Entry	Volume (mL)	[analyte]	I
1	0,000	0,00E+00	1,00E+00
2	0,005	1,23E-05	8,32E-01
3	0,010	2,46E-05	5,99E-01
4	0,015	3,68E-05	3,50E-01
5	0,020	4,90E-05	1,83E-01
6	0,025	6,10E-05	7,41E-02
7	0,030	7,31E-05	3,07E-02
8	0,035	8,50E-05	1,96E-02

TQPO4:

[**TQPO4**] = 0.0000531 M.

[$Cu^{2\oplus}$] = 0.00494 M.

V_{TQPO4} = 2.000 mL

Entry	Volume (mL)	[analyte]	I
1	0,000	0,00E+00	1,00E+00
2	0,005	1,23E-05	8,99E-01
3	0,010	2,46E-05	5,42E-01
4	0,015	3,68E-05	3,20E-01
5	0,020	4,90E-05	1,06E-01
6	0,025	6,10E-05	2,92E-02
7	0,030	7,31E-05	1,80E-02

7.2.5 Chiral Amino Acid recognition

D-Glutamic:
[**TPT**] = 0.0000825 M.
[$Zn^{2\oplus}$] = 0.00483 M.
[L-His] = 0.006419 M.
V_{TPT} = 2.000 mL.
$V_{Zn(II)}$ = 0.0342 mL.
$V_{L\text{-}His}$ = 0.0254 mL.
V_0 = 2.0596 mL.
[D-Glutamic] = 0.008244 M.

Entry	volume (mL)	[analyte]	I first test	I second test	Ī
1	0,000	0,00E+00	1,00E+00	1,00E+00	1,00E+00
2	0,003	1,21E-05	8,85E-01	8,85E-01	8,85E-01
3	0,006	2,42E-05	7,93E-01	7,94E-01	7,94E-01
4	0,009	3,62E-05	7,21E-01	7,18E-01	7,20E-01
5	0,012	4,82E-05	6,54E-01	6,57E-01	6,56E-01
6	0,018	7,21E-05	5,59E-01	5,60E-01	5,60E-01
7	0,024	9,59E-05	4,95E-01	4,95E-01	4,95E-01
8	0,034	1,35E-04	4,22E-01	4,36E-01	4,29E-01
9	0,044	1,74E-04	3,77E-01	3,90E-01	3,83E-01

L-Glutamic:
[**TPT**] = 0.0000825 M.
[$Zn^{2\oplus}$] = 0.00483 M.
[L-His] = 0.006419 M.
V_{TPT} = 2.000 mL.
$V_{Zn(II)}$ = 0.0342 mL.
$V_{L\text{-}His}$ = 0.0254 mL.
V_0 = 2.0596 mL.
[L-Glutamic] = 0.008300 M.

Entry	volume (mL)	[analyte]	I first test	I second test	Ī
1	0,000	0,00E+00	1,00E+00	1,00E+00	1,00E+00
2	0,003	1,21E-05	9,05E-01	8,85E-01	8,95E-01
3	0,006	2,41E-05	8,14E-01	7,86E-01	8,00E-01
4	0,009	3,61E-05	7,37E-01	7,21E-01	7,29E-01
5	0,012	4,81E-05	6,83E-01	6,76E-01	6,79E-01
6	0,018	7,20E-05	5,79E-01	6,02E-01	5,90E-01
7	0,024	9,57E-05	5,18E-01	5,55E-01	5,36E-01
8	0,034	1,35E-04	4,49E-01	4,95E-01	4,71E-01
9	0,044	1,74E-04	4,06E-01	4,57E-01	4,30E-01

D-Aspartic:

[**TPT**] = 0.0000825 M.

[$Zn^{2\oplus}$] = 0.00483 M.

[L-His] = 0.006419 M.

V_{TPT} = 2.000 mL.

$V_{Zn(II)}$ = 0.0342 mL.

$V_{L\text{-}His}$ = 0.0254 mL.

V_0 = 2.0596 mL.

[D-Aspartic] = 0.008392 M.

Entry	volume (mL)	[analyte]	I first test	I second test	$\bar{I}$
1	0,000	0,00E+00	1,00E+00	1,00E+00	1,00E+00
2	0,003	1,23E-05	8,84E-01	8,90E-01	8,87E-01
3	0,006	2,46E-05	7,88E-01	7,98E-01	7,93E-01
4	0,009	3,69E-05	7,11E-01	7,19E-01	7,15E-01
5	0,012	4,91E-05	6,53E-01	6,51E-01	6,52E-01
6	0,018	7,34E-05	5,53E-01	5,56E-01	5,55E-01
7	0,024	9,76E-05	4,82E-01	4,84E-01	4,83E-01
8	0,034	1,38E-04	4,06E-01	4,14E-01	4,10E-01
9	0,044	1,77E-04	3,57E-01	3,60E-01	3,58E-01

L-Aspartic:

[**TPT**] = 0.0000825 M.

[$Zn^{2\oplus}$] = 0.00483 M.

[L-His] = 0.006419 M.

V_{TPT} = 2.000 mL.

$V_{Zn(II)}$ = 0.0342 mL.

$V_{L\text{-}His}$ = 0.0254 mL.

V_0 = 2.0596 mL.

[L-Aspartic] = 0.008452 M.

Entry	volume (mL)	[analyte]	I first test	I second test	$\bar{I}$
1	0,000	0,00E+00	1,00E+00	1,00E+00	1,00E+00
2	0,003	1,23E-05	8,88E-01	9,08E-01	8,98E-01
3	0,006	2,46E-05	7,94E-01	8,15E-01	8,04E-01
4	0,009	3,68E-05	7,18E-01	7,29E-01	7,24E-01
5	0,012	4,90E-05	6,49E-01	6,56E-01	6,52E-01
6	0,018	7,32E-05	5,58E-01	5,53E-01	5,55E-01
7	0,024	9,74E-05	4,89E-01	4,86E-01	4,88E-01
8	0,034	1,37E-04	4,22E-01	4,02E-01	4,11E-01
9	0,044	1,77E-04	3,72E-01	3,51E-01	3,61E-01

Imidazole:

[**TPT**] = 0.0000827 M.

[$Zn^{2\oplus}$] = 0.00483 M.

[L-His] = 0.00288 M.

V_{TPT} = 2.000 mL.

$V_{Zn(II)}$ = 0.0342 mL.

$V_{L\text{-}His}$ = 0.0573 mL.

V_0 = 2.0915 mL.

[Imidazole] = 0.003716 M.

Entry	volume (mL)	[analyte]	I
1	0,000	0,00E+00	9,89E-01
2	0,010	1,77E-05	8,25E-01
3	0,020	3,52E-05	7,05E-01
4	0,030	5,25E-05	6,15E-01
5	0,040	6,97E-05	5,51E-01
6	0,050	8,68E-05	5,21E-01
7	0,060	1,04E-04	5,03E-01
8	0,070	1,20E-04	4,84E-01
9	0,080	1,37E-04	4,81E-01
10	0,090	1,53E-04	4,72E-01
11	0,100	1,70E-04	4,63E-01
12	0,110	1,86E-04	4,56E-01
13	0,120	2,02E-04	4,50E-01

R,*R*-Diaminocyclohexane (DACH):

[**TPT**] = 0.0000827 M.

[$Zn^{2\oplus}$] = 0.00483 M.

V_{TPT} = 2.000 mL.

$V_{Zn(II)}$ = 0.0343 mL.

V_0 = 2.0343 mL.

[DACH] = 0.00451 M.

Entry	volume (mL)	[analyte]	I
1	0,000	0,00E+00	9,91E-01
2	0,005	6,75E-06	9,60E-01
3	0,010	1,35E-05	9,20E-01
4	0,015	2,02E-05	8,77E-01
5	0,020	2,68E-05	8,19E-01
6	0,025	3,34E-05	7,51E-01
7	0,030	4,00E-05	6,84E-01
8	0,035	4,66E-05	6,20E-01
9	0,040	5,31E-05	5,39E-01
10	0,045	5,96E-05	4,71E-01
11	0,050	6,60E-05	3,90E-01
12	0,055	7,25E-05	3,22E-01
13	0,060	7,89E-05	2,61E-01
14	0,065	8,52E-05	2,10E-01
15	0,070	9,16E-05	1,66E-01
16	0,075	9,79E-05	1,35E-01
17	0,080	1,04E-04	1,10E-01
18	0,085	1,10E-04	9,49E-02
19	0,090	1,17E-04	8,56E-02
20	0,095	1,23E-04	8,03E-02

L-Glutamic:

[**TPT**] = 0.0000827 M.

[$Zn^{2\oplus}$] = 0.00483 M.

[*R*,*R*-DACH] = 0.006419 M.

$V_{\mathbf{TPT}}$ = 2.000 mL.

$V_{Zn(II)}$ = 0.034 mL.

$V_{R,R\text{-DACH}}$ = 0.015 mL.

V_0 = 2.049 mL.

[L-Glutamic] = 0.008489 M.

Entry	volume (mL)	[analyte]	I
1	0,000	0,00E+00	9,89E-01
2	0,005	2,07E-05	9,30E-01
3	0,010	4,12E-05	8,49E-01
4	0,015	6,17E-05	7,68E-01
5	0,020	8,21E-05	6,91E-01
6	0,025	1,02E-04	6,24E-01
7	0,030	1,22E-04	5,68E-01
8	0,035	1,43E-04	5,21E-01
9	0,040	1,63E-04	4,74E-01
10	0,045	1,82E-04	4,39E-01
11	0,050	2,02E-04	4,08E-01
12	0,060	2,41E-04	3,60E-01
13	0,070	2,80E-04	3,26E-01
14	0,080	3,19E-04	2,98E-01
15	0,090	3,57E-04	2,81E-01
16	0,100	3,95E-04	2,66E-01
17	0,110	4,32E-04	2,56E-01
18	0,120	4,70E-04	2,49E-01

D-Glutamic:

[**TPT**] = 0.0000827 M.

[$Zn^{2\oplus}$] = 0.00483 M.

[*R*,*R*-DACH] = 0.006419 M.

$V_{\mathbf{TPT}}$ = 2.000 mL.

$V_{Zn(II)}$ = 0.034 mL.

$V_{R,R\text{-DACH}}$ = 0.015 mL.

V_0 = 2.049 mL.

[D-Glutamic] = 0.008414 M.

Entry	volume (mL)	[analyte]	I
1	0,005	0,00E+00	9,89E-01
2	0,010	2,05E-05	9,15E-01
3	0,015	4,09E-05	8,24E-01
4	0,020	6,11E-05	7,39E-01
5	0,025	8,13E-05	6,66E-01
6	0,030	1,01E-04	6,06E-01
7	0,035	1,21E-04	5,53E-01
8	0,040	1,41E-04	5,09E-01
9	0,045	1,61E-04	4,76E-01
10	0,050	1,81E-04	4,47E-01
11	0,060	2,00E-04	4,22E-01
12	0,070	2,39E-04	3,81E-01
13	0,080	2,78E-04	3,53E-01
14	0,090	3,16E-04	3,31E-01
15	0,100	3,54E-04	3,13E-01
16	0,110	3,92E-04	3,00E-01
17	0,120	4,29E-04	2,89E-01
18	0,000	4,65E-04	2,81E-01